

High-Resolution Seismic Investigation of Subsidence from Dissolution

By

Richard D. Miller

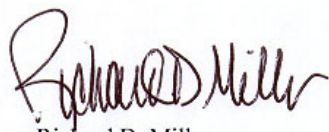
Dissertation submitted to

Department Angewandte Geowissenschaften und Geophysik
Lehrstuhl für Geophysik
Montanuniversität Leoben, Austria

October, 2007

Ich versichere an Eides statt, die vorliegende Arbeit selbständig unter Verwendung der angegebenen Literatur durchgeführt zu haben

I declare upon oath that this dissertation is my own work using only literature referenced in this thesis.

A handwritten signature in dark ink, appearing to read 'Richard D. Miller'. The signature is fluid and cursive, with the first name 'Richard' and last name 'Miller' clearly distinguishable.

Richard D. Miller
Leoben, October 2007

Acknowledgement

I will be forever indebted to Professor Karl Millahn. Agreeing to take me on, as a doctoral student was a bold decision that I deeply appreciate and respect. He has provided guidance and enlightenment, while teaching this 'old dog' a few new tricks and enduring the frustration of having a graduate student who resides 8,000 km (as the plane flies) and seven time zones away. His calm demeanor and keen sense of importance has been an inspiration and will forever shape the way I work and guide my graduate students.

Support provided by the Kansas Geological Survey and encouragement of its Director, Bill Harrison, was absolutely essential to my research and this manuscript, without which this work could never have been completed. With the enormous overall scope of the research effort included in this manuscript, especially the volume of data acquired in route to the unique findings presented here, a great deal of thanks must be extended to my graduate students, co-workers, and colleagues at the KGS current and past (too numerous to mention), who have played various roles in my research program over the last 25 years.

I am sincerely grateful to John Davis who throughout my academic career at the University of Leoben and for many years as a colleague at the University of Kansas has been the voice of wisdom and experience and a true friend, persistently pointing to the light at the end of the tunnel and convincing me it was not a train! Thanks to Günther Hausberger who relentlessly worked, on my behalf, through the mountain of acceptance and enrollment issues/obstacles at the University during the onset of my doctoral program. The logistical and financial talents and creativity of Kathy Sheldon as well as her sincere concern and energy for helping others, minimized many of the personal burdens required to complete this work. Mary Brohammer did a superb job generating publication quality figures, creating an efficient and fluid page layout, and style editing, notably improving the flow and clarity of the presentation. I also appreciate the review of this manuscript provided by Professor Ewald Brückl.

High-Resolution Seismic Investigation of Subsidence from Dissolution

TABLE OF CONTENTS

Table of Contents	iii
List of Tables	vi
List of Figures	vi
 Abstract	
English	xi
German	xiv
 Chapter 1: Introduction	
Sinkholes: Formation and Impact	1-1
 Chapter 2: Regional Framework and Characteristics	
Geologic Setting	2-1
Salt Beds	2-2
Seismic-reflection Setting	2-9
 Chapter 3: Salt Characteristics	
Karst	3-1
Salt	3-1
Salt Stability	3-4
Salt-dissolution Factors	3-5
Dissolution Front	3-7
Natural Salt Dissolution vs. Anthropogenic	3-10
Borehole Access	3-13
Solution Mining	3-16
Brine Disposal	3-17
 Chapter 4: Subsidence Settings	
Subsidence	4-1
Stress Distribution	4-1
Failure Mechanisms	4-4
Failure Rates	4-7
Sinkhole Varieties	4-11
Sinkhole Hazard	4-13
 Chapter 5: Previous Seismic-Reflection Imaging of Subsidence	
Utility of Seismic-Reflection Imaging	5-1
Carbonate Settings	5-2
Pitfalls in Carbonates	5-5
Glacial Settings	5-7
Salt Settings Worldwide	5-8

Salt in Kansas	5-11
Pitfalls of High-Resolution Shallow Seismic Data and Subsidence Structures	5-12
Future	5-16
Chapter 6: Data Processing and Acquisition: Near-Surface Focus	6-1
Keys to High Resolution	6-2
Historical Perspective	6-4
Resolution	6-9
Vertical Resolution	6-11
Lateral Resolution	6-12
Dimensions of Detection and Resolution	6-13
Differences from Conventional	6-14
High Resolution: Acquisition	6-21
High Resolution: Processing	6-24
Chapter 7: Seismic-Reflection Studies of Dissolution	7-1
Anthropogenic	
Mine Collapse	7-2
Disposal Well Breach	7-6
Natural	
Paleosinkholes	
Karst	7-10
Evaporite Karst	7-11
Modern	
Karst	7-12
Evaporite Karst	7-13
Chapter 8: Site-Specific Seismic Investigations of Subsidence Features.....	8-1
Introduction	8-1
Seismic Investigations of Natural Dissolution Subsidence	8-3
Seismic Investigations of Anthropogenic Dissolution Subsidence	8-18
Chapter 9: Seismic-Reflection Characteristics and Models	9-1
Salt Models	9-2
Salt Withdrawal Physical Models.....	9-3
Seismic Characterization of Dissolution and Creep	9-7
Real Data Compared to Physical Models	9-9
Single-episode Subsidence	9-9
Active Leaching and Subsidence	9-11
Paleosubsidence: Reactivation	9-14
Resolution and Structure Anomalies	9-18
Active Anthropogenic Leaching	9-19
Synergistic Discussion	9-20
Complex Subsidence History	9-22
Solution Mine Collapse	9-23
Chapter 10: Observations and Discussion from Seismic Images	10-1
General Process	10-1
Natural Dissolution	10-2
Anthropogenic Catalyst	10-4

Seismic Characteristics	10-6
Key Discussion Points and Unique Contributions	10-7
Appendix A: Glossary of Key Dissolution and Subsidence Terminology	A1
Appendix B: Author-Published Papers Fundamental to Discussions and Concept Development	B1
A. Anthropogenic	
1. Mine Collapse	
Seismic investigation of a surface collapse feature at Weeks Island Salt Dome, Louisiana	B5
Shallow seismic-reflection feasibility study of the salt dissolution well field at North American Salt Company's Hutchinson, Kansas, facility	B17
Detecting voids in a 0.6-m coal seam, 7 m deep, using seismic reflection	B25
Unique near-surface seismic-reflection characteristics within an abandoned salt-mine well field, Hutchinson, Kansas	B39
2. Disposal Well Breach	
Shallow seismic-reflection study of a salt dissolution subsidence feature in Stafford County, Kansas	B45
Seismic investigation of a salt dissolution feature in Kansas	B65
High-resolution seismic-reflection imaging 25 years of change in I-70 sinkhole, Russell, County, Kansas	B81
High-resolution seismic reflection investigations of dissolution sinkholes	B87
B. Natural	
1. Paleosinkholes	
a. Karst	
Seismic techniques to delineate dissolution features (karst) at a proposed power plant site	B93
b. Evaporite Karst	
High-resolution seismic reflection to identify areas with subsidence potential beneath U.S. 50 Highway in eastern Reno County, Kansas	B113
2. Modern	
a. Karst	
Seismic investigation of a sinkhole on Clearwater Dam	B129
b. Evaporite Karst	
High-resolution seismic-reflection investigation of a subsidence feature on U.S. Highway 50 near Hutchinson, Kansas	B149

LIST OF TABLES

Table 4-1.	Angle of draw of surface settlement profiles and sinkholes for underground openings, based on settlement observations	4-3
Table 8-1	Unique and specific characteristics of each study	8-4

LIST OF FIGURES

Figure 1-1.	World map of limestone outcrops	1-3
Figure 1-2.	Worldwide distribution of salt deposits	1-3
Figure 1-3.	Photo of Cargill sinkhole, Hutchinson, Kansas	1-4
Figure 1-4.	Photo of I-70 sinkholes near Russell, Kansas	1-5
Figure 1-5.	Photo of sinkhole along Crooked Creek fault, Meade County, Kansas	1-5
Figure 1-6.	Photo of French sinkhole in Stafford County, Kansas	1-7
Figure 1-7.	Photo of Mosaic sinkhole in Hutchinson, Kansas	1-7
Figure 1-8.	Photo of old mine shaft near Kanopolis, Kansas, after blowout	1-8
Figure 1-9.	Photo of sinkhole at U.S. 50 and Victory Road, near Hutchinson, Kansas	1-8
Figure 1-10.	Photo of Macksville sinkhole	1-9
Figure 1-11.	Photo of brine disposal well feature in Ellsworth County, Kansas	1-10
Figure 1-12.	Photo of Brandy Lake in Reno County, Kansas	1-11
Figure 2-1.	Photo of sinkhole in Winter Park, Florida	2-2
Figure 2-2.	Generalized geologic map of Kansas	2-3
Figure 2-3.	Map of Kansas showing structural provinces	2-3
Figure 2-4.	Map of major salt basins throughout North America	2-3
Figure 2-5.	Isopach of the Hutchinson Salt Member	2-4
Figure 2-6.	Generalized geologic cross section	2-4
Figure 2-7.	Maps showing salt thickness, current depth of salt layer, and surface topography of the salt layer	2-6
Figure 2-8.	Generalized depth section for the northern portion of the salt and generalized depth section for areas investigated in this manuscript along the eastern dissolution edge of the salt	2-8
Figure 2-9.	Maps of (a) the Wellington aquifer and (b) the high-gradient contours of the salt isopach	2-9
Figure 2-10.	Seismic stacked section and synthetic seismic matched to the geologic section	2-12
Figure 2-11.	Geologic column contrasted with synthetic and logs	2-14
Figure 2-12.	Seismic section from 30 km west of dissolution front	2-14
Figure 2-13.	Reflection section targeting top of salt near Inman, Kansas	2-15
Figure 2-14.	Migrated seismic section less than 5 km away from dissolution front compared to a section 10 km west	2-15
Figure 3-1.	Photo of sinkhole in Clearwater Dam, Missouri	3-3
Figure 3-2.	Salt crystal from core of Hutchinson Salt Member	3-4
Figure 3-3.	Classical creep-deformation behavior of salt	3-6
Figure 3-4.	CMP stack of salt interval	3-7
Figure 3-5.	Cartoon of possible natural dissolution front progression	3-8
Figure 3-6.	Failure of casing within intermediate salt interval	3-9
Figure 3-7.	Cartoon of morning-glory structure	3-10

Figure 3-8. Cross section showing extreme topography above the leached-out portion of the salt	3-11
Figure 3-9. Orthophoto with sinkholes circled likely related to natural dissolution	3-12
Figure 3-10. CMP seismic sections from Punkin Center in Reno County, Kansas	3-13
Figure 3-11. Cartoon showing one possible anthropogenic source of salt dissolution and collapse	3-15
Figure 3-12. Photo of Leesburg sinkhole in Stafford County, Kansas	3-17
Figure 3-13. Cartoon of general installation design of single-well facilities	3-18
Figure 3-14. Diagrams of direct and indirect single-well leaching systems	3-18
Figure 3-15. Historic progress of single-well solution mining	3-19
Figure 3-16. Inadvertent formation of a gallery between two wells	3-20
Figure 3-17. Diagram of an engineered gallery in the Detroit area	3-20
Figure 4-1. Cross section of the anatomy of a subsidence trough	4-2
Figure 4-2. Tension dome and distribution of stress	4-4
Figure 4-3. Elements of a voussoir arch	4-4
Figure 4-4. Collapse breccia formed after failure of roof rocks	4-5
Figure 4-5. Overburden failure for small-dimension voids	4-5
Figure 4-6. Sinkhole subsidence feature with segregated layers of collapse breccia	4-6
Figure 4-7. Gradational collapse within the tensional dome	4-6
Figure 4-8. CMP stacked section from Reno County, Kansas, showing drape-type subsidence, and CMP stacked section from Russell County, Kansas, with stoping-and-raveling-style subsidence	4-7
Figure 4-9. Model of deformation from salt dissolution	4-9
Figure 4-10. Photo at Macksville sinkhole in Pawnee County, Kansas	4-10
Figure 4-11. Photo of coal mine collapse sinkhole near Scammon, Kansas	4-14
Figure 4-12. Photo of sinkhole in Bennett Dam, British Columbia, Canada	4-15
Figure 4-13. Photo of sinkhole that formed catastrophically in Guatemala	4-16
Figure 5-1. Interpreted seismic section from Fort George Island	5-3
Figure 5-2. Lake seismic section	5-4
Figure 5-3. Interpreted time-to-depth section	5-5
Figure 5-4. Shot gather from power plant site	5-6
Figure 5-5. Seismic section from a carbonate setting	5-6
Figure 5-6. Section showing a zone of seismic amplitude attenuation beneath a sinkhole	5-7
Figure 5-7. FD time migration section from the Tostedt survey	5-8
Figure 5-8. Shot gathers after NMO correction and top mute	5-8
Figure 5-9. CMP stacked section from Crater Lake, Saskatchewan, Canada	5-9
Figure 5-10. Seismic cross section from English Zechstein basin	5-10
Figure 5-11. Interpreted CMP stacked section across I-70 sinkhole in Russell County, Kansas	5-11
Figure 5-12. CMP section from French sinkhole in Barton County, Kansas	5-13
Figure 5-13. Reprocessed section from Punkin Center in Reno County, Kansas	5-14
Figure 5-14. Reprocessed section from Punkin Center in Reno County, Kansas	5-15
Figure 5-15. Reprocessed section from Punkin Center in Reno County, Kansas	5-16
Figure 5-16. Seismic reflection time slice from industry 3-D	5-17
Figure 6-1. Comparison of coincident gas hydrate data from Canadian Arctic	6-2
Figure 6-2. Contrasting S-wave and P-wave stacked sections from the Mackenzie Delta, northwestern Canada	6-3

Figure 6-3. Photos from Memphis Defense Depot	6-4
Figure 6-4. Optimum offset reflection section from Dryden, Ontario	6-5
Figure 6-5. Profile containing a variety of unique depositional geometries	6-5
Figure 6-6. Photo of device to improve coupling	6-6
Figure 6-7. CDP stacked section	6-6
Figure 6-8. Correlated vibroseis shear-wave shot gather with annotation	6-8
Figure 6-9. S-wave velocity contours from Olathe, Kansas, site	6-9
Figure 6-10. Bed and object separation associated with resolution	6-9
Figure 6-11. Idealized geologic model and seismic response	6-11
Figure 6-12. CMP stacked section compared with a synthetic	6-12
Figure 6-13. Model response illustrating significance of Fresnel zone size	6-13
Figure 6-14. Interpreted CMP stacked section from Cherry Point, North Carolina	6-14
Figure 6-15. AGC scaled field files from Cherry Point, North Carolina	6-15
Figure 6-16. Shot gather with surface wave and refraction interpreted	6-16
Figure 6-17. Example shot gathers	6-16
Figure 6-18. Synthetic wavelets demonstrating the difference between bandwidth and octaves	6-17
Figure 6-19. 240-channel shot gather	6-18
Figure 6-20. Representative shot gather and model	6-18
Figure 6-21. Unprocessed shot gather	6-19
Figure 6-22. Fully processed CMP gather just before stacking	6-20
Figure 6-23. 48-channel seismograph record	6-20
Figure 6-24. Shot gather from 12-gauge Seisgun source	6-21
Figure 6-25. An example of hole conditioning	6-23
Figure 6-26. Ground roll on close offset traces	6-24
Figure 6-27. Generalized processing flow for high-resolution data	6-25
Figure 6-28. Correlated shot gather with reflection events	6-26
Figure 6-29. Sample shot gather	6-27
Figure 6-30. Moved-out shot gather using a 50% stretch mute.....	6-28
Figure 6-31. Clipped shot gather band-pass filtered and scaled	6-29
Figure 7-1. Unmigrated CDP stack with “bow tie” feature	7-2
Figure 7-2. Walkaway noise tests	7-2
Figure 7-3. CMP stacked section along edge of sinkhole	7-3
Figure 7-4. 12-fold CDP stack and geologic interpretation	7-4
Figure 7-5. Migrated CMP stacked section adjacent to sinkhole	7-5
Figure 7-6. CMP stacked section with Stone Corral reflection indicated	7-6
Figure 7-7. Scaled raw data; processed and spectral balanced	7-7
Figure 7-8. Interpreted CMP stack showing salt bed and fault planes within subsidence volume	7-7
Figure 7-9. Stacked section from I-70 sinkhole site showing Witt and Crawford sinkholes	7-8
Figure 7-10. Possible collapse feature and an existing sinkhole	7-9
Figure 7-11. CMP stacked section time-to-depth converted using NMO velocity	7-10
Figure 7-12. Disturbed area within salt and associated non-vertical chimney	7-11
Figure 7-13. Representative shot gather	7-12
Figure 7-14. Interpreted CMP stack showing key layers and abnormalities	7-12
Figure 7-15. CMP stacked section showing sinkhole	7-13

Figure 8-1.	Map of Kansas with outline of areal extent of Hutchinson Salt	8-2
Figure 8-2.	Stacked section highlights paleosubsidence feature geometry	8-3
Figure 8-3.	Migrated nominal 60-fold CMP stacked section crossing a 100-m-wide surface depression	8-7
Figure 8-4.	Interpreted CMP stacked section with disturbed salt interval	8-8
Figure 8-5.	Paleosubsidence feature with no current surface expression	8-9
Figure 8-6.	Interpreted seismic profile from Punkin Center showing undulating Permian reflectors	8-10
Figure 8-7.	Stacked section with interpretation of reactivated subsidence feature	8-12
Figure 8-8.	CMP stacked section from Buerki sinkhole, Sedgwick County, Kansas	8-14
Figure 8-9.	Nominal 60-fold CMP stacked section from Inman area	8-15
Figure 8-10.	Solution-altered wavelets and native reflection from Inman area	8-17
Figure 8-11.	Interpreted CMP stacked section from Conoco disposal well sinkhole	8-19
Figure 8-12.	CMP stack of reflection data acquired at the French sinkhole	8-20
Figure 8-13.	CMP Stacked section showing Witt and Crawford sinkholes	8-22
Figure 8-14.	Portion of the Figure 8-13 stacked section, time flattened on the subsalt reflections	8-23
Figure 8-15.	Interpreted CMP stacked section from Macksville sinkhole (W-E line)	8-24
Figure 8-16.	Interpreted CMP stacked section from Macksville sinkhole (N-S line)	8-25
Figure 8-17.	Nominal 60-fold CMP stacked section at the Leesburg sinkhole	8-26
Figure 8-18.	CMP seismic section from collapsed dissolution salt well in Hutchinson ...	8-28
Figure 9-1.	Synthetic seismic section from salt model	9-2
Figure 9-2.	Model of deformation from salt dissolution	9-5
Figure 9-3.	Conceptual model based on seismic observations of subsidence	9-5
Figure 9-4.	Seismic section from the English Zechstein basin	9-6
Figure 9-5.	Migrated CMP stack along U.S. 50 Highway in central Kansas	9-7
Figure 9-6.	CMP stacked section showing disturbed and undisturbed salt layers	9-8
Figure 9-7.	Paleosubsidence feature with high-angle conical faults	9-9
Figure 9-8.	Interpreted stacked section of a sinkhole caused by an oil-field brine-disposal well	9-9
Figure 9-9.	A portion of Figure 9-7 highlighting subsidence feature geometry	9-10
Figure 9-10.	Seismic section from Witt sinkhole with models	9-12
Figure 9-11.	Migrated CMP stacked section near the natural dissolution front with no surface expression	9-15
Figure 9-12.	Seismic section from the Rayl sinkhole	9-16
Figure 9-13.	Seismic profile from Punkin Center	9-17
Figure 9-14.	Seismic section from around 20 km west of the dissolution front	9-18
Figure 9-15.	Seismic profile of a gradually subsiding feature	9-19
Figure 9-16.	Models compared to seismic data showing subsidence features	9-21
Figure 9-17.	Interpreted seismic profile from Victory Road	9-23
Figure 9-18.	Photo of Mosaic sinkhole	9-24

High-Resolution Seismic Investigation of Subsidence from Dissolution

ABSTRACT

Deformed overburden and abnormalities within the soluble rock interval interpreted on high-resolution seismic-reflection sections provide key insights into formation and development of dissolution voids and associated overburden subsidence processes. Analysis of a large sample (12) of high-resolution seismic-reflection sections over the Hutchinson Salt Member, targeting a variety of subsidence features with different failure mechanisms, rates, and hydrodynamics help unravel some of sinkhole-failure processes and controls. Subtle structures indicative of unique stages of overburden failure and rates can be identified within the collapse-altered volume on high-fidelity and coherent reflection sections.

Development of dissolution voids and associated subsidence features proceeds through several stages based on hydrodynamics, salt stratigraphy, and overburden properties. Dissolution can advance through the salt vertically (top to bottom or bottom to top) or horizontally (along any insoluble barrier within, above, or below the salt). Failure associated with dissolution voids is dependent on the stress regime and rock properties of the salt interval and overburden. Every void that migrates through the overburden has a failure geometry that can be defined by reverse faults (compressional deformation) inside normal faults (tensional deformation). A key consideration applicable to recent subsidence events only is that reverse may be interpretable due to either active dissolution or current stage of development (early or intermediate).

Dissolution from anthropogenic or natural fluid sources results in a wide range of overburden subsidence structures with seismic representations that provide clues but no definitive interpretations as to the complete development history. Seismic-reflection data acquired over 12 different dissolution features provided the study set used to validate and extend the results published in 14 different articles addressing seismic imaging of voids, dissolution-instigated subsidence, carbonate and evaporite karst, mines, and active and paleo features. An underlying difference between anthropogenic and natural that affects seismic interpretations of current and past development is the one-dimensional hydrodynamic system driving the anthropogenic process compared to the three-dimensional process for natural void and subsidence features.

Leaching within the salt interval can be interpreted from traveltime variations related to structures and amplitude and frequency anomalies of reflection wavelets. Voids are interpreted based on the presence of apparent structural variations in interbedded anhydrite and shale layers within the salt. Amplitude anomalies can be interpreted both pre-failure and post-subsidence, related to dissolution zones and alterations of rock from leached intervals. Strong evidence is presented supporting specific changes in reflection attributes (phase, frequency, and amplitude) and interbedded reflection-arrival patterns within the salt interval as characteristic of glide creep with no or only minor associated subsidence of salt. This observation is contrary to previous suggestions that subsidence and creep were indistinguishable processes on seismic sections. Voids formed during dissolution could easily provide the differential pressure and fluid necessary for low-temperature, shallow burial salt flowage.

Seismic interpretation of creep assumes minimal change in material, while subsidence results in material alteration and therefore a notable change in reflectivity.

Deformation in overburden is brittle for these shallow dissolution-driven subsidence structures. Previous interpretations suggestive of ductile (plastic) deformation are actually brittle with apparent bed flexure an artifact of offsets from a series of fracture and fault zones collectively below the resolution limits of seismic-reflection data. Broad synforms defined by gentle dip and a consistent series of coherent reflections above dissolution -altered salt intervals are the result of relatively uninterrupted leaching and associated gradual, downward advance of the overburden.

Seismic-reflection sections with limited coherency, bed offset, scatter, and chaotic energy from within the subsidence structure are clearly representative of the remnants-bed offsets indicative of brittle deformation. Low-pressure settings and brittle overburden materials deform via rupture. Structures imaged possess both imageable bed offset and apparent plastic properties together. Ductile-appearing overburden deformation from a low-pressure setting is an artifact of resolution. Resolution limits also prohibit diffractions from suggested fractures and faults from being recorded.

Compressional and tensional stress with associated strain manifests itself through brittle deformation structures. Juvenile subsidence structures while migrating toward the ground surface have a distinctive shape and amplitude signature. Steep-sided subsidence features predominantly defined by reverse faults are likely undergoing active leaching. Compressional-deformation-evident post-bedrock breakthrough of collapse structure seems conceptually contradictory to stress models. However, once the three-dimensional nature of these features are considered, subsidence within a cylinder defined by the sub-vertical face of the dissolution front will be dominated by matched sets of reverse-fault planes. Several episodes of failure along enlarging sets of concentric reverse-fault planes portray different episodes of dissolution followed by subsidence. With the 3-D nature of the stress field, concentric collapse rings controlled by compressional stress post failure and development of initial throat will be evident for structures with a robust fluid-exchange system.

Seismic images of gradual subsidence features have characteristics of both continuous dissolution and associated small-vertical-scale subsidence of overburden and large void development and upward migration through stoping and raveling, forming a collapse breccia structure geometrically defined as an upward-narrowing inverted cone. Rapid subsidence requires a large sump resulting from dissolution that migrates to the surface via stoping and raveling forming a collapse breccia cone with varying degrees of reflectivity within the breccia or rubble volume.

Subsidence events along the natural dissolution front are generally associated with reactivated leaching within or in close proximity to paleosubsidence structures. Areas characterized by past subsidence and currently experiencing reactivation possess a minimal chance for developing at catastrophic-failure rates. Subsidence is more likely to occur as a reactivation or elongation of an existing dissolution feature than as a new start. The high gradient portion of the natural front has minimal overburden expression but possesses highly distorted salt. In areas west of the dissolution front, a variety of dissolution structures with unique origins and evidence of initial processes are retained in the rock record. Collapse structures east of the dissolution front lack seismically imageable and therefore interpretable structures. These data are dominated by chaotic arrivals, with out-of-the-plane noise and minimal bed coherency. Seismic images of post-dissolution overburden altered with the

passage of the natural dissolution front provide few clues to past dissolution and subsidence processes at this stage. Paleosubsidence structures provide clues to areas with a high risk of future dissolution and potential subsidence.

Predicting or establishing consistent failure mechanisms as a function of subsidence rate or fluid source is not possible. Catastrophic failure is most likely with anthropogenic water sources, where natural sinkhole development is almost exclusively gradual in nature. Seismically this is evident in the isolated nature of the features and 1-D control of the dissolution process. Natural dissolution is generally associated with a history of leaching and complex development geometries.

Several key aspects critical to accurate seismic imaging of subsidence structures must be considered or interpretations can significantly diverge from the real subsurface. Interpretations of reflection below a subsidence feature suffer from sub-salt static and out-of-plane energy generally masking reflections between 100 to 200 ms below the salt interval. Two-dimensional seismic surveys must carefully consider line locations when imaging these small (relative to wavelength) geometrically irregular features for accurate interpretations. High-resolution seismic-reflection data are critical to accurately image subsidence features, but they must be processed using techniques conducive to shallow (upper 100-ms) high-resolution data. Changes in the velocity field within the dissolution and subsidence volume across distances sub-spread length require velocity analysis as a function of offset ranges and time splitting a single CMP gather into offset subsets. Horizontal-resolution limits appear to not accurately represent true potential based on seismic images of steep-sided collapse structures. Seismic investigations using 3-D techniques are critical to continued development of accurate dissolution, creep, and/or subsidence scenarios and processes based on empirical, numerical, and physical models.

ZUSAMMENFASSUNG

Deformationen in den Deckschichten und weitere Anomalien innerhalb löslicher Gesteinschichten, die in hochauflösenden reflexionsseismischen Sektionen sichtbar werden, geben wesentliche Einblicke in Bildung und Entwicklung von Lösungshohlräumen und die damit verbundenen Subsidenzprozesse. Die Analysen von insgesamt zwölf hochauflösenden seismischen Reflexionsprofilen über Strukturen des Hutchinson Salz, die auf eine Vielzahl von Subsidenzerscheinungen mit unterschiedlichen Bruchmechanismen, Absinkraten und hydrodynamischen Prozessen zielen, tragen dazu bei, einige der Mechanismen und kontrollierenden Prozesse der Dolinenbildung zu erschließen. Subtile strukturelle Merkmale, die auf eindeutig identifizierbare Stadien im Versagen der Deckschichten und auf Absinkraten schließen lassen, können auf reflexionsseismischen Sektionen innerhalb des von Absenkungen betroffenen Volumens identifiziert werden.

Die Entwicklung von Auflösungshohlräumen und damit verbundenen Senkungsstrukturen erfolgt in verschiedenen Schritten je nach Hydrodynamik, Salzstratigraphie und Eigenschaften der Deckschichten. Lösungsprozesse können durch das Salz vertikal (aufwärts oder abwärts) oder horizontal fortschreiten (entlang irgendeiner unlöslichen Barriere im, über oder unter dem Salz). Versagen des Gesteins in Verbindung mit Auflösungshohlräumen ist abhängig von Spannungszustand und Gesteinseigenschaften der Salz- und Deckschichten. Jeder Hohlraum, der durch die Deckschichten fortschreitet, hat eine Versagensgeometrie, die durch Aufschiebung (Kompressionsverformung) innerhalb normaler Bruchzonen (tensionale Deformation) definiert werden kann. Als wesentliches Ergebnis, das auf nur neue Senkungsfälle anwendbar ist, ergibt sich, dass gegenläufige Verwerfungsrichtungen entweder an aktiven Lösungsprozessen oder am gegenwärtigen Stadium der Entwicklung definiert werden können (frühe oder mittlere Stadien).

Lösungsprozesse verursacht von anthropogenen oder natürlichen Fluidzuflüssen ergeben ein breites Spektrum von Senkungsstrukturen in den Deckschichten mit seismischen Ausprägungen, die wohl Anhaltspunkte aber keine endgültigen Deutungen hinsichtlich der kompletten Entwicklungsgeschichte zur Verfügung stellen. Reflexionsseismische Daten, gemessen über zwölf unterschiedlichen Strukturen, die auf Lösungsprozesse zurückzuführen sind, lieferten das Material, um in dieser Arbeit die Ergebnisse zu verifizieren und zu erweitern, die in vierzehn unterschiedlichen Publikationen veröffentlicht wurden und die seismische Abbildung von Hohlräumen, von Senkungen, die durch Lösungsprozesse verursacht wurden, von Karbonat- und Evaporit-Karst, von Schächten und sowohl aktiven als auch inaktiven Strukturen ansprechen. Ein grundlegender Unterschied zwischen anthropogenen und natürlichen Ursachen, der die seismische Interpretation von aktueller und zurückliegender Entwicklung beeinflusst, ist das eindimensionale hydrodynamische System, das den anthropogenen Lösungsprozess bestimmt, verglichen mit dem dreidimensionalen hydrodynamischen System für Hohlräume und Absenkungen, die durch natürliche Prozesse entstanden sind.

Auslaugungen innerhalb der Salzsichten können aus Laufzeitänderungen von seismischen Horizonten und aus Amplituden- und Frequenzanomalien von Reflexionssignalen interpretiert werden. Hohlräume werden auf der Basis von scheinbaren strukturellen Änderungen von Anhydrit- und Tonlagen innerhalb des Salzes gedeutet. Amplitudenanomalien können interpretiert werden vor dem Versagen und auch nach der Absenkung in Verbindung mit Lösungs-zonen und Änderungen der Gesteinseigenschaften von bereits ausgelaugten Bereichen.

Deutliche Hinweise werden vorgestellt, die die Vermutung stützen, dass spezifische Änderungen in den Reflexionsattributen (Signalphase, Frequenz und Amplitude) und zwischengeschalteten Reflexionsmustern innerhalb der Salzsicht charakteristisch sind, wenn für Kriechen ohne weitere oder mit nur geringer zusätzlicher Subrosion des Salzes vorliegt. Diese Beobachtung widerspricht früheren Vorschlägen, Subrosion und Kriechen seien in seismischen Sektionen nicht zu unterscheiden. Im Lösungsprozess entstandene Hohlräume könnten ohne weiteres den Differenzdruck und die Fluide zur Verfügung stellen, die für Salzbewegungen bei niedrigen Temperaturen und unter geringmächtiger Sedimentbedeckung notwendig sind. Seismische Interpretation von Kriechen nimmt minimale Änderungen im Material an, während Subrosion zu deutlichen Änderungen führt und folglich signifikante Änderungen im Reflexionsvermögen ergibt.

Deformation der Decksichten verläuft spröde bei diesen flachen von Lösungsprozessen angetriebenen Senkungsstrukturen. Frühere Deutungen, die duktile (plastische) Deformation vorschlugen, sind in Wirklichkeit spröde Deformationen mit scheinbarer Flexur, die als seismische Artefakte entsteht von einer Reihe von Kluft- und Störungszonen, die alle zusammen unterhalb des Auflösungsvermögens der seismischen Reflexionsdaten sind. Breite Synformen, die durch leichtes Einfallen und eine gleichbleibende Reihe kohärenter Reflexionen über lösungsverändertem Salz definiert werden, sind das Resultat von verhältnismäßig kontinuierlichem Auslaugen und damit verbundenem allmählichem Absinken der Decksichten.

Seismische Reflexionsprofile mit beschränkter Kohärenz, versetzten Reflexionselementen, gestreuter und chaotischer Energie innerhalb der Senkungsstruktur sind offenbar repräsentativ für Schichtversatz, der auf spröde Deformation hinweist. Spröde Decksichten verformen sich bei geringem Druck durch Rissbildung. Die abgebildeten Strukturen besitzen sowohl auflösbaren Schichtenversatz als auch gleichzeitig scheinbar plastische Eigenschaften. Duktil erscheinende Deformationen der Decksichten bei geringem Druck sind ein Artefakt der seismischen Auflösung. Die begrenzte Auflösung verhindert auch die Aufzeichnung von Diffraktionen von angedeuteten Klüften und Störungen.

Druck- und Zugspannung mit entsprechender Dehnung zeigen sich durch spröde Deformationsstrukturen. Juvenile Senkungsstrukturen haben, während sie sich in Richtung Erdoberfläche entwickeln, eine unterscheidbare Signatur in Form und Amplituden. Steil stehende Senkungsstrukturen, die überwiegend durch Aufschiebungen definiert werden, sind wahrscheinlich in aktiver Auslaugung begriffen. Kompressive Deformation verbunden mit Durchbruch der Einsturzstruktur in das unterliegende Gestein scheint begrifflich unvereinbar mit Spannungsmodellen. Jedoch sobald der dreidimensionale Charakter dieser Strukturen betrachtet werden, wird Absenkung innerhalb eines Zylinders, der durch die subvertikale Front der Lösungszone definiert wird, durch zusammengehörende Aufschiebungen beherrscht. Mehrere Episoden des Versagens entlang zunehmender konzentrischer Aufschiebungen stellen unterschiedliche Episoden von Lösungsprozessen gefolgt von Absenkungen dar. Mit der dreidimensionalen Struktur des Spannungsfeldes geben die in

konzentrischen Ringen angeordneten Einsturzstrukturen, die durch kompressive Spannungen nach dem Versagen und die Entwicklung von Initialöffnungen gesteuert werden, klare Indikationen für Strukturen mit einem robusten Austauschsystem für Fluide.

Seismische Abbilder von graduellen Absenkungsstrukturen zeigen Charakteristika sowohl für die kontinuierliche Lösung des Gesteins und der damit verbundenen kleinskaligen vertikalen Absenkung der Deckschichten als auch für die Bildung großer Hohlräume und ihr Fortschreiten nach oben durch Einsturz der Firste, wobei eine Einsturzbrekzie gebildet wird, die sich geometrisch als nach oben verjüngender Kegel darstellt. Die schnelle Senkung erfordert einen großen Schachtsumpf. Dieser Sumpf stammt vom Lösungsvorgang, der nach oben fortschreitet. Das gelöste und nachgestürzte Material bildet einen Einsturzkegel mit verschiedenen Graden von Reflexionsvermögen innerhalb des Schuttvolumens.

Senkungsereignisse entlang der natürlichen Lösungsfront sind im Allgemeinen mit der reaktivierten Auslaugung innerhalb oder in nächster Nähe zu Paläosenkungsstrukturen verbunden. Bereiche die durch vorige Senkung gekennzeichnet werden, und die eine Reaktivierung erleben, besitzen eine geringe Wahrscheinlichkeit für weitere Entwicklung mit katastrophaler Bruchrate. Die Subrosion tritt eher auf als Reaktivierung oder Erweiterung einer vorhandenen Lösungsstruktur und weniger als ein ganz neuer Anfang. Der hohe Gradient der natürlichen Lösungsfront hat minimalen Expression in den Deckschichten, besitzt jedoch in hohem Grade verformtes Salz. In den Bereichen westlich der Lösungsfront sind eine Vielzahl der Lösungsstrukturen mit eindeutigem Ursprung und Anzeichen von Anfangsprozessen im Gestein erhalten. Einsturzstrukturen östlich der Lösungsfront fehlen seismisch abbildbare und daher interpretierbare Strukturen. Diese Daten werden durch chaotische Reflexionen mit Störungsenergie, die sich außerhalb der Vertikalebene des Profils ausbreitet, und minimaler Kohärenz der Reflexionen beherrscht. Seismische Abbilder von Deckschichten nach Lösungsprozessen, die durch den Durchgang der Lösungsfront beeinflusst wurden, geben gegenwärtig wenige Anhaltspunkte zu den früheren Lösungs- und Senkungsprozessen. Paläosenkungsstrukturen enthalten Anhaltspunkte und Hinweise zu den Bereichen, die ein hohes Risiko für zukünftige Lösungsphänomene und potentielle Senkungen darstellen.

Vorhersage oder Feststellung konsistenter Bruchmechanismen als Funktion der Senkungsrate oder der Fluidzuflüsse sind nicht möglich. Natürliche Dolinenentwicklung verläuft fast ausschließlich graduell, während katastrophales Versagen in hohem Maße wahrscheinlich ist bei anthropogenen Wasserzuflüssen. Dieses Versagen tritt seismisch zutage in der isolierten Art der Merkmale und der eindimensionalen Steuerung des Lösungsprozesses. Natürliche Lösung ist im Allgemeinen mit einer Geschichte von Auslaugung und komplizierter Entwicklungsgeometrie verbunden.

Einige Hauptaspekte, die zur genauen seismischen Abbildung von Senkungsstrukturen von kritischer Bedeutung sind, müssen beachtet werden, da sonst die Interpretation vom tatsächlichen Untergrund erheblich abweichen kann. Die Interpretationen von Reflexionen unterhalb einer Senkungsstruktur leiden unter Subsalzstatik und seitlich eintreffende Reflexionsenergie; dieser Effekt maskiert im Allgemeinen Reflexionen zwischen 100 und 200 ms unterhalb des Salzintervalls. Bei zweidimensionalen seismischen Messungen muss die Profildführung sorgfältig gewählt werden, wenn die relativ zur Wellenlänge kleinen und geometrisch irregulären Strukturen für genaue Interpretationen abgebildet werden sollen. Hochauflösende Reflexionsseismik ist von wesentlicher Bedeutung, um die Senkungsstrukturen zuverlässig abzubilden, aber sie müssen mit speziellen Processing-

verfahren bearbeitet werden, die Daten aus geringer Tiefe (wenige hundert Millisekunden Laufzeit) und mit hoher Auflösung förderlich sind. Änderungen im Geschwindigkeitsfeld innerhalb des Lösungs- und Senkungsvolumens über Distanzen, die kleiner sind als die Auslage, erfordern eine Geschwindigkeitsanalyse als Funktion von Offset- und Laufzeitbereichen, wobei einzelne CMP-Familien noch weiter unterteilt werden müssen. Die Grenzen der horizontalen Auflösung scheinen das tatsächliche Potenzial eher zu unterschätzen, das auf seismischen Abbildern von steilen Einsturzstrukturen erkennbar wird. Seismische Untersuchungen mit dreidimensionalen Techniken sind essentiell für die weitere Entwicklung von genauen Szenarios für Lösungs-, Kriech- und Subsidenzprozesse und deren empirische, numerische und physikalische Modellierung.

CHAPTER 1

INTRODUCTION

Subsidence related to rock dissolution or subsurface erosion can threaten ground stability in a wide range of geologic settings. Empirically based subsurface models developed for distinct and progressive stages of subsidence can be used with reasonable confidence to estimate growth rates and guide risk estimations for surface activities and structures. Key to the accuracy of these generalized subsurface models is the type, quality, quantity, and reliability of data used to formulate parameters and constraints. A principal product of this study is a sequential set of empirically based subsidence models. These models were developed from a relatively large and representative set of high-confidence and high-resolution subsurface images that have captured a wide range of subsidence features from a variety of settings.

This body of work clearly establishes the utility of high-resolution seismic-reflection imaging for mapping subsidence features at various stages of development with and without surface expression. Images from customized high-resolution seismic-reflection surveys designed, acquired, processed, and interpreted by the author demonstrate the method's applicability and legitimate use in delineating critical and subtle structural components of subsidence features. Seismic images and data characteristics are used to develop/define generalized failure mechanisms and associated controls on subsidence. With the high solubility of evaporites, evolution of subsidence geometries can be captured on time-lapse seismic data at various developmental stages. This work describes subsidence mechanisms and processes predominantly based on evaporite dissolution features, but with general applicability to all subsidence events and resulting structures. Halite's characteristic high solubility allows the progression of subsidence features from juvenile to mature stages in a fluid-rich environment to be observed over reasonable time spans.

Crude conceptual models and interpretations based on very limited, low-resolution data and physical models have historically been the only guides for estimating site-specific subsidence threats and postulating generalized subsidence processes. Unique to this work is the development of comprehensive relationships between subsidence processes and sinkhole geometries founded in dozens of excellent signal-to-noise ratio, high-resolution seismic-reflection profiles. Prior to this study, documented physical and conceptual models (albeit formulated from limited observations) were not completely consistent with observed characteristics and processes at sites experiencing subsidence. Seismic data used in this study were acquired at locations with current or historic salt dissolution, allowing for the first time a series of progressive empirical failure models consistent with the changing stress field, borehole and surface observations, historical conceptual and modern physical models, and dozens of seismic images previously acquired above subsidence features.

Unique dissolution and subsidence concepts with an abundance of supporting seismic data will unfold within the ten chapters and two appendices of this manuscript. These concepts hold true for all documented physical observations and subsurface images and

measurements currently known to exist. Leading into the problems surrounding imaging subsidence features will be a discussion of general areas of concern, with a focus on regional characteristics of the study area. Next, an overview of the geology and key seismic characteristics of this salt will provide a reasonable grasp on the breadth of the problem and establish general constraints on the process. Understanding salt's physical characteristics (creep, solubility, physical properties, seismic characteristics, hydrology of dissolution) and dissolution and subsidence processes (solution mining, borehole fluid access, brine disposal, stress environments, failure mechanisms and rates, sinkhole varieties, hazards) is necessary foundation information and will be drawn from as the many unique observations are presented and formulations developed. Factors that control dissolution and subsidence will be discussed to enlighten and break down the complexities of the processes. A thorough review, and in some cases critique, of published works ensures it is clear that conclusions drawn from interpretations presented here are unique, advance the science, and provide the basis for establishing the significance of this work.

Findings reported in later chapters of this manuscript are built upon 20 years of the author's published works on this topic. Central and key to conclusions and unique observations are the more than a dozen site-specific, high-resolution seismic-reflection surveys woven together with published conceptual and physical models. From this assimilation come generalized empirical models that unveil, with a high degree of confidence and consistency, the progressive history of subsidence features. These models allow predictions of future development associated with either continued dissolution of rock or release of dissolution-induced stress.

Sinkholes: Formation and Impact

Sinkholes are common hazards to property and human safety the world over (e.g., Beck et al., 1999; Johnson and Neal, 2003; Waltham et al., 2005). Their formation is generally associated with subsurface subsidence that occurs when overburden loads exceed the strength of roof rock bridging voids or rubble zones. Subsurface voids are common byproducts of dissolution and mining. Understanding the subsidence process and what controls sinkhole formation and growth rate is key to reducing a sinkhole's impact on human activities, and in the anthropogenic case, potentially avoiding their formation altogether.

A variety of geologic and hydrologic settings are susceptible to dissolution, associated subsidence, and eventual sinkhole development. Caves or voids in soluble limestone, known to be present in outcrop throughout the world, represent varying degrees of risk to life and property (Figure 1-1). Sinkhole formation can result from natural or anthropogenic processes and in general occurs when overburden collapses into voids formed from dissolution of limestone (karst) or evaporites or from mine/tunnel excavations. Most of the world's sinkholes are the result of natural processes that have occurred over geologic time (Waltham et al., 2005). Therefore, most processes and stages of sinkhole development are prehistoric, leaving interpolation and postulation as the primary means to describe formation chronologies.

With the worldwide abundance of limestone, sinkholes from carbonate karst are by far the most commonly encountered and studied (e.g., 10 different *Multidisciplinary Conference on Sinkholes and Engineering and Environmental Impact of Karst* from 1981 to 2005). The more soluble gypsum, anhydrite, and salt underlie little more than 20 percent of the world's land surface (Kozary et al., 1968). Surface subsidence is possible and therefore a risk anywhere soluble rock deposits are present in the subsurface.

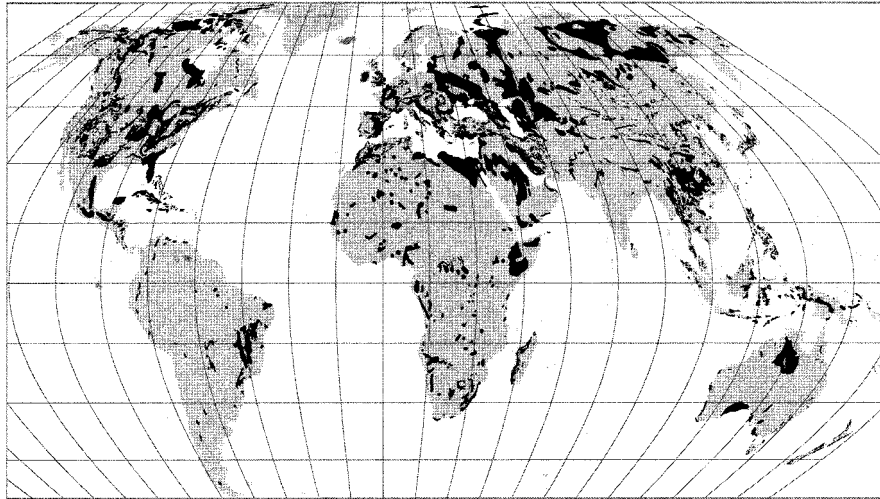


Figure 1-1. Dark areas are locations where limestone outcrops are known to be present and susceptible to dissolution and sinkhole development (Waltham et al., 2005).

An empirically based formation and growth chronology of sinkhole development focusing on the mechanisms and processes influencing both the host rock and overburden could improve how effectively people adapt to and coexist with these geohazards (Figure 1-2). From a geologic time perspective, evaporite dissolution and associated subsidence is extremely fast. Full development of an evaporite dissolution void can occur over periods generally measurable in decades. That characteristic makes the study of evaporite sinkhole progression from pre-juvenile through mature stages amenable. Non-linear changes can be observed within the host rock and during the upward migration of dissolution voids over these humanly manageable time frames. Developmentally at the other temporal extreme are the more globally pervasive carbonate dissolution and subsidence features. Carbonate karst processes require geologic time frames spanning tens to hundreds of millions of years and

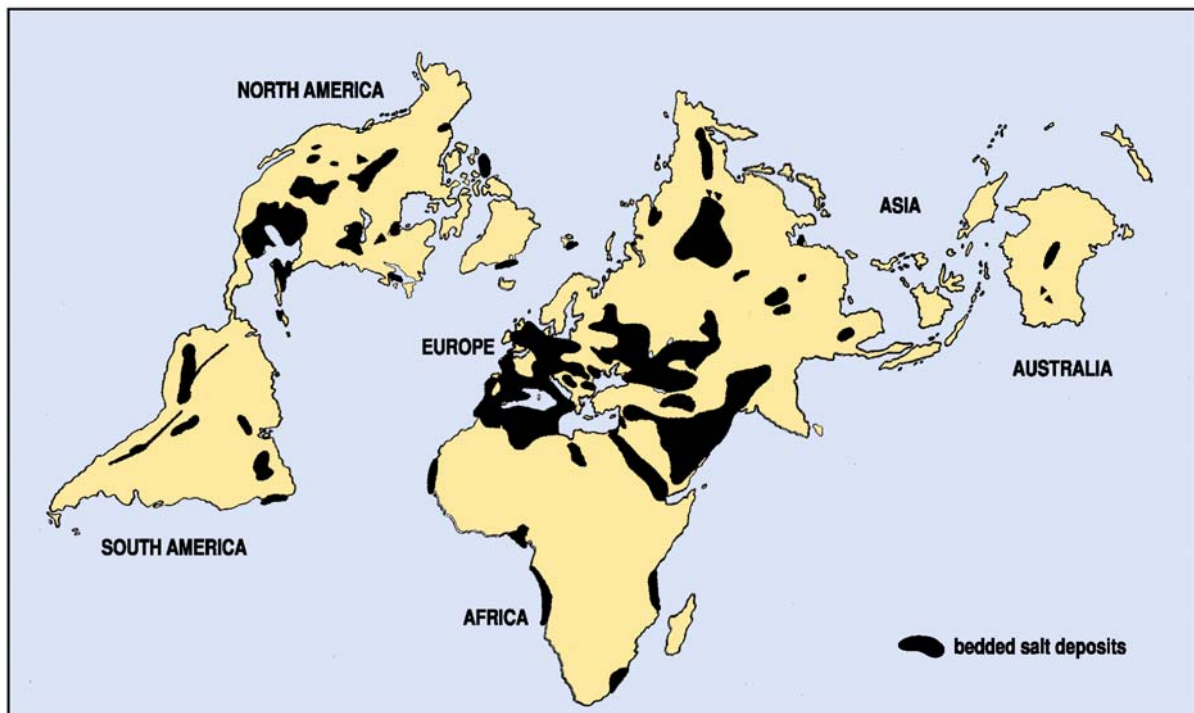


Figure 1-2. Worldwide distribution of salt deposits (modified from Kozary et al., 1968).

therefore necessitate interpolation and speculation to reconstruct site-specific subsidence histories.

The geologic setting of central Kansas provides an outstanding and unequalled test bed for the study of collapse features. Considering the rapid dissolution rates of central Kansas evaporites and associated subsidence, this area represents an excellent subsidence study area and analog for carbonate karst dissolution processes where direct observation is prohibitive within human time frames. Seismic investigations, physical characteristics, and subsurface information from more than a dozen subsidence features with different leaching histories provide the essential framework and details for rudimentary appraisals of risk and prediction of sinkhole development. Fortunately, seismic data used to investigate subsidence targets reported here are truly high-resolution. Techniques described and used in this manuscript are the products of more than 40 years of evolution. What makes the seismic data in this work unique is the successful incorporation of specialized application experience and hardware developments modified and optimized from the petroleum industry.

In central Kansas most sinkholes result from leaching of the Permian Hutchinson Salt Member of the Wellington Formation (Watney et al., 1988). Sinkholes above salt layers have been studied throughout Kansas (Frye, 1950; Walters, 1978), the United States (Ege, 1984), and the world (Kozary et al., 1968) by hydrologists, geologists, engineers, and geophysicists. Studies of subsidence in Kansas related to solution mining of the salt (Walters, 1978) (Figure 1-3), disposal of oil-field brine (Walters, 1991) (Figure 1-4), and natural dissolution through fault/fracture-induced permeability (Frye and Schoff, 1942) (Figure 1-5) have drawn “common sense” conclusions about the mechanism responsible for the observed subsidence geometries and rates based on surface and/or borehole data. Both simple and complex sinkholes have formed catastrophically and/or gradually as a result of limestone or rock salt dissolution by natural and anthropogenic-induced processes in many parts of Kansas (Merriam and Mann, 1957).

It is no surprise that a great number of assumptions and the degree of geologic/mechanical sense must be drawn upon to explain the mechanisms surrounding salt-dissolution-induced sinkhole formation and their potential impact when available information



Figure 1-3. Cargill sinkhole, in Hutchinson, Kansas, formed catastrophically above a solution mine void over a three-day period in 1974 (from Walters, 1978).



Figure 1-4. A stretch of Interstate 70 between Russell and Hays, Kansas, began subsiding in 1967, one year after the highway was opened. Surface subsidence has been consistent and gradual at about 20 cm/year for almost 40 years (photo by R. Miller).



Figure 1-5. Natural sinkhole in Meade County, Kansas, related to Crooked Creek fault formed directly beneath a branch of the Jones and Plummer cattle trail connecting west Texas and Dodge City, Kansas. The sinkhole formed during the month of March in 1879 (Walcott, 1901).

is limited to surface observations and borehole data. High-resolution seismic-reflection profiling has proven an effective tool in defining the subsurface affected volume and estimating future surface growth at active sinkholes (Steeple et al., 1986; Miller et al., 1993, 1995, 1997; Anderson et al., 1995a). Limited penetration depths, low signal-to-noise ratio, and marginal fidelity have inhibited delineating the many subtle secondary features key to extending site-specific studies into more process-related theories.

Salt-dissolution sinkholes in Kansas have been definitively linked to disposal wells (Figure 1-6) designed to inject oil-field brine wastewater, solution-mining wells (Figure 1-7), and abandoned mine shafts (Figure 1-8). Seismic-reflection investigations at a variety of sites throughout central Kansas have already provided defensible correlations between boreholes and sinkholes (Steeple et al., 1986; Knapp et al., 1989; Miller et al., 1995, 1997). Active salt-dissolution sinkholes and areas around active salt-dissolution sinkholes can represent significant geohazards. In some areas sinkholes are a greater risk to the environment than human activity directly. Unquestionably, the subsidence scenario of greatest concern is undetected dissolution of salt with catastrophic failure potential, where people are put at risk. With the high leaching and void-development rates of salt, subsidence risks from induced dissolution are orders of magnitude greater than in carbonate karst settings (Waltham et al., 2005).

Natural dissolution of the Hutchinson Salt Member in Kansas has been ongoing for millions of years (Ege, 1984). Faults extending through Pleistocene sediments have been suggested to act as conduits for freshwater to reach the salt under hydrostatic pressure and instigate dissolution. If this process continues through several periods of subsurface collapse, it eventually results in sinkhole formation (Frye and Schoff, 1942) (Figure 1-5). Sinkholes in Kansas that have formed as a result of natural dissolution of the salt are most commonly observed at the depositional edges on the west and north and erosional boundary on the east (Frye and Schoff, 1942; Frye, 1950; Merriam and Mann, 1957; Anderson et al., 1995a) (Figure 1-9).

Evidence of paleosinkholes that formed prior to Pleistocene deposition was cited based on a single, very poorly processed high-resolution seismic section along the eastern dissolution front (Anderson et al., 1998). High-quality seismic-reflection sections published over the last five years clearly delineate distinct paleosubsidence episodes within a single megafeature (Miller, 2006; Miller and Henthorne, 2004; Miller, 2003). This finding dramatically extended the understanding of the formation history of natural sinkholes in this area. Leaching along the eastern boundary of the salt in Kansas is strongly influenced by subsiding strata along the natural dissolution front and the westward-progressing boundary of the Wellington aquifer (Gogel, 1981).

Subsidence rates, regardless of fluid source, can range from gradual to catastrophic. The rate of subsidence is strongly influenced by the hydrology in and around the salt, the continuity and strength of rock layers above the salt, thickness and composition of the soil layer, and the pre-failure size and geometry of the unsupported span of roof rock and salt void. Ground movement during salt-related sinkhole formation in Kansas can range from near instantaneous (cm/sec) to extremely gradual (sub-cm/year). The complex process of void migration en route to sinkhole formation is influenced by a variety of specific overburden characteristics. Among the most significant are the strength of the caprock, the height of the pre-failure void, characteristics and properties of individual sediment layers above the void, and the pre-failure geometry of the void.



Figure 1-6. Gradual-forming sinkhole centered on an oil-field brine disposal well in Stafford County, Kansas. Surface-subsidence rates for more than 10 years were consistent at around 20 cm/year, recently slowing (photo by R. Miller).



Figure 1-7. Mosaic sinkhole 12 days after catastrophic collapse on January 7, 2005. Obvious in this photograph is solution mining well #19 (left side of sinkhole), an unused gas pipeline suspended across the sink, and a heavily used set of railroad tracks fewer than 25 m north of the sinkhole edge (photo by R. Miller).



Figure 1-8. Old mine shaft used during room-and-pillar mining of rock salt near Kanopolis, Kansas, was plugged by dry-waste loading. Ground-water movement and material failure resulted in a pressure differential that instigated an explosive blowout (photo by G. Ohlmacher).



Figure 1-9. Natural sinkhole began forming in 1998, settling at a rate of about 20 cm/year with a diameter of more than 50 m. No surface expression existed prior to 1998, but seismic data suggested a paleosubsidence feature more than 500 m wide elongated to the east has been present throughout the Quaternary (photo by R. Miller).

Catastrophic failure of the ground surface as a consequence of natural salt dissolution has rarely been documented in Kansas or any other sinkhole-prone area of the world (Waltham et al., 2005) (Figure 1-10). All well-documented, catastrophic, or rapid failures blamed on salt dissolution in Kansas have been in close proximity to a well bore (Walters, 1991; Lambrecht and Miller, 2006), with the possible exception of the 1879 Meade County sinkhole (Walcott, 1901). Gradually subsiding sinkholes have occurred in almost every county in Kansas where the Hutchinson Salt Member is part of the geologic section (Merriam and Mann, 1957). Soil and overburden characteristics in most places above this salt have been shown to support rapid stoping and raveling, forming breccia pipes during upward migration of dissolution voids. This observation supports the assertion that the potential for rapid surface collapse exists regionally.

Voids in salt resulting from leaching are susceptible to closure from salt flowage. Pore space generated by the leaching of salt provides the differential pressure necessary to support creep at a rate dependent on the depth of burial (Le Comte, 1965). However, creep rates relative to dissolution rates are extremely slow (Carter and Hansen, 1983) and therefore, as a rule pore space (void) will enlarge to the point that roof rock strength is exceeded and the unsupported span fails, long before creep becomes a significant component of the salt mechanics.

Seismic investigations, borehole data, and surface observation prior to about 1995 concluded that surface and subsurface maturation of gradually forming sinkholes resembled plastic deformation, with rupture occurring significantly outside the footprint of the dissolution or disturbed zone in the salt (Steeple et al., 1986; Anderson et al., 1995b). These studies suggested sinkhole growth was continuous, with a relatively uniform rate of ground



Figure 1-10. Catastrophic failure of the Macksville, Kansas, sinkhole in July 1988 occurred over hours and resulted in a 10-m-wide opening that was initially over 60 m deep. This photo was taken 10 years after initial failure (photo by J. Charlton).



Figure 1-11. Brine-disposal well in Ellsworth County, Kansas. Growth of this feature has been predicted with seismic data to eventually affect the house and both roads (photo courtesy of Conoco).

sinking coupled with radial expansion. This concept was substantiated by the observed ever-growing bowl-shaped depressions formed with bed geometries and offsets defined by normal fault orientations as interpreted on low-resolution and poor signal-to-noise seismic sections and evident in ground fissures (Figure 1-11). It is generally accepted that gradual surface subsidence is by far the most common rate of sinkhole development regardless of the near-surface setting or overburden material.

Unique stress fields, failure mechanisms, and overburden characteristics have been postulated to be indicative of rapid or catastrophic subsidence and collapse (Davies, 1951; Walters, 1978; Rokar and Staudtmeister, 1985). With the very limited subsurface data and extremely small sample sizes used by investigators to propose these concepts, it is no wonder their reliability is in question. This manuscript combines high-quality seismic-reflection sections from more than a dozen dissolution-instigated sinkholes with research findings of the mining engineering community, physical model studies, and conceptual models to provide a unique and consistent development of the failure processes, gradual and catastrophic.

Seismic-reflection data targeting beds altered by dissolution and subsidence in Kansas have ranged in quality and interpretability from poor (Miller et al., 1995) to outstanding (Miller et al., 1997). Interpretations when data quality is poor, due to low signal-to-noise ratios and limited signal penetration, have unfortunately been relegated to indirect inference of structural processes and subsurface expressions (mainly from interpretations of deformation in layers above the salt). However, dozens of data sets acquired, processed, and interpreted by the author over the last 10 years possess excellent signal-to-noise ratios and resolution potential. These recent data sets allow direct detection and mapping of structures

and geometries that appear characteristic of complex sinkhole development. Resolution potential and signal-to-noise ratio of seismic data presented in this compilation are superior to any previously published that target soluble rock intervals and associated dissolution features below sinkholes. These data provide conclusive images of important structural features with unique characteristics that appear to control/influence sinkhole development.

In the last 25 years imaging quality (signal-to-noise [S/N] and resolution) for specific targets in the upper 1 km has improved by an order of magnitude in S/N and 2 to 3 times in resolution (Miller et al., 2006). Integrating the interpretation of high-resolution seismic-reflection data with physical models (which until this work has never been done for dissolution features with surface deformation) has dramatically improved the details and understanding of the process and maybe more importantly, identified key characteristics indicative of a sinkhole's growth stage and future development potential. Central Kansas, USA, is a premier location to develop and evaluate seismic methodologies for imaging dissolution features and associated deformation.

Concerns for public safety and potential for property damage when sinkholes form in proximity to heavily traveled railroads, highways, and pipelines transporting environmentally hazardous or explosive materials justify careful attention to the condition of overburden rocks (Figure 1-12). Seismic imaging has proven effective delineating overburden deformation in response to the upward migration of dissolution voids. Dozens of seismic images have been obtained above and around sinkholes associated with both anthropogenic and natural dissolution of salt (excessive solution mining, casing failure during disposal of oil-field fluids, failure of annulus seal around well casings, and natural fluid transport via faults and fractures). In all cases, the interpretations of the affected subsurface have lead to an



Figure 1-12. Lake resulting from a natural sinkhole more than 10 km from the dissolution front in eastern Reno County, Kansas. This sinkhole was inactive through the twentieth century until the late 1990s, when about 100 m along the western edge of the heavily traveled U.S. Highway 50 began subsiding (Google Earth, 2006).

improved understanding of site-specific failure mechanisms and predictability. This study brings all those findings together to establish a general understanding and description of the overall process.

To fully ascertain the significance of the problem, problem-specific characteristics, and possible approaches to solve the problem, a familiarity must be established with the geologic setting and associated seismic properties diagnostic of these dissolution features. With the global presence of salt basins, the regionally specific problems of this basin in Kansas are not unique. Establishing the geometry and history of this planar salt is important to understanding some of the constraints on the dissolution and subsidence processes.

Summing Up and To Come

Having just described and shown examples of the kinds of failure surface and subsurface facilities and activities are subject to, the utility is evident for predictive methods or models capable of mitigating much of the speculation about ground movement that is associated with the dissolution of soluble rocks. Natural and anthropogenic dissolution of bedded salt is common within the many-layered salt basins throughout the world. Sinkholes have developed in these basins both gradually and catastrophically, many times developing without surface provocation or advanced warning. Regionally these events represent a potential risk to most surface activities and structures. Advancements in near-surface high-resolution seismic technology have allowed improved resolution and signal-to-noise ratios of subsurface images of subsidence features.

Earth layers characterized as laterally discontinuous both from structural and physical properties perspectives are not ideal for the seismic method. In highly altered rock layers, smearing of the image is a real problem and properties of the reflected wave must be considered when interpreting subsidence features. Even from a high-resolution seismic-reflection perspective, these features change rapidly both laterally and horizontally. In the next chapter key aspects of both the geology and seismic imagery will be reviewed and will be the starting point for examining historical seismic-reflection data that have attempted to image dissolution features. By relating the geology and seismic sensitivities, it is possible to define physical changes expected to be diagnostic of these dissolution features and therefore likely seismic responses.

References

- Anderson, N.L. W.L. Watney, P.A. Macfarlane, and R.W. Knapp, 1995a, Seismic signature of the Hutchinson salt and associated dissolution features; in N.L. Anderson and D.E. Hedke, eds., *Geophysical atlas of selected oil and gas fields in Kansas*: Kansas Geological Survey Bulletin 237, p. 57-65.
- Anderson, N.L., R.W., Knapp, D.W. Steeples, and R.D. Miller, 1995b, Plastic deformation and dissolution of the Hutchinson Salt Member in Kansas; in N.L. Anderson and D.E. Hedke, eds., *Geophysical atlas of selected oil and gas fields in Kansas*: Kansas Geological Survey Bulletin 237, p. 66-70.
- Anderson, N.L., A. Martinez, J.F. Hopkins, and T.R. Carr, 1998, Salt dissolution and surface subsidence in central Kansas: A seismic investigation of the anthropogenic and natural origin models: *Geophysics*, v. 63, p. 366-378.
- Beck, B.F., A.J. Pettit, and J.G. Herring, eds., 1999, *Hydrogeology and Engineering Geology of Sinkholes and Karst—1999*: A.A. Balkema, Rotterdam, 130 p.
- Carter, N.L., and F.D. Hansen, 1983, Creep of rock salt: *Tectonophysics*, v. 92, p. 275-333.
- Davies, W.E., 1951, Mechanics of cavern breakdown: *National Speleological Society*, v. 13, p. 6-43.
- Ege, J.R., 1984, Formation of solution-subsidence sinkholes above salt beds: U.S. Geological Survey Circular 897, 11 p.
- Frye, J.C., 1950, Origin of Kansas Great Plains depressions: Kansas Geological Survey Bulletin 86, pt. 1, 1–20.
- Frye, J.C., and S.L. Schoff, 1942, Deep-seated solution in the Meade basin and vicinity, Kansas and Oklahoma: *American Geophysical Union Transactions*, v. 23, pt. 1, 35–39.
- Gogel, T., 1981, Discharge of saltwater from Permian rocks to major stream-aquifer systems in central Kansas: Kansas Geological Survey Chemical Quality Series No. 9, 60 p.
- Google Earth, 2006 (<http://earth.google.com/>).
- Johnson, K.S., and J.T. Neal, eds., 2003, Evaporite karst and engineering/environmental problems in the United States: Oklahoma Geological Survey Circular 190, 353 p.
- Knapp, R.W., D.W. Steeples, R.D. Miller, and C.D. McElwee, 1989, Seismic reflection at sinkholes; in D.W. Steeples, ed., *Geophysics in Kansas*: Kansas Geological Survey Bulletin 226, p. 95-116.
- Kozary, M.T., J.C. Dunlap, and W.E. Humphrey, 1968, Incidence of saline deposits in geologic time; in R.B. Mattox, ed., *Saline deposits*: Geological Society of America Special Paper 88, p. 43-57.
- Lambrecht, J.L., and R.D. Miller, 2006, Catastrophic sinkhole formation in Kansas: A case study: *The Leading Edge*, v. 25, n. 3, p. 342-347.
- Le Comte, P. 1965, Geological notes—Creep in rock salt: *Journal of Geology*, v. 73, n. 3, p. 469-483.
- Merriam, D.F., and C.J. Mann, 1957, Sinkholes and related geologic features in Kansas: *Transactions of the Kansas Academy of Science*, v. 60, p. 207-243.
- Miller, R.D., 2003, High-resolution seismic-reflection investigation of a subsidence feature on U.S. Highway 50 near Hutchinson, Kansas; in K.S. Johnson and J.T. Neal, eds., *Evaporite karst and engineering/environmental problems in the United States*: Oklahoma Geological Survey Circular 109, p. 157-167.
- Miller, R.D., 2006, High-resolution seismic reflection to identify areas with subsidence potential beneath U.S. 50 Highway in eastern Reno County, Kansas: Symposium on the

- Application of Geophysics to Engineering and Environmental Problems [ext. abs.]: Selected as a best paper from SAGEEP06, presented at Near Surface 2006, Helsinki, Finland, Sept. 4-6, 5 p. (published on CD).
- Miller, R.D., and R. Henthorne, 2004, High-resolution seismic reflection to identify areas with subsidence potential beneath U.S. 50 Highway in eastern Reno County, Kansas: Proceedings of the 55th Highway Geology Symposium, September 8-10, Kansas City, Missouri, p. 29-48.
- Miller, R.D., D.W. Steeples, and J.L. Lambrecht, 2006, High-resolution seismic-reflection imaging 25 years of change in I-70 sinkhole, Russell, County, Kansas [exp. abs.]: Society of Exploration Geophysics.
- Miller, R.D., D.W. Steeples, L. Schulte, and J. Davenport, 1993, Shallow seismic-reflection feasibility study of the salt dissolution well field at North American Salt Company's Hutchinson, Kansas, facility: *Mining Engineering*, October, p. 1291-1296.
- Miller, R.D., D.W. Steeples, and T.V. Weis, 1995, Shallow seismic-reflection study of a salt dissolution subsidence feature in Stafford County, Kansas; in N.L. Anderson and D.E. Hedke, eds., *Geophysical atlas of selected oil and gas fields in Kansas: Kansas Geological Survey Bulletin 237*, p. 71-76.
- Miller, R.D., A. Villella, and J. Xia, 1997, Shallow high resolution seismic reflection to delineate upper 400 m around a collapse feature in central Kansas: *AAPG Division of Environmental Geosciences Journal*, v. 4, n. 3, p. 119-126.
- Rokar, R.B., and K. Staudtmeister, 1985, Creep rupture criteria for rock salt: Sixth International Symposium on Salt, B.C. Schreiber and H.L. Harner, eds., Salt Institute Inc., Virginia, v. 1, p. 455-462.
- Steeple, D.W., R.W. Knapp, and C.D. McElwee, 1986, Seismic reflection investigations of sinkholes beneath interstate highway 80 in Kansas: *Geophysics*, v. 51, p. 295-301.
- Walcott, C.D., 1901, *Twenty-First Annual Report of the U.S. Geological Survey, Part IV—Hydrography*: U.S. Government Printing Office, Washington, D.C., p. 705-711.
- Walters, R.F., 1978, Land subsidence in central Kansas related to salt dissolution: *Kansas Geological Survey Bulletin 214*, 82 p.
- Walters, R.F., 1991, Gorham oil field: *Kansas Geological Survey Bulletin 228*, 112 p.
- Waltham, T., F. Bell, and M. Culshaw, 2005, *Sinkholes and Subsidence: Karst and Cavernous Rocks in Engineering and Construction*: Praxis Publishing Ltd., Chichester, UK, 382 p.

CHAPTER 2

REGIONAL FRAMEWORK AND CHARACTERISTICS

This chapter reviews the geologic setting and characteristics of salt beds and discusses the expected seismic response from the salt interval, overburden, and subsidence-related subsurface features. An understanding of these topics will complement developments in later chapters involving site-specific seismic studies over a variety of different dissolution features. As well, unveiling key aspects of the geology and characteristics of the seismic response relevant to this general study area and targets provides a vital link supporting future developments and conclusions. Important to any discussion of subsurface dissolution features and related processes is not only a general understanding of the geologic setting, but specific lithologic characteristics of overburden rocks as well.

At the beginning of this chapter discussions focus on rock intervals and their associated lithologies and characteristics. Principal emphasis will be directed toward salt stability and upward migration of voids formed in the salt interval. Understanding the deposition process for bedded salt allows an appreciation of the variability in reflection-wavelet characteristics and patterns routinely observed on seismic sections at times consistent with this almost 125-m-thick salt interval. Reconstruction and development of deformation mechanisms rely heavily on the salt history and current setting. It is important to establish an appreciation for the response characteristics of a high-resolution seismic-reflection wavelet from the many diverse structural and lithologic conditions in and above a salt interval both before and after dissolution and subsidence. This appreciation is essential to effectively correlate between a reasonable set of model structures with specific failure mechanisms inferred from seismic data and surface observations. As background, it is important to be familiar with the diversity of wavelet character and reflection sequences that can return from the salt interval.

High-resolution seismic-reflection sections have been used to help unravel a wide range of engineering, geologic, and hydrologic problems throughout the world by the author. For this manuscript, this unique seismic approach is applied in proximity to and focusing on sinkhole volumes and their development. Reference articles published by the author that are included in this work (Appendix B) predominantly target dissolution of the Hutchinson Salt Member in Kansas, USA. Approaches and developments/modifications necessary to optimize seismic data used or displayed in this manuscript were based on the author's 25 years of experience studying and adapting seismic-reflection imaging to a variety of near-surface problems. Kansas was chosen as the test bed for studying the mechanisms and processes associated with collapse structures due to its availability to the author, high rate of sinkhole development in thick bedded salts, and variety of fluid sources and site settings where dissolution with associated subsidence has occurred and is very likely to continue.



Figure 2-1. In 24 hours during 1981, this sinkhole in Winter Park, Florida, opened to 100 m in diameter and 30 m deep, consuming a house, part of a six-lane highway, half of a swimming pool, several cars, and parts of three businesses (Florida Geological Survey) (published in Cobb and Currens, 2001).

Geologic Setting

Subsidence related to dissolution of soluble rocks is a prominent phenomenon world-wide (Ford and Williams, 1989). Most noted subsidence events are karst sinkholes resulting from dissolution of surface and near surface carbonates (Figure 1-1). The emphasis placed on carbonate dissolution is clearly related to their wide distribution, total quantity, and historical relationship with rapid ground failure in populated areas (Figure 2-1). Soluble rocks are bountiful in Kansas, with thick alternating sequences of carbonates and several halite, gypsum, and anhydrite rich zones within 400 m of the ground surface (Zeller, 1968). With soluble rocks and freshwater abundant in the near-surface, karst and subsidence is assured.

The midcontinent of North America has generally been considered the central stable region or stable interior (Snyder, 1968). A stratigraphic sequence across Kansas that ranges from a few hundred to almost 3,000 meters covers the Precambrian basement rocks forming a series of relatively thin veneers (Merriam, 1963) (Figure 2-2). Regionally the sedimentary sequence dips gently to the west at around 4 m/km. The post-Precambrian section in Kansas is only partially present and is represented by a relatively simple succession of thin sedimentary strata that accounts for between 15 and 50 percent of the total section that was once present. Several structural provinces appear relatively consistent throughout the sedimentary section, becoming gradationally less evident in the younger sediments (Figure 2-3). In general, the stratigraphic sequence throughout the Interior Lowlands has been termed the science of gently dipping strata (King, 1959).

With extremely rapid dissolution rates, leaching of a salt deposit can represent a hazard within human time rather than geologic time as is the case for carbonates (Beck, 1988). Several major salt basins exist throughout North America (Ege, 1984) (Figure 2-4).

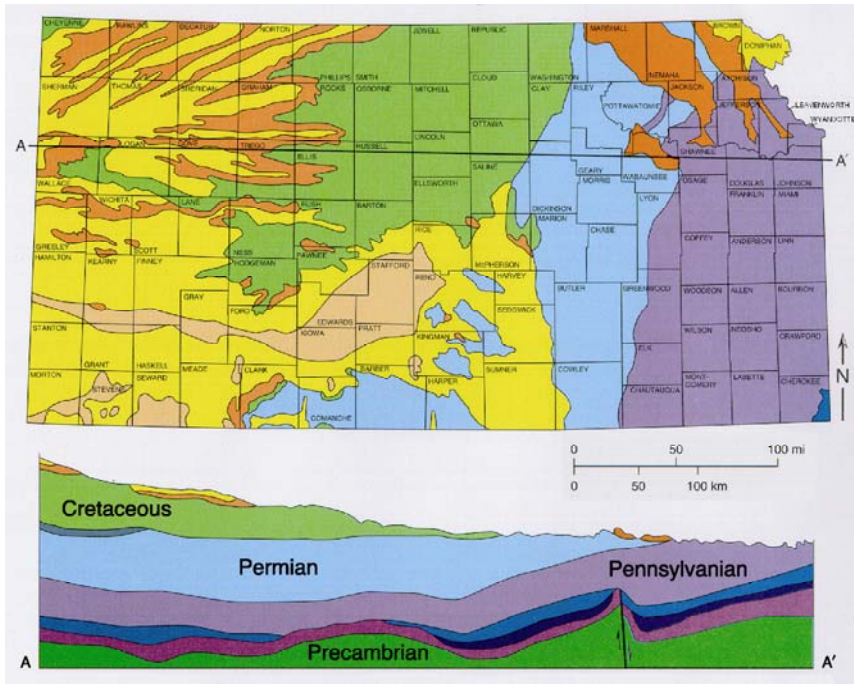


Figure 2-2. Generalized geologic map of Kansas with representative cross section slicing the upper 3 to 4 km from the Colorado border on the west to the Missouri border on the east (modified from Merriam, 1963).

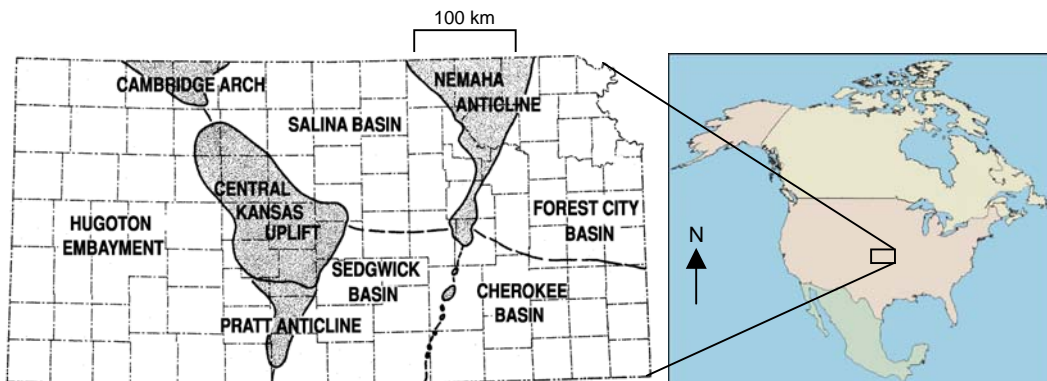


Figure 2-3. Structural provinces are reasonably consistent throughout the sedimentary section in Kansas (modified from Merriam, 1963).

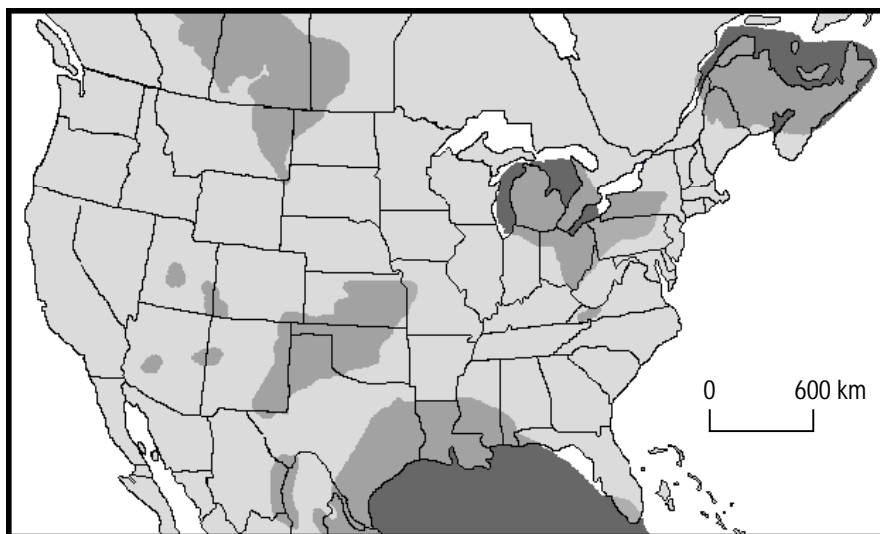


Figure 2-4. Major salt basins throughout North America (Ege, 1984).

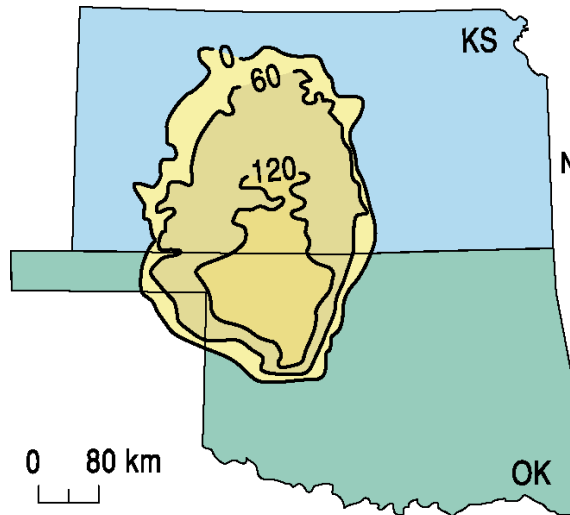


Figure 2-5. Isopach of the Hutchinson Salt Member, showing approximate areal extent and thickness in meters. Clearly evident are the high gradient areas on the east, indicative of the natural dissolution front in Kansas (modified from Walters, 1978).

In the northern extreme of the Permian salt basin (extending from the Texas Panhandle to central Kansas) is the Permian Wellington Formation in central Kansas, which includes the anhydrite- and shale-bounded Hutchinson Salt Member (Figure 2-5). Within the Hutchinson Salt Member interval are laterally extensive, alternating sequences of halite-rich marine cycles that vary quite significantly in thickness and purity across the region (Watney et al., 1988). Due to regional tectonic stability and the relatively impermeable seal provided by the overlying shales, this highly soluble rock has been amazingly stable since deposition almost 260 million years ago (Figure 2-6).

In Kansas, the Hutchinson Salt Member possesses an average net thickness of 75 m, reaching a maximum thickness of over 150 m in the south-central part of the state (Figure 2-5). The increasing thickness of the salt interval toward the center of the basin is due to a combination of increased salt and more and thicker interbedded anhydrites. The distribution and stratigraphy of the salt is well documented (Dellwig, 1963; Holdaway, 1978; Kulstad, 1959; Merriam, 1963; Watney et al., 1988). Deposition occurring during fluctuating sea

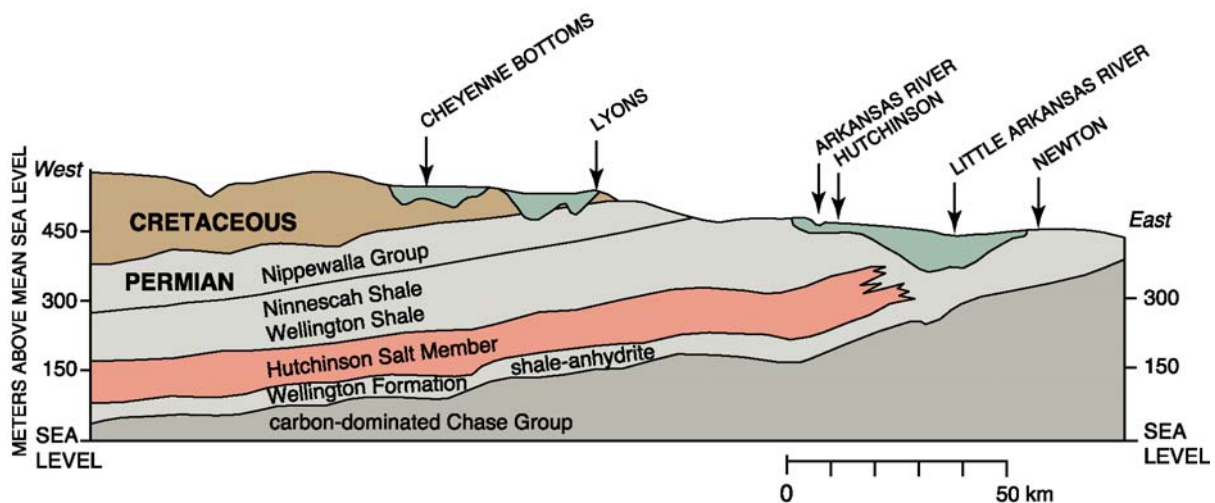


Figure 2-6. Generalized geologic cross section above sea level with major units identified and mapped from well data (modified from Spinazola et al., 1985).

levels resulted in numerous halite beds 0.25 m to 3 m thick alternating with interbedded shale, minor anhydrite, and dolomite/magnesite. Individual salt beds may only be continuous for a few kilometers despite the remarkable lateral continuity of the salt interval as a whole (Walters, 1978). Important to this study is the presence of thin anhydrite beds within the halite succession that generally have a strong acoustic response and once dissolution begins, but prior to overburden subsidence, provide a measure of distortion within the salt interval. Deposition of the Wellington Formation (which includes the Hutchinson Salt Member) was influenced by a broad inland sea that extended north from the modern Gulf of Mexico across current-day Texas and Oklahoma with west, north, and east shorelines in central Kansas. Refreshing of this sea with ocean waters was periodically restricted at the inlet during sea-level fluctuations.

Based on over 3,000 boring logs, the dimensions of the Hutchinson Salt Member can be reasonably well defined (Figure 2-7) (Watney, 2007). From salt thickness contours, depositional edges can clearly be distinguished from dissolution edges (Figure 2-7a). The abrupt reduction in salt thickness from over 75 m to less than 10 m is clearly discernible on the eastern extreme of the bed and interpreted in general as the dissolution front. The exceedingly large area on the east with contours suggesting 0 to 10 m of salt is representative of intermittent, locally randomly distributed remnants of the original salt sheet. Relatively sharp incisions into the salt layer by the interpreted dissolution front on the east are generally indicative of areas with the most active sinkhole development in the region. Evidence of an extensive history of dissolution has been amassed from dozens of seismic profiles and hundreds of surface-subsidence features. Depth of salt burial is consistent with the regional dip (Figure 2-7b). The topographic surface of the salt is intriguing (Figure 2-7c). Valley features on the surface of the salt in proximity to the dissolution front are indicative of more active dissolution zones and are characteristic of more active fluid dynamics and saturation levels well suited for leaching.

The eastern margin of the salt was exposed during late “Tertiary” (Miocene-Pliocene) when natural erosion and leaching began the 30-km westward progression to the front’s present-day location (Bayne, 1956). The ability of the front to migrate while under as much as 100 m of sediments was a direct consequence of a ready access to an abundant supply of ground water (Gogel, 1981; Gillespie and Hargadine, 1986; Johnson, 1981). Contemporaneous deposition of Quaternary alluvium was occurring approximately consistent with the removal of salt and associated overburden subsidence. This Quaternary deposition is responsible for today’s moderate to low-surface relief that masks the extremely distorted (faulted and folded—non-tectonic) rock layers within the upper Wellington Formation and Ninnescah Shale (Anderson et al., 1998). With this migration has come the loss of a significant portion of the rock record. Subsidence of Permian, Cretaceous, and “Tertiary” rocks has continued westward consistent with the migrating natural-dissolution front.

Across the study area the lithology (especially the upper 50 m) varies significantly above the Hutchinson Salt Member (Figure 2-6). Rocks above the salt’s eastern perimeter are predominantly Permian shales with an occasional thin evaporite stringer. Above the north-central edge of the salt, the upper third of the section is dominated by Cretaceous sandstones and shales overlying the shale-dominated Permian section. No significant thickness of Jurassic rocks has been detected at the northern depositional edge of the salt.

Bedrock along the eastern portion of the salt bed is the Ninnescah Shale with the unconsolidated Pliocene-Pleistocene Equus beds making up the majority of the upper 30 m of

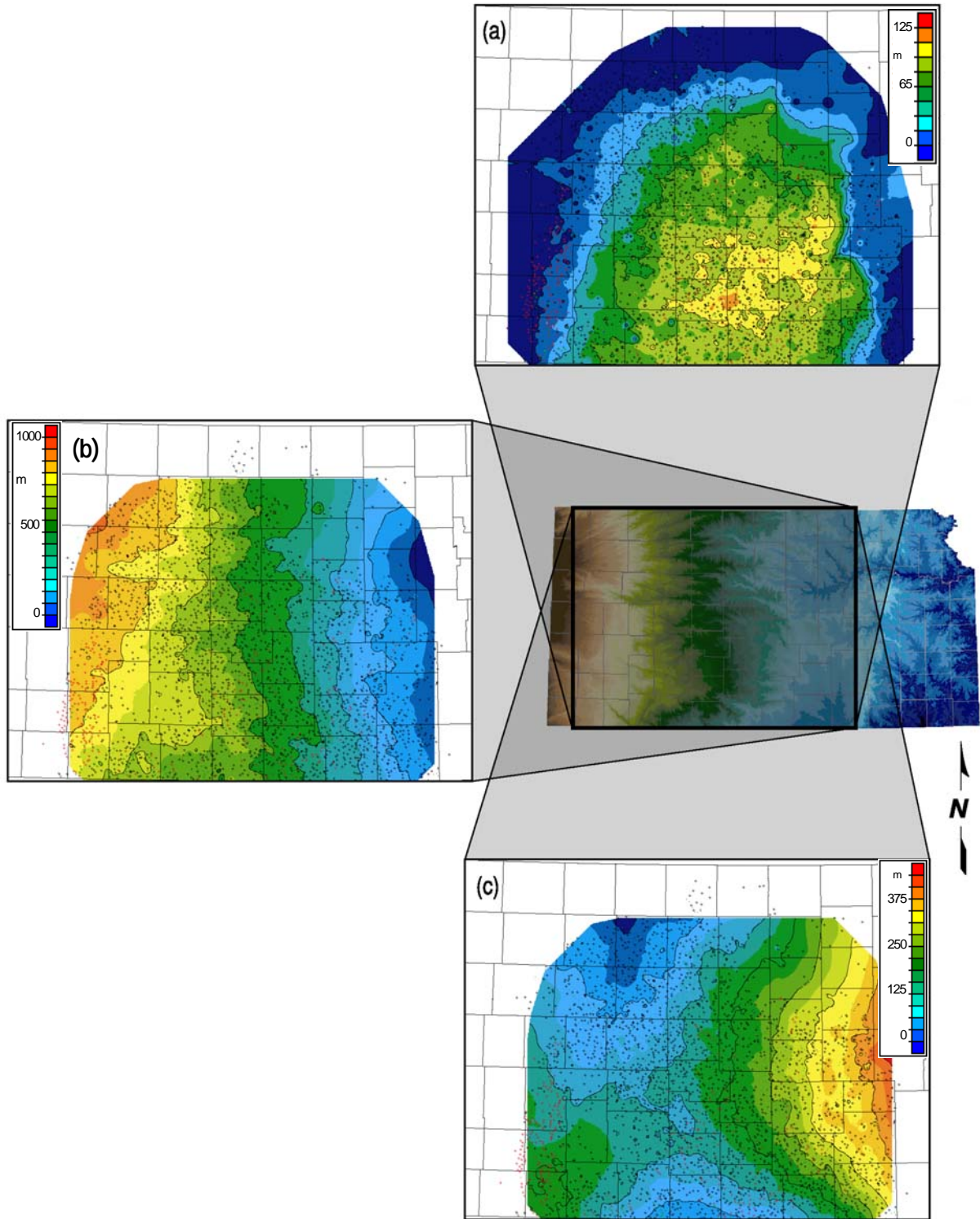


Figure 2-7. Drillhole-mapped salt interval indicating the salt thickness (a), current depth of burial of the salt layer (b), the surface topography of the salt layer (c) (from Watney, 2007), and surface topography (dark-blue 300 m above sea level grading to brown at over 1000 m above sea level).

sediment (Spinazola et al., 1985). Quaternary alluvium fills the stream valleys and paleo-subsidence features that range from 0 to as much as 100 m deep. On the western half of the salt basin, the erosional bedrock surface is Cretaceous Fairport shale with sporadic remnants of ancient valley cut-and-fill features.

Characteristics of the salt caprock are an exceedingly important component of any discussion involving formation of sinkholes from dissolution. The Permian shales (Wellington and Ninnescah) overlaying the Hutchinson Salt Member are generally about 75 m to 100 m thick and characterized as unstable and susceptible to sloughing and collapse when exposed to freshwater (Swineford, 1955). These Permian Ninnescah shales tend to be red or reddish-brown and are commonly referred to as “red beds.” Permian red beds are extremely impermeable to water and have therefore provided an excellent seal between the freshwaters of the Equus beds and the extremely water-soluble Hutchinson Salt Member. The modern-day expanse and mere presence of the Hutchinson Salt Member is largely due to the protection provided by these red beds from fresh water. Directly above the salt/shale contact is an approximately 7-m-thick dark shale with joints and bedding cracks filled with a red halite (Walters, 1978). The red halite is rapidly leached when unsaturated brine comes in contact with this shale layer. In response to fluid contact, the shale layer either begins stoping or simply collapses in total into salt voids. It is not surprising that a key factor in predicting roof-rock failure in salt jugs is the condition of the salt/shale contact and whether it has been exposed to unsaturated brine solution.

Most of the upper 300 m of rock along the eastern boundary of the salt bed is Permian shales (Merriam, 1963) (Figure 2-8). The Permian/Pennsylvanian (Carboniferous) boundary is about 700 m deep and seismically distinguishable as a high-amplitude sequence of cyclic reflecting events. The Chase Group (top at 300 m deep), lower Wellington shales (top at 225 m deep), Hutchinson Salt Member (top at 100 m deep), upper Wellington shales (top at 70 m deep), and Ninnescah Shale (top at 20 m deep) make up the packet of reflecting events easily identifiable and segregated within the Permian. These Permian reflectors must be imaged on seismic data with good signal-to-noise ratios and above the high-resolution threshold to be accurately processed and allow confident interpretation of all the subtle geometric characteristics diagnostic of subsidence features on seismic sections.

Along the northern boundary of the salt bed, most rocks in the upper 600 m are Permian shales and evaporites overlain by Cretaceous sandstones and shales (Figure 2-8). The abundance of fresh-to-brackish aquifers in the Cretaceous section is key to much of the dissolution in the north. Of particular significance are the confined aquifers of the Dakota, Cedar Hills, and Cheyenne (Frye and Brazil, 1943). The presence of the Stone Corral anhydrite in the western half of Kansas is extremely important from a seismic perspective, benefiting all aspects of seismic surveying. This well-known reflector provides a regionally consistent bed with a high reflectivity and an unmistakable reflection signature (McGuire and Miller, 1989).

The most geologically and hydrologically active areas associated with the Hutchinson Salt Member are at the natural dissolution front (processes and characteristics discussed in detail in Chapter 1). This area is prone to and has an extensive history of salt dissolution and sinkhole formation (Merriam and Mann, 1957). In general, natural evaporite dissolution will occur along a dissolution front and preferentially in association with anomalies (faults, fractures, joints, etc.). Transitioning from natural dissolution processes in general to those

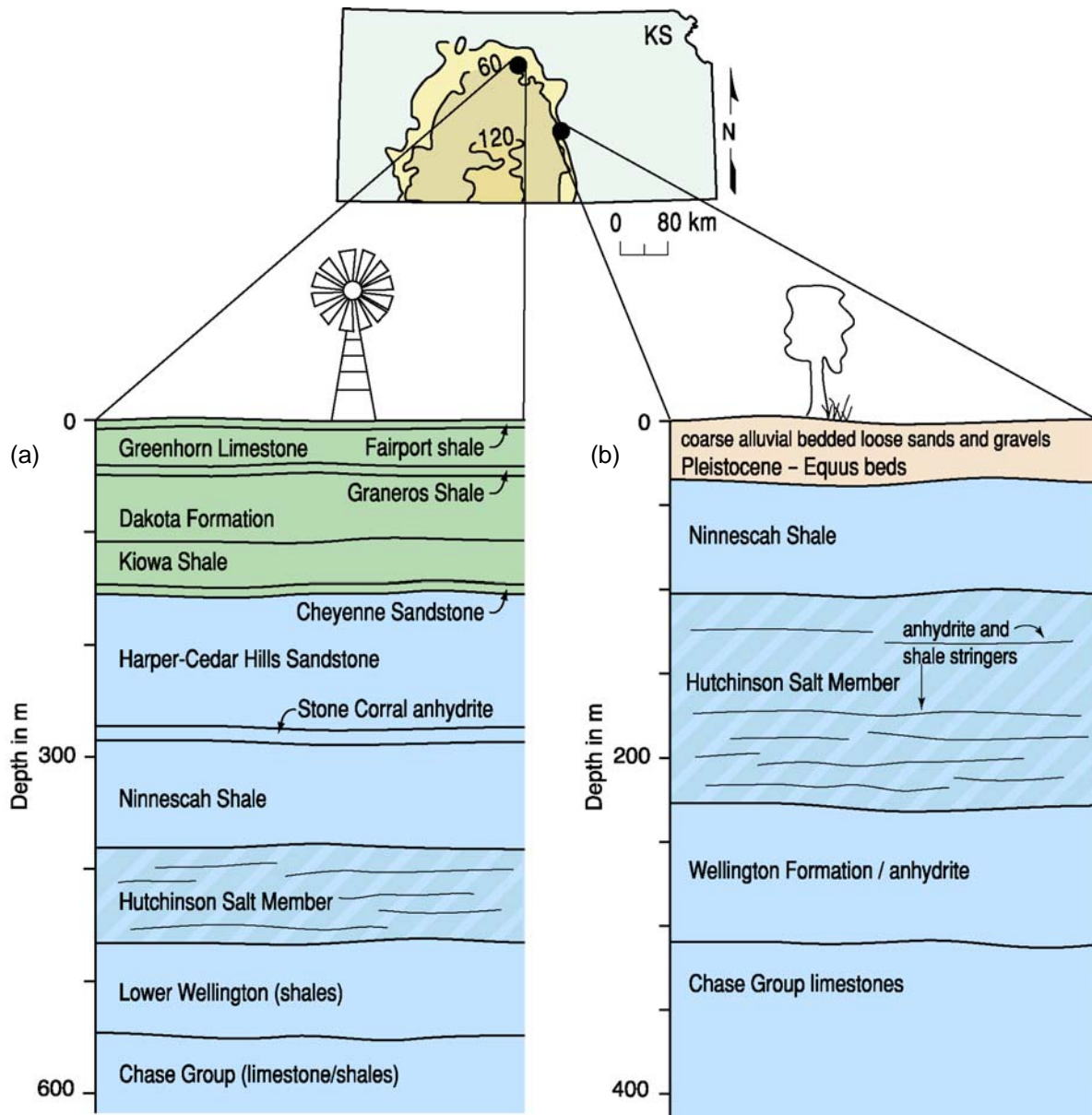


Figure 2-8. (a) Generalized depth section for seismic studies in the northern portion of the salt. (b) Generalized depth section for areas investigated with seismic in this manuscript along the eastern dissolution edge of the salt.

specific to the eastern margin of the bedded salt in Kansas invariably incorporates the influence of the Wellington aquifer (Figure 2-9).

Water flow into and out of the salt layer is key to dissolution and associated subsidence. Structural features tend to represent preferential fluid pathways and correspond to areas most susceptible to natural leaching. Of the nine structural units in Kansas (Merriam, 1963) (Figure 2-3), four are up-arched features separating the four downwarped basins. These structures are all post-Mississippian and have experienced little change since mid-Middle Pennsylvanian (Jewett and Merriam, 1959). Besides risks to surface structures and activities, subsidence features potentially jeopardize the natural segregation of groundwater aquifers, greatly increasing their potential to negatively impact the environment through mixing (Whittemore, 1989, 1990).

Natural, localized leaching of the salt and associated subsidence influenced by structural features forming geologic-based flow systems (such as faults and fractures) have

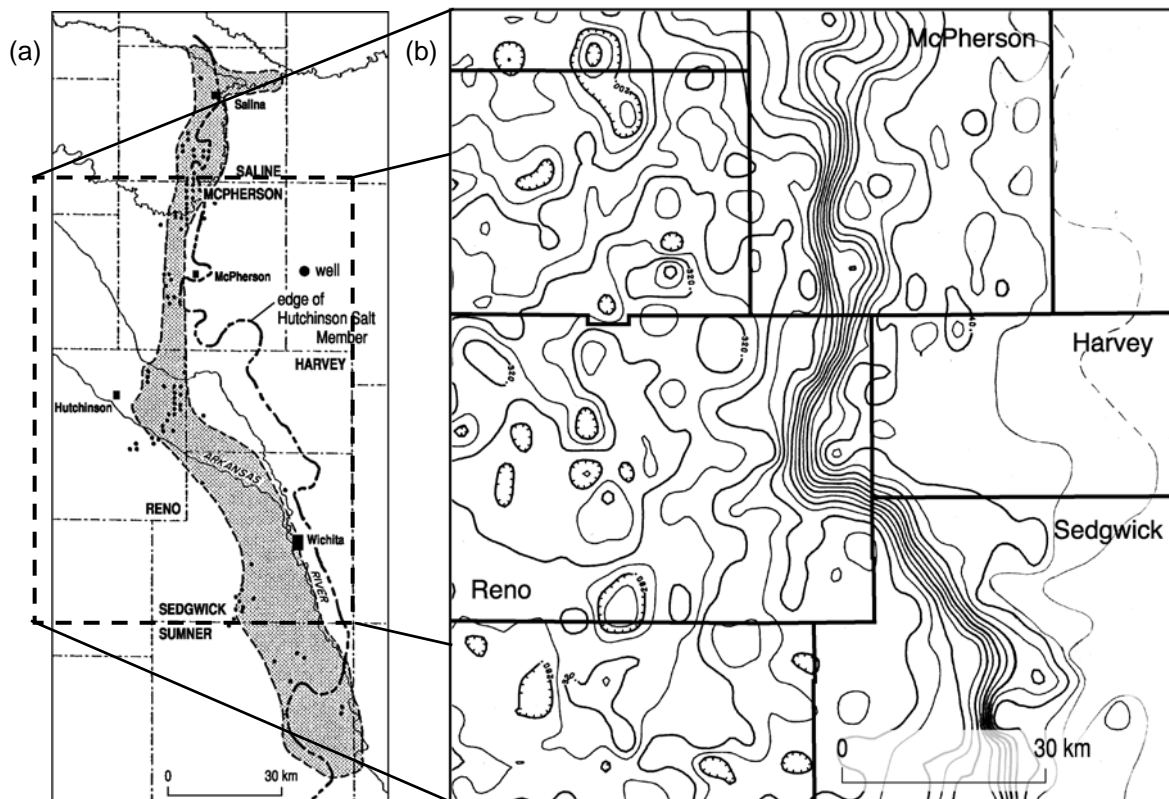


Figure 2-9. Wellington aquifer (a) (from Gogel, 1981) as defined by sinkholes, undrained enclosed depressions, and bedrock folding. The aquifer closely matches the high-gradient contours of the salt isopach (b) (from Watney and Paul, 1980).

been observed west of the main dissolution edge (Merriam and Mann, 1957). Post-depositional uplift and subsidence have provided an assortment of conduits conducive to ground-water circulation. From the many natural dissolution phenomena currently active and those interpreted as “paleo,” these groundwater conduits can lay dormant for millions of years with reactivation driven by undetectable catalysts (Johnson, 2003).

Considering the limited number of known occurrences of natural dissolution of the Hutchinson Salt Member away from the eastern edge since deposition (250 million years), it is reasonable to suggest that most natural dissolution processes have been self-healing (Waltham et al., 2005). Highly detailed exploratory drilling and associated log analysis have allowed the mapping of small-scale incised valleys that cut into the top of the salt and appear to be indicative of limited (maybe single episode) post-deposition leaching more than 40 km west of the natural, active dissolution front (Watney et al., 2003). These incised dissolution valleys appear to be consistent with the crest of a small-scale regional structure. This observation leads to the suggestion that subtle localized structures likely influence natural-dissolution patterns both along the natural front and those likely scattered across the entire salt surface. A dormant pre-Quaternary dissolution and subsidence feature identified on seismic data immediately south of this drill-identified valley feature is consistent with the self-healing process associated with natural dissolution (Miller, 2006).

Salt Beds

Salt deposition in a broad shallow embayment results in horizontal beds (Jackson, 1997). In some settings deformational forces can drive the more buoyant salt to produce diapirs. Deposition of the Hutchinson Salt Member was powered and controlled by

fluctuating Permian sea levels and intermittent restrictions on flow of marine waters into a wide and at times quite shallow inland sea—an inland sea that could occasionally be characterized by extensive tidal mud flats (Walters, 1978). Deposition of halite is typically rapid, resulting in large crystals collecting in beds with initial differences in thickness and quality (purity), a by-product of that deposition (Hovorka, 1994). Changes in environmental conditions affected the percent impurities and interrupted the halite deposition.

Dynamics and configuration of salt beds depend on several aspects of both deposition and post-deposition tectonics. Keys to the characteristics of a bedded salt sequence are the overall thickness of the salt and the thickness, composition, and frequency of insoluble interbedded precipitate (Hovorka, 1994). The quality and initial thickness of the salt intervals are established during deposition. Insoluble interbedded rocks deposited during isolation from marine waters are generally composed of disseminated impurities, mudstones, and anhydrite (Hovorka, 1994). Interbedded shales are added to the salt section during periods when muddy freshwater infiltrates the inland sea, a time characterized by local redissolution of the salt (Dellwig, 1971).

When the inland Permian sea that covered present-day Kansas was isolated from the influx of marine waters and water depths were shallow, evaporation accelerated the precipitation of salt. Halite precipitates to the brine-pool floor as masses or crusts of crystals (Hovorka, 1994). With the influx of new marine waters or rainfall, the pool concentrations decrease and some redissolution of salt occurs on the sea floor. This redissolution leaves impurities from the salt to accumulate on the sea floor as an insoluble layer of lag, later covered by salt precipitate. Dissolution and precipitation of salt and accumulations of impurities at the bottom of the water column during these depositional cycles is influenced by water chemistry, water depths, and cyclicity of new marine water or fresh water (rainfall or ground water).

Both precipitation and dissolution on the sea floor are constrained when the water depths exceed a meter or so (Hovorka, 1994). Denser stratified brine migrates to the bottom of the water column separating the dilution and evaporation process from the brine pool floor. As crystals form at the air/water contact and float on the water surface, they gather to form floating masses that eventually settle as cumulates on the sea floor. Fresh water from rainfall or ground-water infiltrate or less saline marine waters entering the pool will float on the hyper-saturated brine liquid thereby protecting the salt deposit from redissolution. This segregation can accommodate a thick accumulation of halite.

Seismic-reflection Setting

Kansas has a reputation among seismic practitioners as being a “good data area.” This characterization is based on a relatively uniform sedimentary section with abrupt lithologic contacts, gentle structures, and distinctive changes in reflectance at lithologic contacts. In most places in Kansas, topographic and near-surface variability are only minor obstacles to acquisition and processing, and attenuation is minimized by a relatively high Q (quality factor). Therefore, optimizing reflection data for signal-to-noise ratio and more recently for resolution has been possible without sophisticated, assumption-based processing approaches or compromising survey designs.

Seismically, as geologically, where salt dissolution has resulted in subsidence in Kansas all Permian and younger reflectors are important to the accurate interpretation of stacked sections and formulation of a representative subsurface model. Model studies show

significant time delays (static), and geometric distortions are to be expected within recent subsidence features (Anderson et al., 1995). Two-way traveltime “pull downs” of seismic reflections from localized decreases in material velocities are routinely observed and expected within a subsidence structure. The velocity structure, small radius of curvature of the characteristic collapse synforms, narrow diameter of collapse structures, and three-dimensional characteristics of salt dissolution and associated subsidence features produce diffractions and/or highly distort reflections on 2-D vertically incident reflection sections.

Reflections from beneath the salt interval have a subdued expression of reflector that defines salt subsidence structures as a result of bed disruptions and accumulations of collapse breccia, locally reducing the average velocity. On commercial reflection data where deeper petroleum-bearing formations are the principal target, inconsistencies associated with shallow dissolution features have produced debilitating statics problems. Sub-salt reflection imaging represents a challenging subdiscipline all of its own (Colorado School of Mines, 2005). Estimations of subsidence and therefore volume of removed or altered rock salt based on time sections alone (without compensation for reduced and variable velocity) may exceed actual amounts by as much as 25 to 50 percent. Considering the geologic setting in Kansas, it is reasonable when imaging subsidence features to compensate for compaction/subsidence-related static irregularities by “flattening” on the top of the Chase Group (major subsalt reflector). This preliminary approach exposes general characteristics of the real structures. Collapse-induced static must ultimately be compensated for through an improved velocity function (Steeple et al., 1990) because localized structure on the Chase many times is real and accumulated time delay may not correspond solely to velocity anomalies at and above the salt.

Sinkholes from salt dissolution in the western half of Kansas will involve the Stone Corral Formation (anhydrite) in some fashion or another. The Stone Corral is well known as a regionally consistent interface, with a well-earned reputation as a seismic marker bed based on its characteristic high amplitude and frequency-reflection wavelet (McGuire and Miller, 1989). Offset or drape in the Stone Corral reflection can be a key indicator of either subsidence or static. If the Stone Corral is present within the overburden, it will likely be the highest amplitude reflection on the CMP-stacked section and usually isolated on high-resolution data from other reflection events by a cycle or more.

Recording reflections from shale/anhydrite contacts, anhydrite/rock salt contacts, and rock salt/shale contacts is necessary to interpret anomalies and analyze processes within and above the salt interval. An abundance of limestones and sandstones are present throughout the overburden and provide excellent reflection returns. Unfortunately, reflection geometries from within the overburden are more diagnostic of post-void failure and upward migration of the void rather than intersalt distortion, which is indicative of salt-leaching prefailure. On average, an interface defined by an anhydrite in direct contact with a shale or rock-salt layer has a reflectivity of 0.2, compared to a 0.02 for contacts between shale and rock salt. Anhydrite within the salt interval or shale section should produce a relatively high amplitude reflection, while shale layers in the salt interval are expected to have an order of magnitude weaker reflection amplitudes.

Reflection amplitudes from the top of the salt (salt/shale contact) are calculated to be relatively low but the contact is abrupt, and therefore reflections from that interface should be impulsive and distinctive. The abrupt shale/salt contact at the top of the salt is, in fact, quite distinctive on both synthetic and real CMP-stacked sections (Figure 2-10). However,

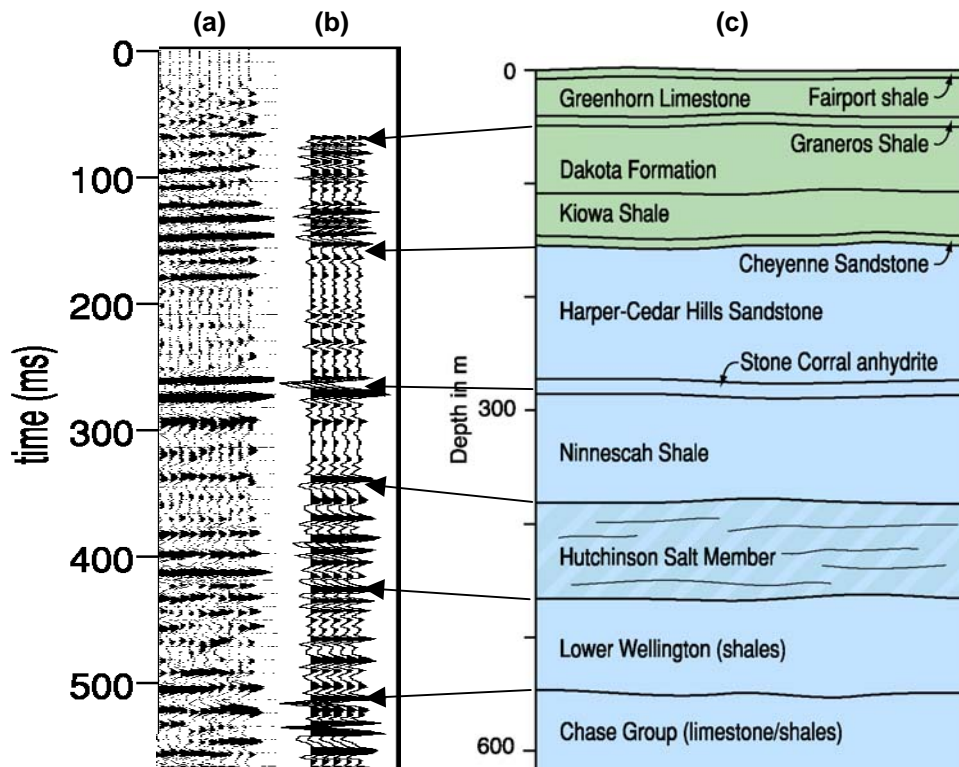


Figure 2-10. Seismic stacked sections (a) from the I-70 line in Russell County, Kansas, compared to synthetic (b) generated from a sonic acquired ~2 km from the seismic data are matched with the geologic section (c).

geophysically distinguishing the reflection from the basal salt contact (salt/shale) is difficult on seismic or electric logs due to its transitional nature. This is evidenced by the thin, highly cyclic anhydrite, shale, and salt sequence that defines the lower few tens of meters of the salt (Dellwig, 1971). Even with the resolution potential of most reflection data in this manuscript, thin bed interpretations within the salt are a challenge because of the small bed separation within the salt interval. These short-wavelength bedding cycles result in a significant amount of tuning and sub-wavelength interference (Knapp, 1990).

Dissolution voids migrating toward the ground surface through progressive roof rock failures represent potential targets for high-resolution reflection surveys. Perturbations in the uniform propagation of seismic energy through this disturbed overburden can range from mild to severe (Miller et al., 1985; Lambrecht and Miller, 2006). Voids formed in overburden rock from bridging during the upward migration of a collapse structure represent areas at greater risk of delayed and accelerated collapse. Microscale seismic model studies have shown with extremely small wavelength energy, voids in a homogeneous earth are interpretable from disturbances in the wavefield (Banks et al., 2006). However, in real world settings geologic noise, heterogeneity of the earth, and the irregularity of void geometries make identifying and separating void signatures from noise nearly impossible, even on high-fidelity borehole seismic data (Rechtien et al., 1995).

In some settings amplitude anomalies can be suggestive of large voids associated with shallow mine cavities (Cook, 1965). It is highly unlikely the upward movement of a salt dissolution void is truly analogous to a mine void; it more likely resembles a rubble zone with elongated geometries and lack of any uniformity. Rubble zones remaining from underground nuclear explosions have been shown through model studies to be potentially indirectly

detectable on portions of the seismic wavefield. However, in a real earth setting where an abundance of geologic noise is routine, subterranean blast zones are clearly undetectable (Larsen and Harris, 1993). It seems unreasonable but not impossible to delineate undercompacted zones or bridged rubble/void volumes within a subsidence structure on high-resolution seismic-reflection sections considering the three-dimensional complexity, relatively small affected volume, and the unlimited number of scatter points, rubble zones, and dipping bed fragments within a collapse volume.

Geophysical data (logs and seismic sections) provide distinctly different seismic character for the salt section from site to site (Figures 2-10, 2-11, 2-12). This variability is directly linked to regional inconsistencies in interbedded insoluble layers within the salt as observed and well documented in core samples/logs and mine inspection (Dellwig, 1971; Walters, 1978; Watney et al., 1988). The observed variability in the reflection signature within the salt interval is geologic in nature and not related to changes in the seismic source signature in response to coupling, energy transmission, or source configuration. Confidently interpreting reflection events as deformed or dissolved salt requires correlation and contrast with reflections from local areas known or at least suspected to be undisturbed. Salt signatures on synthetic and real zero-offset seismic-reflection sections are quite variable from intact salt intervals at different locations around the salt deposit. Seismic investigations at sites with minimal or no deformation of overburden but obvious distortion in bedding within the salt interval help improve our understanding of salt tectonics in settings where pressure gradients are established and by dissolution.

Strong evidence exists supporting observations that natural dissolution (paleo and current) within localized zones along the shale/salt contact at the top of the Hutchinson Salt Member is detectable with seismic-reflection methods (Watney et al., 2003). Changes (amplitude, frequency) in the seismic response at the Hutchinson Salt Member/upper Wellington shale contact would be expected if the acoustic-impedance contrast at that boundary were altered by dissolution. Possible scenarios in this setting include void development along the base of the insoluble caprock, paleovoid development and salt creep or flowage, void development within the salt interval and subsidence of interbedded units near the top of the salt section, dissolution prior to deposition of the upper Wellington shales, or possibly some combination. Clearly changes in reflection character and/or geometry would be diagnostic of significant lateral changes in the material above and/or immediately below the contact. Natural dissolution driven by overburden water sources will likely result in a wide, fairly horizontal zone of leaching (Salzpegel) suggested to be difficult to detect using geophysics (Lohmann, 1972). Seismic-reflection data from near the active dissolution front seem to possess changes in reflection amplitude and arrival time likely characteristic of an isolated leached volume near the top of salt (Figure 2-13).

Changes have been observed in the character (amplitude or phase) and geometry (time) of reflection horizons interpreted to be related to dissolution anomalies (Anderson et al., 1996; Miller, 2003). Conventional seismic data with interpreted salt paleodissolution features at common reservoir depths do not routinely possess changes in reflection wavelet characteristics uniquely attributable to those features (Anderson and Brown, 1991). Disturbed reflections on a single CMP-stacked section located near both the natural dissolution front and an active subsidence area are likely indicative of a leaching remnant (Miller, 2006) (Figure 2-14a). It is not possible to determine uniquely which of the possible scenarios listed in the previous paragraph could have been the cause of this effect. From

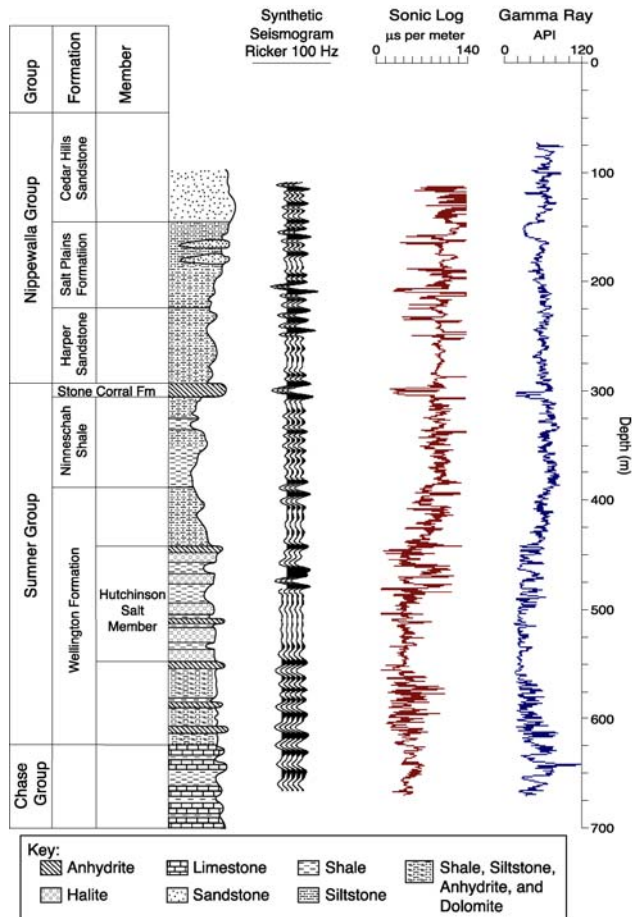


Figure 2-11. Geologic column contrasted with a 100-Hz synthetic, sonic log, and gamma ray log for a well near the Macksville sinkhole, which failed catastrophically as a result of a failed brine-disposal well.

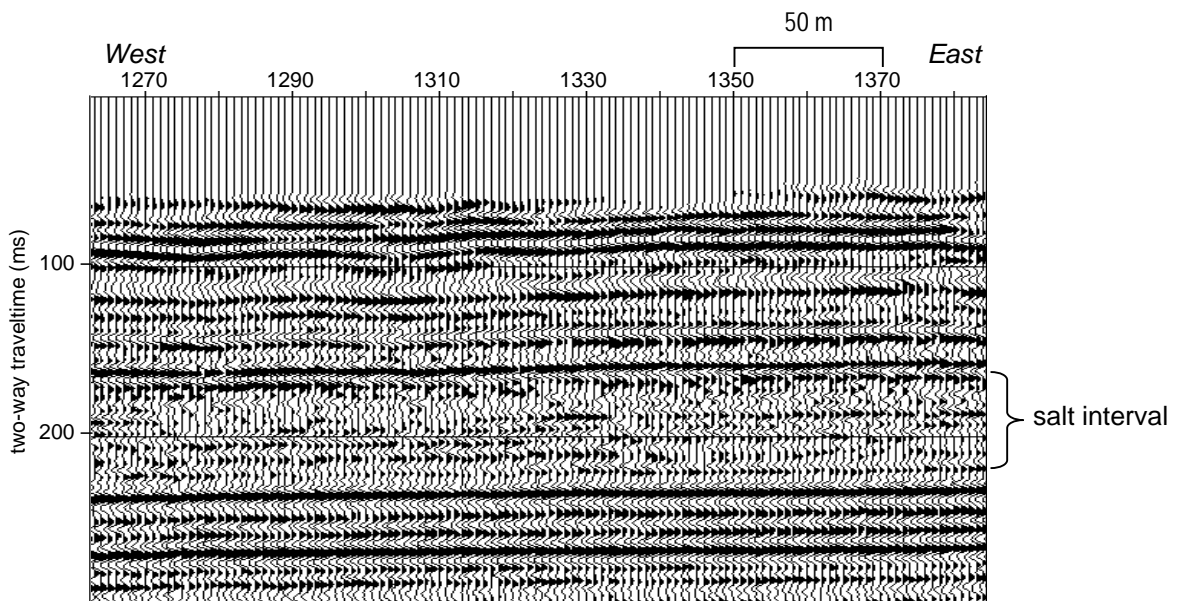


Figure 2-12. Seismic section from more than 30 km west of dissolution front. Reflections from within the salt interval appear discontinuous with features potentially associated with deposition.

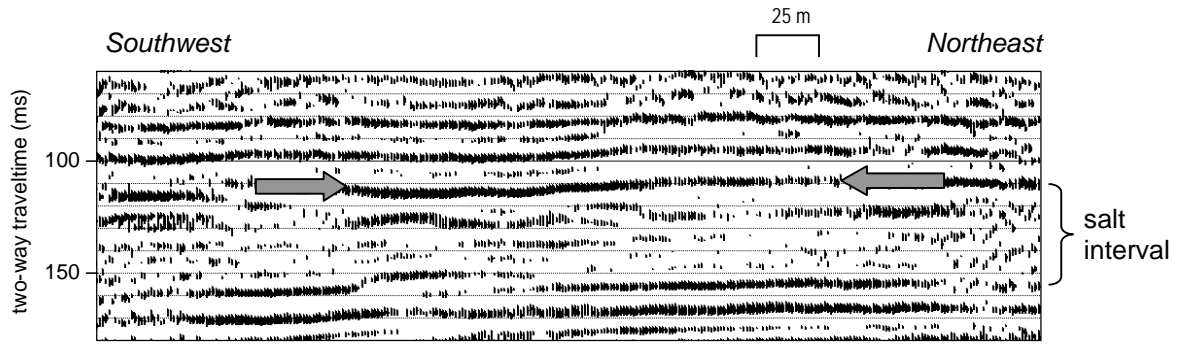


Figure 2-13. Reflection section targeting the top of salt near Inman, Kansas. Increased amplitude and reflection drape above distorted interbedded layers in the salt appear indicative of dissolution and subsidence.

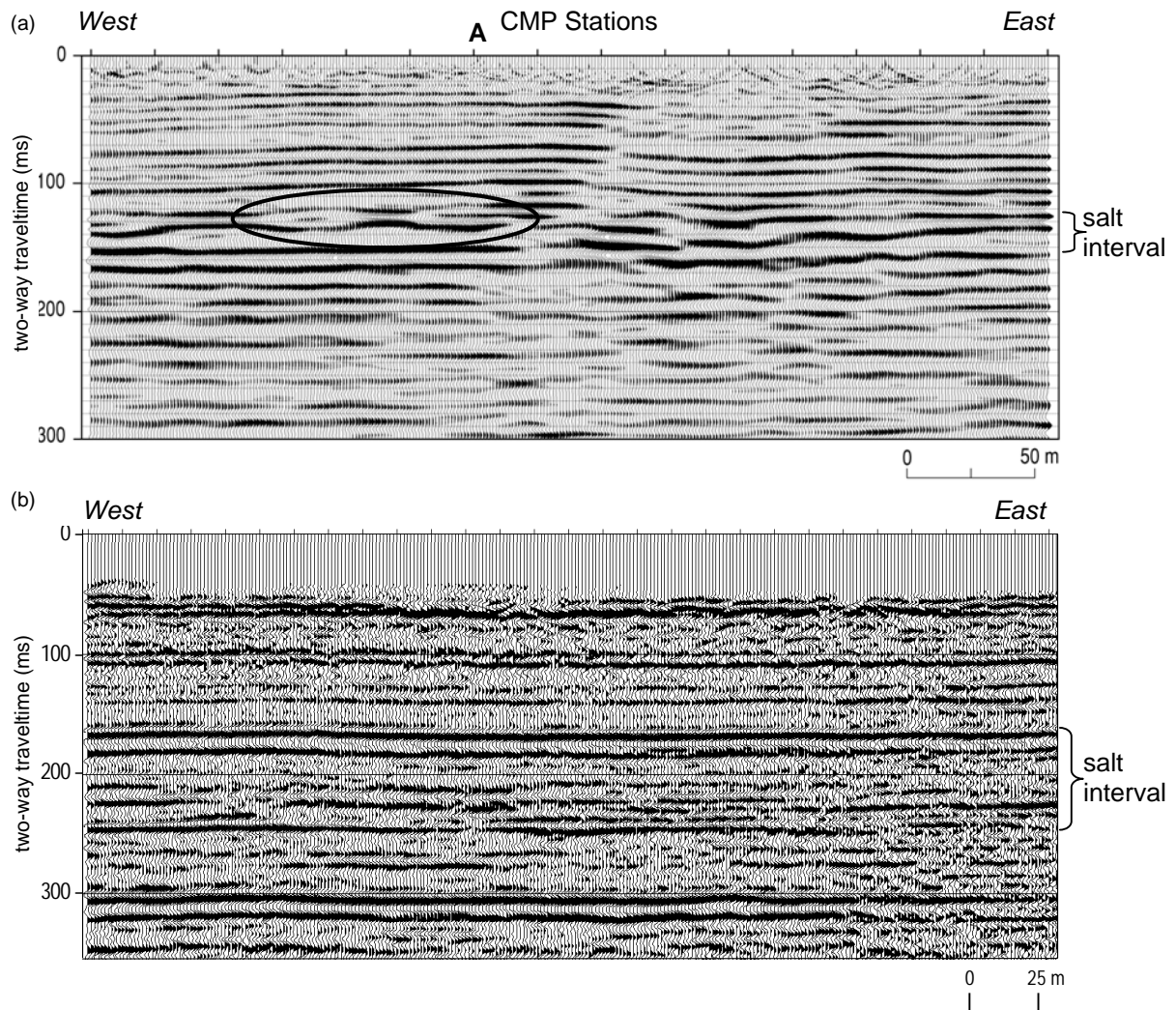


Figure 2-14. Migrated seismic section from area less than 5 km from drill-mapped dissolution front (a) and associated with a paleodissolution feature. Compared to a section 10 km west (b) with very high amplitude and continuous intersalt reflectors. The data in the oval (a) possess character potentially resulting from leaching without collapse or maybe creep.

direct observation it appears undulations in the high-amplitude, lower-frequency reflections from near the top of the salt interval are the dissolution equivalent of cut-and-fill channel features (Figure 2-14a, A). This is a possibility, but based on the decrease in frequency, increase in amplitude, and lack of diffraction or bow-tie distortion in the wavefield (due to the width of the synform relative to reflection wavelength), this apparent undulation is more likely a change in reflection-wavelet phase in response to lithologic changes (possibly a solution zone) directly beneath the shale/salt contact.

Comparing the character of the reflection packet identified as the salt interval near an active dissolution area (Figure 2-14a) with data from a site that appears to have all the original salt in place (Figure 2-14b) leads to the suggestion that complex structures resulting from salt dissolution after deposition of the caprock and unique to the salt interval are detectable on seismic data. Changes in temporal and spatial characteristics of reflection signatures (wavelet attributes) seem to be prevalent on CMP sections within the disturbed section of salt and associated overburden. Seismic wavelets from the disturbed salt interval are much lower frequency and higher amplitude (Figure 2-14a) than those observed in undisturbed salt layers (Figures 2-12 and 2-14b). Considering the reduction in salt thickness and collapse structure just meters away (Figure 2-14a, east of CMP A), distortion within the salt with only minor indications of deformation within the overburden strongly supports an interpretation of possible creep or flowage events driven by the pressure differential inside to outside dissolution voids and accelerated by the fluid present.

Resolution of seismic data is key to discriminating bedding and structures indicative of the different subsidence processes. Horizontal and vertical resolution potential of seismic data is inversely proportional to frequency. Most estimates of resolution potential rely on dominant wavelength, which is inversely proportional to the dominant frequency (Sheriff, 2002). Vertical resolution is routinely estimated using the quarter-wavelength axiom as representing the thinnest separable and smallest detectable distance between beds (Widess, 1973). However, based on an empirical development, it is more realistic to use one-half the dominant wavelength to estimate vertical resolution potential of CMP-stacked seismic-reflection data (Miller et al., 1995). Variations in a reflection wavelet's bandwidth and number of octaves can have little effect on the resolving power of the data, but dramatically affect the interpretability of the reflection section (Knapp, 1990). Horizontal resolution is commonly associated with the Fresnel zone (Sheriff, 2002); however, for broadband data this principle breaks down when the reflector has extremely small lateral extent (Knapp, 1991). In general for high-resolution data, which routinely fight to maintain rich broadband characteristics and with a dominant frequency greater than 80 Hz, horizontal resolution is on the order of $V/2\sqrt{T_0/f}$ or $\sqrt{Vz/2f}$, where V = average velocity, T_0 = vertically incident two-way traveltimes, f = dominant frequency, Vz = velocity at depth z , and z = depth of interest.

Summing Up and To Come

Familiarity with the geologic setting and salt deposition in the context of various observed and possible seismic-reflection wavelet responses was touched on in the previous chapter. Representative seismic images from different subsidence geometries and void/rubble anomalies provide important background for upcoming discussions. From the history of this Permian salt and its susceptibility to both nature and anthropogenic salt dissolution, subsidence features originating within the salt will possess complex structures. Abrupt

changes in seismic characteristics are routinely indicative of these dissolution and collapse structures. Coherent reflections can be strongly influenced by subtle variability of reflectors within the salt interval. The size and complexity of these structures will challenge the fidelity of even high-resolution seismic-reflection data. Sub-wavelength anomalies require interpretations based on changes in seismic-wavelet properties (i.e., reflection amplitude and extreme, yet coherent spatial and temporal changes in frequency and/or phase).

With a solid understanding of the salt and representative samples of seismic responses to undisturbed and disturbed salt, it is prudent to next review the current state of knowledge on salt processes and characteristics as well as salt dissolution and overburden failure mechanisms. In the next chapter discussions will include processes that occur as a result of the extreme properties of salt. Several of these make seismic studies of the salt complicated and sometimes appear more non-unique than would be considered “normal.” An overview of research into salt processes such as stability (creep) and solubility will provide the physical constraints and define a framework for interpreting seismic responses in highly altered portions of the salt interval. As will become obvious, with the high solubility of salt, natural and anthropogenic water sources can leach enough salt in months to instigate overburden failure. This high rate of change makes repeat seismic imaging an ideal tool for capturing the full progression from competent salt to sinkhole all within decades rather than in thousands of centuries, as it is with carbonates.

References

- Anderson, N.L., and R.J. Brown, 1991, A seismic analysis of Black Creek and Wabamun salt collapse features, western Canadian sedimentary basin: *Geophysics*, v. 56, p. 618-627.
- Anderson, N.L. W.L. Watney, P.A. Macfarlane, and R.W. Knapp, 1995, Seismic signature of the Hutchinson salt and associated dissolution features; in N.L. Anderson and D.E. Hedke, eds., *Geophysical atlas of selected oil and gas fields in Kansas*: Kansas Geological Survey Bulletin 237, p. 57-65.
- Anderson, N.L., R.J. Brown, and D.A. Cederwall, 1996, Natural recession of the eastern margin of the Leofnard salt in western Canada: *Geophysics*, v. 61, p. 222-231.
- Anderson, N.L., A. Martinez, J.F. Hopkins, and T.R. Carr, 1998, Salt dissolution and surface subsidence in central Kansas: A seismic investigation of the anthropogenic and natural origin models: *Geophysics*, v. 63, p. 366-378.
- Banks, H.T., N.L. Gibson, and W.P. Winfree, 2006, Pulsed THZ interrogation of SOFI with knit lines in 2D: North Carolina State Univ., Center for Research in Scientific Computation, Technical Report CRSC-TR06-22, 15 p. (www.ncsu.edu/crsc/reports/reports06.htm).
- Bayne, C.K., 1956, *Geology and ground-water resources of Reno County, Kansas*: Kansas Geological Survey Bulletin 120, 130 p.
- Beck, B., 1988, Environmental and engineering effects of sinkholes—The processes behind the problems: *Environmental Geology and Water Sciences*, v. 12, n. 2, p. 71-78.
- Colorado School of Mines, 2005, Workshop on subsalt imaging problems, July, Center for Wave Phenomena.
- Cobb, J., and J. Currens, 2001, Karst: The stealthy hazard: *Geotimes*, v. 46, n. 5, p. 14-17.
- Cook, J.C., 1965, Seismic mapping of underground cavities using reflection amplitudes: *Geophysics*, v. 30, p. 527-538.
- Dellwig, L.F., 1963, Environment and mechanics of deposition of the Permian Hutchinson Salt Member of the Wellington shale: Symposium on Salt, Northern Ohio Geological Society, p. 74-85
- Dellwig, L.F., 1971, Study of salt sequence at proposed site of the national radioactive waste repository at Lyons, Kansas; in Final Report, Geology and hydrology of the proposed Lyons, Kansas radioactive waste repository site: State Geological Survey of Kansas Subcontract No. 3484, p. 85-95.
- Ege, J.R., 1984, Formation of solution-subsidence sinkholes above salt beds: U.S. Geological Survey Circular 897, p. 1-11.
- Ford, D.C., and P.W. Williams, 1989, *Karst Geomorphology and Hydrology*: Unwin Hyman, London, 601 p.
- Frye, J.C., and J.J. Brazil, 1943, Ground water in the oil-field areas of Ellis and Russell counties, Kansas: Kansas Geological Survey Bulletin 50, 104 p.
- Gogel, T., 1981, Discharge of saltwater from permian rocks to major stream-aquifer Systems in Central Kansas: Kansas Geological Survey Chemical Quality Series 9, 60 p.
- Gillespie, J.B., and G.D. Hargadine, 1986, Geohydrology of the Wellington-alluvial aquifer system and evaluation of possible locations for relief wells to decrease saline groundwater discharge to the Smoky Hill and Solomon rivers, central Kansas: U.S. Geological Survey Water Resources Investigations 86-4110, 31 p.
- Holdaway, K.A. 1978, Deposition of evaporites and red beds of the Nippewalla Group, Permian, western Kansas: Kansas Geological Survey Bulletin 215.

- Hovorka, Susan D., 1994, Characterization of bedded salt for storage caverns: Case study from the Midland basin: Bureau of Economic Geology, University of Texas at Austin (<http://www.beg.utexas.edu/enviroqtlty/salt/index.htm>).
- Jackson, J.A., 1997, *Glossary of Geology*, 4th ed.: American Geological Institute, Alexandria, Virginia, 769 p.
- Jewett, J.M., and D.F. Merriam, 1959, Geologic framework of Kansas—A review for geophysicists; in W.W. Hambleton, ed., Symposium on geophysics in Kansas: Kansas Geological Survey Bulletin 137, p. 9-52.
- Johnson, K.S., 1981, Dissolution of salt on the east flank of the Permian basin in the southwestern USA: *Journal of Hydrology*, v. 54, p. 75-93.
- Johnson, K.S., 2003, Evaporite-karst problems in the United States; in K.S. Johnson and J.T. Neal, eds., Evaporite karst and engineering/environmental problems in the United States: Oklahoma Geological Survey Circular 109, p. 1-20.
- King, P.B., 1959, The evolution of North America: Princeton University, p. 1-190.
- Knapp, R.W., 1990, Vertical resolution of thick beds, thin beds, and thin-bed cyclothems: *Geophysics*, v. 55, p. 1183-1190.
- Knapp, R.W., 1991, Fresnel zones in the light of broadband data: *Geophysics*, v. 56, p. 354-359.
- Kulstad, R.O., 1959, Thickness and salt percentage of the Hutchinson salt; in, Symposium on Geophysics in Kansas: Kansas Geological Survey, Bulletin 137, p. 241-247.
- Lambrecht, J.L., and R.D. Miller, 2006, Catastrophic sinkhole formation in Kansas: A case: *The Leading Edge*, v. 25, n. 3, p. 342-347.
- Larsen, S., and D. Harris, 1993, Seismic wave propagation through a low-velocity nuclear rubble zone: Lawrence Livermore National Laboratory, Report UCRL-ID-115729.
- Lohmann, H.H., 1972, Salt dissolution in subsurface of British North Sea as interpreted from seismograms: *AAPG Bulletin*, v. 56, p. 472-479.
- McGuire, D., and B. Miller, 1989, The utility of single-point seismic data; D.W. Steeples, ed., Geophysics in Kansas: Kansas Geological Survey Bulletin 226, p. 1-8.
- Merriam, D.F., 1963, The Geologic History of Kansas: Kansas Geological Survey Bulletin 162, 317 p.
- Merriam, D.F., and C.J. Mann, 1957, Sinkholes and related geologic features in Kansas: *Transactions of the Kansas Academy of Science*, v. 60, n. 3.
- Miller, R.D., 2003, High-resolution seismic-reflection investigation of a subsidence feature on U.S. Highway 50 near Hutchinson, Kansas; in K.S. Johnson and J.T. Neal, eds., Evaporite karst and engineering/environmental problems in the United States: Oklahoma Geological Survey Circular 109, p. 157-167.
- Miller, R.D., 2006, High-resolution seismic reflection to identify areas with subsidence potential beneath U.S. 50 Highway in eastern Reno County, Kansas [ext. abs.]: Symposium on the Application of Geophysics to Engineering and Environmental Problems (selected as a Best Paper). Presented at Near Surface 2006, Helsinki, Finland, Sept. 4-6, 5 p. (published on CD).
- Miller, R.D., D.W. Steeples, and J.A. Treadway, 1985, Seismic reflection survey of a sinkhole in Ellsworth County, Kansas [exp. abs.]: Society of Exploration Geophysicists, p. 154-156.

- Miller, R.D., N.L. Anderson, H.R. Feldman, and E.K. Franseen, 1995, Vertical resolution of a seismic survey in stratigraphic sequences less than 100 m deep in southeastern Kansas: *Geophysics*, v. 60, p. 423-430.
- Rechtien, R.D., R.J. Greenfield, and R.F. Ballard, Jr., 1995, Tunnel signature prediction for a cross-borehole seismic survey: *Geophysics*, v. 60, p. 76-86.
- Sheriff, R.E., 2002, *Encyclopedic Dictionary of Applied Geophysics*, 4th ed.: Oklahoma Society of Exploration Geophysicists, Tulsa, 429 p.
- Snyder, F.G., 1968, Tectonic history of midcontinental United States: *University of Missouri–Rolla Journal*, n. 1, p. 65-77.
- Spinazola, J.M., J.B. Gillespie, and R.J. Hart, 1985, Ground-water flow and solute transport in the Equus beds area, south-central Kansas, 1940-1979: U.S. Geological Survey, Water-Resources Investigations Report 85-4336, 68 p.
- Steeple, D.W., R.D. Miller, and R.A. Black, 1990, Static corrections from shallow-reflection surveys: *Geophysics*, v. 55, p. 769-775.
- Swineford, A., 1955, Petrography of upper Permian rocks in south-central Kansas: State Geological Survey of Kansas Bulletin 111, 179 p.
- Waltham, T., F. Bell, and M. Culshaw, 2005, *Sinkholes and Subsidence: Karst and Cavernous Rocks in Engineering and Construction*: Praxis Publishing Ltd., Chichester, UK, 382 p.
- Walters, R.F., 1978, Land subsidence in central Kansas related to salt dissolution: Kansas Geological Survey Bulletin 214, 82 p.
- Watney, W.L., 2007, work in progress.
- Watney, W.L., and S.E. Paul, 1980, Maps and cross sections of the Lower Permian Hutchinson salt in Kansas: Kansas Geological Survey Open-file Report 80-7, 10 p., 6 plates, map scales 1:500,000.
- Watney, W.L., J.A. Berg, and S. Paul, 1988, Origin and distribution of the Hutchinson salt (lower Leonardian) in Kansas: Midcontinent SEPM Special Publication No. 1, p. 113-135.
- Watney, W.L., S.E. Nissen, S. Bhattacharya, and D. Young, 2003, Evaluation of the role of evaporite karst in the Hutchinson, Kansas, gas explosions, January 17 and 18, 2001; in K.S. Johnson and J.T. Neal, eds., *Evaporite karst and engineering/environmental problems in the United States*: Oklahoma Geological Survey Circular 109, p. 119-147.
- Whittemore, D.O., 1989, Geochemical characterization of saltwater contamination in the Macksville sink and adjacent aquifer: Kansas Geological Survey Open-file Report 89-35.
- Whittemore, D.O., 1990, Geochemical identification of saltwater contamination at the Siefkes subsidence site: Report for the Kansas Corporation Commission.
- Widess, M.B., 1973, How thin is a thin bed?: *Geophysics*, v. 38, p. 1176-1180.
- Zeller, D.E., ed., 1968, The stratigraphic succession in Kansas: Kansas Geological Survey Bulletin 189, 81 p.

CHAPTER 3

SALT CHARACTERISTICS

Conceptual, empirically based models developed from seismic-reflection data will be general in nature as a direct consequence of the variety of viable seismic interpretations that are consistent with both the geophysics and geology at any given site. Unfortunately, the nonuniqueness of seismic-reflection data is both inherent to geophysical data and a consequence of the complex nature of dissolution and associated subsidence features. Leaching or creep interpreted on seismic-reflection sections must be consistent with all current thinking on salt behavior, especially as it relates to physical constraints on each dynamic process. This chapter focuses on the characteristics of salt and processes effecting post-depositional changes in the salt layer.

To formulate a general understanding of the various dissolution frameworks and to secure a broader awareness of the processes, this chapter starts with a basic introduction to karst—emphasizing evaporites—and concludes by establishing key relationships between and unique to different leaching processes. Initial discussions in this chapter explore basic salt properties, focusing on the aspects that influence leaching to the point of overburden destabilization. This chapter also provides a brief review of salt stability under load, a key concept and backdrop to some of the unique discoveries that will be unveiled in later chapters.

The significance of and potential for differential pressure to act as a catalyst for instigating and sustaining salt flow in a fluid-rich environment and at shallow depths will be revealed in this chapter. That discussion will provide the technical basis for suggesting that creep is interpretable at shallow depths on seismic sections and progresses at relatively high rates of speed, a concept rarely discussed and not considered likely in classic manuscripts on salt tectonics. By using *a priori* information, it will be shown that distinguishing creep from dissolution within the salt interval is possible on seismic-reflection data prior to any evidence of overburden failure.

With the early portions of this chapter highlighting salt properties and tectonics or stability, it is logical that latter portions of this chapter include a description of the many possible sequences of events and processes that can influence dissolution. A variety of factors that strongly influence the sequence of events between initiation of leaching and void development of sufficient dimensions for collapse to occur will be discussed. An assortment of fluid catalysts—from meteoric waters channeled by fracture/fault systems to ruptured casing in brine disposal wells—will be elaborated on and the unique aspects of each developed. With the extreme solubility of salt, it is no surprise that the hydrology of a site and/or source and access of fluid to the salt both uniquely and strongly influence both rate of development and extent of affected volume.

Karst

Karst is defined as a terrain with special landforms and drainage characteristics due to a greater than usual solubility of certain rocks in natural waters

(<http://wasg.iinet.net.au/terminol.html>). It is also characterized as landscapes that can be distinguished by their underground drainage; these landforms evolve in response to rainfall and surface water flowing into the ground (Waltham et al., 2005). The term karst is derived from a geographical name in Slovenia (Kar). *Karst terrains* are topography formed chiefly from the dissolution of rock. These terrains are generally underlain by limestone or dolomite, but evaporites such as rock salt or gypsum also are susceptible to karstification and classified as karst in some settings.

Sinkholes, sinking streams, closed depressions, subterranean drainage, and caves are generally synonymous with karst topography (Monroe, 1970). The term “terrain” implies that only the surface is considered, whereas “terrane” includes the surface and subsurface (caves or aquifer) as a single system. More commonly subsurface features associated or resulting from dissolution are considered karst, and therefore karst terrane more accurately represents most settings.

Hydrogeologists define *karst* as a type of terrain, usually associated with carbonate rocks (limestone and dolomite) where ground water has solutionally enlarged openings to form a subsurface drainage system (<http://caveandkarst.wku.edu/>). “Solutionally enlarged openings” is non-size specific and covers a wide range from pore- to cave-size solution features. *Karst aquifers* are those that contain dissolution conduits permitting rapid transport of ground water, often in turbulent flow (White, 1999).

A *karst system*, as commonly characterized by the hydrologic community, relates to the overall hydrology of a soluble rock mass. It is defined as *an integrated mass-transfer system in soluble rocks with a permeability structure that is dominated by conduits dissolved from the rock and organized to facilitate the circulation of fluid in a downgradient direction* (<http://www.ncl.ac.uk/roses/objective1a.html>). Topographic considerations or specific types of patterns (flow or rock voids) are not necessary for a rock mass to be characterized as a karst system. Karst systems are related to fluid transport and interaction with soluble rocks.

Karst systems can be categorized according to attributes affecting ground-water flow and the development of solution features. Hydrogeologic properties diagnostic of karst systems include flow regime, recharge mode and recharge/discharge configurations, ground-water chemistry, and degree of inheritance from earlier conditions. Evolution of karst or a karst sequence can sometimes be linked to and/or identified by relationships with insoluble cover beds. These associations permit identification of factors controlling the origin of particular karst features, including subsidence and its mechanisms.

Types of karst systems significant to this study include:

Open karst, which evolve solely while the soluble rock is exposed at the surface, with limited or no previous dissolution.

Intrastratal karst is developed in rocks covered by younger strata with karstification later than deposition of overburden. Intrastratal karst has several possible stages, including:

deep-seated karst has no evidence at the surface, with no exposure of soluble rock;

subjacent karst occurs when soluble rocks are locally invaded across a small percentage of their thickness and karst features can be observed at the ground surface;

entrenched karst occurs where an entire thickness of soluble rock is exposed along valleys or outcrops but the insoluble cap remains intact; and

denuded karst is where the caprocks are removed and soluble rock is exposed that once was buried beneath younger overburden.

Natural dissolution of rock is most commonly observed as karst in carbonate rocks (e.g., Beck, 1984, 1988; Beck et al., 1999). Worldwide study of karst features resulting from the dissolution of carbonates has been extensive (e.g., Ford and Williams, 1989; White, 1988; Palmer, 1991; Scoffin, 1987). Dissolution of carbonates is relatively slow with passage expansion developing at 0.01 to 0.1 cm/yr (Palmer, 1991). Threats to humans or the environment from the development of new or acceleration of active carbonate dissolution is minimal. With solubility of carbonates around 17 ppm, measurable acceleration of the dissolution process through human interaction is nearly impossible. In the case of dams and other hydraulic structures, changes in the hydrology only change breakthrough of short pathlength structures by a few percent over periods exceeding 100 years (Dreybrodt, 1992, 1996) (Figure 3-1). However, anthropogenic activities in overburden can accelerate and even instigate the formation or growth of sinkholes associated with voids left after the historic dissolution of carbonates (Strum, 1999).

Evaporite karst is less commonly observed and usually results from the dissolution of gypsum ($\text{CaSO}_4 \cdot 2\text{H}_2\text{O}$) or salt (NaCl) (Martinez et al., 1998). Gypsum is 150 times and salt is 7500 times more soluble than carbonates; therefore, subsurface dissolution channels and subsidence features can form in a matter of days in some evaporite settings where features of equivalent size and geometry in carbonates might take millennia (Johnson, 2003). Growth of dissolution features in carbonates progresses at rates of no more than a few millimeters per 100 years (Dreybrodt et al., 2002), while gypsum voids grow at rates around 1 m per 100 years and faster yet are salt-dissolution features, which under similar natural hydrologic conditions can grow at rates approaching 50 to 100 m per 100 years. With dissolution rates this high, voids in evaporite rocks can easily be leached out by unsaturated brine solution



Figure 3-1. Sinkhole in dam formed from piping of dam fill through karst features in bedrock. Backhoe digging out sinkhole in Clearwater Dam, Missouri, USA, to follow throat that was significantly deeper than machine can dig (photo by S. Hartung).

introduced through natural (Gustavson et al., 1980, 1982; Johnson, 1989; Eck and Redfield, 1965) or anthropogenic sources (Walters, 1978, 1991; Dunrud and Nevins, 1981; Ege, 1984) in human time frames.

Like sinkholes in carbonate rocks, evaporite sinkholes can form as a result of either purely natural processes or from human activities. Some have suggested there is no real difference between carbonate and salt karstification processes (Priesnitz, 1969). However, a long and distinguished list of investigators disagree based predominantly on the fact that carbonate dissolution advances in a linear pattern along fissures or softer parts of the formation, whereas leaching salt is more of a frontal attack (Lohmann, 1972). Rock salt dissolves so rapidly, it has its own suite of landforms and conditions (Waltham, 1989) not applicable to carbonate karst (Waltham and Fookes, 2003). Salt-dissolution sinkholes have been observed above most evaporite basins or provinces throughout the world (Gale, 2003). Unlike in carbonates, evaporite sinkholes are rarely dependent on the strength of the evaporite or form due to the “piping” of unconsolidated surface sediments directly into dissolution voids. Strength and hydrology of the overburden is key to evaporite dissolution and associated subsidence progress and processes. Using a strict interpretation of karst, many evaporite subsidence features would not qualify as karst.

Salt

Salt has been classified as both a visco-plastic (Bachu and Rothernburg, 2003) and visco-elastic (Gangi, 1981, 1983) substance with a density generally reported at between 2.1 and 2.6 gm/cm³ (average is 2.2) (Carmichael, 1989) (Figure 3-2). The compressional-wave velocity range for salt is wide but averages from around 3 to 4 km/sec (Carmichael, 1989). Salt has the highest solubility of common rocks at 125,000 ppm and is readily soluble in water (35% by weight; Johnson, 2003) and insoluble or only slightly soluble in most other liquids. It is relatively soft with a low compressibility. Rock or mineral salt is usually less pure and found in large deposits, notably in New York, Michigan, Ohio, Kansas, Texas, and Louisiana, and also in Great Britain, France, Germany, Russia, China, and India.

Rock salt under a large depositional load is almost incompressible, highly ductile, and easily deformed by creep (Baar, 1977). Plastic deformation of the salt associated with glide creep is expected to occur naturally in the presence of large pressure differentials, such as could be the case in close proximity to a void (Miller, 2003; Anderson et al., 1995). In some settings it is impossible to distinguish dissolution from creep when both are active at the same time

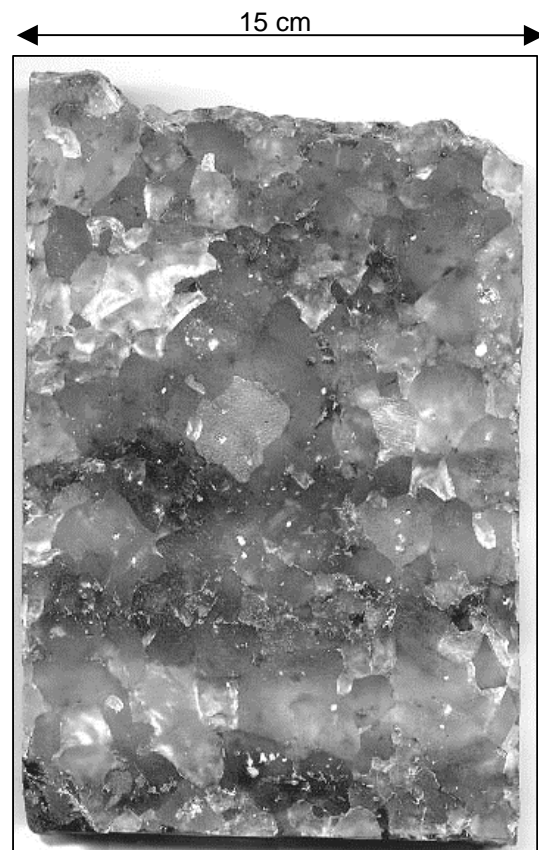


Figure 3-2. Salt crystal from core of Hutchinson Salt Member in Reno County, Kansas, with dark stratification identified as shales (<http://www.kgs.ku.edu/Hydro/Hutch/RockPhotos/index.html>).

(Trusheim, 1960). Thin anhydrite beds within a halite succession will have a strong acoustic contrast and are therefore very seismically distinguishable. These beds provide a relative geometric measure of mechanical deformation within the salt interval. Considering the extreme range of possible strain rates salt can experience during creep deformation, these thin interbeds can experience quite dramatic high-amplitude short-wavelength flexure (undulations) within relatively short horizontal distances.

Due to salt's high solubility and rapid dissolution rates when exposed to freshwater, it only survives at the ground surface in arid environments and in the subsurface where it is protected from unsaturated ground water by insoluble rock layers (Waltham et al., 2005). Salt has very low permeability and therefore saturated brine or non-water-based fluids can be stored in salt voids with little or no potential for migration outside the void walls. Salt voids are commonly used for seasonal storage of a variety of petroleum products (Neal, 2003).

Salt Stability

Salt is incompressible, yet under load it can be extremely mobile, to the point of possessing characteristics of viscous flow. Salt tectonics in sedimentary basins is a global phenomenon with unique mechanics for each individual basin (Jackson and Talbot, 1991). Differential loading drives salt deformation and can impact the evolution of any sedimentary basin where salt is present (Gemmer et al., 2004). Evaporite deposits in general are weak and mobilize and deform much more readily than other sedimentary rocks and are therefore more susceptible to the formation of complex structures. Salt tectonics has drawn a lot of attention over the last four decades as a direct consequence of petroleum exploration (Alsop et al., 1996) and searches for self-sealing, fluid-free long-term nuclear repositories (Munson and Dawson, 1982).

Stress differentials associated with voids in salt provide an ideal setting for the mobilization of pillars and walls in the form of creep. Creep rates and flow characteristics of salt are highly responsive to differential loading (Munson and Dawson, 1982). The characteristics, type, and stage of salt creep are based on a non-linear relationship between vertical axial stress, confining pressure, temperature, and grain size (Le Comte, 1965). Increasing temperature or stress increases creep rate while increasing confining pressure or grain size decreases creep rate. For decades creep and associated distortion of pillars in underground salt mines have been observed and classified as a stability concern.

Stress and temperature conditions strongly influence creep rate and therefore are key to strain predictability. Traditionally, creep is thought to transition through three unique stages (transient, steady state, and tertiary) in response to changes in stress and/or temperature (Munson et al., 1995). These stages can be represented as a function of time versus strain based on a mechanical, non-linear model (Figure 3-3). Different modes of deformation can be distinguished using an extremely complex relationship of temperature versus stress with only a minor dependence on confining pressure and grain size (Munson, 1979).

Under most geologic conditions, dislocation (Wawersik and Zeuch, 1986) and diffusional (Spiers et al., 1990) creep are the prevailing mechanisms to describe salt tectonics (van Keken et al., 1993). Macroscopic scale predictability of creep based on physical models behaving as anticipated from numerical simulations is considered quite good; however, localized and microscopic scale behavior is clearly not fully explained by numerical simulations (Munson and Dawson, 1982).

Differential pressure drives salt evacuation and can lead to overburden instability (van Keken et al., 1993). A rock sequence experiencing differential loading above a salt layer is stable over a range of overburden rock strengths. However, for overburden with strength below a particular threshold, failure will result as a consequence of both insufficient rock strength and the viscous shear forces acting at the base of the overburden (Lehner, 2000).

Depending on overburden characteristics, viscous flow and deformation of the salt can be driven by pressure gradients or gravitational instability (Last, 1988; Vendeville and Jackson, 1992a, 1992b; Poliakov et al., 1993; Jackson and Vendeville, 1994; Kaus and Podladchikov, 2001). Regardless of the deformation mechanism, low-density salt is buoyant beneath denser overburden sediments, as is demonstrated with the development of salt diapirs (Dijk and Berkowitz, 2000).

Axial stress on salt at depth will, of course, vary with overburden load, which is predominantly controlled by deposition and erosion cycles. For bedded salt, confining pressures will be reasonably consistent as long as the salt remains undisturbed. However, with the development of voids comes dramatic decreases in confining pressure and therefore extreme pressure gradients, leading to increased creep rates as a function of void size and geometry. Considering that creep rates have the greatest dependence on axial stress, depositional loading is the dominant driving force to mobilize salt in the presence of a dissolution void. With void development comes creep and the associated distortion of interbedded non-viscous rocks (shales, anhydrites, etc.) and eventually vertical closure in response to overburden loading.

When dissolution forms subfailure-size voids in salt, solution-transfer creep can occur under confining pressure at low strain rates and deviatoric stress (Jackson and Talbot, 1991). These subcritical-size voids provide an environment conducive to differential pressure-instigated creep. Under these conditions, interbedded layers within the salt interval would undergo distortion while overburden remained undisturbed as has been interpreted on seismic data. Once fluids gain access to the salt, mobilization (e.g., through solution-precipitation) via creep becomes a low-temperature, low-pressure drive system (Urai et al., 1986). From interpretations of seismic data, paleodissolution of salt is clearly a discontinuous process, leaving residual brine in dissolution voids, making solution creep a viable flow mechanism at relatively shallow burial depths and therefore low axial stress.

Extreme bed geometry resembling tight folding evident within the salt interval and uniform salt thinning with no associated short wavelength overburden subsidence interpreted on seismic sections have been suggested to represent creep structures (Figure 3-4) (Miller, 2003). Confident differentiation of creep from dissolution is extremely difficult (Trusheim,

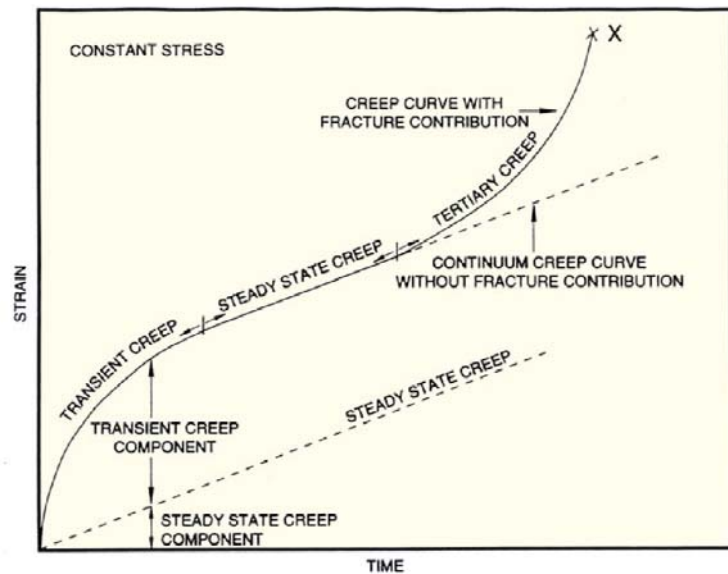


Figure 3-3. Classical creep-deformation behavior of salt (Munson et al., 1995).

1960), especially when both are active coincidentally. Bedded Permian salt in east-central Kansas near the natural dissolution front experienced more than 300 m of burial during the late Cretaceous and around 175 m of subsequent erosion during the Cenozoic. Currently the salt is around 125 m below ground surface in proximity to the dissolution front. Based on changing burial depths since the Permian, creep rates could have varied by an order of magnitude in the last 250 million years.

Paleofolding has been interpreted on seismic data within and unique to the salt interval and near the natural dissolution front. In places

where deformation in the salt bed is present yet no evidence of distortion exists in overburden or basal rock layers, this folding is suggested to result from distinct episodes of dissolution separated by periods of creep. This observation is consistent with the suggestion that leaching along the “active” portion of the natural dissolution front has been intermittent since deposition (Watney et al., 1988). Glide creep in response to differential pressure across a competent salt/void boundary is one possible explanation for the apparent isolation of these paleostructures within the salt interval.

Natural leaching clearly has not been a continuous process along the natural dissolution front in eastern Kansas. Considering the estimated minimal creep rates coupled with extreme geometries and complex interfingering of different interbedded layers within the salt, dissolution activities appear to be better characterized as consisting of intermittent periods with very irregular fluid-exchange rates and locations. Hence, the estimated half-centimeter per year westward migration of the entire dissolution front (Walters, 1978) is clearly a regional average with local movement sporadic and progressing across a wide range of rates. Regional flow of these Permian salts is not likely considering their position and depth of burial within the stable continental setting (Gera, 1972).

For salt-dissolution-induced sinkholes neither stress nor strain in the salt is a significant factor influencing actual sinkhole development, whereas how stress distributes itself in the overburden and the character and magnitude of strain is highly significant to the eventual characteristics of the affected ground surface. Therefore, concerns for salt tectonics are minimal for determining, diagnosing, or describing failure mechanisms associated with sinkhole development. However, salt tectonics and deformation of the salt and less-soluble interbedded layers within the salt are important as they relate to void development: specifically size and rate and long-term stability of dormant voids (no active dissolution-based growth). The predominant aspect of salt tectonics that appears directly interpretable on seismic sections is related to glide creep.

Salt-dissolution Factors

The depositional setting, hydrologic characteristics, and access by unsaturated fluids to the salt are principal factors controlling dissolution of rock salt. As previously noted, thick-bedded salt units are only intact around the world where insoluble and regionally impermeable overburden has provided a barrier to protect the highly soluble salt from

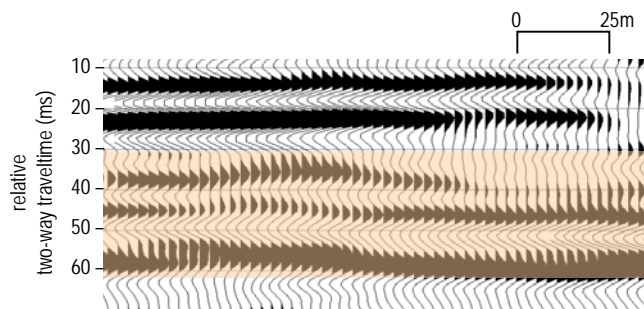


Figure 3-4. CMP stack of salt interval with synform-bedding geometry within the salt (shaded), likely the result of dissolution and glide creep. Trace spacing is 2.5 m with timing lines on 10-ms increments.

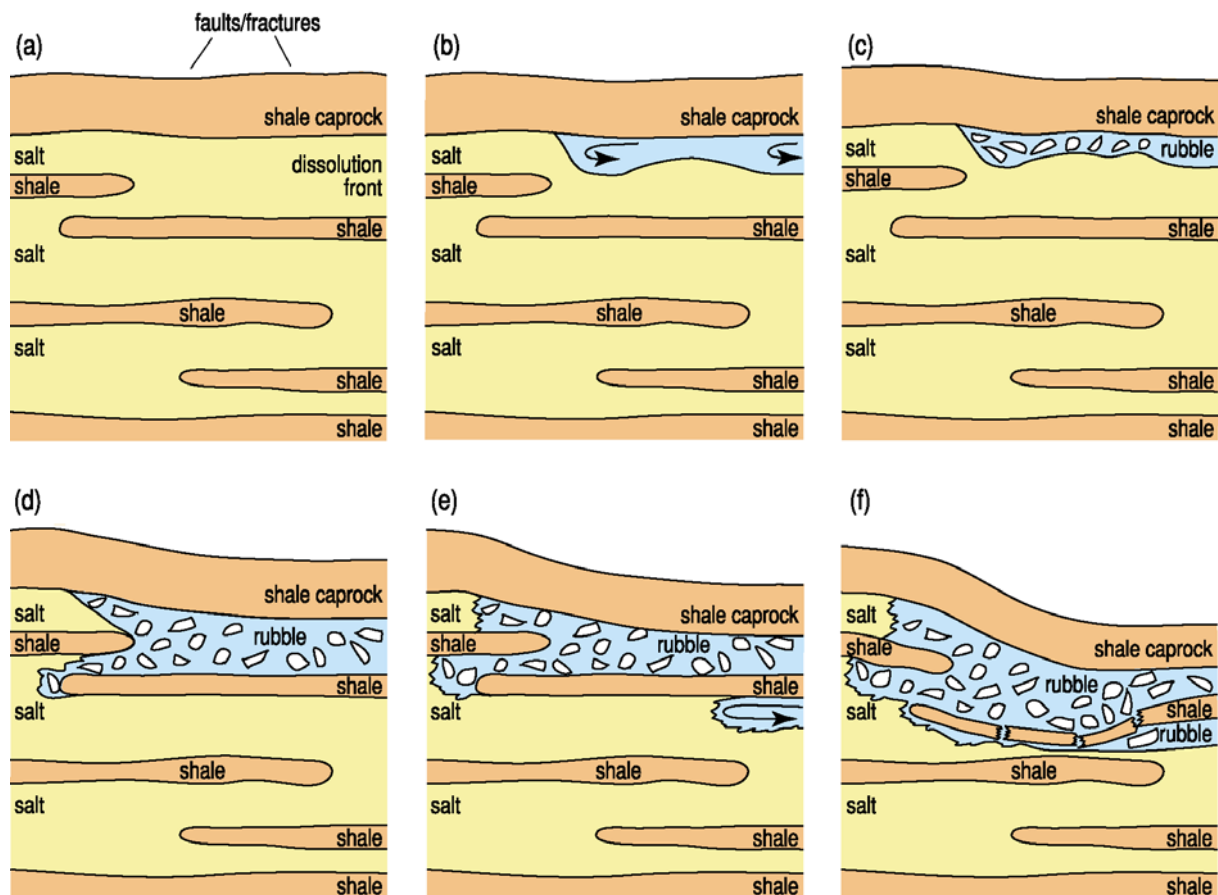


Figure 3-5. Cartoon of possible natural dissolution front progression with fluid moving through the salt interval around rubble zones with collapse of interbedded insoluble layers propagated upwards into overburden.

freshwaters or in highly arid climates (Johnson, 2003). Once fresh to unsaturated brine waters contact bedded salt or a salt diapir, the leaching process can proceed rapidly relative to dissolution rates in other soluble rocks and most geologic processes in general. Dissolution features are dominant structures in any basin where bedded salt has not mobilized to form diapirs (Ge and Jackson, 1998). The dissolution process is strongly influenced by the density of brine at the dissolution front (salt saturation), characteristics of water flow within the salt interval, and barriers to the exchange of saturated with unsaturated brine.

Kinematics of salt dissolution in natural settings are poorly understood. Flow characteristics of water around and within the bedded salt interval are the principal drive for and influence on dissolution and void development. The most active dissolution of salt occurs nearest the freshwater inlet or source where mixing with brackish fluids is minimal. Fresher waters in natural pressure settings will migrate from the inlet to the shallowest part of the water column displacing the denser, more salt-laden fluids, which tend to sink to the bottom of the water column. This density-drive system effectively accelerates leaching near the top of the dissolution volume. Similar preferential zones of leaching are evident in diapirs where most active dissolution is near the top, decreasing down the flanks (Ge and Jackson, 1998).

With the abundance of locally continuous but regionally discontinuous insoluble beds within the Hutchinson Salt Member in Kansas (Walters, 1978), vertical growth of a dissolution volume within the salt will be constrained and guided by these interbedded, insoluble confining surfaces (Figure 3-5). From initial dissolution near the water inlet until

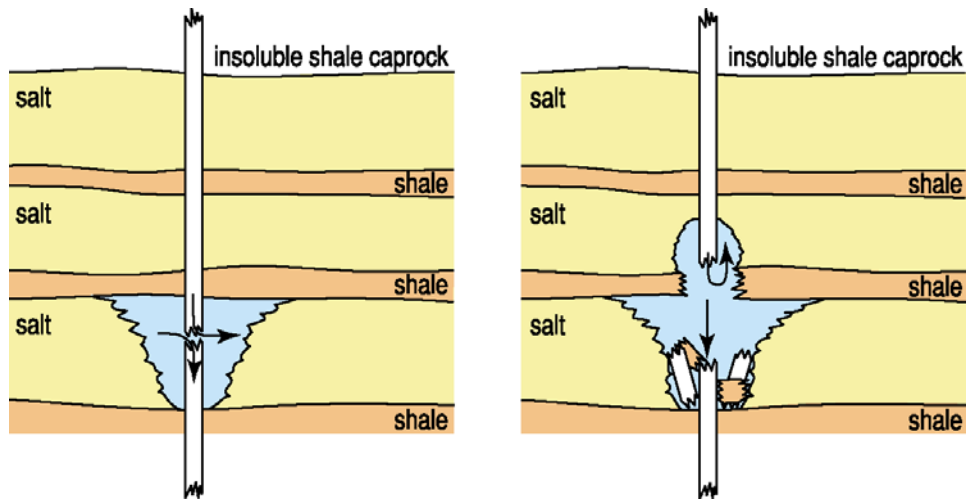


Figure 3-6. Failure of casing within intermediate salt interval, preferentially removing salt along the insoluble interbedded shale/anhydrite.

vertical growth of a void results in contact with an insoluble layer, the geometry of the cavern is controlled by the differential gravity of the fluids, the location of inlet and drain, and velocity and volume of fluids moving through the inlet and drain. The pattern of void growth can be very complex and progress at irregular rates throughout the growth cycle.

Even after the void reaches the base of the caprock or an insoluble layer within the salt, the rate of salt leaching continues highest near the top of the water column where fluid saturation is least. Once contact is made with an insoluble layer, the dissolution front will spread most rapidly in the direction of greatest fluid velocity and therefore highest fluid-exchange rate. This spreading geometry will be strongly influenced by interbed unconformities, structural or stratigraphic ridges or highs, location of drain relative to inlet, faulting or fracturing, and/or continuity of the insoluble roof barrier. Uncontrolled spreading of the dissolution front can remove large volumes of salt immediately below insoluble barriers, thereby exposing expansive segments of unsupported roof rock (Figure 3-6). In natural settings, these rooms generally possess a large real footprint but very limited vertical extent or volume. After failure of the undersupported span of insoluble roof rock, the most active dissolution zones will continue moving preferentially upward.

With the greater density of brine relative to water, active dissolution zones in salt will tend to migrate upward or outward along the base of an insoluble upper confining layer. Voids originating near the top of the salt will generally manifest themselves as relatively thinner, more lenticular features with a larger surface area relative to volume in comparison to voids originating deeper in the salt interval (Figure 3-5). Voids originating deeper in the salt interval will preferentially grow upward, elongating vertically until an insoluble interbed arrests growth. This process is clearly evident in salt jugs that have experienced overmining enlarging the top of the jug to form a morning-glory¹ geometry (Figure 3-7) (Landes and Piper, 1972).

When caprock fails, vertical growth continues progressively upward layer by layer through the overburden as stress exceeds the strength in each successive unsupported span of new roof rock. Maximum potential strain is limited by the void height. As will be discussed in more detail in later chapters, void space available within the salt interval to accommodate

¹A morning glory is a twining plant with funnel-shaped flowers.

roof collapse material is the key characteristic determining whether void movement through the entire overburden rock column proceeds as a rapid continuous process or it progresses as intermittent segments. However, groundwater flow patterns will be altered within the salt interval and affected by overburden lag with each subsequent subsidence event, effectively changing the dynamics of salt harvesting.

Collapse of roof rock instigated by the growth of active dissolution voids will change the hydrologic properties of the system and therefore the leaching rate and location within the salt. Changes in the leaching rate can range from a complete halt to a minor alteration in fluid-flow patterns, thereby directly affecting the dissolution activity along the front. Dramatic changes in fluid-flow characteristics, especially as a result of blockages or restrictions at the inlet and/or drain from collapsed roof rock, are the most likely scenarios responsible for halting the dissolution process at a specific location.

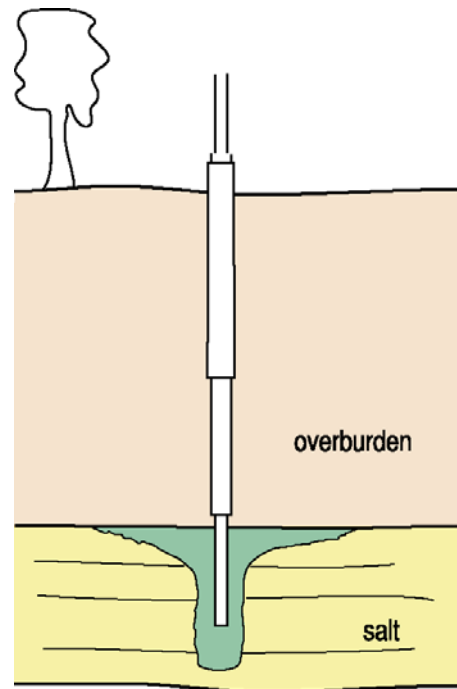


Figure 3-7. Cartoon of morning-glory structure that results from overmining a jug. Unsupported roof span exceeds design maximums and failure is likely.

Dissolution Front

Dissolution along the edges of the massive bedded salts present in dozens of basins throughout the world can occur naturally or through human intervention (Neal, 1995; Anderson et al., 1996; Jenyon, 1985). The massive salt bed that underlies about one-third of the surface area in Kansas and Oklahoma (Figure 2-5) has seen immense quantities of salt harvested by natural processes as well as relatively smaller amounts removed by anthropogenic means (Watney and Paul, 1980). The most active and regionally consistent areas of natural dissolution in Kansas are along the eastern boundary of the Permian Hutchinson Salt Member where the thickness of the updip edge goes from more than 75 m to zero over distances of less than 20 km. From the isopach of the salt (Figure 2-5), an approximately 5-km-wide zone marking the active natural dissolution zone front, commonly referred to as the “dissolution front,” is characterized by an abnormally large thickness gradient that meanders more than 250 km in generally a north/south direction.

This zone of active natural dissolution is characterized by the relative ease with which undersaturated ground water can access the salt face, harvest a full complement of salt, and then migrate away from the front. These natural dissolution zones and associated collapse features are not uncommon. Retreat of the Holbrook Basin natural dissolution front in Arizona, U.S., has left an extensive series of collapse-breccia structures resulting from caprock sinkholes that have collectively become part of a regional bowl subsidence structure (Neal, 1995). In west Texas and eastern New Mexico, the evaporite beds of the Delaware Basin experienced natural subsidence along the western subcrop of an extensive series of salt beds in the Salando and Castile Formations (Martinez et al., 1998). In Kansas, the active natural leaching zone is characterized by highly permeable rubble zones formed through time via collapse of dissolution voids followed by gravity slumping, saturation with brackish waters, and burial by alluvial deposition.

Future westward progression of the salt dissolution front relies heavily on access to the freshwaters abundant in the unconfined Equus Beds aquifer. As collapse of the bedrock surface occurs in response to salt removal, new conduits are created and fresh near-surface waters gain access to the salt face. Once there, this fresh water leaches a full complement of salt and then moves downward and eastward under density drive, providing renewed fresher water access to the salt front. This dynamic fluid system is consistent both in location and permeability with the drill-defined Wellington aquifer (Gogel, 1981) (Figure 2-9). Collapse of the impermeable overburden will continue to migrate the brackish fluids of the “lost circulation zone” (Wellington aquifer) westward. Waters of the Wellington aquifer were once fresh and originated in the Equus Beds aquifer or other unconfined local near-surface water source.

The Wellington aquifer closely tracks the natural dissolution front designated structurally to be along the eastern extreme and consistent with the highest relief portion of the salt bed (Figure 3-8). This aquifer is the source and repository for waters along the natural front that power the dissolution process. As the dissolution front and associated leaching of the salt bed passed from east to west, rocks within the Upper Permian and above the original salt interval underwent brittle deformation and as much as 75 m of subsidence over a several million year period. Progression of the dissolution front (westward retreat of the eastern edge of the salt face) from east to west has been active since at least late Pliocene. Based on drill data, the original eastern depositional edge of the Hutchinson Salt Member was approximately 20 km east of its current location. With the entire Mesozoic section missing over the present eastern third of the Hutchinson Salt Member, it is impossible to estimate when various episodes of dissolution might have occurred and at what rate between the deposition of the Upper Permian shales and Pleistocene. However, since the start of the Pleistocene the dissolution front has retreated west at a rate of 6 km per million years during early Pleistocene and 3 km per million years from late Pleistocene to recent (Walters, 1978).

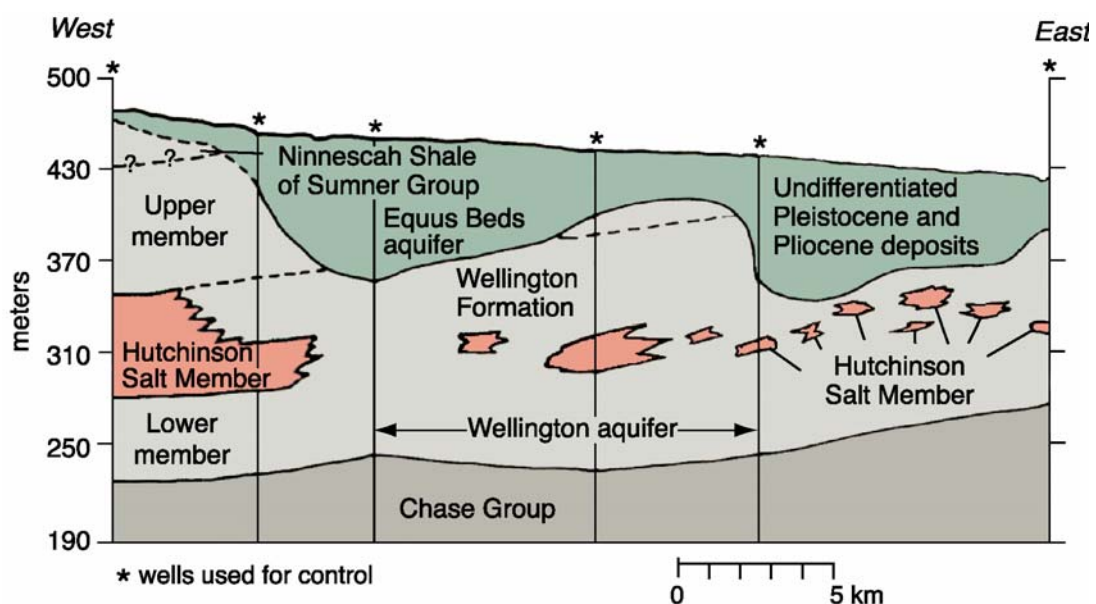


Figure 3-8. Cross section showing the extreme topography above the leached-out portion of the salt relative to flat-surface topography except for river channels. Erratics of salt scattered through the dissolution zone are indications that subsidence is still possible even east of the front (modified from Spinazola et al., 1985).

Remaining above the original salt bed east of the dissolution front are highly folded and faulted layers of rock beneath thick alluvial sequences. These up to 100-m-thick alluvial valleys now represent vital sources of unconfined fresh water for local population centers and agricultural use. These massive valleys are remnants of this retreat and possess basal contacts described as closed lows indicative of subsidence (Walters, 1978). Overburden subsidence formed these large, deep valleys that filled with sediment during the Pleistocene (Watney et al., 1988). Alluvial materials have completely infilled the distinctive karst topography that once marked the passage of the natural dissolution front, leaving the present-day land surface, for the most part, topographically featureless with the exception of the occasional stream or river channel.

Over time increments of millions of years, the progression of the salt-dissolution front along the eastern depositional edge of the basin has been relatively uniform from north to south (Watney and Paul, 1980). Westward intrusions (fingers) of the salt-dissolution front are indicative of zones of more rapid fluid movement that appear to be influenced by higher permeability. These zones of higher permeability are suggested to be structurally influenced (faults, fractures, folds, etc.) and attributable to multiple episodes of uplift via regional tectonic stresses (Watney et al., 2003).

Paleosinkholes identified on seismic-reflection sections (Miller and Henthorne, 2004) more than 20 km from the dissolution front are strong evidence supporting suggestions that natural dissolution extends (fingering) away from the front along corridors of higher permeability (faults, fractures, etc.). As expected, the highest concentration of paleo-subsidence features observed on seismic data are within 5 km of the borehole-mapped dissolution front. However, recent evidence on seismic-reflection sections refutes previous suggestions (Anderson et al., 1998) that natural dissolution is confined to the dissolution front and is responsible for sinkholes in proximity of the front. Patterns distinctive and indicative of natural dissolution of this bedded salt have been observed on seismic images near active sinkholes and by chance captures on seismic sections in areas with no surface expression (Miller and Henthorne, 2004) (Figure 3-9).

Understanding the natural processes (dissolution to roof-rock failure) and resulting structural features imaged on seismic-reflection sections at specific sites is key to characterizing processes associated with different subsidence events and related surface deformation. Defining the potential for sinkhole development and subsidence rates relies heavily on the physical and hydrologic characteristics in and above

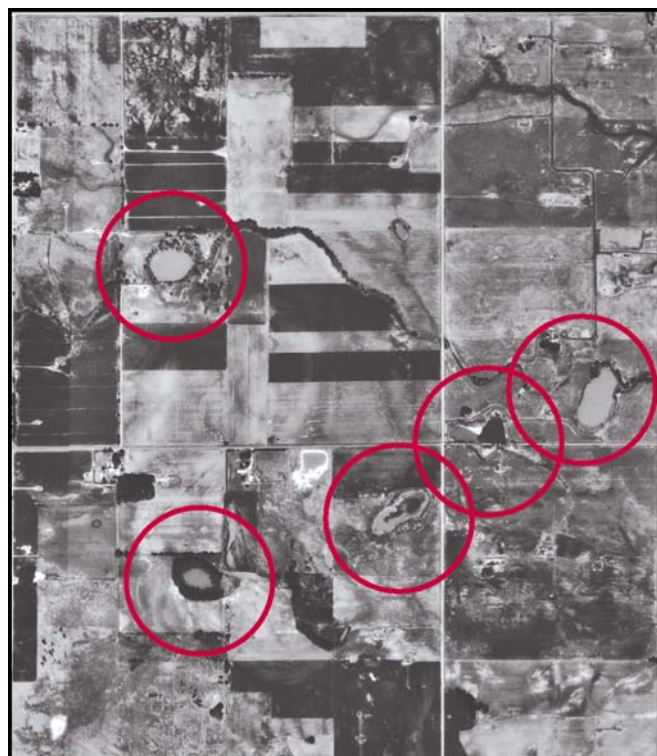


Figure 3-9. Orthophoto with sinkholes circled that are likely related to natural dissolution in Reno County, Kansas, near the dissolution front. Several seismic lines have been acquired in this area with defensible images of paleosubsidence features with and without surface expression.

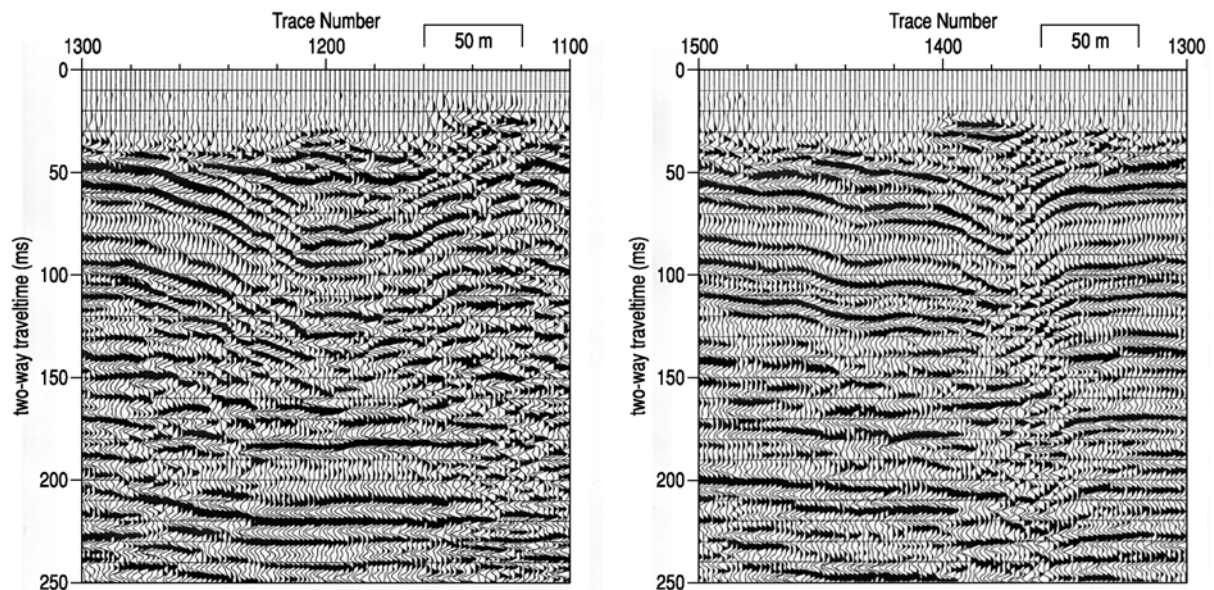


Figure 3-10. CMP-processed seismic sections from Punkin Center in Reno County, Kansas. Obvious solution-induced subsidence has produced dramatic bowl-shaped structures. These features have no surface expression and deposition of pre-Quaternary sediment into these bowl features appears undisturbed, indicative of dormancy.

the layers of soluble rocks. The complexities of a natural-dissolution front in a human time frame are extreme, with an apparent, almost randomness to the development of sinkholes and progression of the dissolution front (Figure 3-8). However, in a more geologic time span (millions of years) the subsidence of salt overburden in response to dissolution voids follows a very well constrained and consistent pattern, progressing at a relatively uniform rate.

Clearly paleosubsidence features interpreted on seismic-reflection data, without current surface expressions, are strong evidence supporting the intermittent nature of dissolution and overburden subsidence processes over the last 250 million years. Most paleofeatures that have been interpreted on seismic-reflection data have no surface expression and therefore have not experienced discernible subsidence over at least the last few thousand years. Dissolution at these sites could be active, but new void space has not grown sufficiently to instigate overburden failure or is too small to be detected with high-resolution seismic reflection.

The Pliocene-Pleistocene Equus beds in Kansas appear undisturbed on seismic sections above massive inactive subsidence features at various locations along the natural dissolution front (Figure 3-10). Shallow horizontal beds above subsidence/collapse structures with no apparent post-deposition distortion evident on seismic sections strongly support the suggestion that the processes responsible for these obvious subsidence/collapse features have been dormant or slowed over the last 2 million years or so. Seismic-reflection images across active sinkholes along the natural dissolution front have been interpreted to show evidence of ties between currently active subsidence areas and distinct yet apparently dormant past cycles of paleosubsidence likely in response to periods of ancient dissolution.

Natural Salt Dissolution vs. Anthropogenic

Natural leaching of evaporites, especially salt, has been documented in both diapirs and bedded salt deposits (Anderson, 1981; Jenyon, 1985, 1986, 1988; Jackson and Seni, 1984). Dissolution and resulting subsidence-related structures have been heavily studied

because of their proven potential as a trapping mechanism for hydrocarbons (Parker, 1967; Swenson, 1967). Natural-transport mechanisms necessary for unsaturated brine to gain access to salt are generally related to regional structures with tectonic origin, salt tectonics, or depositional factors (Ege, 1984). Pathways for ground water to access bedded salt are general regional in nature and therefore represent potentially extensive dissolution networks. The exchange of saturated with unsaturated brine at the natural dissolution front is relatively slow as a result of the complex and low-flow characteristics of most natural ground-water conduits.

Local scale complexities in the hydrogeologic characteristics, salt thickness and geometry, and influence of insoluble residue make site-specific projections of natural dissolution activities nearly impossible. Flow patterns and supply of ground water in proximity to and at dissolution zones will change in response to water chemistry, buildup of insoluble lag, interbedded layer geometry, thickness, separation, and location within salt interval, changes in distance and travel path between freshwater inlet and dissolution front, effectiveness of brine exchange (fresher waters with fully saturated brine), and overburden characteristics (strength, deformation properties, thickness, variability, etc.). Natural leaching and subsidence make the depositional origin of sediments above and around a natural dissolution feature nearly impossible to ascertain due to changes in sedimentary structures, textures, and lithologies (Goodall et al., 2000).

Some of the most dramatic and picturesque landforms on the earth are the result of natural dissolution and subsidence in carbonate rock sequences. Karst features have been directly observed on the ground surface and inferred to exist in the subsurface where soluble carbonate units are present (Franseen et al., 2004). Karst features have been credited with directly or indirectly providing the trapping mechanism for certain petroleum reservoirs (Connelly et al., 1991; Anderson and Franseen, 1991; Surjik and Hobson, 1964). Due in part to the solubility and abundance of carbonate rocks, karst features are common around the world.

Natural dissolution of bedded salt deposits generally occurs along depositional edges (Anderson, 1981; Jenyon, 1985, 1986, 1988). Faults and fractures provide fluid conduits for both bedded and domed (diapirs) deposits and are likely responsible for the zonation of dissolution observed along these structures (Frye and Schoff, 1942; Yiechieli et al., 2003; Jackson and Seni, 1984). Depositional edges in a bedded salt basin are generally regionally extensive and subcrop beneath relatively impermeable caprock (Ege, 1984). If ground water does gain access to the salt along depositional edges, a potentially significant expanse of salt front can be exposed to natural leaching.

Once a natural dissolution front has been established, a bedded salt will begin retreating at a geologically constant rate, leaving a trail of sinkholes with a pockmarked distribution across the zone of active dissolution (Watney and Paul, 1980; Neal, 1995) (Figure 3-9). Sinkholes resulting from natural dissolution of salt can be irregular in shape and grow at very discontinuous rates, generally correlating to periods of active dissolution, dormancy, and then re-activation (Abelson et al., 2003). In most geologic settings natural deposition will subdue and eventually completely mask surface evidence (depressions) as the front progresses and moves on toward the center of the basin.

Little evidence exists to define with confidence the kinematics of salt dissolution in diapirs and development of sinkholes. It is generally accepted based on differential thickness of residual caprock over salt diapirs (Jackson and Seni, 1984) that dissolution is greatest at

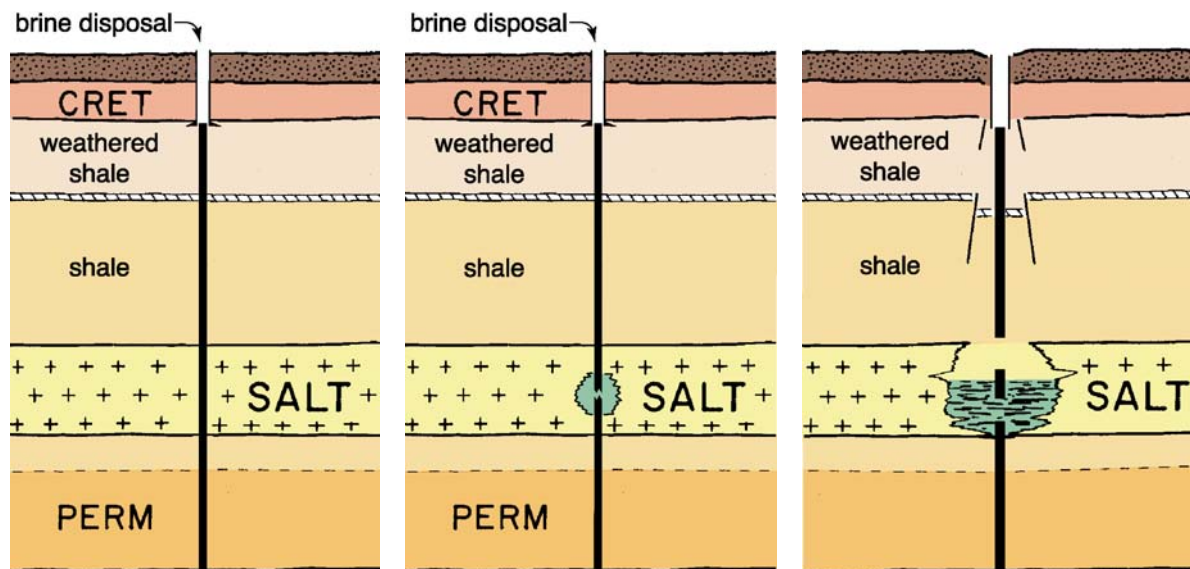


Figure 3-11. Cartoons showing one possible anthropogenic source of salt dissolution and collapse (modified from Walters, 1978).

the crests where salt rises the fastest. It is also accepted that extensional fractures in salt dome caprock provide conduits for fresher waters to access the salt and leach product with dissolution moving downward and inward (Ge and Jackson, 1998). Processes responsible for grabens observed above salt domes are not clearly understood in spite of substantial work looking at both dissolution and tectonics as driving forces (Cater, 1970; Lohmann, 1979; Bacoccoli et al., 1980; Stokes, 1982; Jenyon, 1985, 1986, 1988; Doelling, 1985, 1988; Baars and Doelling, 1987; Chenoweth, 1987; Mart and Ross, 1987; Vendeville and Jackson, 1992a, 1992b; Jackson and Vendeville, 1994; Ge et al., 1995, 1996; Ge, 1996).

Based on the study of dry salt mines (room and pillar) and boring data, it is believed by many that natural dissolution processes in salt are intermittent, generally halting and reactivating on their own in response to fluid restrictions and changing void characteristics (Waltham et al., 2005). In the absence of dissolution, solution voids are likely to undergo closure due to the ductile nature of salt and extreme differential pressures across a salt face. Therefore, once active leaching ends, solution voids and open conduits making a salt face accessible to unsaturated brine may be self-sealing.

Anthropogenic-induced dissolution of salt is completely dependent on establishing a fluid inlet and drain and is generally localized and reasonably well constrained or confined by those fluid passages. Freshwater introduced from an inlet to the salt under hydrostatic pressure moves quickly to the dissolution front (salt face) where it exchanges with denser saturated brine solution that moves to the outlet or drain where it exits the salt interval (Figure 3-11). Unsaturated brine from aquifers or injected fluids from wells that suffer from casing failure or loss of borehole seal interact with the salt in a very uncontrolled fashion. Void geometries resulting from casing breach are strongly influenced by the relative location of the inlet and outlet, velocity and volume of unsaturated brine moving through the solution void, and salt-interval stratigraphy.

Anthropogenic salt dissolution as a means of mining salt from underground ore deposits represents a controlled and safe method under modern oversight and regulations. Historic practices have left oversized voids with failure guaranteed and only when unknown. Considering the fluid pressures and volumes used to produce salt via brining, a slight error

during production could have devastating long-term effects. Dissolution processes are well known to be accelerated as a result of human activities (Newton, 1987).

Borehole Access

Anthropogenic-induced dissolution of salt has occurred both intentionally and accidentally. Mining of salt has produced a multitude of controlled and uncontrolled dissolution events throughout the world (Walters, 1978; Martinez et al., 1998; Landes and Piper, 1972). Abandoned well bores, wastewater disposal wells, and water supply wells have been responsible for many collapse features as a direct result of unintentional dissolution of salt layers penetrated by well bores. The most spectacular and hazardous, and therefore reported and studied, have been from uncontrolled dissolution events that have instigated catastrophic failure of overburden and surface collapse in developed areas. When collapse features threaten public safety, characterization and remedial actions are undertaken immediately to evaluate public risk.

Some of the most spectacular salt dissolution and catastrophic collapse features have resulted from freshwater access to the salt interval via a borehole. Both the salt mining and petroleum industries move fluid into and out of or through the salt interval via boreholes. In the case of the salt industry, controlled dissolution and recovery are the objectives (as will be discussed in the upcoming section), while the petroleum industry uses boreholes penetrating the salt as a conduit to deeper disposal areas or to gain access to deeper hydrocarbon production zones. Either way, when borehole integrity is maintained the process is safe for both the environment and surface activities.

Modern solution mining activities have sufficient levels of monitoring and regulatory oversight to safely and effectively leach salt from natural stores, thereby leaving voids with a geometry and physical characteristics suitable for long-term stability. Modern monitoring includes tight controls on injection and production depths, pressures, and volumes. Sonar surveillance routinely complements integrity-testing practices as part of regulatory oversight. All these controls and oversights are in place to avoid the very problems currently being dealt with at most solution-mine fields that were active in the early half of the twentieth century.

Interaction between boreholes and salt has contributed to or been responsible for surface failures over salt-dissolution mine fields in a variety of settings: in particular, overmining, no salt buffer on jug roof, unstable jug geometry, unintended well-to-well connectivity, casing failure, and improper casing installations within the shale caprock. Ultimately, any one or combination of these factors or conditions could result in instability and surface collapse. Considering the volume of the average jug after conventional solution mining and the poor roof-rock stability and strength of Permian shales in Kansas, failure propagated through the overburden will occur any time no salt buffer exists between the shale and top of the jug. A more complete discussion of solution mining in general will be the focus of the next section in this chapter.

All documented surface subsidence in well fields more than 40 km from the natural dissolution front of the Hutchinson Salt Member in the last 100 years have been the result of well-bore failure or overmining (Figure 3-12) (the only exception is along Crooked Creek fault in southwestern Kansas [Figure 1-5]). Both a concern and an unknown is the number and location of borehole-induced dissolution voids with current failure potential and without surface expression. Equally concerning is not knowing when the upward migration of these voids might begin or continue, eventually forming either a sag or sinkhole. These yet-to-be-



Figure 3-12. Leesburg sinkhole in southern Stafford County, Kansas, formed gradually after containment was lost in an oil-field disposal well. This sinkhole is more than 80 km west of the natural dissolution front and formed in about three years (photo by R. Miller).

discovered anthropogenic dissolution voids could have developed as the result of contact with drill mud, wastewater disposal, or water infiltration via improper seal in annular space. With no hints as to the presence of these hazards from well-bore data or surface expressions, failure could be devastating.

Several publications (Anderson et al., 1998; Walters, 1978) have suggested land subsidence in Kansas is almost exclusively natural, citing less than 10 known anthropogenic sinkholes. A cursory inventory of salt dissolution subsidence features with pronounced surface expression clearly indicates the problem has escalated almost four-fold since these early inventories. Seismic data presented in this report include images from about a half dozen salt dissolution sinkholes that formed since 1980 as a direct result of anthropogenic fluid sources. Since 1978 (Walters, 1978), the number of known well bore-induced sinkholes from oil and gas operations increased from eight to more than 28 (Korphage, 2006). Sinkholes or sags resulting from solution mining have increased from five documented cases in 1978 to currently more than nine (Cochran, 2006). Increasingly these subsidence problems are affecting population centers and putting the environment (especially ground water—a valuable and cherished resource in western Kansas) at risk. Based on the number of boreholes that penetrate the salt, with time and constant or increasing fatigue on overburden rock, this problem is destined to escalate to potentially unmanageable proportions.

Solution Mining

Solution mining of rock salt was first attempted in this region (Hutchinson, Kansas) in 1888 with underground mining starting around 1923 (Sawin and Buchanan, 2005). “Brining” (solution mining) methods and practices throughout most of the twentieth century focused primarily on maximizing production with little thought or effort put into ensuring long-term

surface or subsurface stability (Landes and Piper, 1972; Geertman, 2000). It was not until the later half of the twentieth century that more environmentally sound solution-mining practices began to appear.

Solution mining is common in most places around the world where salt basins are located (Landes and Piper, 1972; Thoms and Gehle, 2000). Mining of the Hutchinson Salt Member in Kansas has generally involved one of three different techniques: single-well, multi-well, and room-and-pillar. During early single-well production of salt in Kansas, many wells were only cased 30 or so meters below the top of the shale bedrock leaving the inner (production) tube suspended in an open borehole as much as 75 m above the top of salt. This configuration allowed fluid contact with the salt and unfortunately the upper Wellington shales as well. In the later half of the twentieth century, regulations required surface casing be placed at or just below the salt/shale contact, thereby protecting the shale caprock (Figure 3-13).

Subsurface remnants of solution mining activities have been responsible for sinkholes all over the world (Landes and Piper, 1972; Martinez et al., 1998). The last documented solution mining sinkhole count in the USA was in 1981, when 10 different major solution-mining sinkholes had been identified (Dunrud and Nevins, 1981). In Kansas, sinkholes associated with dissolution mines have been most prevalent in and around Hutchinson (Walters, 1978). The most dramatic and publicized dissolution mine collapse in Kansas, and the one most often displayed in publications, was at the Cargill plant in 1974 (Figure 1-3). Concerns for ground stability within and around the old Carey Salt Company solution mine field in eastern Hutchinson were substantiated by the catastrophic development of a sinkhole in 2005 that was threatening rail traffic (Cochran, 2005) (Figure 1-7).

Well construction, design, and relative location of a solution mining well is based on the extraction method employed. The two most common methods of brining are conventional and undercut (Landes and Piper, 1972). Conventional production is a single-well method that requires freshwater be forced into the salt with brine returning to the surface as a

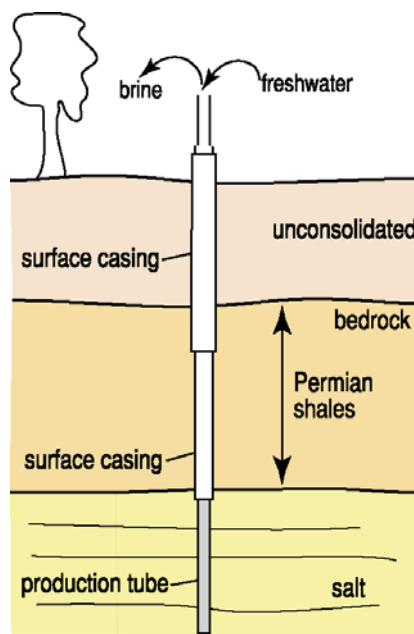


Figure 3-13. Cartoon of general installation design of single-well facilities in the Hutchinson, Kansas, area.

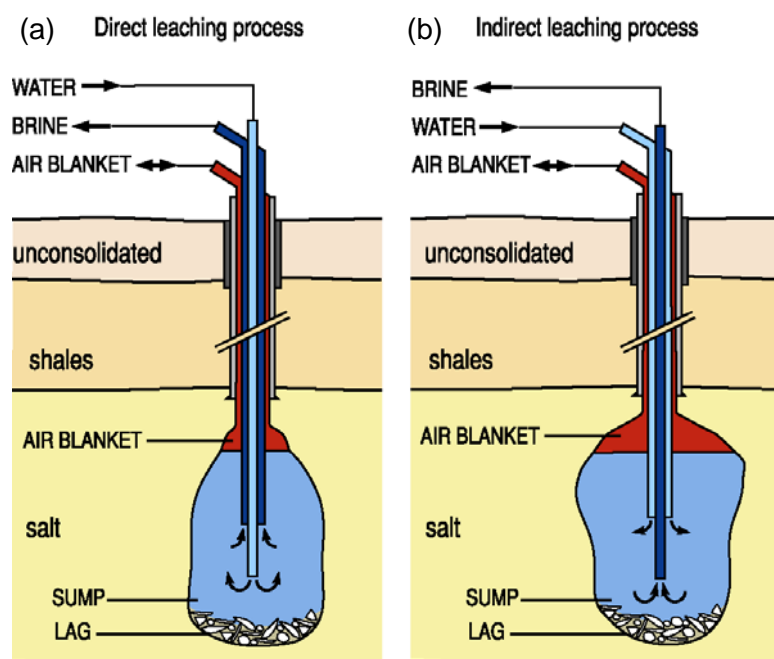


Figure 3-14. Diagrams of direct (a) and indirect (b) single-well leaching systems, which are rarely used anywhere except salt diapirs at this time.

result of this pressure (Figure 3-14). Production tubing was generally installed in the single-well configurations to the maximum designed production depths. Salt caverns formed as a result of this isolated well method are predominantly vertical and called “jugs” (because their vertically elongated shape resembles a jug).

Because brackish water is denser than freshwater, the geometry of the dissolution jug or cavern is highly dependent on whether freshwater is injected near the top or bottom of the salt interval. Direct leaching involves injecting freshwater near the base of the salt (Figure 3-14a), while indirect leaching injects freshwater above the extraction inlet (Figure 3-14b). Ensuring controlled and confined-void development for these conventional production approaches requires appropriate lithology and rock properties with tightly constrained operational ranges. Compressed air is many times used to form a pillow at the top of the dissolution volume, effectively inhibiting vertical progression of the dissolution front. Today conventional solution mining techniques are predominantly used on salt domes.

Unexpected sinkhole appearances within solution mine fields in and around the city of Hutchinson, Kansas, have been reported for more than 90 years (Walters, 1978). These sinkholes, to date, have formed as a result of roof-rock failure associated with conventional mining methods. In general, failure occurs at a single-well installation that has overproduced salt near the salt/shale caprock interface, exposing a span of roof rock that exceeds rock strengths. Problems with the single-hole method in Kansas begin to occur as salt harvesting below interbedded shale or anhydrite stringers extends beyond the point where the unsupported span of these non-soluble layers exceeds what their strength allows (Figure 3-15a). Failure of these beds in proximity to the well bore generally results in rupture of the freshwater tubing and upward movement of the dissolution volume into higher portions of the salt bed (Figure 3-15b). The process becomes much more horizontal when the failure and collapse cycle reaches the top of the salt bed (Figure 3-15c). When a dissolution well field is populated by many conventional production wells in a grid pattern, a gallery can form when the jug of a single-well installation makes contact with the dissolution jug of an adjacent well along the insoluble caprock layer (Figure 3-16). Galleries between wells designed for single-

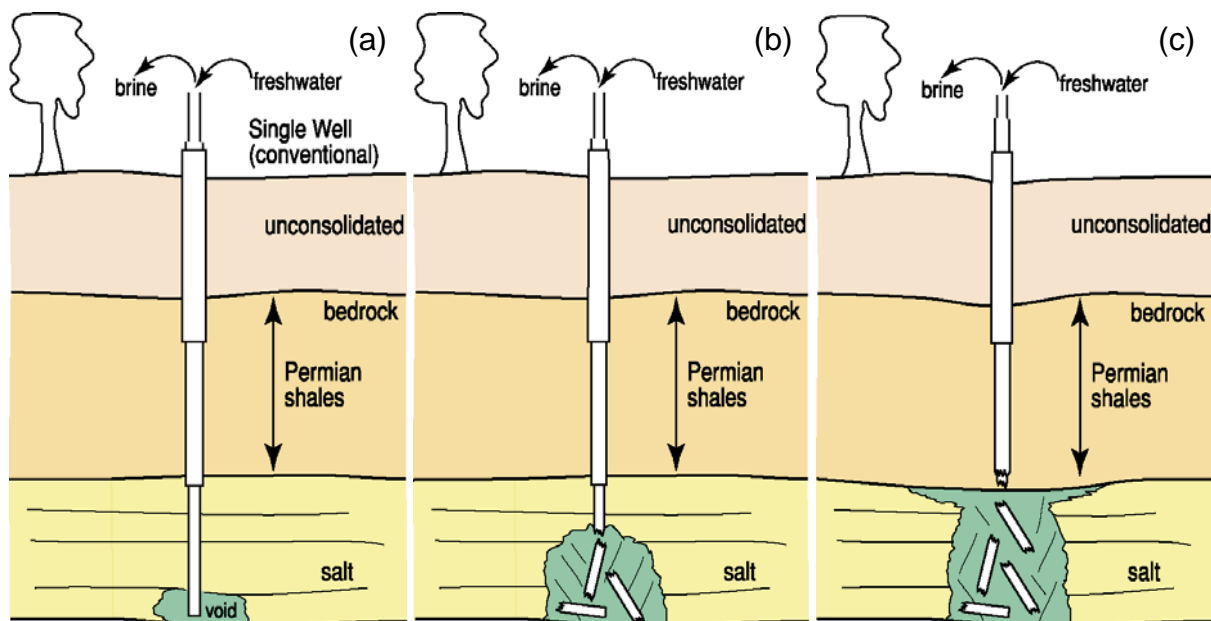


Figure 3-15. Historic progress of single-well solution mining from base of salt (a) through over-production (c) and development of morning-glory structure at the top of salt.

well operations are particularly susceptible to roof-rock failure due to excessive spans of unsupported roof rock.

Solution mining practices most common today in bedded salt involve interconnected multiple wells, called undercut wells (Landes and Piper, 1972). This method of mining requires two or more wells hydrologically connected along the base of the salt interval (Figure 3-17). A multi-well solution mining technique, by design, leaches elongated caverns in salt deposits along interbedded, insoluble layers (e.g., anhydrites, shales). Several interconnected (usually linear) wells define a well field with each well serving as either a producer or injector.

Hydraulic fracturing is commonly used to establish an initial connection between wells. Water is injected into one well and produced from another. Layers of insoluble rock are exposed at the top of the flow corridor with expanses of exposed roof rock continuously enlarging until the insoluble roof rock finally fails, thereby exposing the basal contact of a fresh salt layer, perpetuating the process. Rubble from the collapse of this insoluble interbedded layer (lag) begins to accumulate in the void left by harvested salt. Multi-well fields of this type generally create a single horizontally elongated cavern designed with a width that will not stress pillars/walls beyond the strength limits of the rock serving as the unsupported roof span.

Multi-well solution mining techniques are generally more efficient, but can lead to quite irregular caverns. This lack of uniformity makes estimates of void dimensions difficult. Laterally extensive sags (trough) and elongated sinkholes are a common artifact of a multiwell solution mine field that has been the victim of overmining (Nieto et al., 1983). Mined-out areas usually have a highly irregular geometry and generally track the alignment of wells making up the gallery. Subsidence associated with these solution mine galleries in the Detroit, Michigan, USA, area has manifested itself at the ground surface as both sag and sinkholes (Ege, 1979).

Brine Disposal

Most fluids disposed of by subsurface injection are byproducts of oil and gas production. Large quantities of brine are routinely produced as a consequence of oil and gas extraction from underground reservoirs. A variety of tools have evolved to measure integrity and monitor containment as well as predict containment failure in these wells. Techniques

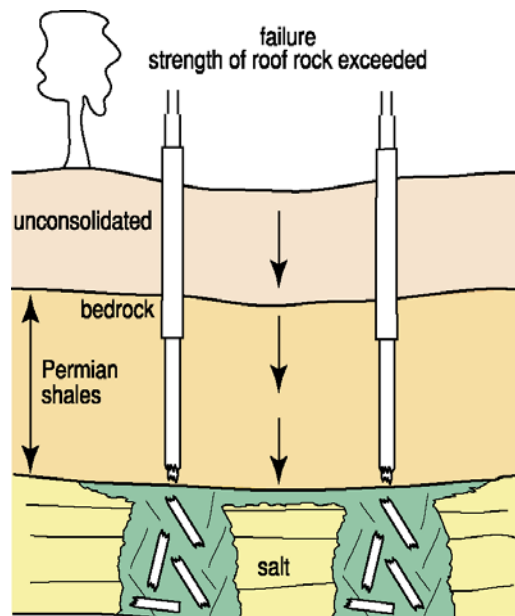


Figure 3-16. Inadvertent formation of a gallery from the joining of two morning-glory structures from adjacent wells and resulting sag.

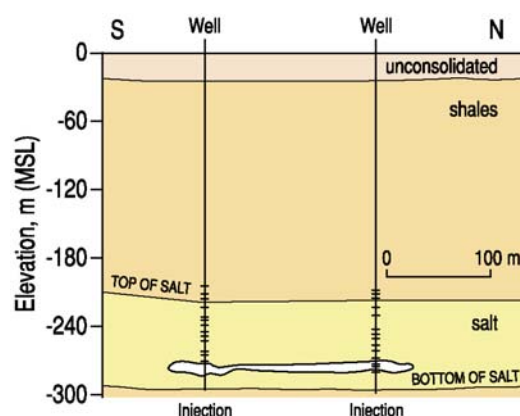


Figure 3-17. Engineered gallery producing salt between two wells in the Detroit area (modified from Fernandez and Castro, 1996).

providing front-line surveillance of injection systems have relied on measurement or estimation of endangering influence, piezometric head, formation transmissivity, pressure fall-off, and water-quality.

Saltwater-disposal (SWD) wells and enhanced recovery wells are synonymous with oil and gas production (McLin, 1986). Since 1859 more than 167,000 wells in the U.S. associated with standard oil-field operations have been converted to SWD or enhanced recovery wells (EPA, underground injection control program, oil and gas injections wells [class II]). Brine injected underground represents the largest single worldwide potential contaminant of potable subsurface waters. More than 2 billion barrels of brine are produced and injected each day in the U.S. In Kansas more than 15,000 wells are used across the state for brine injection with many wells injecting more than 5,000 barrels a day. With brine from oil production containing around 10,000 to 15,000 ppm chlorides, even small leaks can contaminate large volumes of freshwater in an aquifer system or leach away tons of salt under pumping pressures.

In general, underground disposal of liquids into porous rocks can be successful across a range of surface-injection pressures from gravity flow to several tens of MPa, depending on the hydraulic head of the target reservoir. Over the long term and under this range of pressure conditions, well-casing failure due to corrosion or stress does occur. Failure in this setting can place extremely large volumes of brackish fluids in direct contact with potable water or soluble rocks.

A fluid injection well of this type is generally referred to as a “deep well” because historically the proposed destination formation has been located beneath the deepest source of usable water. Any porous and permeable rock formation can act as a disposal reservoir for injected liquids. However, most disposal units already have water present with high concentrations of chlorides, sulfides, or other chemicals that make the reservoir unsuitable for surface use. In Kansas, deep well injection has only been a regulatory requirement for just over 40 years.

Uncontrolled access to the salt interval by unsaturated brine wastewater as a consequence of petroleum exploration and production is not uncommon (Walters, 1978). Insufficient or no seal between the casing and borehole walls and casing failure are the two most common sources of water infiltration into the salt interval as a consequence of petroleum production. For borehole-induced dissolution, the borehole is commonly the inlet and outlet. Therefore dissolution is generally constrained to a volume relatively close to and centered on the borehole. However, there are situations where borehole-induced dissolution has reactivated paleodissolution, affecting the integrity of the overburden in areas where the overburden lost strength during previous subsidence episodes.

Dissolution of the Hutchinson Salt Member via borehole contact with fluid is common. What is extremely uncommon and a bit surprising, considering the total number of drill holes that penetrate the Hutchinson Salt Member in Kansas, is how seldom borehole fluid transfer activities (drilling, production, disposal, etc.) generate dissolution voids large enough to instigate surface subsidence. Drilling mud is usually around 100,000 ppm while salt-saturated solution is 260,000 ppm; therefore, unless a special mud program is utilized some dissolution is inevitable when drilling through the salt. Common wastewater byproducts from oil and gas production contain high concentrations of extremely corrosive H₂S, which accelerates the degradation of casing integrity. Injection of oil-field wastewater

is essential for environmental protection considering how devastating surface disposal of oil-field brines can be to the ecosystem (Otton and Zielinski, 2003).

Summing Up and To Come

Discussion in this chapter revolved around the unique as well as the common properties and characteristics of salt and dissolution, laying groundwork that logically leads to the next chapter's topics which include subsidence, stress environment, failure mechanisms and rates, and sinkhole varieties and hazards. These upcoming aspects or processes of subsidence will help flesh out key concepts and allow a logical progression toward an accurate, empirical understanding of the entire dissolution and subsidence process based on seismic-reflection data mated with surface and borehole observations and drill data.

In general, the next chapter covers subsidence settings and processes, with emphasis on key properties leading to an improved understanding of the relationship between the dissolution and subsidence phenomenon. Specifically, descriptions clarify the types of and subsurface conditions necessary to propagate rock failure from void roof through the overburden. Expanding on unique aspects of the various forces that drive the leaching process and resulting subsidence provides instrumental concepts that are necessary to fully appreciate these subsidence conditions. Topics in the next chapter will include subsidence as a result of void development in salt, failure mechanism including stress regimes and strain geometries, failure rates, sinkhole varieties, and hazards resulting from expected and unexpected sinkhole development.

References

- Abelson, M., G. Baer, V. Shtivelman, D. Wachs, E. Raz, O. Crouvi, I. Kurzon, and Y. Yechieli, 2003, Collapse-sinkholes and radar interferometry reveal neotectonics concealed within the Dead Sea basin: *Geophysical Research Letters*, v. 30, p. 1545.
- Alsop, G.I., D.J. Blundell, and I. Davidson, 1996, *Salt Tectonics*, Vol. 100: Geological Society Special Publication, London.
- Anderson, N.L., and E.K. Franseen, 1991, Differential compaction of Winnipegosis reefs: A seismic perspective: *Geophysics*, v. 56, p. 142-147.
- Anderson, N.L., R.J. Brown, and D.A. Cederwall, 1996, Natural recession of the eastern margin of the Leofnard salt in western Canada: *Geophysics*, v. 61, p. 222-231.
- Anderson, N.L., R.W., Knapp, D.W. Steeples, and R.D. Miller, 1995, Plastic deformation and dissolution of the Hutchinson Salt Member in Kansas; in N.L. Anderson and D.E. Hedke, eds., *Geophysical atlas of selected oil and gas fields in Kansas*: Kansas Geological Survey Bulletin 237, p. 66-70.
- Anderson, N.L., A. Martinez, J.F. Hopkins, and T.R. Carr, 1998, Salt dissolution and surface subsidence in central Kansas: A seismic investigation of the anthropogenic and natural origin models: *Geophysics*, v. 63, p. 366-378.
- Anderson, R.Y., 1981, Deep-seated salt dissolution in the Delaware Basin, Texas and New Mexico: New Mexico Geological Society Special Publication No. 10, p. 133-145.
- Baar, C.A., 1977, *Applied Salt-rock Mechanics I*: Elsevier Scientific Publishing Co., 294 p.
- Baars, D.L., and H.H. Doelling, 1987, Moab salt-intruded anticline, east-central Utah; in S.S. Beus, ed., *Centennial Field Guide: Rocky Mountain Section of the Geological Society of America*, v. 2, p. 275-280.
- Bachu, S., and L. Rothernburg, 2003, Carbon dioxide sequestration in salt caverns: Capacity and long term fate: Proceedings of the Second Annual Conference on Carbon Dioxide Sequestration (CD-ROM), Alexandria, Virginia, May 5-8, 12 p.
- Bacoccoli, G., R.G. Morales, and O.A.J. Campos, 1980, The Namorado oil field—A major discovery in the Campos Basin, Brazil; in M.T. Halbouty, ed., *Giant Oil and Gas Fields of the Decade 1968-1978*: American Association of Petroleum Geologists (AAPG) Memoir 30, p. 329-338.
- Beck, B.F., ed., 1984, *Sinkholes: Their Geology, Engineering, and Environmental Impact*: A.A. Balkema, Rotterdam.
- Beck, B., 1988, Environmental and engineering effects of sinkholes—The processes behind the problems: *Environmental Geology and Water Sciences*, v. 12, n. 2, p. 71-78.
- Beck, B.F., A.J. Pettit, and J.G. Herring, eds., 1999, *Hydrogeology and Engineering Geology of Sinkholes and Karst—1999*: Rotterdam, A.A. Balkema, 130 p.
- Carmichael, R.S., 1989, *CRC Practical Handbook of Physical Properties of Rocks and Minerals*: Boston, CRC Press, 741 p.
- Cater, F.W., 1970, Geology of the salt anticline region in southwestern Colorado: U.S. Geological Survey Professional Paper 637, 80 p.
- Chenoweth, W.L., 1987, Paradox Valley, Colorado: A collapsed salt anticline; in S.S. Beus, ed., *Centennial Field Guide: Rocky Mountain Section of the Geological Society of America*, v. 2, p. 339-342.
- Cochran, M., 2005, Hutchinson sinkhole update: *Underground News*: Kansas Department of Health and Environment, Spring.
- Cochran, M., 2006, personal communication.

- Connelly, D.L., B.J. Ferris, and L.D. Trembly, 1991, Northwestern Williston Basin case histories with 3-D seismic data: *Geophysics*, v. 56, p. 1849-1874.
- Dijk, P.E., and B. Berkowitz, 2000, Buoyancy-driven dissolution enhancement in rock fractures: *Geology*, v. 28, p. 1051-1054.
- Doelling, H.H., 1985, Geologic map of the Arches National Park and vicinity, Grand County, Utah: Utah Geological and Mineral Survey Map 74, scale 1:500,000, 1 sheet, 15 p. text.
- Doelling, H.H., 1988, Geology of Salt Valley anticline and Arches National Park, Grand County, Utah: Utah Geological and Mineral Survey Bulletin 122, p. 1-58.
- Dreybrodt, W., 1992, Dynamics of karstification: A model applied to hydraulic structures in karst terranes: *Applied Hydrogeology*, v. 3, p. 20-32.
- Dreybrodt, W., 1996, Principles of early development of karst conduits under natural and man-made conditions revealed by mathematical analysis of numerical models: *Water Resources Research*, v. 32, p. 2923-2935.
- Dreybrodt, W., D. Romanov, and F. Gabrovsek, 2002, Karstification below dam sites; A model of increasing leakage from reservoirs: *Environmental Geology*, v. 42, p. 518-524.
- Dunrud, C.R., and B.B. Nevins, 1981, Solution mining and subsidence in evaporite rocks in the United States: U.S. Geological Survey Miscellaneous Investigation Series Map I-1298, 2 sheets.
- Eck, W., and R.C. Redfield, 1965, Engineering geology problems at Sanford Dam, Borger, Texas: *Bulletin of the Association of Engineering Geologists*, v. 3, p. 15-25.
- Ege, J.R., 1979, Surface subsidence and collapse in relation to extraction of salt and other soluble evaporites: U.S. Geological Survey Open-file Report 79-1666.
- Ege, J.R., 1984, Formation of solution-subsidence sinkholes above salt beds: U.S. Geological Survey Circular 897, 11 p.
- Fernandez, G., and A. Castro, 1996, Structural stability evaluations of expansion alternatives for solution mining operations at Windsor, Ontario: SMRI Meeting.
- Ford, D., and P. Williams, 1989, *Karst Geomorphology and Hydrology*: Unwin Hyman, London, 601 p.
- Franseen, E.K., A.P. Byrnes, J.R. Cansler, D.M. Steinhauff, and T.R. Carr, 2004, The geology of Kansas—Arbuckle group; in Current research in earth sciences: Kansas Geological Survey, Bulletin 250, part 2 (<http://www.kgs.ku.edu/Current/2004/franseen/index.html>).
- Frye, J.C., and S.L. Schoff, 1942, Deep-seated solution in the Meade Basin and vicinity, Kansas and Oklahoma: *American Geophysical Union Transactions*, v. 23, pt. 1, 35-39.
- Gale, Thomson, 2003, Sinkholes. *World of Earth Science*, K. Lee Lerner and Brenda Wilmoth Lerner, eds. Thomson Gale, 2003. eNotes.com. Sept. 11, 2006 (<http://science.enotes.com/earth-science/>).
- Gangi, A.F., 1981, A constitutive equation for one-dimensional transient and steady-state flow of solids: *Mechanical Behavior of Crustal Rocks*, American Geophysical Union, Geophysical Monograph 24, p. 275-285.
- Gangi, A.F., 1983, Transient and steady-state deformation of synthetic rock salt: *Tectonophysics*, v. 91, p. 137-156.
- Ge, H., 1996, Kinematics and dynamics of salt tectonics in the Paradox basin, Utah and Colorado—Field observations and scaled modeling: Ph.D. dissertation, University of Texas at Austin, Austin, Texas, 317 p.

- Ge, H., and M.P.A. Jackson, 1998, Physical modeling of structures formed by salt withdrawal: Implications for deformation caused by salt dissolution: *AAPG Bulletin*, v. 82, p. 228-250.
- Ge, H., M.P.A. Jackson, and B.C. Vendeville, 1995, Rejuvenation and subsidence of salt diapirs by regional extension: *Gulf Coast Association of Geological Societies Transactions*, v. 45, p. 211-218.
- Ge, H., M.P.A. Jackson, and B.C. Vendeville, 1996, Extensional origin of breached Paradox diapirs, Utah and Colorado—Field observations and scaled physical models; in A.C. Huffman, Jr., W.R. Lund, and L.H. Godwin, eds., *Geology and resources of the Paradox basin: Utah Geological Association Guidebook 25*, p. 285-293.
- Geertman, R.M., ed., 2000, *Proceedings of the 8th World Salt Symposium, May 7-11, 2000*: Elsevier, The Hague, The Netherlands, 1400 pp.
- Gemmer, L., S.J. Ings, S. Medvedev, and C. Beaumont, 2004, Salt tectonics driven by differential sediment loading: Stability analysis and finite-element experiments: *Basin Research*, v. 16, p. 199-218.
- Gera, F., 1972, Review of salt tectonics in relation to the disposal of radioactive wastes in salt formations: *Geological Society of America Bulletin*, v. 83, n. 12, p. 3551-3574.
- Gogel, T., 1981, Discharge of saltwater from Permian rocks to major stream-aquifer systems in central Kansas: *Kansas Geological Survey Chemical Quality Series 9*, 60 p.
- Goodall, T.M., C.P. North, and K.W. Glennie, 2000, Surface and subsurface sedimentary structures produced by salt crusts: *Sedimentology*, v. 47, p. 99-118.
- Gustavson, T.C., M.W. Wiley, C.R. Handford, R.J. Finley, S.P. Dutton, R.W. Baumgardner, K.A. McGillis, and W.W. Simpkins, 1980, *Geology and geohydrology of the Palo Duro Basin, Texas Panhandle—A report on the progress of Nuclear Waste Isolation Feasibility Studies (1979)*: The University of Texas at Austin, Bureau of Economic Geology, Geological Circular 80-7, 99 p.
- Gustavson, T.C., W.W. Simpkins, A. Alhades, and A. Hoadley, 1982, Evaporite dissolution and development of karst features on the Rolling Plains of the Texas Panhandle: *Earth Surface Processes and Landforms*, v. 7, p. 545-563.
- Jackson, M.P.A., and S.J. Seni, 1984, *Atlas of salt domes in the East Texas Basin*: Austin, Texas, University of Texas at Austin, Bureau of Economic Geology Report of Investigations 140, 102 p.
- Jackson, M.P.A., and C.J. Talbot, 1991, *A glossary of salt tectonics*: University of Texas at Austin, Bureau of Economic Geology Geological Circular 91-4.
- Jackson, M.P.A., and B.C. Vendeville, 1994, Regional extension as a geologic trigger for diapirism: *Geological Society of America Bulletin*, v. 106, p. 57-73.
- Jenyon, M.K., 1985, Basin-edge diapirism and updip salt flow in the Zechstein of the southern North Sea: *AAPG Bulletin*, v. 69, p. 53-64.
- Jenyon, M.K., 1986, *Salt Tectonics*: London, Elsevier, 191 p.
- Jenyon, M.K., 1988, Seismic expression of salt dissolution-related features in the North Sea: *Bulletin of Canadian Petroleum Geology*, v. 36, p. 309-324.
- Johnson, K.S., 1989, Salt dissolution, interstratal karst and ground subsidence in the northern part of the Texas Panhandle; in B.F. Beck, ed., *Engineering and Environmental Impacts of Sinkholes and Karst*: A.A. Balkema, Rotterdam, p. 115-121.

- Johnson, K.S., 2003, Evaporite-karst problems in the United States; in K.S. Johnson and J.T. Neal, eds., Evaporite karst and engineering/environmental problems in the United States: Oklahoma Geological Survey Circular 109, p. 1-20.
- Kaus, B.J.P., and Y.Y. Podladchikov, 2001, Forward and reverse modeling of the three-dimensional viscous Rayleigh-Taylor instability: *Geophysical Research Letters*, v. 28, p. 11095-11098.
- Korphage, M., 2006, personal communication.
- Landes, K.K., and T.B. Piper, 1972, Effect upon environment of brine cavity subsidence at Grosse Ile, Michigan, 1971: Solution Mining Research Institute and BASF Wyandotte Corp.
- Last, N.C., 1988, Deformation of a sedimentary overburden on a slowly creeping substratum (Innsbruck 1988); in G.S. Swoboda, ed., *Numerical Methods in Geomechanics: A.A. Balkema*, Rotterdam, p. 577-585.
- Le Comte, P., 1965, Geological notes—Creep in rock salt: *Journal of Geology*, v. 73, n. 3, p. 469-483.
- Lehner, F.K., 2000, Approximate theory of substratum creep and associated overburden deformation in salt basins and deltas; in F.K. Lehner and J.L. Urai, eds., *Aspects of Tectonic Faulting*: Springer-Verlag, Berlin, p. 21-47.
- Lohmann, H.H., 1972, Salt dissolution in subsurface of British North Sea as interpreted from seismograms: *AAPG Bulletin*, v. 56, p. 472-479.
- Lohmann, H.H., 1979, Seismic recognition of salt diapirs: *AAPG Bulletin*, v. 63, p. 2079-2102.
- Mart, Y., and D.A. Ross, 1987, Post-Miocene rifting and diapirism in the northern Red Sea: *Marine Geology*, v. 74, p. 173-190.
- Martinez, J.D., K.S. Johnson, and J.T. Neal, 1998, Sinkholes in evaporite rocks: *American Scientist*, v. 86, p. 38-51.
- McLin, S.G., 1986, Evaluation of aquifer contamination from salt water disposal wells: *Proceedings of the Oklahoma Academy of Science*, v. 66, p. 53-61.
- Miller, R.D., 2003, High-resolution seismic-reflection investigation of a subsidence feature on U.S. Highway 50 near Hutchinson, Kansas; in K.S. Johnson and J.T. Neal, eds., Evaporite karst and engineering/environmental problems in the United States: Oklahoma Geological Survey Circular 109, p. 157-167.
- Miller, R.D., and R. Henthorne, 2004, High-resolution seismic reflection to identify areas with subsidence potential beneath U.S. 50 Highway in eastern Reno County, Kansas: *Proceedings of the 55th Highway Geology Symposium*, September 8-10, Kansas City, Missouri, 29-48.
- Monroe, W.H., 1970, A glossary of karst terminology: U.S. Geological Survey, Water-Supply Paper 1899, 26 p.
- Munson, D.E., 1979, Preliminary deformation-mechanism map for salt: Sandia National Laboratories, Albuquerque, New Mexico, Report SAND 79-0076, 37 p.
- Munson, D.E., and P.R. Dawson, 1982, A transient creep model for salt during stress loading and unloading: Sandia National Laboratories, Albuquerque, New Mexico, Report SAND 82-0962, 55 p.
- Munson, D.E., D.J. Borns, M.K. Pickens, D.J. Holcomb, and S.E. Bigger, 1995, Systems prioritization method—Iteration 2 baseline position paper: *Rock mechanics—Creep*,

- fracture, and disturbed rock zone (DRZ): Sandia National Laboratories, Albuquerque, New Mexico.
- Neal, J.T., 1995, Supai salt karst features: Holbrook basin, Arizona; in B.F. Beck, ed., *Karst Geohazards*: A.A. Balkema, Rotterdam, p. 53-59.
- Neal, J.T., 2003, Sinkholes above the U.S. Strategic Petroleum Reserve Storage Site at Weeks Island salt dome, Louisiana: Recognition, diagnostics, and remediation; in K.S. Johnson and J.T. Neal, eds., *Evaporite karst and engineering/environmental problems in the United States*: Oklahoma Geological Survey Circular 109, p. 347-353.
- Newton, J.G., 1987, Development of sinkholes resulting from man's activities in the eastern United States: U.S. Geological Survey Circular 968, p. 1-54.
- Nieto, A.S., D. Stump, and D.G. Russell, 1983, A mechanism for sinkhole development above brine cavities in the Windsor-Detroit area: Sixth International Symposium on Salt, v. 1, Salt Institute, p. 351-367.
- Ottom, J.K., and R.A. Zielinski, 2003, Produced water and hydrocarbon releases at the Osage-Skiatook petroleum environmental research sites, Osage County, Oklahoma—Introduction and geologic setting; in K. Sublette, ed., 9th Annual International Petroleum Environmental Conference: Albuquerque, New Mexico, October 22-25, 2002, IPEC, 39 p.
- Palmer, A.N., 1991, Origin and morphology of limestone caves: *Geological Society of America Bulletin*, v. 103, p. 1-21.
- Parker, J.M., 1967, Salt solution and subsidence structures, Wyoming, North Dakota, and Montana: *AAPG Bulletin*, v. 51, p. 1929-1947.
- Poliakov, A.N.B., Y. Podladchikov, and C. Talbot, 1993, Initiation of salt diapirs with frictional overburdens: Numerical experiments: *Tectonophysics*, v. 228, p. 199-210. [p. 3-6]
- Priesnitz, K., 1969, Über die Vergleichbarkeit von Lösungsformen auf Chlorid- Sulfat- und Karbonatgestein: Überlegungen zu Fragen der Nomenklatur und Methodik der Karstmorphologie: *Geol. Rundschau*, v. 58, p. 427-438.
- Sawin, R.S., and R.C. Buchanan, 2005, Salt in Kansas: Kansas Geological Survey, Public Information Circular 21, 4 p.
- Scoffin, T.P., 1987, *An Introduction to Carbonate Sediments and Rocks*: Blackie and Son Ltd., Glasgow, 274 p.
- Spiers, C.J., P.M.T.M. Schutjens, R.H. Brzesowsky, C.J. Peach, J.L. Liezenberg, and H.J. Zwart, 1990, Experimental determination of constitutive parameters governing creep of rock salt by pressure solution, deformation mechanisms, rheology, and tectonics; in R.J. Knipe and E.H. Rutter, eds., *The Geological Society Special Publication*: Geological Society, London, v. 54, p. 215-227.
- Spinazola, J.M., J.B. Gillespie, and R.J. Hart, 1985, Ground-water flow and solute transport in the Equus beds area, south-central Kansas, 1940-1979: U.S. Geological Survey Water-Resources Investigations Report 85-4336, 68 p.
- Stokes, W.L., 1982, Geologic comparisons and contrasts, Paradox and Arapien basins; in D. Nielson, ed., *Overthrust Belt of Utah*, 1982 Symposium and Field Conference: Utah Geological Association Publication 10, p. 1-11.
- Strum, S., 1999, Topographic and hydrogeologic controls on sinkhole formation associated with quarry dewatering; in B.F. Beck, A.J. Pettit, and J.G. Herring, eds., *Hydrogeology and Engineering Geology of Sinkholes and Karst—1999*: Balkema, Rotterdam, p. 63-66.
- Surjik, D.L., and G.D. Hobson, 1964, An example of prairie-evaporite mapping in the Minton area of Saskatchewan employing the seismic method: *Geophysics*, v. 29, n. 6, p. 951-956.

- Swenson, R.E., 1967, Trap mechanics in Nisku Formation of northeast Montana: *AAPG Bulletin*, v. 51, p. 1948-1958.
- Thoms, R.L., and R.M. Gehe, 2000, A brief history of salt cavern use: Proceedings of the 8th World Salt Symposium, May 7-11, 2000, R.M. Geertman, ed., Elsevier, The Hague, The Netherlands, 1400 p.
- Trusheim, F., 1960, Mechanism of salt migration in northern Germany: *AAPG Bulletin*, v. 44, p. 1519-1540.
- Urai, J.L., C.J. Spiers, H.J. Zwart, and G.S. Lister, 1986, Weakening of rock salt by water during long-term creep: *Nature*, v. 324, p. 554-557.
- van Keken, P.E., C.J. Spiers, A.P. van den Berg, and E.J. Muzyert, 1993, The effective viscosity of rock salt: Implementation of steady state creep laws in numerical models of salt diapirism: *Tectonophysics*, v. 225, p. 457-476.
- Vendeville, B.C., and M.P.A. Jackson, 1992a, The rise of diapirs during thin-skinned extension: *Marine and Petroleum Geology*, v. 9, p. 331-353.
- Vendeville, B.C., and M.P.A. Jackson, 1992b, The fall of diapirs during thin-skinned extension: *Marine and Petroleum Geology*, v. 9, p. 354-371.
- Walters, R.F., 1978, Land subsidence in central Kansas related to salt dissolution: Kansas Geological Survey Bulletin 214, 82 p.
- Walters, R.F., 1991, Gorham oil field: Kansas Geological Survey Bulletin 228, 112 p.
- Waltham, A.C., 1989, *Ground Subsidence*: Blackie, Glasgow, 202 p.
- Waltham, A.C., and P.G. Fookes, 2003, Engineering classification of karst ground conditions, *Quarterly Journal of Engineering Geology and Hydrogeology*, v. 36, p. 101-118.
- Waltham, T., F. Bell, and M. Culshaw, 2005, *Sinkholes and Subsidence: Karst and Cavernous Rocks in Engineering and Construction*: Praxis Publishing Ltd., Chichester, UK, 382 p.
- Watney, W.L., and S.E. Paul, 1980, Maps and cross sections of the Lower Permian Hutchinson salt in Kansas: Kansas Geological Survey Open-file Report 80-7, 10 p., 6 plates, map scale 1:500,000.
- Watney, W.L., J.A. Berg, and S. Paul, 1988, Origin and distribution of the Hutchinson salt (lower Leonardian) in Kansas: Midcontinent SEPM Special Publication No. 1, p.113-135.
- Watney, W.L., S.E. Nissen, S. Bhattacharya, and D. Young, 2003, Evaluation of the role of evaporite karst in the Hutchinson, Kansas, gas explosions, January 17 and 18, 2001; in K.S. Johnson and J.T. Neal, eds., *Evaporite karst and engineering/environmental problems in the United States*: Oklahoma Geological Survey Circular 109, p. 119-147.
- Wawersik, W.R., and D.H. Zeuch, 1986, Modeling and mechanistic interpretation of creep of rock salt below 200°C: *Tectonophysics*, v. 121, n. 2-4, p. 125-152.
- White, W.B., 1988, *Geomorphology and Hydrology of Karst Terrains*: Oxford University Press, New York, 464 p.
- White, W.B., 1999, Karst hydrology: Recent developments and open questions; in B.F. Beck, A.J. Pettit, and J.G. Herring, eds., 1999, *Hydrogeology and Engineering Geology of Sinkholes and Karst—1999*: A.A. Balkema, Rotterdam, p. 3-21.
- Yiechieli Y., D. Wachs, M. Abelson, O. Crouvi, V. Shtivelman, E. Raz, and G. Baer, 2003, Formation of sinkholes along the shore of the Dead Sea—Summary of the first stage of investigation: Proceedings of the 9th multidisciplinary conference, Sinkhole and the Engineering and Environmental Impacts of Karst, p. 184-494.

CHAPTER 4

SUBSIDENCE PROCESSES

Geologic and hydrologic conditions and processes supporting upward migration of a solution void to the ground surface are developed in this chapter. From the upcoming discussions a reasonable understanding will be gained into the types of subsurface conditions necessary to propagate void roof failure through the overburden and to the ground surface as a result of salt dissolution. This chapter covers a variety of topics that could or do play a role in overburden subsidence, focusing on settings amenable to sinkhole development. Topics will include subsidence as a result of void development in salt, stress regimes and strain geometries, failure mechanisms and rates, sinkhole varieties, and hazards resulting from sinkhole development, expected and unexpected.

Key points to take away from discussions in this chapter will be the characteristics of and controls on various failure scenarios and their associated changing stress fields as a collapse structure matures. Ultimately, this chapter lays the groundwork for future incorporation of seismic images with physical models and characteristics of actual sinkholes in the development of empirically based, conceptually developed models. These models will help predict failure rates and growth geometries, thereby constraining estimates of hazard potential for existing sinkholes or yet-to-form sinkholes resulting from solution void collapse.

Subsidence

Subsidence can be gradual settling or sudden sinking due to subsurface movement of earth materials. Sags and sinkholes are types of subsidence generally related to void collapse (Peng, 1992). *Sags* are generally closed depressions with small settlement slopes. *Sinkholes*, on the other hand, are usually characterized as ground surface depressions with near-vertical walls defining the closed perimeter of a subsurface chimney feature that can be directly linked to the original collapse void. Not all sags or sinkholes are circular. Surface subsidence features resulting from failure of elongated solution voids such as occur in multiwell solution mining operations, will generally produce trough-like depressions (Nieto et al., 1983). Synonymous with the term sinkhole is the Slovene word *doline*, which simply means a closed depression or sinking landform. *Doline* is standard terminology in Europe whereas sinkholes and sag have dominated the literature in the U.S.

Dolines are known to form in almost every area on the planet underlain by evaporites (Martinez et al., 1998). Evaporite sinkholes can only form when four criteria are met: salt or gypsum present, available unsaturated water, fluid inlet and outlet, and energy for water to flow from inlet through the system and exit through the outlet. Missing from this criteria list is duration of fluid exchange. These four criteria must be met long enough for void growth to expose a span of roof rock large enough to exceed overburden strength. Following initial roof failure, the flow dynamics must adjust sufficiently to overcome obstacles or restrictions caused by collapse materials inhibiting the fluid exchange system.

Surface expressions are generally sags for gradual settlement cases (Cording, 2006). These features can be comparably small in areal extent when salt depths are relatively shallow, but with deeper troughs (higher slope angles) than commonly observed when the salt is deeper in the section. Gradually developing sags are by far the most common form of surface depression. The characteristic bowl-shaped geometry of a sag extends outward from the center of the subsurface void a distance defined by the angle of draw relative to the edge of the collapse void (Figure 4-1) (National Coal Board, 1975). When fully mature, sags will consume ground outside the immediate footprint of the disturbed salt zone. The diameter of this fully mature trough can be estimated from an empirical relationship between overburden properties, void depth, and areal extent of the void. The maximum diameter of a surface sag is defined by the angle of draw, dimensions of the dissolution void, and composition and thickness of overburden.

The angle of draw is an empirically defined value predominantly influenced by the rock properties between the void and ground surface. Some dependence on type of void has been observed in cases of mine collapse, but that dependence is more likely related to characteristic mine geometries, host rocks, and ore removal practices of the different mining methods and target resources (Table 4-1) rather than the opening itself. Preferential formation of sags versus sinkholes appears to be predominantly dependent on failure mechanisms and pre-failure void geometry and dimensions.

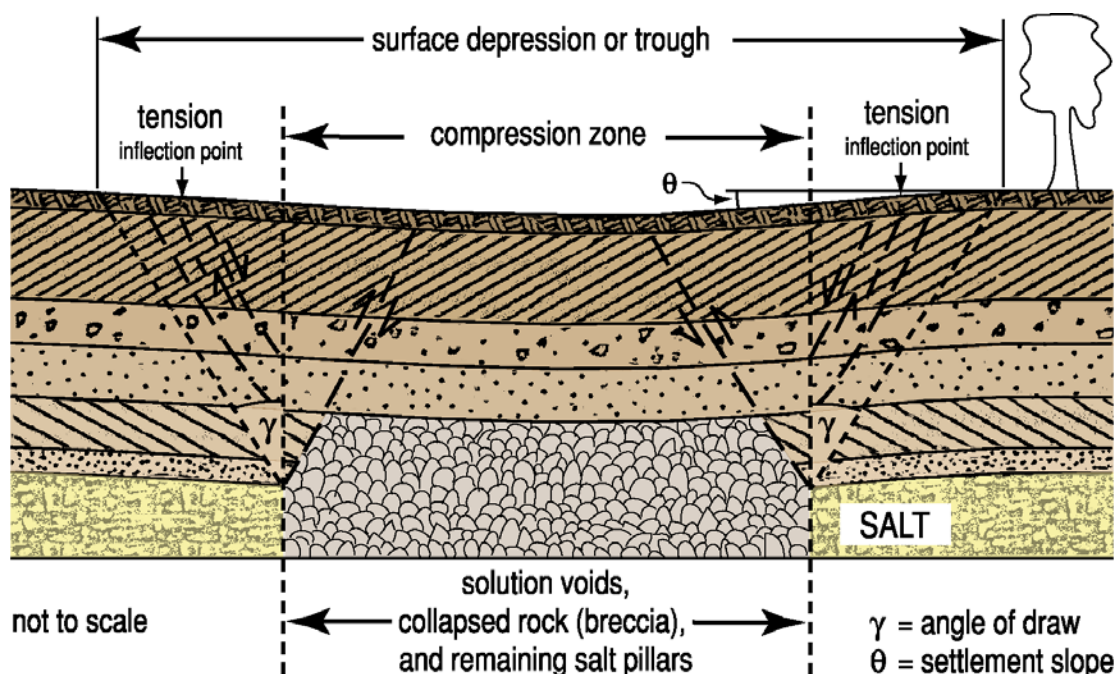


Figure 4-1. Cross section of the anatomy of a subsidence trough showing angle of draw, compression zone, tension zone, and inflection points for a sag feature.

Table 4-1. Angle of Draw of Surface Settlement Profiles and Sinkholes for Various Underground Openings, Based on Settlement Observations

Void	Void Depth	Typical Maximum Surface Settlement	Angle of Draw	Comments
Tunnels in Clay	Typically 10 to 30 m	1 to 6 cm	35° to 45°	Angles of draw for rock will be lower than for clays or sands
Tunnels in Sand	Typically 10 to 30 m	1 to 6 cm	20° to 30°	
Illinois Coal Mines, room and pillar	40-50 m	0.3 to 1 m	33°, 0°, 23°, 22°	Angles of draw are high because of large amount of soil cover
Illinois Coal Mines, room and pillar retreat, and longwall	175 m; Pennsylvanian sh, ss, ls	1 to 1.5 m	10° and 1°	
Room and Pillar Mines in Shale for Propane Storage	125 m; Cavern width: 125 m	1 to 2 m	10° to 15°	Flat bottom of settlement trough and circumferential cracks near edge of the cavern footprint
Long-wall Coal Mines, UK (National Coal Board, 1975)	300 to 500 m; Width = ½ to 1 x depth	1 m	11° to 12°	Based on design charts

Source: Modified from Cording, 2006.

Stress Distribution

As the roof span of a void increases, the stress field enlarges consistent with the tensional dome (Davies, 1951) (Figure 4-2). Distortion within the tensional dome (a volume called the “compressional stress zone”) is consistent with a compressional stress environment. As stress increases inside the dome, strain begins to appear as drape or flexure centered on large unsupported spans of roof rock. From structural analysis, failure of roof rock normally occurs under compressional stress and concentrated where that stress is the greatest (Sofianos, 1996). Apparent drape or flexure geometries of individual rock layers in the overburden will eventually migrate toward the ground surface. How this deformation manifests itself on the ground surface is highly dependent on void geometry, physical condition and strength of roof rock, the characteristics and properties of the rocks that make up the entire overburden section (key is mobility of soil materials), and how effectively the dissolution process proceeds.

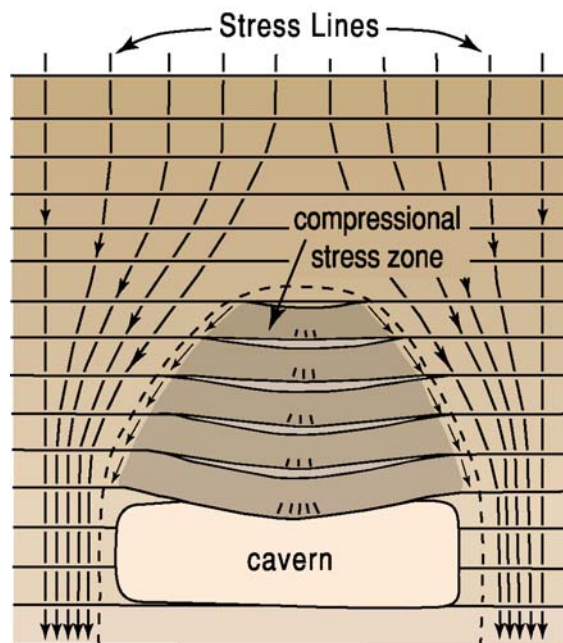


Figure 4-2. Tension dome and distribution of stress lines around a cavern opening in horizontal strata (modified from Davies, 1951).

The load-bearing potential of a void’s roof is strongly dependent on the void’s geometry and roof and pillar material properties. Roof rock can be treated as a beam under flexural stress or an arch in compression (Waltham et al., 2005). Strength of rock is negligible under tension and flexure, but quite high under compression. Therefore, an arched roof geometry provides the greatest roof strength. Rarely does a roof form as unbroken slabs or intact beds; therefore, overburden volumes must be considered fractured rock masses (Kaderabek and Reynolds, 1981). A rock mass above a void is at various stages and under different types of stress depending on location within and structural uniformity of the overburden volume.

Moving upward from the void roof to the ground surface, rock stress changes from tensional to compressional (Figure 4-3). Between the air/rock contact and base of the arch (arch rise), rocks are under tensional stress conditions, which change abruptly within the arch (voussoir) volume where compressional stress concentrates (Waltham et al., 2005). Rocks beneath the arch do not contribute to the load-bearing potential of the roof, and failure of this under-arch rock will occur with little provocation. Above the arch, rocks are under pressure and define what has been previously described as the tensional dome (Davies, 1951). Rocks above the

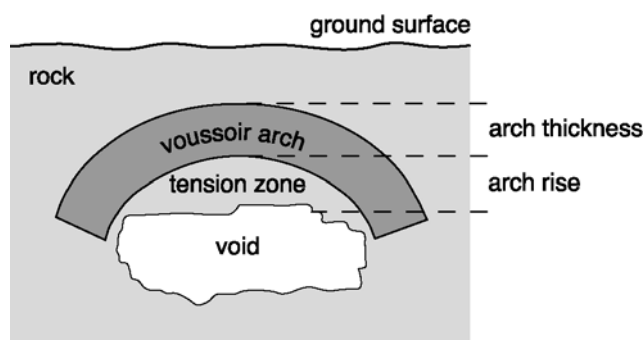


Figure 4-3. Elements of a voussoir arch developed in a fractured rock mass that spans a void (modified from Waltham et al., 2005).

arch constitute the overburden load that is distributed across and must be carried by the arch to avoid failure. Based on structural analysis (Waltham et al., 2005), most void roofs can only be stable if they are treated as an arch under compression and would fail under assumptions of a rock mass under flexural stress (flat-roof load bearing).

Failure of an arched roof under stress (overburden load) will occur when the load exceeds the strength of the arch system or redistribution of load (stress), due to enlargement of unsupported roof span, exceeds strength. Depending on overburden characteristics, failure could involve only the arch and minor amounts of adjacent rock mass or it could constitute complete collapse of the overburden and formation of a sinkhole. When compressional stresses instigate arch failure, brittle rupture will manifest itself along reverse fault planes at the buttress and collapse within the midsection of the arch (Figures 4-4 and 4-5). If only a portion of the overburden collapses, a new arch higher in the section with a reduced span will support the remaining overburden load.

Upward progression of the void's roof is, of course, dependent on the dissolution process and principally influenced by a combination of overburden rock properties and size and shape of the salt void. Void development, resulting geometry, and location within the salt interval dictate which of two processes void migration follows. Migration of roof-rock failure within the tensional dome to the ground surface can be characterized by a column of either breakdown debris called collapse breccia (Figure 4-6) or draping layers of rock that have undergone a series of incremental, short-period slumping events (Figure 4-7).

In the case of collapse breccia, the volume and randomness of rubble is an unmistakable remnant of roof stoping or raveling of cavity walls indicative of caprock or collapse-type failure (Figure 4-6) (Waltham et al., 2005). Throughout North America more than 5000 breccia pipes exist over salt and gypsum deposits (Quinlan et al., 1986). Breccia

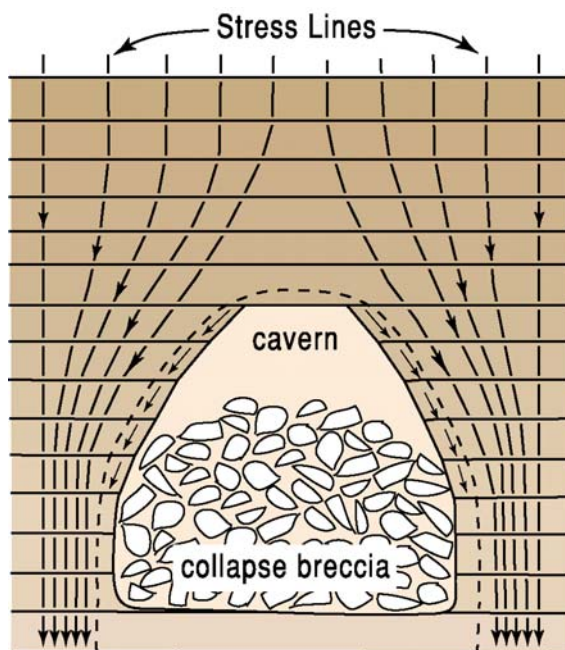


Figure 4-4. Collapse breccia form after failure of roof rocks along tensional dome maximum-stress lines. When cavern volume is large and height-to-width dimensions are large, stoping-and-raveling-type failure dominates (modified from Davies, 1951).

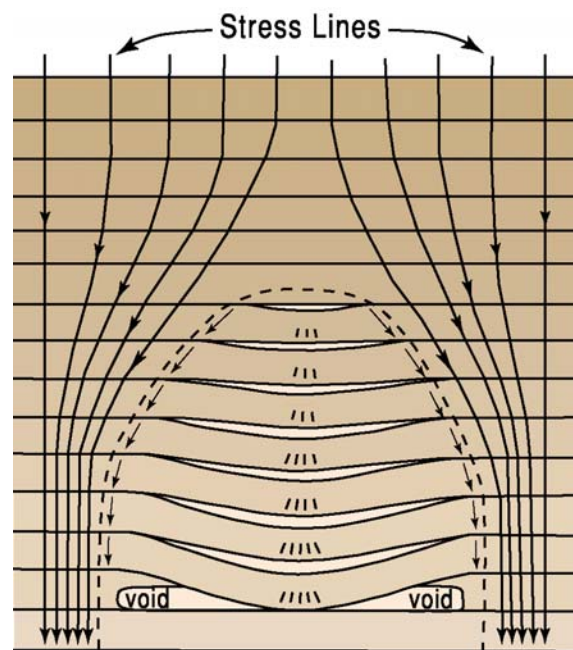


Figure 4-5. Overburden failure for small vertical-to-horizontal dimensions of a void. Layers fail in a more plastic-appearing fashion. However, this being a brittle deformation environment, small-scale fractures and faults likely define this collapse (modified from Davies, 1951).

pipes are the rubble material collapsing or stoping from the roof of an upward-migrating void left after surface subsidence occurs. These roof-rock failure remnants are outstanding indicators of ancient subsidence (Waltham et al., 2005). When a breccia pipe reaches the surface during progressive subsidence, it is many times associated with a very modest depression. Caprock failure is the primary subsidence mechanism producing breccia pipes. Natural dissolution of evaporites buried beneath rock characterized by brittle failure and sediment collapse via stoping or raveling will have these characteristic features.

When compressional stress on a layer exceeds the rock strength for the case of a more horizontal advancing (spreading) dissolution front (draping incremental strain), that layer will rupture and tear away from the rock mass above, subsiding into the available void space (Figure 4-5). Assuming the roof span is wide relative to the height (volume), downwarping (vertical displacement) of the rock layers will only extend over a short distance (maybe on the order of a few meters). Once this brittle failure has occurred, a series of micro-faults (reverse orientation) and fractures will define the compressional portion of the subsidence field. Likewise, a series of very small-scale normal faults will define the tensional zone. Each subsequent layer from top down subsides deeper and deeper into the void, with gradual, continued vertical or horizontal growth acting in response to the harvesting of salt along the dissolution front. Overall this process consumes salt stock as a somewhat hemispherical dissolution front moving predominantly downward toward the basal contact of the salt. With sufficient void development, surface failure occurs as a sag or sinkhole (Figure 4-7). This process can be either continuous through time or sporadic reactivating intermittently, coincident with the availability of water at the salt face.

With the site-specific, irregular nature of the entire dissolution process along the natural front as well as at failed well sites, changes in the characteristics of the tensional dome and stiffness of each rock layer exposed during stoping can alter the subsidence processes. Overburden loading (stress field) on the void roof and pillars (tensional dome) and volume of the sump dictate the dynamics (rate and volume) of void-space propagation from the salt interval to the bedrock surface.

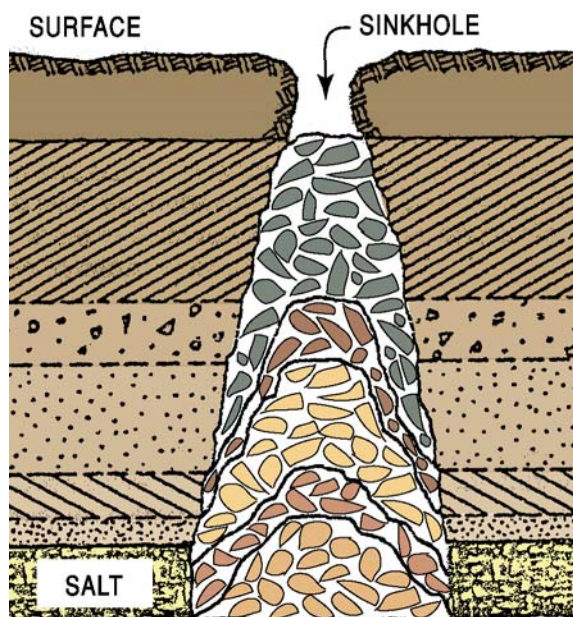


Figure 4-6. Sinkhole subsidence feature with segregated rock layers made up of collapse breccia.

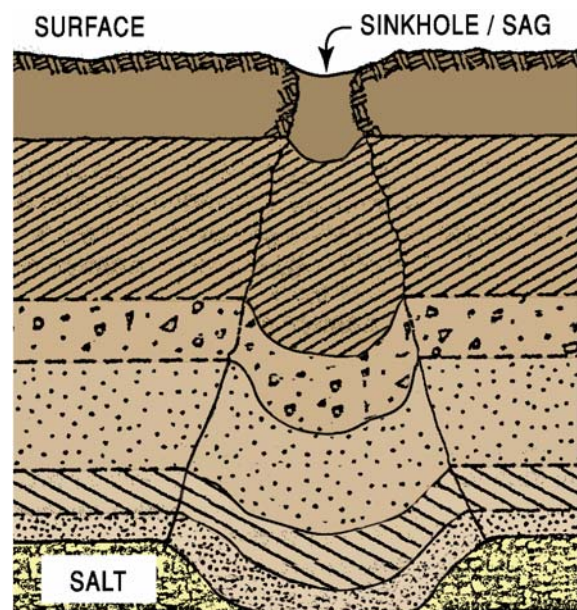


Figure 4-7. Gradational collapse within the tensional dome, resulting in slumping of layers into thin, laterally extensive voids.

Besides the obvious dependence on rock properties, growth of the tensional dome is influenced by the void geometry and dissolution dynamics. As discussed in the previous chapter, dissolution at the early stages of void development is principally controlled by the availability of salt, efficiency of fluid exchange within the system, and ratio of salt to insoluble layer thickness. The thickness of salt-to-insoluble interbedding is one factor that directly affects the overall void space available to act as a sump for collapsed overburden materials or lag. Once strain has propagated throughout the overburden, breaching the bedrock surface, rock layers within the overburden will retain little or no bulk strength. Continued dissolution-induced subsidence within the salt interval will gradually propagate to the ground surface under gravity/compaction drive. The dissolution dynamics as well as overburden rock properties dictate the dimensions of the affected rock mass and growth characteristics of the tensional dome.

Which of these two uniquely different subsidence mechanisms will occur at a given site depends on overburden rock properties, void geometry, and the stress field (tensional dome). Seismically these two distinctly different kinds of subsidence features have uniquely different signatures. Stopping-and-raveling subsidence structures have a more chaotic failure zone, which represents the collapse breccia within the chimney-like structure (Figure 4-8b), while the stopping/drape structure appears as a series of continuous synforms widening as they propagate to the ground surface (Figure 4-8a).

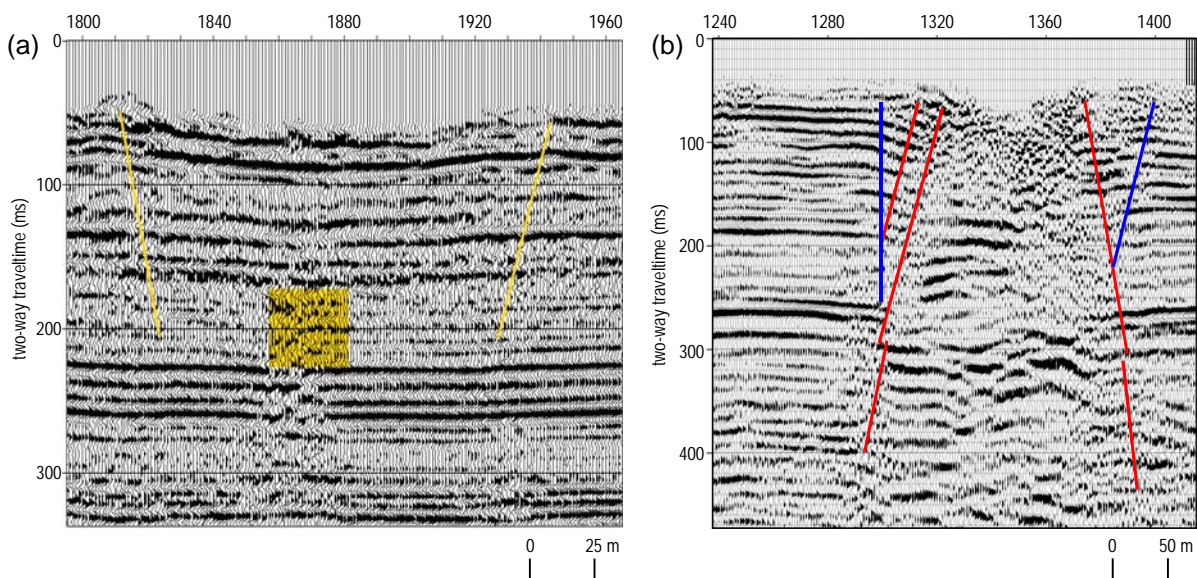


Figure 4-8. (a) CMP-stacked section from Reno County, Kansas, with drape-type subsidence of Permian shale layers above the salt interval between 150 and 210 ms, and (b) CMP-stacked section from Russell County, Kansas, with stopping-and-raveling-style subsidence resulting in a subsidence cone full of material more closely resembling collapse breccia.

Failure Mechanisms

Rock failure in response to collapse of salt-dissolution voids, subsequent subsidence of overburden, and sinkhole formation clearly have two critical controlling components: characteristics of the salt void and overburden rock and soil properties. Void geometry and location within the salt dictates not only the risk of roof-rock failure, but also the vertical growth potential and formation rate of a collapse feature. Foremost, void stability is not threatened until the unsupported roof span exceeds the strength potential of the roof rock.

As well, the void volume and geometry after the leaching of salt must have the capacity and dimensions necessary to act as the sump for overburden material (spoils) stoping or slumping from the void ceiling. Under the more plastic-appearing deformation scenario, void height must be sufficient to accommodate draping of the roof layers, which continues with increasing overburden layer sag as salt is leached away.

Overburden properties dictate the maximum prefailure dimensions of a void's unsupported roof span, the rate of stoping, type of roof deformation, and the potential for arresting the vertical progression of the void. As previously discussed, thickness of the overburden, structural features within the overburden, and lithologic make-up of the overburden contribute in defining the spatially variable sequence of stress and strain relationships. These relationships are instrumental in both defining the rupture characteristics of a particular void's roof and those of the surrounding materials. Deformation of overburden above dissolution voids in most salt basins around the world can be constrained to models for consolidated sedimentary rocks in a low-pressure environment.

Brittle failure generally occurs in response to stress in a low-pressure geologic setting prior to the occurrence of any significant plastic deformation (Carmichael, 1989; Billings, 1972). Tensional, compressional, or shear stress can instigate brittle rock failure and result in a variety of structural features. Subsidence structures associated with a void possess two clearly separate and physically distinct stress fields (Figure 4-1). The presence of both compressional and tensional stress fields is normal during the development of collapse structures. Considering the diametrically opposing characteristics of these two stress relationships, it is unlikely that for a given feature both have equal influence at any point in time. Considering materials have much greater compressional strength than tensional and that roof failure normally occurs under compressional stress, roof-rock failure will reach the surface (bedrock) driven by the compressional stress field (Sofianos, 1996). Once the overburden is fully breached and compressional stresses have dissipated, hanging walls will then begin to undergo strain consistent with remaining tensional stress.

Gradually settling rock layers within the overburden appear on some seismic sections (e.g., Figure 4-8a) to widen upward toward the ground surface in a fashion seeming to violate the previously described basic premise of how strain in these structures is manifested based on the relative pressure environment and stress field. Compressional and tensional portions of the overburden volume above and in proximity to the void should deform by brittle failure defined by reverse faults in the compressional zone and normal faults in the tensional zone. Confusing is what appears to be ductile-looking deformation interpretable on the seismic data (Figure 4-8a). Plastic or ductile deformation, however, is associated with high-pressure settings.

After roof rock fails above horizontally elongated, relatively thin voids (void heights are extremely small), strain can appear plastic on seismic sections without any evidence of rupture in rock layers immediately above the void. Seismic-reflection images of subsidence features interpreted to possess plastic or ductile deformation (Steeple et al., 1986; Miller et al., 1985) are inconsistent with the stress environment and are an artifact of insufficient spatial and vertical resolution. With increasing stress conditions ductile rocks pass the elastic limit and display strain as plastic deformation (Billings, 1972). Rocks that deform ductilely are generally associated with high confining pressures and result in structures with fold-type geometries (Carmichael, 1989). Strain on rock layers beyond the limit of plastic deformation manifests itself as rupture. Therefore strain in this setting is brittle by nature, characterized

by small-scale faults and fractures clearly below the fidelity of the seismic data to distinguish the segments in the caprock's bowl-shaped appearance.

Model studies have shown that subsidence of planar salt beds is smooth, with uniform formation of bowl-like structures generally defined areally as circular to subcircular depressions similar to limestone karst sinkholes (Ge and Jackson, 1998) (Figure 4-9). However, due to the materials used in this physical model to simulate brittle overburden and ductile salt, it is unlikely faults will be evident in some post-drain models. It is possible to generally interpret reverse and normal fault geometries consistent with the subsidence trough that are based on the relative orientation of the bedding and abrupt changes in dip in the settlement zone (Figure 4-1). Faulting and fracturing are likely below the visual resolution provided by this model and are not apparent due to material choices and differences between in situ leaching of salt and a drain-style physical model.

Bed geometries resembling ductile deformation, synonymous with high-pressure settings, seem to be consistent with sags. However, when bed offsets are dramatic, their brittle deformation nature is obvious on seismic data and generally associated with sinkholes. The compressional part of the stress field is defined by reverse faults extending from the cavern/void walls to the ground surface in a chimney-type feature (Figure 4-9). The tensional part of the stress field manifests itself as normal faults ultimately extending out from the wall or edge of the cavern/void consistent with the angle of draw. Sag is a relatively slow process with strain predominantly in the form of tilt rather than angular distortion with lateral extension strains near the outer portion of the settlement feature represented by circumferential tension cracks (Figure 4-10) (Cording, 2006).

Rocks in the overburden susceptible to brittle deformation can experience minimal and very localized plastic distortion but generally, no significant plastic strain occurs prior to rupture (Billings, 1972). In situations that involve voids where brittle roof-rock materials are under stress exceeding the limits of plastic deformation and therefore material strengths, rupture can take many forms including stoping, fracturing, faulting, separation along bedding planes or stratifications, block failure and collapse, discrete layer tilt (torsion), and combinations of types. Elevated stress acting on materials susceptible to brittle failure in a low-pressure environment will generally rupture as faults and/or fractures (Carmichael, 1989).

By definition, roof rock of a void or cavern lacks continuity and uniformity in basal support with pillars or walls acting to carry the overburden load in harvested areas. Unsupported spans of roof-rock materials/ layers under increasing stress due to an enlarging void volume display strain elastically, then plastically, and finally brittle deformation with distension and separation from the surrounding rock. Because most collapse

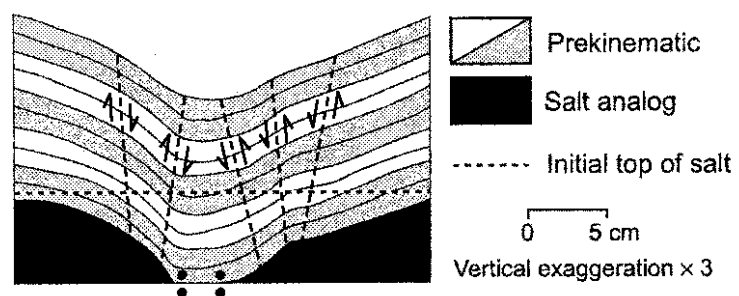


Figure 4-9. Sand and special flowing silicon were used to model deformation from salt dissolution. Silicon, simulating salt, was drained from the bottom of the test tank to allow observation of deformation in brittle overburden (sand simulates brittle rock in this design) (modified from Ge and Jackson, 1998). Vertical exaggeration provides a view of the relative bed geometries and potential micro-fracturing and faulting interpreted to be consistent with the stress model that are likely below the resolution and material potential of this model.



Figure 4-10. Macksville sinkhole in Pawnee County, Kansas, formed catastrophically with the initial chimney-like structure eventually widening in the form of sag forming these tensional tear zones and normal fault-controlled blocks forming terrace-like surface structures (photo by R. Miller).

structures associated with rocks overlying evaporite dissolution features are at relatively shallow (upper few kilometers) depths in sedimentary rock settings, they are in a low-pressure environment and therefore experience brittle material deformation with little or no plastic deformation.

In general, evaporite voids exist in a relatively low-pressure setting and therefore rupture resulting from an excessive span of unsupported roof rock should, under “normal” conditions, be brittle. Broad synfold-like structures inconsistent with brittle deformation appear representative of many subsidence features interpreted on seismic data in this manuscript. As previously noted, the ductile appearance of these subsidence-related structures on seismic sections is an artifact of limited seismic resolution where displacement occurs over a zone that likely includes a multitude of small fracture or fault features. Minimal bed displacement associated with an individual fault or fault zone, bed warping due to small fracture zones, or a series of joint segments would not be distinguishable as individual events on seismic data, but rather smeared horizontally and vertically into what appeared to be a more uniform and continuous fold-type structure.

Once dissolution and resulting subsidence of the overburden have migrated to the ground surface, continued dissolution of salt within the subsidence zone will grow a stress field dramatically different than the initial tensional dome. It seems obvious with failure mechanisms predominantly controlled by the competence of the overburden, once failure occurs and a subsidence trough forms in the overburden, little or no compressional strength would remain in overburden rocks. It would be reasonable to suggest subsidence will,

therefore, migrate upward as an ever-widening bowl-shaped depression much closer to gravity settling and tensional stress environments. A key aspect of subsidence features in salt is their localized nature and generally three-dimensional circular collapse structures. Therefore, when the collapse feature at the bedrock surface possesses a small radius, stress can distribute around the perimeter of this collapse structure, allowing some compressional strength to be maintained in spite of the breach in bedrock surface and the “keystone” missing in the arch (Figure 4-2). This open dome structure can be mechanically stable for a maximum opening size dependent on the overburden material and collapse dimensions (Han and Liu, 2002).

Large-scale faulting and bed rotation or collapse within the overburden correlated to dissolution void failure at or above the resolution limits of seismic data appear predominantly brittle in nature. Ductile-appearing strain apparent in the overburden materials on seismic sections is only possible if deformation is still below the plastic limit, in which case a continuous synform is an accurate interpretation. Plastic strain as an interpretation of these ductile-appearing subsidence structures, however plausible, is highly unlikely to very near impossible.

Stress on roof/wall contacts of a stable void volume increases exponentially when the ratio of void space to pillar volume exceeds 60 to 70 percent, thereby increasing the failure potential (Galvin, 2002). Rock strength decreases over time and under load (Galvin, 2002). Voids within rock that are near the strength limits of the roof rock will eventually fail.

Failure Rates

Surface subsidence rates due to the collapse of dissolution voids and overburden are strongly influenced by the failure mechanisms, void dimensions, and overburden rock properties. Significantly different development processes can result in similar sinkhole characteristics, but with formation rates that vary across a wide range. With the reasonably well-established presence of a stress field reversal along an imaginary upwardly projected cylinder consistent with the void walls (Figure 4-1), it is reasonable to suggest that failure rates for a single sinkhole can change depending on the relative stage of subsidence. Empirically based analysis suggests the volume of affected material within a hollow cone defined by the angle of draw will subside gradually, whereas within the compressional stress volume of overburden (dome or inverted cone) failure rates can range from gradual to catastrophic (Cording, 2006).

The greater the vertical dimension of the dissolution volume relative to the horizontal pre-caprock-failure, the greater the chances for rapid vertical migration of the void through the overburden, resulting in the formation of a surface collapse feature and an associated breccia chimney (Figure 4-6). For relatively rapid migration of the dissolution void to the ground surface, a large sump is necessary to accommodate overburden stoping from the top and sides of the void (Figure 4-4). Contrasting that, gradual subsidence only requires the inlet and outlet (drain) remain open long enough for salt removal to expose a sufficient span of unsupported roof rock to instigate collapse. Under this more gradual scenario, incremental draping or collapse of small volumes of the overburden continues with void growth resulting in a gentle surface sag feature (Figure 4-7).

When sinkhole formation is rapid, initial development is confined to the compressional zone. Catastrophic or rapid failure requires a void to grow to sufficient vertical dimensions and throat capacity to accommodate the overburden material that stopes

down from the ceiling and sifts in from above bedrock surface through the subareal throat. For a sinkhole to form or open rapidly, material at and near the ground surface must move/flow with little resistance into a void (sinkhole throat) that has propagated from the soluble rock formation to very near the ground surface. The ability of the void to act as a sump, the capacity of that sump, and the thickness and flowability of the unconsolidated material over the void dictates the size of the sinkhole after catastrophic failure. The more salt leached prior to initial failure, the greater the potential for catastrophic sinkhole development. This rapid movement of soft sediments into the throat of the collapse structure represents a far greater hazard than the actual narrow opening in bedrock that represents the initial collapse feature.

A salt void capable of supporting rapid sinkhole development in Kansas must have a sump of sufficient volume and vertical extent to accommodate all the bulk or lag generated as stoping proceeds from the salt through the overburden to the ground surface. With the Hutchinson Salt Member generally between 90 and 125 m thick in most places around the state, a solution void that originated near the basal contact of the salt interval, once fully developed, would have the potential for rapid sinkhole development (Watney et al., 1988). The overburden in most areas where the Hutchinson Salt Member is present is less than 400 m thick. The location within the salt interval that dissolution begins, the depth of the salt interval, and the height of the salt void relative to diameter prior to failure of the shale caprock influence the probability that subsidence will proceed in a near-continuous motion to the ground surface. Rapid failure requires the development of a large void with a significant vertical dimension, which is only possible where roof rock possesses adequate compressional strength to be stable across a large span.

Gradual or sag failure results from minimal or no void volume (sump) available when the void subsidence arrives at the ground surface. This most commonly occurs as bulking, which is steady roof failure and associated subsidence that contemporaneously fills the void space created in response to active dissolution in soluble rock. Sag of overburden into void space as it is created via dissolution, if unhalted, can extend the drape characteristics of the roof-rock failure to the ground surface. Reactivation of paleosinkholes is common in areas with natural dissolution potential and structural features (faults, fractures, joints, etc.) that can serve as conduits for water to reestablish contact with the salt. Once rock failure has occurred and subsidence features (faulted or fractured red beds, collapse breccia, etc.) have progressed from the soluble rock to the ground surface, the overburden will not retain sufficient strength to support catastrophic failure. Therefore, areas where subsidence has been responsible for sinkhole development in the past will experience gradual subsidence (gravity settling, sag, drape, etc.) in response to void development in the salt.

Subsidence rates, as previously indicated, are much faster in response to active dissolution of evaporites than carbonates, but the real key to sinkhole-development rates in any setting is less tied to dissolution rates and more related to the overburden lithology and associated strength. Upward movement of voids from their origin to the ground surface progress at rates ranging from seconds to millions of years. Based on accurate subsurface monitoring, a dissolution void moved through 400 m of overburden in just seven months in Russia (Andrejchuk, 2002), and from borehole measurement it was determined a solution void moved 400 m vertically to form a surface expression called the Wink Sink in Texas in 50 years, progressing at a rate of 1 m each 6 weeks (Baumgardner et al., 1982).

Whether gradual or catastrophic, collapse depends on many factors (e.g., dip, stability, homogeneity, fracturing or strength of overlying strata, and speed and direction of the leaching process) (Lohmann, 1972), with no one characteristic in complete control of the process. In geologic time the process is extremely rapid, but in human terms it can seem relatively slow. The high solubility of salt and gypsum permits cavities to form in days to years, whereas cavity formation in carbonate bedrock is a very slow process that generally occurs over centuries to millennia (Waltham et al., 2005).

Sinkhole Varieties

Dissolution, erosion, de-watering, differential ice/permafrost melt, and mining are the principal processes that can produce voids in the earth of sufficient size to instigate overburden subsidence and the formation of sinkholes. Sinkholes are most common where carbonate rocks, rock salt, and coal mines are known to be present in the near surface. Anthropogenic sinkholes, in general, are dwarfed in number and size by natural depression features.

Sinkholes can be divided into six different classes based on failure mechanism and therefore indirectly related to rate of formation (Waltham and Fookes, 2003). Of the six classifications, only four and possibly five are pertinent or applicable to evaporite-dissolution sinkholes. Development rates of evaporite sinkholes could fall under any one or a combination of these classifications. The four clearly applicable are

- dissolution (solution) sinkholes*, which are defined by the gradual lowering or settling of the overburden consistent with the progression of dissolution,
- drop-out sinkholes* result from the formation of large voids beneath stiffer materials until void roof span exceeds material strength and instantaneous collapse results,
- caprock (or cover collapse or collapse) sinkholes* form rapidly as rock layers above the void slope upwards in relation to slowly enlarging voids until the bedrock surface is breeched and soil rapidly fills the void, and
- buried sinkholes*, which form very slowly as changes in near-surface conditions cause ancient or paleosubsidence features to undergo gravitational settlement or reactivation.

One classification that could be interpreted to relate to evaporite dissolution is

- suffusion sinkholes*, which describe subsidence in soil resulting from fluid mobilization into fractures, and which for solution collapse could be an opening at the top of bedrock that accesses a throat above collapse breccia connecting to the dissolution zone.

All these classifications were developed to preferentially describe sinkhole-formation mechanisms associated with carbonate dissolution and therefore lack much of the sensitivity to the speed of dissolution processes in evaporites (rock salt in particular), salt's lack of strength as a roof-rock host, and necessity for an insoluble caprock to separate the evaporite from near-surface water sources.

Engineering classification of karst sinkholes varies based on the complexities and difficulties encountered by foundation engineers (Waltham et al., 2005). Names are related to developmental age and complexity. None of the classification characteristics really relates



Figure 4-11. Sinkhole formed rapidly in association with a coal mine collapse less than 15 m from a main north/south rail line near Scammon, Kansas (photo by D. Steeples).

to evaporite sinkholes, because construction activities rarely if ever actually encounter the areas/volumes where leaching is or has been active. Secondary effects more related to overburden strength and subsidence rates are concerns for foundation engineers in relation to evaporite dissolution. The only real parameter used to classify sinkholes for foundation engineers that is applicable to evaporite sinkholes is distribution density or simply the number of sinkholes per unit area.

Mine collapse and subsidence has resulted in sinkholes around the world and is probably the most common anthropogenic source of sinkholes (Figure 4-11). Dewatering of aquifers or removal of fluid from reservoirs (petroleum production) has resulted in ground subsidence in Texas, California, and South Africa. Internal erosion or piping in levees, dikes, and dams has resulted in sinkholes and represents a threat to the structural stability of these impoundments all over the world (Figure 4-12). Erosion of sediments due to changes in ground-water flow patterns or velocities due to either water removal or natural fluctuations can leave voids of sufficient size to instigate a collapse that forms a sinkhole (Arkin and Gilat, 2000). Insufficient control on dissolution of evaporates during solution mining or uncontrolled dissolution resulting from the loss of well-casing integrity or seal can grow voids large enough to instigate overburden failure and sinkhole development. Solution mining has been responsible for sinkholes around world.

Sinkhole Hazard

Sinkholes are a potential hazard to human activities, infrastructure, and the environment (e.g., Beck et al., 1999; Johnson and Neal, 2003; Waltham et al., 2005; Waltham and Fookes, 2003). Sinkholes represent a risk to life, property and possessions, the environment, and community. Most publicized are sinkholes that interrupt transportation infrastructures



Figure 4-12. Sinkhole with throat extending tens of meters into fill material over impervious core in Bennett Dam, British Columbia, Canada (photo from website). Sinkhole in dam formed from piping of dam fill through karst features in bedrock.

and result in loss of human life (Cobb and Currens, 2001). Pipelines, highways, and rail traffic are all susceptible to ground instability (Kochanov, 1999). Most threatening are sinkholes that form catastrophically and in areas where collapse is either rare or unexpected (Sinclair, 1982) (Figure 4-13). Sinkholes represent a real threat when they affect water-retention facilities and thereby decrease structural integrity and indirectly put life and property at risk downstream (Dewoolkar et al., 2000; Diaz et al., 2000). Least tolerable risk from sinkholes is when it involves threat to life.

Surface risks come in the form of sinkholes and sags. Sinkholes are a potentially immediate threat to safety whereas sags represent a bigger problem for the structural soundness of surface facilities. Risk of rock failure increases when the cover thickness exceeds void width. Most significant in determining risk of sinkhole formation is soil/overburden type, water table, and structures present.

To truly reduce risk from a sinkhole, three components are necessary: risk analysis, risk assessment, and risk management (Fell and Hartford, 1997). Damage from subsidence can range from very slight to total collapse and complete loss. Seismic has proven in this work to be an essential tool for risk analysis and risk assessment, and if used in a time-lapse mode, it could also serve in a limited extent during risk management. Most importantly is the development of an understanding of the process and risk of surface failure at a specific site. In Kansas it is not possible to completely avoid natural subsidence phenomena, but susceptible areas can be identified. As well anthropogenic dissolution and resulting subsidence can be detected prior to surface failure and monitored to maintain an accurate knowledge of the potentially affected subsurface.



Figure 4-13. Catastrophic sinkhole formed without warning in Guatemala in March 2007, killing two people and one person was never found. The sinkhole was 100 m deep with shear walls and about 15 m in diameter (photo from www.cnn.com).

Summing Up and To Come

Key topics covered in this chapter included subsidence, stress distribution, and failure rates and mechanisms as well as sinkhole varieties and hazards. Having gained a general understanding of the various processes and failure characteristics associated with subsidence in this chapter, it is time to move onto seismic-reflection-specific topics as they relate to subsidence. In the next chapter, use of high-resolution seismic reflection for imaging subsidence structures will be the overriding theme of most discussions. Effective use of the seismic-reflection method to delineate collapse features requires maximized resolution and signal-to-noise ratio and a thorough understanding of the detrimental effects rubble or collapse strata can have on seismic velocity and wavelet characteristics. It will be shown how lateral variability in seismic velocities characteristic of these features can be extreme and lead to incorrect interpretations, as well as how attenuative earth and diffractors greatly reduce the effectiveness of the method.

Past attempts by practitioners to image subsidence features with seismic reflection have not always proven effective. Published accounts summarized in the next chapter will highlight some of the problems encountered and successes claimed when trying to image subsidence features in the upper few hundred meters. Contrasting conventional approaches and high-resolution methods clearly reveals significant improvements in resolving power and therefore accuracy of interpreted dissolution structures using a high-resolution approach. Most of the seismic sections displayed in the next chapter have come from published work by other authors in carbonate, glacial, and evaporite settings. In general, the next chapter focuses on historical usage of seismic reflection and attempts to interpret these small-scale, localized, and extremely complex structures.

A detailed critique and associated breakdown of a series of published seismic sections are also incorporated into the next chapter to reinforce the difficulties and pitfalls of working with shallow, high-resolution data. It is essential to maintain an awareness and concern for the uniqueness of the shallow wave field, high-frequency nature of the survey, or low signal-to-noise characteristics of shallow reflection data. Low signal-to-coherent-noise stacked sections have a tendency to entice interpreters into excessive speculation about the coherency and geometry of reflections. Reprocessing by the author unequivocally demonstrates this point. Some of the interpretations displayed in the next chapter lack solid evidence on the original stacked section, but seem reasonably well founded on the reprocessed sections.

References

- Andrejchuk, V., 2002, Collapse above the world's largest potash mine, Ural, Russia: *International Journal of Speleology*, v. 31, p. 137-158.
- Arkin, Y. and A. Gilat, 2000, Dead Sea sinkholes—An ever-developing hazard: *Environmental Geology*, v. 39, n. 7, p. 711-722.
- Baumgardner Jr., R.W., A.D. Hoadley, and A.G. Goldstein, 1982, Formation of the Wink Sink, a salt dissolution and collapse feature, Winkler County, Texas: Bureau of Economic Geology, University of Texas at Austin, Report of Investigations No. 114, 38 p.
- Beck, B.F., A.J. Pettit, and J.G. Herring, eds., 1999, *Hydrogeology and Engineering Geology of Sinkholes and Karst—1999*: Rotterdam, A.A. Balkema, 130 p.
- Billings, M.P., 1972, *Structural Geology*, 3rd ed.: Prentice-Hall Inc., Englewood Cliffs, NJ.
- Carmichael, R.S., 1989, *CRC Practical Handbook of Physical Properties of Rocks and Minerals*: CRC Press, Boston, 741 p.
- Cobb, J., and J. Currens, 2001, Karst: The stealthy hazard: *Geotimes*, May.
- Cording, E.J., 2006, Interim Report: Characteristics of subsidence and sinkholes in salt, Detroit area; A study for the proposed Detroit River International Crossing: E.J. Cording, Geotechnical Consultant.
- Davies, W.E., 1951, Mechanics of cavern breakdown: *National Speleological Society*, v. 13, p. 6-43.
- Dewoolkar, M.M., K. Santichaiant, H-Y. Ko, and T. Goddery, 2000, Effects of sinkholes on earth dams: ASCE Geotechnical Special Publication 101, p. 129-141.
- Diaz, M., L.K. Meeks, and K. Englebrecht, 2000, Assessment and prediction of geologic hazards associated with sinkhole development in karst terrane in Boone County, Missouri [abs.]: Geological Society of America annual meeting, published in *Abstracts with Programs*, v. 32, n. 7, p. 349.
- Fell, R., and D. Hartford, 1997, Landslide risk management; in D.M. Cruden and R. Fell, eds., *Proceedings of the International Workshop on Landslide Risk Assessment, Honolulu*: A.A. Balkema, Rotterdam, p. 51-109.
- Galvin, J., 2002, 6th Kenneth Finlay Memorial Lecture, Oct. 27, University of New South Wales, Australia (<http://www.ferret.com.au/articles/19/0c011F19.asp>).
- Ge, H., and M.P.A. Jackson, 1998, Physical modeling of structures formed by salt withdrawal: Implications for deformation caused by salt dissolution: *AAPG Bulletin*, v. 82, p. 228-250.
- Han, Q., and X. Liu, 2002, Behavior of a single layer spherical dome with openings and large depth-to-span ratio: *Advances in Structural Engineering*, v. 5, n. 3, p. 137-142.
- Johnson, K.S., and J.T. Neal, eds., 2003, Evaporite karst and engineering/environmental problems in the United States: Oklahoma Geological Survey Circular 190.
- Kaderabek, T.J., and R.T. Reynolds, 1981, Miami Limestone foundation design and construction: *Proceedings of the American Society of Civil Engineers*, v. 107, p. 859-872.
- Kochanov, W.E., 1999, Sinkholes in Pennsylvania: Pennsylvania Geological Survey, Educational Series 11, 33 p. (<http://www.dcnr.state.pa.us/topogeo/hazards/es11.pdf>).
- Lohmann, H.H., 1972, Salt dissolution in subsurface of British North Sea as interpreted from seismograms: *AAPG Bulletin*, v. 56, p. 472-479.
- Martinez, J.D., K.S. Johnson, and J.T. Neal, 1998, Sinkholes in evaporite rocks: *American Scientist*, v. 86, p. 38-51.

- Miller, R.D., D.W. Steeples, and J.A. Treadway, 1985, Seismic reflection survey of a sinkhole in Ellsworth County, Kansas [exp. abs.]: Society of Exploration Geophysicists, p. 154-156.
- National Coal Board, UK, 1975, *Subsidence Engineers Handbook*: Mining Department.
- Nieto, A.S., D. Stump, and D.G. Russell, 1983, A mechanism for sinkhole development above brine cavities in the Windsor-Detroit area: Sixth International Symposium on Salt, v. 1, Salt Institute, p. 351-367.
- Peng, S.S., 1992, *Surface Subsidence Engineering*: Society for Mining, Metallurgy, and Exploration, Inc., 161 p.
- Quinlan, J.F., A.R. Smith, and K.S. Johnson, 1986, Gypsum karst and salt karst of the United States of America: *Le Grotte d'Italia*, v. 4, n. 13, p. 73-92.
- Sinclair, W.C., 1982, Sinkhole development resulting from ground-water withdrawal in the Tampa Area, Florida: U.S. Geological Survey Water-Resources Investigations 81-50, 19 p.
- Sofianos, A.I., 1996, Analysis and design of an underground hard rock voussoir beam roof: *International Journal of Rock Mechanics, Mining Science, Geomechanics Abstracts*, v. 33, p. 153-166.
- Steeple, D.W., R.W. Knapp, and C.D. McElwee, 1986, Seismic reflection investigations of sinkholes beneath interstate highway 80 in Kansas: *Geophysics*, v. 51, p. 295-301.
- Waltham, A.C., and P.G. Fookes, 2003, Engineering classification of karst ground conditions: *Quarterly Journal of Engineering Geology and Hydrogeology*, v. 36, p. 101-118.
- Waltham, T., F. Bell, and M. Culshaw, 2005, *Sinkholes and Subsidence: Karst and Cavernous Rocks in Engineering and Construction*: Praxis Publishing Ltd., Chichester, UK, 382 p.
- Watney, W.L., J.A. Berg, and S. Paul, 1988, Origin and distribution of the Hutchinson salt (lower Leonardian) in Kansas: Midcontinent SEPM Special Publication No. 1, p.113-135.

CHAPTER 5

PREVIOUS SEISMIC-REFLECTION IMAGING OF SUBSIDENCE

To this point the focus of this manuscript has broadly revolved around processes and characteristics of dissolution, salt, and subsidence. From here the focus will move more toward high-resolution seismic-reflection images and associated interpretation of these relatively small, yet very complex dissolution and subsidence structures. Principally highlighted in this chapter are past uses of seismic reflection to image subsidence features. Considering research currently underway by the author, it seems prudent to also provide a glimpse at where the future of seismic imaging of subsidence structures could be going. Most of the seismic sections displayed in this chapter have come from published works by authors in pursuit of an improved understanding of collapse structures in carbonate, glacial, and evaporite settings. The message this chapter should leave with the reader is two-fold; first, the body of work this study builds on is relatively small and in some cases of marginal quality, and second, shallow high-resolution seismic-reflection data are unique and require special considerations through all three principal stages of the method (acquisition, processing, and interpretation).

The complex and therefore challenging seismic environment associated with subsidence structures have mystified and frustrated researchers as near-surface seismic technologies developed and instrumentation and computing power has evolved over the last 30 years. As will become evident in this chapter, probably the most underappreciated aspect of collapse structures is their extreme lateral variability in seismic velocities. Previous studies show the need for a thorough understanding of the detrimental effects rubble or collapse strata can have on seismic velocity and wavelet characteristics. This, along with collapse artifacts such as highly attenuative overburden and an abundance of in- and out-of-the-plane scatter events, make these complex structures a daunting seismic challenge, and one that few researchers have fully conquered. In general, the first part of this chapter focuses on historical attempts to image and interpret these small-scale, localized, and extremely complex structures on seismic-reflection sections.

Published accounts summarized in this chapter highlight a condensed history of the use of seismic reflection to map subsidence structures. As well, many of the problems encountered trying to image the upper few hundred meters of these features become evident. An appropriate level of concern for the uniqueness of the shallow wave field, high-frequency characteristics of the wavelet, and low signal-to-noise characteristics of high-resolution data acquired over subsidence features are essential and each could lead to a potential pitfall. Low signal-to-coherent noise stacked sections have a tendency to entice interpreters into excessive speculation as to the coherency and geometry of reflections. Author reprocessing unequivocally demonstrates this point.

Utility of Seismic-Reflection Imaging

Geophysics has been used to characterize the subsurface in and around sinkholes since the late 1940s (Enslin, 1951). Viable attempts to image actively subsiding sinkholes with seismic reflection (Steeple et al., 1983) began appearing in the literature with the development of CDP (CMP) seismic-data acquisition and processing (Mayne, 1962), an awareness that reliable images of the near-surface could be generated with high-resolution seismic reflection (Schepers, 1975), and the availability of software and computers capable of processing CMP seismic-reflection data into 2-D cross sections for engineering and environmental applications (Somanas et al., 1987). Around a dozen attempts to image dormant natural salt-induced dissolution-subsidence features using conventional seismic-reflection approaches appear in the refereed literature between about 1971 and 1982.

Adapting seismic imaging for sinkhole studies demonstrated resolving capabilities sufficient to allow crude interpretations of active subsidence features during early developmental stages (Steeple et al., 1986). As will be seen in later chapters, seismic imaging of the subsurface around and through sinkholes and subsidence features has recently developed to the point different episodes of failure, changes in stress regimes, and zones of dissolution and creep with and without overburden failure can be imaged with past deformation used to postulate future events (Miller et al., 1997, 2006; Miller, 2003; Miller, 2006).

Without question seismic reflection as an imaging and characterization tool has seen monumental growth in application and technology over the last 50 years, fueled predominantly by the petroleum-exploration industry (Lines, 2005). Near-surface high-resolution seismic reflection benefited greatly from that progress. Since seismic reflection was first used to delineate structures in the subsurface around a sinkhole over 35 years ago (Gendzwill and Hajnal, 1971), the tool has been effectively used on a variety of subsidence problems ranging from paleofeatures to salt-mine collapses, from settlement along natural dissolution fronts to evaluation of sinkholes resulting from carbonate karst. Future applications of seismic reflection for delineating subsidence features will surely follow the petroleum industry and exploit the power of 3-D.

Carbonate Settings

Seismic-reflection imaging of sinkholes began finding utility in carbonate karst settings around the world as early as the mid-1980s (Sinclair et al., 1985). Sinkhole sites optimal for seismic reflection are in good supply in Florida where karst is abundant. In northeastern Florida a seismic survey designed to search for and investigate flow paths potentially responsible for the mixing of high chloride waters from deeper aquifers with shallower freshwater benefited from near-ideal seismic-reflection conditions (high water table, fine-grained sediments, well-sorted near-surface sediments, large acoustic impedance contrasts) (Odum et al., 1999). Based on hydrogeologic information, this site was suspected to have a deep-seated collapse feature. From the seismic-reflection section, a zone of draping reflections has been interpreted as a subsidence feature (Figure 5-1). This paleosubsidence feature has been infilled with Quaternary-age sediment with no indication of vertical movement since deposition of these young, unconsolidated sediments.

There appears to be some level of consistency between the interpretation of these data and the collapse and subsidence mechanisms both numerically developed (Davies, 1951), physically modeled (Ge and Jackson, 1998), and empirically verified (Miller et al., 1997).

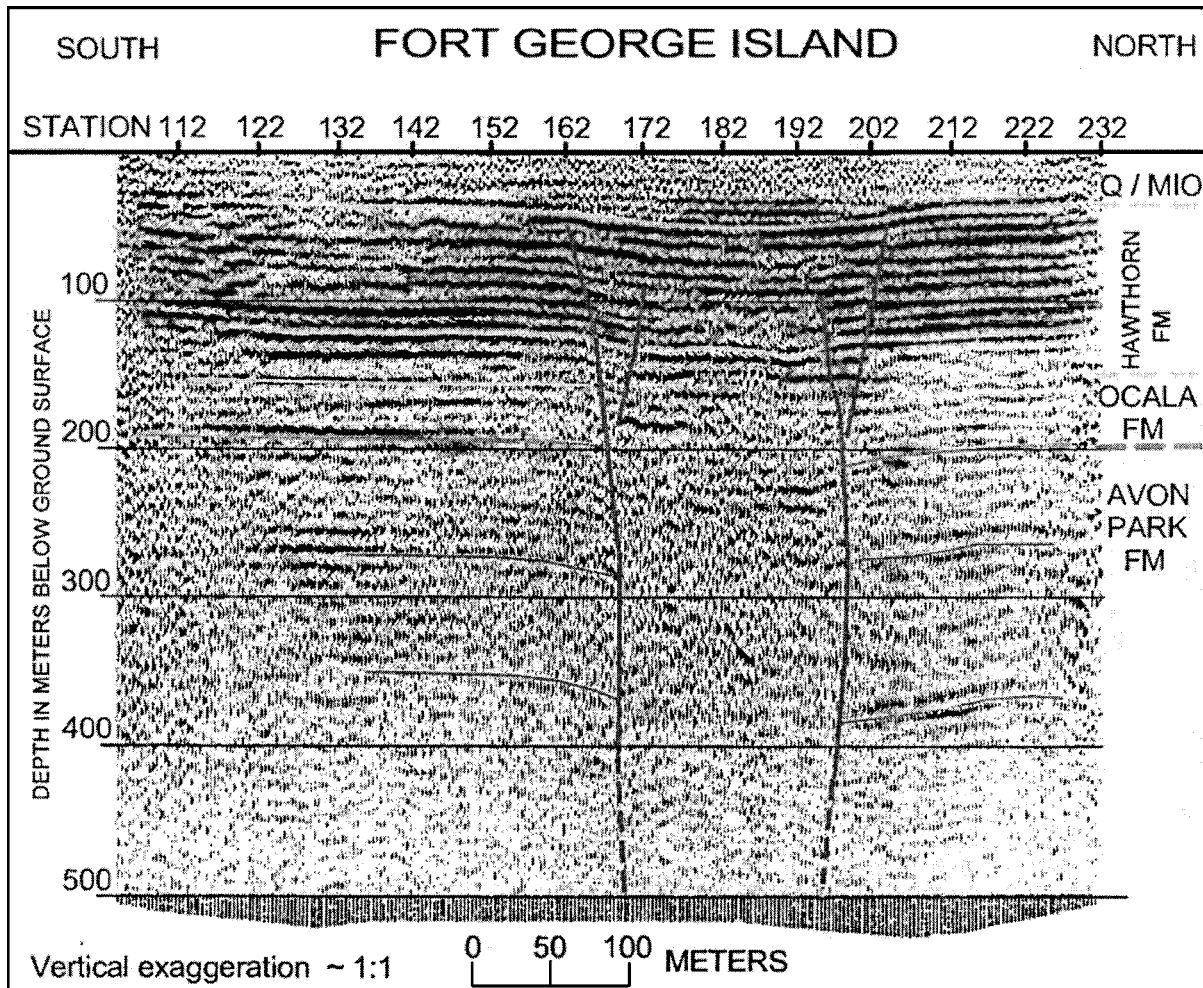
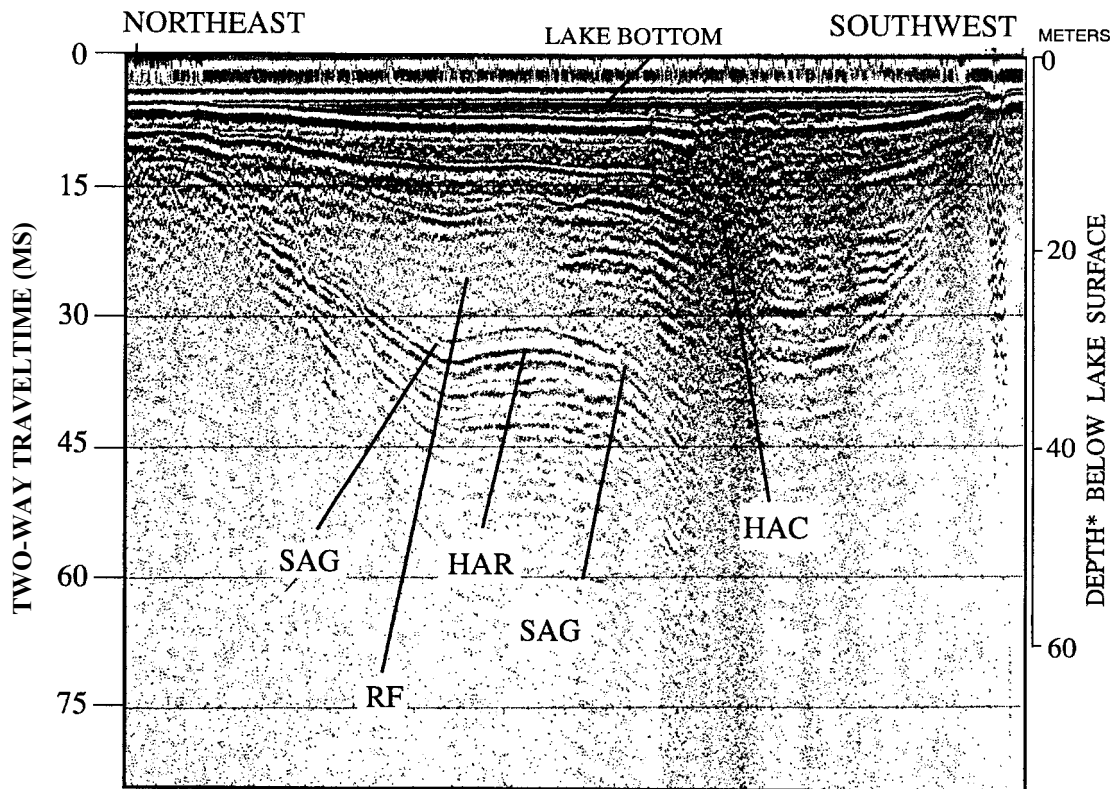


Figure 5-1. Interpretation of Fort George Island high-resolution seismic-reflection profile (Odum et al., 1999).

After careful examination, the series of predominantly tensional fault lines originally interpreted could easily be augmented with compressional strain structures below 100 ms. Interpreting both tensional and compressional events on the same subsidence structure has not been commonly seen and most near-surface practitioners are reluctant to interpret such diametrically opposing strain characteristics on the same localized structure. In general, the bounding faults appear predominantly normal, but offset in beds interpreted between 80 and 200 m below ground surface appear reverse.

The Dead Sea area of Israel possesses a significant regional karst sinkhole problem related to carbonate dissolution; fortunately, it is an area where seismic reflection has shown promise. High-resolution seismic-reflection data have been used to pinpoint areas for enhanced radar imaging to delineate ancient dissolution features (Abelson et al., 2003). Seismic profiles acquired across lineaments along which sinkholes had aligned possess reflection events of moderate quality with prominent discontinuities evident in younger (several thousand years old) sediment interfaces (reflectors). These reflection anomalies mainly consist of diffraction-looking events interpreted to likely originate at a fracture or fault zone that could be in or out of the plane. With the apparent high-frequency nature of the diffraction-looking events, air-coupled wave reflections cannot be ruled out and must also be considered as a possible nonreflection source of these arrivals. These seismic profiles never



* Based on acoustic velocity of 1,800 meters per second.

Figure 5-2. Lake seismic surveys have provided reasonably good quality single-channel data where chimney-like collapse structures can be interpreted. Examples of high-amplitude, concordant reflector package (HAR), with sagging structures (SAG), high-amplitude chaotic zone (HAC), and reflection-free zone (RF) (from Tihansky et al., 1996).

passed over a subsidence structure, only crossed a lineament where sinkholes had a history of development.

Single-channel seismic-reflection profiling in search of subsidence features in lakes has been carried out since the early 1980s and was some of the first seismic-reflection investigation of subsidence features in carbonates (Sinclair et al., 1985; Locker et al., 1988; Snyder et al., 1989; Lee et al., 1991; Sacks et al., 1992; Evans et al., 1994; Kindinger et al., 1994; Tihansky et al., 1996). These aquatic studies have commonly interpreted small vertical “pipes” generally exhibiting vertical relief correlating to bathymetry of the lake (Figure 5-2). Sublake bottom-subsidence features imaged on seismic appear to alter or breach overlying confining units and are interpreted to be the result of karst due to limestone dissolution (Tihansky et al., 1996).

Carbonate karst was the target of a shallow, high-resolution seismic survey at a power plant site in southern Alabama, USA (Miller et al., 2005). Locating sites for power-generation facilities has historically relied on the convergence of three things: fuel-delivery system (pipeline, railroad, harbor, etc.), water (river, lake, etc.), and power grid (high-tension regional distribution electric lines), with concerns for the site geology being secondary or not considered at all. This area of Alabama is well known for surface and subsurface remnants of rapid sinkhole development that have occurred throughout the Quaternary in response to the dissolution of several regional limestone units. Accurate characterization of dissolution features that might be hidden beneath the plant’s proposed footprint and with the potential to

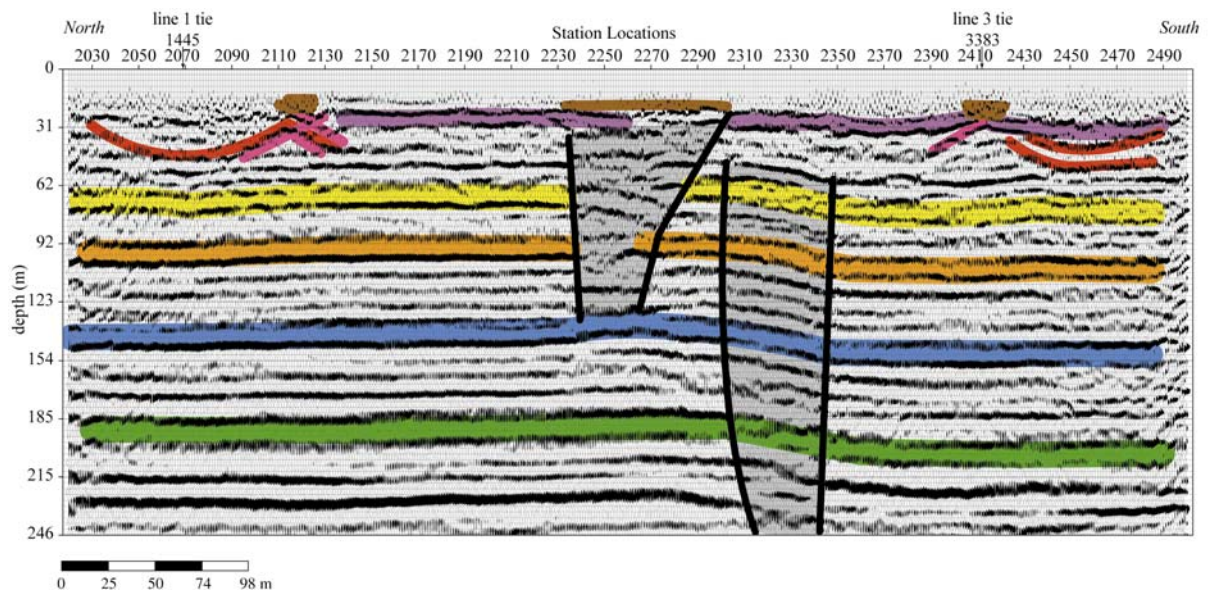


Figure 5-3. Interpreted time-to-depth section converted using NMO velocity calculated during reflection-data processing (from Miller et al., 2005).

jeopardize the stability of critical components is key to engineering-design specifications, cost estimates, and establishing confidence ratings for plant safety.

Seismic images from data acquired and processed using shallow, high-resolution guidelines and workflows are very high quality with dominant-stack reflection frequencies greater than 140 Hz (Figure 5-3). Structures interpreted as either paleosinkholes or paleochannels are evident on seismic images with clear indications of previous earth subsidence and/or high-energy erosion. The paleosinkhole, or more generically synform beneath station 2070 (Figure 5-3), has a remarkable similarity to cut-and-fill channel features observed on seismic data in Miocene sediments along the Atlantic Coastal Plain (Miller et al., 1999). Two high-amplitude reflections interpretable within the paleosinkhole possess distinctly different attributes compared to surrounding “native” reflections (higher amplitude and lower frequency). Absolutely essential for establishing any level of confidence in high-resolution, shallow seismic-reflection data is interpretable reflection on shot gathers (Figure 5-4). This is the only published land seismic study where paleodissolution features without surface expression have been confidently interpreted and then confirmed by drilling.

Pitfalls in Carbonates

Land seismic-reflection surveys targeting karst-related sinkholes in carbonate settings have shown a wide range of effectiveness and success in meeting the goals of individual studies (Lippincott et al., 2000; Shoemaker et al., 1998; Odum et al., 1999; Abelson et al., 2003). Studies in Missouri targeting karst at the bedrock surface where the objectives have ranged from determining potential for collapse to defining actual failure mechanisms and the thickness of overburden soft sediments have provided speculative conclusions and significant postulation based on routinely poor data (Figure 5-5). As is the case on most land CMP stacked sections, events less than 100 Hz in the upper 20 ms are generally stacked refractions (first arrivals). With an acquisition geometry including a 1.6-m receiver spacing and 6.5-m nearest source offset, the wavelet character of the stacked “reflectoid” interpreted as bedrock, and lack of defensible reflections on shot gathers, events above 10 m (45 ms) are no doubt stacked first arrivals (Figure 5-3). This spread configuration makes recording reflections

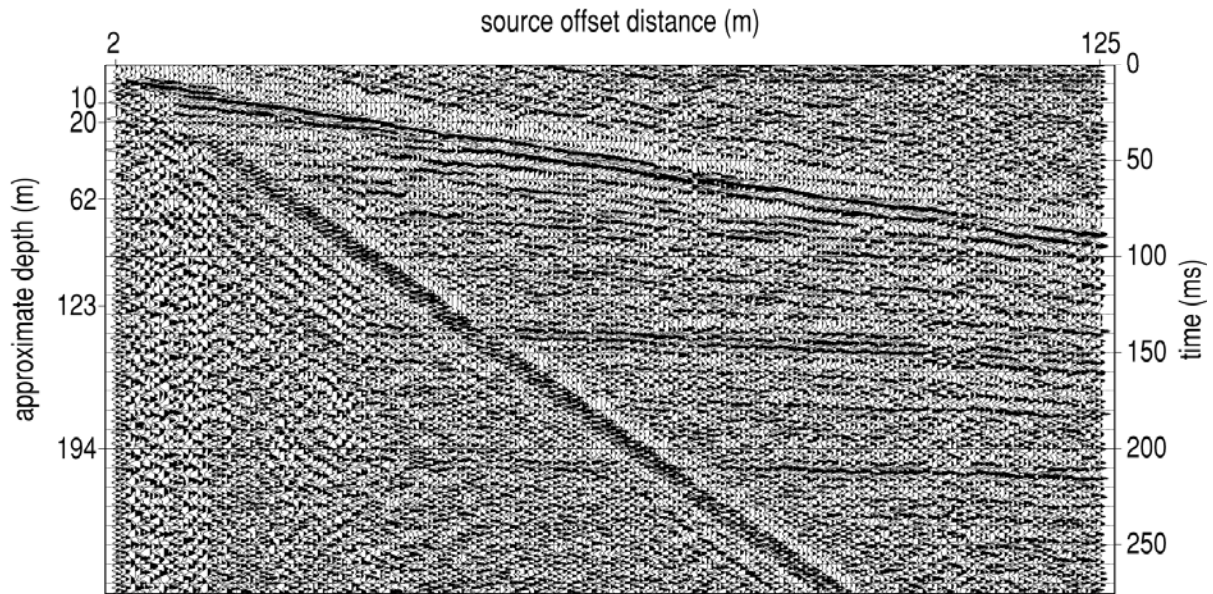


Figure 5-4. Shot gather from 50-caliber downhole seismic source at Alabama power plant site (Miller et al., 2005).

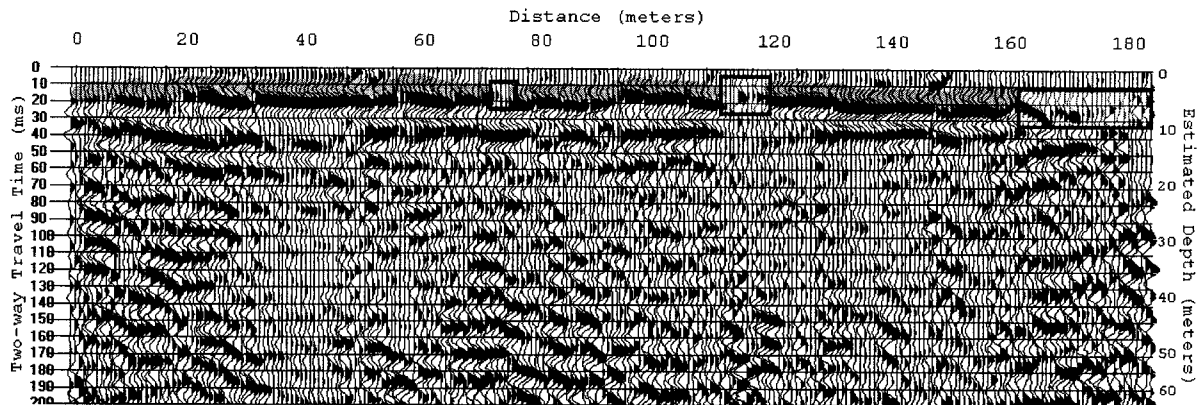


Figure 5-5. Seismic data interpreted to have imaged the solid bedrock interface. High-amplitude, low-frequency event enhanced with CMP processing from first arrivals. Refractions with anomalous arrivals associated with changes in bedrock are stacked as reflections (from Lippincott et al., 2000).

from less than 20 ms impossible. Stacking first arrivals has been a recurrent downfall of many shallow reflection surveys (Steeple and Miller, 1998).

In Australia, sinkhole prone areas along existing and proposed transportation thoroughfares were determined feasible targets for seismic-reflection methods to detect and delineate voids rooted in massive carbonates suspected to be the source rock for sinkhole development (Nelson and Haigh, 1990). CMP stacked seismic sections from this Australian study suffered from many of the same problems researchers in the U.S. were seeing on data of this era (Figure 5-6). A lack of reflection coherency and a relatively narrow stacked bandwidth resulted in CMP stacked sections with a “wormly” appearance. This detrimental artifact required interpreters to highlight horizons excessively for display or even peers could not recognize the suggested coherency. Many of the difficulties were related to minimal recording channels, low A/D converters, and trouble eliminating noise.

These CMP reflection data from Australia lack sufficient evidence to support the interpretation of a subsidence feature below ground surface (Figure 5-6). The purpose of analyzing these seismic data in this manuscript is not to discredit the work but to demonstrate

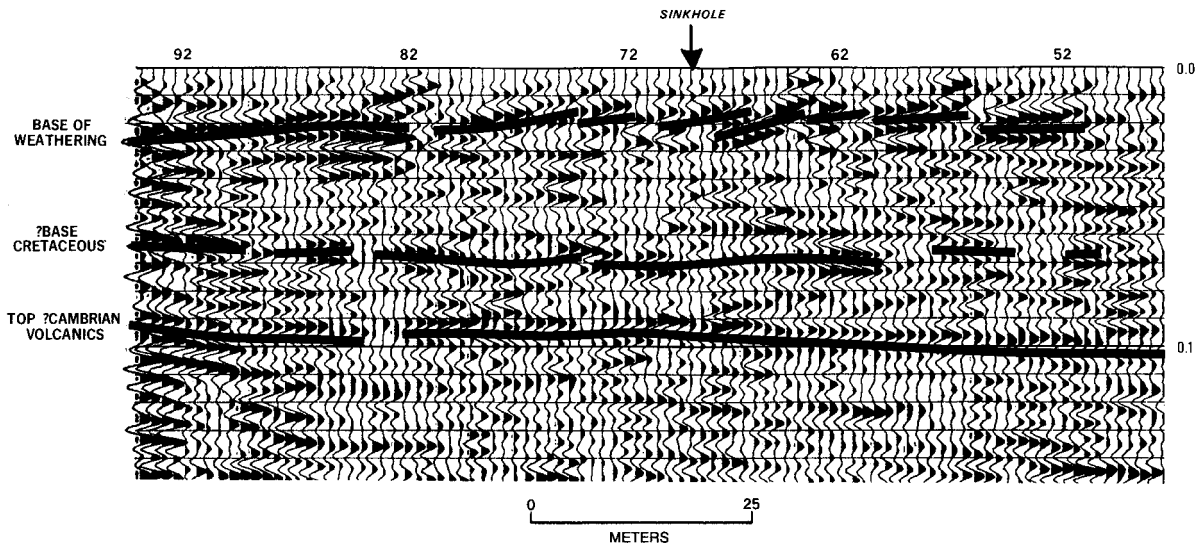


Figure 5-6. There are indications of a zone of seismic-amplitude attenuation beneath the sinkhole (from Nelson and Haigh, 1990). Events interpreted as base of weathering are likely stacked refractions or guided waves. Shingled look to events is due to NMO correction.

the difficulties and inherent problems and obstacles associated with trying to adapt this exploration technology during its early developmental stages. This work (Nelson and Haigh, 1990) passed the scrutiny of peer reviewers because at this time the power of data-processing software and complexity of the near-surface wavefield was not fully understood among practitioners and some researchers alike. As previously shown, not all attempts to use seismic reflections in search of shallow carbonate karst subsidence features have encountered these debilitating difficulties.

Glacial Settings

Subsidence structures associated with active glacial dynamics have been observed and attempts made to image them with seismic reflection (Pyke et al., 2001). Processes associated with glacier termini are deemed important in developing models for landform genesis. Thermokarst sinkholes were interpreted to be present on seismic data, but images of these features were not included in the published version of this high-resolution seismic study of a glacier in Alaska, U.S. (Baker et al., 2003).

Study of glaciated terranes especially related to correlation of lithofacies across characteristic complex depositional environments has been an attractive application of high-resolution seismic reflection since the mid 1980s (Pullan and Hunter, 1990; Green et al., 1995; Lanz et al., 1996; Bükér et al., 1998). Seismic reflection was used to resolve to origin a major closed, bowl-shaped depression buried within a glacial terrain discovered from shallow borings (Wiederhold et al., 1998). With the proximity of a salt diapir to this depression, the question arose as to the feature's origin: glacial erosion or dissolution. A high-quality seismic-reflection profile was acquired across this feature and interpreted to support the feature to be glacial and not the result of dissolution. This interpretation was based on a lack of evidence for subsidence, as would be the case for salt dissolution (Figure 5-7). With the excellent data quality and coherency of stacked reflections, the bowl-shaped structure is obvious and interpreted to be depositional and not characteristic of a subsidence feature.

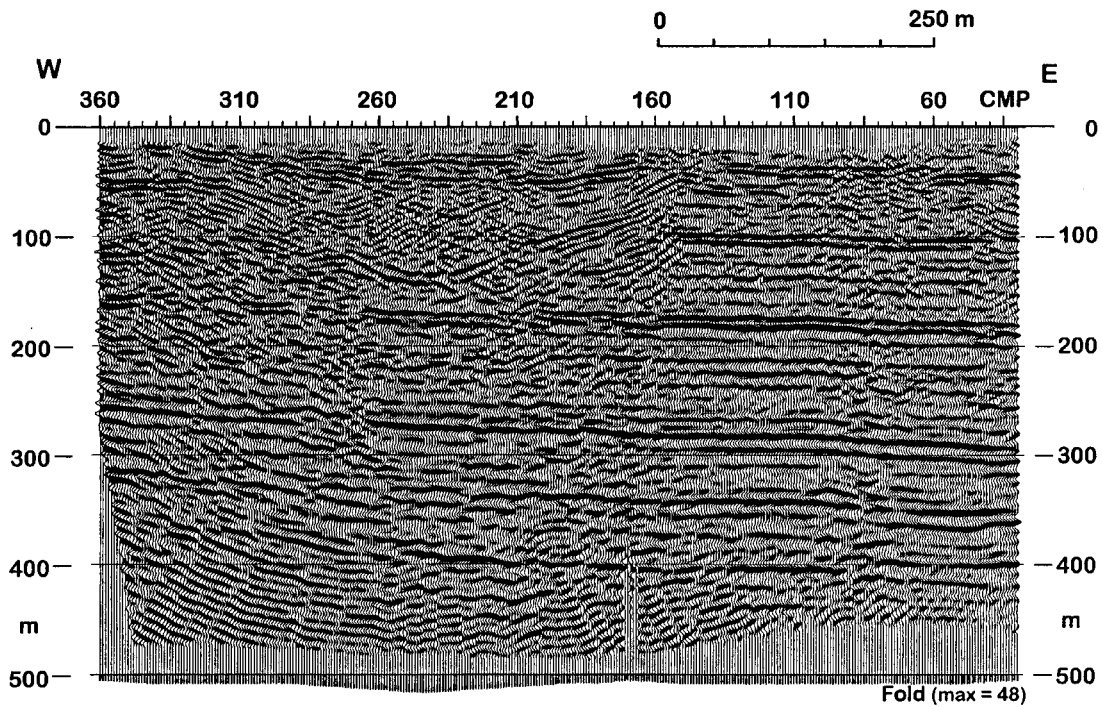


Figure 5-7. FD time migration from the Tostedt survey area. Vertical axis gives two-way traveltime; minimum fold is 14 (from Wiederhold et al., 1998).

Noteworthy is the relative consistency in reflection-time arrivals below this bowl structure, clearly a characteristic indicative of deposition. A significant velocity pull-down is generally associated with dissolution and subsidence. Reflections interpreted on CMP stacked sections at times shallower than 50 ms are not supported by shot gathers and must be viewed with some degree of skepticism (Figure 5-8). With a 50-m closest useable trace offset, at most four traces could have recorded reflected energy during the early time portion of the record, and, based on the processing flow, false (artificially enhanced) coherence is a real risk. Even with the shallow interpretation miscue, this is an excellent high-quality data set.

Salt Settings Worldwide

Seismic images in evaporite settings with sufficient quality to interpret collapse structures are few and far between in the published literature. Most images from pre-1990s surveys are plagued with poor signal-to-noise ratios and therefore lack coherency through the highly distorted collapse zones. Few similarities were observed in seismic-reflection characteristics interpreted to be in response to subsidence features prior to the early 1980s. Important to note here is that apparent collapse processes or mechanisms will have some inherent site to site inconsistency due to the dependence of stress distribution on overburden material. Therefore, even though the large-scale processes may be similar, key geologic and therefore material details and subtleties affecting stress distribution and strain resistance are site dependent and globally inconsistent.

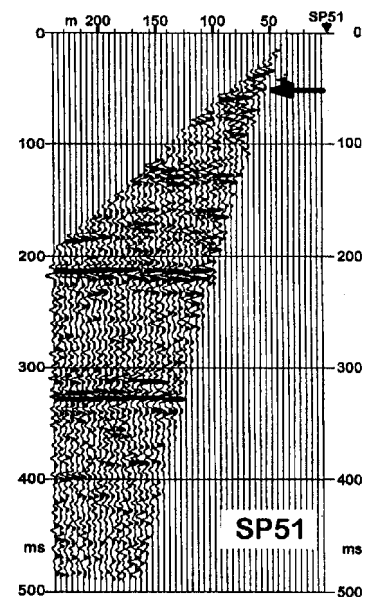


Figure 5-8. Shot gather after NMO correction and top mute (from Wiederhold et al., 1998).

Imaging structures related to bedded salt deposits have proven beneficial for many years in the petroleum industry where paleodissolution and subsidence has provided trapping structures for accumulations of oil and gas (e.g., Connelly et al., 1991; Anderson and Franseen, 1991; Surjik and Hobson, 1964). Structures formed as a consequence of salt dissolution concurrent with depositional changes in lithofacies have hydrocarbon potential. Seismic-reflection amplitude attributes and time-structure maps have shown a great deal of sensitivity to changes in salt thickness and lithologic character. Changes in lithofacies of most reservoir rocks unique to a dissolution structure are many times interpretable from wavelet variations along the salt-reflection horizon.

Most studies prior to 1985 into the structural complexities of subsidence features focused on natural processes and inactive features. One of the earliest investigations where very high quality seismic images were to help understand the structural evolution of dissolution-induced collapse structures was during the study of Crater Lake in Saskatchewan, Canada (Christiansen, 1971). A series of fault blocks appear to form a stair-step structure within the lake itself as defined by two concentric high-angle normal fault zones interpreted using both low resolution and fold, explosive seismic-reflection data and geologic background information (Gendzwill and Hajnal, 1971) (Figure 5-9). Wide trace spacing and an off-line offset

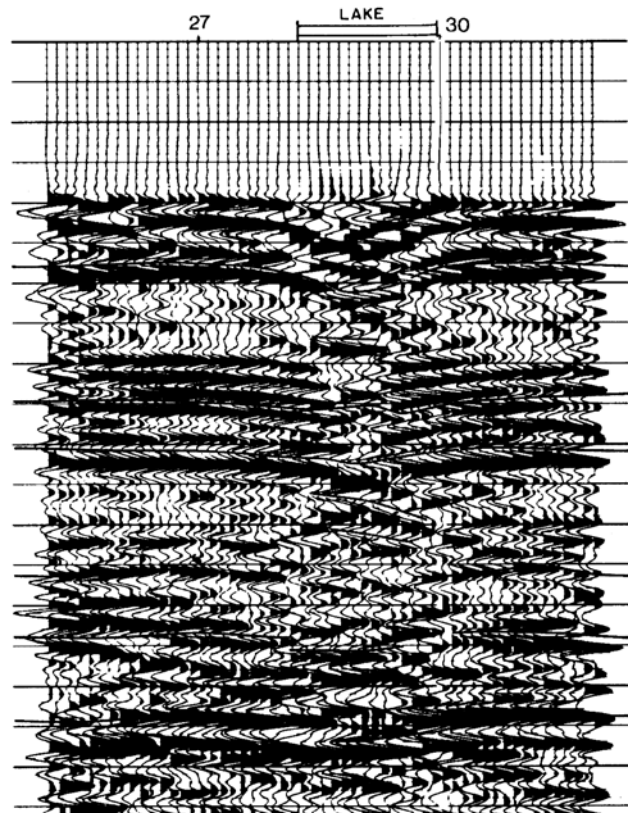


Figure 5-9. CMP stacked section with subsidence feature linked to Crater Lake, Saskatchewan, Canada. This feature has a surface expression, but the 3-fold explosives data recorded on a 12-channel seismograph with 38-m receiver spacing and 152-m source spacing lack the spatial sampling and resolution potential (around 5-Hz dominant frequency) to truly delineate important structural characteristics (Gendzwill and Hajnal, 1971).

(data acquired along perimeter of main surface feature) limited spatial detail and prohibited interpretation of structures or distorted beds within the subsidence zone.

During the same period, marine data from the British North Sea were providing the first glimpse of a salt-dissolution subsidence feature interpreted to possess both normal and reverse fault orientations (Lohmann, 1972) (Figure 5-10). Again, most data of this era lacked the high signal-to-noise ratio and attribute-reconstruction potential of modern data, but the interpretation of the North Sea data as published does appear credible. Without a doubt, these data are clearly suggestive of fault-controlled subsidence and with the two different salt units present and no deep-seated tectonic faulting, shallow forces are a likely drive mechanism.

Even though many papers have been published on salt dissolution in general, detailed seismic images and associated interpretations of structures within the collapse volume were very limited prior to 1995. Historically, seismic sections over non-uniform synform

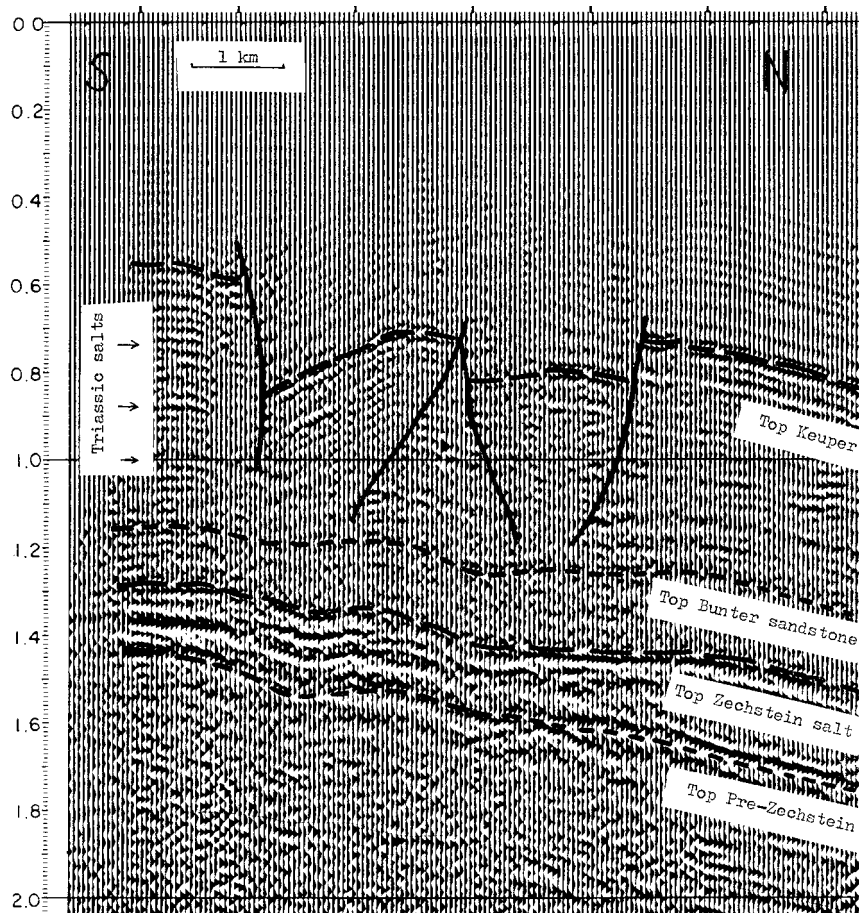


Figure 5-10. Seismic cross section from central part of English Zechstein basin, with two sinkholes formed by dissolution of Triassic salt (Lohmann, 1972). Although the structures do not form the now-accepted narrowing-upward inverted cone with flanking normal faults forming the characteristic large bowl structures, this is the first seismic evidence of both being present on a subsidence feature.

subsidence features have been interpreted with conical normal faults bounding the subsidence bowl (Anderson, 1981; Autin, 1984; Beck, 1984; Jammal and Beck, 1985; Steeples et al, 1986; Anderson et al., 1995; Mullican, 1988). Several of the more well known U.S. subsidence features investigated with seismic reflection (Wink Sinkhole, Texas; Chimney C collapse, New Mexico) lack sufficient coverage and/or data quality to reliably interpret structures within the collapse chimney volume (Baumgardner et al., 1982; Mullican, 1988; Davies, 1985).

Arguably one of the most publicized sinkhole occurrences related to salt removal resulted from roof failure of the 109-year-old, Livingston County, New York, dry salt mine where a passage was flooded by water after the breach of confinement in an overburden aquifer (Gowan and Trader, 2003). High-resolution seismic-reflection was used to evaluate the condition of the bedrock surface beneath almost 150 m of alluvial and glacial sediment. None of the seismic-reflection data from three different surveys at this site have ever been published.

Generalized interpretations of the three seismic surveys at the Livingston County mine have been documented, and, based on those descriptions, the seismic data did not possess sufficient signal-to-noise and/or resolution potential to determine if these large sinkholes (100 m to 200 m in diameter) were the result of collapse due to an enlarged dissolution void in the mine, or if piping through the overburden sediments and into the mine

was the source of the sinkhole. The bedrock in one area was estimated from seismic data to have subsided approximately 1.2 m; drilling in the same location showed the bedrock had dropped more than 2.5 m. Without published data, it is not possible to independently assess and interpret the data, but clearly from all available discussion the seismic data did not allow an interpretation of the entire subsidence feature and therefore were inconclusive.

Salt in Kansas

Seismic investigations of sinkholes have historically been plagued with poor data quality and therefore required “creative” interpretations that have led many to suggest the process was more of an art than science. Studies routinely included 2-D CMP stacked cross sections with reflections manually darkened (highlighting trace-to-trace wavelet “coherency” along a reflecting horizon) to allow a reader to distinguish the suggested reflecting interface from background noise (Anderson et al., 1998). A few examples exist where early seismic sections acquired across sinkholes were interpreted in this fashion and later proved to be extremely accurate (Steeple et al., 1986). As is the case for most near-surface targets, interpretations of seismic sections can be easy to verify with drilling or in this case future surface subsidence. A 1980 vintage seismic section along Interstate 70 was interpreted to have three subsidence features—one of the three had no surface expression (Figure 5-11). Within a few years of interpreting the seismic sections, a sinkhole developed at the predicted location. Detailed, high-fidelity information was not a routine product of early seismic surveys, but many of the interpretations based on those surveys did prove valuable when incorporated into the body of existing geo-knowledge at a subsidence site.

As a result of the faults and implied collapse process interpreted on the Interstate 70 seismic section, a controversy was set into play in Kansas between near-surface seismic pioneers (Steeple et al., 1986) and more classical subsidence disciples (engineers) coming from the dissolution mining community (Walters, 1978). Seismic types argued that based on this first ever “clear” image of an active sinkhole (gradually subsiding in this case), sinkhole development associated with these dissolution features was a relatively continuous collapse processes controlled by tensional stresses defining a large bowl-shaped structure in the subsurface. Normal faults that extend from the original void volume to the ground surface guided the process. Solution mining engineers provided numerical and empirical evidence

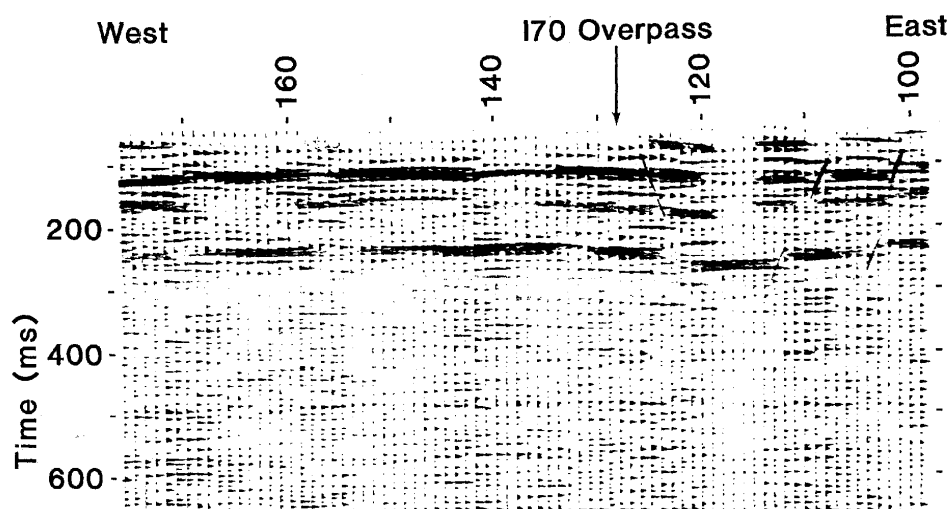


Figure 5-11. Interpreted CMP stacked section across I-70 sinkhole in Russell County, Kansas, in 1980 (Steeple et al., 1986).

from solution mine failures to support the theory that collapse was controlled by the tensional dome, and a compressional environment resulted in upwardly narrowing chimney-like structures defined by reverse fault planes (Davies, 1951).

It was not until 10 years later that seismic researchers in Kansas suggested both mechanisms were possible, depending on the type of subsidence. It was proposed that ductile deformation was characteristic of gradual subsidence and a compressional stress process was associated with catastrophic failure, but poor data quality prohibited interpretable evidence of diagnostic structures (Anderson et al., 1995). This was consistent with the observation that both stress fields had been active at some time based on the 1972 seismic data from the North Sea (Lohmann, 1972). Ductile deformation of the salt was suggested to be associated with dissolution and creep producing bowl-shaped structures (Anderson et al., 1995). Brittle deformation of overburden above salt voids was suggested to occur in situations with no or marginal flowage of salt and rapid migration of collapse to the ground surface. With the exception of ductile deformation (which is not possible in this setting), most of these suggestions are reasonably consistent with engineering, geologic, and seismic images, but they still lacked solid seismic evidence from known failure sites where generalized stress regimes matched the known physical constraints. The myths and reality of these early suggestions and interpretations are sorted out in this study.

Definitive evidence of both tensional and compressional features on CMP stacked sections was a research objective for each new seismic survey undertaken over a dissolution or mine-collapse structure for more than 10 years after the 1986 publication by Steeples et al. (Miller et al., 1985; Steeples and Miller, 1987; Knapp et al., 1989; Anderson et al., 1995; Miller et al., 1995; Miller and Weis, 1995). As the high-resolution seismic method improved in signal-to-noise, resolution, economics (allowing larger channel systems), and source bandwidth, so did the clarity of the structures within collapse volume. A CMP stacked section from data acquired in 1996 over a gradually developing sinkhole that formed due to the accidental and uncontrolled release of brine from an oil-field disposal well provided that first clear strain evidence of a compound stress field (Miller et al., 1997).

For the first time since that initial glimpse on a marine seismic section in 1972, both normal and reverse fault planes were interpretable on CMP sections within the collapse cone (Figure 5-12). Although the 1972 data were reasonably good quality, without the enhancement provided by manual highlighting of the reflection events it would have been difficult to observe the interpreted fault planes. This 1996 finding provided necessary empirical evidence to confirm strain resulting from both compressional and tensional stress environments were distinguishable as discrete components of void collapse and sinkhole development. Unlike the 1972 marine data, the relative orientation and geometry of the fault planes matched both physical and empirical models for a single collapse structure. Early 2-D seismic data were simply too noisy and low resolution to observe these reverse faults within the tensional dome.

Pitfalls of High-resolution Shallow Seismic Data and Subsidence Structures

Complexities associated with processing and interpreting salt subsidence features on high-resolution seismic-reflection data are not always appreciated, even by seasoned, well-published geophysicists. A 4-km-long, high-resolution seismic-reflection profile was acquired across the drill-inferred dissolution edge of the Permian Hutchinson Salt Member in Reno County, Kansas, in hopes of providing a more detailed view and understanding of the

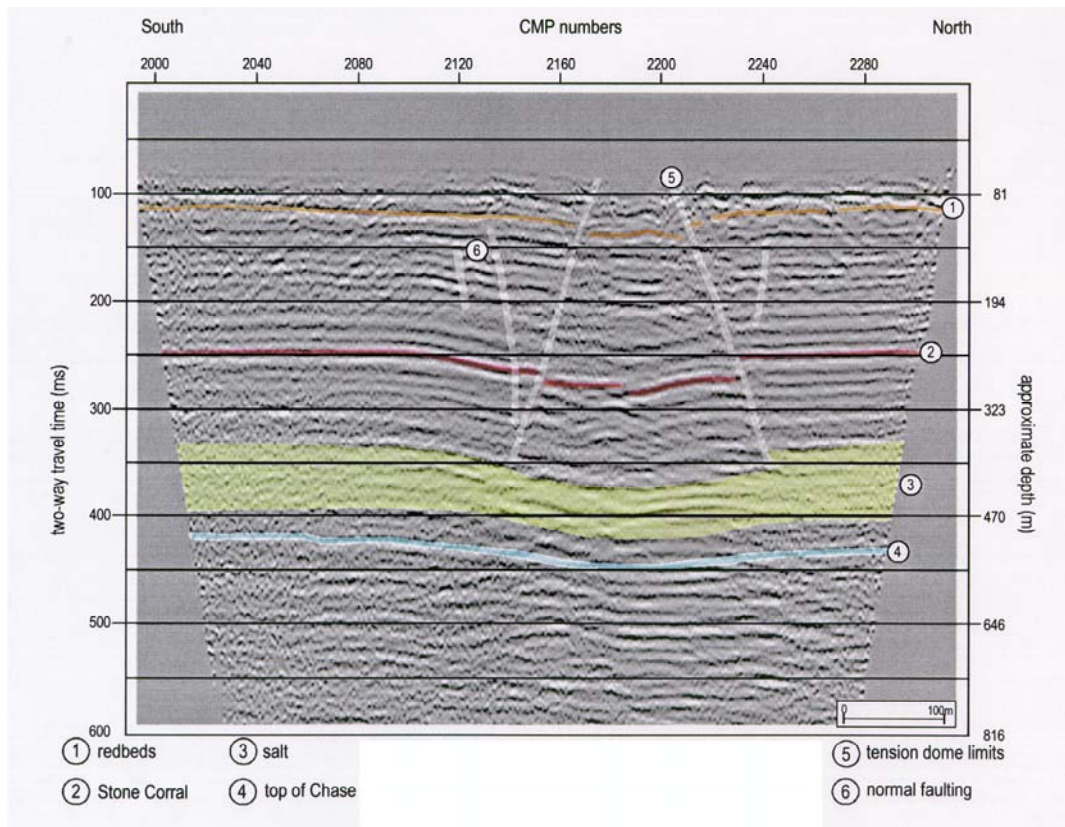


Figure 5-12. CMP section acquired in 1996 across the French sinkhole in Barton County, Kansas. Sinkhole formed due to a leaky disposal well. First high-resolution and high-quality land seismic-reflection section to image both compressional and tensional structures within the collapse chimney in defensible detail.

dissolution process and instigating factors (Anderson et al., 1998). Data from that survey were processed and interpreted using a conventional approach.

CMP stacked sections published in a 1998 *GEOPHYSICS* article (Anderson et al., 1998) examining dissolution processes, catalysts, and structures in general used data from Kansas that were not processed to a level consistent with the data potential (Figure 5-13a). Stacked sections published in this article are contaminated with source noise. Low-frequency ground roll is at a minimum clouding the picture and more likely distorting the interpretation. This is a case where the resulting interpretations are not just incomplete due to poor signal-to-noise ratios or low resolution potential; they are incorrect due to noise contamination and enhancement.

Refraction/first arrival are purposely retained throughout the processing flow in spite of the assumptions of hyperbolic moveout that must be made during the correction for non-vertical incident-reflection ray paths (Miller, 1992). Adding to the processing problems, noise interferes with and violates the basic premise for correlation routines designed to estimate and make optimum static corrections from zero-incident reflections. These published stacked sections are not representative of the subsurface and therefore bring the validity of the authors' (Anderson et al., 1998) discussions and conclusions under question.

Many of the line-highlighted interpretations cycle skip and extend reflections significantly beyond what the data will support. Truncation of the salt as interpreted beneath station 1600 at around 170 ms is not based on correlated trace-to-trace reflection-wavelet coherency for this horizon. Other horizons interpreted around this top-of-salt (TS) event

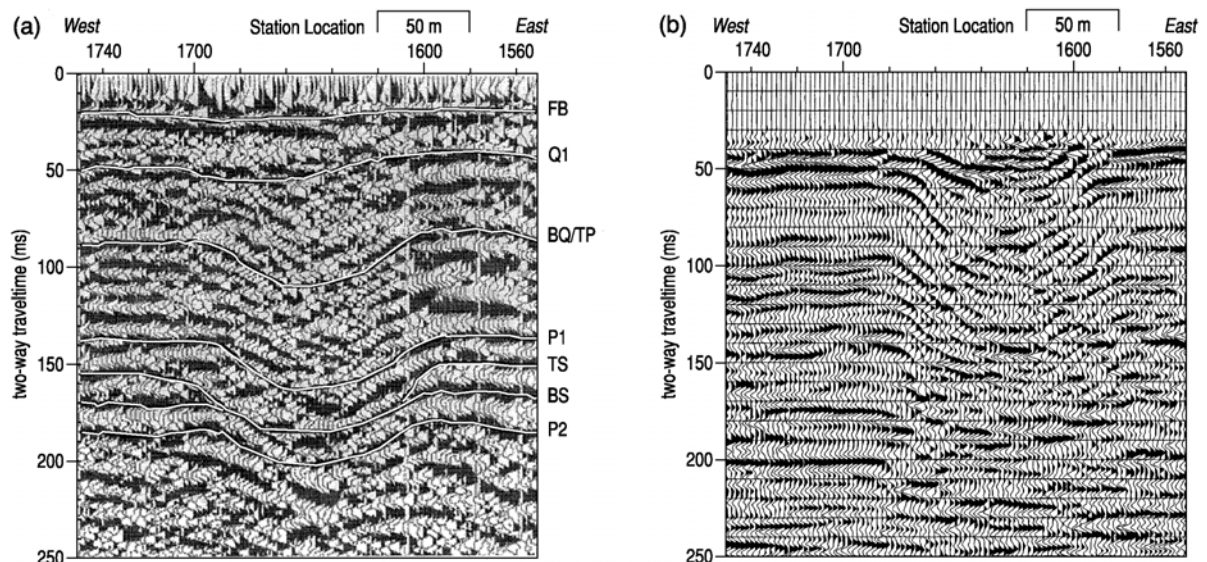


Figure 5-13. Poor-quality data with interpretations forced to fit preconceived model of setting (a) (Anderson et al., 1998). Accurate processing allows for much more accurate and reliable interpretations (b). Most notable are interpreted salt truncations necessary to fit author's model (a) are completely inconsistent with the appropriately processed data.

suffer from the same lack of lateral-event coherency (Figure 5-13). The differences are striking when comparing the data processed using a high-resolution, shallow seismic approach (Figure 5-13b) with a more conventional processing flow (Figure 5-13a). Clearly within the collapse structure on the reprocessed sections there are indications of bedding that has survived subsidence sufficiently intact to return coherent reflections (Figure 5-13b). This interstructure reflection coherency is not consistent with the concept of collapse breccia but similar to the apparent bed drape associated with gradual subsidence. Variability in salt thickness associated with the paleosubsidence features is evident as undulations in overburden reflections relative to flat reflections observed within the deeper Chase Group limestones on the reprocessed sections.

Much of the obvious subsidence is pre-Quaternary as evidenced by the flat-laying reflections, indicative of undisturbed sediments, filling the trough or bowl of the paleosinkhole beneath station 1200 (Figures 5-13b and 5-14b). Also evident is an apparent abrupt truncation of the salt interval on the west side of the reprocessed section around station 1275 at about 150 ms (Figure 5-13b). The very gradational thinning interpreted on the published version of the stacked section (Figure 5-13a) is consistent with the concept that the salt either has undergone plastic deformation (flowage due to creep) or dissolution was active along an elongated sloping front that was over 100 m in length (Anderson et al., 1995). This west dissolution edge on the reprocessed stacked section is relatively sheer with the salt interval decreasing from nearly 20 m to less than 5 m thick across a distance of around 25 m and therefore not a valid example supporting the published concept of creep (Anderson et al., 1998).

Coherent relatively flat reflections evident within the collapse trough below about 70 ms (Figure 5-14b) are likely representative of beds within the initial subsidence cone defined by the tensional dome (Figure 4-2). Based on the apparent intact nature of these intercollapse reflections, it is very probable this failure occurred as thick intervals of roof gradually subsided, as opposed to the collapse breccia that would be expected if stoping were the failure mechanism. An undulation of more than 10 ms has been suggested in the "water

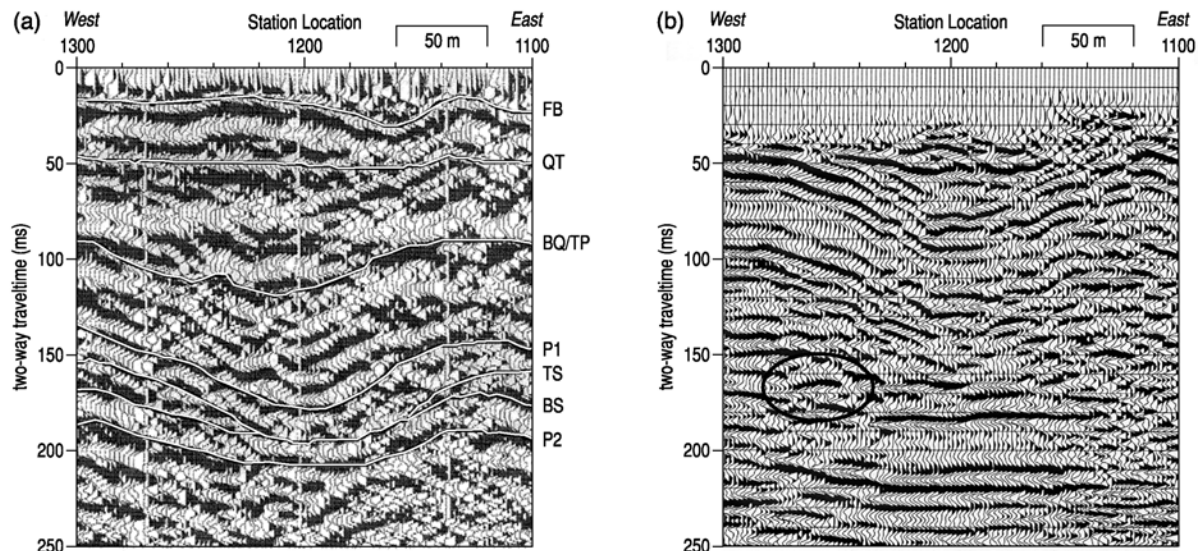


Figure 5-14. Clearly reprocessed data (b) provides a much higher resolution and accurate image than the published version (a) (Anderson et al., 1998). Abrupt change in salt thickness (highlighted inside circle) is consistent with physical and empirical models.

table refraction” (FB) beneath station 1160 (Figure 5-13a). Quaternary materials in this setting hosting the unconfined aquifer are sands and gravels. It is highly unlikely the piezometric surface possesses a 10-ms (more than 5-m) undulation across a horizontal distance of less than 25 m, but rather this artifact is related to processing refractions as reflections. At 10-ms two-way traveltime, this event (FB) is likely a direct arrival and has no bearing on or significance to the geology or hydrogeology beneath station 1160.

Probably discrepancy of greatest concern between the two processed sections is the location of the paleosubsidence feature beneath station 1380 (Figure 5-15b) on the reprocessed section that is interpreted beneath station 1420 on the published stacked section (Figure 5-15a). This difference is dramatic and raises suspicion as to the accuracy (legitimacy) of interpretations and suggestions based on any of the published sections (Figures 5-13, 5-14, and 5-15). Interesting and unique about the collapse structure obvious on the reprocessed section is the uniformity of reflection events east of the paleosubsidence (the direction of rapidly thinning salt based on drilling) (Figure 5-15b). The severity and abrupt nature of the subsidence trough beneath station 1380 on the reprocessed section has the characteristics of a zone with a localized high rate of subsidence, such as would be expected near a freshwater inlet. With this 2-D section alone, it is not possible to determine the type of feature that was feeding this ancient leaching, but clearly the process halted prior to the deposition of the Pliocene-Pleistocene Equus beds, which are interpreted as the flat-lying 30-ms reflection event immediately above the subsidence trough at station 1380.

The salt interval (160-170 ms) seems to be highly disturbed west of the steep-sided subsidence trough with what could be interpreted as a distinct block-type collapse of interbedded insoluble layers within the salt interval. Above these more discrete collapse remnants are smoothly undulating Upper Permian shale reflections. A collapse structure beneath station 1440 is clearly expressed in the salt as a change in reflection character and is translated to drape-looking events (due to resolution limitations) in the affected portion of the overburden. This collapse feature migrated toward the ground surface and either stalled or reached an ancestral ground surface with subsidence halting prior to deposition of the shale

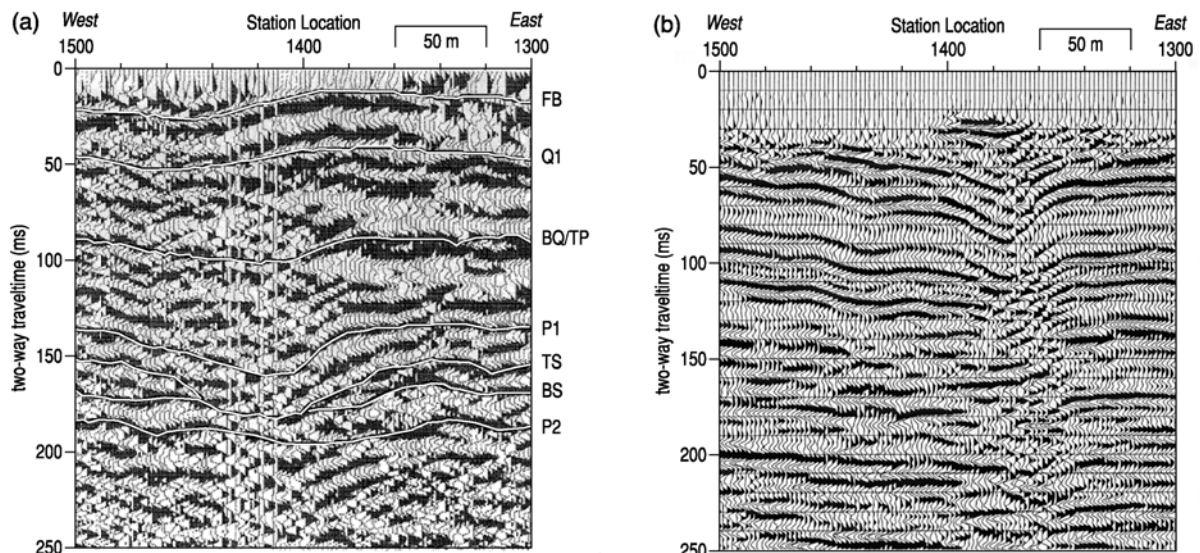


Figure 5-15. CMP stacked section with ground roll, air-coupled, and refraction processed into the image (a) (Anderson et al., 1998). Reprocessed using high-resolution techniques and limitations (b). Troubling is the mislocated paleosubsidence feature on the published data (a) relative to the true location and characteristics on reprocessed data (b).

layers that currently represent bedrock. Attempts at unravelling the subsidence history can clearly be accomplished with confidence using good high-quality seismic-reflection data.

Future

After searching both digital and analog sources of archived subsidence studies, it was very surprising to find so few examples where seismic reflection has been used in attempts to define subsidence mechanisms and growth processes at evaporite dissolution-induced sinkholes. As previously detailed, early applications of seismic reflection were challenged by data quality and resolution issues, with much of the work and therefore conclusions requiring speculation and in some cases extension of interpretations beyond what the seismic-reflection sections would support. Clearly the path ahead is 3-D imaging and use of attributes commonly exploited in petroleum exploration as a principal tool in analyzing these exceedingly complex, 3-D structures many times with areal expressions no larger than the dominant wavelength of the seismic data.

The benefits of 3-D imaging have been exploited by the petroleum industry for more than 25 years with incalculable revenue enhancements from field discoveries and optimization of drill patterns solely attributed to 3-D seismic techniques. Introduction and acceptance of 3-D seismic imaging has been credited with being one of the most significant advancements in increasing oil field discovery rates in the last 50 years (Columbia University, 2005) and the single most significant advancement leading to the growth of reservoir geophysics (Pennington, 2005).

In the future the most important advances leading toward a more complete understanding of the processes and catalysts for salt dissolution and associated subsidence and sinkhole development will come from the use of customized 3-D seismic-imaging techniques. An 820-ms amplitude time slice from a commercial high-resolution 3-D data set acquired in Austria provides an excellent representation of features interpreted as sinkholes from a paleokarst topography in Miocene rocks (Brown, 1999) (Figure 5-16). Clearly, many subsidence structures imaged on 2-D data sets in this manuscript would experience dramatic

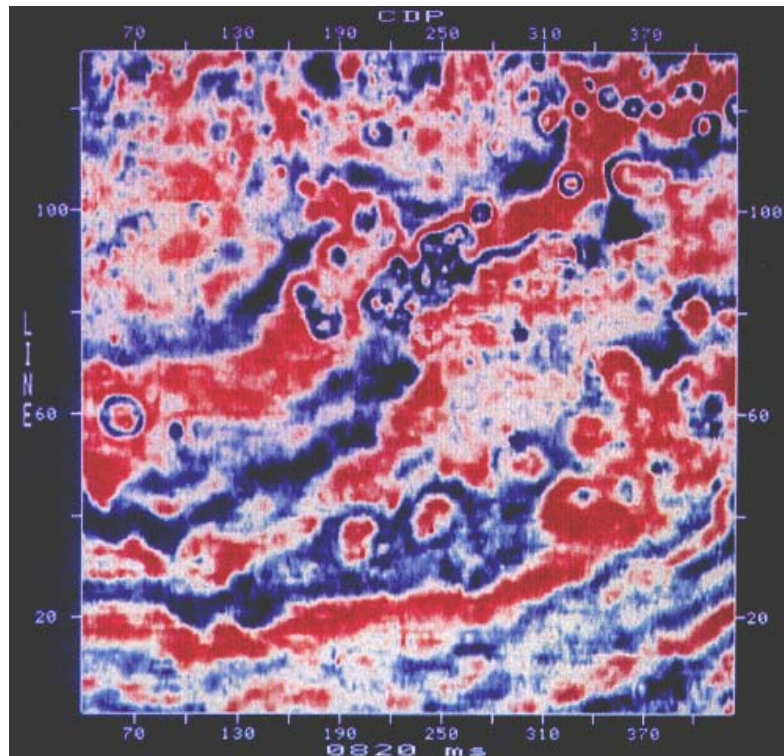


Figure 5-16. Seismic-reflection time slice (820 ms) from industry 3-D with circular features interpreted as sinkhole from Miocene paleokarst topography (Brown, 1999).

improvement in the accuracy and spatial positioning of subtle structural characteristics with 3-D images.

Interpretation tools available for 3-D data and the spatial accuracy of 3-D seismic data would allow the development of more accurate reconstructions of past events and enhanced projections of future subsidence activities. Two-dimensional seismic methods are susceptible to contamination by out-of-the-plane reflected and diffracted energy. With the complex 3-D geometries of dissolution features and the 3-D characteristics of seismic energy, the only way to fully dissect and analyze failure mechanisms, stages of failure, and rate and growth potential is with 3-D seismic methods. Clearly deeper petroleum applications have consistently shown improvement in data quality and associated accuracy and fidelity of interpretations through time and advancements in the methodology.

Seismic reflection has a proven record of success imaging dissolution features for applications ranging from hydrologic to petroleum to public safety. The overall quality and accuracy of interpretations coming from seismic-reflection data over the last 10 years are directly attributable to improved data characteristics (signal-to-noise ratio and resolution). Applications of high-resolution seismic reflection to delineate subsurface structures in and around sinkholes have seen varying degrees of success and regionally spotty effectiveness. Improved quality and understanding of the demands and limitations of high-resolution seismic-reflection data have provided an opportunity to unravel some of the mysteries of the complex mechanical, hydrologic, and geologic process associated with salt dissolution and resulting subsidence.

Until this work no single data set or compilation of data sets available in accessible literature venues have provided sufficient detail to correlate borehole observations with conceptual models from surface observations and relationships (lithologic, structural, and

hydrologic settings) of physical models (developed to simulate subsidence and sinkhole formation) with seismic-reflection images of the subsurface beneath and around sinkholes. Unfortunately some effort was necessary to highlight discussions and interpretations that are not well founded, or are based on misrepresented or inappropriately analyzed data. It is hoped that through the review and critique of previous work presented here the significance of the findings presented in this manuscript can be better appreciated.

Summing Up and To Come

Material presented in this chapter provided a tailored historical overview of some of the earliest interpreted and published seismic images of subsidence features through current work. This chapter highlighted successes and difficulties authors have experienced trying to delineate and unravel localized subsidence phenomena with seismic reflection. Initial discussions marqueeed work in terrain and marine environments with emphasis on key processing and interpretation successes as well as miscues during attempts to image subsidence structures in carbonate settings. Structures examined on published seismic sections from both glacial and salt settings with various subsidence characteristics provide a solid background and foundation for the focused, detailed study to come in later chapters. Overall seismic-reflection images of subsidence features have been sparingly published, possibly due to the complexity and lack of definitive images detailing the problem and lack of publishable seismic sections.

As evident from discussion in this chapter, quality of work imaging salt-dissolution subsidence features has varied dramatically. Studies during the early 1970s provided the first revealing seismic images of subsidence features without major advances in the understanding of these dynamic structures until the mid-1990s. Both reverse and normal fault geometries associated with the same collapse structure but in a relative geometry that did not correlate with any collapse models appeared in the literature on North Sea seismic-reflection data in the 1970s. Only gradational advancements appeared in the seismic literature that helped build a conceptual model with a consistent mechanism or sequence of processes to fully describe subsidence structures. It was not until the mid-1990s that the first land seismic section was published from across an active sinkhole where both normal and reverse faults were clearly interpreted and correlated to the mechanics of collapse and associated stress and strain regimes as observed and modeled for mine collapse in mining-engineering literature of the 1950s.

The difference between conventional and high-resolution seismic-reflection imaging has been repeatedly pointed out during review of previously published seismic sections. It therefore seems logical to follow this historical perspective on seismic-reflection imaging of subsidence features with an overview of the key aspects and procedures that distinguish high-resolution from conventional seismic-reflection acquisition and processing. The next chapter defines and clarifies the subtle and unique characteristic of the shallow (in time) seismic wavefield. First the differences between conventional and high-resolution data are described, with an emphasis on characteristics of the wavetrain and associated velocity field providing the basic background. After the uniqueness of the near-surface wavefield has been defined, the different approaches to and need for special emphasis on various aspects of acquisition and processing are detailed with selected examples from previously published work. Upcoming discussions in the next chapter are based on refereed journal articles by the author and key contributions available in the refereed literature by other near-surface seismologists.

References

- Abelson, M., G. Baer, V. Shtivelman, D. Wachs, E. Raz, O. Crouvi, I. Kurzon, and Y. Yiechieli, 2003, Collapse-sinkholes and radar interferometry reveal neotectonics concealed within the Dead Sea basin: *Geophysical Research Letters*, v. 30, n. 10, p. 1545.
- Anderson, R.Y., 1981, Deep-seated salt dissolution in the Delaware Basin, Texas and New Mexico: New Mexico Geological Society Special Publication No. 10, p. 133-145.
- Anderson, N.L., and E.K. Franseen, 1991, Differential compaction of Winniepegosis reefs: A seismic perspective: *Geophysics*, v. 56, n. 1, p. 142-147.
- Anderson, N.L., R.W., Knapp, D.W. Steeples, and R.D. Miller, 1995, Plastic deformation and dissolution of the Hutchinson Salt Member in Kansas; in N.L. Anderson and D.E. Hedke, eds., *Geophysical atlas of selected oil and gas fields in Kansas: Kansas Geological Survey Bulletin 237*, p. 66-70.
- Anderson, N.L., A. Martinez, J.F. Hopkins, and T.R. Carr, 1998, Salt dissolution and surface subsidence in central Kansas: A seismic investigation of the anthropogenic and natural origin models: *Geophysics*, v. 63, p. 366-378.
- Autin, W.J., 1984, Observations and significance of sinkhole development at Jefferson Island: Department of Natural Resources, Baton Rouge, Louisiana Geological Survey Geological Pamphlet 7, 75 p.
- Baker, G.S., J.C. Strasser, E.B. Evenson, D.E. Lawson, K. Pyke, and R.A. Bigl, 2003, Near-surface seismic reflection profiling of the Matnuska Glacier, Alaska: *Geophysics*, v. 68, p. 147-156.
- Baumgardner Jr., R.W., A.D. Hoadley, and A.G. Goldstein, 1982, Formation of the Wink Sink, a salt dissolution and collapse feature, Winkler County, Texas: Bureau of Economic Geology, University of Texas at Austin, Report of Investigations No. 114, 38 p.
- Beck, B.F., ed., 1984, *Sinkholes: Their Geology, Engineering, and Environmental Impact*: A.A. Balkema, Rotterdam.
- Brown, A.R., 1999, *Interpretation of Three-Dimensional Seismic Data*, 5th ed.: American Association of Petroleum Geologists (AAPG) Memoir 42, 510 p.
- Büker, F., A.G. Green, and H. Horstmeyer, 1998, Shallow seismic reflection study of a glaciated valley: *Geophysics*, v. 63, n. 4, p. 1395-1407.
- Christiansen, E.A., 1971, Geology of the Crater Lake collapse structure in southeastern Saskatchewan: *Canadian Journal of Earth Sciences*, v. 8, p. 1505-1513.
- Columbia University, 2005, 3-D Seismic Reflection Imaging Workshop: Lamont-Doherty Earth Observatory (www.ldeo.columbia.edu/events/workshops/3Dseismic/proposal.html).
- Connelly, D.L., B.J. Ferris, and L.D. Trembly, 1991, Northwestern Williston Basin case histories with 3-D seismic data: *Geophysics*, v. 56, n. 11, p. 1849-1874.
- Davies, W.E., 1951, Mechanics of cavern breakdown: *National Speleological Society*, v. 13, p. 6-43.
- Davies, P.B., 1985, Structural characteristics of a deep-seated dissolution-subsidence chimney in bedded salt; in B.C. Schreiber and H.H. Harner, eds., *Sixth International Symposium on Salt: The Salt Institute*, v. 1, p. 331-350.
- Enslin, J.F., 1951, Some applications of geophysical prospecting in the Union of South Africa: *Geophysics*, v. 20, p. 886-912.
- Evans, M.W., S.W. Snyder, and A.C. Hines, 1994, High-resolution seismic expression of karst evolution within the upper Floridian aquifer system: Crooked Lake, Polk County, Florida: *Journal of Sedimentary Research*, v. B-64, n. 2, p. 232-244.

- Ge, H., and M.P.A. Jackson, 1998, Physical modeling of structures formed by salt withdrawal: Implications for deformation caused by salt dissolution: *AAPG Bulletin*, v. 82, p. 228-250.
- Gendzwill, D.J., and Z. Hajnal, 1971, Seismic investigation of the Crater Lake collapse structure in southeastern Saskatchewan: *Canadian Journal of Earth Sciences*, v. 8, p. 1514-1524.
- Gowan, S.W. and S.M. Trader, 2003, The mechanism of sinkhole formation in glacial sediments above the Retsof Salt Mine [abs.]: Geological Society of America 2002 Annual Meeting, Denver, Colorado, October 27-30, Paper 93-9.
- Green, A.G., A. Pugin, M. Beres, E. Lanz, F. B ker, P. Huggenberger, H. Horstmeyer, M. Grasm ck, R. De Iaco, K. Holliger, and H.R. Maurer, 1995, 3-D high-resolution seismic and georadar reflection mapping of glacial, glaciolacustrine, and glaciofluvial sediments in Switzerland: Symposium on the Application of Geophysics to Engineering and Environmental Problems (SAGEEP 1995), p. 419-434.
- Jammal, S.E., and B.F. Beck, 1985, A self-guided field trip to the Winter Park sinkhole: Orlando, Florida, The Florida Sinkhole Research Institute at the University of Central Florida, Report 85-86-2, 9 p.
- Kindinger, J.L., J.B. Davis, and J.G. Flocks, 1994, High-resolution single-channel seismic reflection surveys of Orange Lake and other selected sites of north central Florida: U.S. Geological Survey, Center for Coastal Geology, Open-file Report 94-616.
- Knapp, R.W., D.W. Steeples, R.D. Miller, and C.D. McElwee, 1989, Seismic reflection at sinkholes; in D.W. Steeples, ed., *Geophysics in Kansas*: Kansas Geological Survey Bulletin 226, p. 95-116.
- Lanz, E., A. Pugin, A.G. Green, and H. Horstmeyer, 1996, Results of 2-D and 3-D high-resolution seismic reflection surveying of surficial sediments: *Geophysical Research Letters*, v. 23, p. 491-494.
- Lee, T.M., D.B. Adams, A.B. Tihansky, and A. Swancar, 1991, Methods, instrumentation, and preliminary evaluation of data for the hydrologic budget assessment of Lake Lucerne, Polk County, Florida: U.S. Geological Survey Water Resources Investigation 90-4111, 42 p.
- Lippincott, T., S. Cardimona, N. Anderson, S. Hickman, and T. Newton, 2000 Geophysical site characterization in support of highway expansion project: Symposium on the Application of Geophysics to Engineering and Environmental Problems (SAGEEP 2000), Arlington, Virginia, February 20-24, p. 587-596.
- Lines, L., 2005, Addressing Milo's challenges with 25 years of seismic advances: *The Leading Edge*, v. 24 (supplement), p. S32-S36.
- Locker, S.D., G.R. Brooks, and L.J. Doyle, 1988, Results of a seismic-reflection investigation and hydrogeologic implications for Lake Apopka, Florida: Center for Near-shore Marine Science, Final Report to the St. John's River Water Management District, 39 p.
- Lohmann, H.H., 1972, Salt dissolution in subsurface of British North Sea as interpreted from seismograms: *AAPG Bulletin*, v. 56, p. 472-479.
- Mayne, W.H., 1962, Horizontal data stacking techniques: Supplement to *Geophysics*, v. 27, p. 927-938.
- Miller, R.D., 1992, Normal moveout stretch mute on shallow-reflection data: *Geophysics*, v. 57, p. 1502-1507.

- Miller, R.D., 2003, High-resolution seismic-reflection investigation of a subsidence feature on U.S. Highway 50 near Hutchinson, Kansas; in K.S. Johnson and J.T. Neal, eds., *Evaporite karst and engineering/environmental problems in the United States: Oklahoma Geological Survey Circular 109*, p. 157-167.
- Miller, R.D., 2006, High-resolution seismic reflection to identify areas with subsidence potential beneath U.S. 50 Highway in eastern Reno County, Kansas: *Symposium on the Application of Geophysics to Engineering and Environmental Problems (SAGEEP 2006)*, Seattle, Washington, April 2-6, Paper 28, 13 p.
- Miller, R.D., and T.V. Weis, 1995, Feasibility and resolution of shallow seismic reflection techniques in northwestern Franklin, southeastern Douglas, and Osage counties in Kansas; in N.L. Anderson and D.E. Hedke, eds., *Geophysical atlas of selected oil and gas fields in Kansas: Kansas Geological Survey Bulletin 237*, p. 83-87.
- Miller, R.D., A. Villella, and J. Xia, 1997, Shallow high resolution seismic reflection to delineate upper 400 m around a collapse feature in central Kansas: *AAPG Division of Environmental Geosciences Journal*, v. 4, no. 3, p. 119-126.
- Miller, R.D., D.W. Steeples, J.L. Lambrecht, and N. Croxton, 2006, High-resolution seismic-reflection imaging 25 years of change in I-70 sinkhole, Russell, County, Kansas [exp. abs.]: *Society of Exploration Geophysicist*, p. 1411-1414.
- Miller, R.D., D.W. Steeples, and J.A. Treadway, 1985, Seismic reflection survey of a sinkhole in Ellsworth County, Kansas [exp. abs.]: *Society of Exploration Geophysicists*, p. 154-156.
- Miller, R.D., D.W. Steeples, and T.V. Weis, 1995, Shallow seismic-reflection study of a salt dissolution subsidence feature in Stafford County, Kansas; in N.L. Anderson and D.E. Hedke, eds., *Geophysical atlas of selected oil and gas fields in Kansas: Kansas Geological Survey Bulletin 237*, p. 71-76.
- Miller, R.D., J. Xia, and C.B. Park, 2005, Seismic techniques to delineate dissolution features (karst) at a proposed power plant site; in D.K. Butler, ed., *Near-Surface Geophysics: Society of Exploration Geophysicists, Investigations in Geophysics No. 13*, p. 663-679.
- Miller, R.D., J. Xia, C.B. Park, and J.M. Ivanov, 1999, Multichannel analysis of surface waves to map bedrock: *The Leading Edge*, v. 18, n. 12, p. 1392-1396.
- Mullican, W.F. III, 1988, Subsidence and collapse at Texas salt domes: *The University of Texas at Austin, Bureau of Economic Geology, Geological Circular 88-2*, 35 p.
- Nelson, R.G., and J.H. Haigh, 1990, Geophysical investigations of sinkholes in Lateritic terrains; in Stan Ward, ed., *Volume 3: Geotechnical: Society of Exploration Geophysicists, Investigations in Geophysics No. 5*, p. 133-153.
- Odum, J.K., W.J. Stephenson, R.A. Williams, W.M. Worley, D.J. Toth, R.M. Spechler, and T.L. Pratt, 1999, Land-based high-resolution seismic-reflection surveys of seven sites in Duval and St. Johns counties, northeastern Florida: *U.S. Geological Survey Open-file Report 97-718*, 61 p.
- Pennington, W.D., 2005, The rapid rise of reservoir geophysics: *The Leading Edge*, v. 24, n. S1, p. S86-S91.
- Pullan, S.E., and J.A. Hunter, 1990, Delineation of buried bedrock valleys using the optimum-offset shallow seismic reflection technique; in Stan Ward, ed., *Volume 3: Geotechnical: Society of Exploration Geophysicists, Investigations in Geophysics No. 5*, p. 89-97.

- Pyke, K.A., G.S. Baker, E. Evenson, and G. Larson, 2001, Multitool geophysical analysis of glacier margin dynamics, Matanuska Glacier, Alaska: Geological Society of America annual conference, Paper 98-0.
- Sacks, L.A., T.M. Lee, and A.B. Tihansky, 1992, Hydrogeologic setting and preliminary data analysis for the hydrologic-budget assessment of Lake Barco, an acidic seepage lake in Putnam County, Florida: U.S. Geological Survey Water Resources Investigation 91-4180, 28 p.
- Schepers, R., 1975, A seismic reflection method for solving engineering problems: *J. Geophysics*, v. 41, p. 367-384.
- Shoemaker, M.L., N.L. Anderson, A.E. Shaw, J.A. Baker, A.W. Hatheway, T.E. Newton, and J. Conley, 1998, Reflection seismic study of previously mined (lead/zinc) ground, Joplin, Missouri; in N.L. Anderson, S. Cardimona, and T. Newton, eds., *Highway Applications of Engineering Geophysics with an Emphasis on Previously Mined Ground*: Missouri Department of Transportation Special Publication, p. 124-135.
- Sinclair, W.C., J.W. Stewart, R.L. Knutilla, A.E. Gilboy, and R.L. Miller, 1985, Types, features and occurrence of sinkholes in the karst of west-central Florida: U.S. Geological Survey Water-Resources Investigations Report 85-4126, 81 p.
- Snyder, S.W., M.W. Evans, A.C. Hines, and J.S. Compton, 1989, Seismic expression of solution collapse features from the Florida platform; in B.F. Beck, and W.L. Wilson, eds., *Proceedings of the Third Multidisciplinary Conference on Sinkholes*: St. Petersburg, Florida, October 2-4, New York, A.A. Balkema, p. 281-298.
- Somanas, C.D., B.C. Bennett, and Y.-J. Chung, 1987, In-field seismic CDP processing with a microcomputer: *The Leading Edge*, v. 6, n. 7, p. 24-26.
- Steeple, D.W., and R.D. Miller, 1987, Direct detection of shallow subsurface voids using high-resolution reflection techniques; in B. Beck and W.L. Wilson, eds., *Sinkholes: Their Geology, Engineering, and Environmental Impact*, 2nd ed.: A.A. Balkema, Boston, p. 179-183.
- Steeple, D.W., and R.D. Miller, 1998, Avoiding pitfalls in shallow seismic reflection surveys: *Geophysics*, v. 63, n. 4, p. 1213-1224.
- Steeple, D.W., R.W. Knapp, and C.D. McElwee, 1983, Seismic reflection surveys of a catastrophically collapsed sinkhole, Ellis County, Kansas [exp. abs.]: Society of Exploration Geophysicists, p. 296-298.
- Steeple, D.W., R.W. Knapp, and C.D. McElwee, 1986, Seismic reflection investigations of sinkholes beneath interstate highway 80 in Kansas: *Geophysics*, v. 51, p. 295-301.
- Surjik, D.L., and G.D. Hobson, 1964, An example of prairie-evaporite mapping in the Minton area of Saskatchewan employing the seismic method: *Geophysics*, v. 29, n. 6, p. 951-956.
- Tihansky, A.B., J.D. Arthur, and D.J. DeWitt, 1996, Sublake geologic structure from high-resolution seismic-reflection data from four sinkhole lakes in the Lake Wales Ridge, central Florida: U.S. Geological Survey Open-file Report 96-224, 72 p.
- Walters, R.F., 1978, Land subsidence in central Kansas related to salt dissolution: Kansas Geological Survey Bulletin 214, 82 p.
- Wiederhold, H., H.A. Bunn, and K. Bram, 1998, Glacial structures in northern Germany revealed by a high-resolution reflection seismic survey: *Geophysics*, v. 63, p. 1265-1272.

CHAPTER 6

DATA PROCESSING AND ACQUISITION: NEAR-SURFACE FOCUS

In various places throughout this manuscript, discussions and developments have been presented that relied heavily on the unique advantages and imaging characteristics of high-resolution seismic-reflection data. To better appreciate those advantages and the unique characteristics of the approach, this chapter has been devoted to providing an overview of high-resolution seismic reflection and why it comes at a high price, but one worth paying. Also summarized in this chapter is a historical development of high-resolution seismic reflection identifying some of the many noteworthy contributions made by key individuals and groups over the last several decades. With high-resolution seismic-reflection imaging being the principal tool of this study, it is prudent to include a section in this chapter defining and clarifying vertical and horizontal resolution potential based on the properties of the wavefield, especially in the context of the shallow subsurface and high frequencies.

Assuming that considerations, concepts, and work flows should scale consistent with frequency seems intuitive; however, that assumption has led to misinterpretations and suggestions that inherent limitations make the seismic-reflection method unreliable at higher frequencies. The high-frequency version of the method does have inherent limitations, but they are related to the earth's preferential attenuation of higher frequencies. As will be shown in this chapter, most misperceptions about the utility of the method are related to a failure to consider the possibility that some approaches and processing schemes reasonable for conventional seismic-reflection data could be inappropriate for high-resolution near-surface data. This chapter tries to highlight the true potential of the high-resolution approach and how that potential can be fulfilled if blind linearity is not assumed for all conventional approaches. Key aspects of both acquisition and processing are presented, focusing on differences between the approaches and the most important considerations and assumptions that distinguish high-resolution from conventional imaging.

This chapter also establishes the basis for the stringent critiques (criticisms) that were leveled in previous chapters against published high-resolution seismic-reflection investigations that failed to pay heed to data-processing assumptions and, in so doing, published results lacking validity. As displayed and discussed in previous chapters, authors sometimes have a tendency to interpret coherent events on CMP stacked sections as reflections without regard to the potential of the data or what transformation the data really made during each processing step. As will become evident in this chapter, most processing and interpretation errors on high-resolution reflection data stem from overlooking assumptions inherent to a process or the fundamental information contained in each trace within a focus time window. In many cases, simply noting the limitations of the acquisition geometry and frequency content of a data set can help avoid impossible assertions about what individual wavelet characteristics truly represent.

Keys to High Resolution

High-resolution seismic data by definition consists of signal with “seismic frequency(ies) above the normal exploration range, recorded with the objective of improving resolution, especially of shallow events. Usually implies frequencies from 80-150 Hz, sometimes to 500 Hz or higher” (Sheriff, 2002). The term high resolution is nonunique in geophysics and has been used to characterize/describe a wide range of geophysical data with higher than “normal” fidelity. Data from seismic reflection (Mair and Green, 1981), seismic refraction (K. Miller et al., 1998), aeromagnetics (McConnell, 1998), gravity (Sandwell and McAdoo, 1990), GPR (Kositsky and Milanfar, 1999; Arcone, 1996), EM (Gibert et al., 1994), to name a few, have all been characterized as high resolution. Just about every geophysical tool that has found its way into the refereed literature has had some subset classified as high resolution by an author. Seismic and aeromagnetics are the only methods that have an accepted, specific, and quantifiable definition for what is required to be classified as “high resolution.”

Distinguishing data types as conventional or high resolution (shallow or near-surface) has gone on longer and by a substantially larger contingent of researchers for seismic reflection than any of the other techniques (Steeple et al., 1995a; 1995b; Miller et al., 2005a) (Figure 6-1). Although high-resolution seismic data are classified by a very concise set of criteria, in general high-resolution has generally been synonymous with shallow or near-surface seismic. At shallow depths seismic reflection must be high-resolution to be applicable; however, high-resolution data are not limited to shallow depths (Hammer et al., 2004). With high-resolution seismic, especially shallow, comes increased potential for pitfalls and inappropriate use of more conventional tools (Gruber and Rieger, 2003).

Criteria and associated definitions for high-resolution seismic-reflection data have historically been based on compressional-wave data. However, in terms of wavelength, lower velocity shear-wave reflection data can have as much as 10 times greater resolving power than compressional-wave data for a given site at equivalent frequencies due to significantly higher compressional-wave velocities (Figure 6-2) (Pullan et al., 1990; Miller et al., 2000). Therefore, at a particular site it is possible for 10-Hz shear-wave reflection data to have equivalent resolving potential as compressional-wave reflection data at 80 Hz or more (Inazaki, 2006). Current requirements for classifying data as high resolution are clearly a bit arbitrary and have been based on empirically derived data characteristics and intuition. Nonetheless, problems exploiting the unique potential higher frequency that shallow-reflection data possess compared to conventional data cannot be overlooked.

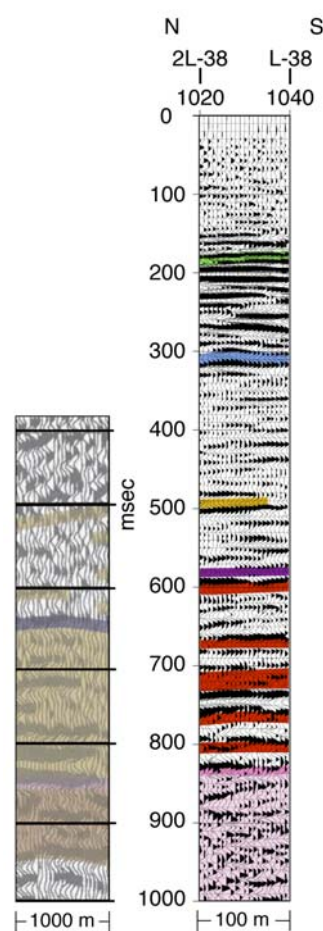


Figure 6-1. Comparison of coincident data at gas-hydrate research site in northwestern Canadian Arctic (from Miller et al., 2005a).

With the improved coupling and reduced attenuation of saturated sediments, most marine seismic-reflection data fall into the classification of high-resolution (Haeni, 1986; Marlow et al., 1996; Hunsdale et al., 1998; Quinn et al., 1998; Seltzer et al., 1998). Applications with penetration depths on the order of 1 to 2 km generally result in reflection sections possessing bandwidths in the 50-Hz to 3-kHz or even higher range in some cases (Barnes and Audru, 1999). Water surveys eliminate many of the obstacles inhibiting or complicating acquisition of high-frequency data routinely encountered during land surveys. The most significant of these obstacles include the attenuative characteristics of dry, unconsolidated surface/near-surface

sediments and lateral variability in velocity and surface elevation manifested in statics. Saturated beach sand provided an ideal test bed for showing the effects of saturated sand vs. dry sand in a natural setting (Bachrach and Rickett, 1999). Reflection events with frequencies in excess of 800 Hz from within saturated sand during low-tide conditions were observed on shot gathers.

Coupling of source and receiver is a principal concern for high-resolution surveys (Hoover and O'Brien, 1980; Miller et al., 1986; Doll et al., 1998; Keiswetter and Steeples, 1995). All else being equal, improving the coupling of receivers increases the high-frequency response (Hoover and O'Brien, 1980; Krohn, 1984, 1985) and coupling geophones to a stiff earth in a saturated environment clearly improves the data resolution (Whiteley et al., 1998). Attempts have been made at various times to artificially simulate these more ideal conditions by physically altering a site (Figure 6-3) (Miller et al., 1994). Researchers have shown that by flooding a dug trench and creating a fluid-coupling scenario, ultra-high-frequency data can be recorded with reflection spectra exceeding 800 Hz (Kim et al., 2001). Changes in coupling through increased spike length, loose soil removal, and increased saturation have only a minor effect on reflection-wavelet characteristics within the lower conventional survey frequency bands.

Source-energy levels and the possible mechanisms used to impart that energy into the ground depend to a large extent on the near-surface setting (Miller et al., 1986; Miller et al., 1992; Miller et al., 1994). Extremely low source energy generally results in broader useable bandwidths and higher dominant-frequency reflected wavelets (Knapp and Steeples, 1986b). Dozens of different types of shallow and high-frequency seismic sources have been developed and used in a variety of near-surface settings. The vast number and types of low-energy seismic sources alone is a key indicator of the unique energy-dissipation

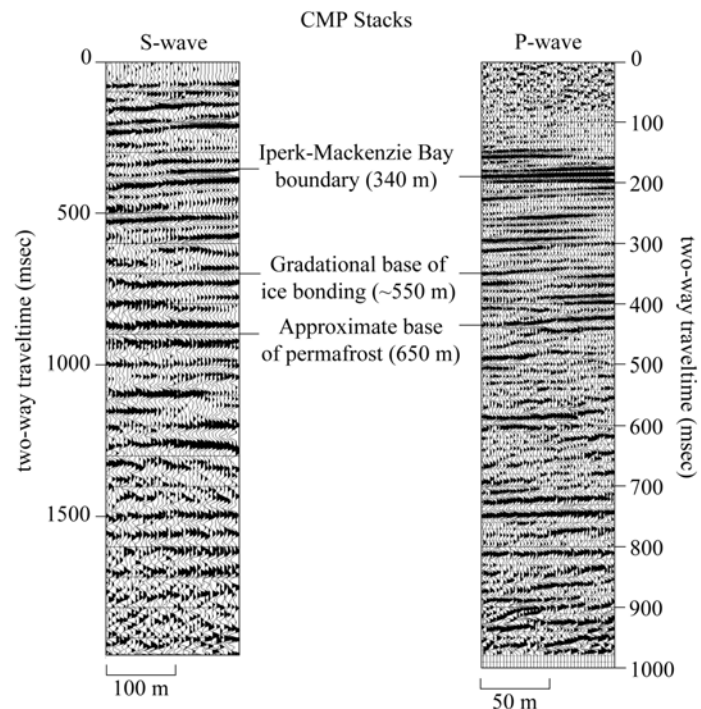


Figure 6-2. Contrasting depth-adjusted shear (S-wave) and compressional (P-wave) stacked sections from northern extreme of the Mackenzie Delta in northwestern Canada (from Miller et al., 2000).



Figure 6-3. Trenches dug through gravel surface at the U.S. Army's Memphis Defense Depot and flooded to improve source and receiver coupling (photos by R. Miller).

characteristics for different near-surface conditions and resolution demands to meet survey goals or targets. Increasing the instantaneous energy levels of a seismic source normally increases the energy-penetration depths but generally reduces the upper corner frequency of the useable bandwidth for a given near-surface reflection event.

Historical Perspective

Effective use of land high-resolution seismic imaging emerged in the latter half of the twentieth century out of heightened interest to better characterize the near surface for various environmental, engineering, and ground-water applications (Steeple and Miller, 1990). Prior to 1980, several researchers demonstrated the technique's potential and orchestrated a vast range of the pioneering, curiosity-driven research projects probing various aspects of high-resolution seismic reflection (Evison, 1952; Pakiser and Warrick, 1956; Mooney, 1973; Schepers, 1975). This early research provided the essential groundwork that opened the door for the broad range of applications and successes the technique enjoys today. Much of this innovative work prior to 1980 was completed with rudimentary equipment, by today's standards, and limited to little or no processing capability.

Three independent research groups emerged in the 1980s, leading the development of high-resolution seismic reflection for shallow applications. First out of the pack was a group led by James Hunter of the Canadian Geological Survey. His group focused on developing methods and approaches that allowed effective use of the seismic-reflection tool by a wide range of geophysicists trying to address shallow problems with notoriously low budgets and

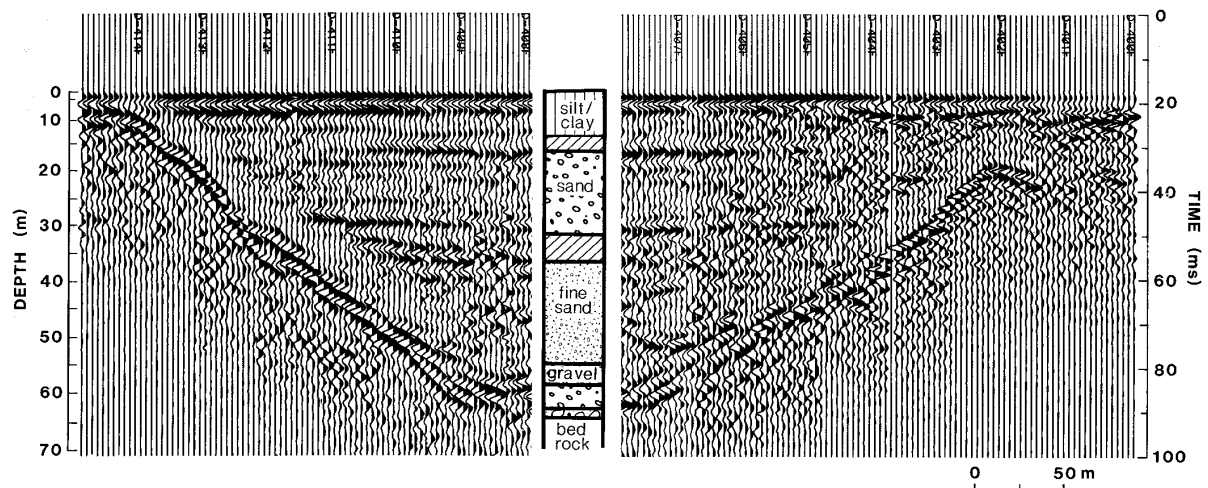


Figure 6-4. Optimum offset reflection section from Dryden, Ontario. This single-fold section shows a steep-sided bedrock valley (from Pullan and Hunter, 1990).

without access to the mainframe computers that were necessary at that time to process conventional seismic data (Hunter et al., 1984). From this group came the “optimum window method” which still finds application today in some settings; however, in most cases it has been relinquished to use as an in-field QC tool (Figure 6-4) (Pullan and Hunter, 1990). Key principles of this single-fold method remain the cornerstone for recording and processing shallow high-resolution seismic-reflection data. The influence of this group reached further into the geotechnical community than any others at this time, with monumental developments in the use of seismic to characterize site response (Hunter et al., 2002).

A second group working in Europe at about the same time under the direction of Klaus Helbig from the University of Utrecht in the Netherlands were pushing the upper limits of resolution through a series of experiments designed to image thin beds at mid-range depths (around 100 m to 1000 m) beneath fully saturated tidal flats (Doornenbal and Helbig, 1983; Jongerius and Helbig, 1988). This group was highly successful in showing the potential of high-resolution seismic reflection and defining the conditions and concerns influencing selection and surveying of a near ideal site (Figure 6-5). By characterizing these near-ideal

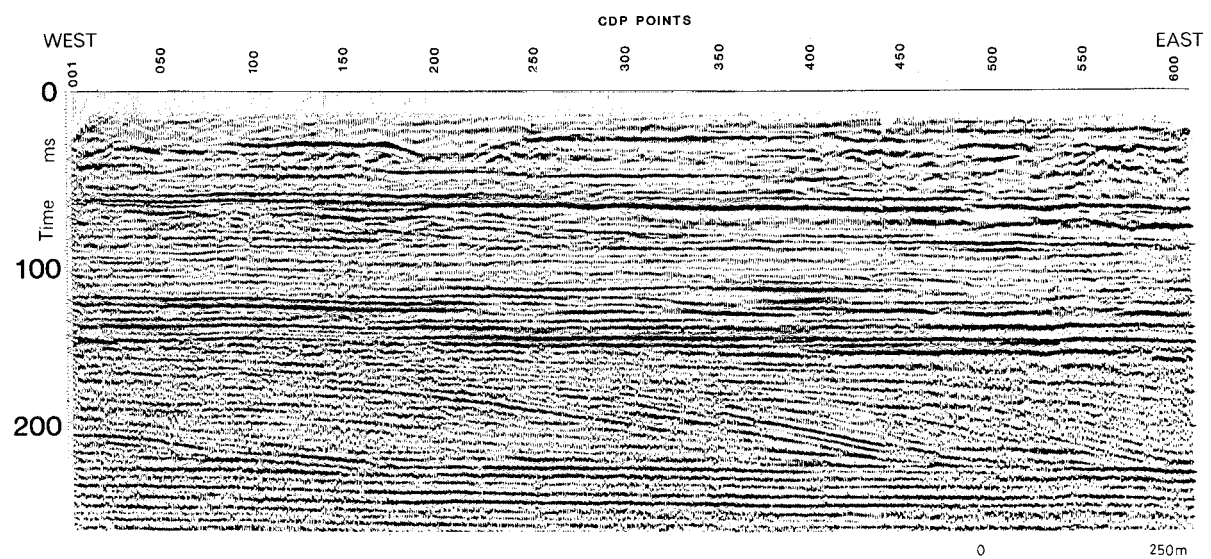


Figure 6-5. This almost 1200-m-long profile captures a variety of unique depositional geometries at unprecedented fidelity for this period (from Jongerius and Helbig, 1988).

conditions and understanding their control on resulting stacked data, appraisals or predictions of likely site response for other areas were greatly improved. Based on this work it became clear that less than optimal sites could be altered and/or procedures modified to better align with and, in many cases, simulate these near ideal conditions (Miller et al., 1994) (Figure 6-6). As an indication of this group's diversity, they were the first to develop an extremely small, high-frequency, electromechanical portable seismic vibrator later marketed by OYO of Japan (Nijhof, 1992; van der Veen et al., 1999).

At this same time a group working under the direction of Don Steeples at the University of Kansas were adapting and applying many of the CMP tools, equipment, and techniques being developed and used at that time by industry in search of petroleum for imaging the near-surface at high resolution (Steeple and Knapp, 1982; Knapp and Steeples, 1986a, 1986b). Unique about this group was their persistence with evaluating and adapting the CMP method to handle real problems at a diverse assortment of difficult sites (Figure 6-7). Conditions in the near-surface at many of these sites were some of the most challenging possible for effective use of the tool; hence, this group uncovered many pitfalls (Steeple and Miller, 1986, 1998) and potential misuse of the method while at the same time pushing the very upper limits of what could be realistically expected across a range of different types of sites (Birkelo et al., 1987; Miller et al., 1989). It was an underlying principle of this group that for any given site, the seismic source could have the



Figure 6-6. A device built by the Kansas Geological Survey to improve coupling by removing unfavorable surface material (photo by R. Miller).

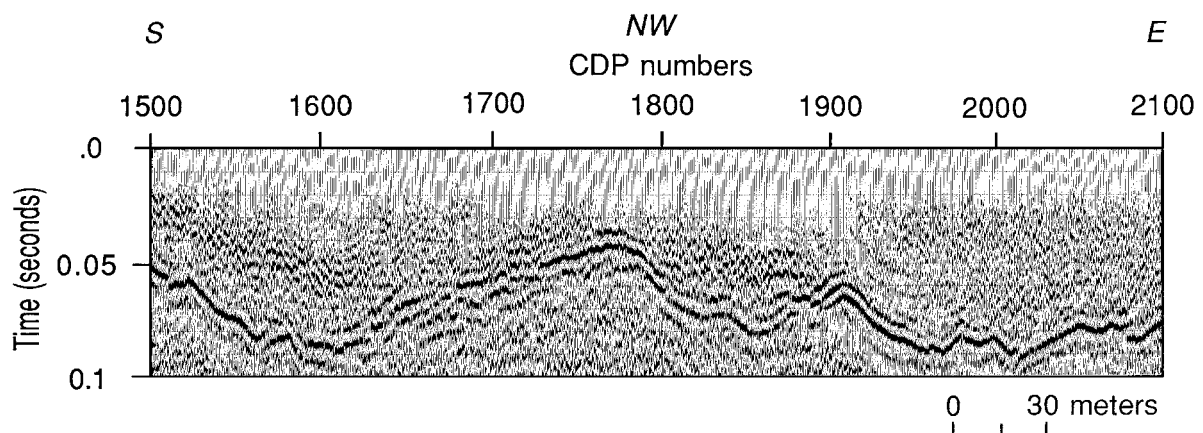


Figure 6-7. This line has a near right-angle bend (compensated for during CDP processing) near CDP 1830 at the highest elevation along the line (modified from Miller et al., 1989). Bedrock is clearly defined, but wavelet inconsistency is obvious and a result of interspread variability. The 10+ m of overburden was dry, unsorted, unconsolidated sand.

most significant influence on the quality and therefore resolution potential of the resulting data; hence, much work was done in source development (Steeple et al., 1987; Miller et al., 1986; Healey et al., 1991; Park et al., 1996).

During the 1990s and early twenty-first century, three groups continued at the forefront of land high-resolution seismic imaging of the near-surface, but the groups and their emphasis changed slightly from those of the 1980s. Research at the Canadian Geological Survey continued to extend the applications of seismic venturing into shear-wave reflection, engineering characterization of the near surface, and borehole seismic characterization (Hunter et al., 1998; Harris et al., 2000; Hunter et al., 2000; Benjumea et al., 2001). The University of Kansas group continued to focus on pushing the resolution potential of the seismic-reflection tool, exploiting more of the seismic wavefield, and improving the efficiency of the entire method (Miller et al., 1995a; Baker et al., 1999; Miller and Henthorne, 2004; Miller et al., 1999, 2003; Steeples et al., 1999; Park et al., 1999). A research group that emerged at ETH Zurich, Switzerland, under the direction of Alan Green, began demonstrating expertise in a wide range of near-surface geophysics applications with a clear emphasis in the application of high-resolution seismic reflection to alpine problems (Büker et al., 1998; Green et al., 1995; Lanz et al., 1996; Roth et al., 1998; van der Veen et al., 2001; Spitzer et al., 2003).

Some of the most significant high-resolution research published in the last decade and a half has come from the ETH Zurich group. Testing the applicability of land streamers for near-surface applications was first undertaken during the late 1990s in Switzerland, where gimbal geophones were mounted to a conveyor belt and dragged in road ditches (van der Veen and Green, 1998). The surge in 3-D imaging throughout the petroleum industry necessitated a detailed evaluation and associated assessment of this volume-based approach to seismic imaging for near-surface and high-resolution targets (Spitzer et al., 1998). The Zurich group was also working to unravel some of the unique components of the wavefield at early times and close offsets in hopes of improving the accuracy of seismic images, specifically fundamental work describing the guided-wave phenomenon (Robertsson et al., 1996a). Recent work by this group has provided a glimpse of where near-surface geophysics in general is headed, with important contributions to joint interpretation of multiple geophysical data sets tailored to a specific target (Green et al., 2006).

Similar research interests on a variety of topics drew the two North American groups into a collaborative partnership during the late 1980s through the early twenty-first century. Some of these research endeavors included source characterization (Miller et al., 1986; Miller et al., 1992; Miller et al., 1994), shear-wave technique development (Hunter et al., 2002; Miller et al., 2000; Harris et al., 2000; Park et al., 2000), high-resolution imaging of non-conventional resources (Miller et al., 2005a), and marine engineering studies (Park et al., 2005). This research alliance tackled problems all over North America, ranging from discrimination of segregated ice in the high Arctic to evaluating optimum source characteristics in the desert-like conditions of southern California. Most of the research articles that have emerged due to this collaboration have unveiled new ideas, answered commonly asked questions, or explained curious observations of past researchers.

Development of the high-resolution seismic method for land applications was not exclusive to these four research groups; innovative applications were showing up in the literature from a variety of authors throughout the latter portion of the twentieth century, specifically in coal exploration, ground-water investigations, and environmental applications.

Outside the contributions of the four major research groups previously mentioned, success and improvements in the method were becoming more widespread. The mining industry invested heavily in high-resolution seismic imaging for coal applications focusing on enhancing resolution (Gochioco and Kelly, 1990; Gochioco, 1991, 1992; Pietsch and Slusarczyk, 1992); improving image accuracy associated with potash mining (Gendzwill and Brehm, 1993); and improving resource assessment for tin mining (Singh, 1984), talc (Urosevic et al., 2002), and diamond mining (Hammer et al., 2004), to name a few. Ground-water studies where high-resolution seismic methods were employed have been more limited outside these four main research groups, but a few good examples of quality research can be found in the literature from other groups around the world (Geissler, 1989; Bachrach and Rickett, 1999; Liberty et al., 1999; Davies et al., 1992; Odum et al., 1999; Olsen et al., 1993; Burow et al., 1997; Shtivelman and Goldman, 2000). A diverse set of high-resolution seismic-reflection approaches have been used by other groups to address environmental problems (Pugin et al., 2004; Guillen and Hertzog, 2004). Critical contributions to high-resolution seismic reflection throughout the 30+ years between 1975 and 2007 came from a diverse group of highly skilled and innovative researchers from around the world.

Shear-wave reflection imaging has not been heavily discussed or exploited by the high-resolution community as a direct consequence of the limited examples of bona fide successes using shear or secondary waves. As previously noted, considering resolution is a function of velocity and frequency, lower shear-wave velocities relative to compressional wave for a given media (as much as 10 times) equate to a much lower frequency threshold for equivalent resolution. A few examples of high-quality shear data have been published through the years with the amazing potential of this transversely polarized body wave clearly evident (Hasbrouck and Padget, 1982; Hasbrouck, 1991; Goforth and Hayward, 1992; Harris et al., 1996; Inazaki, 2006; Pugin et al., 2007) (Figure 6-8). Shear-wave reflection imaging has suffered from minimal use as a direct result of the difficulty in generating and propagating broadband signal and separating Love waves and shear body waves (Miller et al., 2001).

Surface waves, although not generally considered high fidelity, have found application to near-surface imaging and in many cases provide layer discrimination that rivals more mainstream high-resolution reflection imaging (Miller et al., 1999, 2005b) (Figure 6-9). Several researchers developed the numerical basis describing the generation and propagation of these waves (Jones, 1962) and were instrumental in some of the earliest empirical developments of applications for surface waves as an imaging tool (Ballard, 1964). Civil engineers later developed techniques for analyzing the surface-wave arrival characteristics to estimate one-dimensional shear wave velocity (Stokoe et al., 1994).

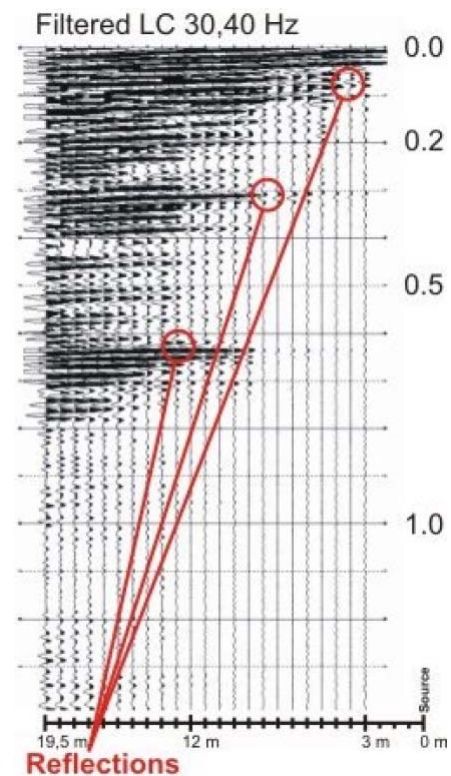


Figure 6-8. Correlated vibroseis shear-wave shot gather with reflections annotated (from Pugin et al., 2007).

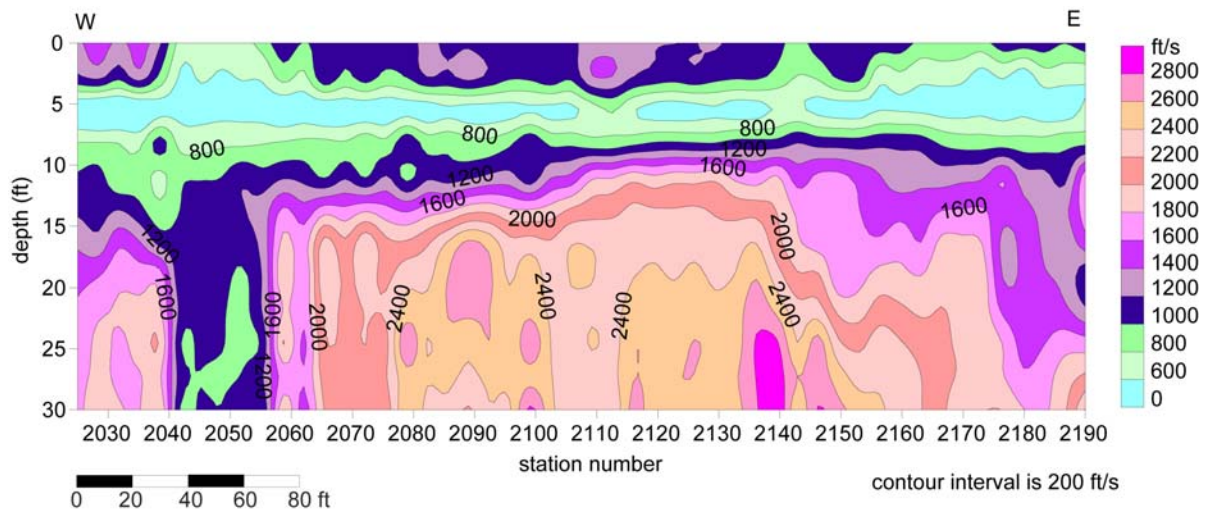


Figure 6-9. S-wave velocity contours at the Olathe, Kansas, site. Low velocity crevice beneath station 2050 is a drill-confirmed fracture zone in limestone with clay infill material (from Miller et al., 1999).

Geophysicists later fully developed surface-wave imaging to facilitate the generation of 2-D cross sections of the shear-wave velocity field (Park et al., 1999; Xia et al., 1999).

Resolution

Seismic resolution is a property of data that defines the minimum distance two layers or objects can be separated and still be distinguishable as unique features; therefore, it is the maximum potential of the data (Figure 6-10). Questions about resolution that need to be asked and will be answered in the context of this manuscript include the following: What are the advantages and disadvantages of high-resolution seismic-reflection data; how are high-resolution data sets different from conventional seismic-reflection data sets; and does high-resolution come at the expense of other data properties and is it worth it? Answers to these questions will highlight many unique properties and essential considerations of high-resolution data. Many of the first-time observations and discussion points raised and addressed about dissolution-induced subsidence features would not be possible without the fidelity seismic-reflection data used in this manuscript possess.

Vertical bed resolution is the most common measure of data fidelity, but for many applications horizontal or lateral resolution can be equally or more important. Vertical resolution is generally equated to the Rayleigh criteria and Widess axiom relating resolution potential to a percentage of the dominant wavelength (Widess, 1973). Lateral resolution, on

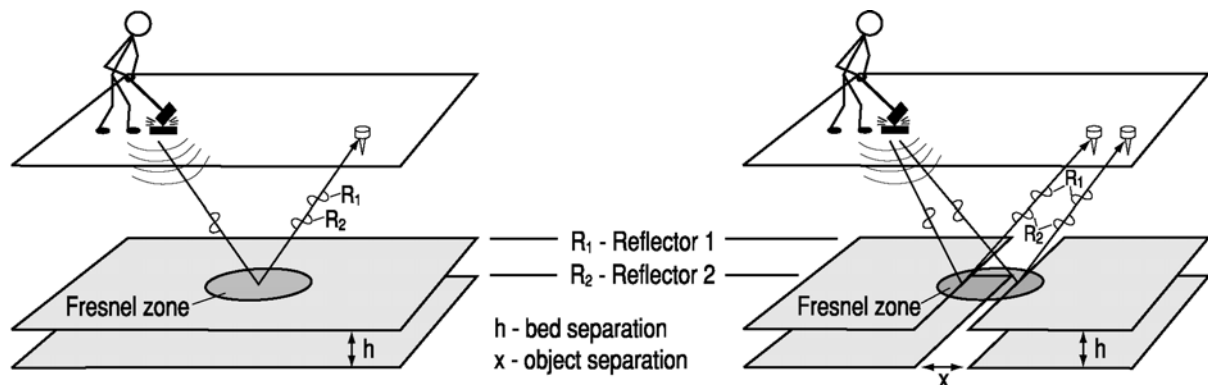


Figure 6-10. Ray diagram defining the bed and object separation associated with resolution criteria.

the other hand, is commonly equilibrated with interference phenomena initially described by the optics community as the Fresnel zone (Hecht and Zajac, 1974). Both vertical and horizontal resolution are considered high when the dominant frequency of the seismic data exceeds 80 Hz. However, the spatial minimum bed or object separation possible with 80-Hz data vary dramatically with different lithologies and target depths.

Fidelity is commonly used interchangeably with resolution although not officially equated in the geophysical literature (Sheriff, 2002). High frequency and high resolution are directly related and many times used in a somewhat equivalent fashion. However, they are not equivalent; a data set can possess high frequencies relative to the “norm” and yet not be high resolution. High resolution is quantitatively defined relative to frequency, whereas “high frequency” is a descriptive nonspecific term. Recently, High Fidelity Vibratory Seismic (HFVS) was developed by researchers formerly at Mobil (now ExxonMobil) to extend the resolution potential of vibroseis data. In general, the technique changes how the source signature is recorded and resulting data processing without changes to the source (Allen et al., 1998; Krohn and Johnson, 2006). As described, HFVS could be high resolution, but it could also just possess higher frequencies than traditional petroleum-industry vibroseis data and not be high resolution. The trend toward high resolution in the petroleum industry continues to gradually push the upper resolution limits of seismic data at common exploration depths fueled by the search for smaller and smaller reserves.

Generally, the minimum horizontal resolution of unmigrated data is restricted to the width of the first Fresnel zone (Yilmaz, 1987), whereas the upper limit of vertical resolution is determined by the dominant wavelength. Key to resolution potential is frequency (dominant and upper corner) and bandwidth (octaves and range) (Knapp, 1990). With the physical measure of resolution based on wavelength, material velocity plays a unique and instrumental role for each and every geologic setting. Common axioms use a fraction of the dominant wavelength as the thinnest resolvable bed limit; reflection wavelet interference, phase, and/or shape are commonly used to discriminate between two distinct layers. Below this wavelength threshold, interpreters must rely on attributes within the amplitude family to suggest interpretable separation between thin beds. Several authors have reported resolution potential as small as one-tenth of a wavelength using a combination of amplitude, wavelet interference, and model guidance (Gochioco, 1992). With resolution dependent on both the frequency characteristics of the recorded signal and the seismic velocity of the rock, amplitude and bandwidth characteristics of body waves imparted into the ground by the source and reliability of receivers to sense the full bandwidth strongly influence a data set’s fidelity.

Spectral properties of recorded seismic signal are influenced by source and receiver characteristics and dependent on near-surface conditions, attenuative properties of the earth, depth of target reflectors, and source-to-receiver offset. High frequencies are attenuated more rapidly than lower frequencies as a consequence of the earth’s natural low-pass tendency. Due to this natural tendency to attenuate high frequencies, increasing the length of the source and receiver raypath (either due to increased source to receiver offset or deeper target depths) reduces the dominant reflection frequency and upper corner of the useable reflection bandwidth. This natural attenuation with depth cannot be compensated for by increasing source energy; generally simply boosting energy levels decreases the high to low frequency ratio (Knapp and Steeples, 1986b; Sheriff and Geldart, 1995).

High-resolution seismic-reflection surveys require acquisition approaches and processing work flows tailored to the unique data characteristics of the shallow depth

intervals (by conventional standards) (Steeple and Miller, 1990; Spitzer et al., 1998; Baker et al., 1998; Jefferson et al., 1998; Henley, 2001; Danbom, 2005). Preservation of reflection wavelets with dominant frequencies greater than 80 Hz can and must be one of if not the highest processing priority for survey success. Spatial and temporal resolution required to map small-scale features demand higher resolution than is usually necessary for conventional seismic surveys and therefore special approaches to acquisition and processing. An example is statics: many high-resolution seismic-reflection targets are within the depth range normally classified as statics or weathered zone on conventional surveys (Cox, 1999; Telford et al., 1976). Although the fundamental theories and concepts are the same, many of the assumptions, the ratios of signal-to-noise, and the characteristics of both signal and noise are markedly different and are generally complicated by a lack of linearity when moving down from conventional scales.

Vertical Resolution

Vertical resolution can be thought of as the designated thinnest layer, in which the top and bottom can be uniquely discriminated on a seismic-reflection section. For a given material type with a characteristic velocity, dominant frequency is the only controllable variable that affects vertical resolution. Theoretical limits have been estimated from elastic models without noise and with uniform wavelet characteristics (Figure 6-11). Practical limits represent reasonable expectations for “normal” data acquisition settings and equipment with noise and real variability in wavelet characteristics.

Model estimates of resolution potential are usually based on minimal or no noise scenarios (Widess, 1973; Gochioco and Kelly, 1990; Gochioco, 1991, 1992). Studies suggest that beds separated by less than one-quarter the dominant wavelength cannot be detected or resolved (Widess, 1973). With the low relative amplitudes of high-frequency seismic signal come reflection wavelets that lack the uniformity and clarity observed in model wavelets. Introducing noise adversely affects the interpretation of thin beds (beds separated by less than a wavelength of the dominant reflected energy) and therefore negatively affects the bed-resolution potential of a data set. Empirical studies have shown that for practical purposes one-half wavelength of the dominant-reflection frequencies is a more realistic estimate of a dataset’s resolution potential (Miller et al., 1995a) (Figure 6-12). Practical resolutions will normally be considerably lower than theoretical values due to the detrimental effects of noise, relatively narrow bandwidth of real data, laterally inconsistent nature of reflection wavelets, and sub-wavelength irregularities in reflecting boundaries.

Vertical resolution can be described using two different, yet commonly used criteria (Knapp, 1990). First, determining the position of a reflection in time or reflector in space is

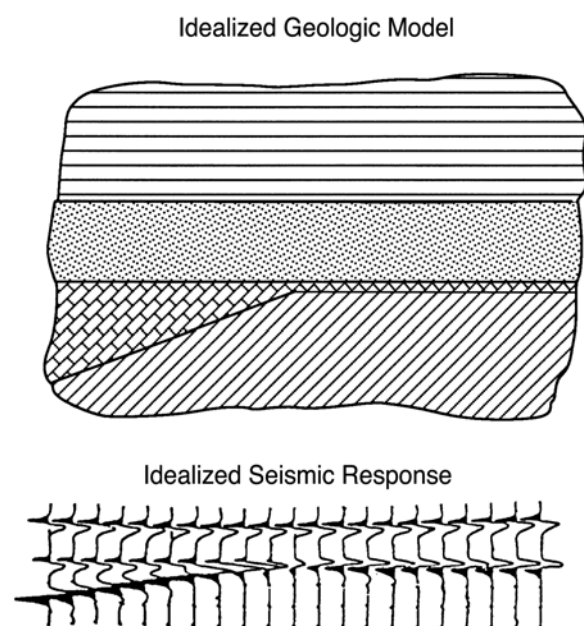


Figure 6-11. Model studies displaying effects of reflection-wavelet interference as a function of bed separation.

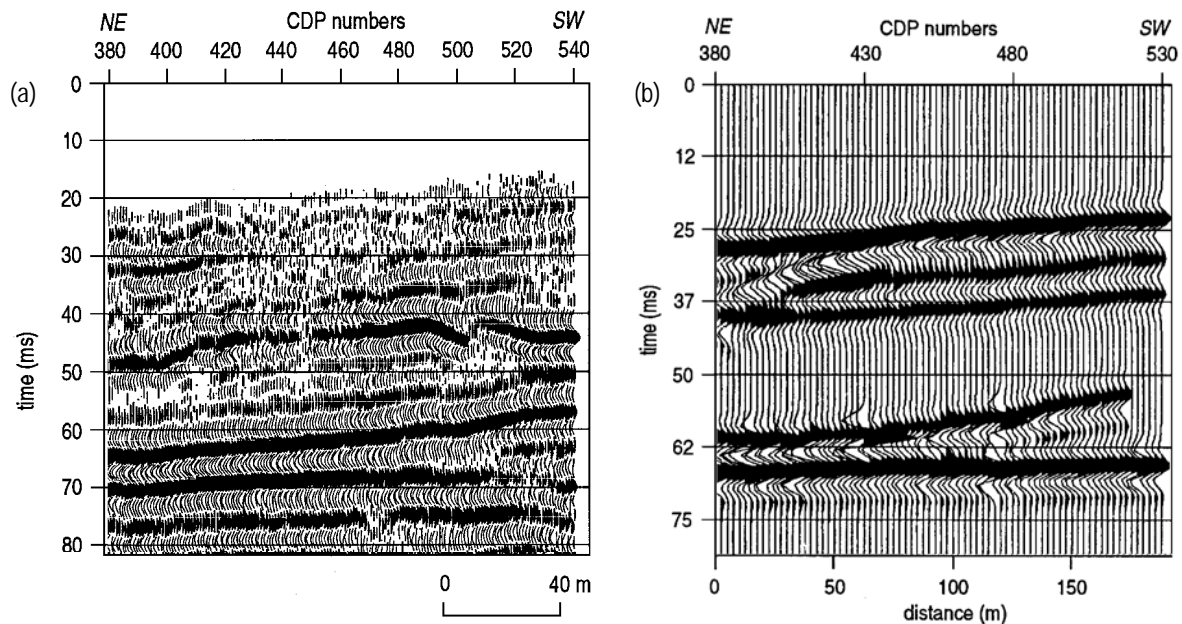


Figure 6-12. CMP stacked section (a) with drill-confirmed bed at 65 ms on the SW end of the section thinning and pinched-out compared to a synthetic (b) based on near identical seismic and geologic properties (from Miller et al., 1995a).

inversely related to the pulse width of the wavelet and is therefore directly related to the bandwidth and center frequency of the energy spectrum. A second and more commonly used criterion determines the minimum separation between the top and bottom of a bed or separation between interfaces that can be distinguished on seismic data. This second description of resolution is related to the Rayleigh criterion, which inversely relates wavelength and resolution. Vertical-resolution potential of seismic data has been suggested to be as small as one-tenth the dominant wavelength (Gochioco, 1991) and as large as half that wavelength (Miller et al., 1995a), but the commonly accepted value is one-quarter the dominant wavelength (Widess, 1973).

Lateral Resolution

Lateral resolution of a seismic-reflection survey is a function of seismic-reflection wavelength, velocity, and target depth with inherent dependence on CMP spacing, generally described as related to the broadband Fresnel radius. An object one-quarter the Fresnel zone appears on reflection data as a diffraction and is considered a point source rather than a reflecting point. Resolving horizontal variations in geometry and/or stratigraphy is more challenging and estimating the resolving potential of reflection data is not nearly as straightforward in the horizontal domain as in the vertical. Horizontal resolution has been described for broadband, zero phase seismic data as a zone of influence (Bruhl et al., 1996) with Rayleigh's criteria used to quantify the minimum distance two objects can be separated and still be distinguishable (Kallweit and Wood, 1982). This distance can be calculated using the relationship

$$r = \sqrt{VZ/2f},$$

where:

r = broadband Fresnel radius,
 f = dominant frequency,
 V = velocity, and
 Z = depth to the reflector (Ebrom et al., 1996).

Decreasing receiver spacing improves the apparent coherency of reflection events, but mathematically does not improve lateral resolution. A minimum receiver spacing approximate one-eighth the radius of the Fresnel zone should be maintained to ensure proper sampling and to optimize the interpretability of small objects on CMP stacked sections (Knapp, 1991) (Figure 6-13).

Lateral resolution can be thought of as the designation of the closest distance two objects can be and still be distinguishable as separate objects on a seismic-reflection section. Increasing the dominant frequency is the only way to improve lateral resolution for a particular material and target depth. Unlike vertical resolution, depth of the target affects lateral resolution.

Horizontal resolution of stacked sections may be improved by migration (Yilmaz, 1987). In practice, migration collapses the Fresnel zone to about the dominant wavelength (Stolt and Benson, 1986). At lower velocities, horizontal resolution of stacked sections may not be improved by migration (Black et al., 1994). Based on model studies for a reflection from a flat surface, about half the first Fresnel zone will interfere constructively (Sheriff, 1977).

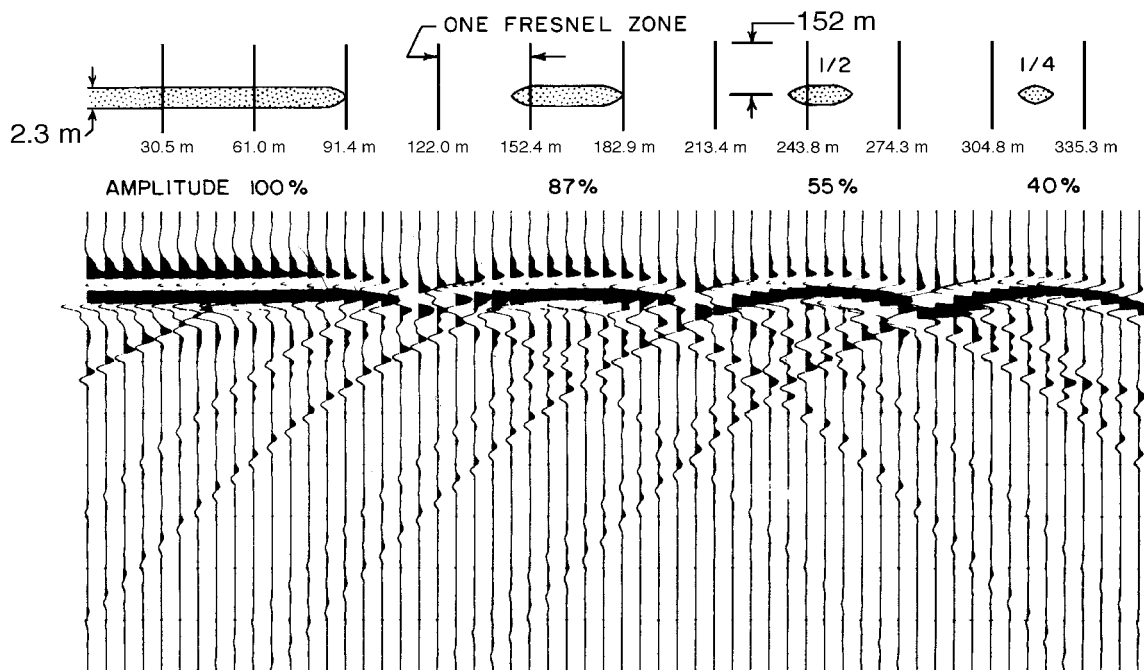


Figure 6-13. Model response for sand lenses of varying lateral extent illustrating significance of Fresnel zone size (modified from Sieck and Self, 1977).

Dimensions of Detection and Resolution

Since spatial resolution potential (minimum resolvable separation between beds or smallest discernible size of an object) is a function of frequency and seismic velocity (as well as depth for horizontal resolution) for a given reflected wavelet, classifications of too thin or

too small to resolve depend on site and target characteristics. Using 80-Hz data and vertical resolution estimates based on the one-quarter wavelength axiom, minimum vertical resolution potential in a carbonate setting will generally be around 16 m. For the same frequency data but in a siliclastic setting, the minimum resolution potential might be around 10 m due to lower velocities. With 80-Hz dominant-frequency reflections, vertical resolution could be as high as 1.5 m within the unsaturated, unconsolidated portion of the geologic section. Vertical-resolution potential for 80-Hz data can therefore range from around 1 m to more than 20 m in commonly encountered near-surface rocks.

To help get a general sense of how large an object needs to be for detection at 1000 m and at 100 m (depths consistent with most data presented in this manuscript), horizontal resolution can be estimated based on the same 80-Hz reflection data and the radius of the Fresnel zone. In the case of carbonates, an object or separation between two objects needs to be around 175 m at 1000 m of depth and 50 m at 100 m deep to be distinguishable. For the same 80-Hz data but in a siliclastic setting, horizontal-resolution potential would be 135 m at 1000 m below ground and 40 m at 100 m underground. In an unconsolidated alluvial setting, the horizontal resolution is 18 m at 100 m. Horizontal resolution based on one-half the radius of the Fresnel zone and possibly even smaller has been suggested possible based on model studies (Meckel and Nath, 1977). In many cases horizontal resolution is not nearly as critical as detection; that is, determining simply whether an object exists or whether a bed truncates or is continuous, such as for determining the possibility of loss of fluid confinement through channel-cut features (Figure 6-14). For detection, the size of the object or separation between two objects can be much smaller than required for resolution.

Differences from Conventional

Reflectors targeted by high-resolution seismic land surveys are predominantly in the shallowest 1 km of the earth crust. This apparent depth dependence or more accurately limitation is directly related to the attenuative characteristics of the earth (Mavko et al., 1979). Therefore, it is not surprising that only a very few high-resolution seismic-reflection

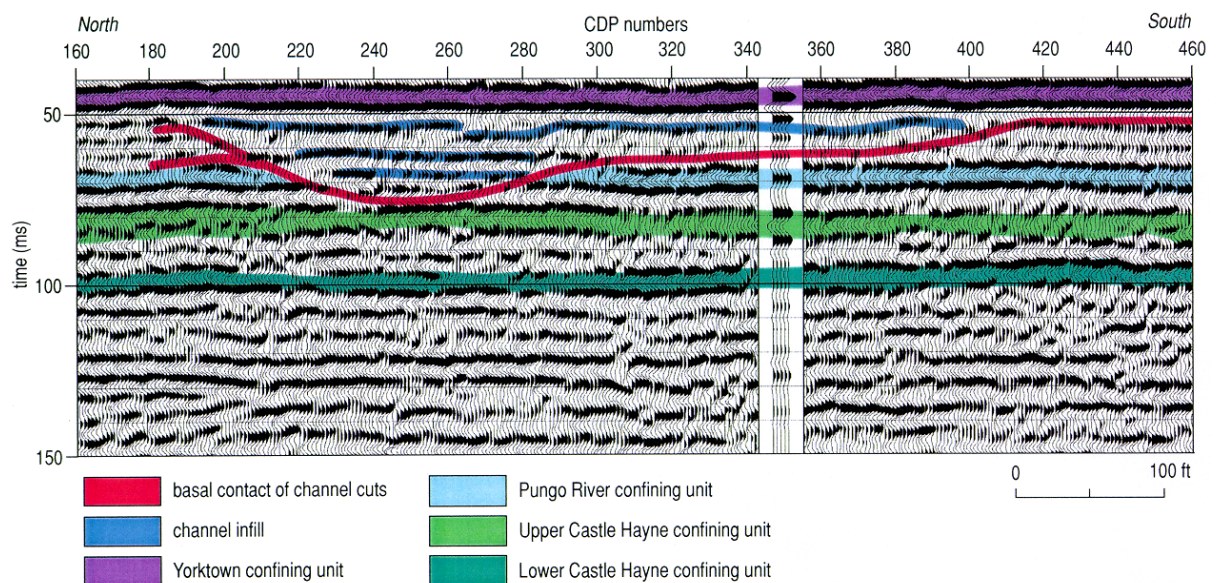


Figure 6-14. Interpreted CMP stacked section with inlaid VSP. Interpretations are based on hydrostratigraphy as defined from well data. Paleochannel breached one confining unit but not the second, which protects the freshwater supply for Cherry Point, North Carolina (from Miller and Xia, 1997).

surveys have attempted and been successful imaging at time depths greater than 700 ms (Hammer et al., 2004; Miller et al., 2005a). Based on the published literature, the overwhelming majority of high-resolution seismic-reflection surveys have targeted depths less than 100 m (Miller et al., 1989; Pullan and Hunter, 1990; Goforth and Hayward, 1992; B ker et al., 1998). Conventional seismic surveys are rarely interested in reflectors less than 1 km and generally focus on time-depths greater than 1 second.

When a seismic source imparts energy (noise and signal) into the ground, the entire wavefield begins propagating away from the source at nearly the same instant. Separation of different energy modes occurs as a function of time, source and receiver spacing, and modal velocity.

Energy arriving on a normal shallow shot gather will include direct arriving energy (direct body waves, air-coupled waves, and ground roll) and indirect (diffracted energy, reflected energy, and refracted energy) (Figure 6-15) (Miller and Xia, 1997). The hyperbolic shape and high apparent velocity of reflected energy is unique (with the exception of diffractions) relative to other components of the wavefield. With increasing two-way travel-time and offset, therefore depth, the separation between first arrivals and surface waves increases (Figure 6-16). Due to distinctly different

velocities, early linear arriving refractions and later arriving surface waves begin to diverge with time and offset from the source. This material-dependent divergence increases the spatial and temporal window available for signal with increasing time. Within the relative early time and short offset portion of the seismogram, non-reflection body-wave noise (Robertsson et al., 1996a) and surface waves (Baker et al., 1998) represent major obstacles to accurate CMP stacked seismic sections.

High-resolution imaging is by nature a tool most suited for shallow targets and therefore suffers from low signal-to-noise ratios that are predominantly the result of the high percentage of source noise at shallow time-depths. With elevated coherent noise come increased difficulties in identifying, separating, and enhancing reflection events during acquisition or processing. A critical criterion for interpreting any stacked reflection with a two-way traveltime less than 50 ms is confident and absolute correlation to an identifiable reflection on shot gathers (B ker et al., 1998; Steeples et al., 1997). Signal-to-noise ratios

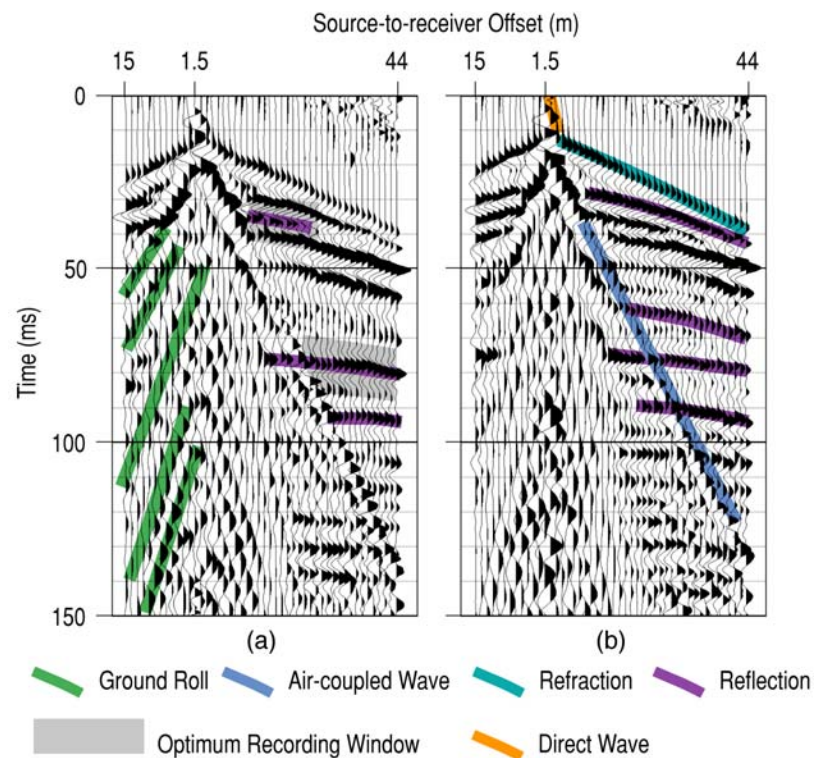


Figure 6-15. AGC scaled field files from two different places on the same line from Cherry Point, North Carolina. Reflection arrivals are apparent on both records. Note the changes in subtle reflections between 50 and 70 ms on (a) and (b) (from Miller and Xia, 1997).

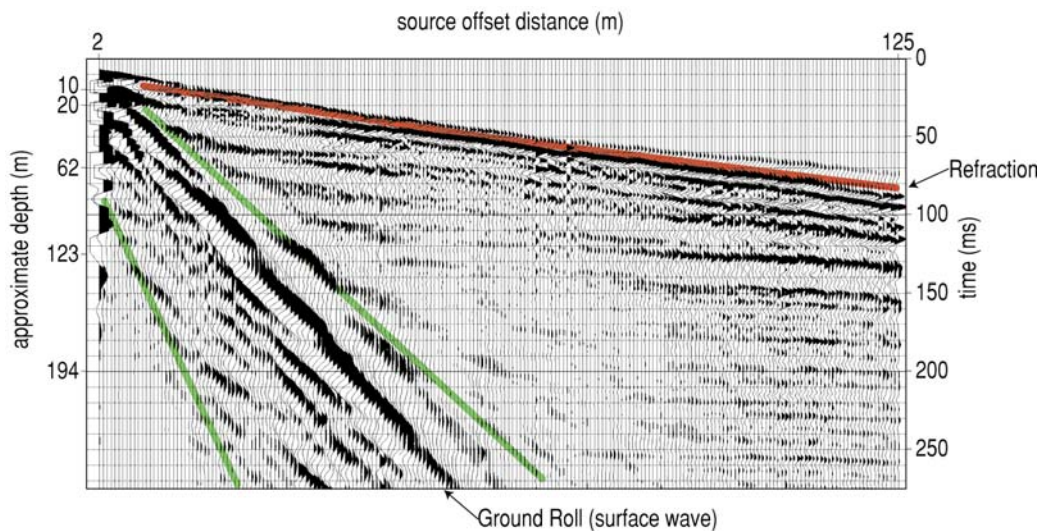


Figure 6-16. Shot gather with surface wave and refraction interpreted to highlight their diverging nature on seismograms (from Miller et al., 2005b).

can vary dramatically for typical high-resolution shot gathers with data characteristics ranging from broadband (multiple octave) with a high percentage of signal (Figure 6-17a) to narrowband (less than one octave) and a high percentage of source noise (Figure 6-17b). As has been demonstrated quite eloquently (Hunter et al., 1984), high-resolution reflection wavelets in the early time portions of a seismogram and with optimal wavelet characteristics will arrive within a limited range of source to receiver offsets and within a relatively narrow two-way travelt ime window.

A common process for enhancing signal-to-noise ratios on high-resolution data is muting. Muting as a technique to remove noise within the wavetrain is only used in conventional processing work flows as a last resort, unlike high-resolution data processing where it is essential (Baker, 1999). Many processing techniques will only operate properly when applied to data with laterally consistent reflection-wavelet characteristics and a high

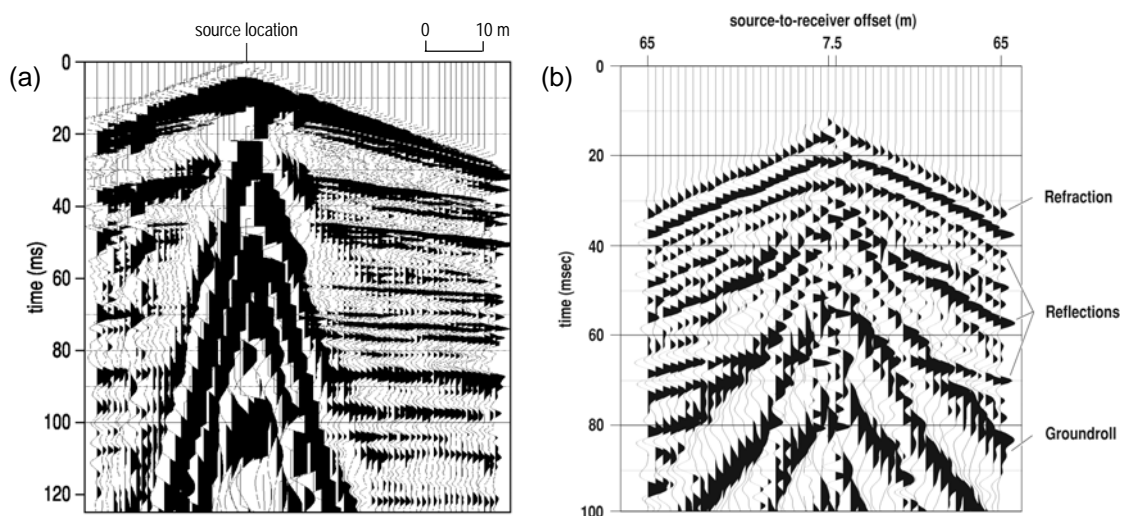


Figure 6-17. This 96-channel shot gather (a) is exceptionally broadband with reflection frequencies from 40 Hz to over 500 Hz (3½ octaves). Display gains are responsible for all clipping outside the ground-roll wedge (from Miller et al., 2007). In contrast, this 48-channel shot gather (b) possesses reflections that are within a narrow frequency band between 100 Hz and 300 Hz (1½ octaves) (from Steeples and Miller, 1993).

percentage of reflected energy to noise. When these requirements/assumptions are not met and elevated levels of coherent source noise are present, many processing routines generate artifacts that can be misinterpreted as reflections (Yilmaz, 1987). Most high-resolution seismic-reflection sections suffer from the adverse affects of guided waves when there is an abrupt seismic contrast (water table or bedrock) in the upper 30 m (Robertsson et al., 1996a). The first arrivals (direct and refracted energy) and their associated guided waves can saturate the optimum reflection window and mask high-resolution seismic reflections within the shallow portion of the section, where on conventional data these coherent noise events are removed with standard top mutes.

Resolution and bandwidth rapidly become a greater and greater issue with increased frequency and therefore increasing data resolution (Knapp, 1990). With increasing dominant frequency it takes a larger frequency range or bandwidth to represent an octave, and clearly the more octaves present in a reflection wavelet the smaller its side lobes (Figure 6-18).

Unlike conventional data where a 60-Hz bandwidth between 10 Hz and 70 Hz equates to almost 3 octaves and therefore a source pulse with minimal side lobes, a 60-Hz bandwidth between 120 Hz and 180 Hz is about half an octave and possesses a “ringy” source wavelet. Hence generating, propagating, recording, and enhancing a bandwidth spanning a couple-hundred hertz is necessary for high-resolution data where as little as 50 or 60 Hz would more than suffice for conventional data (Figure 6-17).

As previously suggested, attenuation of high frequencies is much more severe relative to lower frequencies due to the earth’s low-pass nature (Quan and Harris, 1997). High-frequency body waves traveling through the earth have very short life spans when compared to lower frequency waves (Johnston, 1981). This attenuation phenomenon occurs through both intrinsic (loss through heat) and scatter attenuation. Scatter attenuation is most detrimental to the higher frequency components of the wavefield when layer heterogeneities are smaller than the characteristic wavelengths (Marion and Coudin, 1992). Clearly higher frequency components of the wavefield suffer much more significantly from attenuation than lower frequencies.

The upper few hundred meters of the earth’s crust is the most laterally and vertically inconsistent on a meter-by-meter basis (Figure 6-19). This variability is lumped together on conventional reflection surveys and called the “weathered layer” (Telford et al., 1976), while on near-surface data this is the target interval (Steeple et al., 1997). The complexities of this interval are generally compensated through coherency processing and correlation statics on conventional data sets (Cox, 1999), while on near-surface data extensive velocity analysis and minimal-offset trace processing are necessary to extract reflections that accurately represent the shallow subsurface. In the near-surface, reflections must be identified and enhanced from raw field records through final stacked sections to avoid creating a seismic cross section unrelated to the real earth. Judicious processing with a focus on statics and

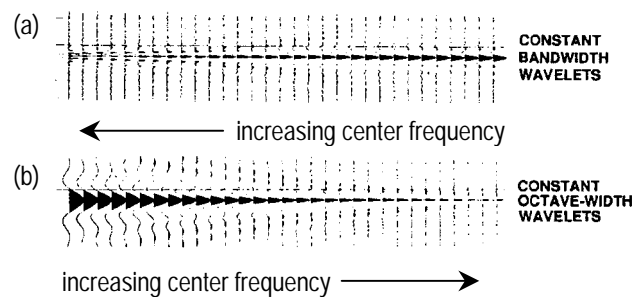


Figure 6-18. Synthetic wavelets demonstrating the difference between bandwidth and octaves. For constant bandwidth data (a), higher frequency ranges produce ringy or cyclic pulses but a constant pulse width, while for a constant number of octaves (b), the pulse shape remains the same while its width compresses (modified from Knapp, 1990).

velocity analysis many times needs to be undertaken on each CMP gather/bin on high-resolution data where grouping of a hundred CMP/bins or more is not uncommon for conventional data sets. Processing in the near surface is a monumentally complex and time-consuming activity if an accurate, high-resolution representation of the subsurface is the objective.

One of the biggest differences and major obstacles to high-resolution profiling, especially as it relates to the very near surface (upper 100 m), is the vertical velocity gradient (Miller and Xia, 1998). Although this phenomenon is intuitively obvious, compensating for it during processing is absolutely overwhelming (Bradford, 2002). NMO curves from events within lower-velocity materials intersect curves from deeper higher-velocity layers due to the dramatic increase in NMO velocity between soil over unconsolidated sediments over saturated unconsolidated sediments over rock (Figure 6-20). Therefore, to properly move out reflections from within the unconsolidated and consolidated materials

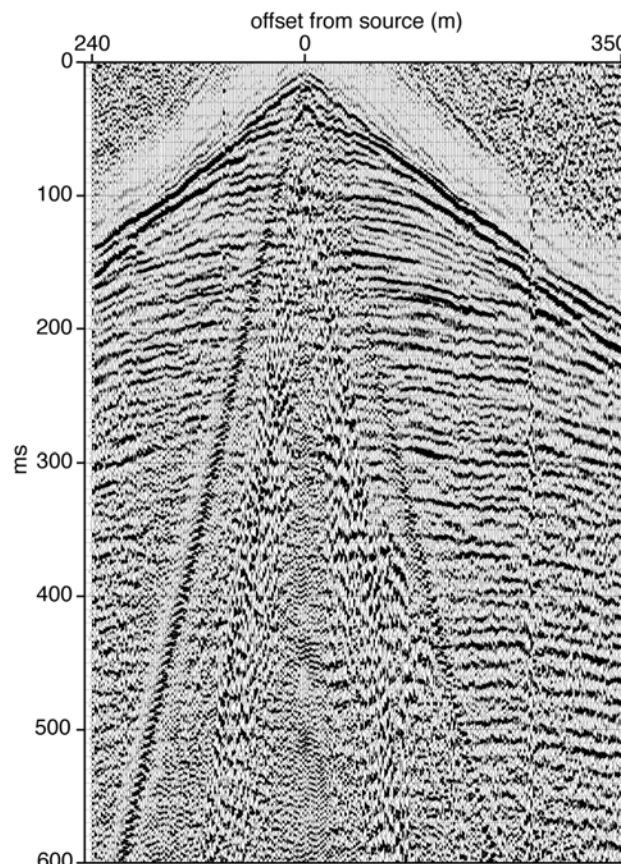


Figure 6-19. 240-channel shot gather with 2.5 m receiver spacing and IVI minivib source, scaled for display. Dozens of reflections are interpretable in the upper 600 ms. Evident in reflections within the upper 100 ms are extreme time undulations suggestive of lateral variations in materials (from Miller, 2003).

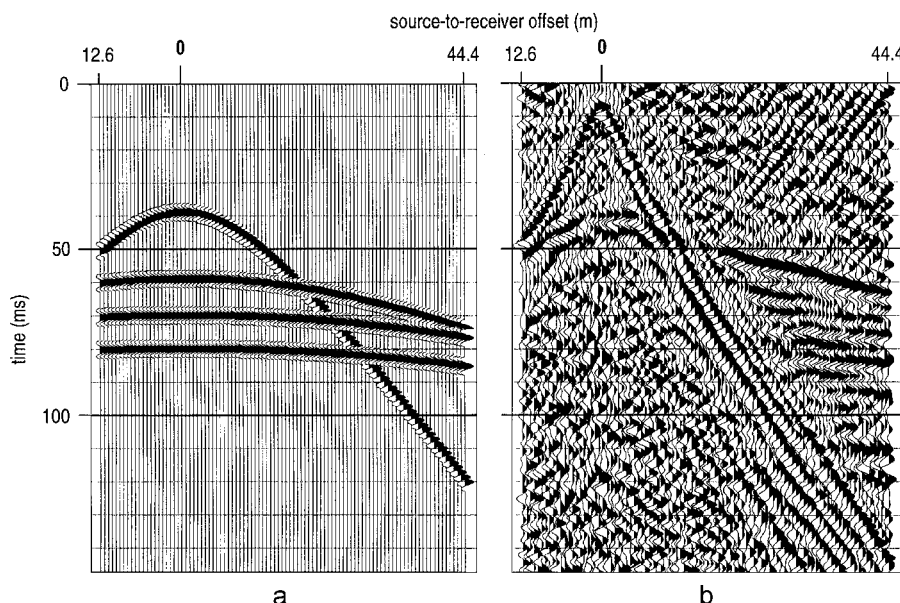


Figure 6-20. Representative shot gather from glacial/alluvial setting in eastern Minnesota. (a) Acoustic model of four reflection events consistent with real data. (b) Digitally filtered and scaled shot gather showing the offset-dependent nature of shallow reflections (from Miller and Xia, 1998).

without generated artifacts and excessive noise from overlapping time shifts, a very severe NMO stretch mute must be applied or different time portions of the data must be run through different and multiple processing flows. Neither solution provides the “correct” answer. At conventional depths, sufficient rock overburden has been included in the normal moveout velocity of the shallowest reflectors of interest that changes in curve geometry between recorded reflections are minimal and never overlap within the recorded spread.

Many seismic-signal processing methods or approaches are violated by the nature and characteristics of shallow high-resolution reflection data. Deconvolution is a tried and true approach that has been in use by the conventional seismic-exploration industry for more than four decades to remove multiples and source signatures (Robinson and Treitel, 1980). Key to the functionality of deconvolution is the assumption that the reflectivity series represents a large number of reflectors that are random and uncorrelated. Also key to the performance of deconvolution is minimum noise, especially coherent noise that interferes with a time-consistent reflection pulse. As reasonable as these assumptions are for conventional data sets, they are almost always violated on shallow, high-resolution data (Figure 6-21). A principal assumption with predictive deconvolution is that the source pulse and reverberations are all broadband and minimum phase. High-resolution data from an impulsive source is for the most part minimum phase, but it is rarely broadband (multiple octaves) (Miller et al., 1986).

Inherent with most shallow high-resolution data is a highly variable time- and offset-dependent fold (Liberty and Knoll, 1998). In the early time portions of a shot gather, the optimum window is significantly smaller than at greater time and source offset.

Therefore a large number of traces at equivalent time samples could have zero sample values (Figure 6-22). Estimating fold by simply adding up the number of traces in a CMP or bin is highly inaccurate and misleading for shallow high-resolution data where that approach is very representative and accepted for conventional data sets. With low signal fold comes insufficient sampling for statistical techniques to effectively and accurately operate (Henley, 2001). Processing methods such as correlation-based statics, horizontal stacking, and slope-type filtering all rely on a large number of samples (traces) within a CMP or bin. It is not uncommon for less than 10% of early times samples of a CMP or bin in high-resolution data to be non-zero. This situation can produce results that unknowingly mislead many processors and interpreters.

High-resolution seismic reflection is governed and defined by the same principles and concepts as conventional approaches, but with a few very important caveats. Most critical are the following:

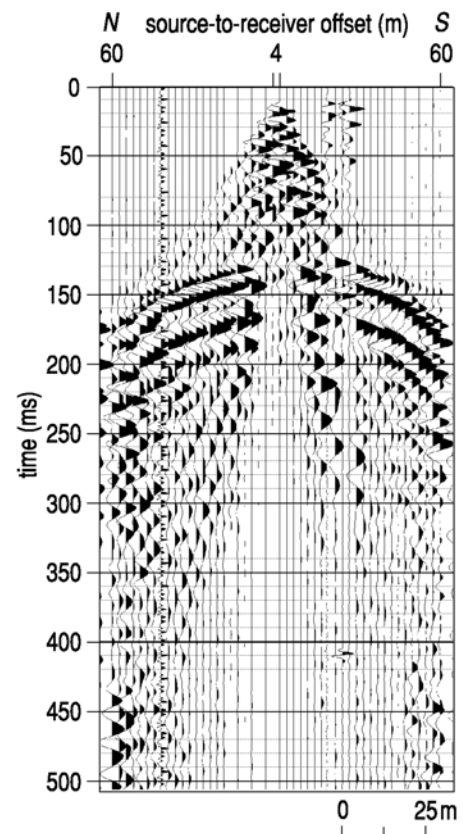


Figure 6-21. Unprocessed shot gathers with reflection ~40 ms beneath the shallowest event. With only two reflections with markedly different wavelet properties, deconvolution would fail miserably if applied to these data (from Miller et al., 1995b).

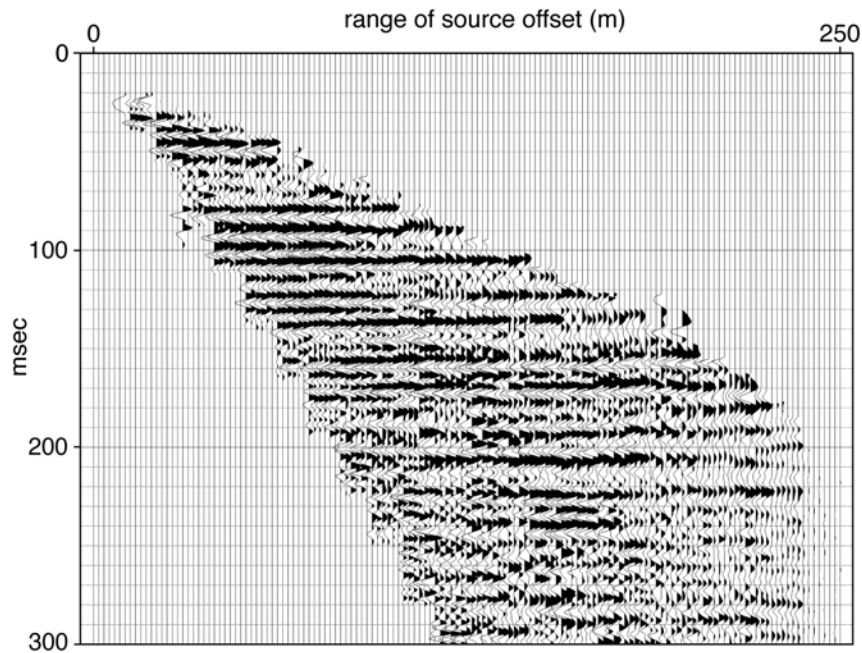


Figure 6-22. Fully processed CMP gather displaying character of the reflection wavelets just before stacking. Even though there are 120 traces that comprise this CMP, with the mutes that have been applied, the fold based on trace count is 120; however, based on traces with data, the reflection at 50 ms is only about 24 (from Miller, 2002).

*potential overwhelming effects of source noise,
 nonlinear nature of the earth's pass band,
 very strong need for an elevated awareness as to the assumptions being made by
 processing methods,
 variable effects of processing approaches
 related to spectra, and
 dramatic effects of large near-surface
 gradients (both velocity and effective fold).*

The early part of a seismogram is not only the most critical on high-resolution seismic-reflection data, but it is where the vast majority of event identification and processing difficulties occur. At early two-way travel times, signal is generally present on an overwhelming minority of traces, thereby making establishing confidence in the mode and classification of an event difficult when using trace to trace coherency. In many near-surface settings the seismic wavefield recorded on a seismogram can consist of more than 70% source noise above 250-ms two-way traveltime and more than 90% source noise earlier than 50 ms (Figure 6-23). On most shallow high-resolution seismograms less than a half dozen traces out of as many as one hundred will have non-zero values contributing to the true fold at a specific two-way traveltime above

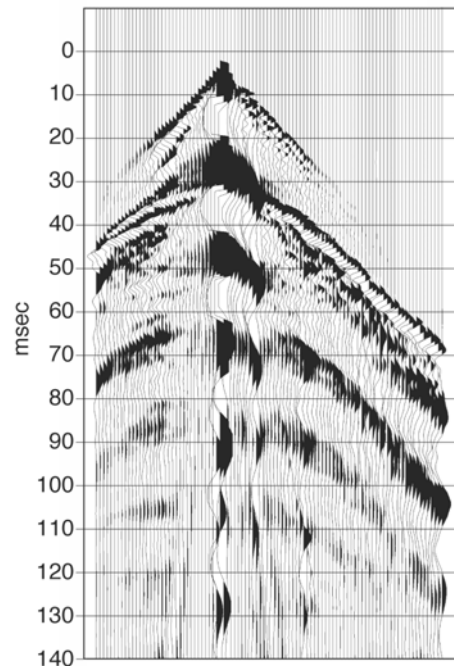


Figure 6-23. 48-channel seismogram record acquired with a seismic source 7.5 m away from the nearest seismic sensors (Miller and Markiewicz, 2001).

100 ms (Figure 6-22). It is much more common for high-resolution seismic-reflection surveys to report unsuccessful attempts to image a near-surface target than a conventional survey being unable to map a reflector package of interest at more commonly investigated depths (Steeple, 2000; Dasios et al., 1999).

High Resolution: Acquisition

For the most part, differences in the approaches to high-resolution and conventional seismic-reflection acquisition are intuitive and linear. For example, high-resolution data acquisition requires increased spatial sampling and reduced spread lengths. As well, bandwidth increases generally come with decreases in source energy (Knapp and Steeples, 1986b). A high dominant-frequency source pulse generally comes at the expense of energy output. However, due to the required close proximity of the source to nearest receivers for shallow high-resolution reflection surveys, operational limits of receivers or seismograph can easily be exceeded with energetic sources (Figure 6-24). Contrary to maintaining a sizable offset between source and receivers for operational reasons is the need for near vertically incident raypaths. Close-offset traces are highly desirable in avoiding NMO stretch issues that plague “longer” offset, high-frequency reflections; therefore, optimizing recorded data necessitates use of lower energy sources.

One problem rarely an issue on conventional surveys, but consistently impacting many shallow high-resolution studies, is a limit on the number of available recording channels. Reduction in spread length is the standard solution to the increased spatial sampling needs of high-frequency

surveys. The compression of the receiver spread effectively constrains the size of the target window, redundancy in sampling, and advantage of split-spread reciprocity in raypaths. The trade-off for most high-resolution data sets is trace-to-trace coherency vs. full-forward and reverse-spread coverage. With very small and sometimes changing optimum offset windows, maximizing the number of traces or receivers within that optimum window is critical to survey success. Reducing spread coverage makes velocity analysis more difficult as well as reduces the effectiveness of pre-stack migration. Because most shallow high-resolution seismic surveys are low budget and low impact, the number of recording channels always seems to be one of the first budget items to be cut.

With minimal channel counts and a narrow optimum offset window comes a major emphasis on and need to keep the spread focused on target reflections. With the high variability of the near surface come dramatic lateral changes in velocity, which will affect the

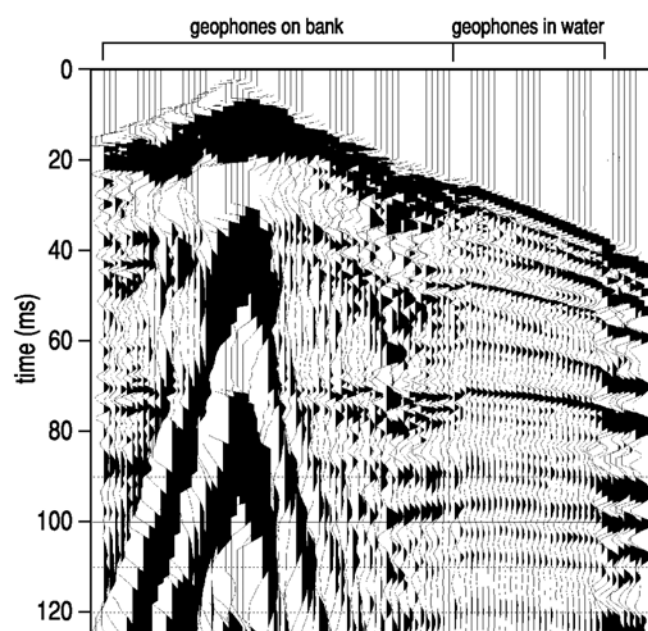


Figure 6-24. 12-gauge Seisgun with some receivers fully submerged and others planted into the creek bank, less than 0.25 m for static water levels. Ground roll has overdriven the near receivers, leaving squared-off wavelets (from Miller et al., 2007).

size and location of the optimum recording offsets. To permit accurate velocity analysis, many times with high-resolution surveys it is necessary to employ asymmetric split-spread geometries to keep high trace counts in optimum offset windows while maintaining necessary longer offsets for deeper event analysis (Figure 6-24). It is more common for high-resolution surveys with their limited channel counts to acquire end-on style data, thereby increasing spatial sampling and source offsets in attempts to ensure the optimum window is captured in spite of velocity changes along a profile.

The philosophy of optimally receiving high-frequency signals (sensors) has generated much controversy, but research results have not been sufficiently compelling to spawn major changes or a clear preferred approach to how (many, placement, wire, etc.) and what (type, grouping, natural frequency, etc.) sensors to deploy for high-frequency surveys. Accelerometers are considered by many to be the ultimate high-frequency receiver with their extremely broad and uniform bandwidth sensitivity (Inazaki and Lel, 2003). Geophones dominate high-resolution seismic-reflection applications because of durability, low noise (accelerometers come with amplifier noise), low cost, and high natural frequency and impedance options that rival integrated accelerometer outputs. High-resolution surveys employ higher natural-frequency geophones generally with more coil windings for improved high-frequency response and signal voltage than customary on conventional surveys.

High-resolution surveys benefit more from receivers with longer spikes (50% or more), clustered arrays, and removal of loose surface organics and soils than surveys designed for conventional frequency ranges. Inadequate coupling (loose) is less of an issue for conventional than high-resolution surveys. Geophone response across common conventional frequency ranges is mildly to not affected by improving cohesive plants (Hoover and O'Brien, 1980). Differences in response from signal above 100 Hz can be dramatic across various surface material types and clearly make selective placement of receivers a significant concern for high-resolution surveys (Krohn, 1985) (Figure 6-24). Receiver spreads designed to attenuate ground roll for conventional surveys attenuate the near-vertical reflection wavelets characteristics of high-resolution surveys (Ziolkowski and Lerwill, 1979; Knapp and Steeples, 1986b). Even with the azimuthal issues of conventional 3-D seismic, receiver arrays are commonly used and designed according to the relationship $fA = V_{int}$, where f is dominant frequency, A is array size, and V_{int} is interval velocity (Vermeer, 2002).

As previously stated, higher frequency signal is synonymous with lower energy sources. Whereas most conventional land surveys use source arrays consisting of several synchronized sources, high-resolution surveys almost exclusively use single-point-source acquisition designs. Hole conditioning has long been known to improve the coupling of high-frequency seismic-reflection data (Figure 6-25) (Miller et al., 1986; Walters et al., 2007). In many cases source selection for high-resolution surveys must facilitate a fine balance between overdriving near-offset receivers and propagating detectable high-frequency signals to longer offset receivers (Figure 6-24) (Miller et al., 2007). Improved source coupling is essential for high-frequency energy generation, but it can prove detrimental to recording unclipped ultra-shallow signal. If clipped waveforms are not identified and properly muted, they can be processed to appear coherent on CMP stacked sections. Without a doubt, stiff, well-sorted surface materials provide the best source environment for high-resolution surveying where these conditions have minimal influential on conventional surveys.

With the low-energy characteristics of high-resolution surveys comes an elevated percentage of environmental noise and airwave to signal levels relative to conventional surveys. Wind, vehicle traffic, pumps and pipelines, as well as livestock and wildlife are noise sources that represent a larger proportion of the recorded data on high-resolution surveys than conventional surveys (Figure 6-26) (Steeple and Miller, 1990). One troublesome noise component more pronounced (relative) on high-resolution data compared to conventional is air-coupled wave (Figure 6-25) (Knapp, 1986). Besides suffering from elevated environmental noise, instrument noise can be a larger component of high-resolution data than commonly observed in conventional data due to the characteristically and necessary lower signal levels of common high-resolution sources.

Frequency deterioration occurs when repeat shots at a single station are vertical stacked without compensating for slight, but ever-present mismatches in time zero and source signature. This problem is more pronounced on high-resolution surveys, where 0.5-ms mismatches can put wavelets 180° out of phase, but on conventional surveys that same 0.5 ms might be only 20° out of phase. This is also a problem for horizontal stacking and unfortunately, a solution is more readily available for the case of vertical stacking—do not vertically stack in the field. By optimizing source characteristics, many times it is possible to minimize or eliminate vertical stacking on high-resolution surveys. Individually recording each impact or source sweep or explosion allows some degree of scrutiny in selecting which records are to be included in a vertical stacked gather, a

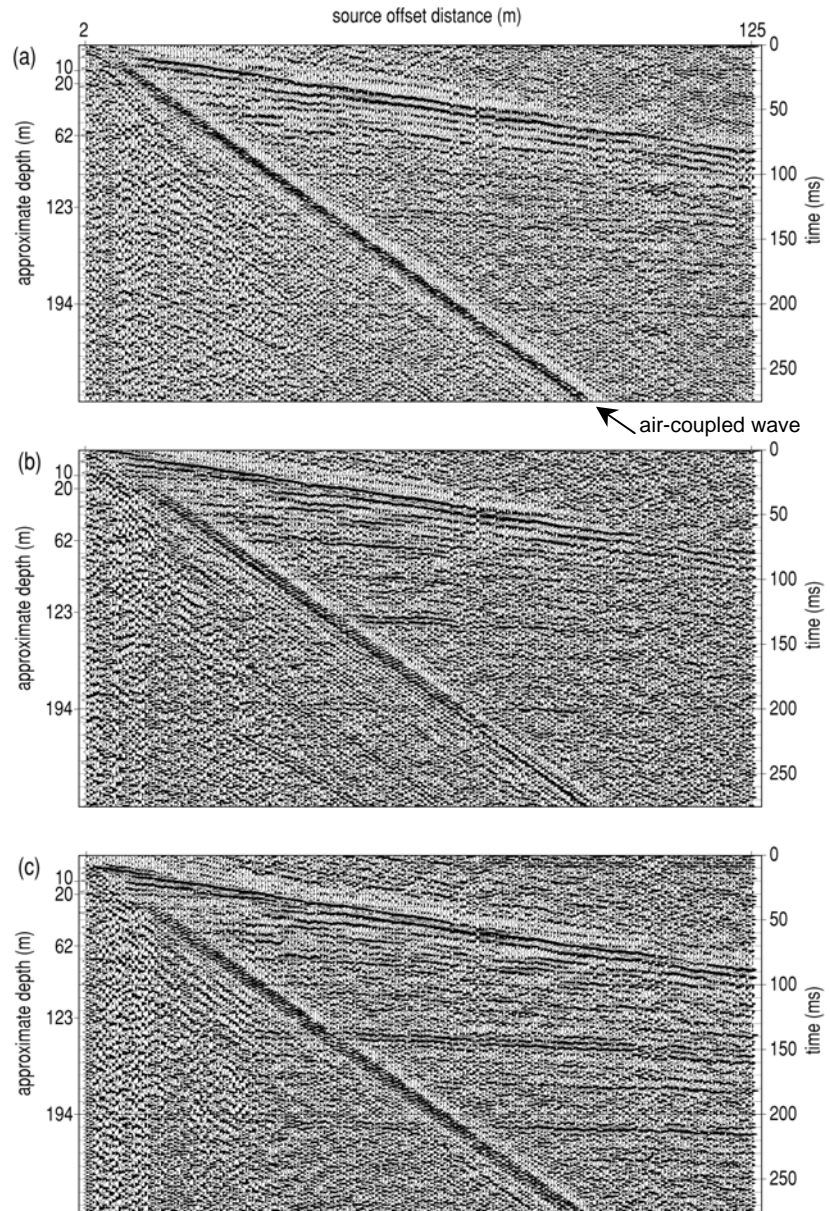


Figure 6-25. An example of hole conditioning. One shot into the hole (a) produces good reflection and refraction arrivals and a strong air-coupled wave component. A second shot into the same hole (b) produces a higher signal-to-noise record. The best data recorded (c) were by the third projectile fired into the same hole (from Miller et al., 2005b).

need more clearly evident on high-resolution surveys compared to conventional.

Acquisition parameters for high-resolution seismic-reflection surveys possess a slightly different set of core prerequisites in comparison to conventional surveys. For both conventional and high-resolution surveys, the utility of forward models based on experience and *a priori* information at the site and about the target is well proven. Conceptual models provide essential spatial and temporal frameworks and geometry of wavefield arrival patterns necessary to help constrain optimum recording parameters for various survey objectives. Final designs of the field geometries need to be consistent with actual data potential (as defined by physical properties derived from test data) avoiding over-optimistic estimations based on no noise, broad bandwidth, or laterally consistent theoretical estimates of resolution (Miller et al., 1995a). Without a doubt, for each new site a walkaway noise test should be conducted at several locations as part of every high-resolution shallow-seismic investigation.

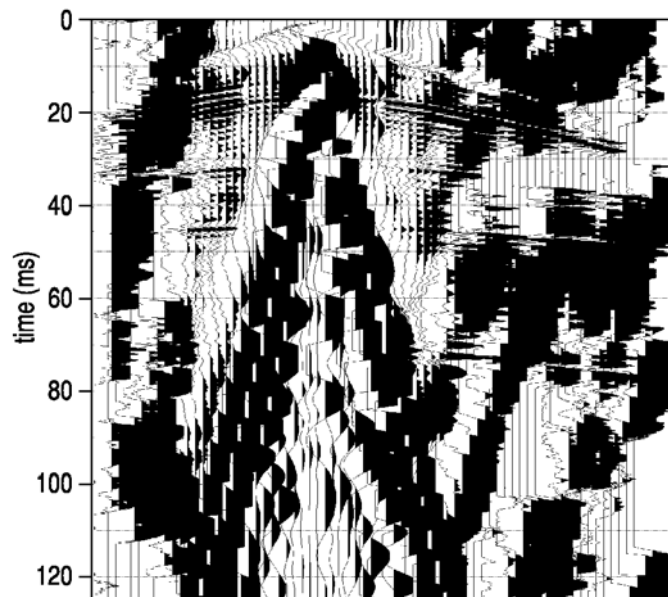


Figure 6-26. Ground roll on close offset traces is overdriven and clipped. Vehicle noise from nearby highway is evident as low-frequency coherent surface wave crossing from right to left across shot gather. Reflections are evident at about 6 ms. Display gains are responsible for all clipping outside ground-roll wedge (from Miller et al., 2007).

High Resolution: Processing

High-resolution seismic-reflection data, by its very nature, lends itself to over-processing, inappropriate processing, and minimal involvement processing. Interpretations of high-resolution shallow-reflection data must take into consideration not only the geologic information available, but also each step of the processing flow, reflection events on raw unprocessed data, and how those events change through the processing flow. Processing high-resolution reflection data must include only operations or processes that enhance signal-to-noise-ratio and/or resolution as determined by evaluation of high confidence reflections interpreted directly on shot gathers. High ratios of coherent source noise to signal is the principal characteristic that makes shallow high-resolution seismic-reflection data exceedingly susceptible to unsuitable manipulation by conventional processing routines and approaches.

From a general workflow perspective, most high-resolution shallow-reflection processing steps can be as simple as the scaling down of conventional approaches and techniques. There is no standardized CMP processing flow; however, the basic architecture and sequence of processing steps is well established for conventional petroleum exploration (Yilmaz, 1987, 2002). To avoid undesirable and misleading artifacts when using conventional methodologies for high-resolution data, it is imperative to maintain extreme attention to parameter details and the statistical assumptions appropriate for and integral to

many operations routinely used on conventional data. To avoid generating artifacts and to achieve accurate images of near-surface structures, some special aspects of processing shallow-seismic data need to be considered. Key components are the identification and enhancement of shallow reflections relative to the source-generated noise, the application of carefully selected top mutes, surgical mutes, normal moveout (NMO) stretch mutes, and the calculation of the static corrections. Each processing flow needs to be customized based on data-specific characteristics and survey objectives.

The primary difference between high-resolution data processing and more conventional flows relates to the necessary levels of QC and awareness of trace-level variability in signal within a CMP or bin (i.e., sub-fold signal windows) (Miller et al., 1989; Steeples and Miller, 1990; Miller and Steeples, 1991). A few of the more significant distinctions between high resolution and conventional relate to the emphasis placed on velocity analysis (Miller, 1992), lack of extensive wavelet processing, care and precision placed on muting, step-by-step analysis of the effects of each operation on reflected energy, limiting statics operations to maximum shifts no greater than one-quarter wavelength of the dominant reflection energy, large correlation windows, trace-specific signal vs. noise for mute zones, and multiple number of cycles of coincident iterative velocity and statics analysis. The sequence and types of basic processing operations performed on CMP reflection data should be relatively consistent throughout the data set.

For most cases, workflows used to process CMP high-resolution reflection data should follow a generalized progression consistent with the methodology (Figure 6-27). CMP processing of seismic-reflection data should focus on increasing the signal-to-noise ratio and resolution potential of CMP stacked sections. Pre-stack processing should attempt to tune spectral properties, remove or at least reduce contributions from noise, adjust reflection arrival times for nonzero source-to-receiver offsets (emulating vertical incidence), compensate for statics (due to variations in near-surface topography and velocity), and minimize artifacts associated with source offset, residual noise, and pre-stack processes.



Figure 6-27. Generalized processing flow appropriate for high-resolution data.

Post-stack processing should be designed to enhance coherent reflection events and their unique properties or attributes while retaining the tie with equivalent coherent reflection events interpreted on pre-stack gathers.

A few of the more challenging processing problems for shallow high-resolution seismic-reflection data can have amazingly adverse effects on the legitimacy of interpretations of CMP stacked sections (Spitzer et al., 2003). Of course the most consistently troublesome and frustrating is source-generated noise. In many cases source noise is extremely difficult to remove without adversely affecting reflections in the early time portions of the section (Figure 6-28). Difficulties separating these different modes of the wavefield are mainly a byproduct of the inherent similarities in phase velocity and frequency of body waves and aliased air-coupled waves.

With the exception of bandpass and f-k filtering, there are few processes that allow enhancement of reflection amplitudes relative to source noise without comprehensive muting. In addition to these filtering routines, spectral balancing or band limited deconvolution can enhance shallow reflections. Most times careful muting of coherent noise is inevitable. Top mutes that extended more than two cycles below the first arrivals do irreparable damage to reflection events. These extended or tailing reverberations continuing after first arrivals are normally guided waves and if not removed can easily stack coherently on CMP sections (Robertsson et al., 1996a, 1996b).

Special emphasis is placed on all noise and coherency analysis portions of high-resolution processing flows but especially during pre-horizontal stack stages. It has been proven necessary and most effective to do velocity, spectral, and on certain occasions deconvolution analysis on every CMP (Steeple and Miller, 1990). Many times variability in near-surface materials and/or conditions require changes in processing parameters across distances less than 20 m (Figure 6-29). Due to the higher percentage of coherent source noise in the shallow portion of the time section more care must be taken to ensure that all coherent events on stacked sections interpreted as reflections are consistent with reflections on shot gathers. Differentiating reflections from direct wave, refractions, airwave, and ground roll in the early portion of a stacked section is an extremely difficult task and must not be taken lightly.

High-quality geologically representative stacked sections generally require velocity analysis of every CMP for high-resolution data. This level of detail and accuracy in the assignment of a velocity function is more important for high-resolution data because most

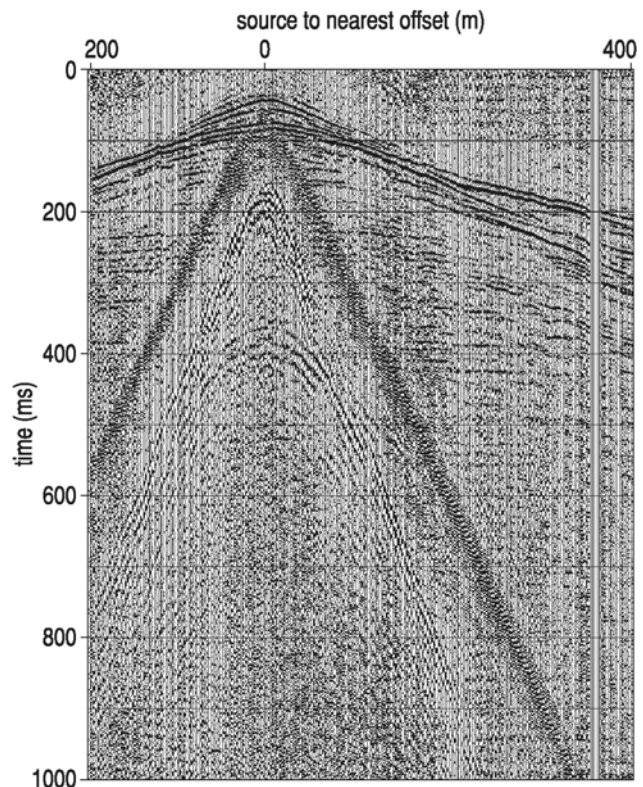


Figure 6-28. Correlated shot gather with reflection events showing diagnostic curvature and high-frequency wavelets. Air-coupled wave, ground roll, and first arrivals all make extracting 60-ms reflection extremely difficult (from Miller, 2006).

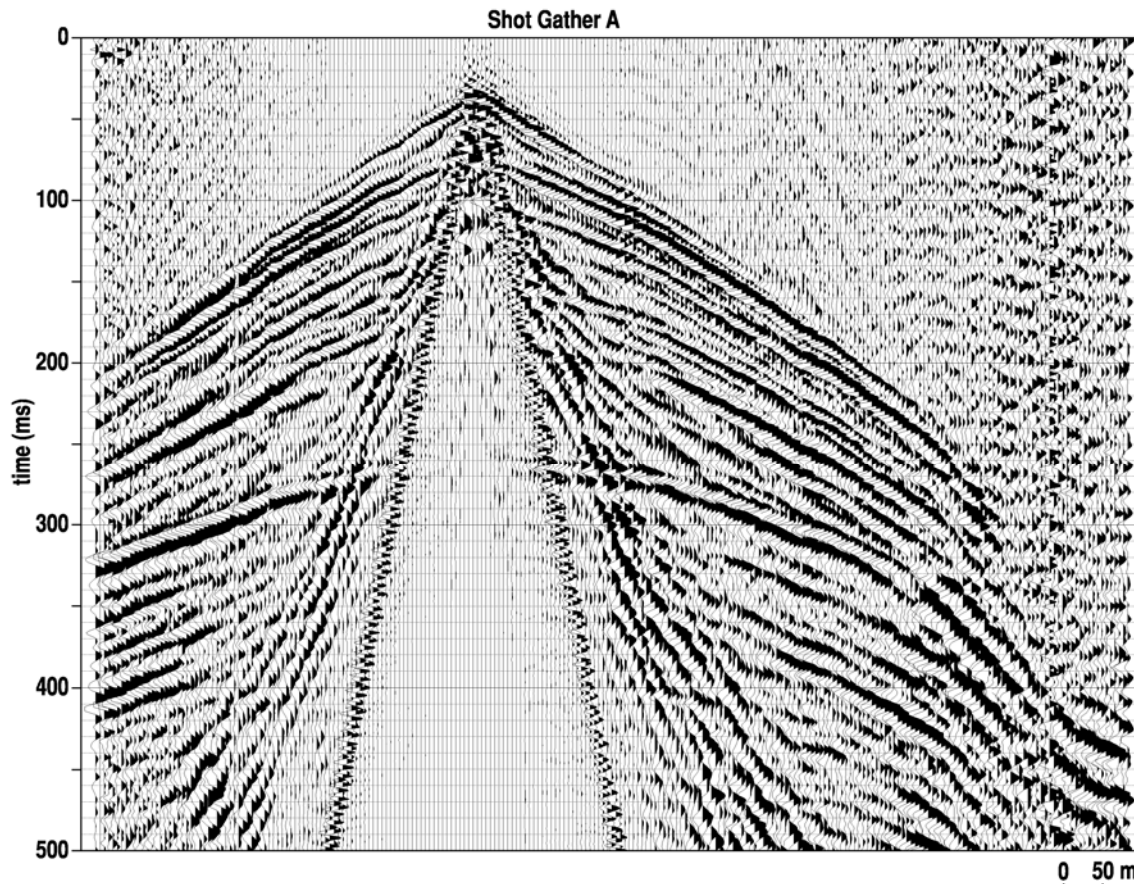


Figure 6-29. Many of the more subtle reflection events on left side of source location do not match (curvature, wavelet properties, static) reflection events on the right side at equivalent time (from Miller et al., 2006).

reflectors are within what is considered the weathered layer on conventional data sets. With the extreme lateral and vertical variability of materials characteristic in most near-surface settings, assignment of a representative normal-moveout velocity function is pivotal to accurate time-to-depth conversions of processed high-resolution seismic-reflection data and is critical to accurate geologic interpretations.

Spectral degradation from CMP stacking of seismic-reflection data is much more prevalent in near-surface high-resolution data than conventional data due to the proportionately larger wavelet stretch necessary to correct reflection wavelets for non-vertical incidence at commonly recorded source to receiver offsets (Miller, 1992). Strange as it seems, in situations with large near-surface velocity gradients (more commonly encountered than might be assumed), a vertically accurate velocity function will result in artifacts due to the geometrical interference of shallow low-velocity reflection wavelets with slightly deeper but much higher velocity shallow-reflection events (Figure 6-30) (Miller and Xia, 1998). Distortion of the wavelet through stretch is necessary to allow horizontal stacking but alters the core properties of the reflection wavelet and therefore the information the wavelet contains. The excessive stretch necessary to correct shallow reflections for nonvertical incidence raises concern about the accuracy and therefore legitimacy of directly using relationships between seismic attributes and rock properties established for conventional data on high-resolution data. Unlike conventional data, stacking of any kind on high-resolution data has an adverse effect on the key characteristic of the data set—spectra.

Correcting for static on high-resolution data is a significantly greater challenge than on conventional data for several reasons including lack of a large statistical set (number of reflections), percent trace to trace time irregularity relative to two-way traveltime of the target-reflection window, source noise interfering and actually influencing correlation routines, topographic changes and replacement velocities relative to reflection depths, and in some settings first arrivals at close offsets can be the air-coupled wave masking trace-specific static. Higher relative variability in velocity within the near surface increases the significance and influence of static corrections on CMP stacked reflection coherency and retention of wavelet information relative to conventional surveys (Cox, 1999).

Refracted arrivals from depths shallow enough to develop a time correction model for statics are not recorded on most near-surface high-resolution surveys due to the minimal spread lengths. Methods have been developed using near-offset refractions (Hatherly et al., 1994), which are reasonably effective on the shallowest velocity irregularities but fall short when key refracting interfaces are more than a quarter to half the spread length deep (Bergman et al., 2004). Simple first-arrival correlation routines designed to maintain a uniform apparent phase velocity do not always meet the statics challenge due to significant travel path differences between first arrivals and deeper reflections recorded on the same trace (Pugin and Pullan, 2000).

Selection of a single flat datum for shallow high-resolution surveys can increase the total error when making elevation corrections by orders of magnitude. Because velocity is estimated across spread length distances using curve-fitting routines, errors can be 10% or more and when velocities possessing errors of that magnitude are used to calculate replacement times for static corrections the time errors increase notably as the thickness of replacement material increases. To minimize the time corrections and therefore minimize error, multiple floating datums have been shown to be highly effective on high-resolution data (Steeple and Miller, 1990; Frei, 1995).

Migration is less effective in general on near-surface data due to the slowness of shallow earth materials (Black et al., 1994). This minimization of the optical distortion is due in part to the near-field perspective provided by a shallow target relative to source and receivers. Migration also has a filtering effect on high-resolution data resulting in the narrowing of bandwidth and reduction in dominant frequency. This filter effect has been shown by some researchers to be advantageous (Ivanov et al., 1998). Due to economics pre-stack f-k migration using a single velocity function is by far the most commonly used

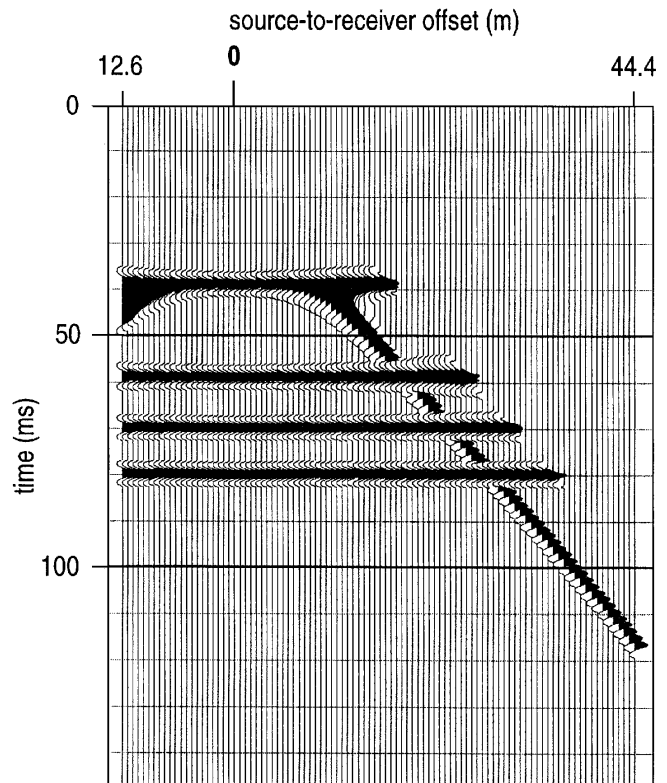


Figure 6-30. Moved-out gather using a time-variable velocity function of 50% stretch mute of Figure 6-20 (from Miller and Xia, 1998).

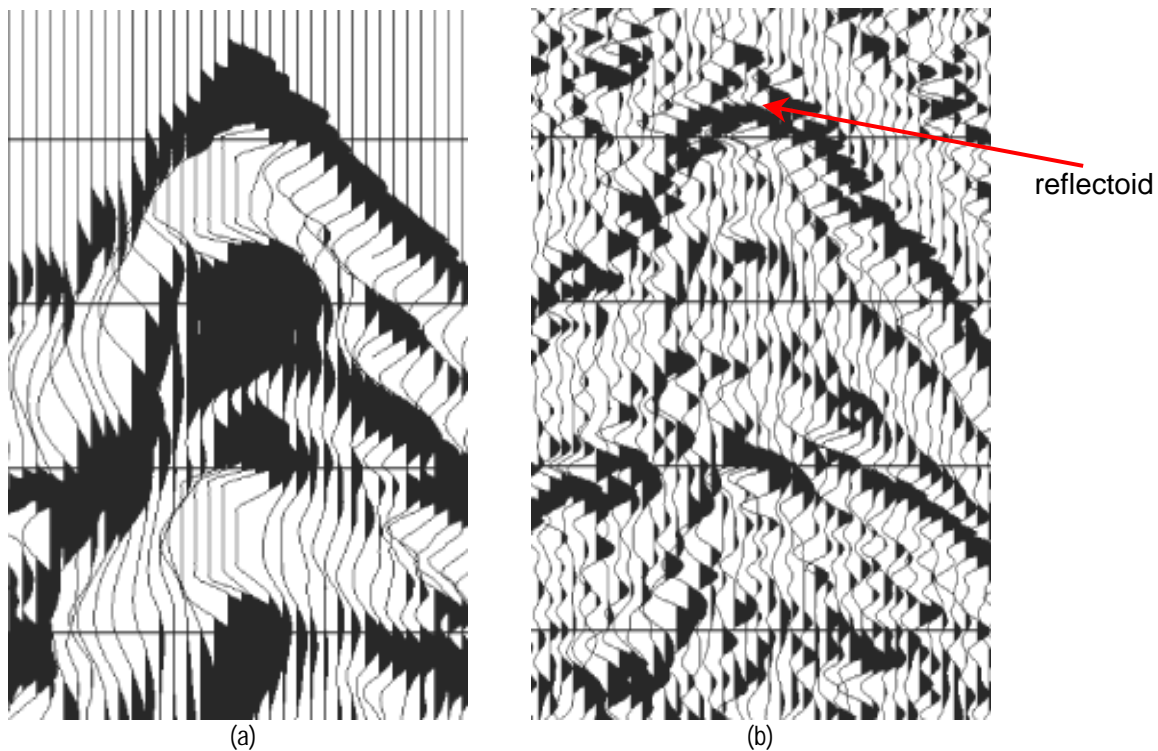


Figure 6-31. Clipped shot gather (a) band-pass filtered and scaled with square wave appearing reflection-like (b).

approach. This simple approach provides a reasonable result for conventional surveys, but, due to the rapidly changing velocity in the near-surface, it is inadequate for most high-resolution surveys.

Bandpass filtering is one of the most commonly used pre-stack data-massaging techniques for QC analysis and event identification on shallow high-resolution data. When applied without an awareness of the target signal, the nature of the noise, energy clipping, or previous muting, bandpass filtering can generate artifacts that process into coherent reflections on CMP stacked sections (Figure 6-31). Unlike conventional data where sufficient separation between reflections and surface wave allow extension of coherent reflections into the noise cone, digital filtering can alias components of the surface wave making them appear reflection-like.

Considering all the differences between conventional and high-resolution seismic-reflection processing, it is not surprising that so many shallow high-resolution seismic-reflection sections suffer from reflection-like artifacts interpreted to be reflections and later proven incorrect. With the power of CMP processing comes an obligation for users to be fully aware of the assumptions and mathematics associated with each operation. Recurrent errors such as 1) processing “signal” out-of-coherent-noise, 2) assuming the number of traces per CMP or bin equals fold, 3) using a sample set too small to meet minimum statistical requirements, 4) the more traces the better philosophy, 5) all coherent events after processing are reflections, 6) all reflections are equal regardless of where the reflector is in the subsurface, 7) the more FFTs per processing flow the better, and 8) within every digital word is the makings of a reflection have generated skepticism and reluctance to generally accept shallow high-resolution seismic reflection in the environmental and engineering community.

Summing Up and To Come

Successful imaging of the shallow subsurface with high-resolution seismic reflection depends on several key subsurface characteristics and acquisition/processing approaches. Foremost among these is the existence of acoustic velocity and/or density contrasts which generally correspond to geologic interfaces. The second relates to the ability of the near surface to propagate high-frequency seismic signals. Finally, the acquisition parameters, recording equipment, and processing flow must be compatible with the proposed target and resolution requirements of the survey. As well, data processing should enhance coherent reflection events, not produce artificial reflections. Regardless of the processes or parameters used to enhance seismic-reflection data, coherent events enhanced throughout processing and presented as reflections on the final stacked sections should correlate to reflections interpreted on shot or CMP gathers.

Now with the uniqueness and complexity of high-resolution seismic reflection clarified, the stage is set for the next chapter where the author's past key contributions and the current significance and applicability of each to high-resolution imaging and, more specifically, subsidence delineation and void detection, are summarized. All the work discussed and concepts developed in this manuscript are based on more than 20 years of experience applying high-resolution seismic reflection to the imaging of anomalies in the shallow subsurface. In the next chapter the author's 12 most influential publications with a subsidence or void detection theme are summarized with key findings highlighted, specifically discussing how contributions from each have advanced the science and understanding of collapse structures. Also, considering some of these works were published more than 15 years ago, it was imperative to duly note discoveries that are still pertinent and applicable today.

References

- Allen, K.P., M.L. Johnson, and J.S. May, 1998, High fidelity vibratory seismic (HFVS) method for acquiring seismic data [exp. abs.]: Society of Exploration Geophysicists, p. 140-146.
- Arcone, S.A., 1996, High resolution of glacial ice stratigraphy: A ground-penetrating radar study of Pegasus Runway, McMurdo Station, Antarctica: *Geophysics*, v. 61, n. 6, p. 1653-1663.
- Bachrach, R., and J. Rickett, 1999, Ultra shallow seismic reflection in depth: Examples from 3D and 2D ultra shallow surveys with application to joint seismic and GPR imaging [exp. abs.]: Society of Exploration Geophysicists, p. 488-491.
- Baker, G.S., 1999, *Processing Near-Surface Seismic-Reflection Data—A Primer*: Society of Exploration Geophysicists, Course Notes Series No. 9, R. Young, ed.
- Baker, G.S., C. Schmeissner, and D.W. Steeples, 1999, Seismic reflections from depths of less than two meters: *Geophysical Research Letters*, v. 26, n. 2, 279-282.
- Baker, G.S., D.W. Steeples, and M. Drake, 1998, Muting the noise cone in near-surface reflection data: An example from southeastern Kansas: *Geophysics*, v. 63, n. 4, p. 1332-1338.
- Ballard, R.F., Jr., 1964, Determination of soil moduli at depth by in situ vibratory techniques: U.S. Army Engineer Waterways Experiment Station Miscellaneous Paper #4-691, Vicksburg, Mississippi, 9 p.
- Barnes, P.M., and J.C. Audru, 1999, Quaternary faulting in the offshore Flaxbourne and Wiararapa basins, south Cook Strait, New Zealand: *New Zealand Journal of Geology and Geophysics*, v. 42, p. 349-367.
- Benjumea, B., J.A. Hunter, R.A. Burns, R.L. Good, and S.E. Pullan, 2001, Use of high-resolution shear-wave-reflection methods for determining earthquake fundamental site period response near Alfred, Ontario: Geological Survey of Canada, Current Research 2001-D3, 10 p.
- Bergman, B., A. Tryggvason, and C. Juhlin, 2004, High-resolution seismic traveltime tomography incorporating static corrections applied to a till-covered bedrock environment: *Geophysics*, v. 69, n. 4, p. 1082-1090.
- Birkelo, B.A., D.W. Steeples, R.D. Miller, and M.A. Sophocleous, 1987, Seismic reflection study of a shallow aquifer during a pumping test: *Ground Water*, v. 25, p. 703-709.
- Black, R., D.W. Steeples, and R.D. Miller, 1994, Migration of shallow reflection data: *Geophysics*, v. 59, p. 402-410.
- Bradford, J.H., 2002, Depth characterization of shallow aquifers with seismic reflection, Part I—The failure of NMO velocity analysis and quantitative error prediction: *Geophysics*, v. 67, n. 1, p. 89-97.
- Bruhl, M., G.J.O. Vermeer, and M. Kiehn, 1996, Fresnel zones for broadband data: *Geophysics*, v. 61, p. 600-604.
- Büker, F., A.G. Green, and H. Horstmeyer, 1998, Shallow seismic reflection study of a glaciated valley: *Geophysics*, v. 63, n. 4, p. 1395-1407.
- Burow, K.R., G.S. Weissmann, R.D. Miller, and G. Placzek, 1997, Hydrogeologic facies characterization of an alluvial fan near Fresno, California, using geophysical techniques: U.S. Geological Survey Open-file Report 97-46, 15 p.
- Cox, M.J.G., 1999, *Static Corrections for Seismic Reflection Surveys*: Society of Exploration Geophysicists, Tulsa, Oklahoma, 531 p.

- Danbom, S., 2005, Special challenges associated with the near surface; in D.K. Butler, ed., *Near-Surface Geophysics*: Society of Exploration Geophysicists, Investigations in Geophysics No. 13, p. 7-29.
- Dasios, A., C. McCann, T.R. Astin, D.M. McCann, and P. Fenning, 1999, Seismic imaging of the shallow subsurface: shear-wave case histories: *Geophysical Prospecting*, v. 47, n. 4, p. 565-591.
- Davies, K.J., R.D. Barker, and R.F. King, 1992, Application of shallow reflection techniques in hydrogeology: *The Quarterly Journal of Engineering Geology*, v. 25, p. 207-216.
- Doll, W.E., R.D. Miller, and J. Xia, 1998, A non-invasive shallow seismic source comparison on the Oak Ridge Reservation, Tennessee: *Geophysics*, v. 63, n. 4, p. 1318-1331.
- Doornenbal, J.C., and K. Helbig, 1983, High-resolution reflection seismics on a tidal flat in the Dutch Delta—Acquisition, processing and interpretation: *First Break*, v. 1, n. 5, p. 9-10.
- Ebrom, D.A., S.A. Markley, and J.A. McDonald, 1996, Horizontal resolution before migration for broadband data [exp. abs.]: Society of Exploration Geophysics, p. 1430-1433.
- Evison, F.F., 1952, The inadequacy of the standard seismic techniques for shallow surveying: *Geophysics*, v. 17, p. 867-875.
- Frei, W., 1995, Refined field static corrections in near-surface reflection profiling across rugged terrain: *The Leading Edge*, v. 14, n. 4, p. 259-262.
- Geissler, P.E., 1989, Seismic reflection profiling for groundwater studies in Victoria, Australia: *Geophysics*, v. 54, n. 1, p. 31-37.
- Gendzwill, D.J., and R. Brehm, 1993, High-resolution seismic reflections in a potash mine: *Geophysics*, v. 58, p. 741-748.
- Gibert, D., B. Tournier, and J. Virieux, 1994, High-resolution electromagnetic imaging of the conductive Earth interior: *Inverse Problems*, v. 10, p. 341-351.
- Gochioco, L.M., 1991, Advances in seismic reflection profiling in U.S. coal exploration: *The Leading Edge*, v. 10, p. 24-29.
- Gochioco, L.M., 1992, Modeling studies of interference reflections in thin-layered media bounded by coal seams: *Geophysics*, v. 57, p. 1217-1227.
- Gochioco, L.M., and J.I. Kelly, 1990, High-resolution seismic survey to map paleochannels in an underground coal mine: *Canadian Journal of Exploration Geophysics*, v. 26, n. 1&2, p. 87-93.
- Goforth, T., and C. Hayward, 1992, Seismic reflection investigations of a bedrock surface buried under alluvium: *Geophysics*, v. 57, p. 1217-1227.
- Green, A.G., H. Maurer, T. Spillman, B. Heincke, and H. Willenberg, 2006, High-resolution geophysical techniques for improving hazard assessments of unstable rock slopes: *The Leading Edge*, v. 25, n. 3, p. 311-316.
- Green, A.G., A. Pugin, M. Beres, E. Lanz, F. Bükler, P. Huggenberger, H. Horstmeyer, M. Grasmück, R. de Iaco, K. Holliger, and H.R. Maurer, 1995, 3-D high-resolution seismic and georadar reflection mapping of glacial, glaciolacustrine and glaciofluvial sediments in Switzerland: Symposium on the Application of Geophysics to Engineering and Environmental Problems (SAGEEP 1995), p. 419-434.
- Gruber, W., and R. Rieger, 2003, High resolution seismic reflection constraints and pitfalls in groundwater exploration: *RMZ—Materials and Goenvironment*, v. 50, n. 1, p. 133-136.

- Guillen, D.P., and R.C. Hertzog, 2004, A survey of Department of Energy–sponsored geophysical research for shallow waste site characterization: *Vadose Zone Journal*, v. 3, p. 122-133.
- Haeni, F.P., 1986, Application of continuous seismic reflection methods to hydrologic studies: *Ground Water*, v. 24, p. 23-31.
- Hammer, P.T.C., R.M. Clowes, and K. Ramachandran, 2004, Case history: High-resolution seismic reflection imaging of a thin, diamondiferous kimberlite dyke: *Geophysics*, v. 69, n. 5, p. 1143-1154.
- Harris, J.B., J.A. Hunter, S.E. Pullan, R.A. Burns, and R.L. Good, 1996, Shallow shear wave seismic reflection profiling in the Fraser River delta, British Columbia [exp. abs.]: Society of Exploration Geophysicists, p. 865-868.
- Harris, J.B., R.D. Miller, J. Xia, J.A. Hunter, C.B. Park, D.R. Laflen, and R.L. Good, 2000, Near-surface shear wave reflection surveys in the Fraser River delta, B.C., Canada [exp. abs.]: Society of Exploration Geophysicists, p. 1327-1330.
- Hasbrouck, W.P., 1991, Four shallow-depth, shear-wave feasibility studies: *Geophysics*, v. 56, p. 1875-1885.
- Hasbrouck, W.P., and N. Padget, 1982, Use of shear wave seismics in evaluation of strippable coal resources: Utah Geological and Mineral Survey Bulletin 118, p. 203-210.
- Hatherly, P.J., M. Urosevic, A. Lambourne, and B.J. Evans, 1994, A simple approach to calculating refraction statics corrections: *Geophysics*, v. 59, p. 156-160.
- Healey, J., J. Anderson, R.D. Miller, D. Keiswetter, D.W. Steeples, and B. Bennett, 1991, Improved shallow seismic-reflection source: Building a better Buffalo [exp. abs.]: Society of Exploration Geophysicists, p. 588-591.
- Hecht, E., and A. Zajac, 1974, *Optics*: Addison-Wesley, Reading, MA, 565 p.
- Henley, D.C., 2001, Challenges in imaging shallow high resolution seismic data [exp. abs.]: Society of Exploration Geophysicists, p. 1373-1376.
- Hoover, G.M., and J.T. O'Brien, 1980, The influence of the planted geophone on seismic land data: *Geophysics*, v. 45, p. 1239-1253.
- Hunsdale, R., J.M. Bull, J.K. Dix, and D.J. Sanderson, 1998, The use of high-resolution seismic reflection profiles for fault analysis in the near-shore environment, Weymouth Bay, Dorset, England, United Kingdom: *Journal of Geophysical Research*, v. 103, n. B7, p. 15409-15422.
- Hunter, J.A., B. Benjumea, J.B. Harris, R.D. Miller, S.E. Pullan, R.A. Burns, and R.L. Good, 2002, Surface and downhole shear wave seismic methods for thick soil site investigations: *Soil Dynamics and Earthquake Engineering*, v. 22, n. 9-12, p. 931-941.
- Hunter, J.A., R.A. Burns, J.M. Aylsworth, and S.E. Pullan, 2000, Near-surface seismic-reflection studies to outline a buried bedrock basin in eastern Ontario: Geological Survey of Canada, Current Research 2000-E13, 7 p. (<http://www.nrcan.gc.ca/gsc/bookstore>).
- Hunter, J.A., M. Douma, R.A. Burns, R.L. Good, S.E. Pullan, J.B. Harris, J.L. Luternauer, and M.E. Best, 1998, Testing and application of near-surface geophysical techniques for earthquake hazard studies, Fraser River delta, BC; in J.J. Clague, J.L. Luternauer, and D.C. Mosher, eds., *Geology and natural hazards of the Fraser River Delta*, British Columbia: Geological Survey of Canada Bulletin 525, p. 123-145.
- Hunter, J.A., S.E. Pullan, R.A. Burns, R.M. Gagne, and R.S. Good, 1984, Shallow seismic-reflection mapping of the overburden-bedrock interface with the engineering seismograph—Some simple techniques: *Geophysics*, v. 49, p. 1381-1385.

- Inazaki, T., 2006, High-resolution S-wave reflection survey in urban areas using a woven belt type land streamer [ext. abs.]: European Association of Geoscientists and Engineers (EAGE) 68th Conference and Exhibition "Near Surface 2006," Vienna, Austria, June 12-15, 4 p. (published on CD).
- Inazaki, T., and X. Lel, 2003, Making of an accelerometer type land streamer and its utilization to near-surface gravity detection: Symposium on the Application of Geophysics to Engineering and Environmental Problems (SAGEEP 2003), p. 1253-1262.
- Ivanov, J., R.D. Miller, and J. Xia, 1998, High frequency random noise attenuation on shallow seismic reflection data by migration filtering [exp. abs.]: Society of Exploration Geophysicists, p. 870-873.
- Jefferson, R.D., D.W. Steeples, R.A. Black, and T. Carr, 1998, Effects of soil-moisture content on shallow-seismic data: *Geophysics*, v. 63, n. 4, p. 1357-1362.
- Johnston, D.H., 1981, Attenuation: A state-of-art summary: Seismic wave attenuation; in M.N. Toksöz and D.H. Johnston, eds., *Geophysics Reprint Series No. 2*: Society of Exploration Geophysicists, Tulsa.
- Jones, R., 1962, Surface wave technique for measuring the elastic properties and thickness of roads: Theoretical development: *British Journal of Applied Physics*, v. 13, p. 21-19.
- Jongerius, P., and K. Helbig, 1988, Onshore high-resolution seismic profiling applied to sedimentology: *Geophysics*, v. 53, p. 1276-1283.
- Kallweit, R.S., and L.C. Wood, 1982, The limits of resolution of zero-phase wavelets: *Geophysics*, v. 47, p. 1035-1046.
- Keiswetter, D., and D.W. Steeples 1995, A field investigation of source parameters for the sledgehammer: *Geophysics*, v. 60, p. 1051-1057.
- Kim, J.S., S.H. Han, H.S. Kim, W.S. Choi, and C.H. Jung, 2001, High-resolution seismic reflection profiling on land with hydrophones employed in the stream-water driver trench: *Geophysical Exploration*, v. 4, n. 4, p. 133-144.
- Knapp, R.W., 1986, Observations of the air-coupled wave as a function of depth: *Geophysics*, v. 51, p. 1853-1857.
- Knapp, R.W., 1990, Vertical resolution of thick beds, thin beds, and thin-bed cyclothems: *Geophysics*, v. 55, n. 9, p. 1183-1190.
- Knapp, R.W., 1991, Fresnel zones in the light of broadband data: *Geophysics*, v. 56, n. 3, p. 354-359.
- Knapp, R.W., and D.W. Steeples, 1986a, High-resolution common depth point seismic reflection profiling: Instrumentation: *Geophysics*, v. 51, p. 276-282.
- Knapp, R.W., and D.W. Steeples, 1986b, High-resolution common depth point seismic reflection profiling: Field acquisition parameter design: *Geophysics*, v. 51, p. 283-294.
- Kositsky, J., and P. Milanfar, 1999, A forward-looking high-resolution GPR system; in *Detection Remediation of Mines and Minelike Targets IV*: Pennsylvania State University, v. SPIE 3710, p. 1052-1062 (<http://citeseer.ist.psu.edu/316077.html>).
- Krohn, C.E., 1984, Geophone ground coupling: *Geophysics*, v. 49, n. 6, p. 722-731.
- Krohn, C.E., 1985, Geophone ground coupling: *The Leading Edge*, v. 4, n. 4, p. 56-60.
- Krohn, C.E., and M.L. Johnson, 2006, HFVSTM: Enhanced data quality through technology integration: *Geophysics*, v. 71, n. 2, p. E13-E23.
- Lanz, E. A. Pugin, A.G. Green, and H. Horstmeyer, 1996, Results of 2- and 3-D high-resolution seismic reflection surveying of surficial sediments: *Geophysical Research Letters*, v. 23, p. 491-494.

- Liberty, L.M., and M. Knoll, 1998, Time-varying fold in stacked seismic reflection data: A new quality control procedure for shallow high-resolution applications: Proceedings of the Symposium on the Application of Geophysics to Engineering and Environmental Problems (SAGEEP98), p. 745-751.
- Liberty, L.M., W.P. Clement, and M.D. Knoll, 1999, Surface and borehole seismic characterization of the Boise Hydrogeophysical Research Site: Symposium on the Application of Geophysics to Engineering and Environmental Problems (SAGEEP 1999), p. 723-732.
- Mair, J.A., and A.G. Green, 1981, High resolution seismic reflection profiles reveal fracture zones within a 'homogeneous' granite batholith: *Nature*, v. 294, p. 439-442.
- Marion, D.P., and P. Coudin, 1992, From ray to effective medium theories in stratified media: An experimental study [exp. abs.]: Society of Exploration Geophysicists, p. 1341-1343.
- Marlow, M.S., P.E. Hart, P.R. Carlson, J.R. Childs, D.M. Mann, R.J. Anima, and R.E. Kayen, 1996, Misinterpretation of lateral acoustic variations on high-resolution seismic reflection profiles as fault offsets of Holocene bay mud beneath the southern part of San Francisco Bay, California: *Marine and Petroleum Geology*, v. 13, n. 3. p. 341-348.
- Mavko, G., E. Kjartansson, and K. Winkler, 1979, Seismic wave attenuation in rocks, *IUGG Quadrennial Report, American Geophysical Union: Reviews of Geophysics and Space Physics*, v. 17, n. 6, p. 1155-1164.
- McConnell, T.J., 1998, Recent advances in high resolution aeromagnetism—Instrumentation: *Canadian Journal of Exploration Geophysics*, v. 34, n. 1&2, p. 1-3.
- Meckel, L.D., Jr., and A.K. Nath, 1977, Geologic considerations for stratigraphic modeling and interpretation; in Charles E. Payton, ed., *Seismic Stratigraphy—Applications to Hydrocarbon Exploration*: American Association of Petroleum Geologists (AAPG) Memoir 26, p. 417-438.
- Miller, K.C., S.H. Harder, D.C. Adams, and T. O'Donnell, Jr., 1998, Integrating high-resolution refraction data into near-surface seismic reflection data processing and interpretation: *Geophysics*, v. 63, n. 4, p. 1339-1347.
- Miller, R.D., 1992, Normal moveout stretch mute on shallow-reflection data: *Geophysics*, v. 57, p. 1502-1507.
- Miller, R.D., 2002, High-resolution seismic reflection investigation of a subsidence feature on U.S. highway 50 near Hutchinson, Kansas: Kansas Geological Survey Open-file Report 2002-17.
- Miller, R.D., 2003, High-resolution seismic-reflection investigation of a subsidence feature on U.S. Highway 50 near Hutchinson, Kansas: in K.S. Johnson and J.T. Neal, eds., *Evaporite karst and engineering/environmental problems in the United States*: Oklahoma Geological Survey Circular 109, p. 157-167.
- Miller, R.D., 2006, High-resolution seismic reflection to identify areas with subsidence potential beneath U.S. 50 Highway in eastern Reno County, Kansas: Symposium on the Application of Geophysics to Engineering and Environmental Problems (SAGEEP 2006), Seattle, Washington, April 2-6, Paper 28, 13 p.
- Miller, R.D., and R. Henthorne, 2004, High-resolution seismic reflection to identify areas with subsidence potential beneath U.S. 50 Highway in eastern Reno County, Kansas: Proceedings of the 55th Highway Geology Symposium, September 8-10, Kansas City, Missouri, p. 29-48.

- Miller, R.D., and R.D. Markiewicz, 2001, High resolution seismic reflection survey at Keechelus Dam: Symposium on the Application of Geophysics to Engineering and Environmental Problems (SAGEEP 2001), Denver, Colorado, March 4-7 (published on CD).
- Miller, R.D., and D.W. Steeples, 1991, Detecting voids in a 0.6-m coal seam, 7 m deep, using seismic reflection: *Geoexploration*, Elsevier Science Publishers B.V., Amsterdam, The Netherlands, v. 28, p. 109-119.
- Miller, R.D., and J. Xia, 1997, Delineating paleochannels using shallow seismic reflection: *The Leading Edge*, v. 16, n. 11, p. 1671-1674.
- Miller, R.D., and J. Xia, 1998, Large near-surface velocity gradients on shallow seismic reflection data: *Geophysics*, v. 63, n. 4, p. 1348-1356.
- Miller, R.D., D.W. Steeples, and M. Brannan, 1989, Mapping a bedrock surface under dry alluvium with shallow seismic reflections: *Geophysics*, v. 54, p. 1528-1534.
- Miller, R.D., J. Xia, and C.B. Park, 2001, Love waves: A menace to shallow shear wave reflection surveying [exp. abs.]: Society of Exploration Geophysicists, p. 1377-1380.
- Miller, R.D., J. Xia, and C.B. Park, 2005b, Seismic techniques to delineate dissolution features (karst) at a proposed power plant site; in D.K. Butler, ed., *Near-Surface Geophysics*: Society of Exploration Geophysicists, Investigations in Geophysics No. 13, p. 663-679.
- Miller, R.D., N.L. Anderson, H.R. Feldman, and E.K. Franseen, 1995a, Vertical resolution of a seismic survey in stratigraphic sequences less than 100 m deep in Southeastern Kansas: *Geophysics*, v. 60, p. 423-430.
- Miller, R.D., J.A. Hunter, W.E. Doll, B.J. Carr, R.A. Burns, R.L. Good, D.R. Laflen, and M. Douma, 2000, Imaging permafrost with shallow P- and S-wave reflection [exp. abs.]: Society of Exploration Geophysicists, p. 1339-1342.
- Miller, R.D., J.A. Hunter, W.E. Doll, B.J. Carr, and T.S. Collett, 2005a, High-resolution seismic imaging of the gas hydrate stability zone at the Mallik L-38 research site; in S.R. Dallimore and T.S. Collett, eds., *Scientific Results from the Mallik 2002 Gas Hydrate Production Research Well Program, Mackenzie Delta, Northwest Territories, Canada*: Geological Survey of Canada, Bulletin 585, 14 p.
- Miller, R.D., R.D. Markiewicz, T.R. Rademacker, R. Hopkins, R.J. Rawcliffe, and J. Paquin, 2007, Advantages of wet work for near-surface seismic reflection [exp. abs.]: Society of Exploration Geophysicists, 4 p.
- Miller, R.D., K. Park, J. Ivanov, C.B. Park, and R.F. Ballard, 2003, A 2-C towed geophone spread for variable surface conditions: Symposium on the Application of Geophysics to Engineering and Environmental Problems (SAGEEP 2003) (published on CD).
- Miller, R.D., S.E. Pullan, D.W. Steeples, and J.A. Hunter, 1992, Field comparison of shallow seismic sources near Chino, California: *Geophysics*, v. 57, p. 693-709.
- Miller, R.D., S.E. Pullan, D.W. Steeples, and J.A. Hunter, 1994, Field comparison of shallow P-Wave seismic sources near Houston, Texas: *Geophysics*, v. 59, p. 1713-1728.
- Miller, R.D., S.E. Pullan, J.S. Waldner, and F.P. Haeni, 1986, Field comparison of shallow seismic sources: *Geophysics*, v. 51, p. 2067-2092.
- Miller, R.D., D.W. Steeples, J.L. Lambrecht, and N. Croxton, 2006, High-resolution seismic-reflection imaging 25 years of change in I-70 sinkhole, Russell, County, Kansas [exp. abs.]: Society of Exploration Geophysicists, p. 1411-1414.

- Miller, R.D., J. Xia, C.B. Park, and J.M. Ivanov, 1999, Multichannel analysis of surface waves to map bedrock: *The Leading Edge*, v. 18, n. 12, p. 1392-1396.
- Miller, R.D., J. Xia, J.W. Deane, J.M. Anderson, D.R. Laflen, P.M. Acker, and M.C. Brohammer, 1994, High resolution seismic reflection survey to image the top and bottom of a shallow clay layer at the Memphis Defense Depot, Memphis, Tennessee; Final report: Kansas Geological Survey Open-file Report 94-18.
- Miller, R.D., J. Xia, R.S. Harding, J.T. Neal, J.W. Fairborn, and D.W. Steeples, 1995b, Seismic investigation of a surface collapse feature at Weeks Island Salt Dome, Louisiana: *AAPG Division of Environmental Geosciences Journal*, v. 2, n. 2, p. 104-112.
- Mooney, H.M., 1973, *Handbook of Engineering Geophysics*: Bison Instruments Inc., Minneapolis, Minnesota.
- Nijhof, V., 1992, A portable high-frequency vibrator and its implementation on a PC-based acquisition system [exp. abs.]: Society of Exploration Geophysicists, p. 942-943.
- Odum, J.K., et al., 1999, Shallow high-resolution seismic-reflection imaging of karst structures within the Floridan aquifer system, northeastern Florida: *Journal of Environmental and Engineering Geophysics*, v. 4, p. 251-261.
- Olsen, H., C. Ploug, U. Nielsen, and K. Sorensen, 1993, Reservoir characterization applying high-resolution seismic profiling, Rabis Creek, Denmark: *Ground Water*, v. 31, p. 84-90.
- Pakiser, L.C., and R.E. Warrick, 1956, A preliminary evaluation of the shallow reflection seismograph: *Geophysics*, v. 21, p. 388-405.
- Park, C.B., R.D. Miller, D.W. Steeples, and R.A. Black, 1996, Swept impact seismic technique (SIST): *Geophysics*, v. 61, p. 1789-1803.
- Park, C.B., R.D. Miller, and J. Xia, 1999, Multi-channel analysis of surface waves: *Geophysics*, v. 64, n. 3, p. 800-808.
- Park, C.B., R.D. Miller, J. Xia, J. Ivanov, G.V. Sonnichsen, J.A. Hunter, R.L. Good, R.A. Burns, and H. Christian, 2005, Underwater MASW to evaluate stiffness of water-bottom sediments: *The Leading Edge*, v. 24, n. 7, p. 724-728.
- Park, C.B., R.D. Miller, J. Xia, J. Ivanov, J.A. Hunter, R.L. Good, and R.A. Burns, 2000, Multichannel analysis of underwater surface waves near Vancouver, B.C., Canada [exp. abs.]: Society of Exploration Geophysicists, p. 1303-1306.
- Pietsch, K., and R. Slusarczyk, 1992, The application of high-resolution seismics in Polish coal mining: *Geophysics*, v. 57, p. 171-180.
- Pugin, A., and S.E. Pullan, 2000, First-Arrival alignment static corrections applied to shallow seismic reflection data: *Journal of Environmental and Engineering Geophysics*, v. 5, n. 1, p. 7-15.
- Pugin, A.J.M., T.H. Larson, S.L. Sargent, J.H. McBride, and C.E. Bexfield, 2004, Near-surface mapping using SH-wave and P-wave seismic land-streamer data acquisition in Illinois, U.S.: *The Leading Edge*, v. 23, n. 7, p. 677-682.
- Pugin, A., J.A. Hunger, D. Motazedian, G. Brooks, K. Khaheshi-Banab, 2007, An application of shear wave reflection landstreamer technology to soil response evaluation of earthquake shaking in an urban area, Ottawa, Ontario: Symposium on the Application of Geophysics to Engineering and Environmental Problems (SAGEEP 2007), p. 885-896.
- Pullan, S.E., and J.A. Hunter, 1990, Delineation of buried bedrock valleys using the optimum-offset shallow seismic reflection technique; in Stan Ward, ed., *Volume 3: Geotechnical*: Society of Exploration Geophysicists, Investigations in Geophysics No. 5, p. 89-97.

- Pullan, S.E., J.A. Hunter, and K.G. Neave, 1990, Shallow shear-wave reflection tests [exp. abs.]: Society of Exploration Geophysicists, p. 380-382.
- Quan, Y., and J.M. Harris, 1997, Seismic attenuation tomography using the frequency shift method: *Geophysics*, v. 62, n. 3, p. 895-905.
- Quinn, R., J.M. Bull, and J.K. Dix, 1998, Optimal processing of marine high-resolution seismic reflection (chirp) data: *Marine Geophysical Researches*, v. 20, n. 1, p. 13-20.
- Robertsson, J.O.A., K. Holliger, A.G. Green, A. Pugin, and R. De Iaco, 1996a, Effects of near-surface waveguides on shallow high-resolution seismic refraction and reflection data: *Geophysical Research Letters*, v. 23, p. 495-498.
- Robertsson, J.O.A., K. Holliger, and A.G. Green, 1996b, Source-generated noise in shallow seismic data: *European Journal of Environmental and Engineering Geophysics*, v. 1, p. 107-124.
- Robinson, E.A., and S. Treitel, 1980, *Geophysical Signal Analysis*: Prentice-Hall, Englewood Cliffs, NJ, 466 p.
- Roth, M., K. Holliger, and A.G. Green, 1998, Guided waves in near-surface seismic surveys: *Geophysical Research Letters*, v. 25, n. 7, p. 1071-1074.
- Sandwell, D.T., and D.C. McAdoo, 1990, High-accuracy, high-resolution gravity profiles from two years of the Geosat Exact Repeat Mission: *Journal of Geophysical Research*, v. 95, n. C3, p. 3049-3060.
- Schepers, R., 1975, A seismic reflection method for solving engineering problems: *Journal of Geophysics*, v. 41, p. 367-384.
- Seltzer, G.O., P. Baker, S. Cross, R. Dunbar, and S. Fritz, 1998, High-resolution seismic reflection profiles from Lake Titicaca, Peru-Bolivia: Evidence for Holocene aridity in the tropical Andes: *Geology*, v. 26, n. 2, p. 167-170.
- Sheriff, R.E., 1977, Limitations on resolution of seismic reflections and geologic detail deliverable from them; in Charles E. Payton, ed., *Seismic Stratigraphy—Applications to Hydrocarbon Exploration*: American Association of Petroleum Geologists (AAPG) Memoir 26, p. 3-14.
- Sheriff, R.E., 2002, *Encyclopedic Dictionary of Applied Geophysics*, 4th ed.: Society of Exploration Geophysicists, Tulsa, 429 p.
- Sheriff, R.E., and L.P. Geldart, 1995, *Exploration Seismology*: Cambridge University Press.
- Shtivelmen, V., and M. Goldman, 2000, Integration of shallow reflection seismics and time domain electromagnetics for detailed study of the coastal aquifer in the Nitzanum area of Israel: *Journal of Applied Geophysics*, v. 44, p. 197-215.
- Sieck, H.C., and G.W. Self, 1977, Analysis of high resolution seismic data; in Charles E. Payton, ed., *Seismic Stratigraphy—Applications to Hydrocarbon Exploration*: American Association of Petroleum Geologists (AAPG) Memoir 26, p. 353-385.
- Singh, S., 1984, High-frequency shallow seismic reflection mapping in tin mining: *Geophysical Prospecting*, v. 32, p. 1033-1044.
- Spitzer, R., F.O. Nitsche, A.G. Green, and H. Horstmeyer, 2003, Efficient acquisition, processing and interpretation strategy for 3-D high-resolution seismic surveying: A case study: *Geophysics*, v. 68, p. 1792-1806.
- Spitzer, R., M. van der Veen, F.O. Nitsche, H. Horstmeyer, and A.G. Green, 1998, Designing 3-D high-resolution seismic surveys [exp. abs.]: Society of Exploration Geophysicists, p. 54-57.

- Steeple, D.W., 2000, Geologic structure detection by high resolution seismic reflection methods near the Custer Hill Landfill: Final report on contract DAMD17-99-2-9053, Report no. A112383, 12 p. (<http://stormingmedia.us/11/1123/A112383.html>).
- Steeple, D.W., and R.K. Knapp, 1982, Reflections from 25 feet or less [exp. abs.]: Society of Exploration Geophysicists, p. 469-471.
- Steeple, D.W., and R.D. Miller, 1986, Some shallow seismic reflection pitfalls [exp. abs.]: Society of Exploration Geophysicists, p. 101-104.
- Steeple, D.W., and R.D. Miller, 1990, Seismic-reflection methods applied to engineering, environmental, and groundwater problems; in Stan Ward, ed., *Volume 1: Review and Tutorial*: Society of Exploration Geophysicists, Investigations in Geophysics No. 5, p. 1-30.
- Steeple, D.W., and R.D. Miller, 1993, Basic principles and concepts of practical shallow seismic reflection profiling (a tutorial): *Mining Engineering*, October, p. 1297-1302.
- Steeple, D.W., and R.D. Miller, 1998, Avoiding pitfalls in shallow seismic reflection surveys: *Geophysics*, v. 63, n. 4, p. 1213-1224.
- Steeple, D.W., G.S. Baker, and C. Schmeissner, 1999, Toward the autojuggie: Planting 72 geophones in 2 seconds: *Geophysical Research Letters*, v. 26, n. 8, p. 1085-1088.
- Steeple, D.W., R.D. Miller, and R.W. Knapp, 1987, Downhole .50-caliber rifle—an advance in high-resolution seismic sources [exp. abs.]: Society of Exploration Geophysicists, p. 76-78.
- Steeple, D.W., C.M. Schmeissner, and B.K. Macy, 1995a, The evolution of shallow seismic methods: *Journal of Environmental and Engineering Geophysics*, v. 0, n. 1, p. 15-24.
- Steeple, D.W., B. Macy, C. Schmeissner, and R.D. Miller, 1995b, Contrasting near-surface and classical seismology: *The Leading Edge*, v. 14, p. 271-272.
- Steeple, D.W., A.G. Green, T.V. McEvelly, R.D. Miller, W.E. Doll, and J.W. Rector, 1997, A workshop examination of shallow seismic reflection surveying: *The Leading Edge*, v. 16, n. 11, p. 1641-1646.
- Stokoe II, K.H., S.G. Wright, J.A. Bay, and J.M. Roësset, 1994, Characterization of geotechnical sites by SASW method; in R.D. Woods, ed., *Geophysical Characterization of Sites*, ISSMFE Technical Committee #10: Oxford Publishers, New Delhi.
- Stolt, R.H., and A.F. Benson, 1986, *Seismic Migration*: Geophysical Press.
- Telford, W.M., L.P. Geldart, R.E. Sheriff, and D.A. Keys, 1976, *Applied Geophysics*: Cambridge University Press, Cambridge, UK, 877 p.
- Urosevic, M., B. Evans, and L. Vella, 2002, Shallow high-resolution seismic imaging of the Three Springs talc mine, Western Australia: *The Leading Edge*, v. 21, p. 923-926.
- van der Veen, M., and A.G. Green, 1998, Landstreamer for shallow seismic data acquisition: Evaluation of gimbal mounted geophones: *Geophysics*, v. 63, p. 1408-1413.
- van der Veen, M., J. Brouwer, and K. Helbig, 1999, Weighted sum method for calculating ground force: an evaluation by using a portable vibrator system: *Geophysical Prospecting*, v. 47, n. 3, p. 251-267.
- van der Veen, M., R. Spitzer, A.G. Green, and P. Wild, 2001, Design and application of a towed land-streamer for cost-effective 2D and pseudo-3D shallow seismic data acquisition: *Geophysics*, v. 66, p. 482-500.
- Vermeer, G.J.O., 2002, 3-D seismic survey design: Society of Exploration Geophysicists, Tulsa, Geophysical References Series No. 4, 205 pp.

- Walters, S.L., R.D. Miller, J.B. Dunbar, and S. Smullen, 2007, Repeatability observations from a 2D time-lapse seismic survey: Symposium on the Application of Geophysics to Engineering and Environmental Problems (SAGEEP 2007), p. 878-884.
- Whiteley, R.J., J.A. Hunter, S.E. Pullan, and P. Nutalaya, 1998, "Optimum offset" seismic reflection mapping of shallow aquifers near Bangkok, Thailand: *Geophysics*, v. 63, n. 4, p. 1385-1394.
- Widess, M.B., 1973, How thin is a thin bed?: *Geophysics*, v. 38, p. 1176-1180.
- Xia, J., Miller, R.D., and Park, C.B., 1999, Estimation of near-surface shear-wave velocity by inversion of Rayleigh waves: *Geophysics*, v. 64, n. 3, p. 691-700.
- Yilmaz, Ö., 1987, *Seismic Data Processing*: Tulsa, Society of Exploration Geophysicists.
- Yilmaz, Ö., 2002, *Seismic Data Analysis—Processing, Inversion, and Interpretation of Seismic Data*: Society of Exploration Geophysicists, Investigations in Geophysics No. 10, S.M. Doherty, ed. (2 volumes).
- Ziolkowski, A., and W.E. Lerwill, 1979, A simple approach to high-resolution seismic profiling for coal: *Geophysical Prospecting*, v. 27, p. 360-393.

CHAPTER 7

SEISMIC-REFLECTION STUDIES OF DISSOLUTION

Previous chapters have focused on describing the characteristics and properties of salt, collapse features, and the high-resolution seismic-reflection method specifically in the context of imaging dissolution-induced subsidence features. Some effort was also made in earlier chapters to describe past efforts by various researchers to seismically image dissolution features associated with site-specific studies. In the previous chapter the high-resolution seismic-reflection tool was differentiated from the more common conventional approach, focusing on the method's uniqueness, limitations, and potential. In staying with that general progression and flow, the objective of this chapter will be to highlight the author's most significant published contributions and findings that are consistent with a seismic-reflection imaging of voids and collapse features theme.

This chapter is a compilation of summaries with key figure(s) extracted from 12 papers written by the author, most refereed, detailing the notable and lasting contributions of each. Considering the diversity of sites and associated features central to each of these published works, this chapter is organized according to key characteristics, catalysts, or settings of each paper. As well, because these papers have been published throughout a period that spans 15 years (1991 to 2006), it is clear that later works have benefited significantly by progressively building on the advancements, discoveries, and experience gained during previous studies. To decisively achieve the goals set for later chapters, it is important and necessary to render each of these 12 papers down to their original, innovative, and key findings and note contributions that are still pertinent today.

Since publication of the oldest paper included in this chapter (1991), the method has seen dramatic improvements in resolution and signal-to-noise ratio due to both equipment and technique enhancements. This evolution is clearly evident when chronologically stepping through this sequence of summarized papers. Each progressively younger work is enriched with more detailed and defined seismic representations and discussions of subsidence processes, mechanisms, and geometries as a direct result of discoveries in earlier papers. Noteworthy about this collection of research works is the diversity of settings and applications with studies ranging from natural dissolution-induced subsidence to roof failure and associated subsidence due to overmining. With this broad range of subsidence targets, common characteristics and principles can be ascertained that enhance the breadth and nonuniqueness of this study.

Of the 12 papers summarized in this chapter, seven have been published in refereed journals; the remaining are proceedings papers and have undergone technical review for correctness and completeness prior to acceptance for presentation at national/international meetings. These selected papers provide the basis for many of the overarching observations and conclusions presented predominantly in Chapter 9 of this work. Reference to and significant findings from each of these papers are strung throughout this manuscript, where they are drawn on as the basis for and in support of various significant conclusions.

Publication venues that are bold and italicized indicate a journal with a minimum of three anonymous reviewers.

Summaries of Published Papers by Author

A. Anthropogenic

1. Mine Collapse

Miller, R.D., J. Xia, R.S. Harding, J.T. Neal, J.W. Fairborn, and D.W. Steeples, 1995, Seismic investigation of a surface collapse feature at Weeks Island Salt Dome, Louisiana: *AAPG Division of Environmental Geosciences Journal*, v. 2, n. 2, p. 104-112.

Surface and borehole seismic-imaging techniques delineate the subsurface expression of an active sinkhole above the former salt mine at Weeks Island, Louisiana, which had been converted for use by the United States Department of Energy's Strategic Petroleum Reserve. The sinkhole, which was originally ~12 m wide and 11 m deep, is directly over the edge of the upper storage chamber and in an area where the salt dome top is 60 m below ground surface. Surface seismic reflections detect a dramatic bowl-shaped depression in a 28-m-deep reflector directly adjacent to the sinkhole (Figure 7-1). Two reflectors (drill-confirmed geologic contacts at 28 and 60 m) interpreted on multichannel vertical seismic profile (VSP) data represent the only velocity and/or density contrasts detected between ground surface and just beneath the salt-dome top. The 28-m reflector identified on both VSP and surface seismic-reflection data (Figure 7-2) is depth-consistent with the piezometric surface. However, because of the high measured permeability and the relative severity of the reflection depression, it is questionable whether the 28-m reflection on surface seismic data is a direct image of the water table. No evidence was discovered to confidently ascertain the mechanism (i.e., fracture from mine activities, shear zone associated with uplift, etc.) responsible for exposing the salt to unsaturated meteoric water.

This work was the first to produce a confidently interpretable image of a subsidence throat approximately equal to the radius of the Fresnel zone and offset from the center of the surface expression. The diffraction and bow tie features are characteristic of abrupt terminations; this is the only seismically imaged, wavelength-size feature infilled with collapse breccia and therefore returning no reflections from within the throat. This image strongly supports an initial compressional failure mechanism.

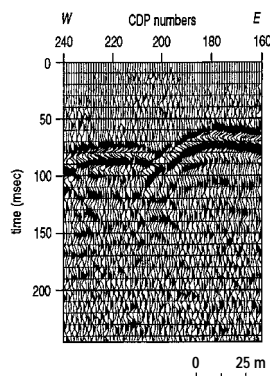


Figure 7-1. Unmigrated CDP stack with clearly developed "bow tie" feature.

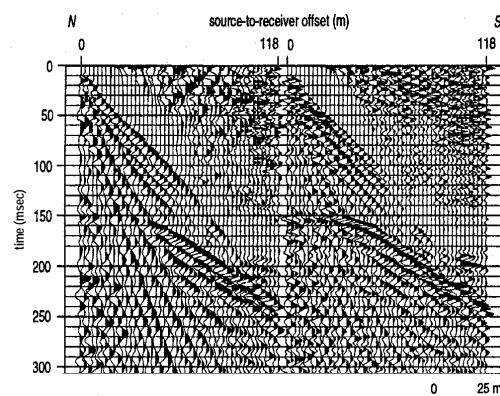


Figure 7-2. Walkaway noise tests conducted along the northeastern end of line 1. The prominent 145-msec reflection possesses textbook curvature and a dominant frequency of greater than 150 Hz. Vertical-resolution potential is less than 1 m.

Miller, R.D., D.W. Steeples, L. Schulte, and J. Davenport, 1993, Shallow seismic-reflection feasibility study of the salt dissolution well field at North American Salt Company's Hutchinson, Kansas, facility: *Mining Engineering*, October, p. 1291-1296.

Shallow seismic-reflection methods were used to delineate the subsurface extent of roof failure associated with the dissolution mining of a 120-m-deep and 60-m-thick salt bed in central Kansas. Three intersecting common depth point (CDP) seismic-reflection profiles, targeting the subsurface around an actively subsiding sinkhole, possess sufficient resolution to delineate the horizontal and vertical extent of subsurface rock failure associated with the subsidence (Figure 7-3). Of principal concern was the railroad spur and secondary city street that passed within 20 m of the sinkhole. The three seismic profiles that surrounded the sinkhole showed a disturbed subsurface area 90 to 150 m in diameter at a depth of between 60 to 75 m. Confirmation drilling verified the interpretation of the seismic data. These seismic-reflection data have the potential to resolve disturbed subsurface areas greater than 23 m in diameter at this site with detection being in the sub-10-m range.

These published data are the first to clearly return a high-resolution seismic-reflection image of a void's stopping roof and associated drape. Because this profile crossed over competent ground immediately adjacent to the sinkhole, overburden imaged above the collapse feature was under stress but did not possess notable strain. These were the first published images of disturbed beds within the tensional dome while the stress regime was fully tensional. These images and study provided critical insights into the failure process in the thick layered shales that overlay the salt. Partial bridging along the intact roof supports collapse material from within the overburden that will eventually fall to the base of the dissolution void to form lag. Advances in the high-resolution seismic-reflection approach include low-fold muting and narrow-window NMO corrections.

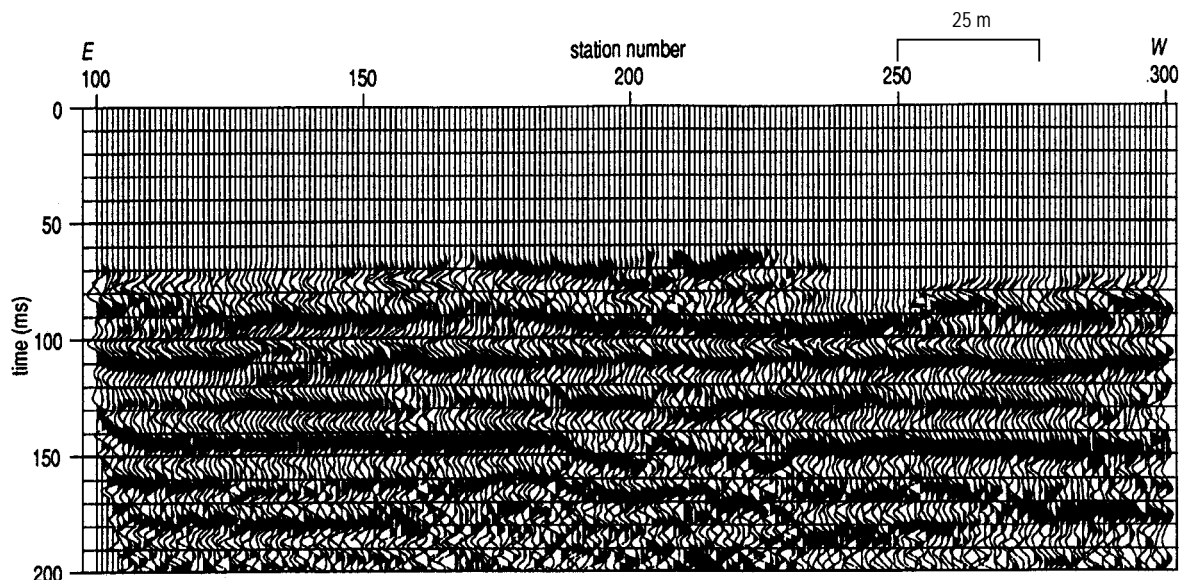


Figure 7-3. CMP stacked section along edge of sinkhole. Distortion in the 140-ms reflection adjacent to the sinkhole is obvious beneath station 200

Miller, R.D., and D.W. Steeples, 1991, Detecting voids in a 0.6-m coal seam, 7 m deep, using seismic reflection: *Geoexploration*, Elsevier Science Publishers B.V., Amsterdam, The Netherlands, v. 28, p. 109-119.

Surface collapse over abandoned subsurface coal mines is a problem in many parts of the world. High-resolution P-wave reflection seismology was successfully used to evaluate the risk of an active sinkhole within 20 m of a main north-south railroad line in an undermined area of southeastern Kansas, USA. Water-filled cavities responsible for sinkholes in this area are in a 0.6-m-thick coal seam, 7 m deep. Dominant reflection frequencies in excess of 200 Hz enabled reflections from the coal seam to be discerned from the direct wave, refractions, air wave, and ground roll on unprocessed field files. Repetitive void sequences within competent coal on three seismic profiles are consistent with the “room and pillar” mining technique practiced in this area near the turn of the century. The seismic survey showed that the apparent active sinkhole was not the result of reactivated subsidence but probably erosion consistent with an old vertical escape or air shaft (Figure 7-4).

Even though this is the oldest paper of the set, it still remains one of the most influential and cited in the field of void detection. Drill-confirmed voids imaged on these seismic-reflection data are the smallest ever detected with this method. Model studies have suggested amplitude variations are key to interpreting beds less than one-quarter wavelength, but this paper provides the first and only empirical data set that possesses clear seismic evidence of a void less than one-tenth the dominant wavelength and less than one-eighth the radius of the Fresnel zone. This paper clearly substantiates the uniqueness of detection versus resolution.

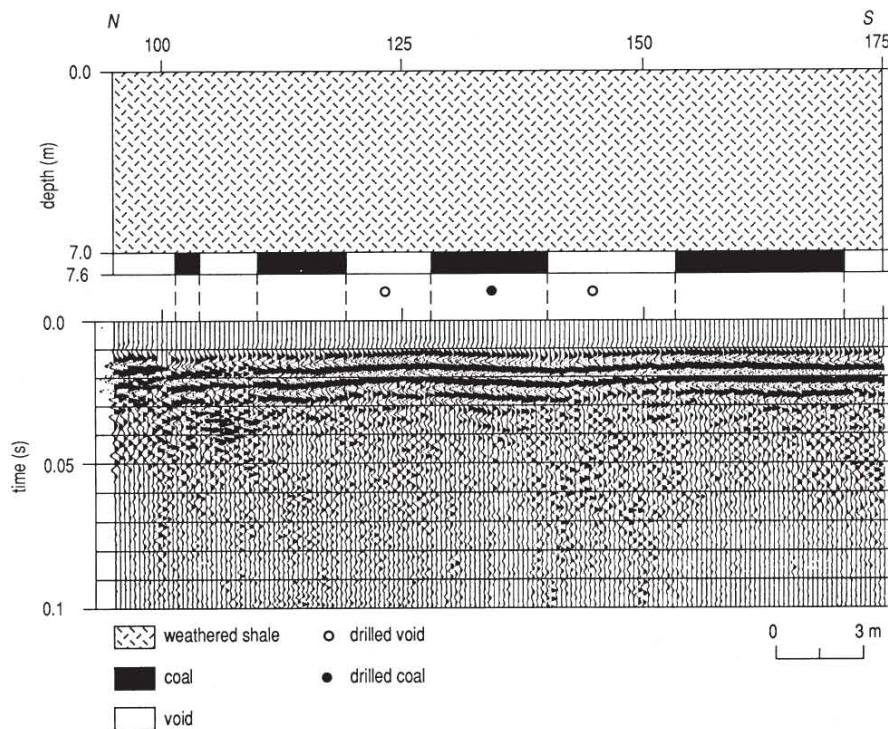


Figure 7-4. Twelve-fold CDP stack and geologic interpretation. Drilling confirmed the presence of the interpreted voids in the competent coal. The first two dominant cycles after first breaks are stacked refraction energy not muted to avoid adversely affecting the reflection arrivals.

Miller, R.D., J. Ivanov, D.W. Steeples, W.L. Watney, and T.R. Rademacker, 2005, Unique near-surface seismic-reflection characteristics within an abandoned salt-mine well field, Hutchinson, Kansas [exp. abs.]: Society of Exploration Geophysicists, p. 1041-1044.

High-resolution seismic reflections have been used effectively to investigate sinkholes resulting from the dissolution of a bedded salt unit found throughout most of central Kansas. A seismic-reflection survey was conducted to investigate the shallow subsurface between a sinkhole that formed catastrophically and a main east/west rail line a few tens of meters away. Data quality was significantly below expectations and not equivalent to other seismic data from this area where acquisition parameters, equipment, and target intervals were similar. Near-surface tomographic and MASW analyses revealed a highly irregular bedrock surface characterized by what appear to be a high concentration of short-wavelength dissolution or erosion features. Data quality is quite good on other seismic-reflection surveys from this general area where these bedrock features are not present. Pronounced static shifts and degradation in spectral characteristics of reflections where these bedrock features are present seem to be isolated to an area suspected to be the crest of a relatively broad regional anticlinal structure. Scattered energy appears as high-angle dipping beds adjacent to the sinkhole around station 1170. Broadband high-resolution compressional-wave energy suffered significantly from this highly irregular bedrock topography (Figure 7-5).

This study demonstrated the adverse effects on seismic data resulting from scatter and wavefield interference associated with sub-Fresnel zone-sized collapse structures outside the plane of the survey.

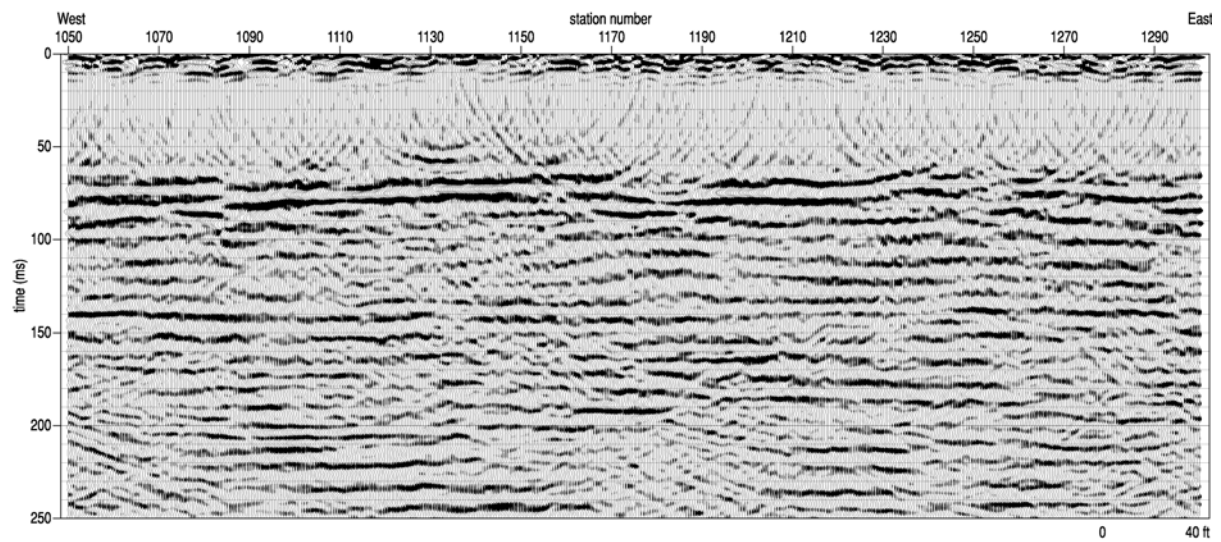


Figure 7-5. Migrated CMP stacked section adjacent to sinkhole and on undisturbed ground. Reduced coherency due to irregular bedrock surface and scatter off the collapse volume from out of the plane.

2. Disposal Well Breach

Miller, R.D., D.W. Steeples, and T.V. Weis, 1995, Shallow seismic-reflection study of a salt dissolution subsidence feature in Stafford County, Kansas; in N.L. Anderson and D.E. Hedke, eds., *Geophysical atlas of selected oil and gas fields in Kansas*: Kansas Geological Survey Bulletin 237, p. 71-76.

Seismic-reflection surveying was successfully used to define subsidence of the Stone Corral anhydrite in Stafford, County, Kansas, in response to dissolution of the 85-m-thick Permian-aged Hutchinson Salt Member at a depth of approximately 340 m. Gradual formation of a surface depression around the Siefkes "A" No. 6 abandoned oil-field-brine disposal well in central Kansas, USA, prompted a 12-fold CDP seismic survey designed to define the potential extent and amount of future surface subsidence. Several reflections interpreted on the CDP stacked sections possess dominant frequencies in excess of 100 Hz. Reflections can be interpreted on stacked sections at two-way times from 80 ms (approximate depth of 70 m) to 220 ms (approximate depth of 200 m). The Stone Corral anhydrite reflection is present at two-way traveltimes between 200 and 220 ms on all seismic lines and possesses a maximum of 20 ms (35 m assuming 1770-m/s seismic velocity) of relative subsidence (Figure 7-6). The perimeter of the subsurface collapse, as defined by structures on the Stone Corral anhydrite, represents a potential four-fold increase in the surface area of the sinkhole, assuming purely vertical upward migration of the disturbed subsurface.

This was the first published attempt to predict future sinkhole growth based on a seismic survey. Still noteworthy today is the observation that surface growth can vary dramatically across the volume of overburden rocks above a salt-dissolution zone. This work set the stage for suggesting that vertical progression of a gradual subsidence feature can be irregular in rate throughout the volume with strain likely to seek a laterally expansive and irregular path to the surface both initially and throughout the life of a subsidence event.

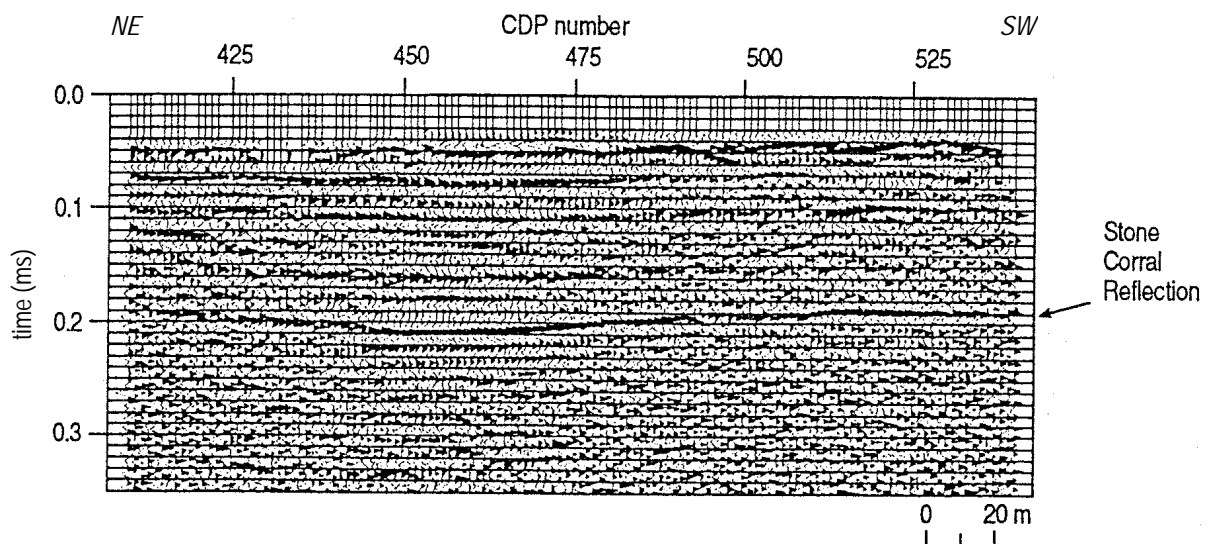


Figure 7-6. CMP stacked section with the Stone Corral reflection indicated. The Stone Corral is a regionally consistent, flat reflector.

Miller, R.D., A. Villella, J. Xia, and D.W. Steeples, 2005, Seismic investigation of a salt dissolution feature in Kansas; in Dwain K. Butler, ed., *Near-Surface Geophysics*: Society of Exploration Geophysicists, Investigations in Geophysics No. 13, p. 681-694.

High-resolution seismic-reflection techniques successfully delineated the main structural and stratigraphic features of a salt-dissolution sinkhole that formed gradually around a brine-disposal well in central Kansas. Subsidence resulted from failure of rock units overlying a void that formed by dissolution in the Permian-aged Hutchinson Salt Member of the Wellington Formation. The surface expression, named the French sinkhole, which currently encompasses approximately 15,000 m² of farm ground, developed at a relatively uniform growth rate (about one-third meter vertical per year). High-resolution seismic images along five profiles captured several reflectors that turned out to be key to unraveling the structural chronology of the French sinkhole, allowing an appraisal of future growth rate, extent, and hazard to surface occupation.

Interpretations of reflections from key stratigraphic horizons suggest multiple phases of loading, failure, and subsidence (Figures 7-7 and 7-8). Initially, rock layers over dissolution voids deformed gradually and appeared to have plastic strain. Once the roof span reached a physical limit defined by the material and span geometry, roof rock failed along reverse-fault planes within a cone-shaped earth volume known as the tensional dome. Currently, relaxation of stress associated with bridged layers outside that dome is occurring along normal faults. These normal faults have minimal vertical connectivity between the successive reflectors and therefore do not form classical fault planes. Oil-field disposal practices provided the original fluids and pathway that initiated the dissolution process, but currently shallower ground water is likely fueling the dissolution process.

This was a landmark paper and the first to seismically image reverse and normal fault planes around a subsidence volume with clear indications of two distinct stress regimes. It was also the first paper to provide strong seismic evidence of multiple, unique subsidence zones throughout the disturbed volume, which differentially affected overburden and asymmetric sinkhole development.

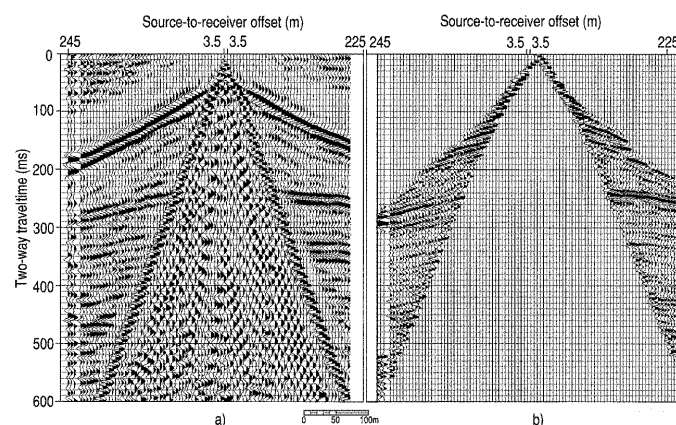


Figure 7-7. (a) Scaled raw data; (b) processed and spectral balanced (a).

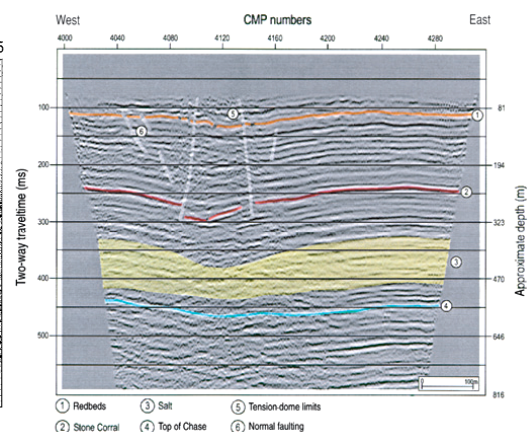


Figure 7-8. Interpreted CMP stack showing salt bed and fault planes within subsidence volume.

Miller, R.D., D.W. Steeples, and J.L. Lambrecht, 2006, High-resolution seismic-reflection imaging 25 years of change in I-70 sinkhole, Russell County, Kansas [exp. abs.]: Society of Exploration Geophysicists (published on CD).

Time-lapse seismic-reflection imaging improved our understanding of the consistent, gradual surface subsidence ongoing at two sinkholes in the Gorham oil field beneath a stretch of Interstate Highway 70 through central Kansas. With subsidence occurring at a rate of around 10 cm per year since discovery in 1966, monitoring has been necessary to ensure public safety and optimize maintenance. A miniSOSIE reflection survey conducted in 1980 delineated the affected subsurface and successfully predicted development of a third sinkhole at this site. In 2004 and 2005, a high-resolution vibroseis survey was completed to ascertain current subsurface conditions including rate and pattern of growth since 1980 and a prediction of continued growth. With time and improved understanding of the salt-dissolution affected subsurface in this area, it appears that these features represent little risk of catastrophic failure (Figure 7-9). However, from an operational perspective, the Kansas Department of Transportation should expect continued subsidence, with future increases in surface area likely at a slightly reduced vertical rate. Seismic characteristics appear empirically consistent with gradual earth-material compaction/settling.

This paper has provided the most detailed view to date of the internal structures and therefore processes of a borehole-induced dissolution feature. Seismic sections in this paper were the first to correlate with the key details and characteristics of physical models. Offset bed geometries indicate two stress regimes with multiple episodes of subsidence and a collapse geometry suggestive of a mid-stage subsidence feature with salt harvesting still active. This work allows an unprecedented glimpse into the internal workings/progression of a subsidence structure and development of point leaching.

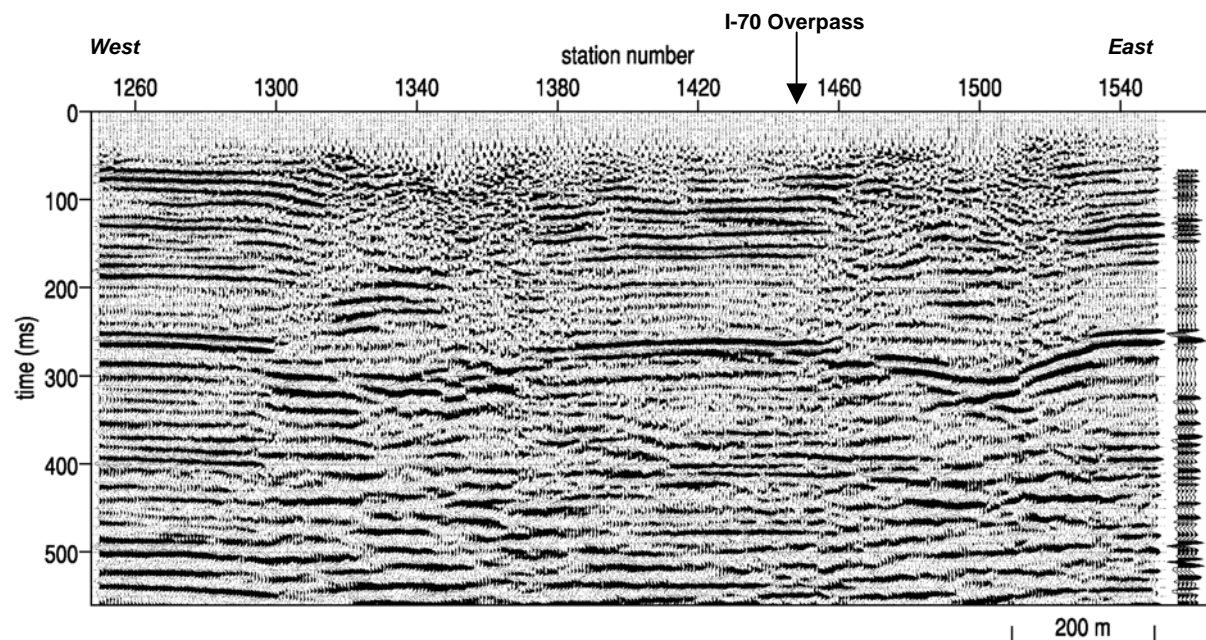


Figure 7-9. Witt sinkhole is located at station 1340 and the Crawford is at 1500. The high-amplitude event at 260 ms is the 300-m-deep Stone Corral anhydrite. Top of salt is at about 340 ms and is approximately 400 m below ground surface. The synthetic at the right verified reflection identification.

Miller, R.D., and K. Millahn, 2006, High-resolution seismic reflection investigations of dissolution sinkholes [ext. abs.]: European Association of Geoscientists and Engineers (EAGE) 68th Conference and Exhibition, Vienna, June 12-15, 4 p. (published on CD).

Seismic reflection images of dissolution-subsidence features that have yet to develop a surface expression provide insights into potential growth mechanisms, development rates, and sinkhole risk. Vertical growth of small depressions or drape in reflectors several hundred meters below ground surface and in proximity to major salt-dissolution sinkholes appears to be remnants of active dissolution at a well unrelated to the known sinkhole location (Figure 7-10). Gradual failure and upward movement of voids characterized by reflector drape are confined to the inverted-cone geometry defining the stress regime or tensional dome. Time-lapse imaging of these yet-to-emerge sinkholes will provide the key insights necessary for improving sinkhole-development models. Ideally, these models would allow prediction of growth rates and eventual areal expressions of sinkholes at the mature stage.

Besides these data, juvenile dissolution-induced collapse structures have only been observed on seismic-reflection data above a salt bed at one other site. The previous image was along the natural dissolution front in central Kansas where early-stage subsidence structures should be relatively common. At the I-70 sinkhole site, the catalyst for the collapse structures has been brine-disposal wells and associated fluids; therefore, the juvenile feature interpreted here is likely related to failed containment in another oil well. This paper provides a very clear view of the conceptual gradual upward movement of the dissolution void with associated bed drape indicative of the void's narrow throat and vertical advancement en route to the ground surface. This is the only seismic image where competent rock layers that appear to have arrested the upward movement of a void can be clearly distinguished from subsidence-altered beds immediately beneath.

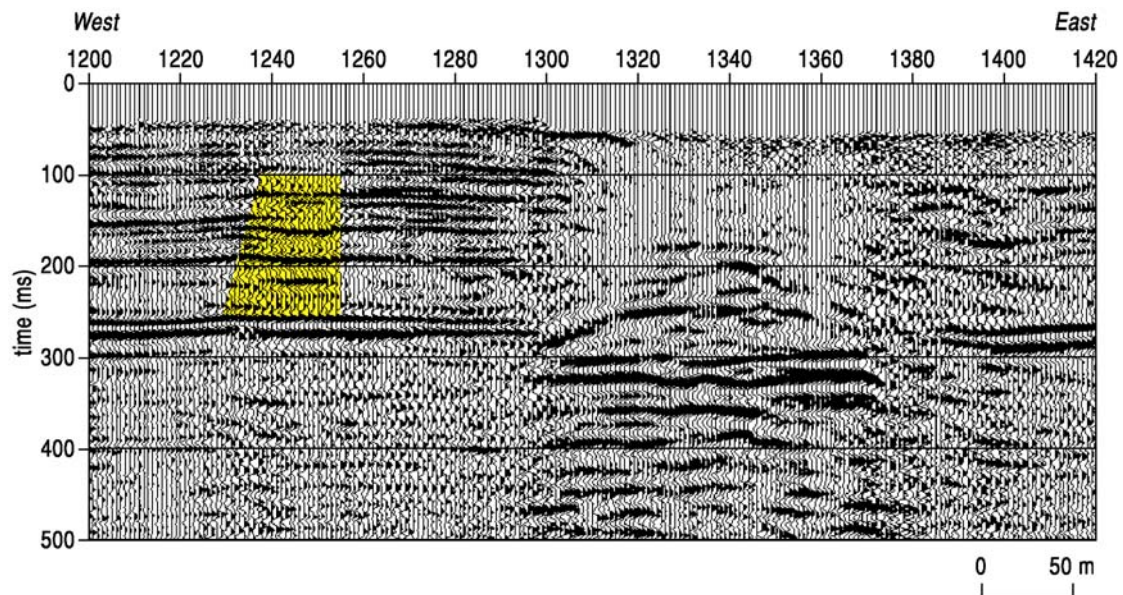


Figure 7-10. Possible collapse feature (highlighted). An existing sinkhole is centered at station 1340.

B. Natural
1. Paleosinkholes
a. Karst

Miller, R.D., J. Xia, and C.B. Park, 2005, Seismic techniques to delineate dissolution features (karst) at a proposed power plant site; in Dwain K. Butler, ed., *Near-Surface Geophysics*: Society of Exploration Geophysicists, Investigations in Geophysics No. 13, p. 663-679.

Shallow seismic techniques produced images that enhanced a grid-drilling program designed to search for limestone-dissolution features that could threaten the precision balance of heavy and delicate equipment planned for Alabama Electric Cooperative's proposed Damascus power plant site. Seismic methods were used to locate and characterize voids, subsurface subsidence, and/or karst features with the potential to affect the stability of the ground surface. High-resolution seismic reflection delineated structures that appear to be either paleosinkholes or paleochannels, currently with no surface expression or inactive at the ground surface, but with clear indications of previous earth subsidence and/or high-energy erosion (Figure 7-11). This two-phase seismic study produced shallow seismic-reflection data capable of detecting dissolution features as small as several meters in diameter at depths from about 15 m to nearly 300 m and shear-wave velocity field images with information about reduced rock strength and risk of subsidence.

These seismic-reflection sections were instrumental in unraveling shallow subsurface layer complexities that inhibited bed-to-bed correlation on borehole data. This paper presents the most complex association of paleodissolution and collapse structures ever deciphered using high-resolution seismic reflection correlated to boring logs. Paleosubsidence features trapped in the shallow geologic record indicate multiple periods of subsidence driven by related but different stress foci. Monumental about this work is the clear indication on seismic-reflection data that natural-dissolution processes—limestone in this case—are active over long periods of time, but change rates, focus, and size dramatically across a single dissolution zone.

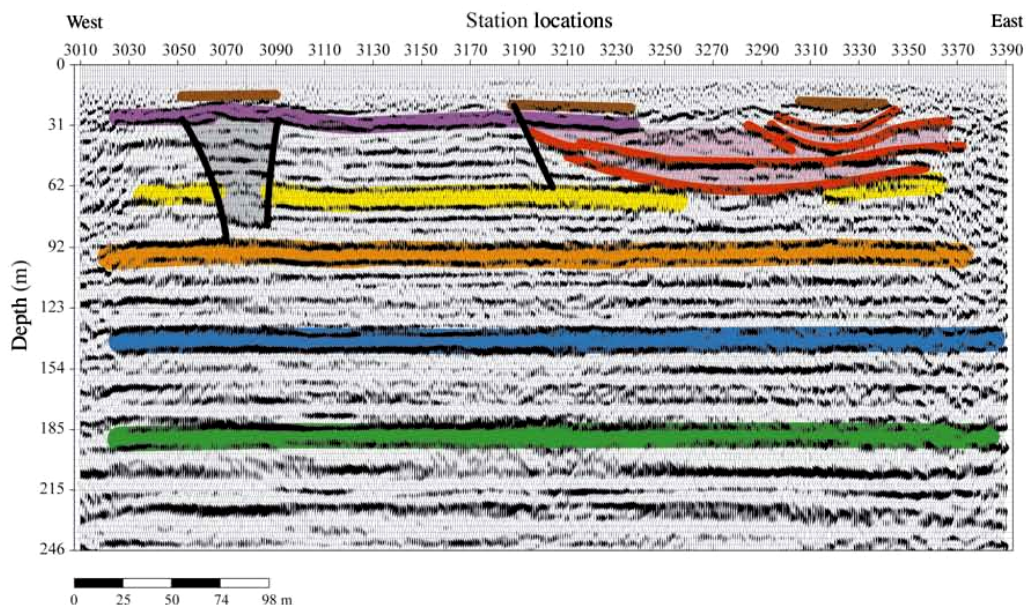


Figure 7-11. CMP stacked section time-to-depth converted using NMO velocity.

b. Evaporite Karst

Miller, R.D., 2006, High-resolution seismic reflection to identify areas with subsidence potential beneath U.S. 50 Highway in eastern Reno County, Kansas: Symposium on the Application of Geophysics to Engineering and Environmental Problems (SAGEEP 2006), Seattle, Washington, April 2-6, Paper 28, 13 p. **Awarded Best of SAGEEP 2006; presented as an invited paper at EAGE NS in Helsinki, Finland, June 2006.**

High-resolution seismic reflections were used to map the upper 200 m along an approximately 22-km stretch of heavily traveled highway in central Kansas, where natural and anthropogenic salt dissolution is known to threaten ground stability. Surface subsidence in this part of Kansas can range from gradual (an inch per year) to catastrophic (tens of feet per second), representing a significant risk to public safety. The high signal-to-noise ratio and resolution of these seismic-reflection data allowed detection, delineation, and evaluation of several abnormalities in the rock-salt layer and overlying Permian sediments. Locations were identified where failure and associated episodes of material collapse were evident due to periodic and localized leaching of the 125-m-deep, 40-m-thick Permian Hutchinson Salt Member. Of particular interest were seismically interpreted features with the potential to migrate to the surface in areas without previous evidence of surface subsidence (Figure 7-12). Anhydrite and shale layers several meters thick within the salt are uniquely distinguishable and appear continuous for distances of several kilometers. High noise levels from the heavy traffic load carried on the highway and maintaining continuous subsurface coverage beneath the Arkansas River presented significant challenges to both the acquisition and processing of these spatially dense data.

With no current surface subsidence apparently active along this profile, the discovery of more than a dozen dissolution-induced collapse structures interpreted to have been active across a wide span of geologic time and with such varying degrees of success reaching the paleo ground surface was unexpected and scientifically significant. Resolution and signal-to-noise ratio of these data are beyond any in the published literature for a target of this type, with such challenging depths and resolution requirements, and where surface conditions were so seismically inhospitable (major highway, 10 m of dry unconsolidated surface and near-surface material, limited to road surface, and undershooting a river). This is the first published image where a subsidence path between a dissolution volume and surface has taken a markedly non-vertical path.

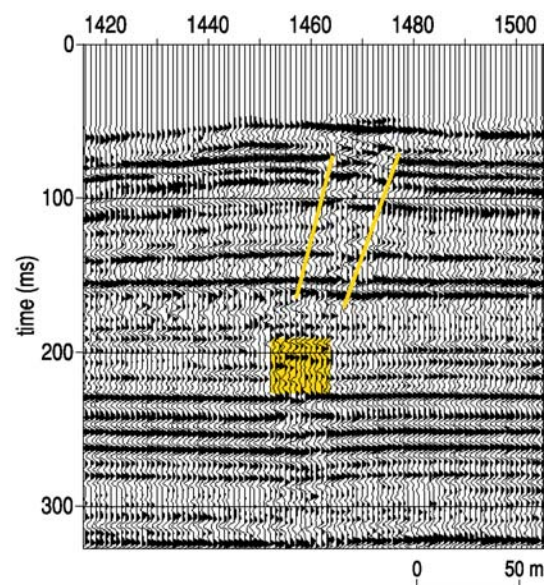


Figure 7-12. Disturbed area within the salt and associated non-vertical chimney where rocks between the salt and bedrock appear altered.

2. Modern
a. Karst

Miller, R.D., J. Ivanov, S. Hartung, and L. Block, 2004, Seismic investigation of a sinkhole on Clearwater Dam: Symposium on the Application of Geophysics to Engineering and Environmental Problems (SAGEEP 2004), Colorado Springs, Colorado, February 22-26, Paper KAR01, p. 1082-1098.

A 3-m-wide and 3-m-deep sinkhole that formed catastrophically approximately 40 m upstream of the crest of Clearwater Dam in southeastern Missouri was the target of a high-resolution seismic-imaging program that included reflection, surface-wave analysis, and crosshole tomography. The primary goals were to determine the general subsidence geometry and integrity of the core and to help ascertain the involvement of bedrock and native alluvium beneath this earthen dam. Reflection data from this survey possess excellent frequency content (dominant >150 Hz) and provide high-resolution images of layers within the pervious shell (Figure 7-13). Based on seismic, construction, drill, and borehole-tracer data, a borehole geophysics program was designed to identify fractures/joints that might provide seepage pathways. Seismic-reflection data detected a large anomalous zone within the bedrock and an associated zone within the pervious fill consistent with borehole-seismic interpretations (Figure 7-14).

These are the only published CMP stacked sections from across the upstream face of a major dam with shot-gather confirmation of the legitimacy of stacked reflections. These data are particularly significant in terms of the methods used and processes followed to compensate for the out-of-the-plane complexity of the collapse feature and dam. The collapse feature was sub-Fresnel zone in diameter and distance from the edge of the dam. With drill confirmation the CMP stacked section breaks new ground for core and sub-core imaging along the upstream slope of an earthen dam.

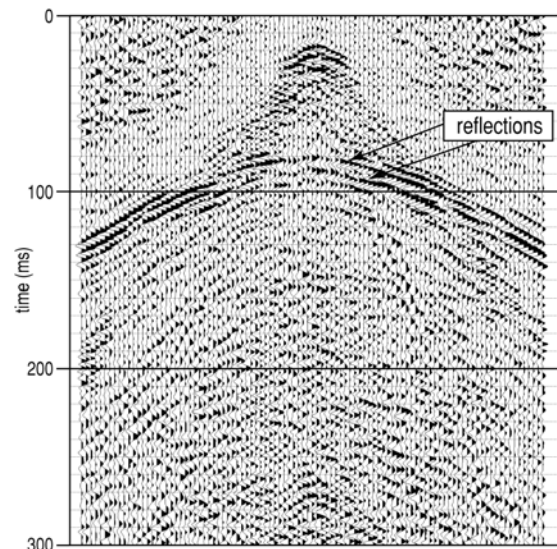


Figure 7-13. Representative shot gather. Reflections are evident on this spectral balanced shot gather. Based on stacking velocities, reflections from 80 msec are approximately 100 ft deep.

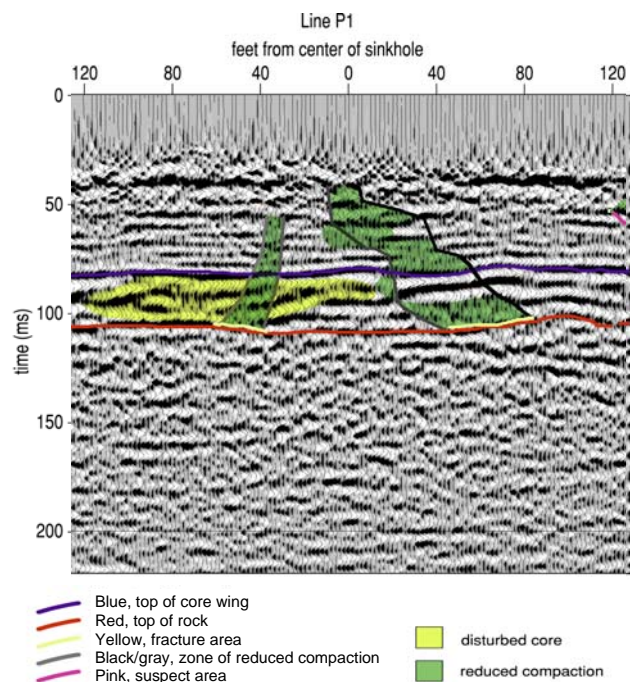


Figure 7-14. Interpreted CMP stack of line P1 showing key layers and abnormalities.

b. Evaporite Karst

Miller, R.D., 2003, High-resolution seismic-reflection investigation of a subsidence feature on U.S. Highway 50 near Hutchinson, Kansas; in K.S. Johnson and J.T. Neal, eds., *Evaporite karst and engineering/environmental problems in the United States*: Oklahoma Geological Survey Circular 109, p. 157-167.

High-resolution seismic reflections were used to map the upper 150 m of the ground surface around and below an actively subsiding sinkhole affecting the stability of a major highway in central Kansas. Primary objectives of this study were to delineate the subsurface expression of this growing salt-dissolution-induced sinkhole and appraise its threat to highway stability and heavy commercial traffic load. The high signal-to-noise ratio and resolution of these seismic reflection data allowed detection, delineation, and evaluation of rock failure and associated multiple episodes of material collapse into voids left after periodic and localized leaching of the 125-m-deep, 40-m-thick Permian Hutchinson Salt Member (Figure 7-15). Mechanisms and gross chronology of structural failures as interpretable from stacked seismic sections suggest initial subsidence and associated bed offset occurred as accumulated stress was rapidly released and constrained to a tensional dome defined by reverse fault planes. As the downward movement (settling, relaxation) of sediments slowed with little or no incremental build-up of stress, gradual subsidence continued, advancing as an ever-expanding bowl that is geometrically defined by normal-fault planes.

Most profound about this manuscript is the high degree of detail and therefore confidence in interpretations. Several episodes of subsidence are evident in several dissolution-related features (current and paleo) imaged on these seismic profiles. This was the first seismically imaged sinkhole where past episodes could be so confidently separated. One of the most fascinating aspects of these data is that the currently developing sinkhole is but a dwarfed expression of a parent subsidence feature with at least three different re-activations during Tertiary and/or Quaternary. This paper provides the first and currently most definitive argument for regional dissolution zones characterized by localized short-lived leaching with rapidly changing areas of active, focused salt harvesting.

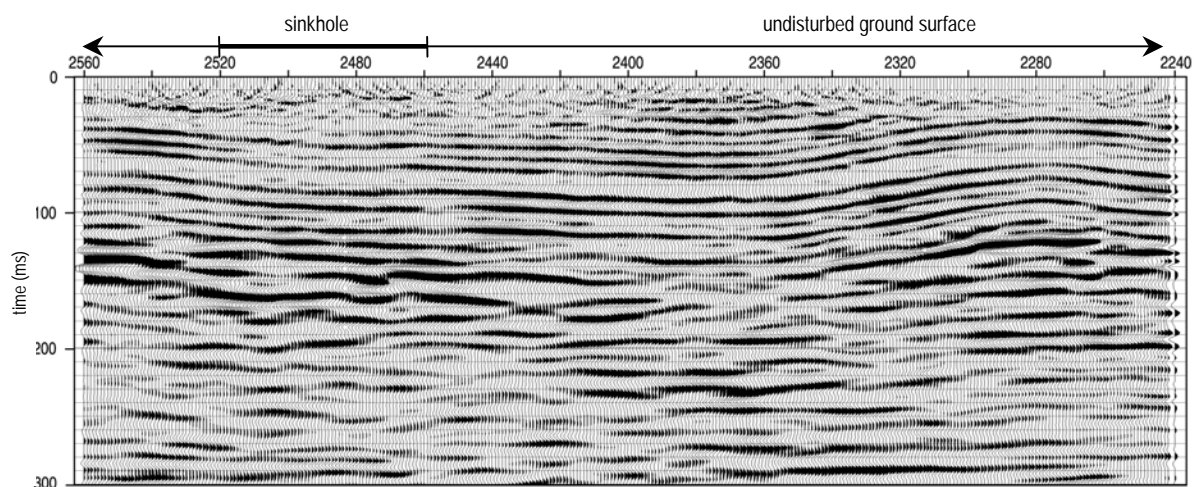


Figure 7-15. CMP stacked section from a portion of line 1. The sinkhole is centered around station 2480 and extends from 2520 to 2460. Migration corrected for much of the optical distortion, but reduced the resolution potential.

Summing Up and To Come

This chapter's overview of the author's more significant contributions to high-resolution seismic investigations of subsidence from dissolution serves as a prelude to and support for the concepts and significant findings developed in later chapters of this study. The common theme of all papers summarized in this chapter has been high-resolution seismic imaging of small (relative to seismic wavelength), anomalous subsurface zones where native materials have been removed and replaced. With the more than 15-year span between the first and last paper in this set, changes in overall data quality are obvious, but for each paper at least one significant contribution to the science and understanding of dissolution-induced subsidence has passed the test of time. The upcoming chapter describes and assimilates the unique and key characteristics of subsidence structures from a concentrated area of central Kansas as they have appeared on seismic-reflection sections.

Attempts to predict subsidence rates and growth characteristics of dissolution-associated sinkholes rely on the overall geology, performance of overburden, and hydrologic properties. All are exceedingly complex and variable at a micro scale, but, based on empirical studies, have definable and somewhat predictable correlations and characteristics at a macro scale. Vertical progression of a gradual subsidence feature can be irregular with strain tending to seek an expansive and at times non-vertical path of least resistance to the surface, both initially and throughout the life of a gradually subsiding sinkhole; this is in contrast to the near-vertical, upward-narrowing tendencies of catastrophic features (Miller et al., 1995; Miller, 2006). Detailed images of the internal structural characteristics of subsidence features have been key to developing an improved and model-consistent understanding of the processes affecting borehole-induced dissolution and subsidence. Interpretations of seismic images correlate extremely well with bed-offset geometries indicating a two-stress regime system and multiple episodes of subsidence as predicted by physical models (Miller et al., 2006).

Isolated dissolution-induced collapse structures associated with natural, active dissolution zones can have their development halted after a very short-lived leaching and subsidence event leaving no surface expression, appearing to then lie dormant though a large span of geologic time (Miller, 2006). Natural dissolution of the Permian Hutchinson Salt Member and subsidence of the overburden in mature areas can involve multiple distinct reactivations of subsidence during the Tertiary and/or Quaternary with isolated active sinkhole-development events represented as a dwarfed expression of the parent subsidence feature (Miller, 2003). This observation supports regional dissolution zones characterized by a collection of localized short-lived leaching foci with rapid changes in rate and location of active salt harvesting. This suggestion can be extended to also include dissolution of limestone bedrock where a single dissolution zone can experience multiple cycles of subsidence and dormancy over long periods of time, each with dramatically different rate, focus, and size of affected area (Miller et al., 2005c).

Key to understanding the subsidence process and the many surface and subsurface observations is unequivocal evidence of reverse- and normal-fault planes within a single subsidence volume, a property necessary to substantiate the two distinct stress regimes observed in physical models (Miller et al., 2005b). Seismic images of juvenile, isolated subsidence features, whose characteristics are obscured on seismic images of mature structures, provide insight into the initial stages of the subsidence process (Miller and Millahn, 2006; Miller, 2003). Interpretations of seismic images of roof failure over mines are

consistent with models of stoping or collapsing beds below an apparently competent roof rock with characteristics of an arched support structure (Miller et al., 1993).

High-resolution data were essential to the findings of all the studies summarized in this chapter. This is especially evident when considering the affected volume and dimensions of salt-dissolution features and the internal geometric and attribute detail necessary to fully appraise the past and then predict the future of dissolution structures. Void detection below the classical one-quarter wavelength axioms is possible based on amplitude variations on high-resolution seismic-reflection wavelets which, from empirical studies is suggested to be less than one-tenth the dominant wavelength and one-eighth the radius of the Fresnel zone (Miller and Steeples, 1991). These detection levels are unprecedented. Seismically imaged bed terminations interpreted to mark the edges of a collapse chimney at around 20 m below ground surface with an approximately equal Fresnel zone radius clearly demonstrates the tool's potential even with extremely small subsidence targets (Miller et al., 1995). As well, this high-resolution tool has a demonstrated ability to detect collapse-breccia zones on the upstream side and tens of meters within an earthen dam at sub-Fresnel dimensions in spite of tremendous out-of-plane interference (Miller et al., 2004). However, a highly irregular bedrock surface resulting in extreme static is beyond what current high-resolution processing approaches could compensate for on the 2-D seismic stacked sections (Miller et al., 2005a).

In the next chapter 12 key high-resolution seismic reflection studies, some summarized in this chapter, will be developed and used as a source of the essential nuggets that will form the framework for overarching observations and suggestions concerning processes and mechanisms showcased in the final two chapters. Components of subsidence studies dealing specifically with catastrophic failure, dissolution and subsidence without surface expression, borehole-induced subsidence, subsidence along the natural dissolution front, and time-lapse investigations of preferential subsidence volumes are just a few of the themes discussed in the next chapter.

References (cited in order presented in this chapter)

- Miller, R.D., J. Xia, R.S. Harding, J.T. Neal, J.W. Fairborn, and D.W. Steeples, 1995, Seismic investigation of a surface collapse feature at Weeks Island Salt Dome, Louisiana: *AAPG Division of Environmental Geosciences Journal*, v. 2, no. 2, p. 104-112.
- Miller, R.D., D.W. Steeples, L. Schulte, and J. Davenport, 1993, Shallow seismic-reflection feasibility study of the salt dissolution well field at North American Salt Company's Hutchinson, Kansas, facility: *Mining Engineering*, October, p. 1291-1296.
- Miller, R.D., and D.W. Steeples, 1991, Detecting voids in a 0.6-m coal seam, 7 m deep, using seismic reflection: *Geoexploration*, Elsevier Science Publishers B.V., Amsterdam, The Netherlands, v. 28, p. 109-119.
- Miller, R.D., J. Ivanov, D.W. Steeples, W.L. Watney, and T.R. Rademacker, 2005a, Unique near-surface seismic-reflection characteristics within an abandoned salt-mine well field, Hutchinson, Kansas [exp. abs.]: Society of Exploration Geophysicists, p. 1041-1044.
- Miller, R.D., D.W. Steeples, and T.V. Weis, 1995, Shallow seismic-reflection study of a salt dissolution subsidence feature in Stafford County, Kansas; in N.L. Anderson and D.E. Hedke, eds., *Geophysical atlas of selected oil and gas fields in Kansas*: Kansas Geological Survey Bulletin 237, p. 71-76.
- Miller, R.D., A. Villella, J. Xia, and D.W. Steeples, 2005b, Seismic investigation of a salt dissolution feature in Kansas; in D.K. Butler, ed., *Near-Surface Geophysics*: Society of Exploration Geophysicists, Investigations in Geophysics No. 13, p. 681-694.
- Miller, R.D., D.W. Steeples, and J.L. Lambrecht, 2006, High-resolution seismic-reflection imaging 25 years of change in I-70 sinkhole, Russell County, Kansas [exp. abs.]: Society of Exploration Geophysicists (published on CD).
- Miller, R.D., and K. Millahn, 2006, High-resolution seismic reflection investigations of dissolution sinkholes [ext. abs.]: European Association of Geoscientists and Engineers (EAGE) 68th Conference and Exhibition, Vienna, Austria, June 12-15, 4 p. (published on CD).
- Miller, R.D., J. Xia, and C.B. Park, 2005c, Seismic techniques to delineate dissolution features (karst) at a proposed power plant site; in D.K. Butler, ed., *Near-Surface Geophysics*: Society of Exploration Geophysicists, Investigations in Geophysics No. 13, p. 663-679.
- Miller, R.D., 2006, High-resolution seismic reflection to identify areas with subsidence potential beneath U.S. 50 Highway in eastern Reno County, Kansas: Symposium on the Application of Geophysics to Engineering and Environmental Problems (SAGEEP 2006), Seattle, Washington, April 2-6, Paper 28, 13 p. Awarded Best of SAGEEP 2006; presented as an invited paper at EAGE NS in Helsinki, Finland, June 2006.
- Miller, R.D., J. Ivanov, S. Hartung, and L. Block, 2004, Seismic investigation of a sinkhole on Clearwater Dam: Symposium on the Application of Geophysics to Engineering and Environmental Problems (SAGEEP 2004), Colorado Springs, Colorado, February 22-26, Paper KAR01, p. 1082-1098.
- Miller, R.D., 2003, High-resolution seismic-reflection investigation of a subsidence feature on U.S. Highway 50 near Hutchinson, Kansas; in K.S. Johnson and J.T. Neal, eds., *Evaporite karst and engineering/environmental problems in the United States*: Oklahoma Geological Survey Circular 109, p. 157-167.

CHAPTER 8

SITE-SPECIFIC SEISMIC INVESTIGATIONS OF SUBSIDENCE FEATURES

Discussions and noteworthy observations have evolved so far through this manuscript from an overview of sinkholes and the generalized mechanics of their formation to highlights in the previous chapter of the author's published work using high-resolution seismic reflection to image anomalous subsurface features. In the past few chapters, in particular, key contributions from a variety of authors have been summarized and represent the starting point for establishing the utility of the seismic-reflection method in defining subsidence-specific characteristics. Those discussions and synthesis are the foundation for this chapter's assimilation of Hutchinson Salt Member-specific seismic studies and development in later chapters of a generalized empirically based concept for dissolution-instigated subsidence. This chapter, in particular, brings together a dozen different high-resolution seismic-reflection studies specifically targeting individual subsidence features with unique characteristics related to salt dissolution.

Many in this chapter's collection of seismic images have never been published, but all possess unique aspects significant to the thesis of this work and therefore justify discussion. Only five of the twelve seismic studies specifically discussed and used in this chapter have been published and included in the previous chapter. This chapter progresses through a sequence of seismically differentiated subsidence features distinguished predominantly by maturity, fluid source, level of current and past activity, and collapse geometries. It is imperative that the empirically based conceptual models developed in later chapters honor the wide range of catalysts, subsidence rates, and geologies of these various subsidence features.

Each of the half-dozen anthropogenic and an equal number of natural subsidence features analyzed in this chapter represent different stages of maturity and relative collapse geometries. Seismic characteristics of these subsidence features will be equated to physical traits and geometries of the rocks and incorporated into conceptual models to allow an improved understanding of likely mechanisms and processes responsible for the imaged structures. Instrumental in this development will be identification of individual attributes consistent with and unique to the collective set. This chapter's compilation of collapse scenarios will establish and retain a common conceptual thread relating all documented and seismically imaged subsidence features discussed in this study. This common thread will be the principal component and justification for the empirically based collapse models to come in later chapters.

Introduction

High-resolution seismic-reflection surveys targeting the Hutchinson Salt Member have collectively provided critical insights and valuable site-specific characteristics of subsidence features throughout Kansas. Significant findings from these various studies are

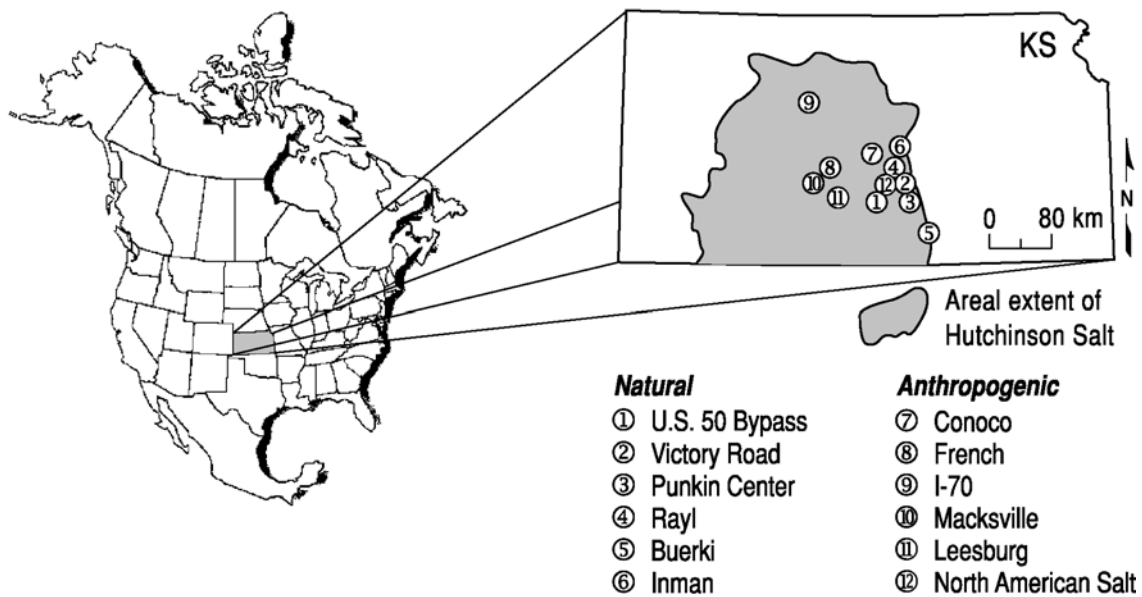


Figure 8-1. Map of Kansas with outline of areal extent of Hutchinson Salt Member. Numerically identified on the map are locations of 12 high-resolution seismic-reflection surveys targeting individual sinkholes. These sites include over 60 km of high-resolution seismic data on 28 different lines, all acquired, processed, and interpreted by or under the direction of the author.

collectively applicable to any region underlain by massive bedded salt layers and in general to any collapse processes in a subsidence-prone setting. A high concentration of seismic profiles has been collected along the natural dissolution front and specific dissolution mine fields where subsidence has threatened transportation and/or population centers. This concentrated area of study in conjunction with several sinkhole investigations scattered around the central part of the state of Kansas allow empirical development of mechanisms and settings controlling and influencing the subsidence process (Figure 8-1).

A range of sinkhole types and locations has been seismically investigated en route to addressing site-specific questions generally related to prediction of future growth rates and affected surface. In part, as a consequence of these focused studies, the high-resolution seismic-reflection method has been refined and, therefore, evolved over the last 15 years to more effectively and accurately image extreme structural anomalies. Sinkholes included in these various studies have formed as a result of salt dissolution both in proximity to well bores (dissolution mining, brine disposal, oil wells, seismic shot holes, etc.) and in areas known to experience natural dissolution with no apparent anthropogenic influences. The eastern boundary of the salt is a natural leaching environment where sinkholes have been forming for millions of years and is significantly less predictable and potentially controllable than subsidence resulting from anthropogenic fluid sources.

Each seismic-reflection study targeting the Hutchinson Salt bed and shallower layers where subsidence was a possibility or has been observed produced seismic images of legacy or active dissolution features generally possessing consistent characteristics and geometries. Twelve seismic investigations originally and individually designed to search for clues amenable to predicting ground stability and associated future sinkhole(s) collectively provide a unique opportunity for joint interpretations in support of a more regional subsidence study with overtones significant to collapse structures worldwide. When considering the limited

number of seismic-reflection surveys specifically designed to delineate collapse structures associated with salt dissolution, it is not surprising that unique scientific contributions can be extracted for every seismic image in this set of 12. Upcoming discussions segregate these 12 subsidence features into anthropogenic and natural (Table 8-1), with the unique characteristics of each described and then assimilated into a collected set of findings for inclusion in an empirical subsidence model.

Seismic Investigations of Natural Dissolution Subsidence

Several natural dissolution features were discovered as a result of a 10-km seismic-reflection investigation along a proposed highway expansion approximately 20 km west of the Hutchinson Salt Member's natural dissolution front (Table 8-1 ④). Many of these dissolution features possess characteristics indicative of different stages of development and duration and number of solution episodes. One paleosubsidence feature imaged during this survey that is of particular interest possesses a very well defined subsidence geometry characteristic of both rapid initial compressional subsidence and the commonly observed broad tensional bowl-shaped feature (Figure 8-2). This distinctive 300-m-wide paleo-subsidence feature has no current surface expression and was totally unexpected this far from the natural dissolution front.

Breaking down this seismic image of a paleosinkhole beyond its two principal subsidence components reveals a variety of unique attributes. This is one of the few known natural dissolution features this far (15 km) from the dissolution front that is not related to regional faulting (Walters, 1980). An increased reflection amplitude along the salt/shale caprock interface (~160 ms) and highly disturbed area in the salt at the apex (trough) (~CMP 1870) of the subsurface synform are both characteristics indicative of subsidence due to dissolution near the salt/caprock contact and collapse breccia within the entire salt volume near the center of the subsidence, both diagnostic of an ancient dissolution feature. Because natural dissolution has a greater tendency to occur along the impermeable and insoluble caprock or at the base of interbedded layers within the salt, the relatively vertical volumetric representation of dissolution at the center of the subsidence feature seems unusual (Figure 8-2). Diffractions within the altered salt volume are consistent and generally

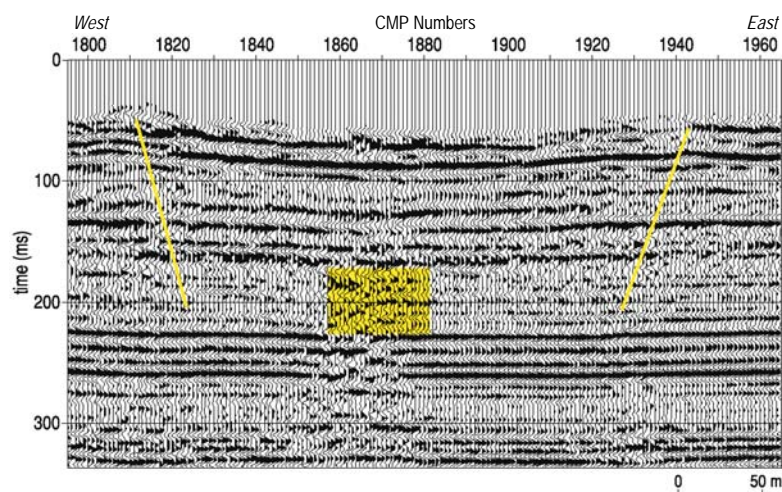


Figure 8-2. A portion of this stacked section highlights the subsidence-feature geometry. The box includes what is interpreted as a dissolution volume, seismic unique with diffractions from bed terminations and low-frequency, more chaotic events.

Table 8-1. Unique and Specific Characteristics of Each Study

NATURAL

Site Name	Parameters		Goal	Scientific Contribution
	Acquisition	Processing		
① U.S. 50 Bypass	19 bit A/D 240 channels 2.5 m receiver 5 m source Vibrator	Spectral balance Gross velocity Severely reduced fold (12-14)	No sinkholes, but search for anomalies above and within salt that might represent collapse risks for proposed highway.	Non-vertical subsidence growth, single episode collapse with central chimney and oversized bowl in near surface (Miller, 2003).
② Victory Road	19 bit A/D 240 channels 2.5 m receiver 5 m source Vibrator	Spectral balance Severe mute NMO velocity Sub-spread static $\frac{1}{4} \lambda$	Recent sinkhole affecting major highway, predict growth and rate and safety for filling.	Dual stress regimes obvious, but multiple reactivations make unraveling complete history impossible. Sinkhole part of larger system (Miller, 2006).
③ Punkin Center	16 bit A/D 48 channels 2.5 m receiver 2.5 m source 8-gauge auger gun	10 CMP velocity Iterative $\frac{1}{4} \lambda$ statics Time-variable bandpass Heavy mute	Determine relationship between oil field and sinkhole in area with multiple natural sinkholes.	Paleosinkholes with steep-sided chimney within an area characterized by dissolution-induced undulating overburden.
④ Rayl	19 bit A/D 240 channels 2.5 m receiver 5 m source Vibrator	NMO velocity Static iteration Severe mute Spectral balance Subspread in sink	Predict sinkhole growth and establish if oil well in portion of sinkhole responsible for dissolution casing subsidence.	Multiple previous episodes of dissolution and paleosubsidence with well asymmetric to dissolution. Complex interfingering.
⑤ Buerki	12 bit A/D 24 channels 2.5 m receiver 2.5 m source 50-cal.	Low-cut filter Detailed noise removal Low-fold overburden	Determine if sinkhole was natural or anthropogenic.	Irregular subsidence pattern proposed to be inconsistent with point-source leaching.
⑥ Inman	19 bit A/D 240 channels 2.5 m receiver 5 m source Vibrator	NMO velocity every CMP Severe mute Spectral balance No vertical stack	No confirmed sinkhole where highway crossing dissolution front. Investigate and delineate any dissolution structures.	Bridging interpreted based on amplitude characteristics, abrupt nature of front not evident at surface.

ANTHROPOGENIC

Site Name	Parameters		Goal	Scientific Contribution
	Acquisition	Processing		
⑦ Conoco	12 bit A/D 24 channels 16 m receiver 16 m source MiniSosie	NMO every 10 CMP Minimum fold processing No wavelet Iterative statics Large CORR window	Predict growth; specifically, potential effect on road and farm house.	Bowl-shaped depression above salt interpreted normal at time, later clearly reverse and normal faults (Miller et al., 1985).
⑧ French	19 bit A/D 96 and 120 channels 5 m receiver 5 m source Vibrator	Velocity function highly detailed Static w/multiple replacement velocities Multiple statics iterations	Evaluate failure potential of ground inside sinkhole for plugging operations. Predict growth rate and extent of sinkhole.	First dual-stress field sinkhole with confidently interpretable reverse and normal faults that match physical models (Miller et al., 1997).
⑨ I-70	19 bit A/D 240 channels 5 m receiver 16 m source Vibrator	Spatial variable CMP High-density velocity Spatial variable mute–compressed CMP spread	Evaluate dissolution change and estimate growth potential and rapid subsidence risk.	Majority reverse with minor normal matching physical models for active dissolution beyond surface collapse (Miller et al., 2006).
⑩ Macksville	19 bit A/D 240 channels 5 m receiver 10 m source Vibrator	Detailed NMO velocity Reduced trace count to option Heavy mute	Establish growth characteristics of sinkhole and unique properties of catastrophic initial failure that is currently gradual.	Active subsidence areas associated with dissolution move laterally, generally in a reverse fault geometry at the active face (Lambrech and Miller, 2006).
⑪ Leesburg	19 bit A/D 240 channels 5 m receiver 16 m source Vibrator	Migration filter Time-variable filter Spectral balance High kill to balance trace window	Predict future surface growth and develop concept related to apparent multi-well involvement.	Most geometrically distorted feature with extensive subsurface expression relative to surface—first multi-source anthropogenic dissolution features.
⑫ North American Salt	12 bit A/D 24 channels 2.5 m receiver 2.5 m source Downhole 50-cal.	Tight bandpass Severe muting Minimal fold Detailed NMO High stretch mute	Determine potential and extent of future subsidence, especially beneath road and railroad.	Delineated collapse roof halted within dome, roof material tensional under dome, dome undisturbed (Miller et al, 1993).

synonymous with irregular features or layer discontinuities such as voids, faults, or bed terminations.

The apparent vertical elongation of this paleodissolution feature within the salt interval is unusual and likely due to the presence of localized fractures oblique to the orientation of the seismic line. There is no seismic evidence to support faulting as a possible conduit for fluid migration at this location. Any discontinuity in the subsalt layer could have acted as a thoroughfare for ground water to access the salt interval. Considering the increase in fluid density with increased salinity, one possible explanation for this localized leached volume is the migration of unsaturated fluids vertically from the base of the salt interval through the salt and expansion along the salt and overlying shale contact (morning-glory structure). With the interbedded nature of the salt, individual solution voids must have grown to the point they were large enough at the base of each interbedded shale and anhydrite layer to precipitate failure, thereby creating the pathway necessary to accommodate vertical fluid migration and eventual development of this disturbed salt volume. Alternately, because these interbedded layers are known not to be laterally continuous over a distance more than a few kilometers, this volume could be consistent with the coincident termination of several interbedded units.

It appears from the seismic image that once fluid contacted the massive insoluble shale caprock, leaching was constrained and guided along this contact. Vertical migration was halted at the base of the shale caprock and the dissolution front began spreading radially from the disturbed salt volume at the center of the present synclinal feature. Gradual and incremental subsidence continued until the leaching process ended, leaving the collapse structure as interpreted on the seismic section extending from CMPs 1820 to 1940 (~300 m). At this point, the hydrodynamics of this feature apparently changed and the dissolution and subsidence process appears to have at least temporarily ended.

Seismic characteristics of the draping beds and intersalt disturbances are key to and help build the foundation for suggestions concerning the dissolution and collapse history of this feature. Reflections immediately below the salt interval possess a distinctive velocity or static pull-down relative to undisturbed rock on either side. This pull-down is due to the reduced overburden velocity within the subsidence-affected area. Significant to the validity of this interpretation are the very well shaped and relatively undisturbed diffraction events originating from within the salt and predominantly near the apex of the subsidence synform. Also noteworthy with respect to the top of salt reflection is the decrease in dominant frequency. Wavelet changes associated with the top of the salt within this dissolution feature are consistent with theoretical developments for void/rubble replacement of competent rock beneath a caprock.

An alternative interpretation of fluid migration critical to development of this dissolution feature puts the inlet or source within the overburden. If fluid entered from above the salt, dissolution would have also preferentially occurred near the top, expanding along the insoluble caprock, consistent with the location of the fluid outlet. Considering the predominantly vertical dissolution volume interpreted on seismic data from within the salt, fluid exiting through the salt and into the substrata would have been heavily laden with salt, likely fully saturated, thereby leaching within the salt would have been minimal. Saturated fluid moving through the salt would not enlarge the dissolution volume. Critical to this fluid movement scenario is the clear passage through the salt. Because this feature is natural and

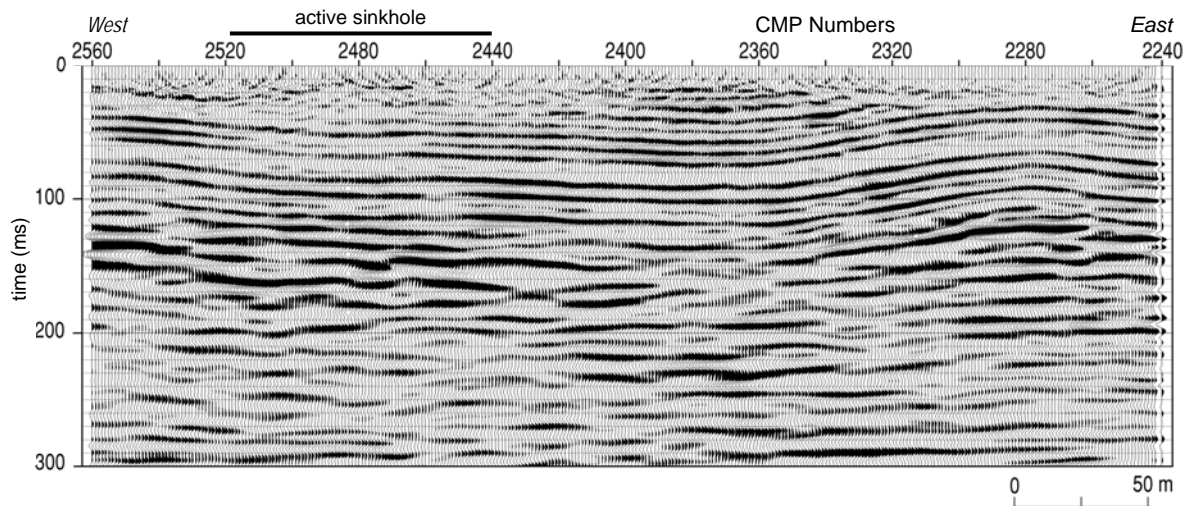


Figure 8-3. Migrated nominal 60-fold CMP stacked section crossing a 100-m-wide surface depression centered on station 2480. The Hutchinson Salt Member interval has been correlated with nearby borehole logs and is between 120 ms and 160 ms two-way travel time. With no surface expression except the 100-m-wide sinkhole at 2480, it is reasonable to interpret a paleosubsidence feature that is at least 400 m wide.

likely structurally controlled, the three-dimensional aspects of the fluid conduit must also be considered, making fractures a potential controlling influence.

This single-episode subsidence feature is interpreted to be an example of the initial stage in the maturation of a natural dissolution-induced subsidence feature. Multiple-episode subsidence structures that have been seismically imaged possess significantly more complex reflection geometries and are influenced by numerous reactivations of leaching, generally followed by periods of dormancy and/or continued leaching through newly established localized fluid pathways. These multi-episodal superstructures can be kilometers in diameter and active throughout an extensive period of leaching with a multitude of distinct voids in various stages of migration toward the ground surface.

A study designed to investigate the subsurface beneath a 100-m-wide sinkhole near the natural dissolution front uncovered one of these massive subsidence features without surface expression and acting as the parent structure to the small active sinkhole targeted by this particular investigation (Table 8-1 ②). High signal-to-noise ratio and high-resolution seismic-reflection data allowed detection, delineation, and evaluation of rock failure associated with multiple episodes of material collapse after periodic and localized natural leaching of the 125-m-deep, 40-m-thick Permian Hutchinson Salt Member (Figure 8-3). Mechanisms and gross chronology of structural failures as interpretable from stacked seismic sections were principally influenced by pre-Pliocene-Pleistocene to current dissolution. Dating the structural progression of this entire feature is in part based on the relatively flat appearance of shallow reflections above highly altered rock; this observation implies subsurface stability since deposition of the shallowest Quaternary material.

Collapse of the consolidated overburden sediments (predominantly shale) responsible for the currently active sinkhole appears to have been strongly influenced by the maximum stress lines associated with the tensional dome model. As leaching continued, the radius of failure progressively increased with subsidence predominantly controlled or at least defined by concentric sets of reverse fault geometries interpreted from offset in overburden rock layers (Figure 8-4). This series of sub-parallel reverse-fault planes geometrically matches the

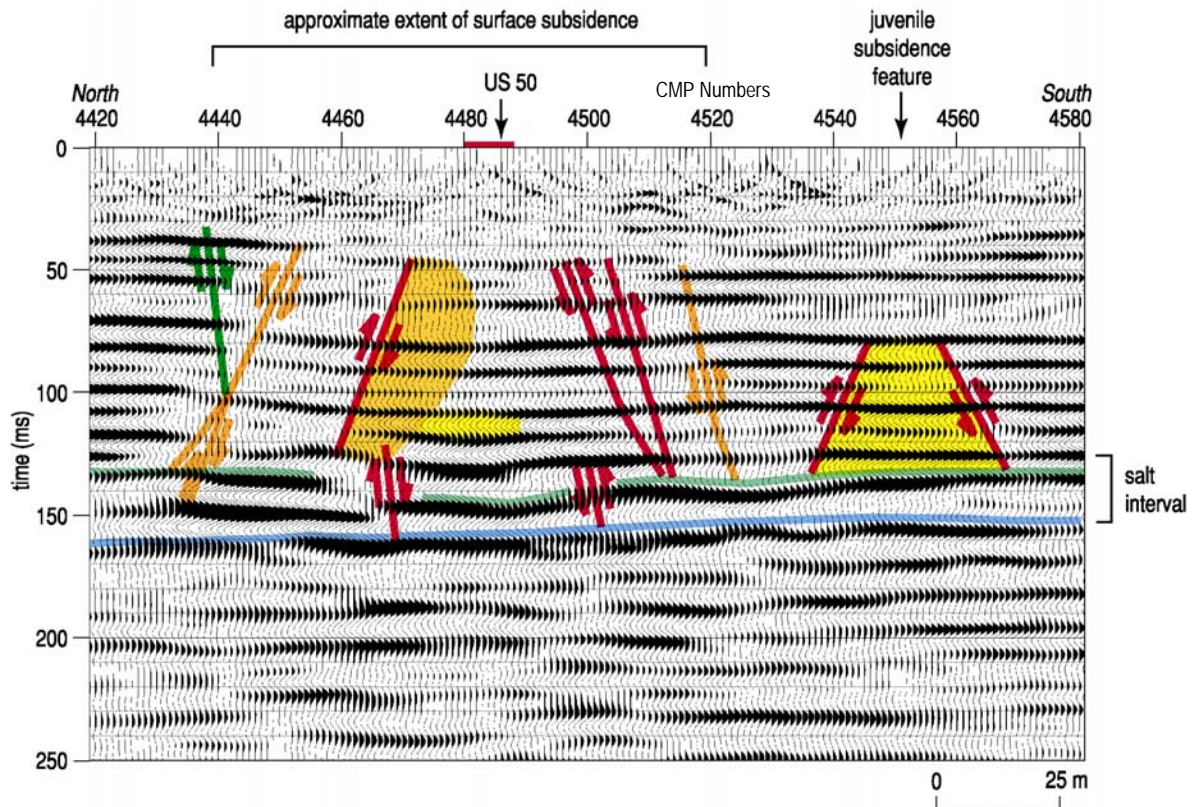


Figure 8-4. Interpreted CMP stacked section with disturbed salt interval at about 120 ms to 160 ms two-way traveltime. Several possible interpretations would be valid for this migrated section. Of particular interest is the small juvenile subsidence feature interpreted beneath station 4550 about 70 ms deep. Red bar near 4480 is location of highway crossing line at nearly a right angle.

lines of stress that would define the initial failure tensional dome. At least two distinct episodes of collapse along groupings of reverse faults define this active subsidence structure, with the beginnings of a third and likely final collapse phase indicated by normal faults at the extreme outside of this feature. Enlargement of the collapsed overburden volume appears to have progressed in this fashion with several periods of dissolution at each of several smaller structures across this massive large-scale structure.

Once the salt void growth ended and so the undercutting of competent overburden along the perimeter of the dissolution volume also ended, overhanging layers or ledges of rock (hanging wall) were left under significant extensional stress. These ledges extend around the perimeter of the cone/chimney structure supporting an upward-thickening, relatively undisturbed volume of rock through the upper Permian section. Relative movement of rock layers around the outer portion of the subsidence feature is interpreted to have been influenced by faults with normal orientations or geometries. This suggests the stress environment in and around this subsidence feature took on more extensional characteristics at this point. Hence, after dissolution concluded, downward movement (settling, relaxation) of sediments around the perimeter of the initial subsidence volume appears to have been driven by gravity and controlled/influenced by weakened rock layers above and on the perimeter of the dissolution zone.

With the termination of salt-void growth, little or no incremental accumulation of stress occurred and gradual subsidence continued advancing radially as an ever-expanding

bowl (synform), geometrically defined by normal fault planes. Based on the reflection geometries, expansion beyond the perimeter defined by the edges of the dissolved salt and associated reverse-fault planes has resulted from extensional stress, gravity slumping, and differential compaction of the solution void that was at least partially filled with collapse breccia during initial failure. Normal fault geometries define a bowl-shaped structure near the perimeter of the collapse feature while a series of upward-narrowing cones defined by the reverse-fault planes are evident near the center of the subsidence feature. This sequence of events both explains and is consistent with the rock geometries defined by these seismic data and known geology.

Captured on these seismic data is what has been interpreted as a juvenile subsidence feature (Figure 8-4). Beneath CMP station 4550 there appears to be a subsidence feature with subtle drape in the 80-ms reflection and a triangular shape (on this 2-D section) defined by relative bed offsets consistent with reverse faults. This fault geometry was previously described as characteristic of initial roof failure of a void with reverse fault planes equated to lines of equivalent stress above an unsupported span of roof rock. One of the keys to this postulated juvenile subsidence feature is the slight increase in amplitude of and time delay in the shallowest salt reflection, characteristics interpreted to be consistent with dissolution along an acoustic-impedance contrast (reflector). It is not clear whether this subsidence is active or dormant, but it does seem to be a likely location for future subsidence along this profile.

As seen on the previous data set from U.S. 50 Highway, this profile also inadvertently crossed a paleosubsidence feature (Figure 8-5). This seismic profile provides dramatic evidence supporting the seismically inferred failure processes and resulting bed geometries. At the eastern extreme of this buried collapse structure is an abrupt and intact reverse fault interpreted above the salt interval and bounding the eastern edge of the synform. On the western extreme of the synform, the slopes are gentle and characterized by a block defined by

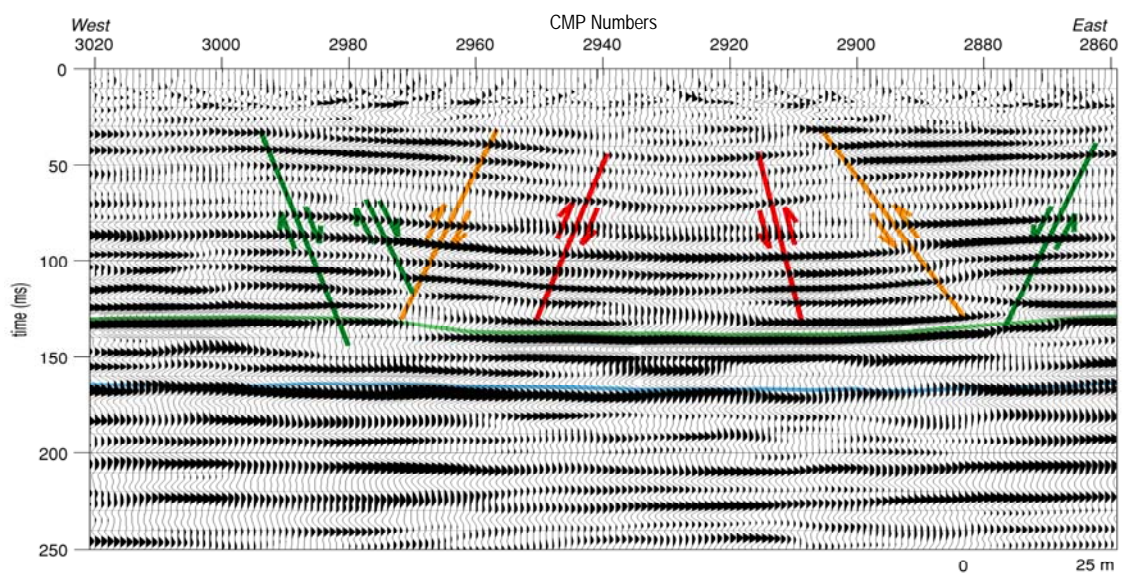


Figure 8-5. Paleosubsidence feature with no current surface expression. Dissolution of the upper portion of the salt is evident, with a high-amplitude reflection interpreted to be the top of salt. Failure likely occurred from middle of the feature out with the two pairs of reverse faults defining initial failure that occurred while the dissolution process was active, with normal-oriented offset beds in response to compaction into the dissolved and disturbed volume.

normal faults. This asymmetry leads to the suggestion that the west side formed during initial subsidence and then overburden displacement halted, whereas the east side continued after initial subsidence to experience extensional stress and associated strain over a much longer time period.

Current sinkhole development at this site is related to the reactivation of natural leaching activities that originally produced the seismically imaged, 530-m-wide subsidence superstructure interpreted to have been active during the Tertiary and/or Quaternary. Alternately, recent surface subsidence could have resulted from localized failure of upper Permian rock layers previously bridging voids or settling of an undercompacted zone that formed while this paleosubsidence event was last active between the Tertiary and Quaternary.

Multiple episodes of natural dissolution and resulting subsidence can be localized, as in the previous two cases, or very expansive extending substantial distances along the regional natural dissolution front. Seismic investigation of a sinkhole located along the natural dissolution front and coincident with an active oil field uncovered an extensive history of dissolution and associated subsidence. A portion of these seismic data almost 1 km west of the target sinkhole captured an extensive area of natural leaching that left a Permian rock sequence between the salt and bedrock surface that, while very irregular and distorted, retained sufficient trace-to-trace coherency to correlate reflections across the profile (Figure 8-6). Several chimney-collapse structures appear superimposed on a subsidence terrain characterized by short-wavelength undulations in overburden indicative of karst. These uniquely contrasting features and formation processes were clearly active at different times, but no signs are evident to suggest any current activity. In general, the ground surface in this area is topographically featureless and consistent with a broad alluvial-valley depositional environment.

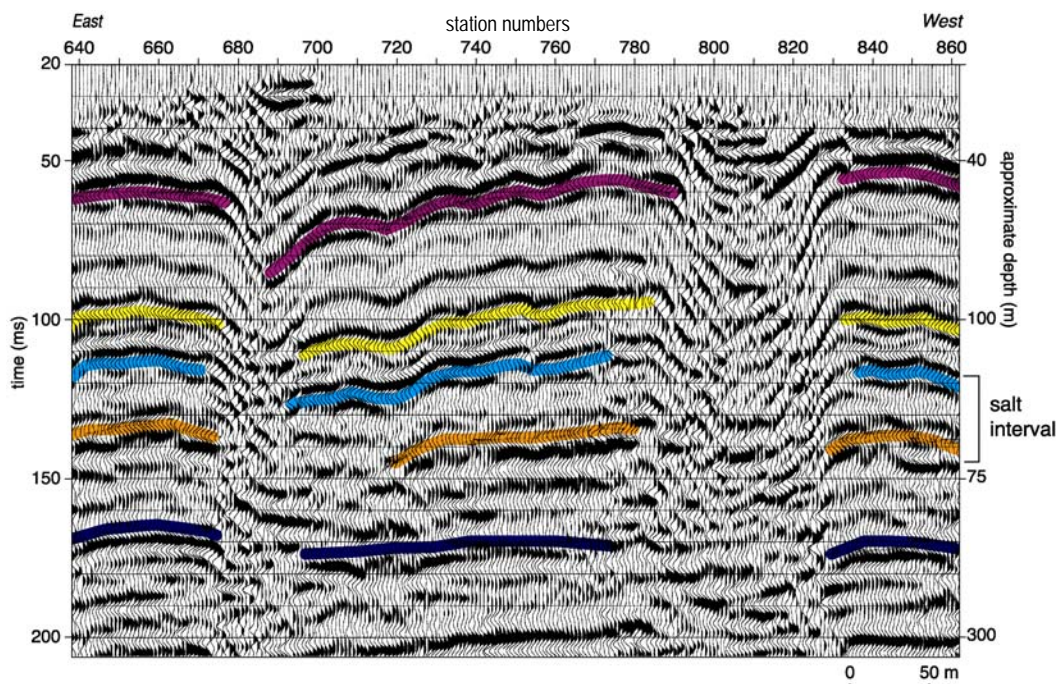


Figure 8-6. Complex paleosubsidence events spanning a distance of about 300 m located near the town of Punkin Center, Kansas. Undulating upper Permian reflectors are representative of a very gradual subsidence process involving repetitive cycles of dissolution and subsidence.

These distinctive and abrupt paleosinkholes are within the upper Permian portion of the section (above the salt interval). Subsidence geometries of these chimney-type failure structures appear to narrow very subtly in diameter between the salt and ground surface. Chimney-style features of this kind are routinely observed above salt-dissolution mines and borehole-induced dissolution failures where collapse was either rapid or dissolution hydrology was limited to a point source/exit. This seismic section captured the only known example of a highly disturbed and predominantly vertical failure feature that can be undeniably classified as a paleosubsidence event. Also of significance on this CMP stacked seismic section is the short wavelength, laterally undulating reflections and dipping beds that appear representative of a completely different dissolution and/or failure mechanism relative to the distinctive steep-sided chimney structures (centered on CMPs 690 and 810). For both the chimney and undulating drape-style failure features, no surface expression exists and the shallowest interpreted reflection events (Pliocene-Pleistocene Equus beds) appear flat with no expression of these underlying subsidence features, a situation indicative of subsidence dormancy since near the beginning of the Quaternary.

Clearly the overwhelming difference between this site and most others west of the dissolution front is the lateral extent of the highly distorted, short-wavelength undulation in the salt overburden. The presence of both styles of subsidence is suggestive of a changing hydrology, change in dominant leaching direction (vertical to form chimney and horizontal to form undulating reflections), and/or presence of zones within the salt susceptible to rapid vertical dissolution. Considering fluid densities and availability of fresher waters, it is reasonable to suggest natural leaching is predominantly active near the top of the salt. Normally interbedded shale and anhydrite layers act as permeability barriers where they tend to channel fluids more horizontally within the salt. These very vertical chimney features likely correlate to more solution-susceptible zones that have allowed enhanced fluid access and vertical movement in the otherwise locally continuous interbedded shale and anhydrite layers. No strong evidence exists on the seismic data to suggest tectonic forces have played a role here.

These steep-sided solution zones beneath stations 810 and 680 appear consistent with areas of depleted or nearly depleted salt volumes. Leaching likely originated at these locations along fractures prior to the predominantly horizontal dissolution that resulted in the more laterally consistent low-amplitude, short-wavelength undulations in the overburden. The horizontal leaching as evident from overburden subsidence has all the characteristics of a gradual process. Areas of greater solutioning are likely coincident with the troughs in the overburden reflection. Dissolution likely began at 810 prior to starting at 680, as evidenced by the overall gradual overburden-bed dip from west to east.

Based on reflection geometries, an alternate chronology is possible to explain these dramatic bed geometries. Reflections in very close proximity to the chimney features appear to correlate reasonably well across the chimney features. This observation could suggest the chimney-collapse structures occurred after or during the slower more laterally uniform dissolution and subsidence process. Alternatively, these short-wavelength bed undulations could be the result of different processes: dissolution, glide creep, and subsidence after the chimney features formed. This natural setting could provide the fluid and overburden pressure differential necessary to support either mechanism.

Multiple episodes of natural dissolution and subsidence evident on the Punkin Center (Figure 8-6) and the Victory Road seismic profiles (Figure 8-3) can be separated into different subsidence episodes based on unique characteristics and geometries, and therefore it is reasonable to speculate as to rates and affected volumes associated with each subsidence event. Seismic-reflection sections from the Rayl sinkhole appear to tell a tale of an area influenced by several episodes of paleodissolution, each characterized by distinct and seemingly disconnected subsidence locations as imaged throughout the overburden as distorted beds. These Rayl sinkhole data are suggestive of a very complex hydrologic past with multiple collapse features appearing to be the result of unrelated leaching activity spanning a generally large feature.

The Rayl sinkhole formed within several kilometers of the subcrop of the natural salt-dissolution front, gradually and inoffensively growing until it began affecting a county road, house, and an abandoned oil-field disposal well (Table 8-1 ④). Post-subsidence well integrity tests showed the casing of the disposal well was intact with no evidence to suggest it had lost containment or was responsible for this subsidence event. Seismic data clearly captured remnants of a complex subsidence history (Figure 8-7).

Surface subsidence tracked with ground-elevation surveys correlates the surface expression and its growth with the eastern edge of a paleodissolution feature captured on seismic data. The seismically imaged salt interval appears disturbed further east than evident in distorted reflections from the overburden layers or ground surveys. Time delays and elevated reflection amplitudes from the top of salt along the eastern edge of this feature are consistent with the seismic characteristics of active dissolution in the salt. Rocks directly above the eastern dissolution front and immediately outside the volume defined by the

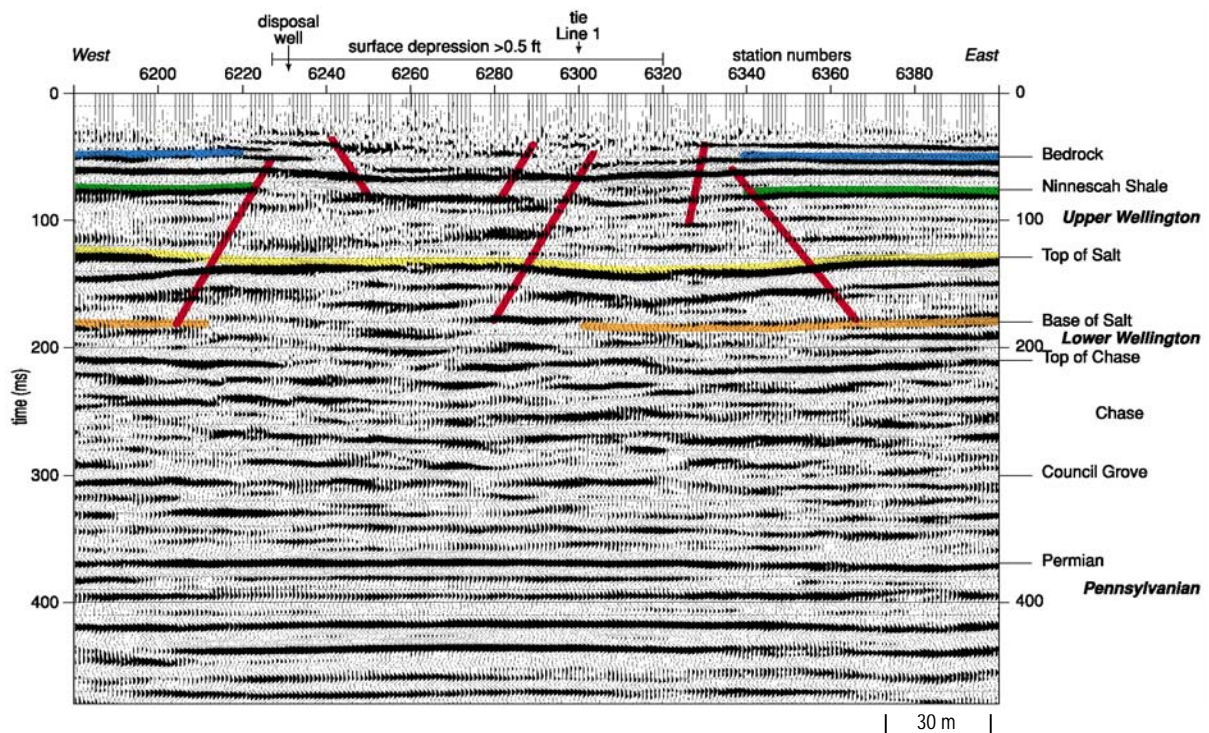


Figure 8-7. CMP stacked section with interpretation of reactivated subsidence feature beneath and immediately west of a house and major north/south county road. Current subsidence along eastern edge of dissolution zone is defined by reverse faults and is likely indicative of active leaching of salt beneath this section of line.

reverse-fault planes (tensional dome) are likely under stress due to the apparent bridging of rock layers immediately above the salt interval. A large portion of the overburden rock imaged by the seismic section appears perched upon unsupported or poorly supported rock layers forming what geometrically resembles a hanging wall. Stress within this hangwall will eventually manifest itself as strain after failure and formation of a normal fault-defined bowl-shaped subsurface structure.

Disturbed layers between the top of the salt and the ground surface and the undulating reflecting surfaces within the salt itself on the west half of the seismic image are indicative of past dissolution and subsidence or creep events. Based on the subsurface history as interpreted from the seismic data, this area has undergone several episodes of natural dissolution of the salt and subsequent overburden subsidence. This extensive and complex subsidence history is not visible at the ground surface and therefore likely occurred prior to deposition of existing Quaternary surface cover. The well bore is located in the extreme western part of the affected subsurface and appears to be unrelated to current subsidence.

As will be shown later in this chapter, most dissolution sinkholes resulting from casing failure occur as a single, continuous dissolution and subsidence event that is centered on the failed casing. Based on the competency of the overburden and seismic-wavelet characteristics (velocity delays and elevated amplitudes at contact between dissolved salt volume and caprock or interbedded rock layers), dissolution responsible for the current sinkhole at the Rayl site is or was last active within a relatively small area along the eastern edge of what appears to be a large reactivated paleosubsidence feature.

Subsidence histories of active dissolution volumes are difficult to decipher when most or all of the salt have been leached away during multiple reactivations and hydrologic changes. As evident from the sequence of subsidence features presented so far in this chapter, with continued reactivation and depletion of salt stock seismically imaged subsidence structures begin to lose their individual character and blend into a mass of distorted layers with only the personality of the whole remaining. A gradually subsiding sinkhole located near the natural dissolution front began affecting a house and barn and was accused of being the offspring of dissolution induced by an early twentieth-century seismic exploration shot hole (Table 8-1 ⑤). Shot holes of this type and era and in this area were deep (into the 50-m-deep salt) to optimize frequency and energy. They were rarely plugged, thereby providing a conduit for freshwater from near-surface aquifers to access the salt.

With the exception of a drop in signal-to-noise ratio near the middle of the section (location of the sinkhole), reflections from the upper 150 ms are coherent with geometries consistent with subsidence and bed distortion as observed at other sinkholes in close proximity and on the east side (minimal salt side) of the natural dissolution front (Figure 8-8). Reflections from above the salt have geometries indicative of a relatively uniform subsidence history with predominantly brittle deformation. The general appearance and geometries of reflections above the salt are consistent with those observed on seismic data from the Punkin Center area (Figure 8-6) and Victory Road (Figure 8-4), more than 100 km north and equally close to the dissolution front.

These data have been flattened on the subsalt, Chase Group limestone, to compensate for the extreme lateral variability in near-surface velocities that result from the irregular dissolution of the salt and associated overburden collapse. Based on the time difference between the Chase at about 130 ms and reflections within the Ninnescah Shale, located

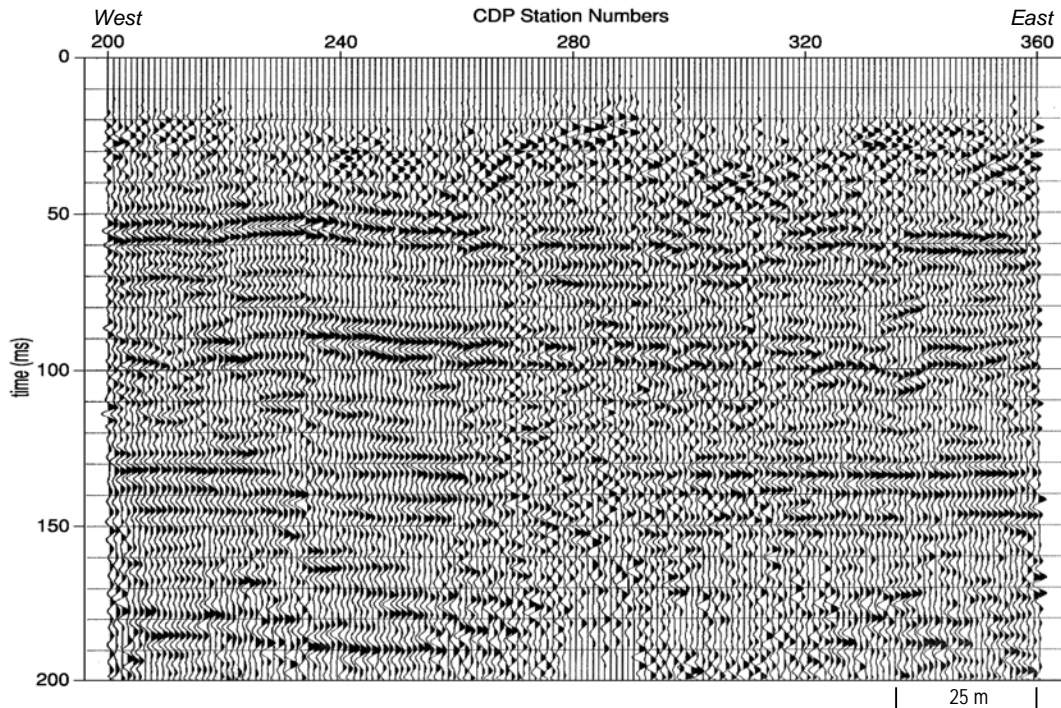


Figure 8-8. Twelve-fold CMP stacked section from Buerki sinkhole in Sedgwick County, Kansas. Reflection from base of salt flattened to compensate for near-surface velocity irregularities. Reflection undulations consistent with those seen on Figure 8-6 where natural dissolution resulted in similar gradual subsidence features.

immediately above the Hutchinson Salt Member, some salt still remains at this site. There appears to be as much as 10 ms more salt at the west end of the profile relative to the east end. From the very erratic nature of the reflections above salt, small-scale (50-m radius) dissolution of the salt varied noticeably across this site. Reflection geometries are suggestive of overburden collapse influenced by meandering fluid pathways altered as each subsequent roof section collapsed into leached voids. Plastic-looking deformation is consistent with horizontally elongated leach zones large enough to instigate roof failure followed by upward migration of the void through each layer with successive roof failure. Individual vertical collapse distances are likely quite small, resulting in very localized fractures and fault zones with offsets below the horizontal resolution of these data and therefore the plastic appearance of the bed deformation.

Natural dissolution features on the basinward (toward the thicker salt interval) side of the regional dissolution front are much better preserved than those on the east, allowing more confident event chronologies to be interpreted from seismic-reflection data. In areas near the dissolution front and on the west side, like the Punkin Center site and Victory Road sinkhole, the salt is still relatively thick, with dissolution and subsidence still in the early stages. In an area 20 km north of the Punkin Center and Victory Road seismic profiles, the dissolution front is defined by an extremely high salt-isopach gradient transitioning from full salt thickness (125 m) to less than 10 m in less than 1 km, based on well data.

A site where this high-gradient dissolution front is mapped to cross the planned construction of a new superhighway prompted a high-resolution seismic-reflection study (Table 8-1 ©). Special emphasis was placed on locations where rigid structures (bridges and overpasses) were planned. Of primary concern were locations with the potential for

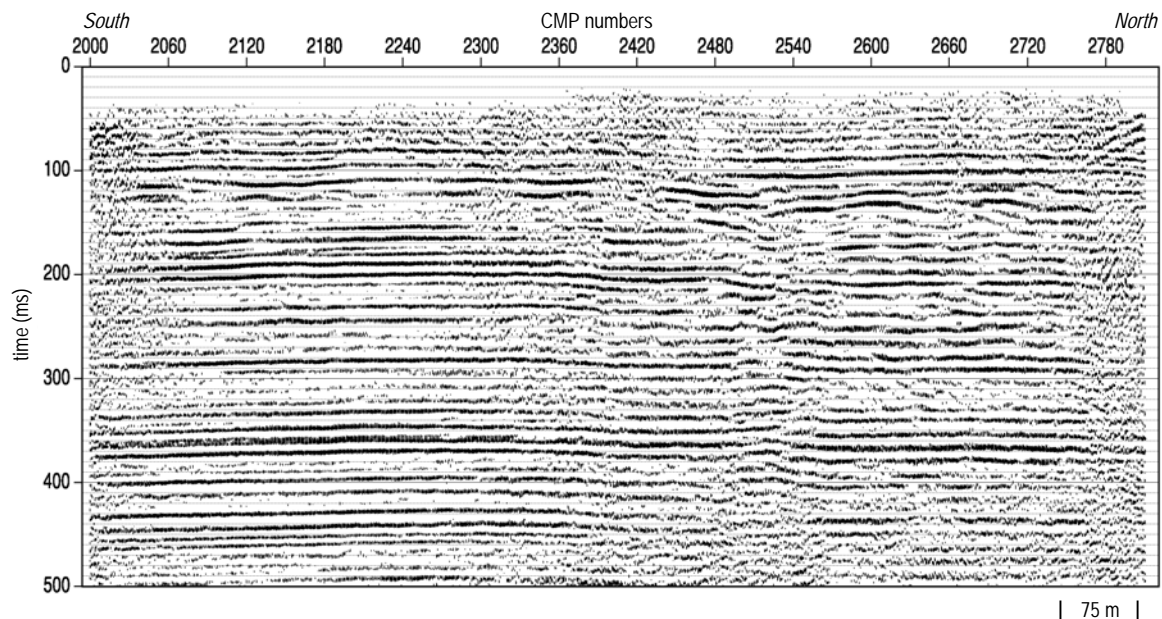


Figure 8-9. Nominal 60-fold CMP stacked section from Inman area. The drill-inferred dissolution front along the eastern edge of the Hutchinson Salt Member is evident based on appearance of highly distorted reflection with obvious static associated with a laterally variable velocity profile.

catastrophic surface collapse as inferred from voids and disturbances interpreted on seismic sections from the salt, anomalous reflection characteristics in the shallow portion of the section, or areas where seismic-reflection wavelet properties are consistent with active dissolution. However, in general, the objective was detection of any subsurface feature that could threaten highway stability and public safety. Considering the relative proximity of this Inman profile to the regional dissolution front, characteristics of seismically imaged dissolution structures were expected to be similar to those observed on two previous studies at Punkin Center and Victory Road. The 10-km-long survey was designed for optimal subsurface imaging oblique to the high-gradient contours of the salt isopach.

Consistent with the zone projected by well data to possess the most rapid thinning of the salt layer, seismic data imaged a highly altered near-surface geology (Figure 8-9). An abrupt change in reflection characteristics at CMP 2300 likely marks the western edge of the rapidly thinning salt interval defined as the natural dissolution front. The transition is obvious and characterized by relatively well-behaved reflections to the south changing to highly altered reflection events within the 70-m-thick salt over a distance of less than 100 m. As expected, the salt topography changes very abruptly, with undulations in reflections (nodes) as high as 100 m over distances as short as a 250 m. This very ragged nature of the dissolution front has been suggested but never imaged (Spinazola et al., 1985).

Reflections interpreted within the Permian shales and above the dissolution-altered inter-salt reflection events, appear indicative of only minor overburden subsidence immediately above the leached salt section at this location. Reflection events above the altered salt possess minimal drape or deformation in response to what seismically resembles significant dissolution and deformation within the salt interval. The reflection immediately above the salt at approximately 80 ms possesses a maximum of 10 ms of time change across a broad synclinal structure approximately 700 m in length. This 10-ms drape on the 80-ms overburden reflection is likely in response to the over 20 ms of subsidence and bed

aberrations evident within the salt interval over a distance of around 400 m. As well, the 80-ms reflection possesses a very smooth synclinal geometry consistent with relatively small-scale brittle deformation along subresolution fault and/or fracture zones. Contrasting this smooth 80-ms overburden reflection with salt reflections immediately below that appear irregular—steeply dipping in some places—and that possess unequivocal brittle deformation characteristics are indicative of a transition from high energy within the salt interval to a low-energy environment in the predominantly shale overburden. Deformation above the salt has a plastic appearance when, in reality, distortion of these beds has occurred through brittle deformation; but as previously stated, data resolution is not sufficient to detect small-scale faults and fractures.

Based on the appearance and severity of the dissolution-altered salt reflections between 100 ms and 150 ms, more short-wavelength synclinal-shaped subsidence features were expected than observed in the upper 80 ms of overburden along the interpreted dissolution edge north of CMP 2360. These expected short-wavelength subsidence geometries were observed on the Punkin Center line, Victory Road line, and Buerki line. It appears initially at the very edge of the highly active dissolution front, shale layers in the overburden tend to distribute deformation over a larger distance, resulting in a more plastic-appearing subsidence in spite of the fact microscale faults and fractures are responsible for these structures. Deformation in the salt layer is more isolated and rugged interpreted around void areas where leaching appears to have been more aggressive with deformation focused within the salt. Clearly this plastic-appearing deformation in the overburden is a symptom of the minimal strength these shales possess as roof rock and a high density of small-scale fractures and faults.

Layers within the solution-disturbed salt appear to have failed in a brittle fashion, forming a series of highly distorted reflections that lack geometric consistency and possess notable diffraction events. These bed-termination characteristics suggest the permeability barrier these interbed layers once represented are likely breached at various locations across the dissolution front and have allowed fluids greater freedom to move through the salt. This suggestion is consistent with the two different dissolution and associated deformation mechanisms observed beneath the Punkin Center profile with the more horizontal, gradual subsidence preceding the more rapid, vertically elongated compressional-style chimney failure.

Estimating the amount of subsidence would best be accomplished using an accurate time-to-depth converted seismic section; however, due to the extreme distortion in reflecting events, CMP stacking velocities calculated from these data lack the necessary accuracy. Two different velocity aberrations present problems for developing depth-based geologic models in subsidence areas. First, the dissolution zone itself has significant void space and rubble in areas where surrounding rock is competent and consolidated. This results in a lower average or bulk velocity, which manifests itself as reflection pull-downs on CMP stacked sections below the dissolution zone. Reflections from below the dissolution zone appear to possess subdued structures (deeper time-depth than the dissolution zone) that mimic those from above the dissolution zone. If an accurate, subsurface-length velocity function could be determined, the seismic two-way traveltime section could be converted to a depth section with accurate geological and structural interpretations of the rock layers in the subsidence zone. This has been problematic for many petroleum-exploration seismic surveys where evaporites are present above the reservoir.

A second velocity abnormality unique to and complicating interpretations of subsidence features on time sections is reduced average velocity above the dissolution zone due to settling and degradation of the rock matrix from fracturing, distortion, and differential compaction. Unlike the shadow effect that dissolution and related subsidence have on deeper events, this velocity effect is related to true rock properties and geometries within the affected portion of the seismic section. A consequence of these inaccurate velocities is unrealistic time-to-depth conversions. In spite of structurally misleading seismic-depth sections, the general geometry of these physically altered layers as depicted on CMP stacked time sections do reasonably represent the subsurface. Interpretations of events above the dissolution zone from time sections alone are reasonably consistent with the true geology (although slightly exaggerated).

Immediately south of the edge of the dissolution front (~CMP 2300) is a relatively small (~150 m wide), yet distinct seismic feature centered on CMP 2150 (labeled A on Figure 8-10). This reflection, interpreted to be from or at least near the top of the salt, has wavelet characteristics consistent with expectation based on models and previous seismic studies for the dissolution-altered top of salt. Most notable is the very subtle yet vertically isolated synclinal shape of the single reflection from the top of the salt (~110 ms) (labeled A on Figure 8-10). Maximum time displacement of the salt reflection at the center of this bowl (synform) feature is around 5 ms. This subtle drape in the top of the salt reflection is consistent with other seismic observations associated with leaching near the natural dissolution front.

This feature provides the first opportunity to correlate seismic-wavelet characteristics and reflection geometries to dissolution, using proximity and models as guides. Consistent with theory, amplitude is the attribute keenly sensitive to voids and/or altered zones beneath continuous spans of roof rock or interbedded layers. Comparison of the salt-reflection wavelet amplitude from within the interpreted subsidence feature centered on CMP 2150 with the same reflection from what geometrically and from velocity analysis appears to be an

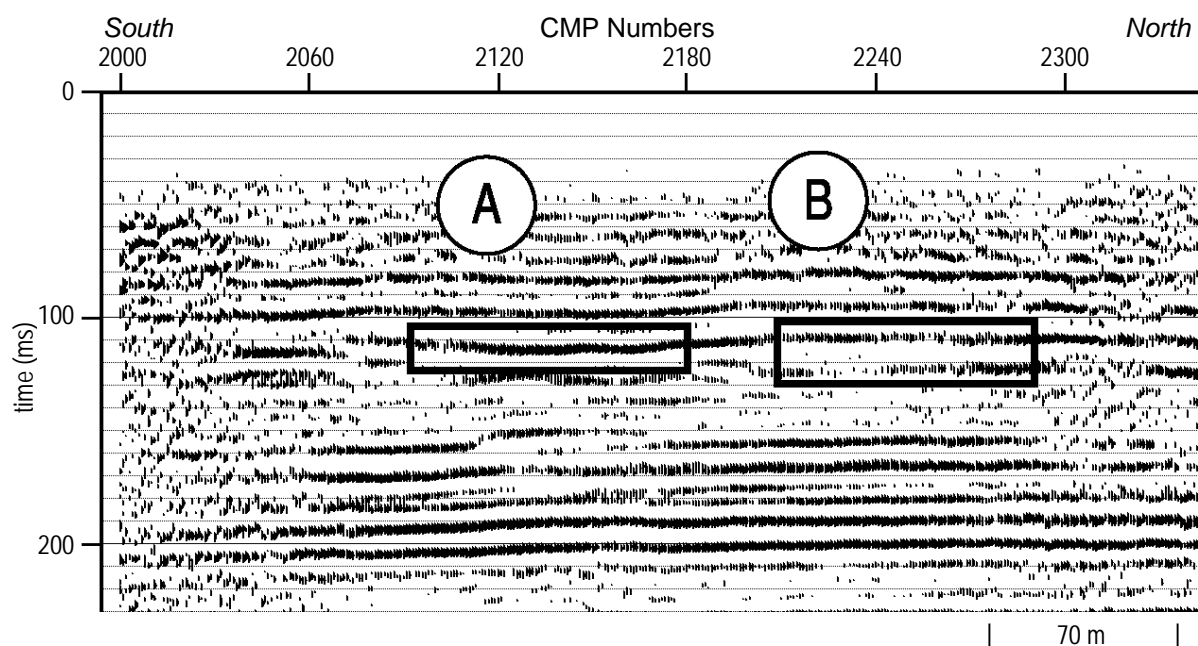


Figure 8-10. (A) Solution-altered reflection wavelet; (B) native from Inman seismic profile.

undisturbed section of salt centered on CMP 2240 (labeled B on Figure 8-10) highlights a marked increase in amplitude inside the bowl-shaped subsidence feature. This same phenomenon was noted on reflections from U.S. 50 (Figure 8-2), Victory Road (Figure 8-3), and Rayl (Figure 8-7).

Some evidence exists on these data that frequency might also be affected by changes due to minimal localized leaching. This frequency characteristic would be expected in reflections from the shadow zone below void areas. The rubble zone should both scatter and attenuate greatly the high frequency portion of the spectrum relative to equivalent energy traveling through competent rock immediately adjacent to the subsidence-altered rock. Some of the most compelling evidence supporting many of the concepts developed in this manuscript describing the natural dissolution process has been based on reflection-amplitude anomalies associated with dissolution at the salt/shale caprock interface.

Seismic Investigations of Anthropogenic Dissolution Subsidence

Hydrology is the component of dissolution-instigated subsidence that most significantly distinguishes anthropogenic from natural processes. With the fluid-access points (inlet and exit) fixed for the anthropogenic-induced dissolution case, the process is clearly constrained to a volume of salt commensurate with the dynamics of the fluid and available salt stock. Although in general the processes are identical, resulting structures, fluid volumes/velocities, and time frames are dramatically different. Consistent with the previous section, where discussions focused on seismic investigations of natural subsidence features, the remainder of this chapter will highlight seismic investigations and associated findings at anthropogenic dissolution sites, starting with simple single-stage collapse structures and working toward complex subsidence structures with multiple collapse episodes and changing stress regimes.

A gradually subsiding sinkhole centered on a saltwater disposal well formed between a major highway, a set of railroad tracks, and a farmstead and posed a potential risk to public safety (Table 8-1 ⑦). A set of seismic-reflection profiles acquired directly over the sinkhole were used to identify the sinkhole's subsurface expression (Figure 8-11). This sinkhole and associated subsurface feature is symmetric about the failed borehole and clearly possesses two different subsidence geometries. Based on this and previous sinkholes studied, initial failure was confined between reverse-fault planes inferred to be consistent with the lines of stress in the overburden above a void volume just prior to initial roof-rock failure and associated overburden collapse. Once this initial failure occurred, collapse of rock layers within the overburden continued along more normal fault planes defined by bed offsets. This extensional failure mode (secondary) is consistent with the change in stress field after initial collapse, assuming the salt void did not experience continued dissolution growth.

This interpreted sinkhole chronology clearly fits the empirically derived model where initial roof-rock failure is controlled by the stress field and strength of roof rocks. Subsequent failure/relaxation of overburden appears consistent with an extensional setting where compaction, rock strength, and overburden load dictates bed failure, geometries, and subsidence rates. Using the current working theory suggesting once secondary subsidence begins to occur (bed offsets mapped with normal fault geometries) and void growth slows or halts, this sinkhole's horizontal growth should be slowing and subsidence rates decreasing. Seismic images of the post-failure subsurface at this sinkhole are consistent with a single

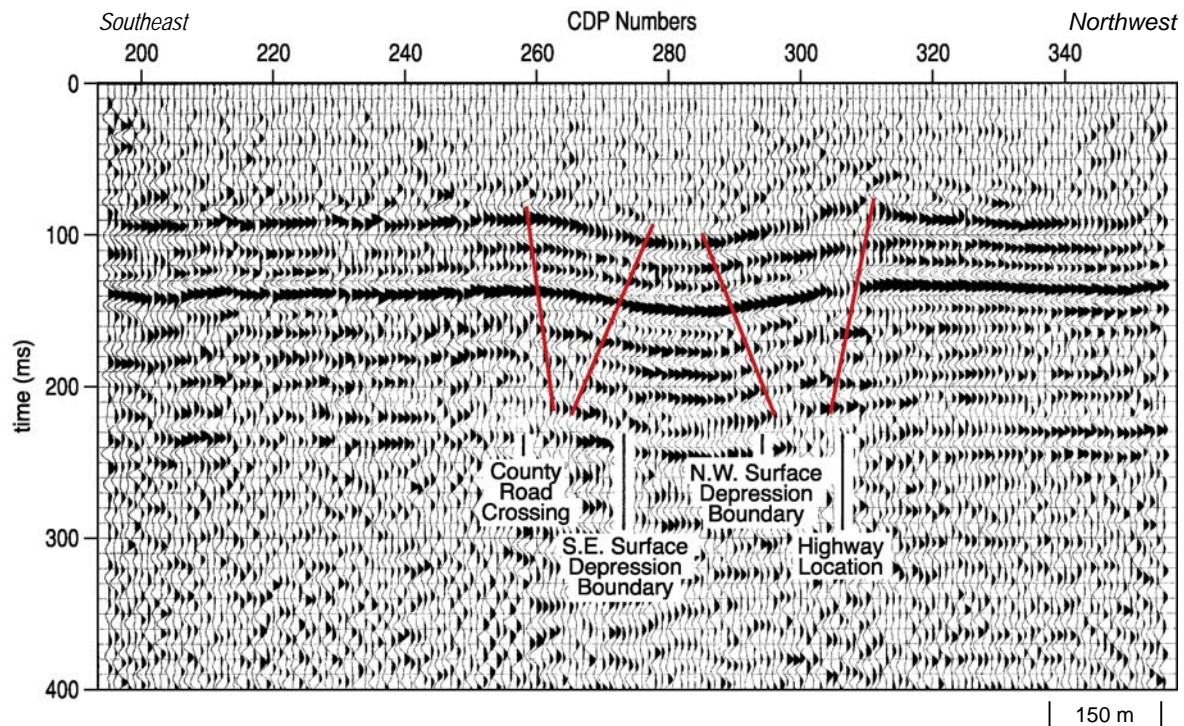


Figure 8-11. CMP stacked section with 12-fold redundancy from Conoco disposal well sinkhole in Ellsworth County, Kansas. Symmetric subsidence structure and excellent reflection coherency from rock layers above the salt interval at about 240-ms two-way travelttime.

episode of dissolution and then failure, beginning with compressional and ending with tensional.

Induced dissolution (anthropogenic) is generally characterized by a relatively localized disturbed volume and symmetry about the borehole. As in the previously documented sinkhole and associated seismic image, the growth rate of surface subsidence is generally relatively uniform. A subsidence event clearly related to a failed disposal well displaying asymmetric rates of subsidence, and with the culprit well significantly offset from the center of the sinkhole, provides more empirical details of these stealthy hazards (Table 8-1 ©). Observations related to a lack of symmetry were of sufficient concern to prompt authorities to investigate the subsurface with a low-fold 3-D seismic-reflection study and five 2-D profiles encompassing the surface depression. Results from this seismic study were intended to establish some degree of confidence in the safety of crews commissioned to reoccupy the borehole and plug the casing below the salt interval.

From the CMP stacked section the subsidence chronology and current potential for rapid failure within the collapse feature can be diagrammed (Figure 8-12). Based on previous studies of subsidence induced from salt-dissolution mining and seismic images acquired at the very early or active dissolution stages, it is reasonable to interpret two different collapse periods/mechanisms. First, the salt void grew beneath an impermeable, insoluble layer of shale or anhydrite (could have been at the top of the salt or one of the interbedded layers) until the unsupported span of roof rock exceeded the strength of the roof rock and failed consistent with the tensional dome. Vertical migration of the void proceeded through each successive layer of rock, moving ever closer to the ground surface. Collectively these successive bed ruptures manifested themselves in an upward-narrowing chimney-type geometry consistent with reverse faulting. As noted in previous chapters, this phenomenon

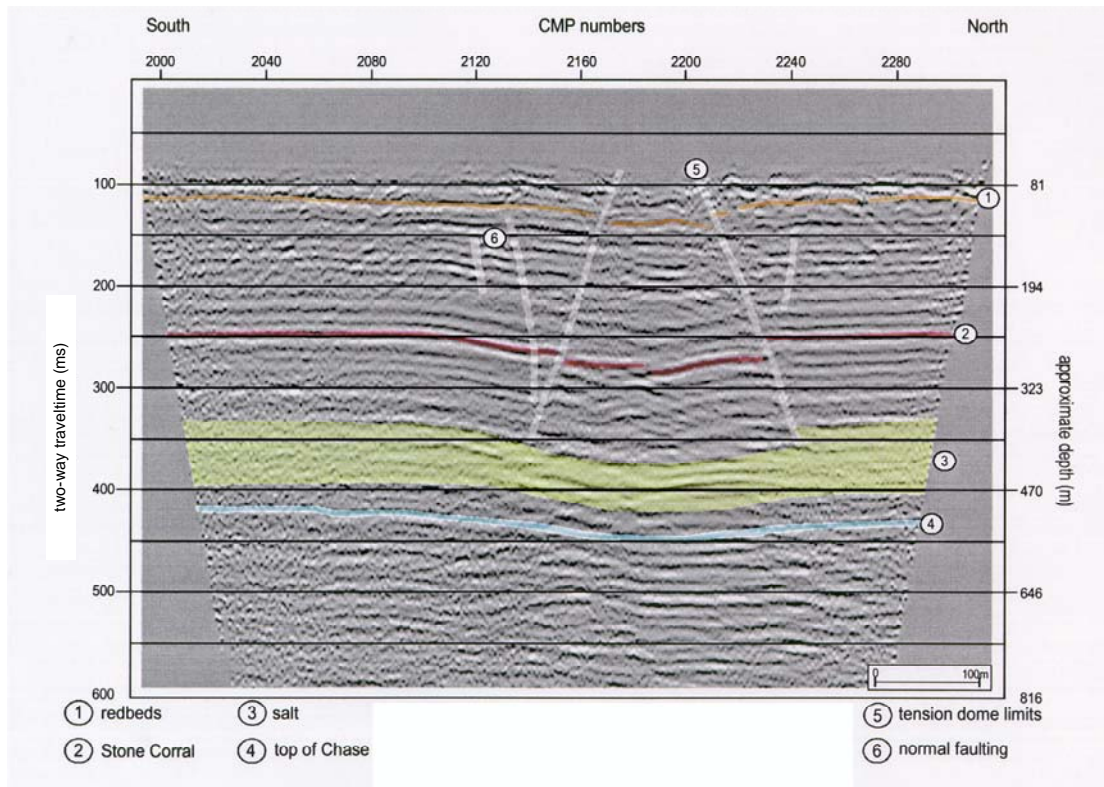


Figure 8-12. Nominal 48-fold CMP stack of reflection data acquired around and through the French sinkhole. Strain geometries are very evident with reverse faults defining subsidence near the center of the feature and normal relative bed movement in the outer part of the subsidence features.

has been detected by borehole interrogations at sites where sinkholes had formed from catastrophic collapse of salt jugs.

Seismically imaged rock layers around the perimeter of the collapse structure show evidence of bed-offset geometries consistent with normal faulting. Normal faults, interpreted on these seismic sections outside the central reverse faults, are indicative of a complete reversal of stress marking the termination of the compressional stress and buildup of extensional stress. This change is completely consistent with the concept of an extensional stress environment being established once there is no longer horizontal growth via dissolution of the salt interval. Surface subsidence at this site slowed to less than 1 cm/year from over 20 cm/yr over a 10-year period starting with the initial formation of the depression.

Borehole-induced dissolution and resulting subsidence as described by the previous two examples was clearly a single-episode event with initial upward migration of the dissolution void defined by compressional-stress-induced roof stoping and bed collapse followed by what appears was a uniform transition to extensional-stress-controlled failure and lateral expansion. For both anthropogenic and natural dissolution induced subsidence, seismic images appear to consistently provide evidence supporting both compressional and extensional failure modes. The one key characteristic that distinguishes these two hydrologic classifications is the episodal nature of natural versus the somewhat continuous progression through the stages for anthropogenic-induced subsidence. To continue improving the working model, seismic images of a subsidence event with an active sinkhole currently undergoing salt dissolution and therefore possessing a complex stress regime will be considered. This next setting tests the theory that movement along both reverse and normal

faults can be active simultaneously when leaching along the dissolution-void perimeter is active.

Seismic-reflection imaging provided an enlightened view of the subsurface beneath two distinct, circular, and gradually subsiding sinkholes first discovered in 1966 in the Gorham oil field beneath a stretch of four-lane highway (I-70) crossing north-central Kansas (Table 8-1 ©). Considering the average square kilometer in this oil field has more than 50 documented well locations, subsidence associated with abandoned oil or disposal wells should not be unexpected and could occur almost anywhere, at any time, along this several-kilometer stretch of highway. Around 10 cm per year of subsidence has been measured at the primary sinkhole (Crawford) since discovery. Seismic data acquired in 1980 and again in 2005 provided important information concerning sinkhole development and potential future growth projections.

The seismic expressions of the two principal sinkholes are as obvious on the CMP stacked section as they are on the ground surface (Figure 8-13). A unique characteristic of these two sinkholes, at least compared to the two previously discussed borehole-induced dissolution and subsidence features, is the very vertical nature of the bed offsets. Images of reflectors below both these active sinkholes appear to possess the same chimney-style, vertical-collapse structures observed and interpreted on seismic data over salt jugs after roof failure, and consistent with initial failure along the lines of equal stress, to define the tensional dome.

Based on drilling completed during the late 1990s, the ruptured casing at both these sites is actively moving fluids out of the salt interval. Bed-offset geometries observed on the CMP stacked sections associated with these sinkholes are consistent with previous interpretations of initial failure on seismic data from other borehole-induced dissolution and collapse structures. From interpretations of paleosubsidence features captured on seismic sections near the natural dissolution front (e.g., Figure 8-4), episodic reverse-fault-controlled subsidence appears to be coincident with unique periods of reactivated leaching with associated stress release. It is, therefore, reasonable to assume that subsurface subsidence structures with steep-sided, chimney-type structures (consistent with the tensional dome model) are indicative of either active or very recently active dissolution. Neither of these subsidence features possesses reflections with significant bed offsets displaying normal-fault orientations. It is, however, plausible to suggest a few bed offsets can be interpreted with normal-fault orientations in the upper 200 ms and within about 50 m of the extrapolated intersection of the ground surface and reverse-fault planes. Extending that interpretation one step further, it is reasonable to suggest dissolution has halted when subsidence can clearly be defined by normal-fault planes that extend from the salt to the ground surface on seismic-reflection images.

A small sinkhole centered at approximately CMP 1700 appears uniquely different relative to either of the seismically imaged larger active sinkholes (Figure 8-13). Beneath both the two large active sinkholes, the high-amplitude reflection event at approximate 260 ms (Stone Corral Formation) has either failed or has been distorted beyond what these data can resolve. As well, an abundance of diffraction events can be interpreted from around the perimeter of the large subsidence features, indicative of bed terminations. Also the interpreted offset geometry of reflectors within these two sinkholes is consistent with the previously described reverse-fault model. Subsidence features imaged on the eastern third of

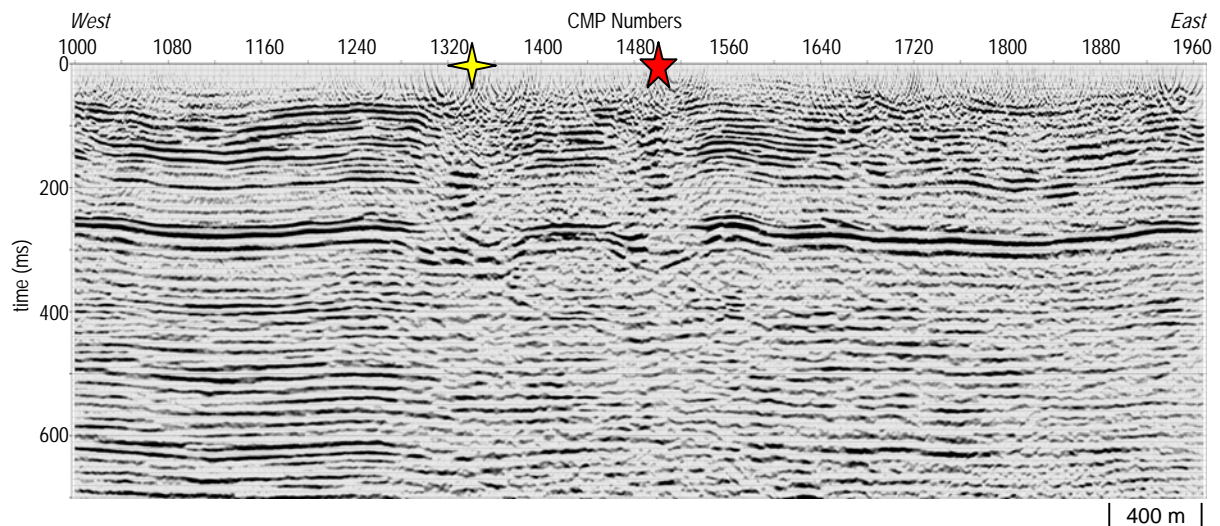


Figure 8-13. I-70, migrated CMP stacked section: Witt sinkhole is at station 1340 ✦ and Crawford is at 1500 ★. The high-amplitude event at 260 ms is the 300-m deep Stone Corral Formation. Top of salt is at about 400 ms and approximately 400 m below ground surface. Static effects from lateral variability in velocity are evident on the Stone Corral as a result of both dissolution and near-surface deposition.

the 5-km-long seismic profile possess subtle drape with a general appearance more consistent with the single-episode borehole-induced subsidence feature introduced at the start of this section (Figure 8-11). It is, therefore, reasonable to suggest the subsidence and/or dissolution mechanism or process in this third subsidence area is somehow different from either of the two large active sinkholes to the west.

Closer study of this small sinkhole uncovers evidence of another subsidence feature centered on about station 1840 that has not yet made a depression at the ground surface. For both these smaller sinkholes, the Stone Corral Formation (immediately above the salt interval) possesses about 20 to 30 ms of drape or flexure. The fact that this layer has not ruptured sufficiently to distinguish bed offsets on seismic data suggests either dissolution has been predominantly horizontal in nature (much like that suggested for natural dissolution) or it has been very localized and has not yet produced an unsupported span of roof rock large enough to exceed the strength of the immediate overburden layers in the Cretaceous portion of the section. One more possibility is that the dissolution process here has been halted due to an interruption in fluid movement.

As previously discussed, with the dramatic drop in localized velocity within the disturbed rock volume during the upward migration of a dissolution void comes significant statics problems, and, without a highly detailed velocity function, time-depth conversions are extremely inaccurate. So to more accurately represent the time structures above these subsidence features, reflections between the base of the salt and basement were time flattened. This process reduces any static effects and more accurately represents the time structure of the synclinal features evident on the 260-ms-deep Stone Corral Formation (Figure 8-14). Reflections above the 330-ms salt are obviously distorted across most of the eastern half of the profile while the reflection events below 400 ms are flat with no evidence of near-surface static.

Several distinctive episodes of subsidence can be inferred from the small, unique synclinal structures that appear to distort the Stone Corral Formation and overlying shales

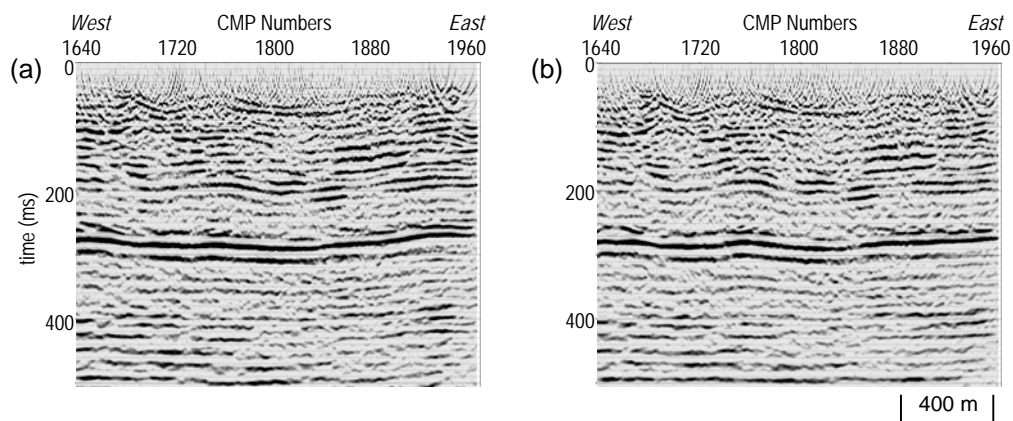


Figure 8-14. A portion of the CMP stacked section from Figure 8-13 (a) has been time-flattened on the subsalt reflections (b). Artificially flattening reflections immediately below the salt interval reduces the effect of velocity variability and focuses reflector structures above the base of the salt.

and sandstones in the upper Permian and lower Cretaceous. Considering the well density in this oil field, it is likely the subsidence features observed on seismic data on the eastern half of the line are the result of wells that have either leaked or with annular space that did not hydraulically isolate the salt from aquifers throughout the upper 1.5 km. Hence, dissolution of the salt was active for shorter periods of time, less fluid was available to enlarge voids sufficiently to consume enough overburden to form a significant collapse structure, or leaching was predominantly in thin zones along the top of individual salt layers.

Subsidence artifacts imaged beneath the two active sinkholes that are interfering with the four-lane I-70 highway in north-central Kansas are distinctly different compared to the previous two anthropogenic cases where dissolution had halted and subsidence was occurring within an extensional environment. The I-70 sinkholes appear to be forming under the influence of active dissolution and therefore a compressional-stress environment seems to still be present. Consistent among these last three sinkhole studies is the symmetry of formation. In all the previous studies these seismic-reflection images of the subsidence structures have suggested a relatively uniform radial development. In the next study, time-lapse seismic images provided the first-ever glimpse of a borehole-induced subsidence feature that formed catastrophically and continued to develop along an elongated solution-controlled alley.

Formation of the Macksville sinkhole was catastrophic and anomalous; therefore, it has generated a lot of interest and speculation as to the formation mechanism and subsurface chronology (Table 8-1 ⑩). This sinkhole formed catastrophically around an abandoned oil-field brine-disposal well. Failure at this site came with no warning and in a portion of the oil field that had been shut-in for over two decades. Concern for ground water in this area and risk of ground movement beneath surface installations supporting active oil production prompted the seismic investigation of this sinkhole.

Due to the large pond (approx. 2500 m²) in the center of the sinkhole, which was approximately centered on the disposal-well location, seismic lines were acquired off sinkhole center and for the west/east profile along a stretch of ground with little to no surface expression. The extremely steep-sided nature of this sinkhole on the south, west, and north restricted optimum placement of seismic lines. However, key subsurface characteristics of this actively growing sinkhole were interpreted in spite of the less-than-ideal line placement. Clearly this subsidence feature can be characterized by well-defined reverse faults defining

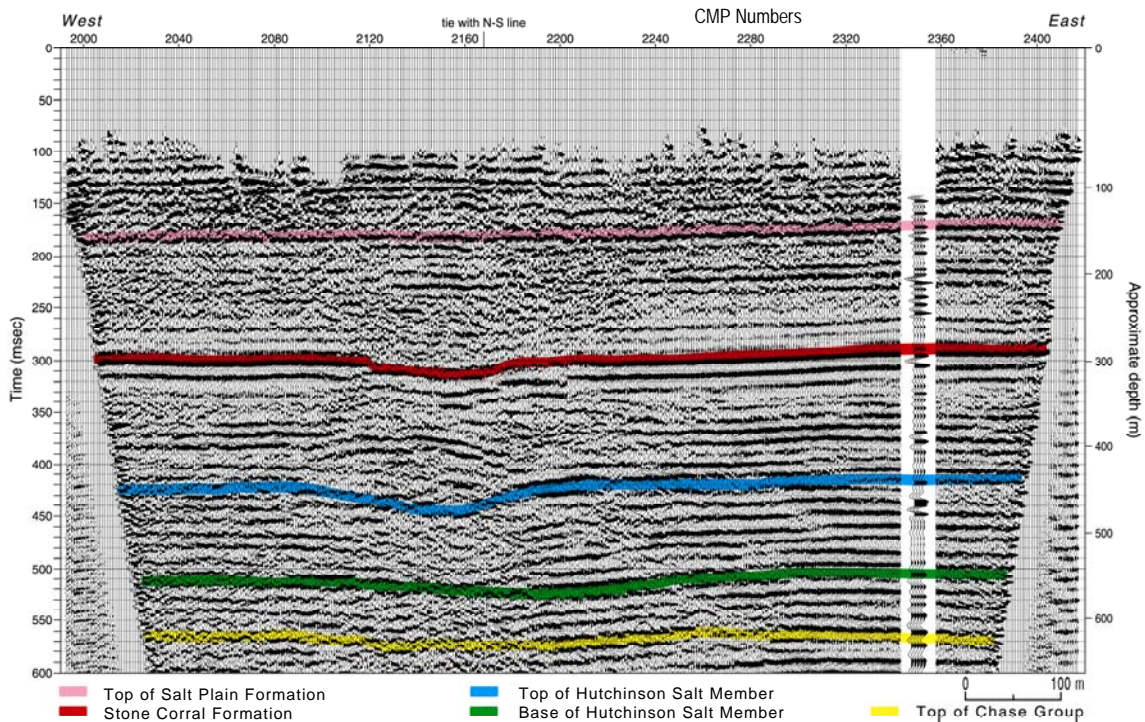


Figure 8-15. Nominal 60-fold interpreted CMP stacked section from the Macksville sinkhole. Shallow reflections are from rock layers yet unaffected by the subsidence feature while deeper rocks are clearly suggestive of a reverse-fault offset geometry in reflection from the top of salt to about 200 m.

the subsurface boundary of the initial failed rock layers (Figure 8-14). On this CMP stacked section, there is no clear indication that bed-offset planes are consistent with normal-fault geometries. Considering this sinkhole formed more than 10 years prior to the seismic survey, it is a bit surprising that the active/current failure mechanisms for this sinkhole are still characterized by bed offsets with reverse-fault orientations.

As expected, the shallowest layer imaged on the west-to-east line shows no indication of subsidence (Figure 8-15). This is consistent with the fact that this survey line was immediately south of the surface rupture in an area with no topographic expression of the sinkhole. Clearly the root of the sinkhole extends under the 2-D profile line and, based on the increasing diameter with depth of this feature, the subsidence geometry is still dominated by reverse faulting. Consistent with inferences from studies previously detailed in this section, this apparent compressionally dominated stress regime is likely indicative of active leaching and void building. Once dissolution stops and active void growth ends, the dominant-offset orientation of rock failure should be extensional.

Along the eastern end of the sinkhole the topography changes gradually enough to allow the north/south line to be acquired within the eastern rim of the sinkhole trough (Figure 8-16). The reverse-fault bed offsets defining the core of this subsidence feature are well imaged and easily interpreted. Unique about this profile relative to the west/east section (Figure 8-15) is the apparent normal faulting (CMP 4120) that can be interpreted immediately north of the upthrown side of the outermost reverse faults. By incorporating observations from previously studied sinkholes, it is reasonable to suggest migration of the dissolution front to the north has ended, as indicated by the apparent change in the stress regime in that quadrant. Migration of the dissolution front appears active to the west, south, and east. This

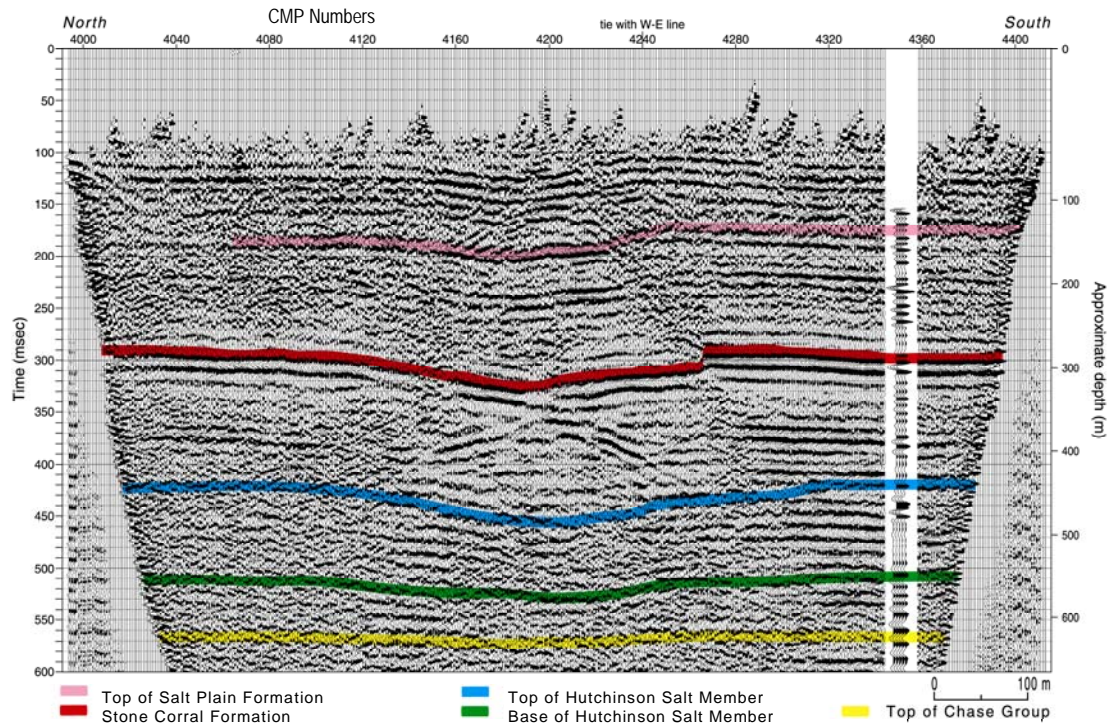


Figure 8-16. Nominal 60-fold interpreted CMP stack of north/south line at Macksville sinkhole. Drapes in reflections is evident to the top of the section consistent with the location of this line, which crossed over the east edge of the sinkhole. Reverse-fault geometries dominate the interpreted bed offsets.

subsurface observation is in complete agreement with surface-elevation surveys that have been carried out each year since the sinkhole first formed.

Borehole-induced dissolution and resulting subsidence features provide ideal settings for studying the controlling processes and characteristics of leaching interpreted from reflector-defined collapse structures (in a few cases where time-lapse surveying has played a role; changes in those geometries). Seismic images of reflectors beneath a sinkhole are a compilation of interrelated clues that can be used to unravel the history of the process. By carrying forward lessons learned during study of progressively more complex cases, an evolutionary chain of events develops that can guide empirical models used for predicting future growth scenarios as well as giving insights into the past. In this section discussions started from the simple first-order continuous subsidence feature and have advanced to a complex subsidence feature defined by a non-uniform geometry and active salt harvesting well after catastrophic sinkhole formation. Emerging from a synthesis of the past four cases is a definable pattern and series of events that seem to collectively describe the many types of active processes. The next sinkhole and associated subsidence structure discussed adds a significant level of complication through the involvement of more than one well bore and communication between those wells.

A loss of well-bore confinement was observed during standard pressure tests, cluing regulators into a potential problem isolating well-bore fluids from surrounding evaporite layers at a disposal well in south-central Kansas (Table 8-1 ①). Attempts to plug the well and seal the borehole failed. With the casing severed, borehole fluids were moving easily through the salt, leaching of that salt was apparently uncontrolled, and a gradually subsiding and expanding sinkhole was developing. It was soon discovered that a second borehole less than

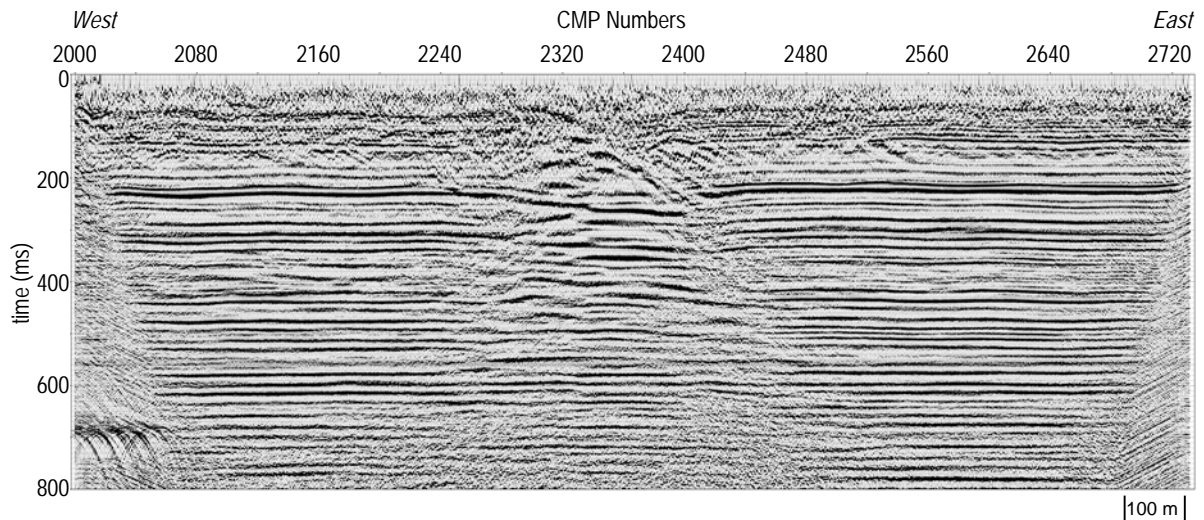


Figure 8-17. Nominal 60-fold CMP stack at the Leesburg sinkhole. Asymmetry of the collapse structure is unusual for a subsidence feature from borehole-induced dissolution. East side of profile clearly defined by reverse-fault geometry.

100 m from the first had also lost containment and the two were hydraulically connected. Based on well-bore tests the worst case was discovered; fluid was moving within the salt interval between the two wells.

Reflections in proximity to and beneath the sinkhole were highly distorted with a collapse structure well defined in the subsurface (Figure 8-17). Subsidence geometry of the 220-ms-deep Stone Corral Formation is unique compared to previously studied single-well sinkholes where salt was at a similar depth and dissolution was instigated by oil-field well-casing failure. At this site it appears the Stone Corral Formation failed as large, relatively intact blocks with the largest segment measuring around 150 m to 200 m in length and down-dropped around 40 m (after compensation for the reduced average velocity within the disturbed near-surface) located immediately beneath the sinkhole. Other large pieces of this anhydrite layer appear to have tilted in response to progressive leaching of the salt and expansion of the dissolution front.

Interpreted bed offset geometry/orientation is unique to this subsidence feature and provides important clues to possible growth mechanisms. Faults interpreted as defining layer displacement resulting from failure are different on one side of the subsidence feature relative to the other. As with all other subsidence features studied in this chapter, opposing reverse faults clearly define the initial failure cone and are centered on the current sinkhole at about CMP 2360. Based on surface-elevation data, the most rapid vertical growth is along the eastern side of the sinkhole, while very little vertical growth has been observed to the west; the sinkhole clearly possesses a very gentle ground surface slope toward the sinkhole center from all directions.

It is reasonable to correlate future surface growth with the unique reflection geometries on opposing sides of this subsidence feature. Gradual expansion in the radius of the sinkhole to the west is consistent with normal-fault offset geometries in bedding as would be anticipated during gradual relaxation of the accumulated stress after salt leaching has ceased. The predominantly vertical growth evident throughout this structure is interpreted to correlate with subsurface sediments that are subsiding along reverse-fault planes during initial formation. The asymmetry in rock geometries apparent within the overburden on

seismic images is a bit unusual for a single borehole-induced dissolution void. Future surface growth will likely correlate with this non-linear radial-growth pattern observable in the subsidence-altered reflections beneath the sinkhole.

Unique to this sinkhole is the two-well hydrologic system and the nonsymmetrical reflection and bed offset geometries about the principal well bore. It is likely these two unusual situations/characteristics are cause and effect, respectively. This lack of verticality, normally observed in well-induced subsidence features, is also a likely result of this two-well system. The hydrostatic head of the completion units (geologic) for each well would dictate fluid-flow direction (artesian or gravity) and volumes. With the enhanced potential for fluid transport, this two-well system could eventually lead to leached volumes and a subsequent sinkhole significantly larger than any single-well sinkhole currently known to exist.

Careful study of geometries prevalent in this seismic image provides important clues to sinkhole growth and factors influencing areas of active leaching. Bed offsets on the east are markedly different in orientation and general geometry relative to the west side of the structure. Building on the observations on seismic-reflection surveys at subsidence sites previously discussed in this chapter, the more reverse-fault-dominated east side of the structure is likely to support the majority of future subsidence. Implications from previous sites would support the suggestion that normal-fault-controlled subsidence on the west is the response to gradual relaxation of stress over an area without current leaching. On the east, however, the reverse-fault architecture bounding the outermost perimeter of the subsidence volume is one indicator of active leaching and potentially higher subsidence rates resulting in a much larger surface expression.

Working through this collection of borehole-induced dissolution and subsidence features, various development scenarios appear consistent for all structures. First, initial failure occurs along offset planes with reverse (hanging wall above footwall) orientation. Second, based on a single site that was known to have formed catastrophically, a reverse-fault volume defining the chimney structure contains collapse breccia that was generated as a result of rapid material failure. Third, active dissolution and void development with associated collapse will constrain itself predominantly to reverse-fault bed offsets, but during secondary failure these reverse faults will splay off small-scale normal faults near the ground surface. Fourth, during periods of extensional strain, void growth is unlikely and this stage generally appears to represent a decaying energy state. With no confirmed seismic images of subsidence features at the pre-sinkhole development stage and post-initial collapse stage, the migration process toward the surface must be deciphered from available post-sinkhole clues. An investigation of a solution salt-mine roof failure provides images of rock distortion that are likely indicative of roof stopping during compressional-stress-driven failures before sinkhole development.

Catastrophic development of a sinkhole in a dissolution-well field threatening a nearby city street and railroad spur prompted a subsurface investigation which included three 200+-m-long seismic-reflection profiles acquired adjacent to the sinkhole (Table 8-1 ©). The salt interval at this site was about 100 m thick with the top of the salt about 125 m below ground surface.

A clearly definable void-looking feature can be interpreted on the seismic-reflection section beneath station 210 (Figure 8-18). Seismic characteristics of this void are quite unique relative to the rest of the reflection events on these data and consistent with expectation

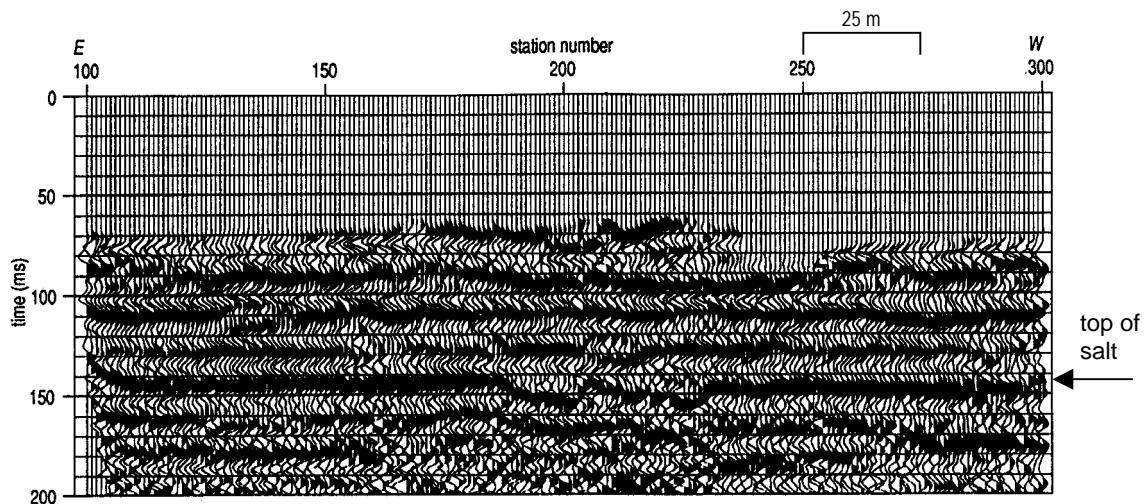


Figure 8-18. Twelve-fold, CMP seismic section from collapsed dissolution salt well in Hutchinson, Kansas. Disturbed top of salt is evident beneath station 210 at a two-way travelttime of 140 ms, equating to a depth of about 125 m.

(diffractions, scatter energy, out-of-the-plane events, draping-reflection horizons, etc.). The seismic profile was acquired immediately adjacent to the sinkhole but in an area where the ground surface had not yet subsided. Rocks between the salt void and ground surface (overburden) imaged as part of the seismic survey show no evidence of distortion related to the salt void. Considering the seismic-reflection survey only sampled a 2-D slice between the sinkhole and city street, strong seismic evidence exists to suggest this void extends beneath the city street and railroad spur. Drill data designed to ground truth these seismic data corroborated the seismic interpretation.

Considering the proximity of the seismic line to the sinkhole and the clearly distinguishable seismic signature of the top of the mined salt “jug,” it is reasonable to suggest rock failure between the jug and ground surface was constrained to a very narrow chimney significantly smaller in diameter than the jug. This subsidence geometry is consistent with the concept that initial failure over a void or cavity occurs along the lines of greatest stress defined by the tensional dome. Subtle indications of drape in the imaged overburden appear to narrow as the disturbance moves toward the ground surface—an observation consistent with reverse-fault-controlled subsidence associated with initial failure during leaching and void growth.

Failure of another salt jug in this same mine field (less than 0.5 km away) occurred approximately 10 years after this failure. Seismic and drill data confirmed the sinkhole was the surface manifestation of cylindrical and near-vertical failure in the overburden above a known salt jug. The collapse of consolidated overburden was isolated to a relatively narrow chimney feature (smaller in diameter than the salt jug and narrowing upward) connecting the salt jug with the bedrock surface. This geometry is consistent with the suggestion that initial failure was along or coincident with the lines of equal stress present in rocks above and around a void. Rapid initial growth of the sinkhole after catastrophically appearing was the result of gravity slumping of unconsolidated materials into the 4-m-wide opening at the bedrock surface some 20 m below ground surface.

Summing Up and To Come

This chapter presents essential contributions that are en route to the development of an empirically based subsidence model honoring all high-resolution seismic-reflection imaged subsidence examples. The set of 12 high-resolution seismic-reflection studies discussed in this chapter highlight key components both unique and similar. Previous chapters have provided background information and established the technical basis for deductions and interpretations presented in this chapter. A more diverse, inclusive, thorough, and conclusive collection of seismically investigated subsidence features has never been amassed. This group of six anthropogenic and six natural dissolution-induced subsidence features allows the first-ever data-based development chronology detailing the migration of voids through the overburden. Each subsidence site investigation in this chapter had particular seismic characteristics or properties unique to the specific dissolution-induced collapse structure, from the simplest to the very complex.

Working through this collection of natural and borehole-induced dissolution and subsidence features presented in this chapter, various development scenarios appear consistent for all structures. First, initial failure occurs along reverse-style offset planes (hanging wall above footwall). Second, multiple groupings of reverse-fault planes relate to episodic collapse due to active dissolution. Third, the innermost reverse-fault pair maps the tensional dome and initial chimney feature possessing catastrophic-collapse potential. Fourth, during secondary failure associated with active leaching reverse faults will splay off small-scale normal faults near the ground surface. Fifth, normal-fault geometries designate a low-energy stage in terms of active dissolution and collapse rates. Sixth, during periods of extensional strain, void growth is unlikely and this stage generally appears to represent a decaying energy state. Juvenile subsidence structures inferred from seismic images have characteristics that support the upward migration of a dissolution void as interpreted from drill investigations at dissolution mines and deciphered from seismic images of post-failure structures.

In the upcoming chapter the seismically defined characteristics and processes associated with dissolution-induced subsidence just described will be combined with physical-model studies and ancillary seismic-data properties, geometries, and attributes to formulate a conceptual model that honors all data and models based on realistic parameters. Physical models have predominantly focused on salt domes as a direct result of their petroleum significance, but aspects of those results provide key insights into observations on seismic sections imaging real subsidence structures in bed salt. Using these physical models, the large gaps between instigation and maturation of seismically imaged subsidence structures can be filled with underlying processes consistent with all developed subsidence features. Combining all these key pieces to form a more detailed conceptual model of the collapse process will allow enhanced predictions at any site with sinkhole potential.

References

- Lambrecht, J.L., and R.D. Miller, 2006, Catastrophic sinkhole formation in Kansas: A case study: *Leading Edge*, v. 25, n. 3, p. 342-347.
- Miller, R.D., 2003, High-resolution seismic-reflection investigation of a subsidence feature on U.S. Highway 50 near Hutchinson, Kansas; in K.S. Johnson and J.T. Neal, eds., *Evaporite karst and engineering/environmental problems in the United States: Oklahoma Geological Survey Circular 109*, p. 157-167.
- Miller, R.D., 2006, High-resolution seismic reflection to identify areas with subsidence potential beneath U.S. 50 Highway in eastern Reno County, Kansas: Symposium on the Application of Geophysics to Engineering and Environmental Problems [ext. abs.]: Selected as a best paper from SAGEEP06, presented at Near Surface 2006, Helsinki, Finland, Sept. 4-6, 5 p. (published on CD).
- Miller, R.D., D.W. Steeples, and J.L. Lambrecht, 2006, High-resolution seismic-reflection imaging 25 years of change in I-70 sinkhole, Russell, County, Kansas [exp. abs.]: Society of Exploration Geophysicists, Tulsa.
- Miller, R.D., D.W. Steeples, and J.A. Treadway, 1985, Seismic reflection survey of a sinkhole in Ellsworth County, Kansas [exp. abs.]: Society of Exploration Geophysicists, Tulsa, p. 154-156.
- Miller, R.D., A.C. Villella, and J. Xia, 1997, Shallow high-resolution seismic reflection to delineate upper 400 m around a collapse feature in central Kansas: *Environmental Geosciences*, v. 4, n. 3, p. 119-126.
- Miller, R.D., D.W. Steeples, L. Schulte, and J. Davenport, 1993, Shallow seismic reflection study of a salt dissolution well field near Hutchinson, Kansas: *Mining Engineering*, October, p. 1291-1296.
- Spinazola, J.M., J.B. Gillespie, and R.J. Hart, 1985, Ground-water flow and solute transport in the Equus beds area, south-central Kansas, 1940-1979: U.S. Geological Survey Water-Resources Investigations Report 85-4336, 68 p.
- Walters, R.F., 1980, Solution and collapse features in the salt near Hutchinson, Kansas: Geological Society of America, South-central Section, Field Trip Notes, 10 p.

CHAPTER 9

SEISMIC-REFLECTION CHARACTERISTICS AND MODELS

Throughout the previous eight chapters, theories, discussions, and developments have been presented, orchestrated, and assembled expressly to support observations and conclusions that will be formulated in this chapter and summarized in Chapter 10. This chapter brings together high-resolution seismic-reflection-based interpretations, correlations, and speculation offered in previous chapters with various published physical and empirically based dissolution models. This fusion of theory and data provides the most comprehensive workup to date of concepts responsible for and driving the collapse processes, specifically for salt dissolution but also applicable to collapse in general. Finally, general and several case-specific conceptual models will be presented in Chapter 10 based on the merger of documented concepts and principles with basic behavioral traits derived from the dozens of high-resolution seismic-reflection investigations of collapse structures unveiled and detailed in this manuscript.

Yet to be discussed as part of this development are models. Detrimental to populating numerical models for these kinds of collapse structures is the overwhelming complexity of the collapse process due mainly to the multitude of rock types and properties, material heterogeneities, and lack of structural uniformity. These real-earth complexities inhibit the level of detail and in many cases accuracy of assigned model properties, and thereby hinder how faithfully numerical models represent the collapse process and can serve as predictive tools. Developing a single site-specific numerical model could take years and require prohibitive quantities of computing power. For these highly complex structures, empirical and physical models provide more realistic and practical representations of site-specific collapse structures. By matching processes and geometries at various stages of model development with observations on real data, key controlling characteristics and settings can be defined and used as indicators of various potential collapse scenarios. These conceptual models can guide the classification of various temporal stages of failure, especially at the point where a collapse structure poses a risk to people or property.

Each of the previous chapters has maintained a common, yet unique topical thread, whether dissolution processes, failure mechanism, or high-resolution seismic reflection; each chapter has been organized and focused to support the principal imaging and subsidence thesis of this manuscript. This chapter is no exception; here many of the processes and ideas described or developed in previous chapters will be spun together to form the fabric of an empirically based conceptual-subsidence model that will be fully described in Chapter 10. En route to this culmination, existing physical models will be matched with previously discussed seismic-reflection images. This matching will be based on structural characteristics and overall bed geometries. Correlating real data with models allows not only the sequence of events leading up to the current reflector geometries to be postulated, but the future of these structures as well can be mapped out with some degree of confidence. Predicting the most likely development scenarios can then be based on various hydrologic scenarios

incorporated with case studies of subsidence features in similar settings. Interpretation of seismic-reflection sections greatly benefits and confidence is heightened through model correlations.

Salt Models

Interest in numeric modeling of salt structures began with the recognition that deformation associated with dissolution of salt diapirs can be an indicator of subsalt and salt-flank hydrocarbon traps (Parker, 1967; Swenson, 1967). The utility of scale physical model data became evident with the necessity to validate numerical seismic-response models (synthetic) after altering model parameters based on site-specific characteristics (e.g., Ladzekpo et al., 1988; Lu and Herbert, 1989). With the addition of real data components like noise, source sensitivity, and full 3-D response, testing new acquisition designs and data-processing routines became much easier and cheaper with numerical models without compromising realism (Ebrom et al., 1990), but validation still required physical models designed for scale seismic imaging.

Model simulations of seismically complex salt structures showed that reflection-arrival patterns observed on real data were indeed related to the highly variable geometries and large velocity and density (acoustic impedance) contrasts (Chen and McMechan, 1993). These first physical models provided a test bed for developing new approaches to acquisition and processing with the potential for pseudo ground truthing. However, these tests were very limited due to the complexity of true salt structures and, therefore, overly simplistic.

A vast library of synthetic seismic data was generated using the numerical SEG/EAGE salt model (SEG/EAGE, 3-D Modeling Committee, 1994). This digital data set made the need for a complex, full-scale physical model evident and its construction a viable and necessary undertaking. A physical model of the SEG/EAGE numerical model was built specifically to test imaging and specialized processing techniques designed to address complex and highly variable velocity structures represented in the numerical model and based on what was known



Figure 9-1. Synthetic seismic section from salt model. Vertical slice through 3-D prestack depth-migrated seismic volume (from Wiley et al., 1996).

about salt structures (Wiley et al., 1996) (Figure 9-1). Models designed to simulate these salt-diapir characteristics do not accurately represent processes associated with or structures resulting from removal of stock from a bedded salt and subsequent subsidence. Effort and resources expended to develop this one SEG/EAGE numerical salt model were immense and not practical for site-specific simulations.

In most cases model “systems” (numerical and physical) are rudimentary and designed specifically for evaluating particular salt-body characteristics significant to a single petroleum-exploration problem or situation (Chon and Turpening, 1990). Extreme bed

geometries and complex velocity structures are the principal challenge to these simplistic models. Unfortunately, growth or failure of beds under the stress of active salt tectonics has been difficult to address with models of any kind due to the complexity and economics of designing and constructing suitable scale models.

Salt Withdrawal Physical Models

Dynamics, geometric complexities, minimal physical size (relative to wavelengths), and rate of change make salt-dissolution features a unique and challenging imaging problem. Due to the influences of the petroleum industry, the most commonly studied and economically significant salt tectonic features are associated with diapir growth and dissolution of the crown (bulb). Little modeling and few studies have investigated the various seismic responses to dissolution or removal of salt and development of collapse structures in bedded salt deposits. Structures and growth-related stratigraphy above salt domes have been studied for more than 80 years, with most research targeting faulting above actively growing diapirs (Link, 1930; Parker and McDowell, 1951; Currie, 1956; Withjack and Scheiner, 1982; Lemon, 1985; Brewer and Groshong, 1993). Only one physical model study prior to 1998 investigated the effects of bedded salt dissolution and showed overburden subsidence due to brittle failure could be characterized by both high-angle normal- and reverse-fault planes (Parker and McDowell, 1955).

A physical model study recently undertaken to evaluate the effects of dissolution and resulting subsidence provided high clarity, conclusive model results using basal withdrawal of salt as an analog to dissolution (Ge and Jackson, 1998). This “withdrawal” approach is suggested to be equivalent to and consistent with gradual dissolution and associated overburden subsidence. This particular physical model study provided the first robust, detailed, and material equivalent look at collapse structures analogous to dissolution of various bedded and diapir salt scenarios. Models were designed specifically to maintain similar dynamics, rates, and distributions as dissolution and subsidence processes observed in nature. With the structural evolution of these models intended to be a close match to nature, comparing various physical subsidence models to high-resolution seismic-reflection data seemed a reasonable and beneficial undertaking en route to an improved understanding of the natural process. If distinguishable, differences expected between natural and anthropogenic induced dissolution and resulting subsidence could provide important clues about and therefore an understanding of both processes. No scale seismic data were acquired over these withdrawal physical models, so correlation of the physical models with the time-seismic data do not have the benefit of ideal pseudo-synthetic seismic sections.

Physical model cross sections of subsidence features, published in *Physical Modeling of Structures Formed by Salt Withdrawal: Implications for Deformation Caused by Salt Dissolution* (Ge and Jackson, 1998), are based on the withdrawal of a silicone polymer mass (salt analog) and designed with a geometry and volume consistent with a specific salt setting. Salt bodies constructed as part of the physical model study were buried beneath a dry quartz sand (sediment analog) in a 33-cm-long and 23-cm-wide containment vessel (tank). Testing focused on different shape diapirs of various heights, withdrawal rates, and symmetries. Of the 15 experiments run as part of the physical model study, the tabular, rectangular wall, and cylindrical stock models provided the most reasonable analogs to bedded salt stock features and overburden as interpreted on seismic-reflection data present in this manuscript.

A simple, tabular-shape bed designed to represent either autochthonous bedded salt or an allochthonous sheet of salt should be reasonably and generally consistent with the Hutchinson Salt Member in Kansas (an autochthonous bedded salt). It is not intuitively obvious how analogous draining a salt model is to real in situ dissolution processes, but it will be assumed for this study that most situations in nature can be simulated by draining (e.g., void development from top of salt would clearly have some significant differences). With the relative regularity of fluid flow when dissolution is driven by anthropogenic sources, it seems most probable that subsidence patterns will correlate best with this model at sites where a casing breach instigates dissolution (point fluid source, steady flow rates, and a point outlet) at a depth near the base of the salt. Natural dissolution could also develop structures within the salt and overburden that are reasonably consistent with this model and its withdrawal process if natural conduits and fluid orifices remain open over an extended period of time (even a series of individual dissolution episodes at nearly the same point and subsidence events on a single feature) and are confined to a small area. The real disconnect between the physical model processes and natural processes is that, in natural settings, flow characteristics and water chemistry are generally altered when insoluble interbeds and overburden subside into active dissolution zones.

It is unlikely any physical model using these materials and drain system will reasonably approximate the subsidence phenomena observed for solution-mine voids (or any salt void formed similar to solution-mined jugs) and affected overburden. With the speed and controlled nature voids develop during solution mining and the need for roof stability under the stress applied by overburden or upper salt layers, salt removal physical models need much greater control of micro (in this case) level processes, over a significantly smaller withdrawal volume. The physical scale of these physical models is not consistent with most anthropogenic processes (Ge and Jackson, 1998). For purposes of this manuscript, the tabular-shape diapir model will reasonably match the gradually subsiding overburden above continuous and uniform leaching in a real earth setting (Figure 9-2).

Post-deformation, the tabular physical model is dominated by a broad, gentle syncline formed by focused drainage and significant flowage of the bounding salt (Figure 9-2). Flowage outside the withdrawal cylinder is distinguishable by a definitive change in slope that transitions from a flat-bottomed, steep-sided bowl above the drained area to monocline flexures extending away from the drained volume (Figure 9-2b). Because these models were designed to approximate natural processes and structures, clearly a principal assumption is that material response to differential pressure will be in the form of creep proceeding at rates consistent with dissolution in nature. Natural dissolution rates are generally extremely slow relative to anthropogenic rates (Martinez et al., 1998). This suggestion is consistent with the observation that the large bowl-shaped subsidence structure model possesses well-defined breaks in slope interpreted to mark the change from dissolution to flowage (Figure 9-2b). The bed geometries of this model do not fit the natural chimney-style collapse structures such as those observed on the Punkin Center seismic-reflection section (Figure 8-6).

The general appearance of this tabular salt-subsidence model is generally consistent with the conceptual model of a mature natural paleosubsidence feature (Figure 9-3) conceived based on a single, low-resolution, single-fold seismic-reflection sections from the British North Sea (Figure 9-4) (Lohmann, 1972). This conceptual earth model of subsidence due to natural dissolution is based on a single snapshot in time provided by a single-fold

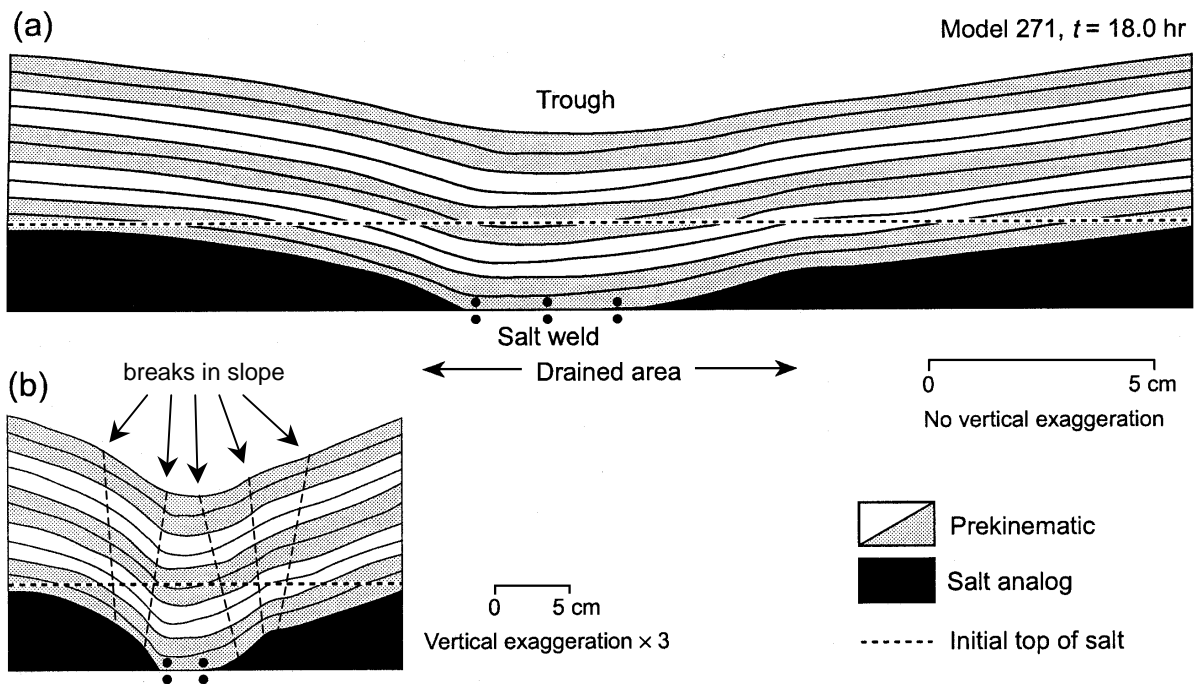


Figure 9-2. Sand and special flowing silicon were used to model deformation from salt dissolution. Silicon, simulating salt, was drained from the bottom of the test tank to allow observation of deformation in brittle overburden (sand simulates brittle rock in this design) (from Ge and Jackson, 1998).

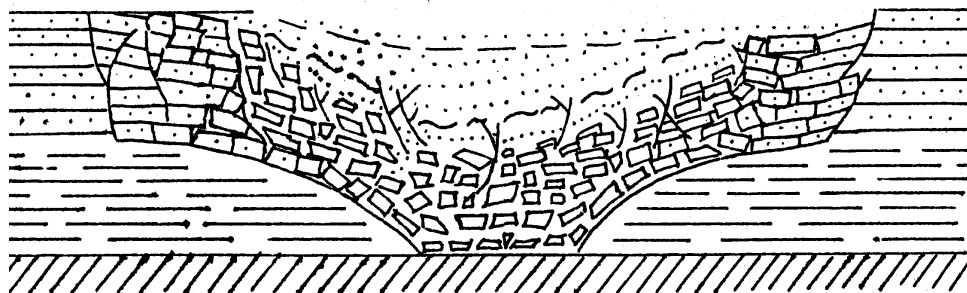


Figure 9-3. Conceptual model developed based on seismic observations of subsidence in British North Sea (modified from Lohmann, 1972).

seismic-reflection section (Figure 9-4). This conceptual model assumes leaching alone is responsible for this structure and does not consider creep an option.

Conceptual models developed from borehole studies of collapsed solution mines (Walters, 1978) do not agree with the deformation displayed in this North Sea conceptual model or physical models of collapse structures and associated progression (Figure 9-2). Clearly, for the tabular physical model to emulate a solution-mine subsidence structure (Figure 3-11), a stable void must grow beneath the overburden, culminating in predominantly vertical failure and development of a fault-controlled collapse breccia column. Growing and maintaining a stable void is not possible with this physical model design (Ge and Jackson, 1998).

The geometry of the principal withdrawal volume appears consistent with a complex cone (Figure 9-2). No clear fault offsets were observed in the overburden strata of the physical model (Ge and Jackson, 1998), and a wedge-shaped radial reduction in salt thickness is evident with increasing offset from the drain holes (Figure 9-2). Obvious is a striking

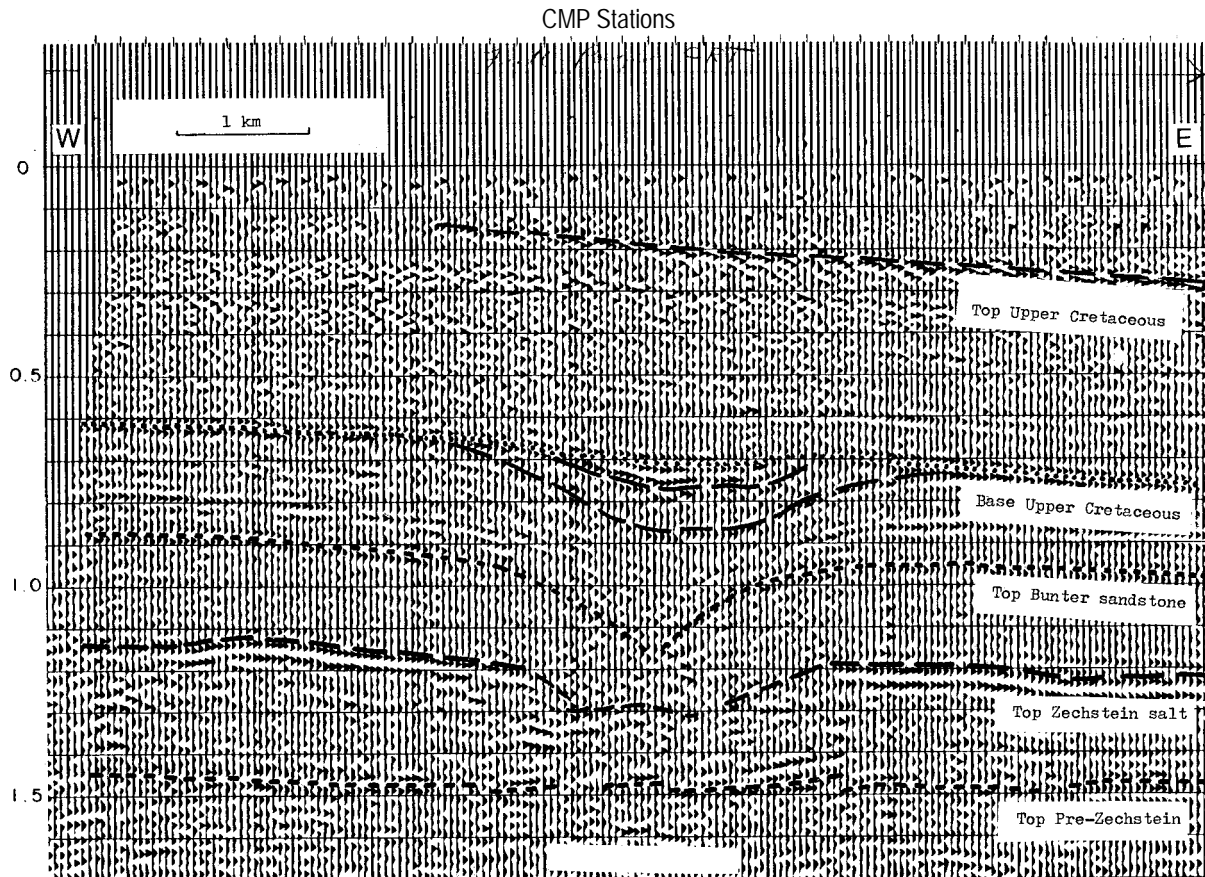


Figure 9-4. Common offset seismic section from the northern part of English Zechstein basin. Subsidence feature resulting from salt dissolution and failure pre-deposition of the Upper Cretaceous units (Lohmann, 1972).

similarity between the tabular physical model and the mature stage of the subsidence feature diagrammed from the single North Sea seismic section (Figure 9-3). Without intermediate stages of the physical models available (Figure 9-2), it is not possible to determine how or if even a very small void formed during the development of the collapse structure in the physical model and, if it did form, if it underwent stable growth prior to roof failure and subsidence of overburden strata. Uniform growth analogous to sand through an hourglass is the most likely physical model formation scenario, a process that would be inconsistent with solution mining or borehole-induced dissolution and collapse. Clearly the physical models do not address the complexities of non-uniform failure of individual beds.

Critical to how a void grows and overburden subsides in all these models is the initiation point of leaching (water inlet or source point) and exit point(s) or drain geometry. Based on the lack of faults and uniformity of the layered strata (overburden) in the physical model (Figure 9-2) it is reasonable to suggest overburden subsidence en route to the displayed physical model was volumetrically and temporally consistent with salt withdrawal. Previously suggested differences between the physical model and conceptual processes are non-trivial, but do not negate the legitimacy of developing generalized, ideal collapse and subsidence scenarios for various settings and hydrologies using these withdrawal-based physical models as a means to improve the understanding of subsidence processes.

Seismic Characterization of Dissolution and Creep

It has been suggested that halokinetics and subsrosion are difficult to distinguish when both phenomena occur together in nature (Lohmann, 1972). Because halokinetics is a specific gravity drive form of halotectonics, it is reasonable in this case to equate the two. Based on the materials used and drain approach taken for the physical models, it would be plausible to suggest either leaching or creep could be responsible for the salt geometry outside the drain cylinder. Suggesting it difficult to distinguish natural dissolution from creep is not surprising considering that a single seismic example of subsidence appears to be the basis for that statement. The physical models referenced and compared in this manuscript do not allow distinction between leaching and creep due to the drain style of salt removal.

Differences between creep and natural leaching are suggested in this manuscript to be distinguishable on high-resolution seismic data when data fidelity allows delineation of subtle changes in reflectivity of the salt/overburden contact and/or where interbedded insoluble rocks appear distorted or displayed marked changes in attributes (Figure 9-5). It is not common to observe extreme folding and dramatic amplitude changes in the top of salt reflection or reflections within the salt interval but away from the collapse volume. This statement comes after studying a large number of seismic images of natural subsidence features with analysis focused on reflection-wavelet characteristics and reflection deformation. Even considering the most optimistic creep rates for anthropogenic solution features, creep is not a viable and seismically observable process associated with currently active sinkholes.

Changes in seismic character as a response to dissolution are likely similar to changes suggested to be predominantly the result of creep (Figure 9-6). It is reasonable to interpret amplitude anomalies and irregular bed geometries within the salt interval as the result of dissolution and/or creep when drape is obvious in the Stone Corral Formation and other

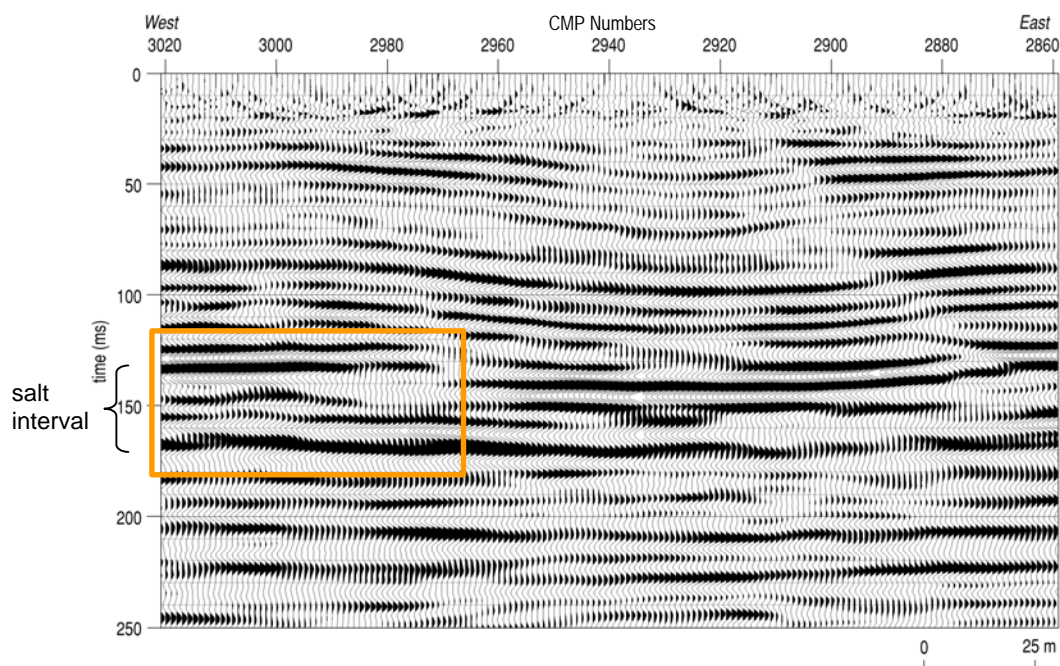


Figure 9-5. Migrated CMP stack along U.S. 50 Highway in central Kansas. Paleosubsidence feature beneath station 2930 has no expression on the ground surface. The orange box highlights a segment of the salt interval where undulating reflections are isolated to only within the salt. With no overburden effects from these disturbed reflections, creep is suspected.

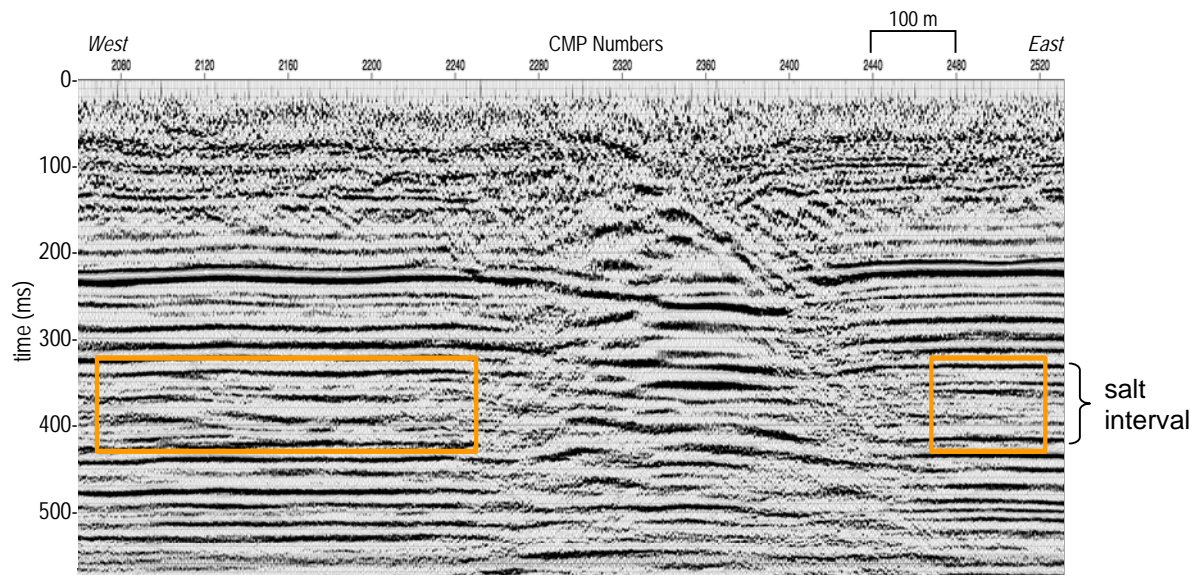


Figure 9-6. CMP stacked section with disturbed salt boxed on the left and undisturbed salt indicated on the right. Surface depression is between stations 2280 and 2400.

prominent reflections immediately above the salt, while reflections from below the salt (Chase Group) are uniform. Comparing undisturbed salt reflections (east end) to reflections with prominent drape indicative of subsidence (west end) provides an excellent empirical model of a possible reflection-wavelet response to dissolution and subsidence (Figure 9-6). No surface expression or evidence of subsidence exists within the Cretaceous and Quaternary portion of the section (upper 120 ms) in areas west of the sinkhole edge (station 2240) where Permian beds are disturbed. Because leaching at this site was instigated by at least two failed disposal wells, it is reasonable to interpret these seismic anomalies and subsidence in the Stone Corral Formation reflection a response to dissolution as indicative and representative of dissolution only and not creep.

Drape in the Stone Corral and Upper Permian shales at some sites will match temporally and spatially with synforms observed in the deeper salt layer (Figure 9-6 west), while extreme fold geometries within the salt interval at other sites can appear to correlate with only subtle and in some case no undulations in the overlying Upper Permian shales (Figure 9-5 west). These differences seem to be uniquely related to different natural and anthropogenic dissolution, subsidence, and/or glide creep interpretations. Considering the horizontal scales of these two sections (Figure 9-5 and 9-6), short wavelength folding (Figure 9-5) with no apparent expression in the overburden is suggestive of creep and characterized by reflections with marked changes in frequency (possibly phase) and amplitude. These wavelet characteristics are similar to models of tuning effects associated with cyclic thin beds (Knapp, 1991). Structural characteristics of insoluble layers within the salt interval that are mirrored in the overburden and not present below the salt layer are likely the effect of dissolution and subsidence (Figure 9-6). Extreme geometric distortion of rock layers within the salt interval but without associated deformed overburden are strong candidates for classification as creep structures driven by differential pressure and wetting during the development of dissolution voids.

Real Data Compared to Physical Models

Single-episode Subsidence

Contrasting the geometry of the tabular salt physical model (Figure 9-2) and real data examples with simple and reasonably uniform geometries reveals several obvious similarities and differences. It appears formation of broad subsidence structures in overburden with synform geometry begins with the development of a relatively small collapse breccia or chimney feature within the salt. In time the overburden forms a broad, gently draping synclinal structure significantly larger than the initial void's lateral extent (Figures 9-7 and 9-8). The consistency and similarity in deformation geometries of these single-episode dissolution and subsidence structures is quite compelling evidence supporting the physical

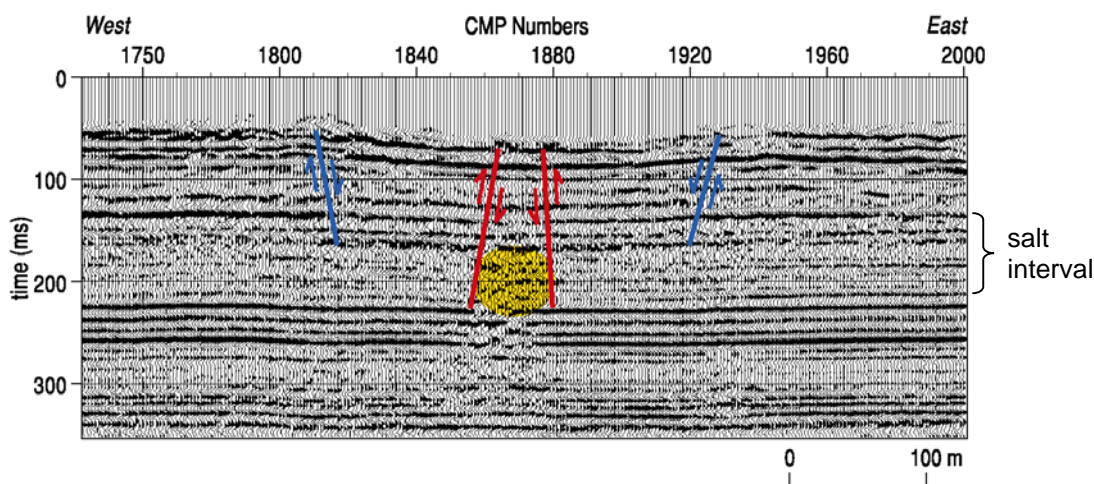


Figure 9-7. Paleosubsidence feature with high-angle conical faults defining a broad, synclinal subsidence geometry and dissolution that appears to be concentrated in a small area directly beneath the center of the bowl-shaped subsidence depression.

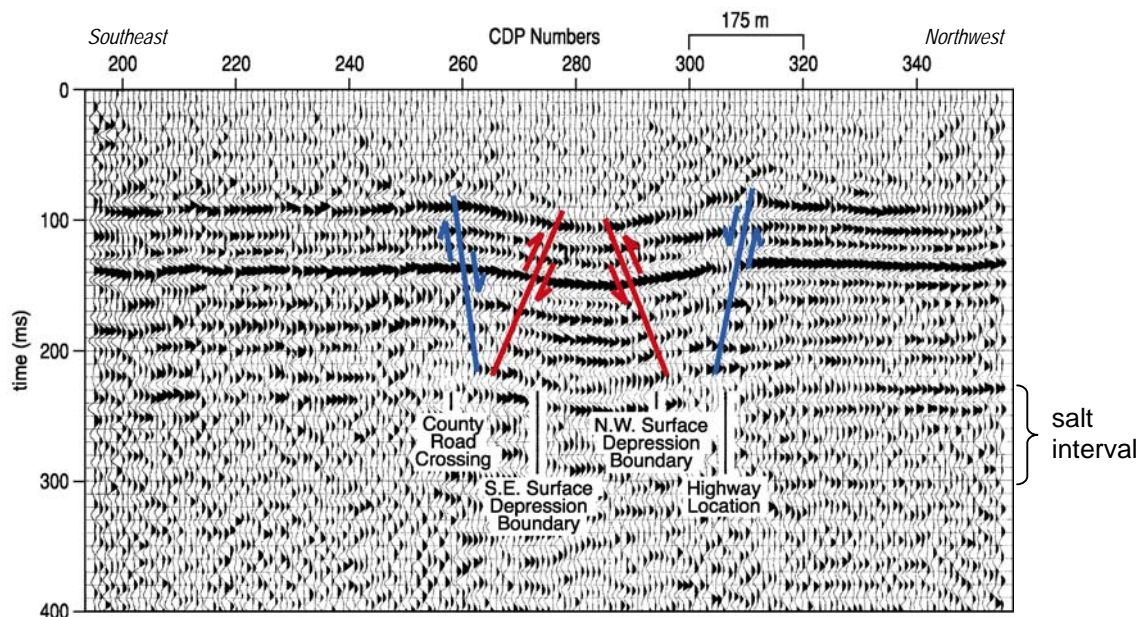


Figure 9-8. Oil-field brine-disposal well with over 200 m of surface depression defined by a gentle sag-like feature that formed at a gradual yet consistent subsidence rate. Broad synclinal subsidence feature clearly appears to be the result of ductile deformation; however, with the resolution of these data, faulting as interpreted and fractures associated with bed flexure would not be obvious. Based on mechanical models and stress scenarios, these structures are highly likely.

model. However, several questions still exist with respect to the changing stress fields and associated change in apparent fault control evident in the real data and suggested not to be observed in the physical models. Both real data examples can, in general, be characterized by broad synclinal structures with apparent high-angle normal faults defining and controlling radial expansion. Curious is the fact that these two subsidence features are the result of dissolution by completely different sources and associated processes—one is the result of natural dissolution with paleosubsidence and no surface expression (Figure 9-7), while the other is related to an oil-field brine-disposal well breach with an actively subsiding surface depression (Figure 9-8).

Resolution potential of the CMP stacked section from the failed brine-disposal well (Figure 9-8) is significantly lower (about half) than data from the natural feature (Figure 9-7), while possessing similar reflection geometries and data quality. Adding to the difference in fidelity is the four-times difference in the spatial sampling interval. Also noteworthy is the very limited depth of seismic-energy penetration at the oil-field brine-disposal well site with reflection returns limited to time-depths less than around 250 ms (Figure 9-8). CMP data over the paleostructure possess high-quality reflection returns evident at time-depths in excess of 350 ms (Figure 9-7). This highlights the improvements in data quality related to resolution, signal-to-noise, and penetration depths for near-surface applications across the 15-year time span between 1984 and 1999.

This natural dissolution feature (Figure 9-7) possesses structures generally similar to representations at the mature stage of both physical (Figure 9-2) and conceptual subsidence models (Figure 9-3). A disturbance in the coherency of reflections within the salt interval near the center of the synclinal-shaped structure is interpreted to be a narrow deeply leached volume (Figure 9-9). Coherent reflection events interpretable in this narrow zone possess a lower dominant frequency and higher amplitude than stratigraphically equivalent reflections in areas with no apparent deformed overburden. These unique reflection-wavelet characteristics are likely related to either collapse breccia or localized dissolution along insoluble layers. With the very narrow, almost fracture-looking appearance of this dissolution volume in the salt, it seems unlikely significant amounts of unsaturated brine made contact with the salt as it passed through this vertical zone. Fluid exchange under gravity drive likely forced a saturated brine with minimal to no capacity for harvesting more salt through the salt interval.

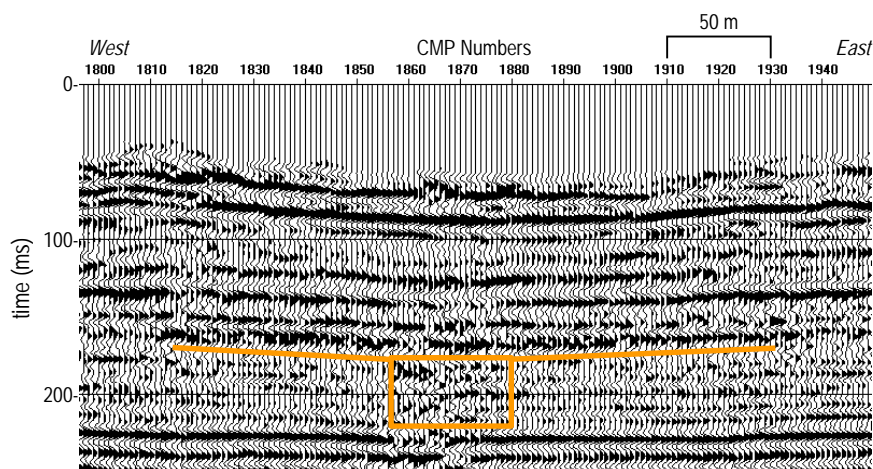


Figure 9-9. A portion of Figure 9-7 highlighting the subsidence-feature geometry. The box includes what is interpreted as a dissolution volume, seismic unique with diffractions from bed terminations and low-frequency, more chaotic events.

Diffractions indicative of bed terminations are evident and likely from insoluble interbedded layers within the salt interval. A marked difference between these data and the model is that a significant volume of salt is still present beneath the synform.

Thinning along the top of salt is evident and indicative of leaching along the base of the shale caprock likely from water sources structurally above the salt interval (Figure 3-5). A broad, more than 200-m-wide, relatively thin “morning glory” or Salzpegel-shaped dissolution void likely formed and failed, allowing the top of salt to drop around 10 m at the trough center to zero at the rim of the bowl structure. Apparently this collapse sealed the inlet or outlet, and the dissolution process was arrested. The physical model (Figure 9-2) lacks any distinguishable properties at the salt/overburden contact that would justify the observed reflectivity change and resulting amplitude anomaly in the salt-reflection wavelet on the real seismic data (Figures 9-7 and 9-9).

Alternatively, but extremely unlikely, after the development of the near-vertical dissolved volume, differential-pressure-instigated glide creep could have mobilized the salt in an extremely uniform fashion along the salt/shale contact, resulting in the bowl-shaped geometry and increased thinning of salt toward the drain (dissolution volume). Without some deformation in interbedded salt layers, this salt mobilization seems unlikely. As well, fluid could have entered from below the salt and leached upward until contact with the caprock, when dissolution was redirected radially away from the more vertical dissolution volume.

Synform bed geometries and apparent failure mechanisms interpreted from seismic data across these two uniquely different subsidence features (Figures 9-7 and 9-8) do not appear to relate or distinguish according to dissolution rate or instigating fluid source (natural vs. anthropogenic). Both subsidence examples here have large bowl-shaped structures that impact overburden horizons with more than an order of magnitude larger areal extent than the interpreted dissolution zone. Structures within these subsidence features appear to have ductile-type deformation (of course, as previously discussed, this phenomenon is related to seismic-resolution limitations) defined by both normal- and reverse-fault planes consistent with the changing stress regimes. With both features evident as large bowl-shaped depressions in the overburden beds—one subsidence feature related to a failed brine-disposal well and a second likely related to faults or fractures and a natural water source—no apparent relationship or common denominator exists relating fluid sources with failure processes or subsurface-reflection geometries at this point in time.

Active Leaching and Subsidence

One of the most enlightening and highest quality seismic sections included in this manuscript was acquired across an active sinkhole that formed as a result of a failed plug in an (or possibly unplugged) abandoned oil well in north-central Kansas (Figure 9-10). This seismic section effectively imaged beneath an active sinkhole during an intermediate stage of dissolution and subsequent subsidence. Structural characteristics depicted are diagnostic of stress regimes and structural growth that appear to contradict the tabular-salt physical model (Figure 9-2). Considering this is an active sinkhole (deepening), the near-vertical collapse structure imaged on seismic data, and data from a borehole drilled into the sinkhole in the late 1960s, dissolution must be progressing from top to bottom in the salt bed. As the dissolution face has moved deeper into the salt interval, the associated dissolution volume appears to have maintained a predominant inverse conical geometry (narrowing-upward chimney) with the areal extent of the dissolution-altered salt horizon larger than the subsidence-affected

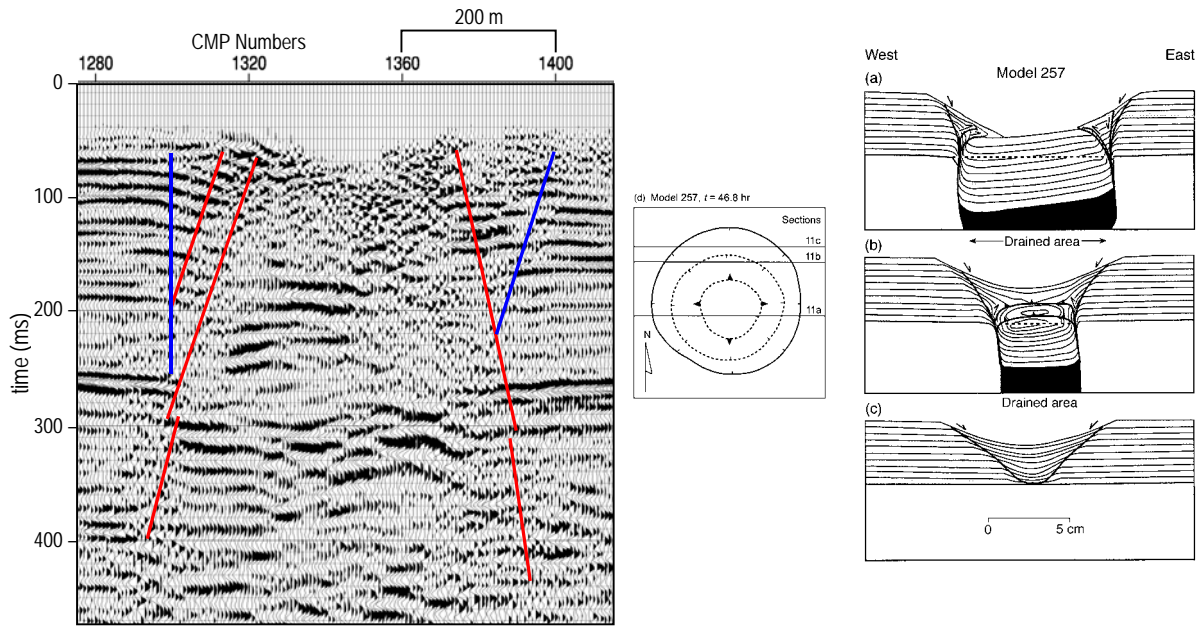


Figure 9-10. Seismic-reflection section from Witt sinkhole in central Kansas, interpreted with faults indicating bed offset and relative movement. A salt-diapir model with several cross sections demonstrating structures highly dependent on relative location (models from Ge and Jackson, 1998).

overburden. Subsidence structures appear more vertically focused on these seismic-reflection data than most active features discussed in the previous chapter. Initial development of the natural subsidence structure previously discussed in this chapter was predominantly vertical with dramatic lateral growth during later stages of development (Figure 9-9).

The physical-withdrawal model for bedded salt (tabular model) (Figure 9-2) appears to reasonably represent both the natural and anthropogenic subsidence features previously discussed, but fails to match the seismic representation of this active sinkhole's subsurface expression (Figure 9-10). There is no clear difference between the two anthropogenic sites (Figures 9-8 and 9-10) that would account for the different failure mechanisms based only on an initial inspection of the seismic data. A profound difference is that one is active (Figure 9-10) and the other is dormant (Figure 9-8). Active dissolution began near the top of the salt interval at the Witt sinkhole (Figure 9-10) and, based on drill investigations, progressed downward, forming a hemispherical dissolution pattern en route to the base of the salt interval.

Subsidence within this feature as interpreted from seismic data is predominantly controlled by a series of reverse faults representative of compressional strain (Figure 9-10). Radial growth within the salt interval is, of course, limited by fluid dynamics, primary fill (collapse breccia), and chemistry of waters. With the original petroleum borehole likely acting as the outlet for saturated brine moving into the solution volume from the overburden, leaching will concentrate around the borehole, extending radially away from that outlet as far as fluid exchange will allow. Access to fresher waters at the dissolution front/face will become increasingly more problematic as the salt stock in close proximity to the borehole is harvested.

It is obvious from studying seismic energy reflected from the salt interval that dissolution has been confined to a volume consistent with the location of the abandoned well. Based on drill and seismic data, the old well bore is providing the outlet for saturated brine to

move into deeper, lower-head confined aquifer units. Inlet for the fresher waters could be any one or combination of seismically imaged faults that now breach the confining units originally acting to isolate the many Cretaceous aquifers. Unique to this subsidence feature relative to the previous two in this section (Figures 9-7 and 9-8) is the vertically confined nature of the subsidence structure. Simplistic models suggest once breakthrough at the bedrock surface occurs, compressional stress is relieved and extensional forces become dominant, resulting in radial growth of the bowl-like structure. The width of this subsidence volume and relative location of the bounding (furthest from center of subsidence structure) reverse-fault planes in combination with the gradual-subsidence history suggests compressional strain has continued to build after initial bedrock failure.

The hemispherical dissolution front of this subsidence feature (Figure 9-10) is likely still advancing downward following the old drill hole, and based on the geometry as interpreted on the seismic-reflection data, it has not yet encountered the basal contact of the salt. This progression pattern can explain the structural similarity between the seismic interpretation and the diapir dissolution model (Figure 9-10a, b, c). If fluid exchange at the dissolution front is still possible once contact is made with the basal reflector and vertical growth is arrested, horizontal growth will be concentrated along that basal reflector and near the top of the salt interval, continuing until fluid exchange is no longer possible.

Dissolution will likely be most active near the top of the salt interval because fluids near the overburden inlets are the freshest. Fluid salinity will increase with increasing time spent in the salt interval. During this horizontal growth stage, significant radial expansion of sag will occur at the ground surface within a region defined by the angle of draw. Subsurface development will continue as a bowl-shaped depression forms consistent with the bedded-salt physical model. Once dissolution halts near the top of salt due to hydrologic changes, the ground sinking near the center of the surface depression will slow, with movement becoming more a function of overburden compaction.

It is therefore possible using the findings of this study to suggest that the dissolution feature on I-70 (Figure 9-10) will continue to subside at its current gradual rate of 10 to 20 cm/year until the downward-progressing dissolution front either encounters the basal contact of the salt or loses fluid exchange. If dissolution continues after the dissolution front contacts the basal interface of the salt, this sinkhole will begin to spread radially consistent with the angle of draw, which will likely mean ground sag will extend out almost 500 m from the center of the sinkhole.

Contrary to the generally accepted concept that dissolution will normally be most pronounced near the top of the salt as a direct consequence of the density of saturated brine, this subsidence structure (Figure 9-10) is overwhelmingly vertical. Based on compressional strain interpreted on seismic data, this structure appears to be actively leaching from top down into deeper layers of the salt stock. Seismic images presented in this manuscript have documented preferential leaching near the top of the salt or along an insoluble contact within the salt bed. It is a process that has been suggested in previous work (Salzpegel) as dominant in cases of natural dissolution (Lohmann, 1972). However, seismic images of this anthropogenic dissolution feature appear to contradict that as the principal drive process.

After considering the fluid dynamics, this vertical-growth setting is simply the result of a fluid outlet near the bottom of the salt interval with minimal or no flow restrictions. For natural features fluid exchange is slow and freshwater spends more time near the inlet (normally at the top of the salt), thereby enhancing leaching near the top with fluid migration

more under the influence of density than pressure. For many anthropogenic cases the borehole provides a high-velocity flow outlet, thereby minimizing the time unsaturated brine dwells near the top of the salt and reducing the percent dissolved solids in the fluid when it reaches the dissolution front closer to the outlet. The overall width of the dissolution-affected salt is likely directly related to fluid velocity exiting the dissolution volume.

Evident from the physical model (Figure 9-10a, b, c) is the complexity and changes in the cross sectional character and controlling structures as the position of the cross sectional profile over the dome structure changes. This implies a significant level of concern and consideration needs to be given to line locations relative to the dissolution volume and overburden-subsidence structure when investigating and interpreting these relatively small (in comparison to seismic wavelengths) dissolution features with 2-D seismic. Obvious here (Figure 9-10), if this seismic profile would have been acquired along an edge of the sinkhole (necessary in many cases because of access problems), the structures imaged on seismic data would have appeared more like the wide bowl structures observed on previous sections (Figure 9-4 and 9-7) and more consistent with a bedded-salt physical model (Figure 9-2) (the difference being distinct bed offsets and steeper-sided structures).

The major difference between the bedded-salt physical model (Figure 9-2) and the physical diapir model (Figure 9-10) for seismic lines over the subsidence-altered overburden, but off-centerline of the dissolution volume, is the presence of bed offset and therefore the implication of faulting. Faulting appears evident within the subsidence cone of the diapir physical model even off to the side of the dissolution volume, while the bedded-salt model shows no evidence of faulting, only ductile-appearing deformation. It is reasonable, then, to suggest that many previous studies of dissolution sinkholes imaged with seismic and interpreted to have only high-angle normal faulting may have simply been positioned inappropriately to image all key structural components. Physical models of salt-bed dissolution depict radial expansion in post-surface-failure subsidence structures related to radial expansion as dominated by tensional strain. The predominantly reverse fault nature of structures beneath the I-70 (Witt) sinkhole is unexpected and likely diagnostic of the stage of development, fluid dynamics, and site-specific geology.

It is unlikely that horizontal dissolution and/or creep has played a major role at this stage in the Witt sinkhole development as evidenced by the excellent match between the seismic-imaged structures beneath the Witt sinkhole and the physical model of a salt diapir. Salt material available for removal in the diapir physical model was limited to a cylindrical volume bounded by immobile material. Structures on seismic sections compared to physical models of diapirs (cylindrical salt model) are amazingly similar during the active middle dissolution stages of anthropogenic development. In the real-earth setting a laterally continuous volume of salt is available, but dissolution is limited to the model equivalent of a cylinder.

Paleosubsidence: Reactivation

As previously demonstrated, the bedded-salt physical model correlates well to both natural and anthropogenic subsidence features. Paleosubsidence features near the dissolution front have been interpreted on seismic data to have structural components with compressional and tensional strain (Figure 9-11). A particular paleofeature with no surface expression is characterized by resolvable bed offset along both reverse- and normal-fault planes and has physical evidence of recent inactivity. From reflections above the paleostructure, it appears

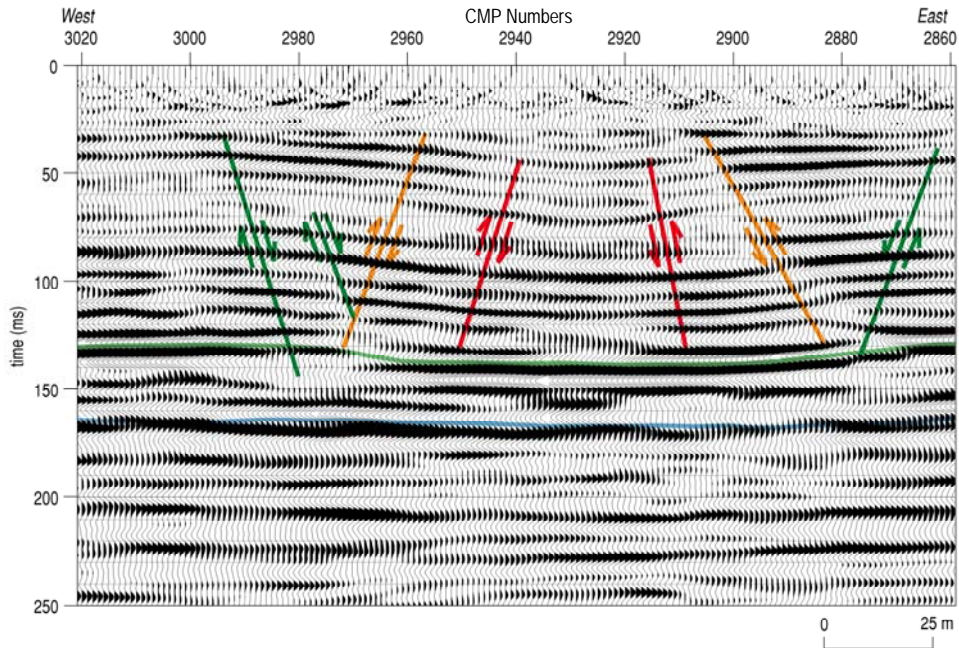


Figure 9-11. Migrated CMP stacked section near natural dissolution front with no surface expression clearly displays at least two episodes of reverse faulting with associated normal faults.

this feature has been dormant since at least deposition of nearly 20 m of Quaternary fill. Therefore it is reasonable to assume this feature has been stable for more than 2 million years.

With clearly discernable bed offsets in the overburden, this inactive, natural feature (Figure 9-11) is not consistent with the apparent smooth, offset-free, bowl-shape geometry observed in the bedded-salt physical model (Figure 9-2). These differences are clearly not specific to inactivity or natural versus anthropogenic hydrologic factors because examples of natural, inactive subsidence structures (Figure 9-7) less than 20 km from this site appear reasonably consistent with the bedded-salt physical model. Obviously there is a wide range of possible variables that influence structural development of these subsidence features beyond just subsidence rate and fluid source. Principal differences between these two dissolution features (Figures 9-7 and 9-11) are salt lithology and thickness and fluid chemistry and rate of flow. Clearly these variables could dramatically change the mechanics of a subsidence event. This paleoevent (Figure 9-11) possesses strain characteristics resembling those observed on physical models of diapirs, implying limited horizontal salt harvesting during initial stages of development.

Reactivation of dormant natural dissolution features introduces complexities that physical models are just not capable of emulating. Natural features can experience multiple episodes of dissolution and resulting subsidence with each session halted or initiated based on changes in fluid dynamics and fluid source and exit points (Figure 9-12). Physical models available to compare with seismic-imaged subsidence features were all developed during one continuous withdrawal stage that halted after removal of the entire salt interval above the drain zone. Clearly this scenario is not applicable for thick bedded salts with interbedded insoluble layers capable of altering the hydrology and dissolution rates. Changes in reflection character as a result of subsidence are quite noticeable in amplitude, coherency, and subsalt noise. Differentiating structural components related to different periods of dissolution and associated subsidence is beyond the potential of two-dimensional seismic data, but disturbed

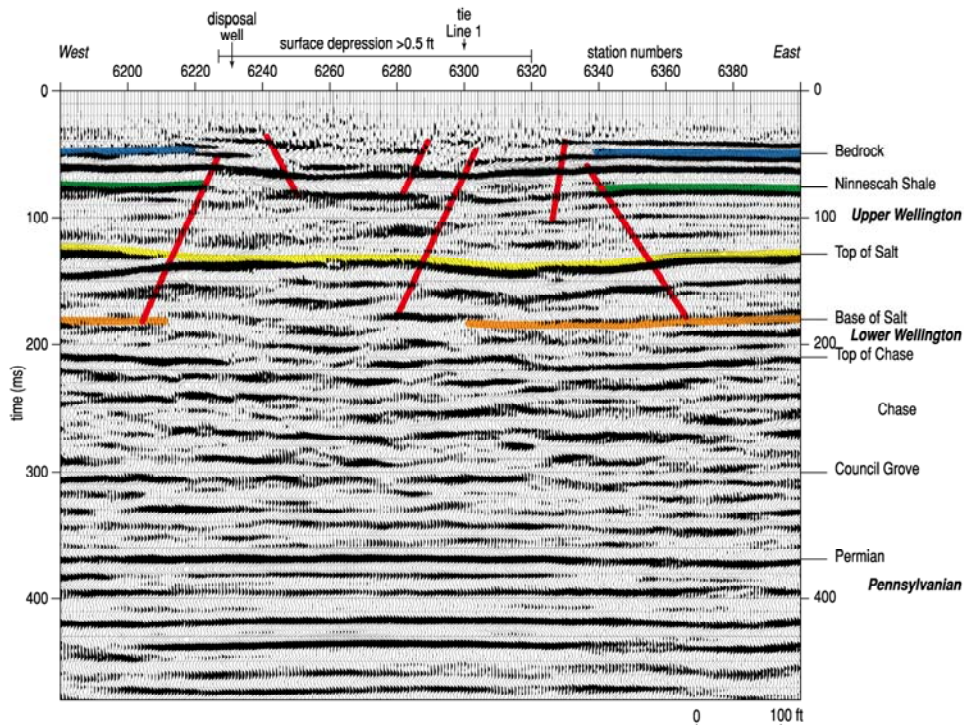


Figure 9-12. Rayl sinkhole in central Kansas, where subsidence began at a gradual rate of around 10-20 cm/year. Juxtaposition of a saltwater-disposal well concerned the landowner and prompted questions relating to the fluid source for this feature. This seismic-reflection section clearly imaged several previous episodes of subsidence from natural causes.

shallow reflections indicative of current subsidence are clearly distinguishable and geometrically unique. Collapse structures and bed distortion associated with multiple episodes of dissolution and different areas of active leaching results in a highly chaotic reflection pattern with significant out of the plane energy that simply cannot be delineated on two-dimensional seismic data.

From previous discussions, rate of subsidence and leaching likely have significant impact on deformation style and duration of a single dissolution episode, especially for natural processes. Based on the geometry of the overburden strata at the Punkin Center site in central Kansas, dissolution of the salt interval occurred in a very irregular yet generally continuous fashion (Figure 9-13). Unlike the previous site (Figure 9-12), where subsidence was active during distinct periods separated by extended periods of dormancy, at Punkin Center the pre-Quaternary subsidence appears to have been active throughout most of the dissolution process, leaving the altered subsurface without apparent uniformity in bed distortion associated with individual failure events.

From coherent reflection events alone, the variability in fold amplitude and wavelength is evident and indicative of changes in forces and/or processes likely driven by variable leaching rates and fluid controls. With limited reflection coherency within the salt interval itself, it is not possible to distinguish creep from dissolution-reflection geometries or characteristics as proposed earlier in this chapter. Due to data limitations, nondepositional distortion in overburden-reflection patterns cannot be correlated to interbedded insoluble layers within the salt and therefore several subsidence scenarios are possible with no chance of identifying or designating the subsidence history.

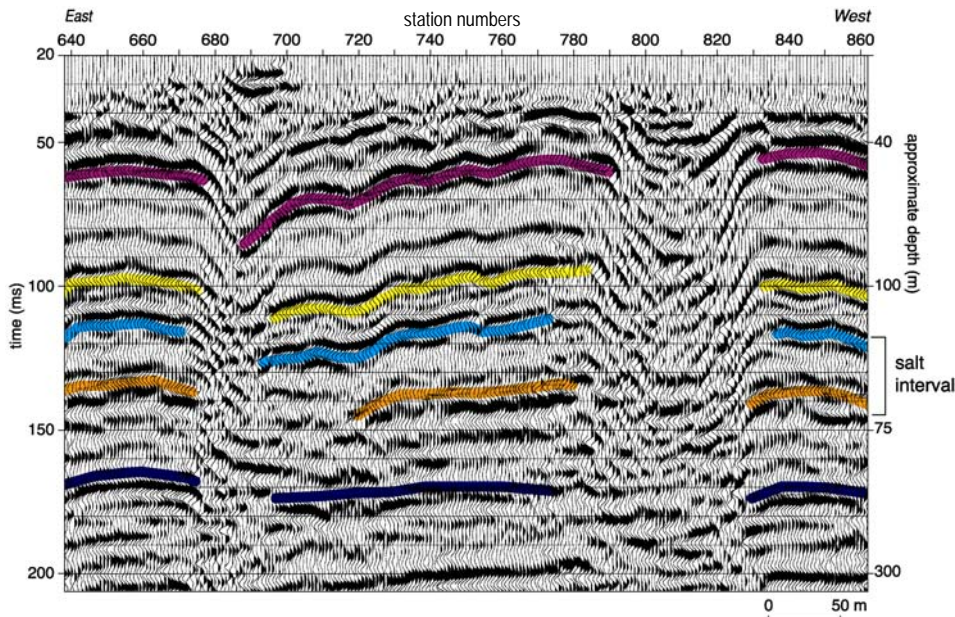


Figure 9-13. Punkin Center seismic profile in central Kansas. Two uniquely different subsidence geometries suggestive of a complex dissolution process.

Some interesting commonalities emerge when comparing the physical model for a bedded salt (Figure 9-2) with these paleofeatures (Figure 9-13). As suggested in the previous chapter, deeper and steeper-sided subsidence features beneath 810 and 680 are likely zones where, if not the complete salt interval, a large percentage of the salt has been removed. Once the base of salt was reached, the dissolution face/front began spreading along this basal contact and initiated dissolution along the edge and top of the salt around the perimeter of these steep-sided paleofeatures. These two deeper steep-sided subsidence volumes were likely active at different times with the youngest responsible for the current dip direction. Under that scenario the deeper more severe subsidence feature beneath station 810 is likely the older, with the collapse feature at 680 active most recently and therefore affecting the local dip of overburden beds between these two collapse structures.

Matching the proposed Punkin Center site subsidence history with the physical models highlights several marked similarities and likely keys to the progression of subsidence events captured in this seismic snap shot (Figure 9-13). The void responsible for the subsidence feature beneath 810 likely moved downward as a hemispherical front until vertical leaching was arrested at the base of salt. With the clearly interpretable beds within the collapse chimney, it is unlikely the subsidence feature formed catastrophically; this is mainly suggested due to the lack of chaotic energy arrivals associated with collapse breccia. At that milestone in this collapse feature's past, minimal to no horizontal leaching along the top of salt progressed with minimal extensional stress until a structure resembling the diapir physical model (Figure 9-10) and single-episode natural dissolution (Figure 9-9) had developed. At this point the dissolution activities at this feature likely halted. At some point later in time, the same sequence of events began beneath station 680. Based on the relative general dips in reflections between station 680 and 810, these collapse chimneys were distinct and separate events.

Alternately based on reflection-wavelet character, these two different subsidence structures (one type being deep-seated subsidence [680 and 810], the other being the apparent highly folded (undulating) beds between these structures) could have formed through

completely different processes than previously suggested. It is possible that active dissolution and subsidence began beneath stations 680 and 810 with glide creep in the salt between the structures responsible for the short wavelength folds. As previously suggested, considering the time duration that these processes could have been active at this site, the extreme pressure differential between the dissolution volume and adjoining salt layers, and the presence of fluid, localized glide creep is possible even under these low confining pressures.

Resolution and Structure Anomalies

Resolution potential of these Punkin Center data is excellent with a dominant frequency easily in excess of 150 Hz (Figure 9-13). Radius of the Fresnel zone, and therefore horizontal-resolution potential, is on the order of 30 m for reflectors around 300 m deep at this site. Reflection synforms representing the steep-sided chimney features possess severe curvatures with radii around 25 m. The entire deep-seated subsidence structure is only on the order of 50 m across. Dips on the apparent collapsed altered reflectors representing the sides or lips of the structure appear to be more than 70° in some places. An example of the severity of these very abrupt transitions from relatively horizontal to steeply dipping reflections is along a stretch of seismic line west of station 840 where reflections go from nearly horizontal to 65° dip at station 810. At station 670 these severely dipping events make this high-angle transition across a distance (25 m) significantly less than should be resolvable based on classic estimates of resolution potential. These unmigrated data possess characteristics that seem to exceed theoretical and practical horizontal-resolution limits. However, how much of the apparent reflection geometries are related to true reflectors and how much is an artifact of the extreme dip or bed terminations is not clear.

Faults and fractures are the most probable conduits for transporting the life-giving fluid necessary to instigate and sustain natural dissolution. However, faults are not diagnostic of dissolution. The most pronounced fault on any of the seismic sections displayed in this manuscript is interpreted to fully intersect and offset the salt interval but has no obvious associated dissolution (Figure 9-14). With the full 125 m of salt present at around 150 ms,

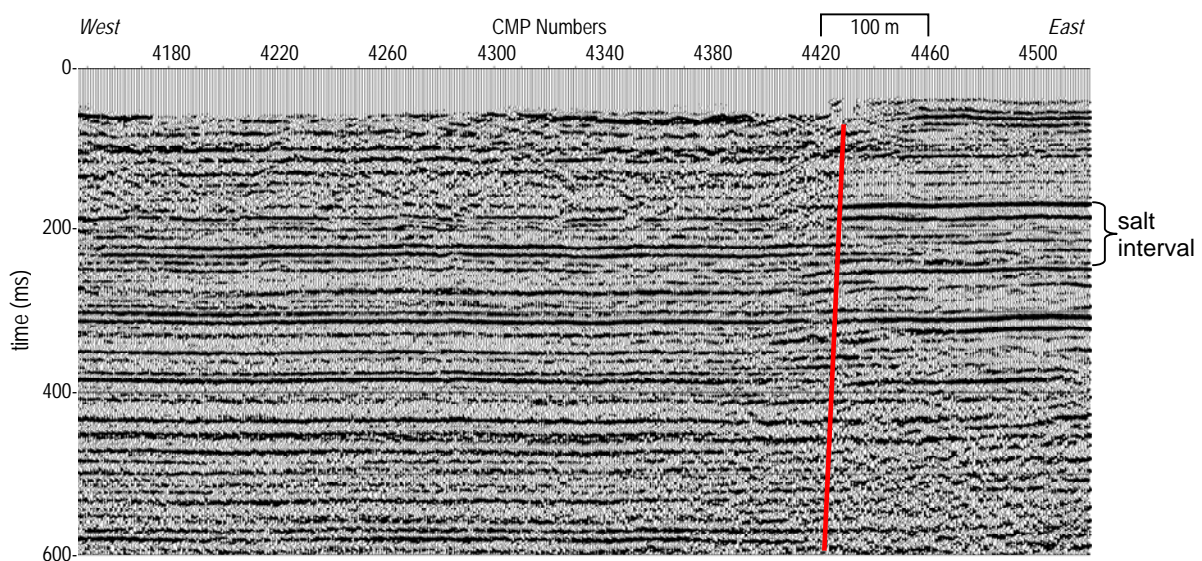


Figure 9-14. Seismic-reflection section from central Kansas around 20 km west of the dissolution front. Bed offset, diffractions, and notable difference in wavelet character across a feature that intersects the entire section is interpreted to be a fault suspected to be strike-slip.

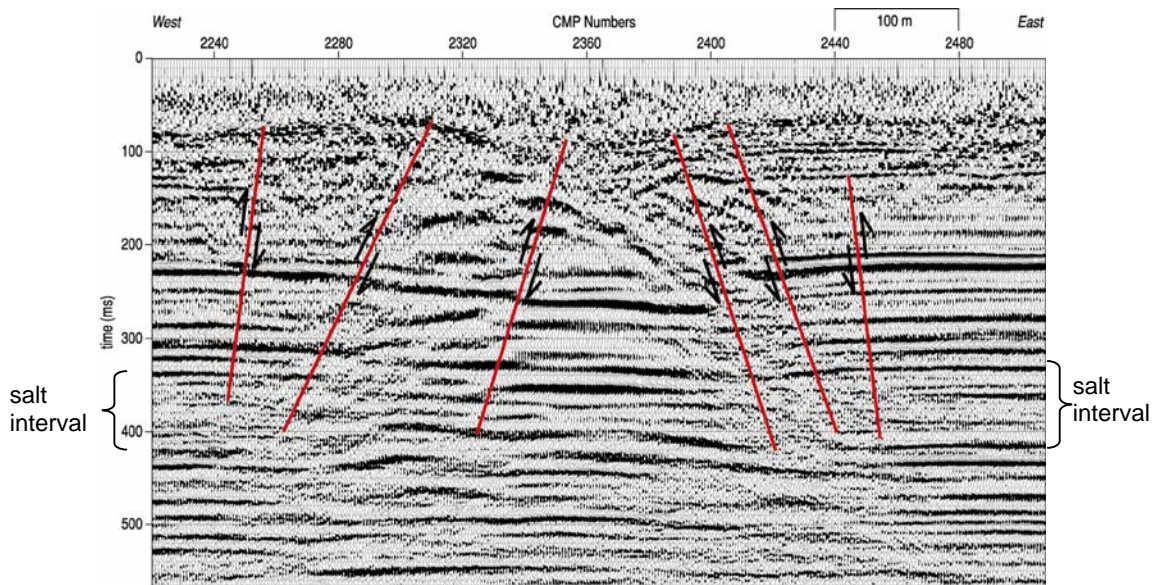


Figure 9-15. Gradually subsiding feature in south-central Kansas associated with at least two oil-field wells with lost containment. A majority of affected salt is west of the dissolution-induced collapse structure.

the fault at station 4425 should provide an excellent conduit for the freshwaters of the unconfined Equus Beds aquifer to directly access salt. No surface expression in the Quaternary-aged alluvial sediments can be directly linked to this lineament. This might be an example of the absolutely essential and pivotal role fluid dynamics plays in dissolution of any kind; one role possibly is that fluids can access the salt interval but no outlet is available, and therefore the exchange of saturated and unsaturated fluids might not be possible.

Active Anthropogenic Leaching

Complex flow patterns and large fluid volumes increase the rate of dissolution and appear to result in clearly brittle, block-type deformation (Figure 9-15). At this sinkhole site the subsurface affected area is orders of magnitude larger than surface disturbance. With more than 500 m of dissolution-altered salt and a surface expression less than 100 m in diameter, clearly the upward progression of the void is strongly influenced by compressional failure and reverse-fault planes. Subsidence has been constrained to an inverted-cone structure defined by concentric pairs of reverse faults in relatively close proximity to the responsible well bores. This offset geometry has formed a series of horst-like structures that have retained sufficient strength around the perimeter of a domed roof to continue to support compressional stress.

The salt-diapir physical model with non-uniform withdrawal provides a picture (Figure 9-10) resembling the gross structure within the subsidence volume (Figure 9-15). Correlating the model (Figure 9-10) with the seismic image (Figure 9-15) suggests more salt was initially leached on the east, resulting in a deeper dissolution volume. Based on reflection geometries, rapid leaching likely led to the development of irregular void geometries supported by sporadic pillars. With more than one well involved, a complex gallery likely formed intermittent and irregular pillars that were left to support the roof after the dissolution front/face passed. Asymmetric failure was likely strongly influenced by the location of these more resistant salt volumes that remained after passage of the main dissolution front. Rotational block-type failure is consistent with the characteristics of the

diapir physical model. Subsidence was likely initially instigated by the failure of one or more salt pillars.

Unique to this particular structure is the distinct, concentric series of matched reverse-orientation faults (Figure 9-15). With no obvious tensional strain, this feature is clearly too young to fit the physical models, but it is strain consistent with the early developmental stage of the solution-mine model (Figure 3-11) and the I-70 subsidence geometry (Figure 9-10). Failure is obviously along these three sets of reverse-fault planes relative to the sinkhole and deepest part of the subsidence structure. This failure sequence means the dissolution void within the salt continued growing even after initial subsidence reached the bedrock surface. This continued dissolution-void growth along the perimeter of the collapse feature created large unsupported overhangs that collapsed along reverse-fault planes during at least two different episodes.

Conceptually, once failure migrated through the entire section of overburden and affected surface failure and subsidence, intuitively compressional stress should not be reestablished across the collapse structure (Figure 4-6). Based on the simplistic arch model, once the center roof block fails the stress regime should switch to extensional. This void failure concept is analogous to a doorway arch when the keystone fails; connectivity between the two sides is lost and therefore compressional stress cannot be maintained and a single pair of reverse faults should be present from the salt to the bedrock surface defining the chimney-collapse feature.

This and other seismic sections have been interpreted to possess multiple matched sets of reverse faults near the center (relative to the collapse chimney) of the collapse structure. This apparent inconsistency is easily explained by considering the three-dimensional nature of the earth and the two-dimensional representations on seismic images and models used to view and describe these features. In a three-dimensional world, compressional stress can be established around the perimeter of a failure chimney structure analogous to an open ceiling in a domed-roof structure. Concentric reverse faults are the result of secondary collapse following subsequent build-ups in compressional stress around the rim of the opening in a domed roof remaining after initial failure. These concentric groupings of reverse faults define the throat of the chimney structure at different stages of enlargement prior to the eventual transition to an extensional stress regime.

Classic models of dissolution and stress distribution, both physical and conceptual, reasonably represent the stages of dissolution for uniform salt and subsidence of overburden. However, in nature variations in temporal and spatial characteristics of the controlling factors will be a strong influence on the development of these features and may help to understand why seismically imaged subsidence structures do not always match the configurations portrayed by these models.

Synergistic Discussion

With the rapid development of anthropogenic subsidence features, it is possible to seismically sample these features at various stages of development and correlate those to physical models and other subsidence features at the same stage but in different geologic settings. The collective data set analyzed in this manuscript provides the first ever opportunity to match up subsidence models with real data across a range of developmental stages (Figure 9-16). Interpreted seismic sections and overburden structural characteristics

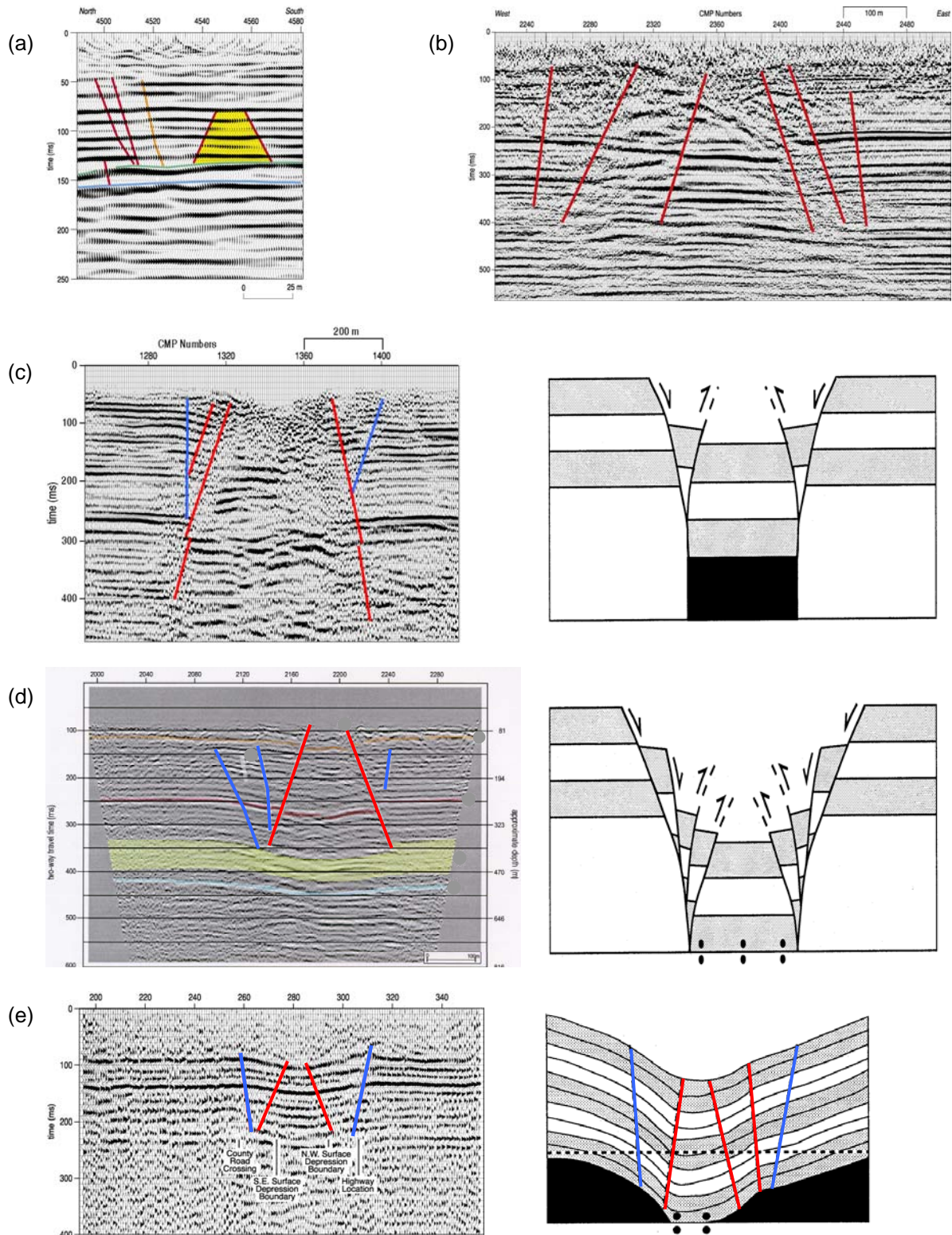


Figure 9-16. Models from Ge and Jackson (1998) compared to seismic data showing subsidence features at (a) Victory Road (Figure 8-4), (b) Leesburg (Figure 9-15), (c) I-70 (Figure 9-10), (d) French (Figure 5-12), and (e) Conoco (Figure 9-8). Each stage of subsidence maturity is correlated between real data examples and appropriate physical models. All real data examples used here except (a) are from brine-disposal-well failures.

from early stages of dissolution and subsidence (Figure 9-16a, b, c) reasonably match the diapir (salt stock) physical model. This suggests when initial dissolution begins near the top of the salt and advances predominantly downward, it will be confined to a cylindrical volume similar in shape to a diapir with fluid dynamics and flow portals as the dominant control variables.

Early stages of subsidence will be limited to an area equal to or less than the areal expression of the salt-dissolution volume. Once a dissolution void begins its upward migration to the ground surface, it will be characterized by compressional deformation. Surprising on many seismic images is the appearance of several episodes of reverse-fault deformation forming horst pairs (sets of reverse faults approximately equal distance from the center of the sinkhole and with similar angles) within the leached-salt volume (Figure 9-11 natural dormant feature and Figure 9-15 anthropogenic active feature). It appears these reverse-fault pairs form in succession, developing from the initial bedrock breakthrough and continuing throughout the active leaching period. Normal faults interpreted from near the top edge of the leached volume to the ground surface are generally at or near the angle of draw, signaling the termination of void growth (leaching) and the beginning of tensional deformation and radial-subsidence expansion (Figures 9-11 and 9-16c, d, e). From this point in time until a new episode of dissolution begins, subsidence will be limited to gravity settling and associated compaction with extension forming radial-tension fissures (circumferential and tensional cracks).

Estimating dissolution and subsidence rates and continuity of the process for natural events is difficult. Unlike anthropogenic-induced dissolution where generally a point source (1-D), like a well, represents the inlet and outlet, natural processes involve faults and fractures with complicated (3-D) geometries and flow patterns. With the apparent similarities between physical models and seismically imaged uniform, gradual anthropogenic induced dissolution and subsidence features, it is reasonable to speculate about rates for natural events with similar seismic representations through those stages. For paleosubsidence features with chaotic reflection and scattered energy returning from the breccia pipe, it is plausible to suggest a relatively rapid raveling and/or stoping of roof rock above a solution void. Where reflections represent a gentle draping overburden and either minor faulting or no apparent faulting, the entire process appears to have progressed gradually, taking years to centuries or longer to develop.

Complex Subsidence History

Fractures, faults, and folds provide weak zones susceptible to encroachment of meteoric waters. These linear fluid-exchange systems result in sporadic, localized leach zones that generally remove enough salt to propagate a subsidence event into the overburden (Figure 9-12). However, as salt is leached from layers where insoluble interbeds and impurities exist, these insoluble materials collapse into the dissolution zone thereby altering the fluid dynamics and leaching efficiency. Eventually enough lag builds up to halt or divert fluid flow. Also, post-collapse overburden rubble can act to restrict fluid movement. With the water source still present and faults, fractures, or folds acting as conduits, the process is likely to start up again along these permeable discontinuities in close proximity to previously leached areas, targeting a fresh exposure of the salt face. Hence most active natural dissolution features are a composite of multiple episodes of dissolution resulting in a complex pattern of collapse and deformed strata (Figure 9-17).

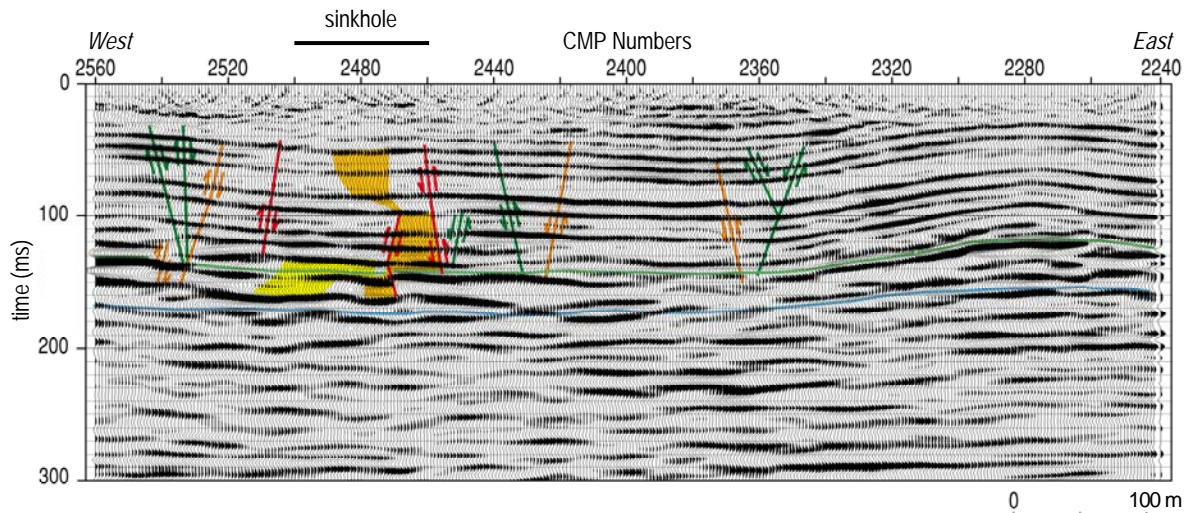


Figure 9-17. Victory Road east/west. Interpretation is speculative, but is based on models, other seismic profiles from area, and surface expression. Sinkhole is about 100 m wide from CMP 2500 to 2460. Several episodes of dissolution and subsidence have been active over the last several million years. Flat reflections beneath station 2400 at about 20-ms time-depth are Pliocene-Pleistocene Equus beds, indicating subsidence beneath that station is more than 2 million years old.

Solution Mine Collapse

Physical models previously discussed and compared to seismic images of collapse structures associated with sinkholes are not analogous to solution-mining void-collapse structures. Solution-mining voids are susceptible to rapid failure due to the large brine-filled volume of jugs and high vertical to horizontal dimension. Unlike the uncontrolled or natural dissolution voids, solution-mining jugs are by design large cisterns with the capacity to instantly consume tens to hundreds of cubic meters of overburden. Failure of a solution jug will progress analogous to a room and pillar mine collapse or carbonate karst-collapse sinkhole. All solution-mine collapse structures seismically imaged have been interpreted to initially fail through the consolidated rocks along reverse-fault-controlled chimney or conical structures with the size and failure characteristics of this initial surface expression dictated more by the properties and thickness of the unconsolidated material above bedrock than the subsidence features below bedrock.

Stopping and raveling are the principal failure mechanism, with the top of the void or collapse volume (roof rock) imageable on seismic sections. Once the sump represented by the dissolution jug is full of collapse breccia, subsidence ends and the overburden stabilizes. Through time, compaction of collapse breccia or raveling of the walls can destabilize the roof rock (excess compressional stress) and roof collapse resumes. If the bedrock surface is breached and the associated chimney-throat diameter at the bedrock surface increases sufficiently to no longer sustain compressional stress, tensional stress begins to control the gradual radial growth in the final stage in sinkhole development. Sag will extend a measurable distance from the sinkhole center as determined by the angle of draw and overburden material. The size of the affected surface (sag) can be several orders of magnitude larger than the sinkhole for deeper voids. Identification of void wall and estimation of the angle of draw are therefore critical to public safety and a challenge seismic has met on various occasions.

Features resulting from catastrophic failure of voids leached from salt have been seismically studied at two sites both with anthropogenic origin (Macksville and Mosaic). Neither of these sites possesses characteristics that distinguish them from gradual subsidence

structures or fail to correlate with the current physical models. In both cases the subsurface collapse structures are extremely complex, and access directly over the sinkhole was not possible (Figure 9-18). As shown on the physical model for the diapir, cross sections from off-center lines display a dramatically different image than those directly over the dissolution-affected salt (Figure 9-10a, b, c). Images acquired off-center of the dissolution-affected salt interval will be plagued by dramatically reduced signal-to-noise ratio as a result of complex out-of-the-plane energy reflecting and diffracting from the subsidence throat and collapse breccia.



Figure 9-18. Mosaic sinkhole growing radially at about 1 m/day 12 days after catastrophic collapse on January 7, 2005. Obvious in this photograph is solution-mining well #19 (center of photo), an unused gas pipeline suspended across the sink, and a heavily used set of railroad tracks fewer than 25 m north of the sinkhole edge. Also pictured is the seismic crew and recording vehicle (yellow cover) (photo by R. Miller).

Summing Up and To Come

This chapter introduced various physical models and then integrated those models with seismic sections to formulate empirically based concepts and processes associated with dissolution of a bedded salt and resulting overburden-collapse structures. Most of the information presented in the previous eight chapters was drawn on and merged together in support of the observations and interpretations of specific dissolution and collapse processes. Information in the previous chapters also served as the framework for extending the very limited understanding of the developmental stages of collapse structures and settings that influence key processes. No single physical model possessed post-dissolution structures that matched all the subsidence geometries imaged on seismic sections. This empirical-to-

physical-model-data mismatch allows some latitude in the development of concepts and processes for these real, seismically imaged collapse features.

A combination of planar salt and salt-diapir physical models provided the best fit to the collapse images interpreted on seismic-reflection data. This divergence from expected collapse progressions on either model is indicative of the model's accuracy replicating the process. A mismatch in overburden-material properties and lack of interbeds within the salt layer of the models are the likely culprits. Regardless, the similarity between the intermediate stages of well-bore-induced dissolution and subsidence and the diapir model provides outstanding support for suggesting the presence of a compressional-stress regime and resulting structures are key indicators of active leaching. It can also be stated, based on these comparisons, that strain structures formed in an extensional stress setting are likely indicative of dissolution dormancy. These model studies support the suggestion that multiple collapse episodes while in an active leaching environment can be defined by conical pairings of reverse faults around the initial collapse-chimney structure.

Throughout the lifetime of natural dissolution-instigated collapse structure, a sequence of dissolution, subsidence, dormancy, and reactivation results in the formation of an extremely complex series of overlapping and interlaid subsidence structures. During intermediate stages of salt harvesting, these features can possess a dozen or more unique, distinguishable collapse episodes, which are all but erased once the subsidence structure reaches maturity and the salt stock is nearly depleted. Based on the post-collapse geometries of these subsidence structures, predictions can be made as to future growth with reasonable confidence.

Physical models and real seismic images of collapse structures are not completely consistent with respect to fault locations and orientations, but they do match in terms of relative offset and therefore the implied stress regimes. Faulting was not evident on the planar-salt physical model, and analogous real-reflection images possessed structures with bed drape consistent with the model; therefore, based on resolution consideration, seismic images of collapse structures were interpreted with faults. Faults in these overburden materials are responsible for all bed deformation due to the low-pressure environment and the basic principles of material failure. Due to limitations in the model design, salt jugs and associated roof failure of those structures cannot be accurately modeled using the previous setup. A drain design and negative-pressure withdraw does not allow a void to form and therefore negates solution-well models. As well, based on the two proposed examples of juvenile subsidence structures (pre-sinkhole), seismic images do not possess sufficient information to estimate or predict failure rates.

In the next chapter, all the significant and noteworthy developments and postulations made in the first nine chapters of this manuscript will be brought together and discussed as a collective compilation of subsidence concepts and processes. This next chapter will provide a summary of the key findings, but will by no means fully represent all the important and applicable finds of this work. Chapter 10 is a discussion and not a conclusion section. The intent of Chapter 10 will be to extract more interesting characteristics and properties of dissolution-instigated subsidence and to pose interesting questions that still need resolution.

References

- Brewer, R.C., and R.H. Groshong, Jr., 1993, Restoration of cross sections above intrusive salt domes: *AAPG Bulletin*, v. 77, p. 1769-1780.
- Chen, H-W., and G.A. McMechan, 1993, 3-D physical modeling and pseudospectral simulation of seismic common-source data volumes: *Geophysics*, v. 58, p. 121-133.
- Chon, Y.T., and W.R. Turpening, 1990, Complex salt and subsalt imaging: A seismic physical model study in 2-D and 3-D [exp. abs.]: Society of Exploration Geophysicists, p. 1569-1571.
- Currie, J.B., 1956, Role of concurrent deposition and deformation of sediments in development of salt-dome graben structures: *AAPG Bulletin*, v. 40, p. 1-16.
- Ebrom, D.A., R.H. Tatham, K.K. Sekharan, J.A. McDonald, and G.H.F. Gardner, 1990, Hyperbolic travel time analysis of first arrivals in an azimuthally anisotropic medium: A physical modeling study: *Geophysics*, v. 55, p. 185-191.
- Ge, H., and M.P.A. Jackson, 1998, Physical modeling of structures formed by salt withdrawal: Implications for deformation caused by salt dissolution: *AAPG Bulletin*, v. 82, p. 228-250.
- Knapp, R.W., 1991, Fresnel zones in the light of broadband data: *Geophysics*, v. 56, p. 354-359.
- Ladzekpo, D.H., K.K. Sekharan, and G.H.F. Gardner, 1988, Physical modeling for hydrocarbon exploration [exp. abs.]: Society of Exploration Geophysicists, p. 586-588.
- Lemon, N.M., 1985, Physical modeling of sedimentation adjacent to diapirs and comparison with late Precambrian Oratunga breccia body in central Flinders Ranges, South Australia: *AAPG Bulletin*, v. 56, p. 472-479.
- Link, T.A., 1930, Experiments relating to salt-dome structures: *AAPG Bulletin*, v. 14, p. 483-508.
- Lohmann, H.H., 1972, Salt dissolution in subsurface of British North Sea as interpreted from seismograms: *AAPG Bulletin*, v. 56, p. 472-479.
- Lu, L., and V. Herbert, 1989, Depth imaging of physical model data [exp. abs.]: Society of Exploration Geophysicists, p. 1187-1188.
- Martinez, J.D., K.S. Johnson, and J.T. Neal, Sinkholes in evaporite rocks: *American Scientist*, v. 86, p. 38-51.
- Parker, J.M., 1967, Salt solution and subsidence structures, Wyoming, North Dakota, and Montana: *AAPG Bulletin*, v. 51, p. 1929-1947.
- Parker, T.J., and A.N. McDowell, 1951, Scale models as guide to interpretation of salt-dome faulting: *AAPG Bulletin*, v. 35, p. 2076-2086.
- Parker, T.J., and A.N. McDowell, 1955, Model studies of salt-dome tectonics: *AAPG Bulletin*, v. 39, p. 2384-2470.
- SEG/EAGE, 3-D Modeling Committee, 1994, Progress report from the SEG/EAGE 3-D Modeling Committee: *The Leading Edge*, v. 13, n. 2, p. 110-112.
- Swenson, R.E., 1967, Trap mechanics in Nisku Formation of northeast Montana: *AAPG Bulletin*, v. 51, p. 1948-1958.
- Walters, R.F., 1978, Land subsidence in central Kansas related to salt dissolution: Kansas Geological Survey Bulletin 214, 82 p.
- Wiley, R.W., R.S. McKnight, and K.K. Sekharan, 1996, Salt canopy 3-D physical modeling project: *The Leading Edge*, v. 15, n. 11, p. 1249-1251.
- Withjack, M.O., and C. Scheiner, 1982, Fault patterns associated with domes—An experimental and analytical study: *AAPG Bulletin*, v. 66, p. 302-316.

CHAPTER 10

OBSERVATIONS AND DISCUSSION FROM SEISMIC IMAGES

In this final chapter, the most significant and noteworthy developments and concepts formulated through the first nine chapters are brought together and discussed collectively with focus directed toward the subsidence processes as illustrated on high-resolution seismic-reflection sections. At this point in this manuscript a wide range of processes, observations, and data samples have been introduced pointing out and expanding on characteristics integral to the thesis of this work. This chapter is designed to summarize key findings, but by no means is it intended to provide a full representation of all the important and applicable aspects of this work. The upcoming sections in this chapter are discussion-based and not intended to be conclusions. These discussions should entice a sundry of intriguing and expansive thoughts, hopefully drawing out curious questions that remain unanswered or that have arisen as a consequence of this work.

General Process

Key to in situ dissolution of any soluble earth material is the chemistry, rate, and volume of unsaturated fluids moving through the dissolution zone. Any change in the hydrodynamics within the dissolution zone and/or high-permeability layers in contact with the evaporites will alter the rate and pattern of the dissolution.

High-resolution, high signal-to-noise ratio seismic-reflection surveys over the last decade have provided images with sufficient fidelity and clarity to infer distinctly different episodes of subsidence related to changing hydrologic characteristics. Clearly the process involves two stages; the first is void development, overburden failure, and vertical migration through the overburden. During this part of the process, salt is leached from an exposed face to form a solution void of ever-increasing size, exposing a larger and larger span of unsupported roof rock. Once the stresses on the roof rock from overburden load exceeds material strengths, failure occurs. Physical properties of overburden material, pre-failure dimensions of the salt void, and continuity of fluid dynamics are the predominant controls on the upward progression of the void to the ground surface.

Incrementally and progressively the subsidence/failure event makes its way to the ground surface. Each successive layer of rock above the initial salt void acts for some period of time as roof rock, failing once the stresses along the rock layer (especially at the support contacts between the roof rock and pillars or intact substratum) exceed the strength of the roof rock within the tensional dome. This process can move from salt to ground surface gradually in segments or rapidly in a single complex motion. Either way, the initial collapse volume defined by the geometry of the failed rock layers is consistent with a pyramid, chimney, or dome structure, with a shape defined by fault or rupture planes consistent with reverse-fault orientations/geometries.

After a sinkhole forms, subsidence rates within the conical-shaped volume of overburden characterized by ruptured, rubble, and distorted rock layers are controlled by both continued dissolution and void development in the salt and differential compaction and slumping of weakened rock layers along the perimeter of the initial failure volume. Continued dissolution and void development will manifest itself as either additional failure planes with reverse-fault relative displacement forming at a rate approximately equivalent to the rate of dissolution or increased displacement along initial reverse-fault planes.

Contributing to both the total sinkhole volume and subsidence rate of the sinkhole are secondary voids within the salt not filled by overburden rock during initial collapse and/or voids formed within the collapse volume not filled during subsidence of the overburden rock layers. Roof rock over these secondary voids can fail catastrophically, roof rock can gradually slump into the void, or, if the geometry or material properties are conducive, they may remain intact forming a bridge. Considering the lack of stiffness in these post-failure overburden rock layers, they will likely propagate through the remaining overburden, manifesting themselves at the ground surface as gradual subsidence events any time after the initial subsidence (possibly millions of years after initial subsidence). With only two sinkholes known to have formed catastrophically, this concept is postulated with only limited data and lacks a robust development.

Independent of any active salt dissolution, undersupported rock layers at the edge of the tensional dome fail sequentially in segments, progressively increasing the radius of the bowl-shaped sinkhole. The surface area of the sinkhole tends to increase at a gradual rate and under differential compaction and slumping controlled by an extensional stress regime outside the initial failure volume. This slow, yet persistent, subsidence process occurs from the salt interval upward as weakened rock layers left suspended over voids (hanging wall) during the initial reverse-fault-defined collapse begin failing as the unsupported span increases or fatigue decreases roof strength. Extensional stress results in strain characterized by circumferential cracks on the ground surface affecting an area consistent with the angle of draw and normal-oriented subsurface faults. As a result, this second stage of sinkhole development usually involves the radial growth of the sinkhole defined in the subsurface by normal-fault planes and beds that dip toward the center of the ever-widening sinkhole.

If dissolution is still active post-initial collapse (first phase), small void spaces within the salt interval will form, undercutting the volume of rock within the hanging wall. Unless initial collapse has grossly altered the hydrodynamics driving the dissolution process, failure will likely occur along fault or failure planes consistent with the stress lines and sub-parallel to the reverse faults defining the initial collapse. Considering the reduced strength of the overburden after initial failure and therefore the limited size and shape to which a void can grow before exceeding roof-rock strengths, collapse of material into these secondary leached voids will likely result in gradual surface subsidence.

Natural Dissolution

Overburden sediments above or in close proximity to the dissolution front in central Kansas are highly disturbed and irregular from a local or site-specific perspective but regionally relatively uniform, thickening to the west over a distance generally less than 7 km. Seismic investigations across the most active portion (based on sinkhole development) of the dissolution front near Victory, Punkin Center, and Buerki provided images with sufficient

clarity to piece together with reasonable confidence the natural process. Surface topography along the dissolution front is minimal; however, rock layers between the salt interval and ground surface can possess extreme, localized relief (Watney and Paul, 1980). Based on seismic data presented in this manuscript, in some areas near the natural dissolution front, burial depth of a marker bed in the upper Permian can vary more than 30 m across distances less than a kilometer and reflections in many places along the front can be characterized by obvious bed distortion and cyclic, short-wavelength, irregular-fold-style geometries.

The overall regional uniformity of the dissolution front across Kansas (Bayne, 1956), in contrast to the extreme structural irregularity of rock layers immediately above the salt interval imaged at specific sites, suggests the salt-leaching process is regionally uniform, concentrated along an active zone, and progressing westward at a slow and somewhat consistent rate. This consistency implies overall uniformity in the hydrologic setting and hydrostatic pressures over the millions of years that this regional dissolution process has been active. However, from a local perspective and in a human time frame, dissolution and associated subsidence is extremely irregular, unpredictable, and while active, progresses rapidly.

Coincident analysis of the natural and anthropogenic dissolution processes and associated failures evidenced in seismic and historical data provide excellent support for suggesting natural dissolution along the eastern edge of the Hutchinson Salt Member is strongly influenced by hydrodynamics. Natural dissolution along the eastern subcrop is more susceptible to lateral extension of the leaching process as opposed to the more vertical growth within the salt interval observed when boreholes drive the process. Ultimately the natural process depends on the regional hydrodynamics, suggesting changes in fluid chemistry and movement in one location along the dissolution front will be compensated for at another location. The non-point-source nature of fluid dynamics in the natural process is responsible for the apparent very discontinuous sinkhole development and sporadic and unpredictable dissolution patterns along the natural dissolution front.

Seismically investigated active sinkholes identified as natural in origin (based on location, geometry, and no history of drilling) appear generally to be associated in some fashion with paleosinkholes. Assimilated interpretations of seismic images acquired across active sinkholes and geologically within areas known to be at risk of natural dissolution, support suggesting current natural dissolution and subsidence is likely the most recent of several distinct, local episodes. Most previous periods of dissolution have distinctly altered the paleo-ground surface. Evidence in overburden rocks suggests dissolution was active in the salt interval as far back as Pliocene-Pleistocene. Progression of the dissolution front appears to be characterized by short periods of active dissolution halted by flow-altering events related to collapse and reactivation of nearby paleoleaching sites. This cyclic leaching activity is locally irregular but regionally very methodical and persistent.

Most of these seismically studied natural dissolution sinkholes can be attributed to reactivation of leaching within very specific zones of a massive paleosubsidence feature. No seismic evidence exists to confidently suggest paleosinkholes imaged with high-resolution seismic reflection were active throughout late Quaternary deposition. This observation is clearly related to the fact that by investigating only currently active natural sinkholes we have incompletely sampled this historical record. Also a factor is the problem interpreting the shallowest portion of the seismogram, an area key to recent subsidence that has been silted

over in the last few centuries. Apparent reactivation of a portion of a massive paleo-subsidence feature is consistent with the idea that the hydrology within the salt interval is extremely dynamic at a small scale, yet consistent regionally and over periods of geologic time.

It is clear that rapid isolation and re-exposure of ground-water flow to different locations within the salt interval is common on these very local scales and in the context of geologic time. With the very localized nature of seismic observations and the regional consistency of this zone identified as the dissolution front from borehole data, it is reasonable to suggest significant fluid movement and exchange within the ground-water system is prevalent along the dissolution front. This suggestion is also consistent with point-source well data from within the “lost circulation zone” located along the eastern edge of the dissolution front (Gogel, 1981).

When unsaturated brine fluids come in contact with the salt layer along the dissolution front through natural sources, preferential leaching generally occurs near the top of the affected salt interval (Whittemore, 2000). This tendency to dissolve salt near the top of the bed is related to fluid densities and availability of ground water from shallower aquifers. As dissolution continues and the brine solution becomes heavily laden with dissolved solids (salt), its density increases and fully saturated brine settles to the lowest levels in the fluid column. As fresher waters enter the salt interval, more brackish fluids settle and must exit the salt interval for the process to continue. This keeps fresher waters near the top of the salt interval and, therefore, encourages preferentially horizontal void growth confined by the caprock or less soluble interbedded layers. This predominantly horizontal void growth enlarges the unsupported span of roof rock to the point of failure, but does not provide a sufficient vertical column to allow extensive upward movement of the collapse episode.

Deposition of the salt layer in shallow Permian seas has produced geometries at the edges of the salt basin consistent with the thinning observed in near-shoreline settings (Schumaker, 1966). This thinning precludes estimates of total salt removed by dissolution based on unknown original salt thickness along the eastern dissolution front. The only method of determining the amount and extent of natural dissolution along this front is seismic imaging or direct borehole measurements. Subtle changes in wavelet characteristics and overburden layer geometry appear to be interpretable and correlatable to missing salt or salt-void collapse.

Site-specific seismic images over the Hutchinson Salt Member suggest the threat to surface activity from unexpected subsidence is real. Elevated maintenance costs associated with unstable ground above dissolution-prone rock layers is a reality in many parts of world. It is unlikely any location with paleo-expressions of salt dissolution and associated subsidence in rocks overlying the salt will experience catastrophic failure due to salt dissolution. Natural dissolution processes in salt settings tends to result in gradual settlement forming large synforms with gentle dips.

Anthropogenic Catalyst

Subsidence volumes studied are associated with a single well-bore failure have consistently been geometrically symmetric on both seismic and topographic data. Elongated surface depressions with directionally preferential growth have been routinely observed in dissolution-collapse structures interpreted as natural and generally in proximity to or

associated with paleosubsidence features. One example does exist of catastrophic failure at a well bore and the development of a non-symmetric sinkhole that has been correlated to what appears on time-lapse seismic data as geologic-structure-controlled, preferential dissolution of the salt (Lambrecht and Miller, 2006). All modern catastrophic failure above this bedded salt has been related to anthropogenic influences.

Leaching by fluids released into the salt through casing failure is strongly influenced by the hydrostatic head in the completion (injection) interval and post-casing failure injection history (Walters, 1978). Initially, after a disposal well's casing integrity is breached, injected fluids escaping through the ruptured pipe interact with the salt and then re-enter the casing with increased salinity and therefore density after dynamic exposure to the salt face. This process enlarges the salt void, eventually to the point that segments of casing breaking free from the casing string, thereby increasing the separation between the fluid entry and exit points and increasing fluid exposure to the fresh salt face. Once injection has halted and brine is no longer being injected at high pressures directly into the salt via the casing rupture, the dissolution rate slows and differential pressures based on the piezometric surface and fluid densities in the completed zone (disposal interval) drive the process at a much slower rate.

Roof-rock failure through the subsidence process is strongly influenced by the stress field originally defined by the tensional dome just before initial breakthrough at the top of the overburden. Based on the interpretation of seismic data and field measurements, it appears failure of rock layers and offset geometries continue to be consistent with reverse-fault orientations, even after initial surface subsidence, as long as leaching is active along the salt face and compressional stress can build around the bedrock opening of the subsidence throat.

Because wells designed in the first half of the twentieth century for dissolution mining of salt generally had a single entry and exit point for fluids, once injection of fluid from the surface was halted, salt dissolution ended (Landes and Piper, 1972). Stress on roof rocks should not change in these dissolution voids barring cement-bond failure in the annular space between the casing and well bore and changes in void-confining pressures. However, the void (jug) formed in the salt interval as a result of mining dramatically changes the natural stress field in the roof rock and, in conjunction with subtle changes in void pressures and/or encroachment of jug fluids into the walls and roof, can all set up scenarios that instigate collapse. Considering the vertically elongated nature of dissolution voids resulting from single-well-based mining, initial roof failure will generally be predominantly vertical with little or no horizontal component extending beyond the footprint of the void itself. Horizontal growth at the ground surface after initial failure generally results from the gravity slumping due to tensional stress occurring post-sinkhole formation.

Anthropogenic dissolution of the salt has almost exclusively occurred in proximity to boreholes. Entry and exit of brine waters has been controlled by the boring, casing-rupture characteristics, and fluid properties. The vertical nature of a boring and the inevitable penetration of the interbedded shale and anhydrite layers within the salt predicate predominantly vertical dissolution with horizontal growth increasing post-failure. Barring structural features that complicate the dissolution pattern, uniformity in growth relative to the boring is common and generally results in symmetric surface depressions and subsurface expressions.

Evident from salt-dissolution mine borings and documented occurrences of rapid vertical subsidence, catastrophic collapse is most prominent when the dissolution process begins near the base of the salt interval and progresses upward to the top of the interval. This provides the maximum vertical space possible for sediments to fill during upward progression of the dissolution void through stoping once roof-rock failure begins. The location within the salt interval initial where dissolution takes place is key to the failure rate through the overburden. Once the void comes in contact with the impermeable layers, it begins to spread horizontally, controlled by the strength of that impermeable layer and the size and orientation of the void space. When the void gets large enough to exceed the strength of the rock, failure occurs. This failure process occurs throughout the salt. At the point the void encounters the top of salt roof rock, if the void area is relatively small but has a significant vertical component capable of retaining large volumes of overburden rocks, the chances increase that initial failure will progress nearly instantaneously, manifesting itself as a steep-sided, deep sinkhole.

Subsidence rates, affected volume, failure mechanisms, and risk are all strongly dependent on void geometries and origin within the salt interval and overburden lithologies and structures. Natural dissolution tends to occur along the upper boundary of the salt and impermeable caprock. Leaching in this fashion produces a large span of unsupported roof rock and a relatively small void volume. Borehole-instigated dissolution generally advances symmetrically about the fluid inlet, moving upward through the salt interval. Unsaturated brines can enter the salt layer from above or below depending on the hydrostatic head of the disposal zone. The deeper in the salt layer the breach or original injection point, the greater the potential for catastrophic collapse.

Seismic Characteristics

Seismic characteristics are key indicators of salt and overburden conditions. Significant changes in reflection amplitudes along interbedded layers within the salt or caprock are strong indicators of current or previous dissolution. Competent salt is replaced by brackish solution or rubble along these contacts increasing the reflectivity (R) from 0.23 to 0.47 across those interfaces. In places where interbedded shales or anhydrites have collapsed into voids resulting from leaching, reflection amplitudes increase as indicated

$$R = \frac{\rho_2 V_2 - \rho_1 V_1}{\rho_2 V_2 + \rho_1 V_1} \quad (1)$$

and the geometry of the interbed is altered quite significantly. Changes in seismic characteristics of this nature are not only easily interpreted but easily explained.

Once subsidence occurs the average seismic velocity of previously competent overburden decreases sufficiently to result in an anomalously low-velocity zone within the subsidence-altered overburden. It is extremely difficult to differentiate true synclinal structures from velocity pull-down in proximity to and below subsidence-altered rock. Standard velocity analysis is not sufficient to distinguish small-scale folding or bed flexure associated with unsupported roof rock from velocity pull-downs associated with reduced velocity after failure and subsidence.

Interpreting bed or reflector offsets from reflections that appear continuous is neither intuitively obvious nor is it possible based on a single reflecting event. Two conditions must exist in order to justify interpreting faults across bedding planes that appear continuous on reflection data. First, the bed offset must be minimal in comparison to the dominant wavelength, on the order of less than a quarter-wavelength change in offset between adjacent traces. Second, the spatial sampling or trace spacing must be high with respect to the radius of the Fresnel zone. Considering that the radius of the Fresnel zone is at best an order of magnitude larger than the trace spacing for high-resolution data, each reflection wavelet represents an average response from a span of the reflector the adjacent 10 receivers are also sampling. This oversampling and smearing of discrete sample points into areas results in the elongation of bed terminations across several traces.

When bed offset is less than a wavelength (cycle for seismic time sections) or is offset across a fault zone, discrete bed separation is difficult to distinguish from dip. With spatial sampling extremely small relative to most fault zones and with the size of the sampling area for most high-resolution reflection investigations, smearing is not only possible it is inevitable. One of the major interpretation challenges of high-resolution data is distinguishing faults from folds from small-scale depositional features. Key to inferring faults is vertical consistency in total offset throughout the section and a fault surface that is clearly not vertical. The non-vertical requirement is a direct consequence of the similarity of vertical faults and velocity statics. When the offset is a fraction of a wavelength and the data are recorded with a high spatial-sampling interval relative to the Fresnel zone, reflections will appear to smoothly transition across a discrete vertical-offset reflector.

Key Discussion Points and Unique Contributions

Seismic reflection has proven not only an effective tool in delineating the subsurface extent of dissolution features—and therefore plays an important role in predicting surface risk areas—it also has provided a variety of important clues as to dissolution and resulting subsidence processes and controls. Catastrophic collapse is rare, but represents the most obvious risk to public safety. Predicting catastrophic collapse represents one of the most significant potential accomplishments for a seismic investigation of one of these extremely active phenomena. Failure rates and growth patterns of sinkholes are controlled by a combination of salt stock, hydrodynamics, and overburden-material properties.

Seismic reflection has attempted to address those aspects, with greater success in overburden structural evaluations and predictions and seismic stratigraphic delineations than defining the fluid processes active within and associated with the salt interval. Time-lapse seismic has begun to provide significant enhancements to our thinking about the process. Continued study of the more than a dozen sinkholes in Kansas related to salt dissolution will provide key insights in pre-surface failure predictions, growth modeling, and eventual stagnation of the leaching of the salt.

Lateral variations in the amplitude of reflections from the salt/shale caprock interface and from interbedded shales and anhydrites within the salt interval are a key indicator of dissolution. Based on reflectivity models the reflection amplitude could increase by as much as 100% where solution/rubble void areas are in contact with shale/anhydrite caprock rather than the native competent salt. This characteristic is not unexpected, but it has never been observed and interpreted on seismic data and used as a dissolution indicator until now.

Several examples have been shown in data presented here where this subtle yet consistent attribute was synonymous with dissolution.

Dissolution of bedded salt is a process driven by availability of unsaturated brine fluids and flow. As a brine solution becomes more saturated, its density increases and the freshest waters migrate to the top of the fluid column. Leaching will therefore be most active along the top or roof of a salt dissolution void. For bedded salts like the Hutchinson Salt Member, interbedded shales and anhydrites represent boundaries to the unimpeded vertical progression of solutioning through the full salt interval. Therefore once unsaturated brine solution comes in contact with an interbedded layer or the shale caprock, active dissolution will predominantly follow the contact between the salt and this insoluble layer. This phenomenon is routinely observed in dissolution mining when a salt jug is over-mined, producing what is termed a “flower structure.”

Predominantly horizontal dissolution can generate void areas along the salt/shale contact with spans of unsupported roof rock sufficient to exceed roof-rock strength and propagate collapse, while providing a very limited volume available to accommodate collapsed overburden. This phenomenon is interpreted on seismic data along the eastern boundary of the salt interval as a stacked sequence of laterally coherent reflections with pronounced short-wavelength undulations. The wavelength or severity of the geometries is related to size of individual collapse features in the salt. Under this scenario fluid accessing the top of salt at the shale contact (caprock) salt would leach salt from top to bottom with each collapse changing the hydrodynamics but continuing to move fluid downward in the salt until an insoluble barrier was encountered.

Interbedded layers of shale and anhydrite within the Hutchinson Salt Member are laterally continuous for distance generally less than a few kilometers. Sporadic breaks in the lateral continuity of beds within the salt provide fluids migration pathways into deeper salt layers and opportunities to continue the leaching process along the basal contact of the insoluble layer and underlying salt. Hence collapse of overburden as a result of natural dissolution near the eastern boundary of the salt will generally produce minimal collapse volumes, without the potential to propagate the collapse rapidly through the overburden and to the ground surface. Once failure has occurred and subsidence is evident at the ground surface or at least throughout the consolidated part of the section, overburden rocks will not possess sufficient strength to support overburden above voids large enough to migrate to the ground surface during a single collapse event. Hence catastrophic failure is highly unlikely.

Research and modeling of cave and mine collapse has established failure mechanism associated with stress lines around unsupported spans of roof rock termed the “tensional dome.” This phenomenon is consistent with physical measurements and descriptions of collapse structures associated with failed dissolution mined salt jugs. Seismic data provide an opportunity to image the reverse faults that define this upward-narrowing chimney feature associated with initial failure. Some seismically imaged subsidence features can be defined by multiple concentric sets of reverse-fault-plane geometries. For many sinkholes there appears to be several reverse-fault-controlled subsidence episodes near the center of the feature with bed offset near the perimeter of the subsidence feature displaying normal-fault geometries. This perimeter of failure (edge of the collapse structure relative to competent, intact, unaltered rock) is proposed to be key to the current state of dissolution.

If fluids are still available and mobile after the initial failure occurs and overburden materials fill the leached void, continued dissolution along the fresh salt face will enlarge the void area thereby increasing the span of roof rock supporting the hanging wall. The rock ledge supporting the hanging wall and associated overburden will act as a moment arm. Continued undercutting of this ledge of intact roof rock will eventually accumulate sufficient torque at the salt-face/roof-rock contact due to increasing overburden load and unsupported span to precipitate collapse. This secondary collapse and associated offset in reflectors in the overburden appears to be consistent with reverse-fault geometries. Roof-rock failure that is instigated by leaching of the fresh salt face around the perimeter of the dissolution volume will be characterized by reverse faults progressively moving away from the initial failure volume.

When fluids are no longer available at the salt face (dissolution front), subsidence will continue, but now as a result of differential compaction and extensional stresses. As sediments pack ever tighter into the void and rubble zones, shallower layers of overburden begin failing along geometries consistent with normal faulting. These fault geometries are consistent with an extensional stress environment, which matches expectation that differential compaction of sediments in the void area and originally affected overburden is the driving force behind these sediment movements. Normal faults at the perimeter of the subsidence-altered volume are a key indicator that gradual settling has begun and sinkhole growth will be sedate.

All the documented catastrophic failures above the Hutchinson Salt Member in Kansas have had anthropogenic origins. Rapid failures have been most frequent in salt-dissolution mine fields where the dissolution process begins near the bottom of the salt and progresses vertically maintaining a relatively fixed affected radius. The radius of the dissolution jug is designed and developed to represent an unsupported span of roof rock that will not exceed the rock's strength. Catastrophic failure requires a void of sufficient volume to accommodate all the overburden rocks within the upwardly narrowing chimney-shaped collapse structure. The greater strength the roof rock possesses the larger the salt void can get before failure and the more likely all the overburden within the collapse chimney can be accommodated by the jug. Depending on where within the salt a casing breach occurs in an oil-field disposal well determines the potential rate of failure at the ground surface. Dissolution salt mines have the greatest potential for catastrophic failure because the dissolution begins at the base of the salt by design.

Salt voids that result from dissolution starting deep in the salt interval and advancing upward through the salt represent the greatest risk for catastrophic failure. The vertical dimension of the salt void at the time of roof-rock (shale marking the top of salt) failure represents the key characteristic influencing the failure rate of this predominantly shale overburden. Natural dissolution along the eastern boundary of the salt is principally fueled by relatively freshwater aquifers above the salt. This in conjunction with the seismically interpreted, undulating short-wavelength reflection patterns in overburden reflections that result from dissolution and subsidence make it appear unlikely that fresher water routinely gains access to the bottom portion of the salt, necessary to create deep voids that are capable of containing the entire overburden column within the collapse chimney. Therefore, catastrophic failure from natural dissolution is highly unlikely.

Summing Up

Deformed overburden and abnormalities within the soluble rock interval interpreted on high-resolution seismic-reflection sections provide key insights into formation and development of dissolution voids and associated overburden subsidence processes. Analysis of a large sample (12) of high-resolution seismic-reflection sections over the Hutchinson Salt Member, targeting a variety of subsidence features with different failure mechanisms, rates, and hydrodynamics helps unravel some of sinkhole-failure processes and controls. Subtle structures indicative of unique stages of overburden failure and rates can be identified within the collapse-altered volume on high-fidelity and coherent reflection sections.

Development of dissolution voids and associated subsidence features proceeds through several stages based on hydrodynamics, salt stratigraphy, and overburden properties. Dissolution can advance through the salt vertically (top to bottom or bottom to top) or horizontally (along any insoluble barrier within, above, or below the salt). Failure associated with dissolution voids is dependent on the stress regime and rock properties of the salt interval and overburden. Every void that has migrated through the overburden has a failure geometry that can be defined by reverse faults (compressional deformation) with normal faults (tensional deformation) bounding the initial reverse-fault-defined central cone. A key consideration is for recent subsidence events where only reverse may be interpretable due to either active dissolution or the current stage of development (early or intermediate).

Dissolution from anthropogenic or natural fluid sources results in a wide range of overburden subsidence structures with seismic images providing clues but still lacking definitive interpretations as to the complete development history. Seismic-reflection data acquired over 12 different dissolution features provided the study set used to validate and extend the results published in 14 different articles addressing seismic imaging of voids, dissolution-instigated subsidence, carbonate and evaporite karst, mines, and active and paleofeatures. An underlying difference between anthropogenic and natural that affects seismic interpretations of current and past development is the one-dimensional hydrodynamic system driving the anthropogenic process compared to the three-dimensional process for natural void and subsidence features.

Leaching within the salt interval can be interpreted from traveltime variations related to structures and amplitude and frequency anomalies of reflection wavelets. Voids are interpreted based on the presence of apparent structural variations in interbedded anhydrite and shale layers within the salt. Amplitude anomalies can be interpreted both pre-failure and post-subsidence, related to dissolution zones and alterations of rock from leached intervals. Strong evidence is presented supporting specific changes in reflection attributes (phase, frequency, and amplitude) and interbedded reflection-arrival patterns within the salt interval as characteristic of glide creep with no or only minor associated subsidence of salt. This observation is contrary to previous suggestions that subsidence and creep were indistinguishable processes on seismic sections. Voids formed during dissolution could easily provide the differential pressure and fluid necessary for low-temperature, shallow-burial salt flowage. Seismic interpretation of creep assumes minimal change in material, while subsidence results in material alteration and therefore a notable change in reflectivity.

Deformation in overburden is brittle for these shallow dissolution-driven subsidence structures. Previous interpretations suggestive of ductile (plastic) deformation are actually brittle with apparent bed flexure an artifact of offsets from a series of fracture and fault zones

collectively below the resolution limits of seismic-reflection data. Broad synforms defined by gentle dip and a consistent series of coherent reflections above dissolution-altered salt intervals are the result of relatively uninterrupted leaching and associated gradual, downward advance of the overburden.

Seismic-reflection sections with limited coherency, bed offset, scatter, and chaotic energy from within the subsidence structure are clearly representative of the remnants of bed offset, indicative of brittle deformation. Low-pressure settings and brittle overburden materials deform via rupture. Structures imaged appear to possess both detectable bed offset and apparent plastic properties together. Ductile-appearing overburden deformation from a low-pressure setting is an artifact of resolution. Resolution limits also prohibit diffractions from the suggested small-scale fractures and faults from being recorded.

Compressional and tensional stress with associated strain manifests itself through brittle deformation structures. Juvenile subsidence structures, while migrating toward the ground surface, have a distinctive shape and amplitude signature. Steep-sided subsidence features predominantly defined by reverse faults are likely undergoing active leaching in an intermediate stage of development. Compressional-deformation-evident post-bedrock breakthrough of collapse structure seems conceptually to contradict stress models. However, once the three-dimensional nature of these features are considered, subsidence within a cylinder defined by the subvertical face of the dissolution front will be dominated by matched sets of reverse-fault planes. Several periods of failure along enlarging sets of concentric reverse-fault planes portray different episodes of dissolution followed by subsidence. With the three-dimensional nature of the stress field, concentric collapse rings controlled by compressional stresses post-failure and development of initial throat will be evident for structures with a robust fluid exchange system.

Seismic images of gradual subsidence features have characteristics of both continuous dissolution and associated small-scale vertical subsidence of overburden and large void development and upward migration through stoping and raveling, forming a collapse-breccia structure geometrically defined as an upward-narrowing inverted cone. Rapid subsidence requires a large sump resulting from dissolution that migrates to the surface via stoping and raveling forming a collapse-breccia cone with varying degrees of reflectivity within the breccia or rubble volume.

Subsidence events along the natural dissolution front are generally associated with reactivated leaching within or in close proximity to paleosubsidence structures. Areas characterized by past subsidence and currently experiencing reactivation possess a minimal chance of catastrophic-failure rates. Subrosion is more likely to occur as a reactivation or elongation of existing dissolution features than as a new start. The high-gradient portion of the natural dissolution front has minimal overburden expression but possesses highly distorted salt. In areas west of the dissolution front, a variety of dissolution structures with unique origins and evidence of initial processes are retained in the rock record. Collapse structures east of the dissolution front are not seismically imageable and therefore lack interpretable structures. These data are dominated by chaotic arrivals, with out-of-the-plane noise and minimal bed coherency. Seismic images of post dissolution overburden altered with the passage of the natural dissolution front provide few clues to past dissolution and subsidence processes at this stage. Paleosubsidence structures provide clues to areas with a high risk of future dissolution and potential subsidence.

Predicting or establishing consistent failure mechanisms as a function of subsidence rate or fluid source is not possible. Catastrophic failure is most likely with anthropogenic water sources, whereas natural sinkhole development is almost exclusively gradual in nature. Seismically this difference is evident in the isolated nature of the features and one-dimensional nature of the dissolution process for anthropogenic processes, while natural dissolution is generally associated with a multi-million-year history of leaching and complex structural-development geometries.

Several key aspects critical to accurate seismic imaging of subsidence structures must be considered or interpretations can significantly diverge from the real subsurface. Interpretations of reflections below a subsidence feature suffer from subsalt static and out-of-plane energy, generally masking reflections between 100 to 200 ms below the salt interval. Two-dimensional seismic surveys must carefully consider line locations when imaging these small (relative to wavelength) geometrically irregular features for accurate interpretations.

High-resolution seismic-reflection data are critical to accurately image subsidence features, but it must be processed using techniques conducive to shallow (upper 100 ms) high-resolution data. Changes in the velocity field within the dissolution and subsidence volume across distances less than the spread length require velocity analysis as a function of offset ranges and time, splitting a single CMP gather into offset subsets. Horizontal resolution limits appear to not accurately represent true potential based on seismic images of steep-sided collapse structures. Seismic investigations using three-dimensional techniques are critical to continued development of accurate dissolution, creep, and/or subsidence scenarios and processes based on empirical, numerical, and physical models.

Continued study of more than a dozen “type section” sinkholes in Kansas related to salt dissolution will continue to enhance these key insights into both pre-surface failure predictions and growth modeling and eventual stagnation of the leaching of the salt. These 12 examples represent unique sites in a similar regional setting but diverse local geologies and physical characteristics that have been responsible for the imaged and observed subsidence features.

Gross structures and reflection characteristics of sediments above and within the dissolution zone appear to provide clues to roof-rock-failure mechanisms and information that can be used to generally estimate vertical-propagation rate of strain, post-sinkhole formation. However, pre-failure dissolution and subsidence features have not been captured on seismic data in sufficient quantity to formulate specific criteria for predicting failure rates in the many diverse settings where dissolution-instigated subsidence has been documented. Detailed interpretations and analysis of small-scale features within the subsidence zone on post-subsidence seismic-reflection images provide clues to their subsidence history.

Physical characteristics of subsidence features can be interpreted to varying degrees from seismic data. Based on seismic interrogation of both paleo and modern dissolution-induced earth subsidence, pre-failure predictions of subsidence rates (catastrophic or gradual) might now be possible if the timing and placement of seismic profiles were coincident with a pre-failure void.

References

- Bayne, C.K., 1956, Geology and ground-water resources of Reno County, Kansas: Kansas Geological Survey Bulletin 120, 130 p.
- Gogel, T., 1981, Discharge of saltwater from Permian rocks to major stream-aquifer systems in central Kansas: Kansas Geological Survey Chemical Quality Series 9, 60 p.
- Lambrech, J.L., and R.D. Miller, 2006, Catastrophic sinkhole formation in Kansas: A case study: *The Leading Edge*, v. 25, n. 3, p. 342-347.
- Landes, K.K., and T.B. Piper, 1972, Effect upon environment of brine cavity subsidence at Grosse Ile, Michigan, 1971: Solution Mining Research Institute and BASF Wyandotte Corp.
- Schumaker, R.D., 1966, Regional study of Kansas Permian evaporite formations: Unpublished M.S. thesis, Department of Geology, Wichita State University, 87 p.
- Walters, R.F., 1978, Land subsidence in central Kansas related to salt dissolution: Kansas Geological Survey Bulletin 214, 82 p.
- Watney, W.L., and S.E. Paul, 1980, Maps and cross sections of the Lower Permian Hutchinson salt in Kansas: Kansas Geological Survey Open-file Report 80-7, 10 p., 6 plates, map scale 1:500,000.
- Whittemore, D.O., 2000, Identification of natural and anthropogenic sources of chloride and sulfate: Kansas Geological Survey Open-file Report 2000-63, 7 p.

APPENDIX A

Glossary of Key Dissolution and Subsidence Terminology

APPENDIX A

Glossary of Key Dissolution and Subsidence Terminology

Alluvial	Relating to, composed of, or found in the clay, silt, sand, gravel, or similar detritus material deposited by running water.
Anhydrite	A mineral, anhydrous calcium sulfate (chemical formula CaSO_4), occurring naturally in salt deposits. Anhydrite is much less soluble than salt, so anhydrite solids must be removed from brine before the brine can be disposed of in the ocean or injected into underground wells.
Aquifer	A body of rock or soil that is capable of transmitting ground water and yielding usable quantities of water to wells or springs. A permeable region of rock or soil through which ground water can move.
Autochthonous salt	Salt body resting on the original strata or surface on which it accumulated by evaporation.
Allochthonous salt	Sheetlike salt bodies emplaced at stratigraphic levels above the <i>autochthonous</i> source layer. Allochthonous salt lies on stratigraphically younger strata.
Borehole	A hole made by drilling into the ground to study stratification, to release underground pressures, or to construct a production well, a disposal well, or a storage cavern in salt rock.
Breccia pipe	Column of breakdown debris above a collapsed cave chamber.
Brine	Water with a salt concentration greater than 35 parts per thousand. Sea water has a similar average concentration. In comparison, discharged brine has a typical concentration of 263 parts per thousand.
Brittle	Structural behavior in which a material deforms permanently by fracturing.
Brittle limit	The stress limit beyond which a material fractures, rather than behaving in a ductile or elastic fashion.
Caprock	A comparatively impervious stratum immediately overlying an oil- or gas-bearing rock.
Caprock sinkhole	Sinkhole in insoluble rock formed by collapse into underlying cavernous rock.

Casing	Steel pipe used in oil wells to seal off fluids from the borehole and to prevent the walls of the hole from sloughing off or caving. There may be several strings of casing in a well, one inside the other.
Cavern	An underground chamber or cavity created in a salt dome by solution mining and used for storing petroleum.
Collapse chamber	Cave chamber modified by wall and roof collapse.
Collapse sinkhole	Sinkhole formed by collapse of rock into a cave passage or chamber.
Compaction	Reduction of pore space between individual particles as the result of overlying sediments or of tectonic movements.
Compression	Squeezing a material from opposite directions.
Creep	The time-dependent deformation of materials. The very slow, generally continuous movement of material under the influence of gravity or pressure. In engineering usage, creep is any general, slow displacement under load.
Differential loading	Creation of lateral pressure gradients on salt caused by lateral variations in thickness, density, or strength of the overburden. Such variations may be sedimentary (for example, fans, deltas, or lobes) or structural (for example, thinning by rifting or thickening in growth-fault hanging walls).
Dissolution front	Area of active salt leaching where unsaturated brines harvest salt, pregnant brines transport that salt away from the salt face, with unsaturated brines refreshing fluids at the salt face. Fluids necessary to form a dissolution front can be from either natural or anthropogenic sources.
Dissolution sinkhole	Same as solution sinkhole or doline.
Doline	Closed depression in karst, often known as a sinkhole. The most representative landform of the karst surface. The name derives from the word <i>dolina</i> , a Slav term indicating any depression in the topographical surface.
Ductile	Structural behavior in which a material deforms permanently without fracturing.
Elastic	Non-permanent structural deformation during which the amount of deformation (strain) is proportional to the stress.

Evaporite	A mineral or rock deposited directly from a solution (commonly seawater) during evaporation. For example, gypsum and halite are evaporite minerals.
Fault	The surface of rock rupture along which there has been differential movement of the rock on either side.
Foot wall block	The body of rock that lies below an inclined fault plane.
Halokinetic	Form of salt tectonics where salt flow is powered entirely by gravity—that is, a total lack of lateral tectonic forces.
Hanging wall block	The body of rock that lies above an inclined fault plane. Compare foot wall block.
Head (hydraulic)	The level to which ground water in the zone of saturation will rise.
Karst	A terrain with special landforms and drainage characteristics due to greater solubility of certain rocks in natural waters than is common.
Leaching	The removal of soluble constituents from a rock or soil by moving ground water or hydrothermal fluids.
Normal fault	A dip-slip fault on which the hanging wall block is offset downward relative to the foot wall block. Compare reverse fault.
Permeability	Capacity for transmitting a fluid a given distance through an interval of time.
Pipe	Cylindrical or conical mass of clay and sand that fills a solution sinkhole, shaft, or cave.
Radial fault	A fault belonging to a system that radiates from a point.
Ravelling	Breakdown and disassociation of soil that falls away from the roof and walls of a ground cavity.
Reverse fault	A dip-slip fault on which the hanging wall block is offset upward relative to the foot wall block. Compare normal fault.
Sag	Generally refers to as an enclosed subsidence zone, loosely circular in nature, that forms as a result of bed deformation associated with mine or void collapse. Elongated subsidence zone associated with subsurface collapse or settlement is referred to as a trough.

Salt diapir	A mass of salt that has flowed ductilely and appears to have discordantly pierced or intruded the overburden.
Salt dome	A subsurface geologic structure consisting of a vertical cylinder of salt that may be anywhere from 0.5 to 6 miles (1 to 10 kilometers) across and up to 20,000 feet (6,100 meters) deep. Domes are formed when salt from buried salt pans flows upward due to its buoyancy.
Salt reduction	Mass transfer of salt over time, resulting in an obvious change in salt area in cross section.
Salt sheet	Allochthonous salt whose breadth is several times greater than its maximum thickness.
Salt tectonics	(syn. halotectonics) Any tectonic deformation involving salt, or other evaporites, as a substratum or source layer; it includes <i>halokinesis</i> .
Shear strength	The resistance of a body to shear stress.
Shear stress	The stress on an object operating parallel to the slope on which it lies. Angle of draw—angle of inclination from the vertical of a line.
Shear zone	A tabular area of rock that has been crushed and broken into fragments by many parallel fractures resulting from shear strain; often becomes a channel for underground fluids and the seat of ore deposition.
Sinkhole	Depression in ground surface caused by collapse into a cave below. Small closed depression in karst, also known as a doline. A depression in the land surface that results from the collapse or slow settlement of underground voids produced by solution weathering. The rock being dissolved is normally limestone but can also be salt, gypsum, or dolostone.
Slump	Downward and outward rotational movement of earth materials traveling as a unit or series of units.
Solution mining	The process of creating space in rock salt by dissolving the salt with injected water and removing the resultant brine.
Solution sinkhole	Sinkhole formed by dissolutional lowering of the rock surface in and around zones of drainage into a cavernous rock.
Strain	Change in the shape or volume of a body as a result of stress.
Strength	The ability to withstand a stress without permanent deformation.

Stress	The force per unit area acting on any surface within a solid; also, by extension, the external pressure that generates the internal force.
Stoping	Progressive collapse of roof rock that causes a cavern to migrate upwards.
Subrosion	Subsurface solution of salt. Dissolution of subsurface rock salt due to ground water flow.
Subsidence	The geological sinking or downward settling of an area on the earth's surface, resulting in the formation of a depression.
Sump	The space below the bottom end of a well pipe where liquid collects.
Tension	A stress that tends to pull a body apart.
Tensional dome	An area within the subsurface defined by the stress field associated with a void or rubble zone with a span of unsupported roof rock. Rupture of rock layers above a void occur along an arch where stress radiating toward the ground surface from support structures (pillars) is the greatest.
Tumor sinkhole	Collapse sinkhole formed by undermining, where no large chamber ever existed.
Turbulent flow	Fluid flow in which the flow lines are confused and mixed. Fluid moves in eddies and swirls.

Sources

Definitions for many of these terms came from <http://geology.com/geology-dictionary.shtml>.

Jackson, M.P.A., and C.J. Talbot, 1991, A glossary of salt tectonics: Texas Bureau of Economic Geology Geological Circular 91-4, 44 p.

Waltham, T., F. Bell, and M. Culshaw, 2005, *Sinkholes and Subsidence: Karst and Cavernous Rocks in Engineering and Construction*: Praxis Publishing Ltd., Chichester, UK.

APPENDIX B

Author-Published Papers Integral to Discussions and Concept Development

APPENDIX B

Miller, R.D., J. Xia, R.S. Harding, J.T. Neal, J.W. Fairborn, and D.W. Steeples, 1995, Seismic investigation of a surface collapse feature at Weeks Island Salt Dome, Louisiana: *AAPG Division of Environmental Geosciences Journal*, v. 2, no. 2, p. 104-112.

Seismic Investigation of a Surface Collapse Feature at Weeks Island Salt Dome, Louisiana

RICHARD D. MILLER,* JIANGHAI XIA,* RICHARD S. HARDING,†
 JAMES T. NEAL,‡ JOHN W. FAIRBORN,§
 and DON W. STEEPLES||

* *Kansas Geological Survey, 1930 Constant Avenue, Lawrence, KS 66047-3726*

† *Sandia National Laboratories, P.O. Box 5800, Albuquerque, NM 87185*

‡ *WellSeismic Computing Services, 1021 East Balboa Boulevard, Balboa, CA 92661*

|| *Department of Geology, 120 Lindley Hall, University of Kansas, Lawrence, KS 66045*

ABSTRACT ●

Surface and borehole seismic imaging techniques delineate the subsurface expression of an active sinkhole above the former salt mine at Weeks Island, Louisiana, which was converted for use by the United States Department of Energy's Strategic Petroleum Reserve. The sinkhole, which originally was ~12 m wide and 11 m deep, is directly over the edge of the upper storage chamber and in an area where the salt dome top is 60 m below ground surface. Surface seismic reflections detect a dramatic bowl-shaped depression in a 28-m-deep reflector directly adjacent to and centered on the sinkhole. A vertical seismic profile (VSP) provides time-to-depth relationships and assists correlation of reflections with drill-confirmed geologic contacts. Two reflectors (28 and 60 m) interpreted on multichannel VSP data, represent the only velocity and/or density contrasts detected between ground surface and just beneath the salt dome top. The 28-m reflector identified on both VSP and surface seismic reflection data is depth consistent with the piezometric surface. However, because of the high measured permeability and the relative severity of depression in the reflector, it is questionable whether the 28-m reflection on surface seismic data originates at the water table. The 60-m salt reflection, evident on VSP, can be interpreted on selected processed surface seismic shot gathers but is difficult to identify confidently on common depth point stacked sections. The sinkhole lies along a northeast-trending acoustic lineament, possibly related to or associated with salt dissolution. The acoustic expression of the sinkhole suggests a localized, predominantly vertical feature. No

evidence was discovered to ascertain confidently the mechanism (i.e., fractures from mine activities, shear zone associated with uplift, etc.) responsible for exposing the salt to unsaturated meteoric water.

INTRODUCTION ●

Subsurface dissolution of salt can not only compromise the hydrologic and geologic stability of an area but could also represent a potential hazard to surface and subsurface structures in many parts of the world. Dissolution and subsidence is not uncommon in areas with domal (Neal, 1994) or bedded salt (Walters, 1977), and in many cases sinkhole development is inevitable (Ege, 1984). Subsurface subsidence is generally unpredictable and can occur gradually or catastrophically with little or no warning. Sinkhole development in areas with perched water tables, confined aquifers, and/or contaminant plumes can threaten the hydrologic and geochemical properties of public water supplies. The environmental impact of sinkholes can range from minimal to devastating, resulting in everything from safety hazards to conduits for contaminant transport to habitat destruction.

This study was conducted to detect and delineate geologic or hydrologic features associated with a small sinkhole discovered on May 18, 1992 directly over the edge of the Weeks Island mine, operated by the U.S. Department of Energy Strategic Petroleum Reserve (SPR). A secondary purpose for the surface seismic survey was to identify other areas above the SPR storage cavities potentially susceptible to future collapse/subsidence. The underground oil storage occupies two levels of a former room and pillar salt mine which were holding 11.6 million kL (73 million bbl) of crude oil during this survey. The mine ranges in depth from 154 m to more than 215 m below ground surface (BGS). The top of the salt dome is ~60 m BGS at the sinkhole. The 38-m topographical high that distinguishes Weeks Island from the surrounding coastal marshland results from the upward movement of the salt mass during dome formation and is within 2 km of the shore-

This report was prepared as an account of work sponsored by an agency of the United States Government. Neither the U.S. Government, nor any agency thereof, nor any of their employees makes any warranty, express or implied, or assumes any legal liability or responsibility for the accuracy, completeness, or usefulness of any information, apparatus, product, process, or service by trade name, trademark, manufacturer, or otherwise does not necessarily constitute or imply its endorsement, recommendation, or favoring by the U.S. Government or any agency thereof. The views and opinions of the authors expressed herein do not necessarily state or reflect those of the U.S. Government or any agency thereof.

line of the Gulf of Mexico. The piezometric surface near the sinkhole is nominally the same as mean sea level (MSL), or 28 m BGS. Absence of a consolidated sedimentary cap rock leaves the salt boundaries of this dome in direct contact with overlying unconsolidated sediments, reducing to some degree the long-term hydrologic stability of the dome (Martinez et al., 1977). At the time of this survey, the sinkhole was 11 to 12 m in diameter, slightly more than 11 m deep, and within 15 m of the south side of Morton Road (Figure 1). Continued dissolution and subsidence could possibly breach the integrity of the dome, allowing crude oil movement out of the contaminant cavities.

The Weeks Island salt dome is one of five island domes that are located along the Intracoastal Waterway of southern Louisiana. All five domes have been mined for salt, but only three are operating; the other two were flooded—one accidentally and the other intentionally. The base of the salt layer that is the source of the island chain is ~5000 m deep (Martinez et al., 1977). A nondistinct sequence of Pleistocene deltaic alluvium of the ancestral Mississippi River overlies the dome (Neal and Myers, 1995). Based on mapped closed structures, growth of the Weeks Island salt

dome was likely a result of upward movement of salt layers through subvertical pipeline conduits 1 m (only a few ft) in diameter but possibly as much as 1 km (several thousand ft) long (Balk, 1949; Kupfer, 1962). Growth rates for similar domes in Louisiana and East Texas averaged 0.03 mm/yr during Cenozoic and Cretaceous (Netherland and Associates, 1976) periods with little or no uplift detectable during the Quaternary. Weeks Island has measured rise of 3 mm/yr, which is consistent with the observed geological units. Neal and Myers (1995) reported that salt creep closure at the Weeks Island SPR results in approximately one-fifth of a percent per year reduction in the approximate storage volume of 25,440 kL (160,000 bbl).

Dissolution features associated with evaporite beds at other locations have produced easily interpreted signatures on shallow seismic sections (Steeple et al., 1986; Steeples and Miller, 1987; Miller et al., 1993). Seismic reflection techniques are commonly used to image salt sediment contacts in the exploration for petroleum reserves (see *The Leading Edge*, 1994). Dome structures can possess very irregular salt/sediment contacts on seismic sections (Black and Voigt, 1982). Direct detection of the salt/sediment contact at Weeks Island has proven challenging (G. L. Kinsland, 1994, personal communication). Imaging dissolution or stress-related structures above or on the surface of the salt is potentially useful in risk determination and reclamation planning at this site. Incorporation of several acoustic imaging methods should enhance both the resolution and confidence in interpreted geology.

DATA ACQUISITION

Surface Seismic Reflection

The surface conditions included heavily wooded ground (hand-cleared, 1.5-m-wide path), manicured lawns, and asphalt roads. The extremely variable near-surface conditions complicated interpretations and were likely responsible for some subtle apparent reflection irregularities. The ground surface was characterized by several significant topographic and cultural obstacles including ditches, relatively steep terraces, and partially buried foundations from previous surface structures, resulting in ~17 m of relative elevation change across the study area. The ground was also damp during the survey.

Data for the seismic reflection study were acquired on a 48-channel Geometrics 2401X seismograph using an 8-gauge auger gun (Healey et al., 1991) and arrays of three L28E 40-Hz geophones. On-site walkaway wave testing concentrated on source/receiver geometries and recording parameters. A strong reflection with a zero-offset time of ~140 to 150 msec can be interpreted on all walkaway files (Figure 2). Selection of a source-receiver geometry and recording parameters was based on analysis of direct waves, refractions, ground roll, reflections, and air-coupled

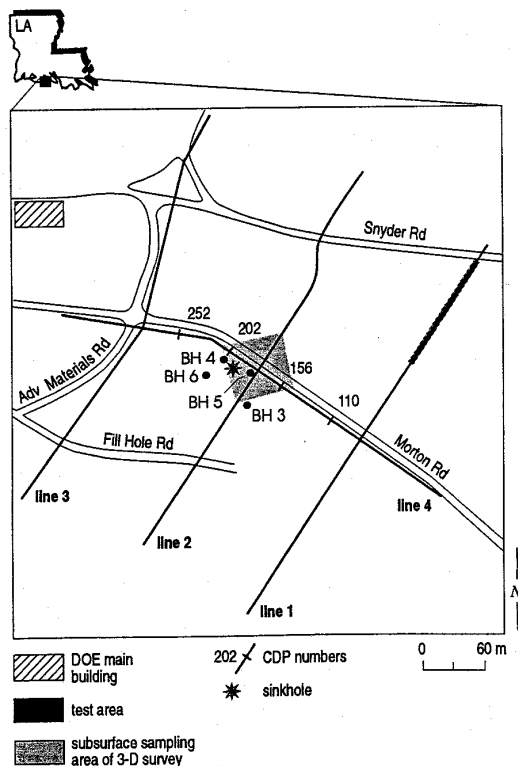


FIGURE 1: Site map indicating the relative location of Weeks Island and the layout of the survey. The four seismic lines are annotated with both survey distance measurements and CDP numbers. The shaded area represents the subsurface footprint of the 3-D test survey. The four boreholes included in the VSP and tomography are indicated.

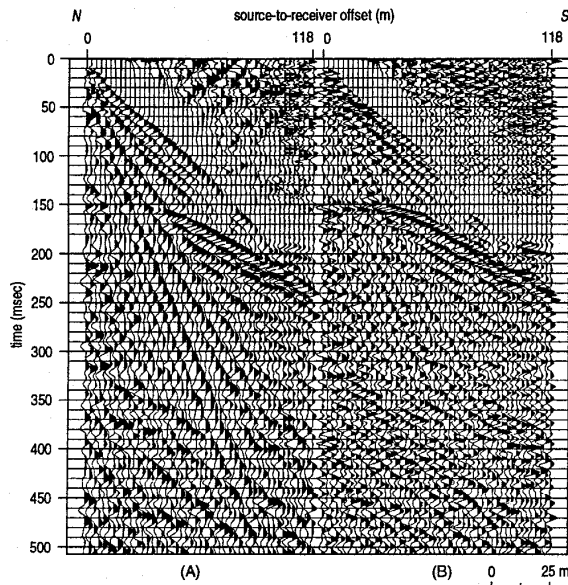


FIGURE 2: Walkaway noise tests conducted along the northeastern end of line 1. The four files were acquired with the same geophones and source location but different analog low-cut filters (A) out and (B) 100 Hz. The prominent 145-msec reflection possesses textbook curvature and a dominant frequency of greater than 150 Hz on the 100-Hz low-cut file. Vertical resolution potential is less than 1 m.

wave arrival patterns and wavelet characteristics. To enhance and balance the higher frequency components of the reflection energy and therefore the resolution potential, data were shaped with 50-Hz analog low-cut filters. This emphasis on spectral shaping (Steeple, 1990) was necessary to maximize the chance of separating the 28-m reflector from reflections from the top of the salt.

Borehole Seismic Survey

Data for the vertical seismic profile (VSP) were acquired in borehole BH-5 by using a 336-cm³ (20 in³) airgun deployed at the surface as the seismic energy source (Figure 3). This seismic source provided ample energy for observing both first arrival and reflected events. The borehole receivers were vertically separated by 0.75 m and occupied the interval from 1.5 to 71 m BGS. Using this recording geometry, the construction of a time-depth curve assists correlation of reflected arrivals with geologic units. The travel time curves allow accurate conversion of surface reflection two-way times to depth.

DATA PROCESSING

Data processing has been carefully executed without a priori assumptions. Extreme care was taken to enhance reflections that can be identified on raw data.

Surface Seismic Reflection

For most basic shallow high-resolution seismic reflection data, the processing procedures are a simple scaling

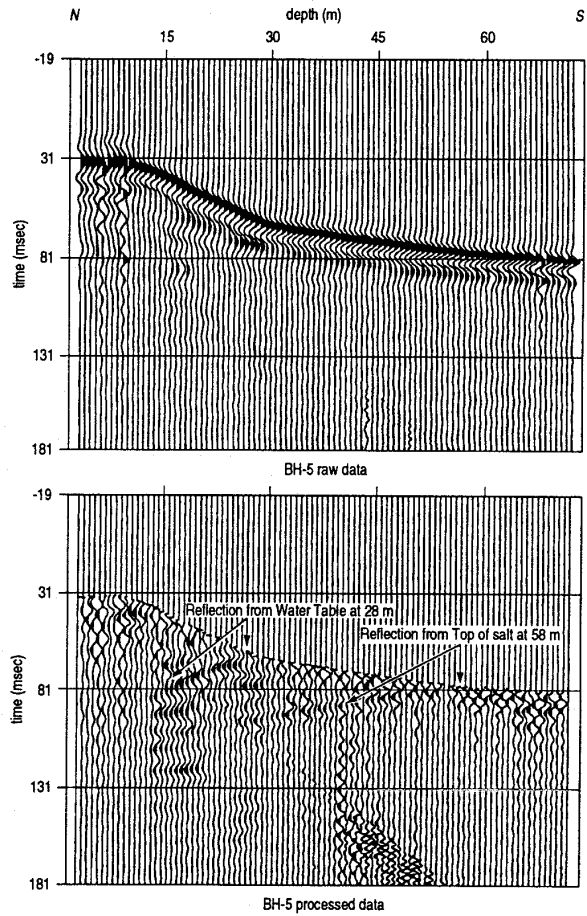


FIGURE 3: Time-depth displays of raw and processed VSP data from BH-5 clearly show the break in curvature indicative of the change in velocity at the water table. The processed VSP (bottom) has easily interpretable reflections from the water table and salt.

down of established petroleum-based processing techniques and methods (Yilmaz, 1987; Steeples and Miller, 1990). Multifold reflection data were processed on an Intel 80486-based microcomputer using a set of commercially available algorithms. The processing flow used was similar to routine petroleum exploration seismology methodologies (Yilmaz, 1987). The data were used to migrate, correct for minimal geometric distortion (Black et al., 1994), and focus the bow-tie feature prominent on stacked data. The main distinctions between the processing flow used for these data and routine petroleum flows relate to the extremely conservative use and application of correlation statics, the precision required during velocity and spectral analysis, and the accuracy of muting operations.

Vertical Seismic Profile

These VSP data are processed to allow direct correlation of drill-determined geologic contacts with reflections interpreted on common depth point (CDP) stacked sec-

tions. The raw data are shown in the top display of Figure 3. The reflections shown on the lower display were obtained by subtracting the direct arrival from the raw data and then applying a mild bandpass filter with 3-db cutoffs at 20 and 250 Hz. The direct arrival waveform was estimated by a running 7-trace average along the direct arrival trajectory.

RESULTS

Unequivocal identification of reflection energy on shot gathers is basic to effective use of shallow surface seismic reflection. Confident separation of signal from coherent noise is essential for accurate interpretation of CDP stacked sections. Raw field files acquired during the production portion of this survey have reflection events identifiable between 70 and 150 msec (Figure 4). These reflection events have an average dominant frequency of ~ 80 Hz and an apparent stacking velocity ranging from 400 to 650 m/sec. The average depth to the primary reflector is 28 m. Theoretically, the average vertical resolution of recorded data to 28 m should be less than 1.5 m (Widess, 1973) but in practice may be as large as 3 m (Miller et al., 1995); below 28 m the theoretical resolution increases to over 6 m with a practical resolution of as much as 12 m.

Horizontal resolution is often equated to the radius of the first Fresnel zone. The radius of the first Fresnel zone is 8 m for the 28-m reflector, increasing to over 24 m at 60 m, which makes delineation of a 10-m dissolution feature on the top of the salt impossible with these surface seismic data. At most, two reflections can be interpreted on selected unprocessed field files (Figure 4). The signal-to-noise ratio of this data set is very good and allows confident identification of the prominent 28-m reflection on 90% of unprocessed shot gathers.

The structure apparent in the MSL reflection between CDP 180 and 210 on line 4 is almost certainly related to the sinkhole approximately centered on and 15 m south of CDP 200 (Figure 5). This bowl-shaped depression in the reflection is the most striking acoustic feature of the surface seismic reflection survey. Considering the size of the Fresnel zone, the diameter of the subsurface depression beneath line 4 is nearly 70 m across. The well-defined "bow tie" feature evident on unmigrated data not only confirms the authenticity of the structure, but also suggests the sloping sides of the bowl structure are real and not edge effects from reflector termination (Figure 6). Based on time/depth conversions, the MSL reflector indicates 3 to 6 m of subsidence 15 to 20 m north of the sinkhole center. Extrapolating the subsurface affected area to the ground surface reveals a potential growth area more than 20 times the present expression, including space presently occupied by Morton Road. The horizontal extent of the bowl structure interpreted on the MSL reflector is more

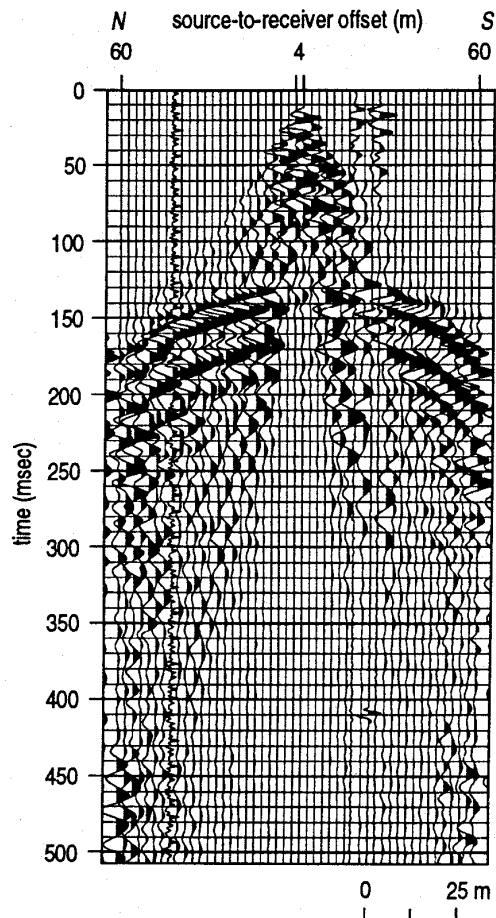


FIGURE 4: Unprocessed shot gathers selected based on potential reflection ~ 40 msec beneath the shallowest event.

than an order of magnitude larger than the expression on either the ground surface or the top of the salt.

Several fairly localized and abrupt changes in wavelet character and depth on north/south lines 1, 2, and 3 suggest significant offset, steep monoclines or horst/graben structures (Figure 7). Most of these structures do not correlate to any observed surface feature. The absence of energy scatter or diffractions associated with these very irregular reflector surfaces is consistent with the suggestion of near-surface velocity changes as the source of these features. Careful examination of unstacked data, however, provides no evidence for significant lateral changes in near-surface velocity. Lineaments or shear zones inferred from remote sensing data acquired at Weeks Island could be related to apparent structural features (Martinez et al., 1976). Most of the structural features uniquely suggested by the seismic data are probably associated with either the formation or dissolution and subsidence of the dome.

The axis of an apparent monocline lies along a lineament seismically defined by a distinct wavelet change and

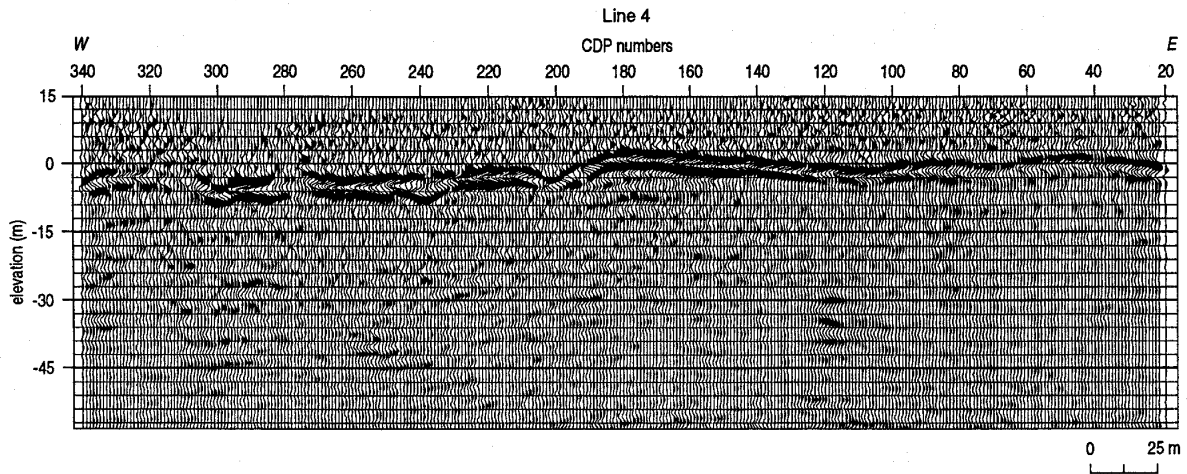


FIGURE 5: Line 4, 24-fold, CDP stacked and migrated section using a stacking velocity of 610 m/s.

a 3- to 6-m depth change (Figure 7). The interpreted axis of this monocline intersects lines 1, 2, and 3 at CDP 140, 190, and 200, respectively (Figure 8). Water seeps, vertical chimneys, and highly folded black salt identified along the southern perimeter of the Weeks Island salt mine prior to petroleum storage use have been related to a shear zone boundary (Martinez et al., 1977). The seismically interpreted lineament (monocline) is generally consistent with the vertical projection of the mine face for both the upper and lower cavities. Significant to the overall dome stability, the tensional environment resulting from salt removal

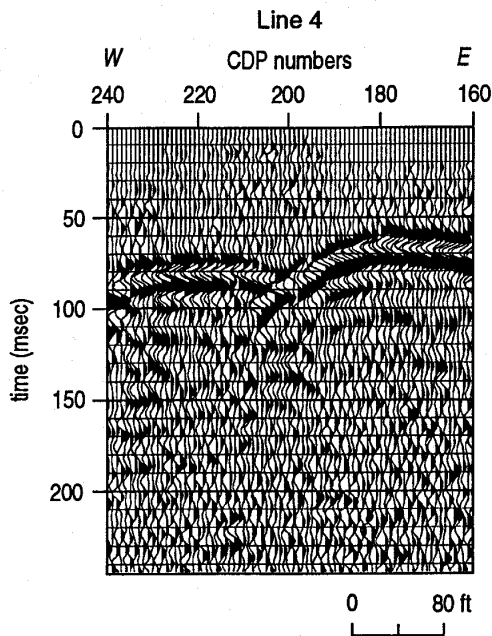


FIGURE 6: Unmigrated CDP stacked portion of line 4 showing the clearly developed "bow tie" feature characteristic of distortion due to short wavelength folding.

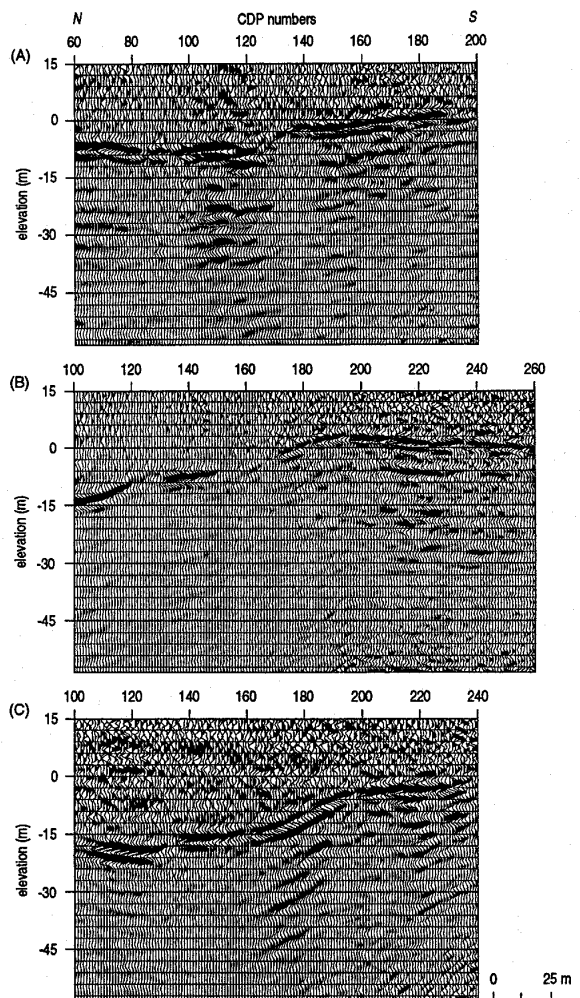


FIGURE 7: Portions of 24-fold, CDP stacked sections from line 1 (A), line 2 (B), and line 3 (C). The depth change associated with the MSL reflection is dramatically represented on each section.

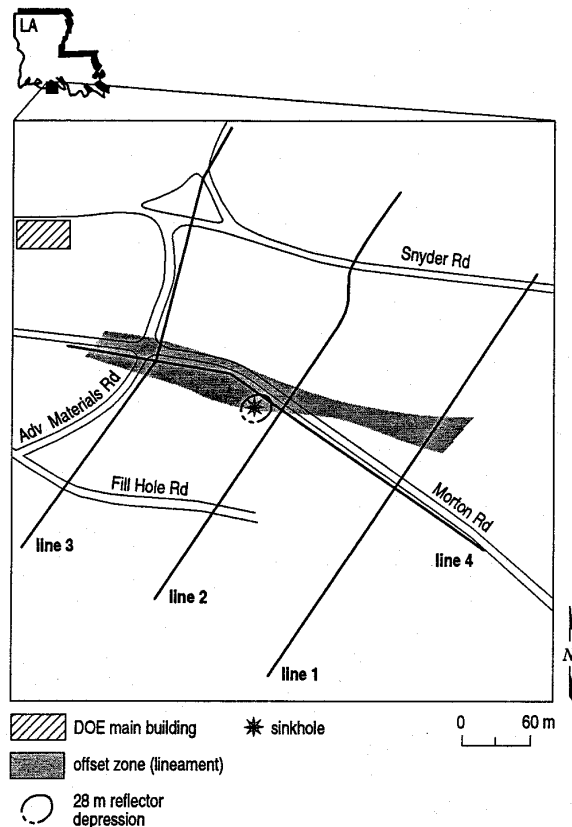


FIGURE 8: Linear surface projection of apparent offset and wavelet change on seismic lines 1, 2, 3, and 4. The lineament intersects the sinkhole and the steep-sided ditch on line 1. Based on projections from mine maps, the lineament is consistent with the mine face of both the upper and lower cavities.

has resulted in predicted fractures near the mine perimeter (Ehgartner, 1993). The close proximity of the acoustic lineament, sinkhole, shear zone (identified by remote sensing and physical mine properties), and perimeter fractures (predicted by modeling) is likely more than a coincidence, with each anomaly probably related through a cause-and-effect process. Regardless of the presence or lack of a relationship between the monocline, shear zone, and stress fracturing, active dissolution and subsidence along the mine's southern perimeter is likely to continue. Dissolution and subsidence, at least in part, are influenced by fluid management in the cavity.

The lower amplitude of salt reflections on both VSP and surface seismic data is consistent with expectations based on acoustic impedance and angle of incidence. VSP and sonic data demonstrate that the strongest velocity contrast occurs at a depth of 28 m (Figure 3). Above this depth, the interval velocity is 513 m/sec. Below 28 m, the interval velocity increases to nearly 2000 m/sec, almost a factor of 4. At the salt, velocity increases from 2000 to 4000

m/sec, or only a factor of 2. Likewise, a bulk density increase would be expected when passing from unsaturated to saturated soil, although direct measurement to verify this was not conducted. The bulk density contrast from saturated soil to salt should not be particularly large. The significantly higher amplitude of the 28-m reflection in comparison to salt reflections is consistent with the fact that amplitude is directly related to acoustic impedance contrast (i.e., a product of seismic velocity and bulk density).

The angle of incidence also contributes to the low amplitude and in most cases absence of the salt reflection on surface seismic stacked sections and most field files. Energy impinging on the water table interface with incident angles greater than $\sim 20^\circ$ should experience a high percentage of reflectance. Classically, the water table interface in an unconsolidated (e.g., alluvial/colluvial/glacial) setting possesses a high acoustic contrast and can be effectively imaged with seismic reflection, many times at the expense of deeper units (Hunter et al., 1984; Birkelo et al., 1987). However, in settings with a low velocity near-surface (i.e., < 600 m/sec) and a water table depth > 10 m, penetration of high frequency energy through the water table has proven challenging (Merey et al., 1992).

Confident identification of the geologic interface responsible for the prominent MSL reflection event is not possible using VSP data and drill logs. The reflector is near MSL elevation at the south end of lines 1, 2, and 3 and the east end of line 4. Near the sinkhole, drilling encountered uniform nondistinct sediments through the upper 30+ m. Static water table was measured at 28 m in a borehole near the sinkhole. Permeabilities of sediments in the upper 30 m near the sinkhole averaged 60 Darcies (Ostensen, 1994). An impulsive change in velocity was also noted from 554 to 1500 m/sec at 28 m of depth. Sustaining a drawdown in the piezometric surface significantly below sea level for any length of time for an area as large as the bowl-shaped structure interpreted on surface seismic data is unlikely considering the high permeability of the sediments above the salt.

Forty-five shotpoints of one-fold three-dimensional (3-D) data were acquired with the profile centered on the intersection of lines 2 and 4 (Figure 1). The data quality (i.e., signal-to-noise) of the 3-D survey was sufficiently high to allow a confident interpretation when displayed in a volumetric wiggle-trace diagram (Figure 9). Many of the processing parameters were based on two-dimensional (2-D) data analysis near the intersection of lines 2 and 4. The lack of redundancy would have inhibited accurate processing of the 3-D data without the 2-D data. These resulting data clearly show the depression on the surface of the prominent reflector identified on line 4.

A symmetric and localized dissolution and subsidence

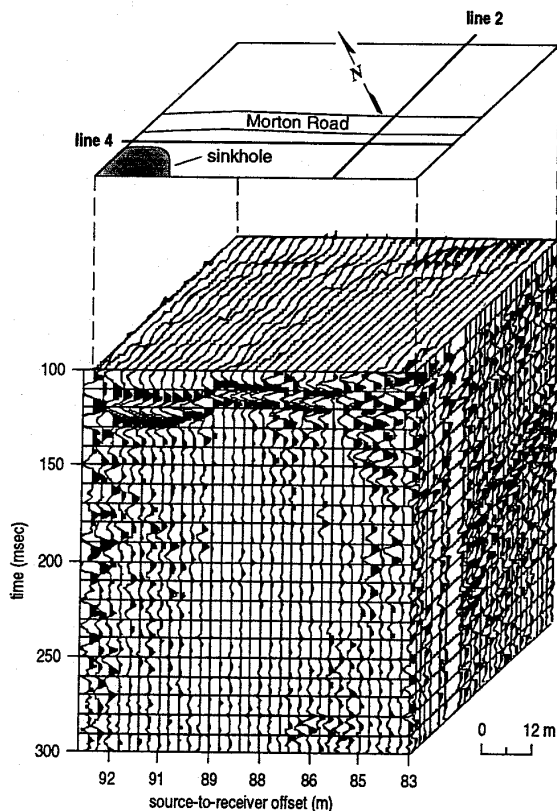


FIGURE 9: Onefold, 3-D volumetric seismic section with the relative location of the sinkhole and Morton Road overlain. This 3-D slice clearly traces the subsurface expression of the sinkhole. Processing parameters including velocity correction, statics, muting, and filtering were assigned based on analysis of the 2-D data in the immediate area.

feature is interpreted on a volumetric representation of the subsurface (Figure 10). The disturbed area interpreted on the 28-m reflector is more than an order of magnitude larger than either the surface expression or the dissolution area at the top of the salt. This large apparent subsidence area seems inconsistent with the near-vertical side-walls of the sinkhole and the physical properties of the native alluvium as well as the small dissolution area on top of the salt. A subsidence plug or chimney feature missing from the 28-m reflector could only be detected if its diameter was greater than ~ 10 m and the seismic surface line passed directly over the feature. It is not possible with seismic data (2-D or 3-D seismic) from this survey to detect a chimney-type (intermittent bed termination) feature in the 28-m reflector less than ~ 20 to 25 m in diameter. The expression at the salt surface is nearly centered on the sinkhole and slightly smaller in diameter than the disturbed area on the MSL reflector. Extrapolations between the known subsurface points (as interpreted from drill and geophysical data) result in a relatively symmetric cylindrical structure with conical ends. Incorporating the interpretations of 2-D reflection, VSPs, drilling, and 3-D reflec-

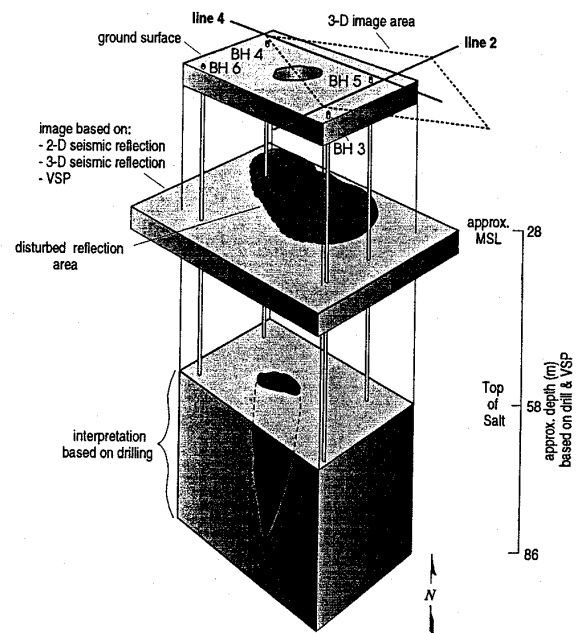


FIGURE 10: Volumetric representation of the sinkhole/subsidence from ground surface to almost 90 m. This representation is the result of combining surface observations, 2-D seismic reflection, 3-D seismic reflection, borehole geology, VSPs, and cross-hole tomography.

tion data presents a picture of the subsurface closely resembling a subsidence plug.

CONCLUSIONS •

Geophysical methods and drilling effectively delineate the subsurface expression of the Weeks Island sinkhole and detect an anomalous zone possibly related to the origin of subsidence. Both the 24-fold 2-D and onefold 3-D reflection data display a single coherent reflection at two-way times between 0.090 and 0.155 sec. A VSP provides depth control, assists in reflector identification, and images the salt surface. The geologic interface responsible for the prominent reflection cannot be confidently determined from borehole investigations near the sinkhole site. The piezometric surface was encountered at 28 m; however, measurements of high permeability minimize the possibility of sustaining drawdown to the degree imaged by the seismic data. Seismic velocity information derived from VSP data place the reflector at 23 to 46 m BGS across the study area. The MSL reflection undergoes a significant depression or time delay adjacent to the surface expression of the sinkhole. The "bow tie" effects in conjunction with other acoustic evidence allows confidence in the depression structure interpretation. These 2-D data alone are insufficient to delineate completely the lateral extent of this subsidence feature. Incorporation of onefold 3-D seismic and borehole seismic data with multifold 2-D data

substantially improves the ability to determine the lateral extent of the collapse feature in the subsurface.

Borehole seismic surveys are consistent with and dramatically improve interpretations of reflecting events. The geometry of the dissolution feature can be determined with certainty by incorporating the extensive areal coverage of the surface seismic reflection survey and the high-resolution, focused aspects of borehole imaging. Considering the geophysical image of the area around the sinkhole and assuming a consistent hydrologic setting, continued subsidence is likely. Based on Neal and Myers (1995), the sinkhole has been filled with locally available sands and a fluid injection system installed to allow introduction of saturated brine directly into the geophysically and drill-defined throat of the subsidence feature. The injected, saturated brine limits salt dissolution, stabilizing the subsidence. Studies by U.S. Department of Energy are ongoing to determine appropriate procedures and precautions necessary to relocate the oil from the mine. A freezeway was constructed around the sinkhole in the latter half of 1995 and oil relocation began in November 1995.

ACKNOWLEDGMENTS •

This work was supported by the United States Department of Energy under Contract DE-AC04-94AL85000 through Sandia National Laboratories. We thank Pat Acker for her quality graphics, Mary Brohammer for her work in manuscript preparation, and Brett Bennett for assistance with data conversions. We also thank Pat, Mary, Joe Anderson, Jeff Erickson, and David Laflen for their work in the field, and Ross Black for his help in planning this project. Jeff Treadway of Union Pacific Resources provided invaluable counsel on 3-D data acquisition, processing, and display.

REFERENCES •

- Balk, R. (1949). Structure of Grand Saline salt dome, Van Zandt County, Texas. *Am Assoc Petrol Geol Bull*, 33, 1791-1829.
- Birkelo, B. A., Steeples, D. W., Miller, R. D., and Sophocleous, M. A. (1987). Seismic reflection study of a shallow aquifer during a pumping test. *Ground Water*, 25, 703-709.
- Black, R. A., Steeples, D. W., and Miller, R. D. (1994). Migration of shallow seismic reflection data. *Geophysics*, 59, 402-410.
- Black, W. E., and Voigt, J. O. (1982). The use of seismic refraction and mine-to-surface shooting to delineate salt dome configuration and map fracture zones. In *Proceedings of the 1982 annual meeting of the Society of Exploration Geophysicists*: Tulsa, OK, Society of Exploration Geophysicists, pp. 465-466.
- Ege, J. R. (1984). Formation of solution-subsidence sinkholes above salt beds. *Geol Surv Circ*, 897, 11.
- Ehgartner, B. L. (1993). *Weeks Island stress prediction and relationship to sinkhole formation*. Sandia National Laboratories Department 6113 internal memorandum, Albuquerque, NM.
- Healey, J., Anderson, J., Miller, R. D., Keiswetter, D., Steeples, D. W., and Bennett, B. (1991). Improved shallow seismic-reflection source: Building a better Buffalo. In *Proceedings of the 1991 annual meeting of the Society of Exploration Geophysicists*: Tulsa, OK, Society of Exploration Geophysicists, pp. 588-591.
- Hunter, J. A., Pullan, S. E., Burns, R. A., Gagne, R. M., and Good R. S. (1984). Shallow seismic-reflection mapping of the overburden-bedrock interface with the engineering seismograph—Some simple techniques. *Geophysics*, 49, 1381-1385.
- Kupfer, D. H. (1962). Structure of Morton Salt Company Mine, Weeks Island salt dome, Louisiana. *Am Assoc Petrol Geol Bull*, 46, 1460-1467.
- The Leading Edge*. (1994). Special issue on subsalt imaging. *Soc Explor Geophys*, 13.
- Martinez, J. D., Thoms, R. L., Kupfer, D. H., Smith, C. G., Jr., Kolb, C. R., Newchurch, E. J., Wilcox, R. E., Manning, T. A., Jr., Romberg, M., Lewis, A. J., and Rovik, J. E. (1976). An investigation of the utility of gulf coast salt domes for the storage or disposal of radioactive wastes. Office of Waste Isolation, Union Carbide Corporation—Nuclear Division, U.S. Energy Research and Development Administration Report ORNL-Sub-4112-25, Baton Rouge, LA, Institute for Environmental Studies, Louisiana State University.
- Martinez, J. D., Thoms, R. L., Smith, Jr., C. G., Kolb, C. R., Newchurch, E. J., and Wilcox, R. E. (1977). An investigation of the utility of gulf coast salt domes for the storage or disposal of radioactive wastes. Office of Waste Isolation, Union Carbide Corporation—Nuclear Division, U.S. Energy Research and Development Administration Report Y/OWI/SUB-4112/37, Baton Rouge, LA, Institute for Environmental Studies, Louisiana State University.
- Merey, C., Miller, R. D., Ticken, E. J., and Lewis, J. S. (1992). Hydrogeologic characterization using a shallow seismic reflection survey at Fort Ord, California. In *Proceedings of the 1992 annual meeting of the Society of Exploration Geophysicists*: Tulsa, OK, Society of Exploration Geophysicists, pp. 370-373.
- Miller, R. D., Steeples, D. W., Schulte, L., and Davenport, J. (1993). Shallow seismic-reflection feasibility study of the salt dissolution well field at North American Salt Company's Hutchinson, Kansas, facility. *Mining Eng*, Oct, 1291-1296.
- Miller, R. D., Anderson, N. L., Feldman, H. R., and Franseen, E. K. (1995). Vertical resolution of a seismic survey in stratigraphic sequences less than 100 m deep in South-

- eastern Kansas. *Geophysics*, 60, 423-430.
- Neal, J. T. (1994). Surface features indicative of subsurface evaporite dissolution: Implications for storage and mining. Deerfield, IL: Solution Mining Research Institute Archives.
- Neal, J. T., and Myers, R. E. (1995). Origin, diagnostics, and mitigation of a salt dissolution sinkhole at the U.S. Strategic Petroleum Reserve Storage Site, Weeks Island, Louisiana. In *Fifth international symposium on land subsidence*. The Hague, Netherlands: International Association Science Hydrology.
- Netherland, S., and Associates. (1976). Geologic study of the interior salt domes of northeast Texas salt-dome basin to investigate their suitability for possible storage of radioactive waste material as of May 1976. Report prepared for the Office of Mine Isolation, Union Carbide Corporation, Nuclear Division, Energy Research and Development Administration.
- Ostensen, R. W. (1994). Permeability inferred from Weeks Island well tests. Sandia National Laboratories Department 6113 internal memorandum, Albuquerque, NM.
- Steeple, D. W. (1990). Spectral shaping during acquisition of seismic-reflection data. In *Proceedings of the 1990 annual meeting of the Society of Exploration Geophysicists*: Tulsa, OK, Society of Exploration Geophysicists, pp. 917-920.
- Steeple, D. W., and Miller, R. D. (1987). Direct detection of shallow subsurface voids using high-resolution reflection techniques. In B. Beck and W. L. Wilson (Eds.), *Sinkholes: Their geology, engineering, and environmental impact* (2nd Edition) (pp. 179-183). Boston, MA: A. A. Balkema.
- Steeple, D. W., and Miller, R. D. (1990). Seismic reflection methods applied to engineering, environmental, and groundwater problems. In S. H. Ward (Ed.), *Investigations in Geophysics*, No. 5, Volume 1: *Review and Tutorial* (pp. 1-30), Tulsa, OK: Society of Exploration Geophysicists.
- Steeple, D. W., Knapp, R. W., and McElwee, C. D. (1986). Seismic reflection investigations of sinkholes beneath interstate highway 70 in Kansas. *Geophysics*, 51, 295-301.
- Walters, R. F. (1977). Land subsidence in central Kansas related to salt dissolution. *Kansas Geol Surv Bull*, 214, 82.
- Widess, M. D. (1973). How thin is a thin bed? *Geophysics*, 38, 1176-1180.
- Yilmaz, O. (1987). Seismic data processing. In S. M. Doherty (Ed.), *Investigations in Geophysics* No. 2. Tulsa, OK: Society of Exploration Geophysicists.

Miller, R.D., D.W. Steeples, L. Schulte, and J. Davenport, 1993, Shallow seismic-reflection feasibility study of the salt dissolution well field at North American Salt Company's Hutchinson, Kansas, facility: *Mining Engineering*, October, p. 1291-1296.

Shallow seismic reflection study of a salt dissolution well field near Hutchinson, KS

R.D. Miller, D.W. Steeples, L. Schulte and J. Davenport

Abstract — *Shallow seismic reflection methods were successfully used to delineate the subsurface extent of roof failure associated with the dissolution mining of a 120-m (400-ft) deep and 60-m (200-ft) thick salt bed in central Kansas. Surface subsidence at North American Salt's Hutchinson, KS, salt-dissolution well field represents a potential risk to surface structures and transportation facilities. Three intersecting common depth point (CDP) seismic reflection profiles, targeting the subsurface around an actively subsiding sinkhole, possess sufficient resolution to delineate the horizontal and vertical extent of subsurface rock failure associated with the subsidence. The three seismic profiles showed a disturbed subsurface area 90 to 105 m-diam (300 to 350 ft-diam) at a depth of between 60 to 75 m (200 ft and 250 ft). Confirmation drilling verified the interpretation of the seismic data. The seismic reflection method has the potential to resolve disturbed subsurface areas greater than 23 m-diam (75 ft-diam) at this site.*

Introduction

Subsurface dissolution of salt beds is a potential hazard to surface and subsurface structures in many parts of the world. Naturally or artificially induced surface subsidence can occur either gradually or catastrophically. Determining the potential extent of continued surface subsidence allows more accurate damage estimates and rehabilitation requirements. Seismic reflection techniques have successfully detected the presence and extent of subsurface salt dissolution before and during surface subsidence at other locations in Kansas (Steeple et al., 1986, 1987; Miller et al., 1985; Knapp et al., 1989).

Seismic reflection is a powerful method of imaging portions of the subsurface in the vicinity of some sinkholes. The successful use of the technique depends on several key conditions. Foremost among these is the existence of acoustic velocity and/or density contrasts at geologic interfaces in the subsurface. The second relates to the ability of the near-surface to propagate high frequency seismic signals. Finally, the acquisition parameters and recording equipment must be compatible with the proposed target and resolution requirements of the survey.

A shallow seismic reflection survey, designed to determine the extent of subsurface collapse around a catastrophically developed sinkhole with continuing gradual subsidence, was conducted within a salt dissolution well field in Reno County, KS (Fig. 1). The three interconnecting seismic lines were processed into three CDP stacked sections with a 2.4-m (8-ft) trace spacing. Orientation, length and number of seismic lines were designed to maximize the effectiveness of the entire study.

Geologic setting and subsidence

Several major salt basins exist throughout North America (Fig. 1) (Ege, 1984). The Hutchinson Salt Member of the Permian Wellington Formation underlies a significant portion of southcentral Kansas (Fig. 1) (Walters, 1977). The thickness of the salt increases from depositional edges on the west and north, an erosional edge on the east and a facies change on the south to a maximum of more than 167 m (550 ft) in central Oklahoma. This increasing thickness from the edges to the center of the salt bed is due to increased quantities of salt and more and thicker interbedded anhydrites. Overlying the salt is the Permian Stone Corral anhydrite and about 120 m (400 ft) of Permian shale sequences.

Salt dissolution can result in surface subsidence at various rates. The dissolution process remains active as long as unsaturated brine solution or fresh water is in contact with a salt bed. This contact generally results in dissolution of the salt and the formation of a void within the salt bed. In most cases, sufficient data (geologic or geophysical) do not exist to predict subsidence before the surficial expression of subsurface dissolution.

Natural dissolution of the Hutchinson Salt is not uncommon in Kansas and has been occurring for millions of years (Ege, 1984). Faults extending up to Pleistocene sediments containing fresh water under hydrostatic pressure are postulated as the conduits instigating the salt dissolution that eventually resulted in the Meade County sinkhole (Frye and Schoff, 1942). Paleosinkholes resulting from dissolution of the Hutchinson Salt before Pleistocene deposition have been discovered with high-resolution, seismic reflection surveys (Miller et al., 1985).

Land subsidence associated with salt mining and petroleum-related brine disposal has been documented in Kansas for at least 70 years (Walters, 1977). In cases related to solution salt mining, sinkholes generally have been the result of over mining and subsequent roof rock failure. Oil well casing failure or faulty surface grouting has allowed oil-field brine disposal wells to

R.D. Miller, and **D.W. Steeples**, member SME, are assistant scientist and associate research director, respectively, with the Kansas Geological Survey, University of Kansas, Lawrence, KS. **L. Schulte** and **J. Davenport** are vice president, environmental safety and quality control, and Kansas production manager, respectively, with North American Salt Co., Hutchinson, KS. SME nonmeeting paper 91-207 A. Manuscript Feb. 22, 1991. Discussion of this peer-reviewed and approved paper is invited and must be submitted, in duplicate, prior to Dec. 31, 1993.

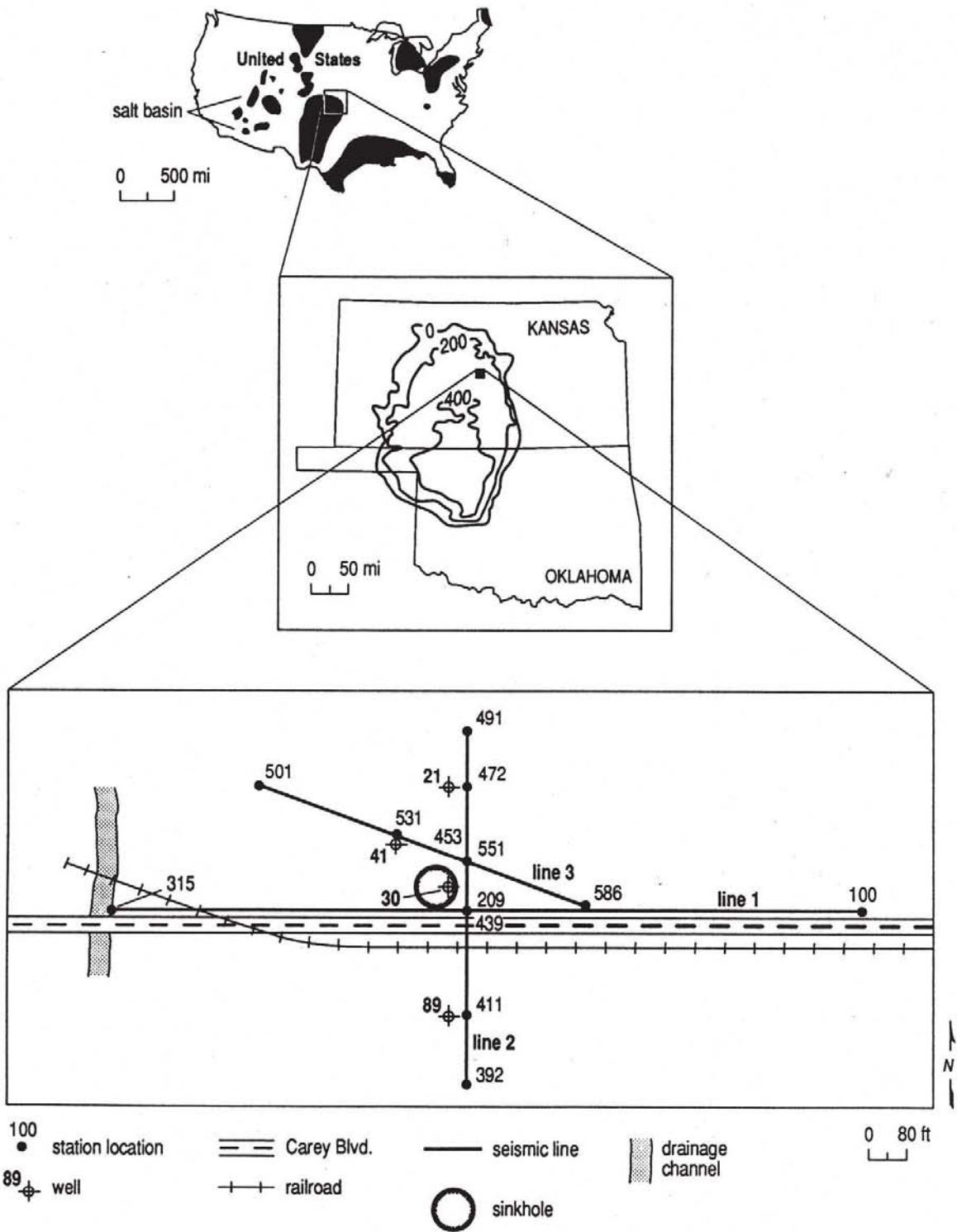


Fig. 1 — Major salt basins of North America (top, Ege, 1984); areal extent and thickness of Hutchinson Salt Member (middle, Walters, 1977) and site map indicating location of three seismic lines and approximate areal extent of the sinkhole (bottom).

become conduits to the Hutchinson Salt for unsaturated brine solutions. Sinkholes related to brine disposal wells result from roof failure similar to sinkholes associated with solution mining of salt.

Field parameters

Three CDP seismic reflection lines were acquired with nominal 12-fold redundancy (Fig. 1). The lines, which intersect less than 6 m (20 ft) northeast of well 30, were laid out to maximize subsurface coverage near the sinkhole. No surface expression suggesting subsurface collapse was observed at any of the five dissolution wells within about 150 m (500 ft) of line 1.

A series of tests designed to maximize the effectiveness of available equipment with existing surface and near-surface conditions was conducted before acquisition of production seismic lines. The proven spectral and energy characteristics of the downhole .50-cal. seismic source (Steeple et al., 1987) made it the source of choice at this site for this geologic target. The .50-cal. is seismic energy equivalent to that from about 0.013 kg (0.29 lb) of dynamite and possesses similar spectral properties (Miller et al., 1992). The downhole placement of the .50-cal. barrel greatly reduced the source-generated, air-coupled waves and the thickness of low velocity, highly attenuative, near-surface material through which the seismic energy must travel. The receiver array consisted of 3-40 Hz geophones equally spaced over 1 m (3 ft) and centered on each station. The receiver array was designed in an attempt to attenuate some of the source-generated noise. The seismograph was a 24-channel, 12-bit Input/Output DHR 2400. Analysis of the noise tests allowed acquisition parameters and equipment to be optimized for the site conditions, principal target and available equipment.

Equipment, target depths and required resolution were considered before selecting an optimum offset (Hunter et al., 1984) and receiver station spacing. The target reflection (shale-salt interface) can be identified on field data at about 110 ms. Maximizing the 110 ms target reflection on 24 recording channels compromised potential coherency and velocity determination of deeper events. Reflections deeper than 150 ms possessed as little as three-fold redundancy as a result of the very focused approach to acquiring and processing of this data set. The entire survey was designed to enhance the primary target of this survey (the 110 ms reflection). All other information arriving between 80 and 200 ms was of secondary importance.

Production lines were acquired using an end-on source/receiver geometry. Test data allowed determination of an optimum source-to-nearest-receiver offset of 19.5 m (64 ft) and source-to-farthest-receiver offset of 75.5 m (248 ft). A very attenuative near surface, consisting of weathered shales and windblown material, limited the maximum source-to-receiver offset from which high signal-to-noise ratio information could be recorded. One shot was fired into each 24-channel spread. After each shot was recorded, the 24-channel spread and shot location were uniformly moved forward a single station interval (2.4 m or 8 ft). This standard common depth point (CDP) roll-along acquisition procedure resulted in nominal 12-fold redundancy for individual sampled points in the subsurface (Steeple and Miller, 1993, in following paper).

Data processing

The processing flow was similar to that used in routine petroleum exploration, except for the severity and precision of the surgical muting processes and emphasis placed on near-

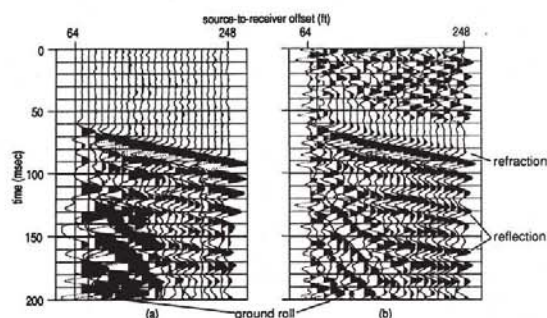


Fig. 2—24-channel field file: (a) raw, (b) filtered and scaled. Reflections, refractions and ground roll are identified.

surface velocity analysis. Care was used during the editing processes to ensure removal of all nonseismic energy that could be misinterpreted as reflections on stacked data or that hampered interpretation of real reflection events. Velocity analysis incorporating iterative constant velocity stacking with detailed surface-consistent statics improved accuracy of velocity corrections and time/depth conversions on interpreted cross sections. Adjacent 12-fold CDPs were summed to increase the signal-to-noise ratio and apparent fold of final stacked sections. This processing flow resulted in 24 traces being summed to form each CDP-stacked trace.

Results

Reflection energy can be identified on raw field files in a time window between about 80 and 190 ms (Fig. 2a). Differentiation of reflection energy from seismic noise on field files is essential for confident and consistent interpretations on stacked seismic sections. Refraction arrivals, present as first breaks (earliest recorded source-generated energy) on seismograms, were removed surgically by a muting process. Low-velocity, low-frequency linear arrivals, identified on field files as ground roll, saturated the A/D conversion process. They were also removed by muting along with the source generated air-coupled waves. The dominant frequency of the reflection energy is about 75 Hz.

Digital filtering and trace balancing of the raw field files sufficiently increased the signal-to-noise ratio to allow identification of reflections on most field files (Fig. 2b). Reflection events are easily identified by their distinctive hyperbolic curvature at times between about 80 and 180 ms on traces with source-to-receiver offsets of more than 30 m (100 ft). Depths calculated from reflection events on field files range from 45 m to more than 90 m (150 to 300 ft).

The three seismic lines intersect about 4.5 m (15 ft) east of well 30 (Fig. 1). The intersection points can be used to correlate reflections from one seismic section to the next. Lines 1 and 2 tie at stations 209 and 439. Lines 2 and 3 tie at stations 453 and 551. Tie points allow time compensation for subtle static mistakes between lines associated with near-surface irregularities.

Reflection irregularities and decreased coherency on seismic line 1 suggest a subsurface disturbance interpreted to be about 45 m (150 ft) in radius centered near well 30 (Fig. 3). The disturbed appearance of the 140 ms reflection, calculated to be from a depth of about 76 m (250 ft), is probably associated with roof collapse into void(s) left as a result of dissolution. The 110 ms reflection appears to be undisturbed by the collapse of units deeper in the section. This suggests roof failure and associated collapse has not progressed upward past about 60 m (200 ft).

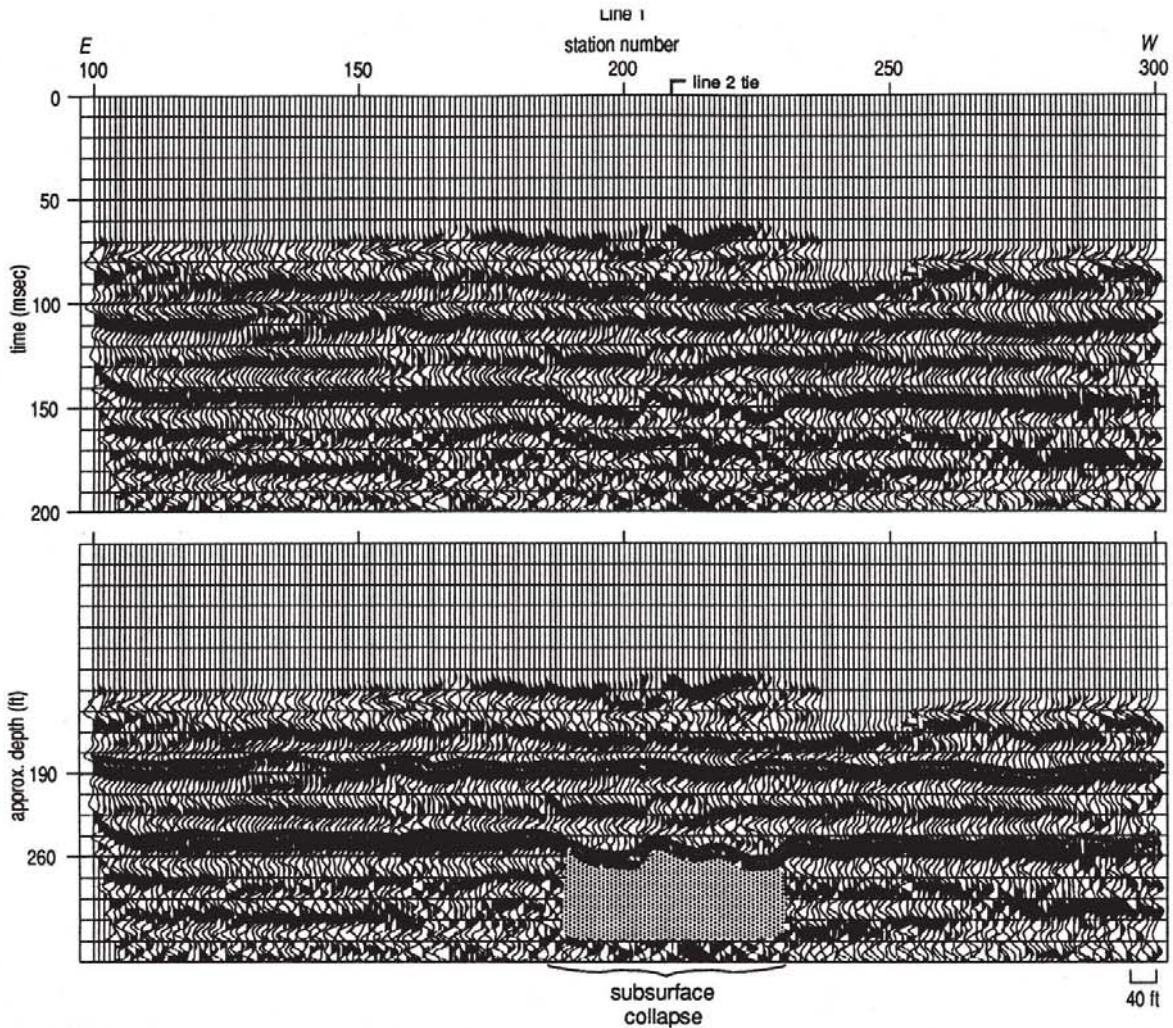


Fig. 3 — CDP stacked section of line 1 on top and an interpreted version of the section on the bottom. The affected subsurface is stippled.

The non-uniform appearance of reflections that probably correlate to collapse features is consistent with seismic interpretations from other dissolution sinkholes in this area (Knapp et al., 1989).

The key interpreted feature on line 2 is the disturbed zone centered on station location 440 (Fig. 4). The disturbed zone is acoustically similar to the collapse feature interpreted on line 1 and centered on station 210 (Fig. 3). The interpreted subsurface extent of the dissolution is from station 418 to at least station 460 on line 2. Well 30 is located about 4.5 m (15 ft) off line at about station 450. Some slumping can be observed in the reflection at 110 ms. The slumping interpreted in the 110 ms reflection suggests collapse has begun beneath line 2, as shallow as 58 m (190 ft). The short length of line 2 does not allow good identification of the exact boundaries of the subsurface disturbed zone.

From line 3 data, the subsurface appears to be disturbed from station 520 to station 560 (Fig. 5). Reflections deeper than 150 ms are disturbed as a result of collapse near well 30. The 110 ms reflection, however, appears relatively coherent with no strong indications of collapse. The general character of seismic energy within the interpreted disturbed area on line 3 is consistent with the other seismic lines.

Lens-type features directly above the subsurface collapse area on line 1 (Fig. 3) — at about 125 ms deep at station location 210 and at 110 ms deep at station location 137 — are related to

either the stratigraphy or the effects of the dissolution mining process. The general seismic appearance of the features is consistent, suggesting a similar subsurface environment. The interpreted lens features could be early indicators of future collapse around a well head if they are related to roof failure.

The approximate amount of subsidence and relative size of the interpreted disturbance in the subsurface is consistent for all three lines. General seismic characteristics, line-to-line consistency and abruptness of interpreted boundaries are probably indicative of a dissolution front. The subsurface disturbed area is about 98 m (320 ft) across with almost 6 m (20 ft) of calculated subsidence of the 140 ms reflector.

The interpreted seismic data suggest the sinkhole associated with well 33 could expand to encompass not only the paved road but also the railroad spur and well 41 (Fig. 6). Assuming no further dissolution, surface expression of the sinkhole will probably grow horizontally to about 90 m-diam (300 ft-diam). The subsurface disturbance is slightly elongated to the northwest and approximately centered on well 30. Evidence on seismic data suggests wells 30 and 41 may be connected in the subsurface.

A test hole about 2.5 m (8 ft) south of the railroad spur in line with wells 30 and 89 encountered a void at about 80 m (260 ft) (Fig. 6). The electrical and geological logs suggest a relatively normal stratigraphic section down to about 90 m (260 ft) where

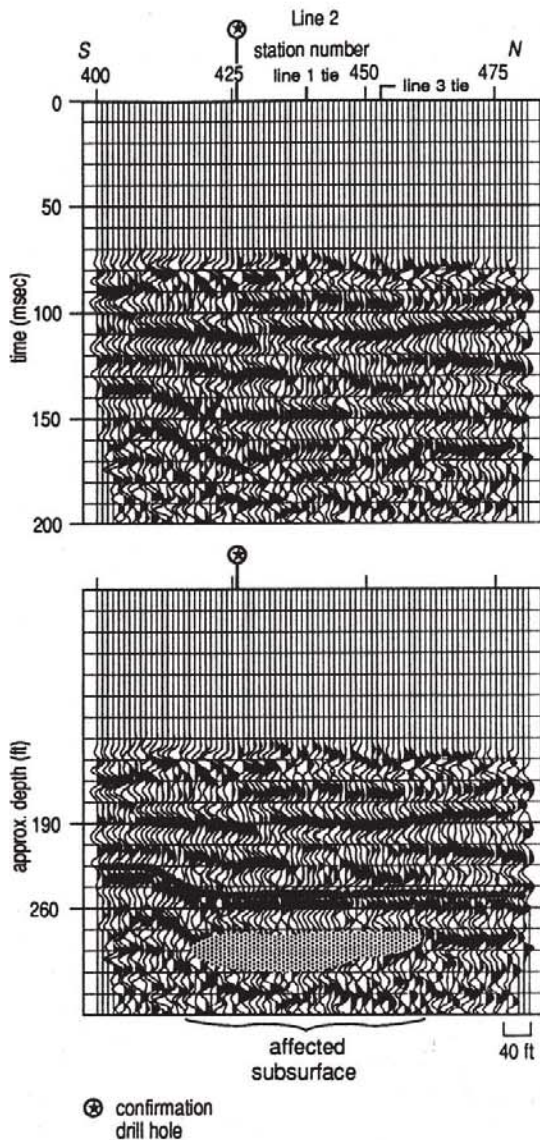


Fig. 4—CDP stacked section of line 2 on top and an interpreted version of the section on the bottom. The affected subsurface is stippled

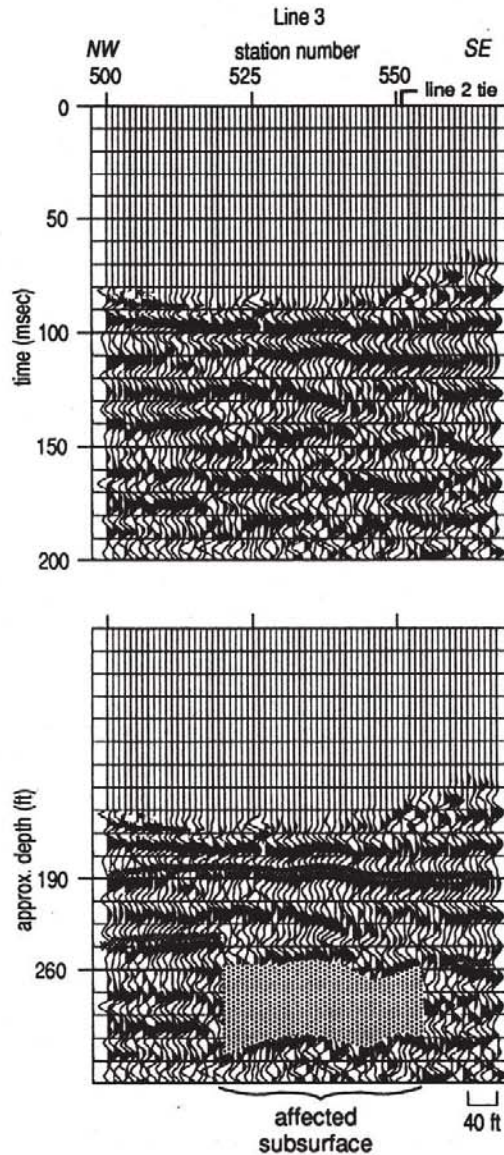


Fig. 5—CDP stacked section of line 3 on top and an interpreted version of the section on the bottom. The affected subsurface is stippled.

circulation was lost and drilling was halted. Placement of the confirmation hole and associated proposed drilling depth was based on seismic data presented here.

Presence of active dissolution cannot be ascertained from a single seismic survey. The disturbed area identified on seismic lines 1, 2 and 3 could be a remnant of previous mining activity. A second survey, reoccupying the same stations, could be used for comparison to determine the levels of dissolution activity as well as preferential growth directions during the time elapsed between the two surveys.

Conclusions

The surface subsidence associated with well 30 correlates to a disturbed subsurface area that includes not only Carey Blvd.,

but also the railroad spur on the south side of the road and well 41 to the north. Drilling confirms the interpretation of the seismic data. Extrapolation of the present subsurface collapse boundaries (as interpreted from the 140 ms reflection) to the ground surface results in a potential 16-fold increase in the surface area of the present day sinkhole. Evidence exists to suggest a subsurface tie exists between wells 30 and 41. Subsidence of the 140 ms reflector at the present time is elliptical with the major axis trending northwest-southeast.

The present subsurface subsidence rate cannot be determined without a second comparative seismic survey. From comparison of the 140 ms reflection on two seismic data sets, the rate of subsidence could be approximated. The relatively coherent, high amplitude signal recorded from the 140 ms reflector and the 16-fold difference between surface expression and interpreted subsurface disturbed

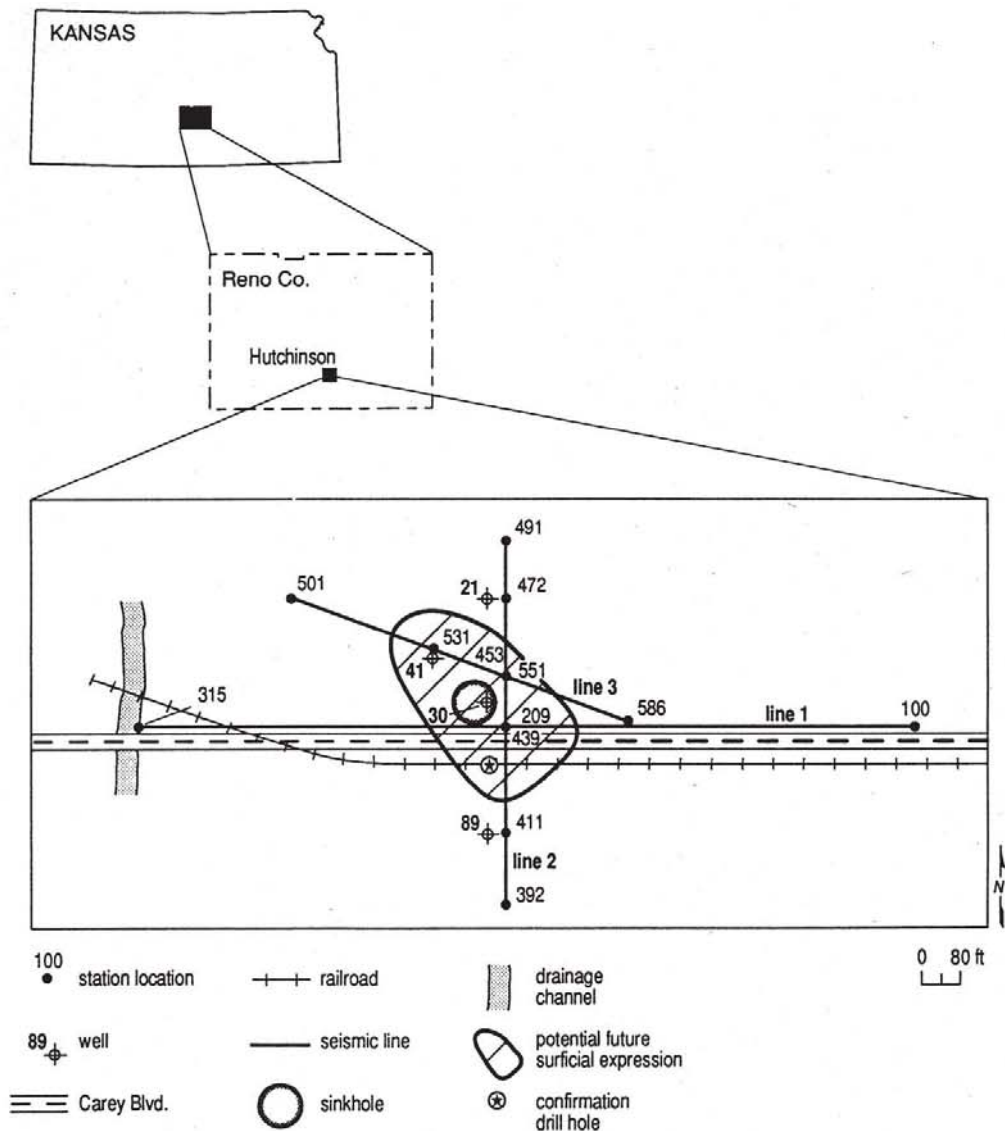


Fig. 6 — Inferred areal extent of the subsurface collapse zone. Extrapolating the drill confirmed subsurface-affected area to the surface Carey Blvd. and the railroad spur will be affected by the roof collapse of dissolution salt well No. 30.

area probably indicates a gradual subsurface collapse and eventual surface expansion. Based on confirmation of the seismic interpretation by drilling, areas with a similarly disturbed subsurface could be identified before surface expression. ♦

Acknowledgments

Support for this study was provided by North American Salt Co. Field assistance was given by Dean A. Keiswetter, Fabian T. Wimkar and William P. Hudnell. The authors thank Esther Price, Wilma Baruth and Mary Brohammer for their work in manuscript preparation. Pat Acker's graphics and Rex Buchanan's editorial comments and suggestions are greatly appreciated.

References

Ege, J.R., 1984, "Formation of solution-subsidence sinkholes above salt beds," US Geological Survey Circular 897, 11 pp.
 Frye, J.C. and Schoff, S.L., 1942, "Deep-seated solution in the Meade Basin and vicinity, Kansas and Oklahoma," *American Geophysical Union Transactions*, Vol. 23, part 1, pp. 35-39.

Hunter, J.A., et al., 1984, "Shallow seismic reflection mapping of the overburden-bedrock interface with the engineering seismograph-some simple techniques," *Geophysics*, Vol. 49, pp. 1381-1385.
 Knapp, R.W., et al., 1989, "Seismic reflection surveys at sinkholes in central Kansas," *Proceedings, Symposium on Geophysics in Kansas*, D.W. Steeples, ed., Kansas Geological Survey Bulletin 226, pp. 95-116.
 Miller, R.D., Steeples, D.W. and Treadway, J.A., 1985, "Seismic reflection survey of a sinkhole in Ellsworth County, Kansas," *Technical Program Abstracts and Biographies, 55th Annual Meeting, Society of Exploration Geophysics*, Washington, DC, pp. 154-156.
 Miller, R.D., et al., 1992, "Field comparison of shallow seismic sources near Chino, California," *Geophysics*, Vol. 57, pp. 693-709.
 Steeples, D.W., Knapp, R.W. and McElwee, C.D., 1986, "Seismic reflection investigations of sinkholes beneath Interstate Highway 70 in Kansas," *Geophysics*, Vol. 51, pp. 295-301.
 Steeples, D.W., Knapp, R.W. and Miller, R.D., 1984, "Examination of sinkholes by seismic reflection," *Sinkholes: Their geology, engineering, and environmental impact*, B. Beck, ed., A.A. Balkema, Boston, pp. 217-224.
 Steeples, D.W., Miller, R.D. and Knapp, R.W., 1987, "Downhole .50-caliber rifle an advance in high-resolution seismic sources," survey of a sinkhole in Ellsworth County, Kansas," *Technical Program Abstracts and Biographies, 57th Annual Meeting, Society of Exploration Geophysics*, pp. 76-78.
 Walters, R.F., 1977, "Land subsidence in central Kansas related to salt dissolution," *Kansas Geological Survey Bulletin* 214, 82 pp.

Miller, R.D., and D.W. Steeples, 1991, Detecting voids in a 0.6-m coal seam, 7 m deep, using seismic reflection: *Geoexploration*, Elsevier Science Publishers B.V., Amsterdam, The Netherlands, v. 28, p. 109-119.

Detecting voids in a 0.6 m coal seam, 7 m deep, using seismic reflection

Richard D. Miller and Don W. Steeples

Kansas Geological Survey, The University of Kansas, Lawrence, KS 66047, USA

(Received September 20, 1990; accepted after revision February 25, 1991)

ABSTRACT

Miller, R.D. and Steeples, D.W., 1991. Detecting voids in a 0.6 m coal seam, 7 m deep, using seismic reflection. *Geoexploration*, 28: 109–119.

Surface collapse over abandoned subsurface coal mines is a problem in many parts of the world. High-resolution P-wave reflection seismology was successfully used to evaluate the risk of an active sinkhole to a main north–south railroad line in an undermined area of southeastern Kansas, USA. Water-filled cavities responsible for sinkholes in this area are in a 0.6 m thick coal seam, 7 m deep. Dominant reflection frequencies in excess of 200 Hz enabled reflections from the coal seam to be discerned from the direct wave, refractions, air wave, and ground roll on unprocessed field files. Repetitive void sequences within competent coal on three seismic profiles are consistent with the “room and pillar” mining technique practiced in this area near the turn of the century. The seismic survey showed that the apparent active sinkhole was not the result of reactivated subsidence but probably erosion.

INTRODUCTION

Detection of subsurface cavities by methods other than drilling is of interest to geologists and engineers in many parts of the world. Recent advances in high-resolution reflection seismology can be applicable to shallow cavity detection (Hunter et al., 1984; Branham and Steeples, 1988; Steeples and Miller, 1987, 1990). Recorded energy with a dominant frequency greater than 100 Hz is needed to detect targets shallower than 30 m using P-wave reflection seismology. High frequencies increase the resolution of the survey allowing shallower, smaller features to be detected and possibly delineated (Widess, 1973). These higher-than-normal frequencies have been attained in nonmarine environments using nonstandard seismic sources and severe low-cut analog filtering (Jongerijs and Helbig, 1988; Birkelo et al., 1987; Miller et al., 1989; Pullan and Hunter, 1990). The extreme contrast of elastic properties between a void (water or air-filled) and the surrounding rocks provides an excellent reflecting interface.

Gradual earth subsidence forming shallow sinkholes is common in heavily undermined areas of southeast Kansas. The gradual collapse of near-surface material into voids commonly less than 5 m in diameter in the 7–10 m deep and 0.6–1.0 m thick Weir–Pittsburg coal generally results in sinkholes less than 3 m in diameter and 0.3 m deep. Most of these subsurface voids are remnants of the “room and pillar” mining method commonly used in this area.

The accelerated rate of subsidence of a previously dormant sinkhole within 20 m of a set of heavily used railroad tracks near Scammon, Kansas, USA, represented a potential risk to rail traffic. An approximately four-fold increase in the surface area of this sinkhole, predominantly toward the railroad tracks over a period of two months, suggested possible reactivation of subsid-

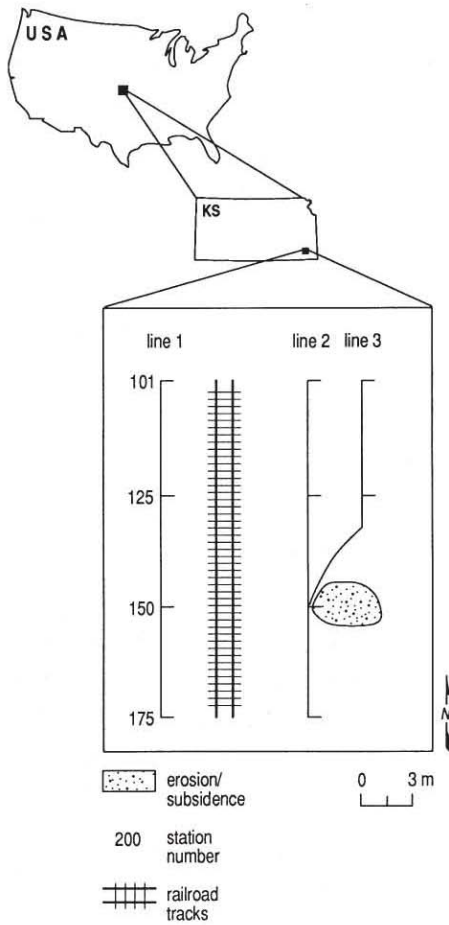


Fig. 1. Location map showing surface subsidence feature with respect to the seismic lines and railroad tracks.

ence. To determine appropriate remediation and ensure the structural integrity and safety of the tracks, it was necessary to locate precisely the mine shaft responsible for the sinkhole.

A seismic survey was designed to maximize the potential for locating horizontal shafts associated with the observed subsidence that might cross beneath the north-south railroad tracks (Fig. 1). A preliminary seismic profile was collected to determine the optimum acquisition parameters for future production lines. Two production lines (lines 1 and 2) were then acquired parallel to and on opposite sides of the tracks, centered on the active sinkhole. The acquisition parameters used on the two production lines were designed to allow direct detection of any subsurface void present beneath the seismic lines. Confident correlation between the two production seismic lines is possible if the trend, size, and distance between horizontal shafts crossing beneath the tracks are relatively consistent.

GEOLOGICAL SETTING AND FIELD PROCEDURES

The Weir-Pittsburg coal bed has an average thickness of 1 m in southeastern Kansas. It is located within the lower portion of the Cabaniss Formation, which is part of the Pennsylvanian (Carboniferous) Cherokee Group. The various phases of the Cherokee cyclothems are best interpreted as facies of alluvial-deltaic complexes, the repetitive nature being due to delta shifting and distributary abandonment (Heckel et al., 1979). The Cherokee coals are the culmination of aggrading sedimentation of delta plains. The Weir-Pittsburg coal bed was extensively mined until about 1940 by both subsurface and strip-mining methods. As a result of the subsurface mining, large areas of southeastern Kansas are underlain by a maze of interconnected cavities.

The data were collected using a standard CDP acquisition method. The source-and-receiver spacings were 0.6 m. The source was a downhole .30-06 single-shot rifle with its barrel 0.1 m below the ground surface in a 3 cm diameter borehole about 0.2 m deep. The receivers were two 100 Hz geophones on 14 cm spikes, connected in series with a 0.3 m in-line spacing. The optimum recording window (Hunter et al., 1984) and acquisition parameters (Knapp and Steeples, 1986) were selected from walkaway tests with source-to-receiver spacing ranging from 0.3 m to 37 m on 0.3 m intervals and low-cut filters of 240 Hz, 340 Hz, and 480 Hz. Maximum recordable reflection frequencies were maintained partly as a result of careful attention to source-and-receiver ground coupling throughout the acquisition phase.

The data were recorded on an I/O DHR-2400 seismograph. The fixed-gain data were converted analog-to-digital (A/D) into an 11-bit plus sign value and then stored on magnetic tape in modified SEG-Y format. The recording system amplifiers have 72 dB of dynamic range with a 120 nV RMS noise level. The anti-alias filters used have a 60 dB/octave roll-off with a -60 dB

point of 2000 Hz. A pre-A/D low-cut filter with a 24 dB/octave roll-off and a -3 dB point of 340 Hz was used to maximize potential resolution and reduce the effects of ground roll. The selected low-cut filters were essential to the quality and success of this survey.

DATA PROCESSING

The data were processed on a Data General MV-20,000 computer (using basic CDP seismic-processing techniques). Special emphasis was placed on defining and applying a digital bandpass filter optimizing the spectral difference between voids and intact coal. A subtle difference can be observed on the CDP stacked sections between the dominant frequency of reflections from the coal seam and reflections, or a lack of them, from the interpreted void area. This observation is consistent with other documented studies in this area (Branham and Steeples, 1988). The primary processing procedures performed on the seismic data were focused on enhancing reflection information identified within the upper 40 ms on field files (common shot gathers).

Surgical muting of noise would have been detrimental to the reflection information, which was concentrated in time and offset windows rich in refraction, direct-wave, and air-wave energy. Changes in reflection wavelet characteristics between coal and void are difficult to identify and analyze on unprocessed field files. Reflection energy (or lack of it) from voids is not sufficiently distinctive to isolate it from random noise on field files. The lack of muting demands careful attention during each of the data processing phases to avoid misidentification and possible enhancement of non-reflection energy.

Digital bandpass filtering proved to be the key to enhancing reflection energy (or lack of it) from the coal seam and voids. The CDP stacking process alone did not enhance reflections from coal or void in the upper 40 ms. A digital low-cut filter with zero percent amplitude point in excess of 200 Hz was necessary to isolate reflections definitively from within the coal seam on the CDP stacked sections.

Static anomalies associated with variable near-surface velocity can be observed on some field files (Fig. 2). A surface-consistent statics routine was used to minimize the effects of near-surface irregularities. Static problems on most field files were subtle and did not represent a significant obstacle in producing accurate CDP stacked sections.

Normal moveout (NMO) sample stretch was less than or equal to 15 percent. The NMO stretch mute was selected through iterative analysis. All samples were zeroed when relative stretch greater than 15 percent of the sample interval after NMO correction was encountered. Incorrect maximum sample stretch can decrease the dominant frequency as well as apparent amplitude and distort phase sufficiently to hamper the interpretation of the coal-seam reflection.

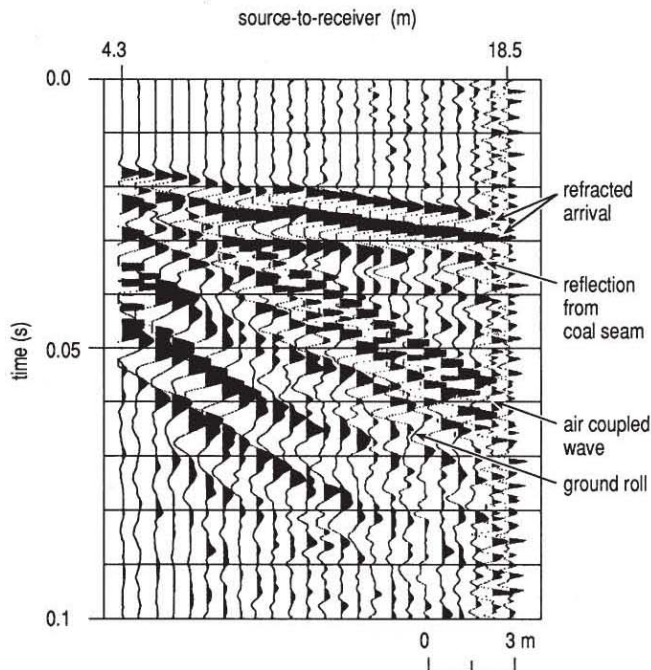


Fig. 2. Unprocessed field file with identified reflection, refraction, air wave, and surface wave. Confident identification is possible due to the unique characteristics and arrival pattern of the coal reflection.

RESULTS

Reflections from the coal seam can be interpreted from raw field-files (Fig. 2). The coal reflection has a unique frequency spectrum and hyperbolic arrival pattern that separates it from refracted-wave, direct-wave, and air-wave energy. The dominant reflection frequency is in excess of 200 Hz. Two-way arrival time of the coal reflection is consistent with the one-way travel time observed in an uphole survey. Reflection energy from voids lacks trace-to-trace consistency in frequency content.

The voids can be separated from competent coal according to frequency, amplitude, coherency, phase, and reflection-wave character on the 12-fold CDP, stack of line 2 (Fig. 4). The first three positive amplitude arrivals between 10 ms and about 22 ms on line 2 are refractions. As previously mentioned, refractions were not muted to avoid disturbing the reflecting arrivals that closely trail the refractions (Fig. 2). The difference in the seismic characteristics of voids and intact coal are obvious when the drill-confirmed voids on line 2 at station 123 and 144 are compared with the drill-confirmed coal at station 135 on line 2. The coal reflection at station 135 is higher in ampli-

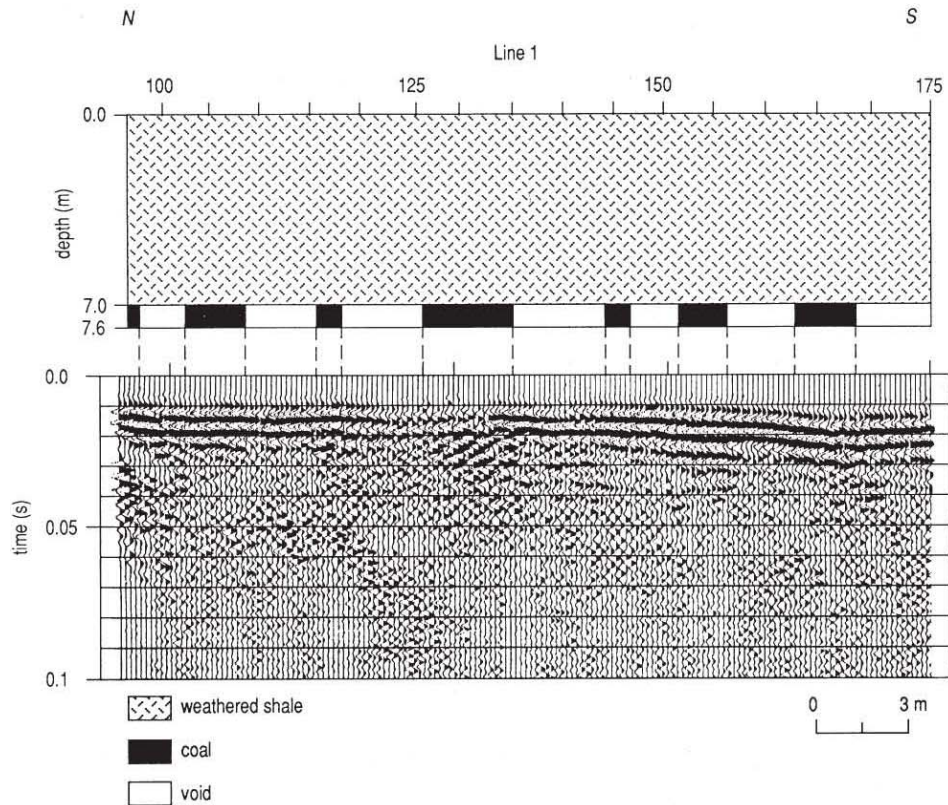


Fig. 3. Twelve-fold CDP stack and geologic interpretation of line 1. The first two dominant cycles after first breaks are stacked refraction energy not muted to avoid adversely affecting the reflection arrivals. Rooms and pillars, as indicated on the geologic cross-section, are remnants of a coal-mining technique commonly practiced in this area around 1900.

tude, more coherent, and lower in frequency than the reflection energy of the bounding voids.

The drill-confirmed criteria for identifying voids in the coal from line 2 were used to interpret lines 1 and 3 (Figs. 3, 4, and 5). Consistent emphasis was placed on each of the various seismic characteristics in defining location and extent of void areas in the subsurface. Voids are seismically represented on stacked sections as either an increase in the dominant frequency (location 125 on line 3; Fig. 5) or a loss of coherency resulting in a chaotic zone (location 125 on line 1; Fig. 3). The repetitive nature of the void/coal patterns on all three lines is consistent with the “room and pillar” mining technique as shown on old mine maps from this area.

Reflection events can appear continuous across abrupt discontinuities when subsurface sample points are closer together than the diameter of the first

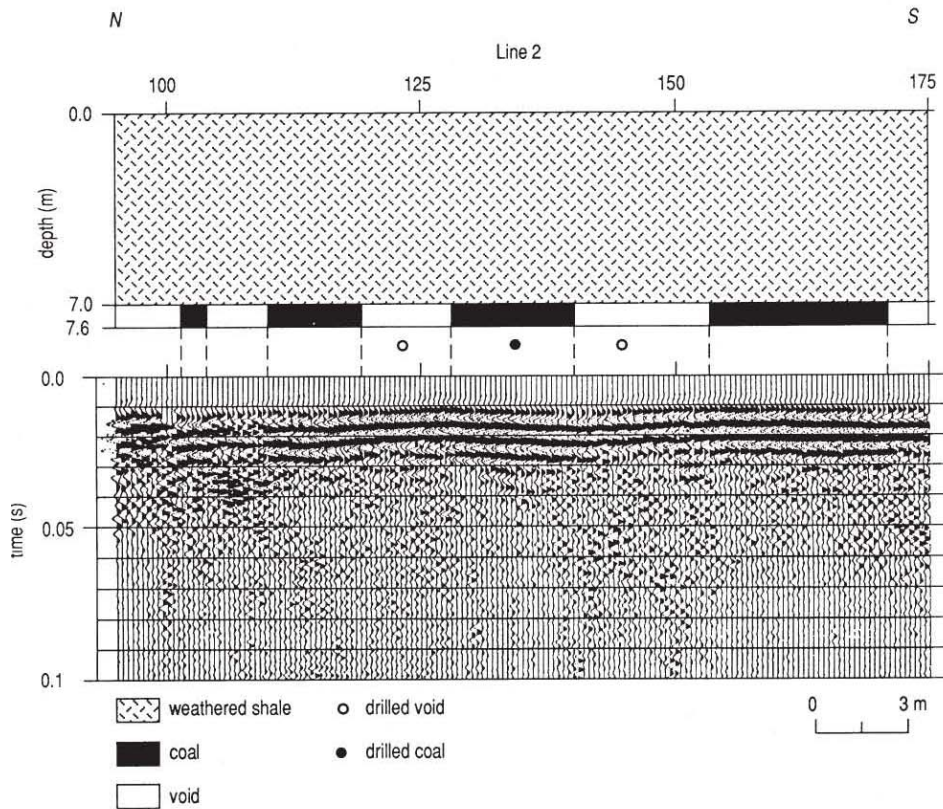


Fig. 4. Twelve-fold CDP stack and geologic interpretation of line 2. Drilling on line 2 confirmed the presence of the interpreted voids in the competent coal. The first two dominant cycles after first breaks are stacked refraction energy not muted to avoid adversely affecting the reflection arrivals.

Fresnel zone (Waters, 1987; Miller et al., 1990). Oversampling of the first Fresnel zone resulted in diffused boundaries between voids and competent coal on all three CDP stacked sections. The boundaries between coal and void identified on the geologic cross-sections are subjective and were selected based on localized relative amplitude and frequency changes. Horizontal focusing of subsurface features occurs as the spatial sampling interval approaches the radius of the first Fresnel zone. The oversampling on this data set was necessary to maintain good coherency on the coal seam reflection.

The sinkhole's migration path toward the railroad tracks does not appear to directly correlate to interpreted voids having sufficient volume to yield over 3 m of surface subsidence (Fig. 6). Voids interpreted on lines 1, 2, and 3 all possess consistent seismic character, approximate void size, and "room and pillar" grid patterns. It would be speculative, due to the isolated and

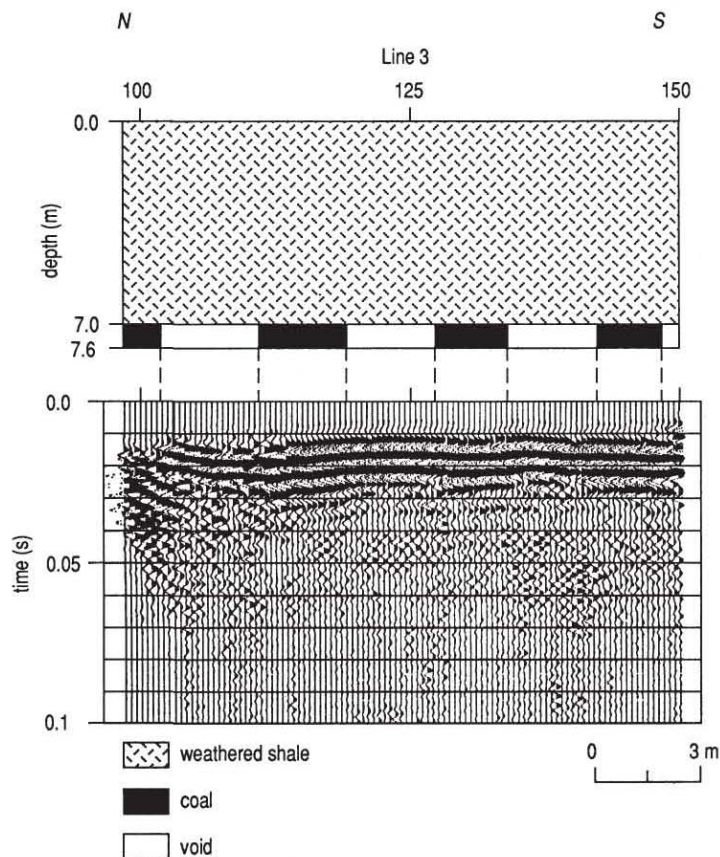


Fig. 5. Twelve-fold CDP stack and geologic interpretation of line 3. Line 3 was a preliminary test line intended to determine the feasibility of the CDP reflection technique at this location. The first two dominant cycles after first breaks are stacked refraction energy not muted to avoid adversely affecting the reflection arrivals.

sometimes chaotic nature of mine works in this area, to extrapolate the voids interpreted on this data set beneath the tracks without more supporting evidence. The surface location and migration path of the sinkhole suggests a room at least 3 m in height, and approximately 3 m in diameter beneath stations 145–155 on lines 2 and 3. The seismic sections show no voids meeting these criteria at that location. The mechanism responsible for the accelerated growth rate of the sinkhole, both horizontal and vertical, is apparently not related to subsidence.

Subsequent surface investigation revealed a correlation between the migration path of the sinkhole walls and the local drainage pattern of surface water (Fig. 6). The original formation of the sinkhole was probably from surface collapse of material surrounding a vertical shaft. The recent reactivation and

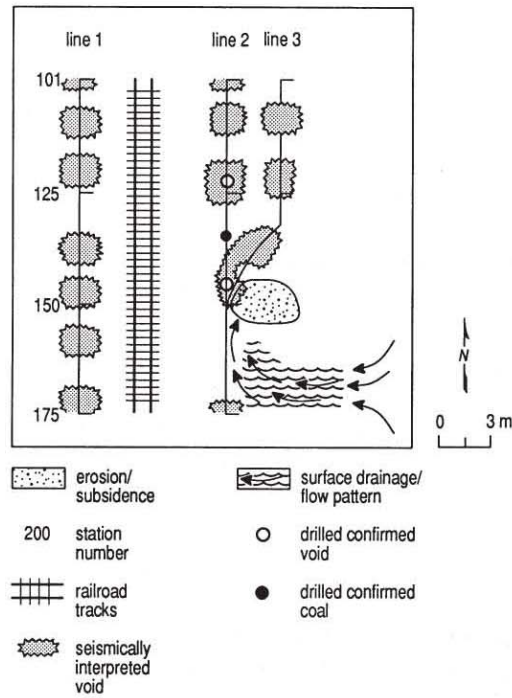


Fig. 6. Map view interpretation of the voids (rooms) and competent coal (pillars) interpreted on each of the three lines. Confident correlation of this grid-mining technique (as interpreted on the CDP stacked section) between lines would be speculative. The erratic nature of the orientation of the “rooms and pillars” as indicated by many mine maps from this area discourages line-to-line ties (with the exception of lines 2 and 3 near CDP 150). Surface drainage, as indicated, is responsible for the drop in the ground surface previously attributed to subsidence.

resulting expansion of the sinkhole perimeter is focused predominantly along a topographic low that is acting as a channel for surface-water runoff. The erosion associated with the water flow has lengthened the sinkhole along the drainage channel. Absence of water in the sinkhole indicates that surface water is probably escaping through the reopened vertical shaft. The accelerated rate of subsidence and growth direction of the sinkhole should remain consistent with the amount and drainage pattern of surface-water runoff in the immediate area.

CONCLUSION

High-resolution seismic-reflection methods were successfully used to evaluate the risk to rail traffic of an active sinkhole within 20 m of the tracks. Voids were interpreted on the seismic sections. The remnants of “room-and-pillar” mining can be clearly interpreted on stack seismic sections. Drill data

and an uphole survey agreed with the seismic-reflection data on depth-to-coal, location of intact coal, location of voids in the coal seam, and two-way travel time from the surface to the coal and back to the surface. The geologic interpretation is based on information acquired through confirmation drilling along the seismic-reflection profile and on uphole travel times. The correlation of the drill information and the seismically derived interpretation of line 2 justifies confidence in the overall interpretation (Fig. 6). The areal expansion of the sinkhole was determined from seismic data not to be related to the collapse of a horizontal mine shaft. The accelerated growth is probably a result of erosion.

As a result of the seismic survey and interpretive geologic cross-section, the recommendation was made to fill the active sinkhole with impermeable material and reroute surface drainage away from the hole. These recommendations were accepted and completed by the railroad, ending the apparent sinking and the immediate danger to the railroad tracks.

ACKNOWLEDGEMENTS

The development of this application of the seismic-reflection method was supported in part by the U.S. Office of Surface Mining under Assistance Agreement No. J-5150055. We would like to thank Esther Price for her work in manuscript preparation, Rex Buchanan for his perceptive editorial suggestions, and Pat Acker for the quality graphics. We also appreciate the efforts of George Coyle, Randie Grantham, Greg Hildebrand, Andrew Kalik, and Tonja Nuss during data acquisition.

REFERENCES

- Birkelo, B.A., Steeples, D.W., Miller, R.D. and Sophocleous, M.A., 1987, Seismic-reflection study of a shallow aquifer during a pumping test. *Ground Water*, 25: 703-709.
- Branham, K.L. and Steeples, D.W., 1988, Cavity detection using high-resolution seismic-reflection methods. *Min. Eng.*, 40: 115-119.
- Heckel, P.H., Brady, L.L., Ebanks, W.J. and Pabian, R.K., 1979, Pennsylvanian cyclic platform deposits of Kansas and Nebraska, Ninth Int. Congr. of Carboniferous Stratigraphy and Geology, Guidebook Series 4, pp. 79.
- Hunter, J.A., Pullan, S.E., Burns, R.A., Gagne, R.M. and Good, R.L., 1984, Shallow seismic reflection mapping of the overburden-bedrock interface with the engineering seismograph—some simple techniques. *Geophysics*, 49: 1381-1385.
- Jongierius, P. and Helbig, K., 1988, Onshore high-resolution seismic profiling applied to sedimentology. *Geophysics*, 53: 1276-1283.
- Knapp, R.W. and Steeples, D.W., 1986, High-resolution common depth point seismic-reflection profiling: field acquisition parameter design. *Geophysics*, 51: 283-294.
- Miller, R.D., Pullan, S.E., Waldner, J.S. and Haeni, F.P., 1986, Field comparison of shallow seismic sources. *Geophysics*, 51: 2067-2092.

- Miller, R.D., Steeples, D.W. and Brannan, M., 1989, Mapping a bedrock surface under dry alluvium with shallow seismic reflections. *Geophysics*, 54: 1528–1534.
- Miller, R.D., Steeples, D.W. and Myers, P.B., 1990, Shallow seismic reflection survey across the Meers fault, Oklahoma. *Geol. Soc. Am. Bull.*, 102: 18–25.
- Pullan, S.E. and Hunter, J.A., 1990, Shallow shear-wave reflection tests. Expanded Abstracts of the Technical Program with Authors' Biographies, Vol. I. Society of Exploration Geophysicists sixtieth Annual Int. Meeting & Exposition, September 23–27, San Francisco, CA. *Soc. Explor. Geophys.*, Tulsa, OK, pp. 380–382.
- Steeples, D.W. and Miller, R.D., 1987, Direct detection of shallow subsurface voids using high-resolution seismic-reflection techniques, in: B.F. Beck and W.L. Wilson (Editors) *Karst Hydrogeology: Engineering and Environmental Applications*, Balkema, Boston, pp. 179–183.
- Steeples, D.W. and Miller, R.D., 1990, Seismic-reflection methods applied to engineering, environmental, and ground-water problems. In: S. Ward (Editor), *Soc. Explor. Geophys. Volumes on Geotechnical and Environmental Geophysics*. Vol. 1. Review and Tutorial, pp. 1–30.
- Waters, K.H., 1987, *Reflection Seismology—A Tool for Energy-Resource Exploration*, 3rd ed. Wiley, New York, 538 pp.
- Widess, M.B., 1973, How thin is a thin bed? *Geophysics*, 38: 1176–1180.

Miller, R.D., J. Ivanov, D.W. Steeples, W.L. Watney, and T.R. Rademacker, 2005, Unique near-surface seismic-reflection characteristics within an abandoned salt-mine well field, Hutchinson, Kansas [exp. abs.]: Society of Exploration Geophysicists, p. 1041-1044.

Unique near-surface seismic-reflection characteristics within an abandoned salt-mine well field, Hutchinson, Kansas

Richard D. Miller,*† Julian Ivanov,† Don W. Steeples,‡ W. Lynn Watney,† and Theresa R. Rademacker†

†Kansas Geological Survey, University of Kansas, Lawrence, Kansas

‡Department of Geology, University of Kansas, Lawrence, Kansas

Summary

High-resolution seismic reflections have been used effectively to investigate sinkholes resulting from the dissolution of a bedded salt unit found throughout most of central Kansas. A seismic reflection survey was conducted to investigate the shallow subsurface between a sinkhole that formed catastrophically within a few tens of meters of a main east/west rail line. Data quality was significantly below expectations and not equivalent to other seismic data from this area where acquisition parameters, equipment, and target intervals were similar. Near-surface tomographic and MASW analyses revealed a highly irregular bedrock surface characterized by what appear to be a high concentration of short wavelength dissolution features. These bedrock features are below about 20 m of unconsolidated sediments with physical dimensions several meters deep and several meters wide. Data quality is quite good on other seismic reflection surveys from this general area where these bedrock features are not present. Pronounced static shifts and degradation in spectral characteristics of reflections where these bedrock features are present seems to be isolated to an area suspected to be the crest of a relatively broad anticlinal structure where surface fractures could have provided a conduit for fresh water to access shallow, thin evaporite layers within the thick shale sequence in the upper 200 m. Broadband high-resolution compressional-wave energy suffered significantly from this highly irregular bedrock topography.

Introduction

Concerns for public safety and the threat of property damage from a sinkhole that formed catastrophically within 40 m of a heavily traveled east/west railroad main line prompted a high resolution seismic reflection investigation of the subsurface between the sinkhole and the railroad tracks. Findings of this particular survey were inconclusive and prompted a more in-depth investigation to ascertain the reasons for the diversity in seismic responses observed at these different sites all within east central Reno County, Kansas.

Four seismic data sets, each from different sites in east central Reno County, Kansas, all targeting the upper several hundred meters of earth (including the Hutchinson Salt), were acquired because of the formation or threat of formation of a sinkhole (Figure 1). Of these four seismic data sets, two (① and ②) are from investigations of collapse structures associated with brine wells for salt mining, one (③) is a reconnaissance survey in an area with no sinkholes—but at high risk of future subsidence, and a fourth (④) is in an oil field where a brine disposal well was suspected of containment failure, dissolution, and collapse. These four profiles were acquired with

different equipment and using different techniques, but all are less than 10 km apart. One survey used vibroseis, two were impulsive using a 50-cal projectile source, and the fourth was impulsive employing an 8-gauge auger gun downhole source. Acquisition occurred over a 15-year period between 1990 and 2005.

Evidence exists throughout eastern Reno County for paleosinkholes not visible at the ground surface, which is an indication that fresh water has had access to the salt and a pathway to carry salt away from the dissolution front. Several naturally forming sinkholes in this area have seen recent reactivation and formation of surface depressions. No evidence existed prior to this seismic survey for karst type bedrock topography in this area that is a direct result of evaporite dissolution from rock layers other than the Hutchinson Salt.

Geologic Setting

Several major salt basins exist throughout North America. The Permian Hutchinson Salt Member occurs in a large portion of the Great Plains, and is prone to dissolution and subsequent formation of sinkholes. In Kansas, the Hutchinson Salt possesses an average net thickness of 76 m and reaches a maximum of over 152 m in the southern part of the basin. Deposition occurring during fluctuating sea levels caused numerous halite beds, 0.15 to 3 m thick, to be formed interbedded with shale, minor anhydrite, and dolomite/magnesite. Individual salt beds may be continuous for only a few miles despite the remarkable lateral continuity of the salt as a whole (Walters, 1978).



Figure 1. Site map, Reno County, Kansas.

Seismic-reflection characteristics within an abandoned salt-mine well field

Most of the upper 700 m of rock at the sites investigated here is Permian shales (Merriam, 1963). The Chase Group (top at 250 m deep), Lower Wellington Shales (top at 175 m deep), Hutchinson Salt (top at 125 m deep), Upper Wellington Shales (top at 70 m deep), and Ninnescah Shale (top at 25 m deep) make up the packets of reflecting events easily identifiable and segregated within the Permian portion of the section. Bedrock is defined as the top of the Ninnescah Shale with the unconsolidated Plio-Pleistocene Equus Beds making up the majority of the upper 30 m of sediment. Thickness of Quaternary alluvium that fills the stream valleys and paleosubsidence features goes from 0 to as much as 100 m, depending on the dimensions of the features.

Seismic Data Sets

① Principal Profile—Railroad Collapse

A continuous profile approximately 200 m long was centered on a sinkhole that formed catastrophically along an east-west railroad mainline in Hutchinson, Kansas (Figure 2). These data were acquired under significant site access restrictions, mainly related to physical limitations of working in a railroad drainage ditch along an active subsidence feature on one side and a railroad yard on the other. Data were recorded on a 240-channel Geometrics StrataView using two 40 Hz Mark Products geophones per station and a downhole 50-cal seismic source. Source spacing was 1.25 m and receiver stations were separated by 0.6 m. Data processing using *WinSeis* followed a very routine, proven high-resolution processing flow. These data possessed very limited bandwidth and raised concerns for data quality based on comparisons of data acquired just 2 km south of this railroad collapse site.

First arrivals and surface wave energy from the reflection data were processed to improve on the characterization of the shallow subsurface. Based on static effects observed on the shot gathers, poorer than expected data quality was blamed on static shifts between bedrock and ground surface, a distance of about 20 m. Turning-ray tomography and MASW cross sections suggest an extremely altered bedrock surface, with what appears to be a karst-type topography.

② Comparison Profile—Salt Mine Well Collapse

After catastrophic development of a sinkhole above a salt mine dissolution well field became a threat to a nearby city street and railroad spur in the early 1990s, a 200 m seismic reflection profile was acquired adjacent to the sinkhole intersecting both the road and railroad spur (Figure 3; Miller et al., 1993). Data were acquired with a 24-channel I/O seismograph and three 40 Hz Mark Products geophones, and a downhole 50-cal was used for the seismic energy source. Shot and receiver stations were separated by 2.5 m. Processing followed a very routine flow for near-surface reflection data and produced several lower resolution reflections on CMP stacked sections. Reflection bandwidth was relatively narrow, with little to no reflection energy returning from the bedrock.

To investigate the possibility that extreme bedrock topography could be responsible for static irregularities that have inhibited maximizing the CMP stacked sections along this line, these data were processed using turning-ray tomography and MASW analyses to image the upper 30 m. As with the site immediately northwest along the railroad tracks, the bedrock under this line is also very irregular with very irregular bedrock topography.

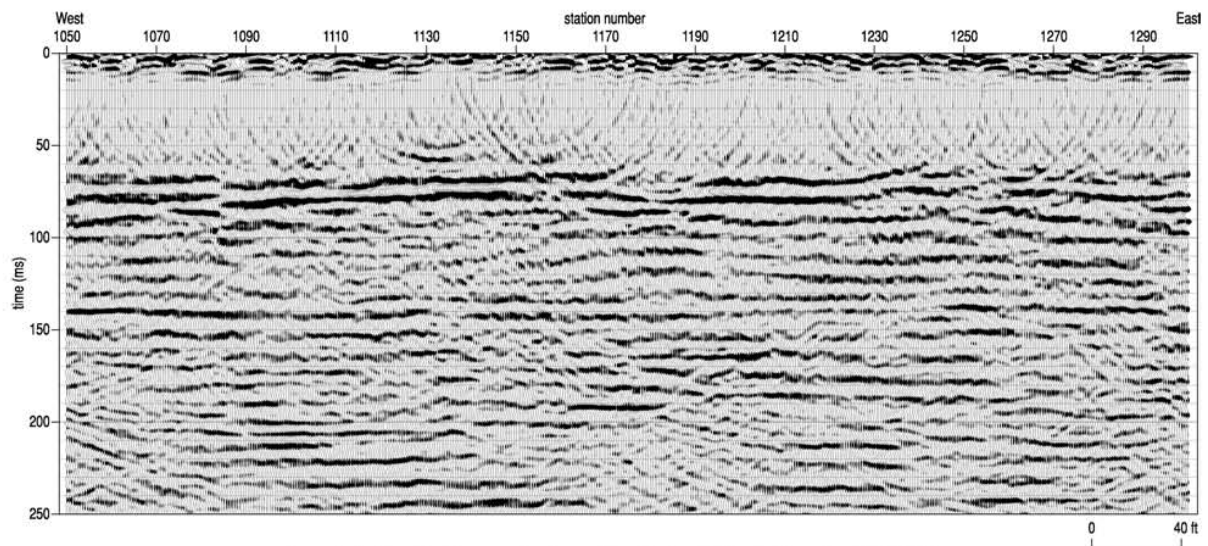


Figure 2. Railroad collapse seismic profile within salt dissolution mine field (①).

Seismic-reflection characteristics within an abandoned salt-mine well field

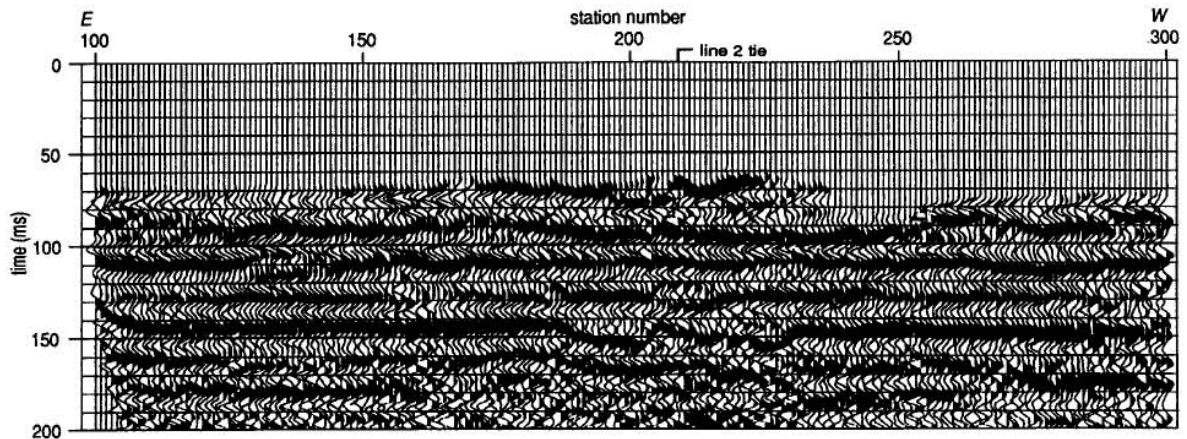


Figure 3. Salt mine collapse from early 1990s for comparison with recent collapse (②).

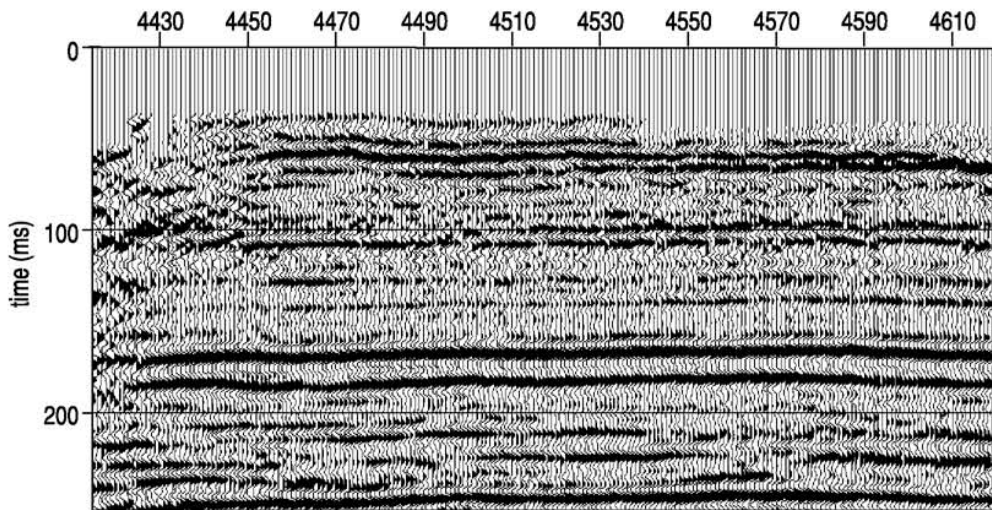


Figure 4. U.S. 50-bypass seismic profile less than 2 km south of salt mine collapse (③).

③ Undisturbed Surface Profile—U.S. 50 Highway

A continuous profile over 10 km in length was acquired along the existing U.S. 50 Highway right-of-way around Hutchinson, Kansas (Figure 4; Miller and Henthorne, 2004). This survey was designed to explore areas within or above the salt that could threaten future highway stability. A segment of this profile passed within 2 km of the brine well field where the primary and comparison profiles were acquired. Acquisition parameters and some of the equipment was different, but comparisons were still reasonable and possible. Data were acquired using the vibroseis technique, a 240-channel Geometrics StrataView and StrataVisor, and two 40 Hz Mark Products geophones. Receiver stations interval was 2.5 m with a 5 m source station spacing. Processing of these data was

very basic with a minimal flow. Reflections are broadband and high frequency. Overall the signal-to-noise ratio is quite good with a practical resolution potential of around 5 m within the salt interval.

Following the notion that data quality issues observed at the salt mine collapse sites are from static irregularities related to bedrock surface topography, a selected portion of this profile was subjected to turning-ray tomography and MASW analyses. Contrasting the non-reflection analysis between the datasets clearly suggests the extremely irregular bedrock surface is isolated to the salt mine collapse site and the degree of lateral variability observed would dramatically alter any body wave traveling incident to the bedrock surface.

Seismic-reflection characteristics within an abandoned salt-mine well field

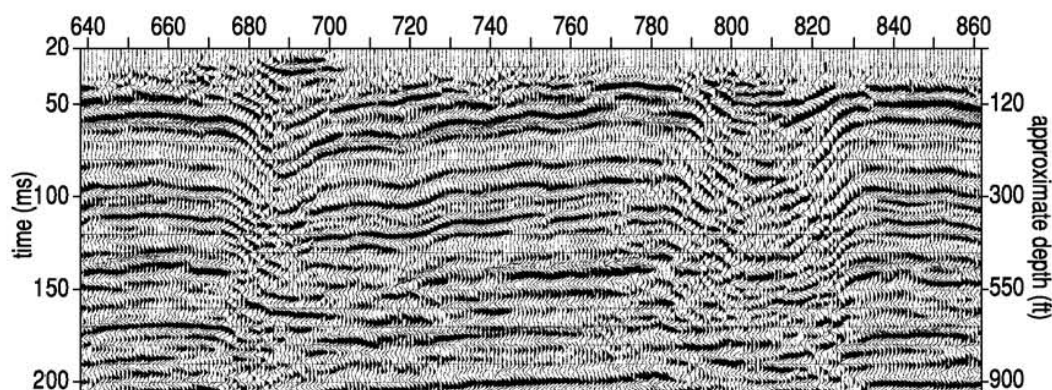


Figure 5. Paleosubsidence features from profile less than 10 km from salt mine collapse (④).

④ Paleosinkhole Profile—Disposal Well Collapse Site

A single seismic profile approximately 3 km long was acquired along the eastern dissolution front of the Hutchinson Salt in eastern Reno County to discern the origin of a sinkhole that formed around an oil field brine disposal well (Figure 5; Miller et al., 1998). Data were acquired using an impulsive 8-gauge auger gun source, 48-channel Geometrics ES-4801 seismograph, and three 40 Hz Mark Products geophones. Both source and receiver station intervals were 2.5 m. Processing was limited to a basic flow using *WinSeis*. These data were very high quality with a resolution potential less than 5 m within the salt interval.

Along the dissolution front, natural leaching of the salt is expected and paleosinkholes are common. Along this profile several paleosinkholes were imaged, resulting in a very irregular and distorted Permian rock sequence between the salt and bedrock. However, as evident from turning-ray tomography and MASW analysis, the bedrock surface is relatively uniform with only long wavelength undulations associated with the paleosubsidence. Clearly the overwhelming difference between this site and the salt mine collapse sites is the highly distorted, short wavelength undulation in the bedrock surface. There is no doubt the extremely inconsistent shallow bedrock velocities resulted in both spectral degradation and static problems.

Discussion

Differences in uniformity of rock in the upper several meters of bedrock at the salt mine collapse site has dramatically altered the signal quality and potential of the high-resolution seismic reflection data collected to investigate the sinkhole that formed catastrophically above an abandoned salt dissolution well. This very distorted bedrock surface seems to be regionally unique to this site. Seismic reflection data targeting the salt in other parts of this county do not suffer from the same poor data quality and do not possess the same highly irregular bedrock surface. The uniqueness of the bedrock topography and the associated seismic artifacts could be related to a

regional anticlinal structure suggested to extend beneath the central part of Reno County.

With the high evaporite concentrations within the Permian shale sequences between the bedrock surface and the top of the Hutchinson salt, if fractures formed along the crest of this structure during its formation, fresh surface and shallow subsurface waters could have gained access to interbedded evaporites close to the bedrock surface. If sufficient fluid movement was possible, dissolution voids could have formed consistent with the fractures, resulting in subsidence features and the karst topography apparent on the bedrock surface.

An extreme topography of the nature described would have an overwhelming impact on both the spectral and velocity characteristics of seismic reflection data. Using the tomography and MASW data velocity reconstruction is possible with improvements to static correction processes. Attenuation and interference of higher frequency components of the reflection wavelets cannot be recovered.

Acknowledgements

The authors thank Mike Cochran of the Kansas Dept of Health and Environment, the City of Hutchinson and especially Fire Chief Kim Forbes, for their assistance with site logistics during acquisition. Thanks also to the field crew from the Kansas Geological Survey: David Lafien, Joe Anderson, David Thiel, Brett Wedel, and Andrew Newell; also Mary Brohammer for help with manuscript preparation.

References

- Merriam, D.F., 1963, The geologic history of Kansas: Kansas Geol. Survey Bulletin 162, 317 p.
- Miller, R.D., and R. Henthorne, 2004, High-resolution seismic reflection to identify areas with subsidence potential beneath U.S. 50 Highway in eastern Reno County, Kansas: Proceedings of the 55th Highway Geology Symposium, September 8-10, Kansas City, Missouri, p. 29-48.
- Miller, R.D., D.W. Steeples, L. Schulte, and J. Davenport, 1993, Shallow seismic-reflection feasibility study of the salt dissolution well field at North American Salt Company's Hutchinson, Kansas, facility: Mining Engineering, October, p. 1291-1296.
- Miller, R.D., J. Xia, and D.W. Steeples, 1998, Shallow reflection does not always work [Exp. Abs.]: Soc. Explor. Geophys., p. 852-855.
- Walters, R.F., 1978, Land subsidence in central Kansas related to salt dissolution: Kansas Geological Survey Bulletin 214, p. 1-32.

Miller, R.D., D.W. Steeples, and T.V. Weis, 1995, Shallow seismic-reflection study of a salt dissolution subsidence feature in Stafford County, Kansas; in N.L. Anderson and D.E. Hedke, eds., Geophysical atlas of selected oil and gas fields in Kansas: Kansas Geological Survey Bulletin 237, p. 71-76.

[Reformatted from 11" x 17" size, as published, to fit this page format. No content has been changed.]

Shallow Seismic-reflection Study of a Salt-dissolution Subsidence Feature in Stafford County, Kansas

Richard D. Miller¹, Don W. Steeples², and Thomas V. Weis³

¹Kansas Geological Survey, The University of Kansas, Lawrence, KS 66047;

²Department of Geology, The University of Kansas, Lawrence, KS 66045; and

³formerly with Kansas Geological Survey, now with Normandy Exploration Limited, Kent Town, Australia

Abstract

Seismic-reflection surveying was successfully used to define subsidence of the Stone Corral anhydrite in Stafford County, Kansas, in response to dissolution of the 85-m (279-ft)-thick Permian-aged Hutchinson Salt at a depth of approximately 340 m (1,116 ft). Gradual formation of a surface depression around the Siefkes "A" No. 6 abandoned oil-field-brine disposal well in Stafford County, Kansas, led to a 12-fold CDP seismic survey to define the potential extent and amount of future surface subsidence. Several reflections interpreted on the CDP stacked sections possess dominant frequencies in excess of 100 Hz. Reflections can be interpreted on stacked sections at two-way times from 80 msec (approximate depth of 70 m; 230 ft) to 220 msec (approximate depth of 200 m; 656 ft). The Stone Corral anhydrite reflection is present between 200 and 220 msec on all three seismic lines and possesses a maximum of 20 msec (35 m assuming 1,770 m/sec seismic velocity) of relative subsidence. The March 1990 subsurface dissolution boundary, as defined by the Stone Corral anhydrite, suggested a potential four-fold increase in the surface area of the sinkhole encompassing part of both an east-west and a north-south county road.

Introduction

Subsurface dissolution of salt beds represents a hazard to surface and subsurface structures in many parts of the world. Natural or anthropogenic subsidence can occur either gradually or catastrophically (Walters, 1977). Determination of potential extent of future surface subsidence allows more accurate damage estimates and rehabilitation requirements.

Seismic-reflection techniques have successfully detected the presence and extent of subsurface dissolution prior to and during surface subsidence (Steeple et al., 1986, 1987; Miller et al., 1985; Knapp et al., 1989). The technique offers a powerful method of imaging portions of the subsurface in the vicinity of some subsidence features. The successful use of the technique depends on several key conditions. First and foremost is the existence of acoustic velocity and/or density contrasts between geologic units in the subsurface. The Stone Corral anhydrite fulfills this condition, having a large acoustic velocity and density contrast with surrounding siltstones, silty sandstones, and shales. The second condition relates to the ability of the near-surface to propagate a high-frequency seismic signal. Finally, the acquisition parameters and recording equipment must be compatible with the proposed target and required resolution of the survey.

Geologic Setting and Subsidence

Several major salt basins exist throughout North America (fig. 1) (Ege, 1984). The Hutchinson Salt Member of the Permian Wellington Formation underlies a significant portion of south-central Kansas (fig. 2) (Walters, 1977). The thickness of the salt increases from depositional edges on the west and north, an erosional edge on the east, and a facies change on the south to a maximum thickness of over 170 m (558 ft) in north-central Oklahoma. The increased thickness of the Hutchinson Salt is due to increased quantities of salt as well as more and thicker interbedded anhydrites. Thick-

ness of the salt in the vicinity of the Siefkes subsidence is approximately 75–85 m (246–279 ft) (figs. 3 and 5) (Watney, 1980). Cross section A–A' shows the distribution of salt along an east-west profile located 6 mi (9.6 km) north of the Siefkes subsidence feature (fig. 6) (Watney, 1980). The Siefkes subsidence is located approximately 120 km (72 mi) west of the Hutchinson Salt dissolution front (figs. 3 and 6) (Watney, 1980).

The stratigraphic section overlying the Hutchinson Salt Formation at the Siefkes well location is the target of this seismic-reflection survey (fig. 5). Overlying the salt are approximately 70 m (230 ft) of the upper Wellington Formation shales with minor carbonates, 80 m (262 ft) of the Ninnescah Shale with minor carbonates, and 6 m (20 ft) of Stone Corral anhydrite at a depth of 186 m (610 ft). The Stone Corral is a key seismic marker horizon in central Kansas. The depression of the Stone Corral, resulting from dissolution of the underlying Hutchinson Salt, is used to map the lateral extent of the Siefkes subsidence feature in the subsurface. Overlying the Stone Corral is approximately 70 m (230 ft) of Harper Sandstone, 80 m (262 ft) of Salt Plain Sandstone, and 41 m (135 ft) of Quaternary unconsolidated sediments.

Salt dissolution can result in various rates of surface subsidence. The dissolution process remains active as long as flowing unsaturated brine solution or freshwater is in contact with a salt bed. This results in the formation of a void, generally water filled, within the salt bed. Depending on the size of the void and the competency of the overlying sedimentary section, either a void or a closed collapse feature migrates upward at varying rates. The result is a catastrophic collapse or gradual subsidence when the effect of the dissolution feature reaches the surface.

Natural dissolution of the Hutchinson Salt is not uncommon in Kansas (Ege, 1984). Surface subsidence associated with natural salt dissolution occurred in Meade County, Kansas, in 1879. Faults extending through the Pleistocene sediments (sediments containing freshwater under hydrostatic pressure) are postulated as the conduits for flow instigating the salt dissolution that eventually resulted in the Meade County sinkhole (Frye

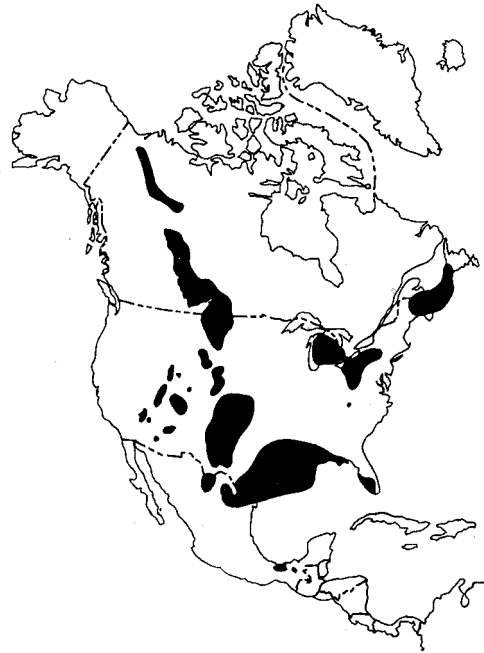


FIGURE 1—MAJOR SALT BASINS OF NORTH AMERICA (Ege, 1984).

and Schoff, 1942). Paleo-sinkholes resulting from dissolution of the Hutchinson Salt prior to Pleistocene deposition have been discovered with high-resolution seismic-reflection surveys (Steeple et al., 1984). Natural dissolution of the Hutchinson Salt may have been occurring to some degree in some localities since deposition.

Land subsidence associated with salt mining and petroleum-related brine disposal has been documented in Kansas for at least the last 70 years (Walters, 1977). In cases related to solution salt mining, sinkholes generally have been the result of roof rock failure. Casing failure or faulty surface grouting have allowed petroleum by-product disposal wells to become conduits to the Hutchinson Salt (unsaturated brine solutions). Sinkholes related to brine-disposal wells result from roof failure similar to sinkholes associated with solution mining of salt.

Siefkes Subsidence Feature

The Siefkes subsidence feature is located in NE NE NE sec. 3, T. 22 S., R. 12 W. in Stafford County, Kansas (fig. 3). The gradually forming, anthropogenic subsidence feature is centered on the plugged Siefkes "A" No. 6 saltwater-disposal well (fig. 4). A rough visual estimate of surface subsidence as of 1990 indicated the feature had approximate dimensions of 75 m by 85 m (246 ft by 279 ft) laterally with about 0.5 m (1.6 ft) maximum vertical displacement (fig. 4). This is a minimum estimate since visually determining the outer edges of a shallow subsidence feature is difficult.

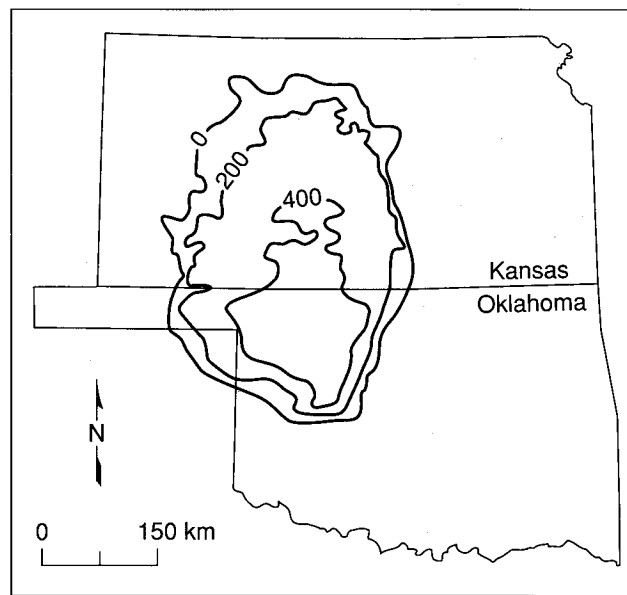


FIGURE 2—AREAL EXTENT AND THICKNESS OF HUTCHINSON SALT MEMBER (Walters, 1977).

The Siefkes "A" No. 6 drillhole was completed in November 1939. It penetrates the Hutchinson Salt Member of the Wellington Formation from 344 m to 416 m (1,129 ft to 1,365 ft) in depth. The drillhole has a total depth of 1,100 m (3,609 ft) and terminates in the Arbuckle Formation. The well was converted to a saltwater-disposal well in 1950 (Korphage, personal communication, 1992). Unsaturated fluids eventually reached the Hutchinson Salt either through corroded casing or along the outside of the casing. The well passed a mechanical integrity test as late as 1986, but due to evidence of surface subsidence, it was plugged in 1988 (Morris, personal communication, 1992). The onset of dissolution of the Hutchinson Salt and the time required for the subsidence to have developed a noticeable surface expression is unknown.

Field Parameters

Three CDP seismic-reflection lines were acquired with nominal 24-fold redundancy (fig. 4). The lines were roughly centered on and intersect at the Siefkes "A" No. 6 inactive brine-disposal well. Lines 1 and 2 were acquired during March 1989 with line 3 acquired in March 1990. The original two lines (1 and 2) were collected with extremely dry near-surface conditions and abnormally high winds. It was determined after digital processing of data from lines 1 and 2 that more subsurface information was needed east

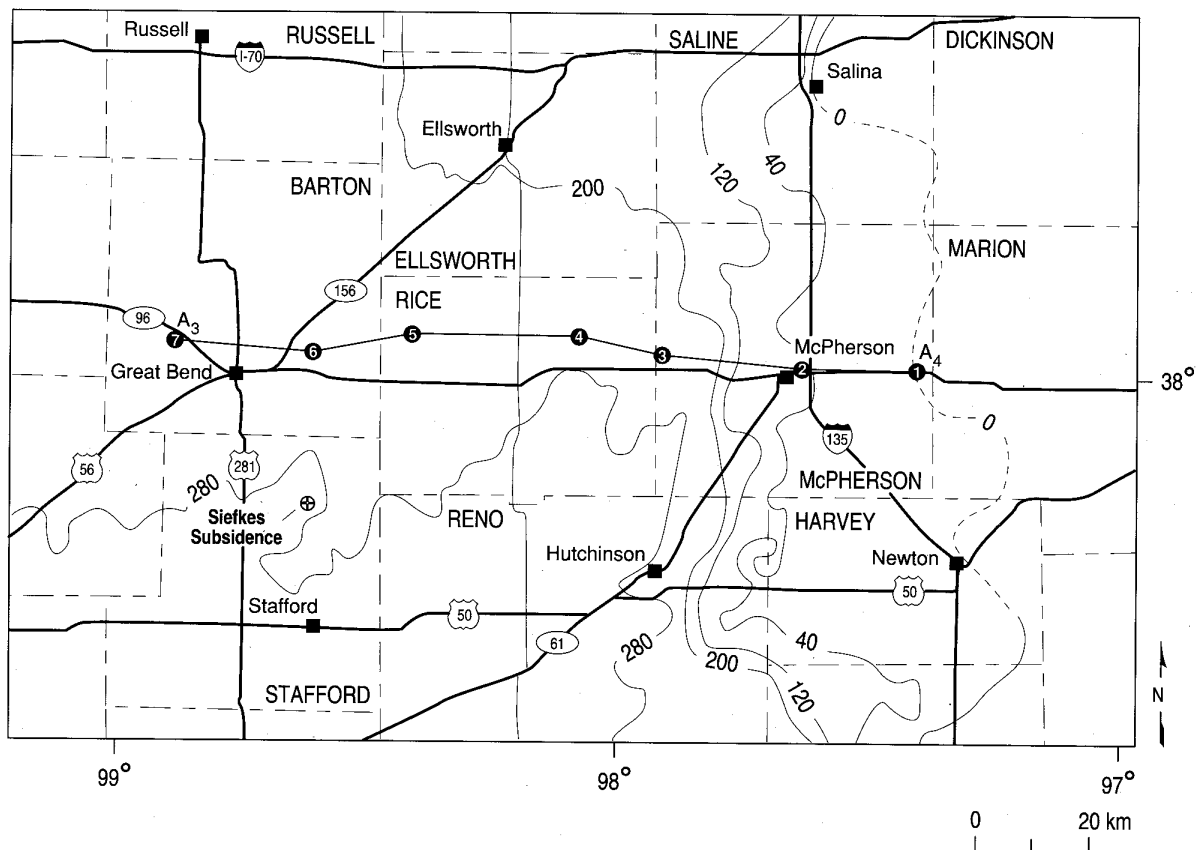


FIGURE 3—SIEFKES SUBSIDENCE LOCATION MAP, INCLUDING HUTCHINSON SALT THICKNESS CONTOURS and drillhole cross section location (Watney, 1980).

of the north-south county road. The third line was then acquired using the results of lines 1 and 2 to determine line length and location.

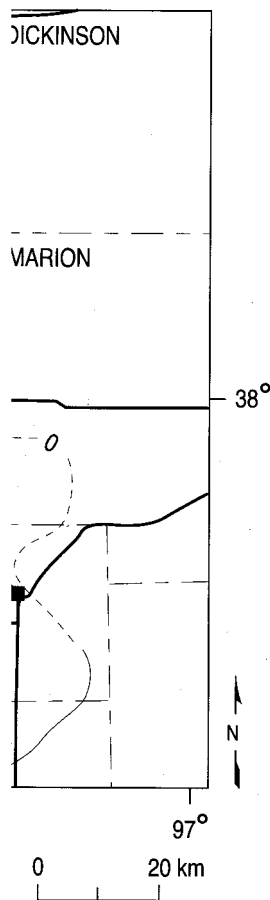
An extensive series of walkaway-noise tests was conducted prior to production acquisition (table 1). The compacted near-surface material made it impossible to use the downhole .50-cal seismic source (the source of choice at this site, for this geologic target) and forced the use of an above-ground silenced .50-cal gun. The .50-cal silencer reduces source-generated air-coupled waves and acts as a containment device for stray debris. The surface configuration of the .50 cal is less energetic and does not generate the high frequency and broad bandwidth signal possible with the .50 cal in the downhole mode (Steeple et al., 1987). The receiver array consisted of three 40-Hz geophones equally spaced over approximately 1 m (3.3 ft) and centered on each station. The receiver array was designed in an attempt to attenuate the source-generated noise. The acquisition parameters and equipment for lines 1 and 2 were optimized for the less-than-ideal site conditions.

Significant changes in the near-surface conditions during the March 1990 survey necessitated a new set of walkaway-noise tests for line 3 (table 1). Improved near-surface conditions allowed the use of the .50-cal downhole gun. In the downhole configuration of the .50 cal, the gun barrel is lowered down an augered hole approximately 6 cm (2.4 inches) in diameter and 0.6 m (2 ft) deep. The downhole placement of the barrel greatly reduces both the source-generated air-coupled waves and the thickness

of low-velocity, highly attenuative near-surface material through which seismic energy must travel. Station spacing was identical to the 1989 survey as were the receiver arrays and source/receiver geometries. Consistent with the 1989 survey, the acquisition parameters and equipment were optimized to the site conditions and geologic target.

The source/receiver geometry on all three lines resulted in a nominal 24-fold data set. Most shot locations were occupied twice, once pushing the 24-channel spread from low-numbered stations to high-numbered stations and then reversed, pushing the same spread from high-numbered stations to low-numbered stations. This acquisition procedure results in a pseudo 48-channel symmetric (with respect to the source location) split-spread geometry with two consecutive groups of 24 channels separated by three stations.

The 24-channel data were analog-filtered, amplified, A/D-converted (11 bit plus sign), and recorded on an Input/Output DHR-2400 seismograph. Analog low-cut filters helped to enhance the data bandwidth by decreasing the amount of low-frequency noise, allowing increased gaining of incoming post-filtered high-frequency signal. The analog low-cut filters selected have a 24 dB/octave roll-off with a -3 dB point of 110 Hz for line 3 and 55 Hz for lines 1 and 2. The relatively severe analog low-cut filtering increased the dominant reflection frequencies and therefore improved the potential vertical- and horizontal-bed resolution.



the cross section location

TABLE 1—CRITICAL ACQUISITION PARAMETERS.

	3/90	3/91
Station increment	5 m (16.5 ft)	same as 3/90
Receiver array length	1.5 m (4.9 ft)	same as 3/90
Split-spread intervals*	10 - 125 m (33–412.5 ft)	same as 3/90
Source downhole	.50 cal surface	.50 cal
Receivers	L28E Mark Prod.	same as 3/90

*Source-to-nearest-and-farthest-receiver distance

TABLE 2—CDP SEISMIC PROCESSING STEPS.

Format to SEG-Y
Dead and noisy trace edit
Trace balancing (AGC)
First-arrival muting
Surgical muting of coherent noise
CDP sort
Datum statics correction
NMO correction
Surface-consistent statics
Bandpass filtering
CDP stack

Data Processing

The CDP data were processed at the KGS using a proprietary set of algorithms developed by Sytech Co. The processing flow was very similar to routine petroleum sequences with the exception of the severity and accuracy of the muting processes and the emphasis placed on near-surface velocity analysis (table 2). Extreme care was used during the editing processes to ensure removal of all non-seismic energy that could either be misinterpreted as reflections on stacked data or that hampered interpretations of real reflection events. Velocity analysis incorporated iterative constant velocity stacking with detailed surface-consistent statics to improve both accuracy of velocity corrections and time/depth conversion on interpreted cross sections. The general processing flow resulted in a nominal 24-fold CDP stacked section for each of the three survey lines.

Results

Reflection energy can be identified on raw field data in a time window between about 80 msec and 400 msec (fig. 7). Differentiation of reflection energy from seismic noise on field files is essential for confident and consistent interpretation of stacked seismic sections. Refraction arrivals, present as the first breaks (first source-generated energy recorded) on seismograms, were removed with a severe first-arrival mute. Low-velocity linear arrivals that can be identified on the nearest-to-the-source trace at about 50 msec and on the farthest-from-the-source trace at about 400 msec are source-

generated air-coupled waves. Air-coupled waves were surgically removed from all shot gathers. Ground roll is the low-frequency energy clearly visible on inside traces between 10 m and 40 m (33 ft and 131 ft) source offset. The low-frequency characteristics of the ground roll make attenuation with a properly designed bandpass filter very effective. Dominant frequency of reflection energy is in excess of 100 Hz.

Reflections from the Stone Corral anhydrite can be clearly identified at about 210 msec on most field files (fig. 7). The apparent reverse moveout on the Stone Corral reflection on this field file is interpreted to be the result of roof failure of a previous salt-dissolution void. Stone Corral reflections on seismograms from areas with competent salt would appear hyperbolic with a very subtle downward curvature at increasing receiver-to-source offsets. The reflection energy interpretable on this seismogram clearly indicates subsurface collapse. A synthetic seismogram calculated from the nearby Sittner "A" No. 1 acoustic-velocity log supports the interpretation of the field file (fig. 8). The strongest reflector on the synthetic seismogram is the Stone Corral. The absolute two-way travel time of the Stone Corral reflector calculated from the synthetic seismogram is unknown because the acoustic log used to generate it was not recorded above a depth of 76 m (250 ft). However, the amplitude of the Stone Corral reflection is

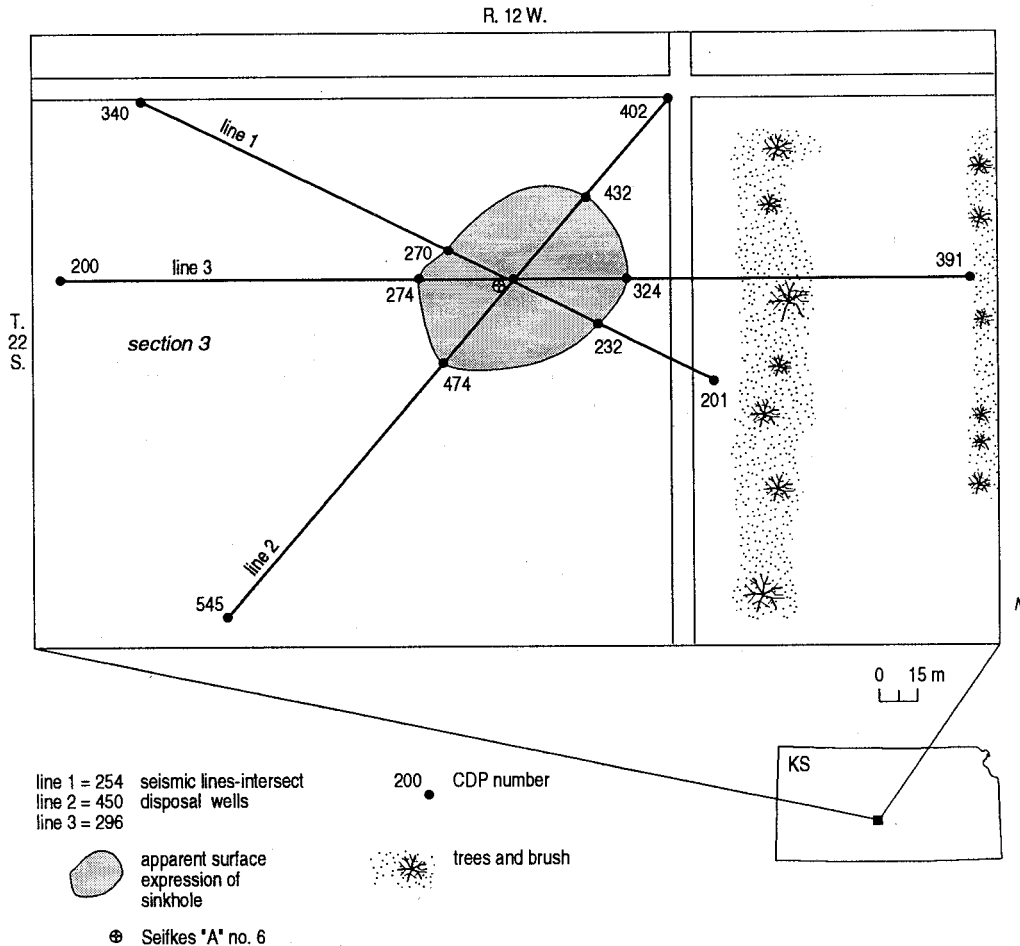


FIGURE 4—SITE MAP INDICATING LOCATION OF THREE SEISMIC LINES AND APPROXIMATE AREAL EXTENT OF THE SUBSIDENCE.

significantly larger than any other reflection occurring between 76 m (250 ft) and 457 m (1,500 ft) on the synthetic seismogram. This supports the interpretation that the large amplitude 210-msec reflections observed on lines 1, 2, and 3 (figs. 9, 10, and 11) are from the Stone Corral. By comparing the drill log (fig. 5) with the field file plot (fig. 7), a stacking velocity of 1,800 m/sec is calculated. This is consistent with the results of the velocity analysis carried out during processing.

The top of the Hutchinson Salt does not generate a large amplitude reflection on the synthetic seismogram (fig. 8). In fact, it is a weaker reflector than is indicated by the synthetic seismogram because the low density-high velocity combination of salt results in a small acoustic-impedance contrast with the surrounding low velocity-high density shales. No density log is available for the Sittner "A" No. 1 drillhole, so the large acoustic velocity of the salt is not modified by the salt's low density, and the synthetic seismogram overestimates the salt response. Figure 7 confirms that the top of the Hutchinson Salt is not a good reflector.

Seismic line 1 was acquired with a maximum record length of 250 msec (fig. 9). The target on line 1 was the top of the Stone Corral. Faulting and subsidence interpreted on the Stone Corral is assumed to be the result of dissolution of the salt. Normal faults forming horst and graben structures can be interpreted from the 12-msec depression of the Stone Corral reflection. Subtle coherent reflection events observed between CDPs 225 and 275 above the Stone Corral are most likely from within the Harper and Salt Plain Sandstones. The lack of coherent events between the Stone Corral and the surface from CDPs 275 to 325 is related to the poor near-surface and environmental conditions. Dissolution in the subsurface extends from approximately CDPs 220 to 320 on line 1.

Seismic line 2 was acquired with a maximum record length of 500 msec (fig. 10). Coherent reflection information is identifiable between approximately 70 and 320 msec. The overall data quality on line 2 is better than line 1 due to decreased wind noise. The near-surface conditions were consistent for both lines 1 and 2. The Stone Corral reflection can be identified across the entire line. A depression of up to 20 msec is observed on the Stone Corral reflector. Several reflection events between the Stone Corral and the surface are interpreted as coming from within the Harper and Salt Plain Sandstones and are across the entire expanse of line 2. The interpretative line drawing clearly shows the extent of faulting and the relatively uniform nature of the subsidence in the subsurface. The severity of reflector slump observed on line 2 appears to increase with depth. This apparent decrease in subsidence upward from the salt is probably related to differential expansion, although it could be related to velocity anomalies related to slumping into the cavity. The predominant structural features on line 2 are the series of normal fault blocks that bound the graben formed as a result of dissolution and subsidence.

Line 3 was acquired east-west and is the most conclusive of the three seismic lines (fig. 11). The dominant frequency of the Stone Corral reflection is clearly in excess of 100 Hz. Subsurface subsidence on line 3 extends from CDP 250 to 340. Normal faults offset the Stone Corral reflection across the entire subsidence area. The maximum depression of the Stone Corral reflection is 20 msec. Only the normal fault interpreted at approximately CDP 325 offsets the 80-msec reflecting event. The 80-msec reflection is the shallowest interpreted reflector at a depth of approximately 50 m (164 ft). Several high-frequency events are interpreted between the 80-msec reflection and the approximately 200-msec Stone Corral

reflection. The relatively uniform, gradual slump of reflectors overlying the dissolved salt can be observed on all three lines.

The 20-msec depression of the Stone Corral reflector visible on lines 2 and 3 (figs. 10 and 11) represents the Siefkes subsidence feature in the subsurface. By using an 1,800-m/sec stacking velocity, calculation of a 35-m (115-ft) maximum vertical displacement of the Stone Corral is possible. If the stacking velocity within the zone of subsidence is reduced by the collapse and fracturing of the sediments overlying the salt, the resulting vertical displacement would be proportionately less than 35 m (115 ft).

The potential future surficial expression of dissolution voids in the Hutchinson Salt can be extrapolated from interpretations on the Stone Corral reflection (fig. 12). The dashed portions of the interpreted future sinkhole represent speculative interpolation between control points on the associated seismic lines. The apparent eastward elongation of the future sinkhole along line 3 indicates subsidence of the Stone Corral reflector was probably active along the eastern edge between March 1989 and March 1990. This ongoing subsidence of the Stone Corral may be indicative of active dissolution or delayed roof failure along the eastern portion of the salt void.

Conclusions

Optimum recording parameters for each line were selected after two separate extensive series of walkaway-noise tests, one for each survey (table 1) (Steeles and Miller, 1990). Adverse near-surface and environmental conditions, detrimentally affecting both geophone plants and propagation of high-frequency seismic-reflection information, strongly contributed to a low signal-to-noise ratio on the 1989 survey. Improved site conditions on the 1990 survey allowed use of the downhole .50-cal gun and 110-Hz low-cut filters, which (in comparison to the 1989 survey) resulted in reduced levels of recorded environmental, instrument, and non-seismic reflection noise.

The subsurface subsidence associated with this Siefkes subsidence feature (at least as indicated by the Stone Corral anhydrite) seems to have been active as of March 1990. Extrapolation of the present subsurface dissolution boundaries (as interpreted from the Stone Corral reflection) suggests a potential four-fold increase in the surface area of the present-day sinkhole. At some time in the future, this sinkhole could include part of the east-west and north-south county roads. Dissolution of the salt, as interpreted from seismic data, appears to be

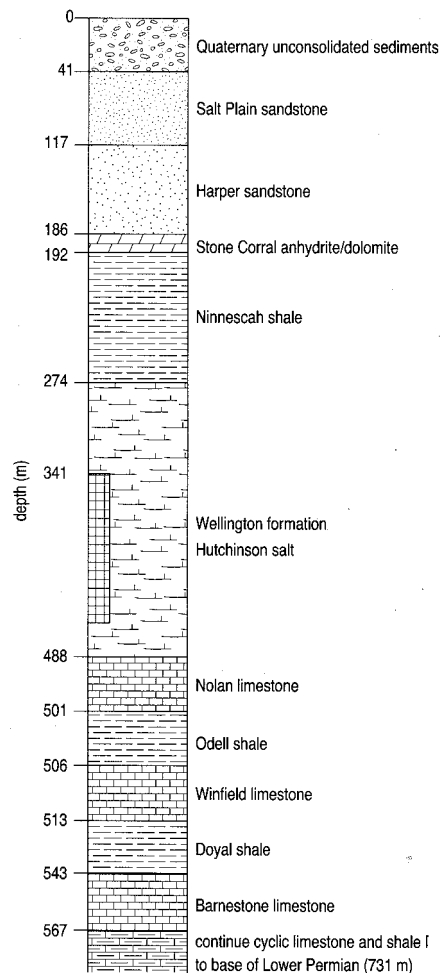
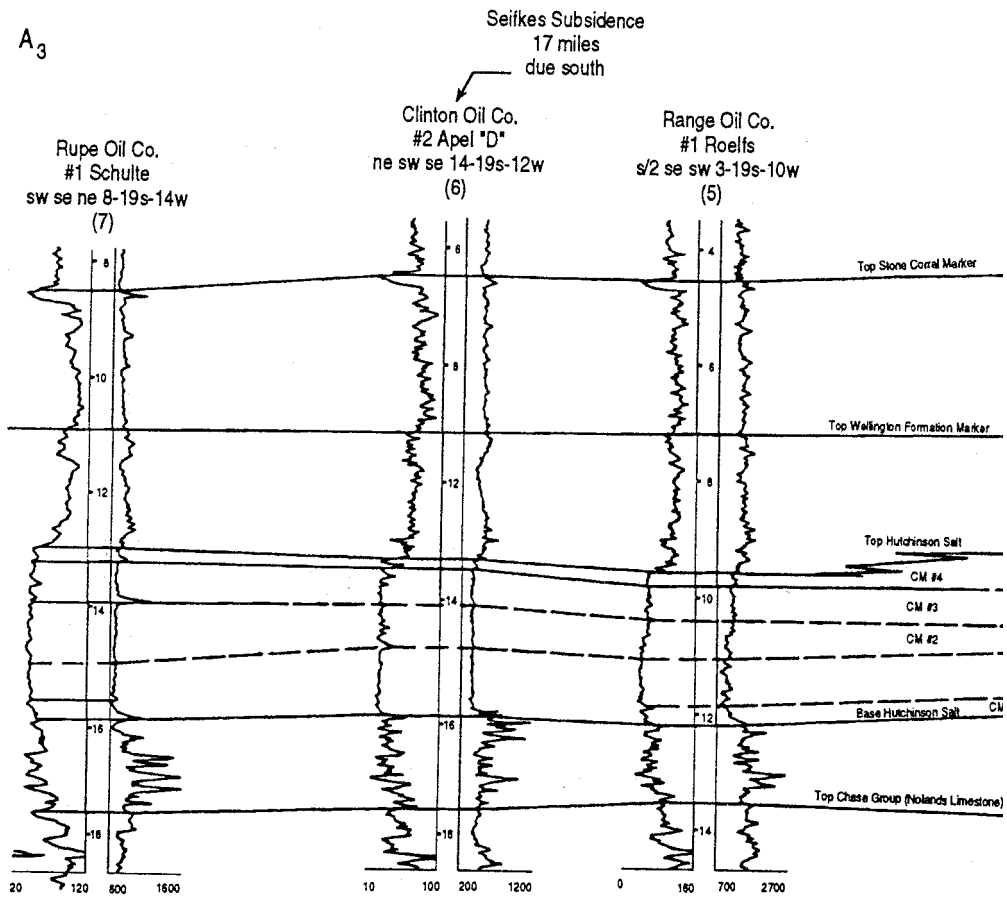
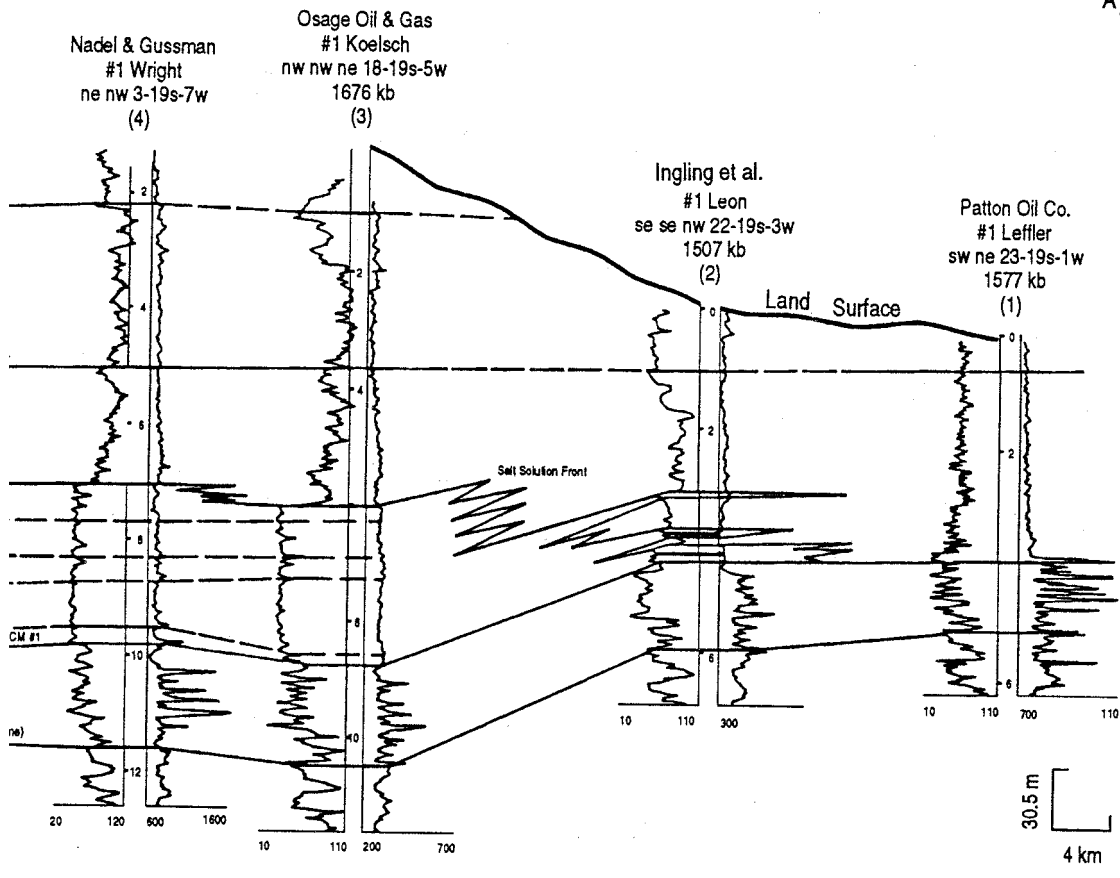


FIGURE 5—STRATIGRAPHIC SECTION FROM SIEFKES "A" No. 6 GAMMA RAY/NEUTRON LOG.



Open file August, 1980
W. L. Watney
Kansas Geological Survey

FIGURE 6—DRILLHOLE CROSS SECTION A₃—A₄ THROUGH BARTON, RICE, AND MCPHERSON COUNTIES, KANSAS (



West to east stratigraphic cross section
Scott County to McPherson County, Kansas
Hutchinson Salt Member, Wellington Formation
Datum: Top Wellington formation marker
Logs: Gamma Ray-Neutron (API Units)

(Watney, 1980).

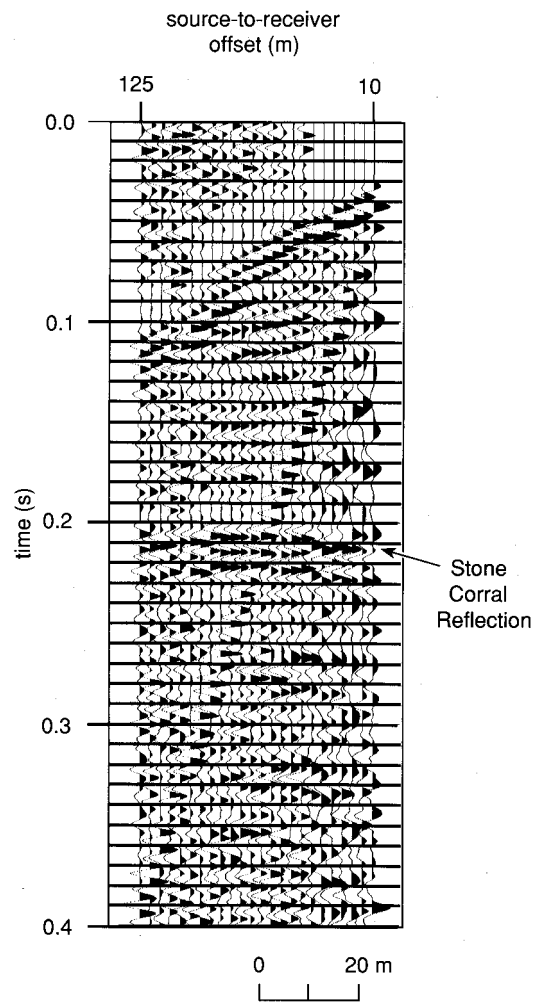


FIGURE 7—24-CHANNEL FIELD FILE WITH STONE CORRAL REFLECTION INDICATED.

slightly asymmetric to the west with respect to the surface location of the abandoned disposal well.

There is no reason to suspect the apparent eastward growth of the subsurface dissolution front has terminated. The actual subsurface dissolution front could be well east of the north-south county road that intersects line 1. It is also not unreasonable to suggest that the northeast boundary (as interpreted from line 2) may now be several tens-of-meters closer to the intersection of the two county roads. No seismic evidence exists (on the three seismic lines reported here) to suggest the surficial expression of the subsurface subsidence will reach the intersection of the north-south and east-west county roads. The north-south county road will eventually be affected by the salt dissolution which has already resulted in subsurface subsidence (as interpreted on the Stone Corral anhydrite) several tens-of-meters east of the road.

The interpreted subsurface subsidence on the western boundary appears to be consistent over the span of time between the two seismic surveys. Topographic evidence seems to suggest surface subsidence is presently active along the western boundary. There is no seismic evidence to suggest westward expansion of subsurface subsidence.

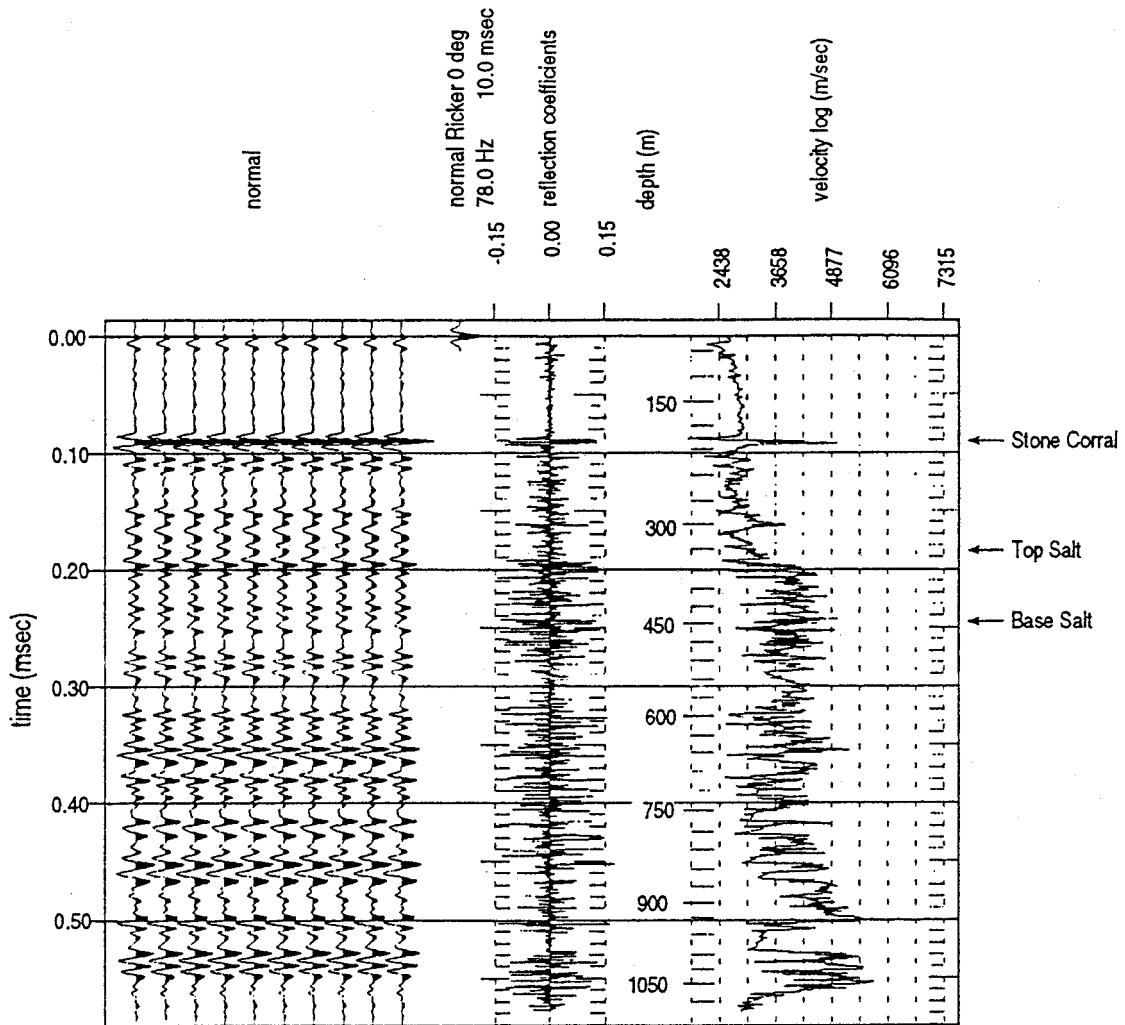


FIGURE 8—SYNTHETIC SEISMOGRAM CALCULATED FROM SITTNER "A" No. 1 ACOUSTIC VELOCITY LOG. The Stone Corral reflection is indicated.

The apparent subsurface growth of the dissolution front to the east with no apparent associated surface subsidence suggests delay between roof failure of the salt unit and surficial expression. The apparent elongation of the surface expression of the sinkhole to the west between the two seismic surveys with no obvious associated subsurface growth is probably related as well to a delay. The delay between roof collapse and surface subsidence is probably not uniform for all parts of the sinkhole. Alternatively, the rate of dissolution may vary with azimuth from the center of the sinkhole, in which case the elongation noted above may not be indicative of active dissolution.

The results derived from interpretations of the three seismic lines suggest a continued gradual subsiding of the surface around the abandoned disposal well. Due to the apparent active nature of the subsurface subsidence, the maximum future surficial expression of the salt voids and associated roof collapse cannot be ascertained from the three seismic lines collected between March 1989 and March 1990. There appears to be either continued subsurface growth of salt voids to the east or delayed roof failure of previously existing voids in the salt. A return visit to this site in approximately two to three years with the intent of acquiring data along line 3 should yield far more insight into subsurface growth and rate of roof failure.

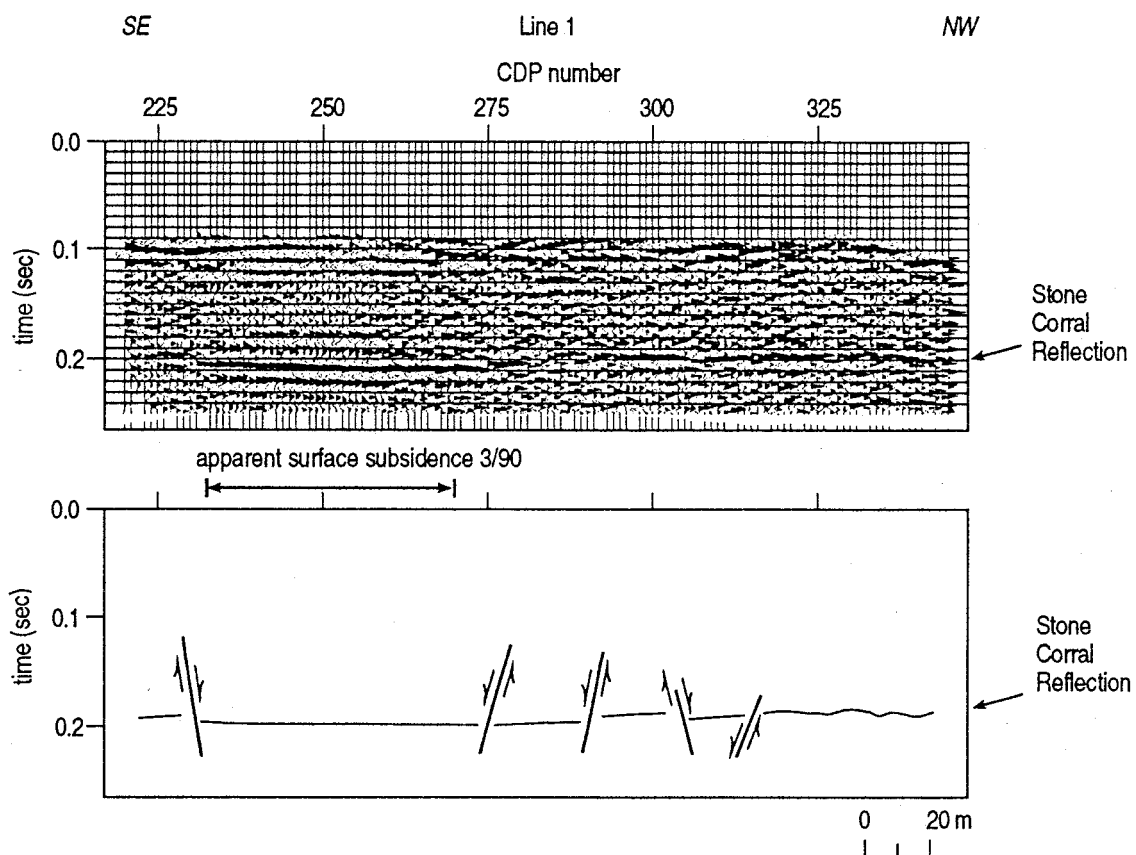


FIGURE 9—PSEUDO 24-FOLD STACK SEISMIC SECTION OF LINE 1 WITH ASSOCIATED INTERPRETIVE LINE DRAWING. The Stone Corral reflection is indicated.

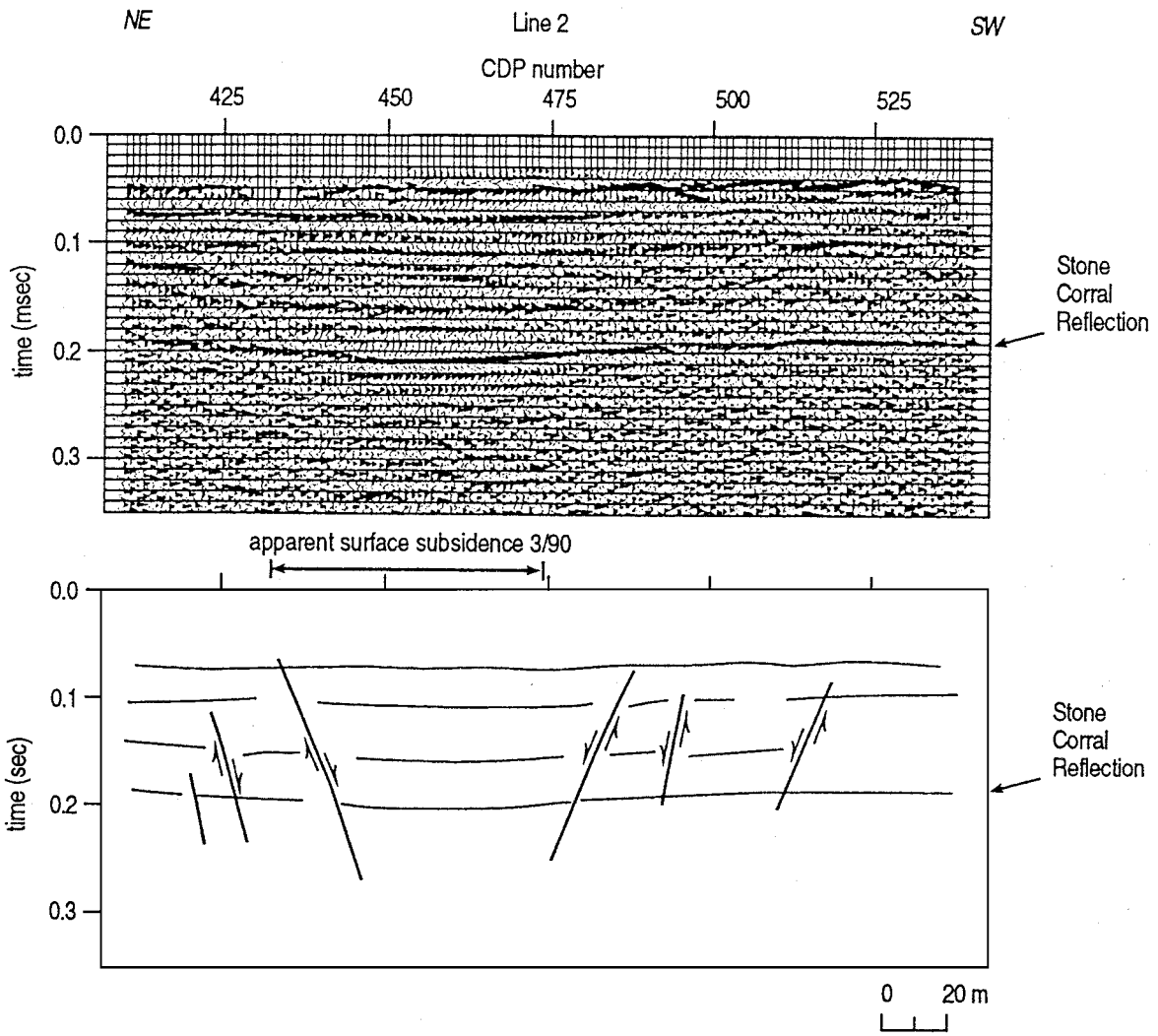


FIGURE 10—PSEUDO 24-FOLD STACK SEISMIC SECTION OF LINE 2 WITH ASSOCIATED INTERPRETIVE LINE DRAWING. The Stone Corral reflection is indicated.

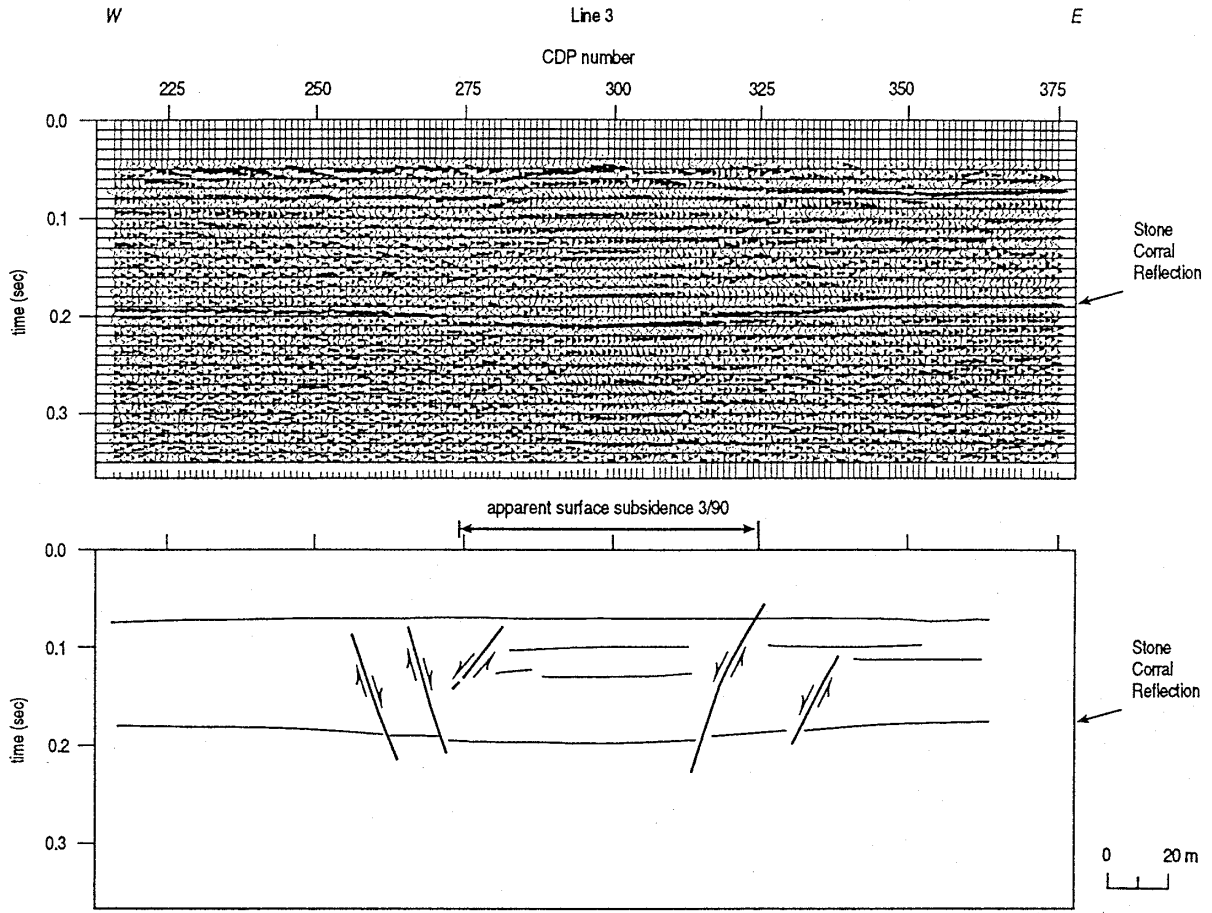


FIGURE 11—PSEUDO 24-FOLD STACK SEISMIC SECTION OF LINE 3 WITH ASSOCIATED INTERPRETIVE LINE DRAWING. The Stone Corral reflection is indicated.

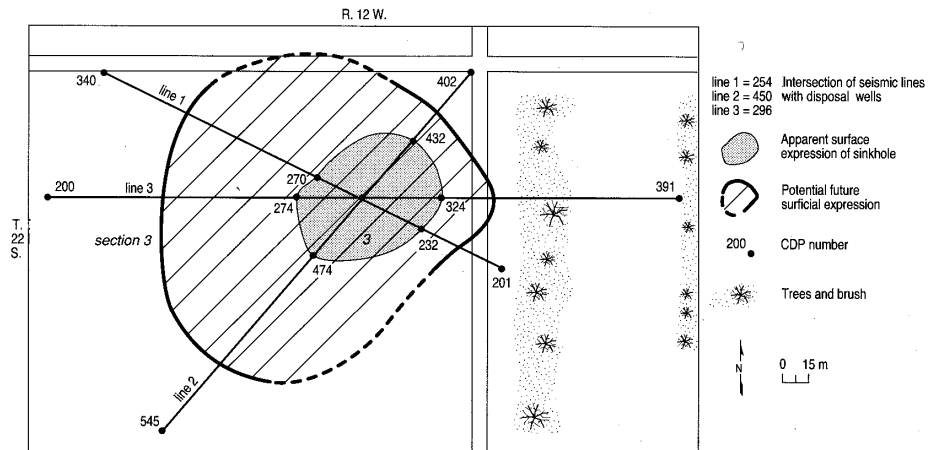


FIGURE 12—SITE MAP SHOWING PRESENT AND POTENTIAL SURFACE SUBSIDENCE AT SIEFKES.

ACKNOWLEDGMENTS—We wish to thank Randie Grantham, George Coyle, and Mubarik Ali for their assistance with data acquisition. We would like to extend a special thanks to Dean A. Keiswetter for his assistance during acquisition. Also, the work of Esther Price and Mary Brohammer in manuscript preparation and Pat Acker's quality graphics are greatly appreciated. Funding was provided in part by a contract with Quinoco Petroleum.

References

- Ege, J. R., 1984, Formation of solution-subsidence sinkholes above salt beds: U.S. Geological Survey, Circular 897, 11 p.
- Frye, J. C., and Schoff, S. L., 1942, Deep-seated solution in the Meade basin and vicinity, Kansas and Oklahoma: American Geophysical Union, Transactions, v. 23, pt. 1, p. 35–39
- Knapp, R. W., Steeples, D. W., Miller, R. D., and McElwee, C. D., 1989, Seismic reflection surveys at sinkholes in central Kansas; *in*, Geophysics in Kansas, D. W. Steeples, ed.: Kansas Geological Survey, Bulletin 226, p. 95–116
- Miller, R. D., Steeples, D. W., and Treadway, J. A., 1985, Seismic-reflection survey of a sinkhole in Ellsworth County, Kansas: Society of Exploration Geophysicists, 55th annual meeting, Washington, D.C., Technical Program Abstracts and Biographies [Exp. Abs.], p. 154–156
- Steeple, D. W., Knapp, R. W., and Miller, R. D., 1984, Examination of sinkholes by seismic reflection; *in*, Sinkholes—Their Geology, Engineering, and Environmental Impact, Barry Beck, ed.: A.A. Balkema, Boston, p. 217–224
- Steeple, D. W., Knapp, R. W., and McElwee, C. D., 1986, Seismic reflection investigations of sinkholes beneath Interstate Highway 70 in Kansas: *Geophysics*, v. 51, p. 295–301
- Steeple, D. W., Miller, R. D. and Knapp, R. W., 1987, Downhole .50-caliber rifle—an advance in high-resolution seismic sources [Exp. Abs.]; *in* Technical Program Abstracts and Biographies: Society of Exploration Geophysicists, 57th Annual Meeting., p. 76–78
- Steeple, D. W., and Miller, R. D., 1990, Seismic reflection methods applied to engineering, environmental, and groundwater problems: Society of Exploration Geophysicists, volumes on Geotechnical and Environmental Geophysics, Stan H. Ward, ed., Vol. 1: Review and Tutorial, 1–30
- Walters, R.F., 1977, Land subsidence in central Kansas related to salt dissolution: Kansas Geological Survey, Bulletin 214, 82 p.
- Watney, L., 1980, Maps and cross sections of the Lower Permian Hutchinson Salt in Kansas: Kansas Geological Survey, Open-file Report 80–7

Miller, R.D., A. Vilella, J. Xia, and D.W. Steeples, 2005, Seismic investigation of a salt dissolution feature in Kansas; in D.K. Butler, ed., *Near-Surface Geophysics*: Society of Exploration Geophysicists, Investigations in Geophysics No. 13, p. 681-694.

Chapter 29

Seismic Investigation of a Salt Dissolution Feature in Kansas

Richard D. Miller¹, Ana Villeda¹, Jianghai Xia¹, and Don W. Steeples²

Introduction

Sinkholes are common hazards to property and human safety the world over. Their formation can be initiated by natural or anthropogenically induced dissolution processes. Understanding the process responsible for sinkhole formation is key to reducing the risk of their unexpected development and, if they do form, their impact on human activities. Shallow high-resolution seismic investigations have successfully imaged salt dissolution sinkholes in central Kansas over the last 20 years (Steeple et al., 1986; Knapp et al., 1989; Miller et al., 1993; Miller et al., 1997). In almost all cases, previous studies unfortunately have been relegated to indirect inference of structural processes and subsurface expression in the salt interval (mainly from interpretations of structural deformation in layers above the salt). Resolution potential and signal-to-noise ratio of seismic data from this study enables interpretation of important structural features and unique characteristics within the salt interval controlling sinkhole development.

Brine disposal in shallow and deep well systems has been responsible for localized dissolution of the Hutchinson Salt in south central Kansas and north central Oklahoma for nearly a century (Figure 1). Petroleum produced from reservoirs in central Kansas comes from wells that must penetrate the salt section. Drilling with muds without appropriate chloride saturation routinely enlarges boreholes within the salt layers, which by itself does not represent a particularly strong risk for subsidence, but does complicate borehole completion. When the salt interval is not properly isolated due to inadequate grout or faulty casing, disposal brines—or worse yet, fresh water—can access the salt and cause uncontrolled leaching of the salt. If the unsaturated brines maintain contact with the dissolution front long enough to enlarge the salt void beyond a

distance the roof rock can support, void development will usually culminate with subsidence and, in many cases, sinkhole development.

A sinkhole that formed gradually around the French “A” no. 1 disposal well in Stafford County, Kansas, is the focus of this study and the target of a Kansas Corporation Commission plugging operation designed to stop fluid movement in the salt interval by sealing the failed borehole at the base of the salt. Previous seismic reflection investigations around old disposal or oil wells with surface subsidence in central Kansas have produced subsurface images that generally depict normal fault controlled reflection offset and reflections draping into voids or disturbed areas (Knapp et al., 1989; Miller et al., 1995). Usually the dominant reflection is from the Stone Corral anhydrite (which overlies the salt in most areas of central Kansas), which is used to quantify and delineate bed-associated failure geometries above and around dissolution voids. How beds above the salt are disturbed is indicative of and a key to understanding roof rock failure and deformation. Most theories concerning the process of sinkhole formation relate failure of rock layers to excessive undersupported rock load. The mechanisms and processes observed here are consistent with that idea. However, the specifics of the process and how the failure progresses can be unique for each setting. Different stress regimes are present throughout the time from initial failure until total relaxation occurs. There has never been clear seismic evidence allowing delineation of the entire mechanism and how subsidence processes changed with time and size of the dissolution front.

Geologic Setting

The upper portion of the Lower Permian section encompasses all the major geologic units that play a role in the formation and growth of salt-dissolution sinkholes throughout central Kansas. Dissolution of the Hutchinson salt is responsible for the development of the French sinkhole, where the salt is approximately 385 m below ground surface (BGS) and just over 100 m thick. Units within the

¹Kansas Geological Survey, 1930 Constant Avenue, The University of Kansas, Lawrence, KS 66047-3726, E-mail: rmiller@kgs.ku.edu.

²Department of Geology, University of Kansas, Lawrence, KS 66047, E-mail: dsteeple@ku.edu.

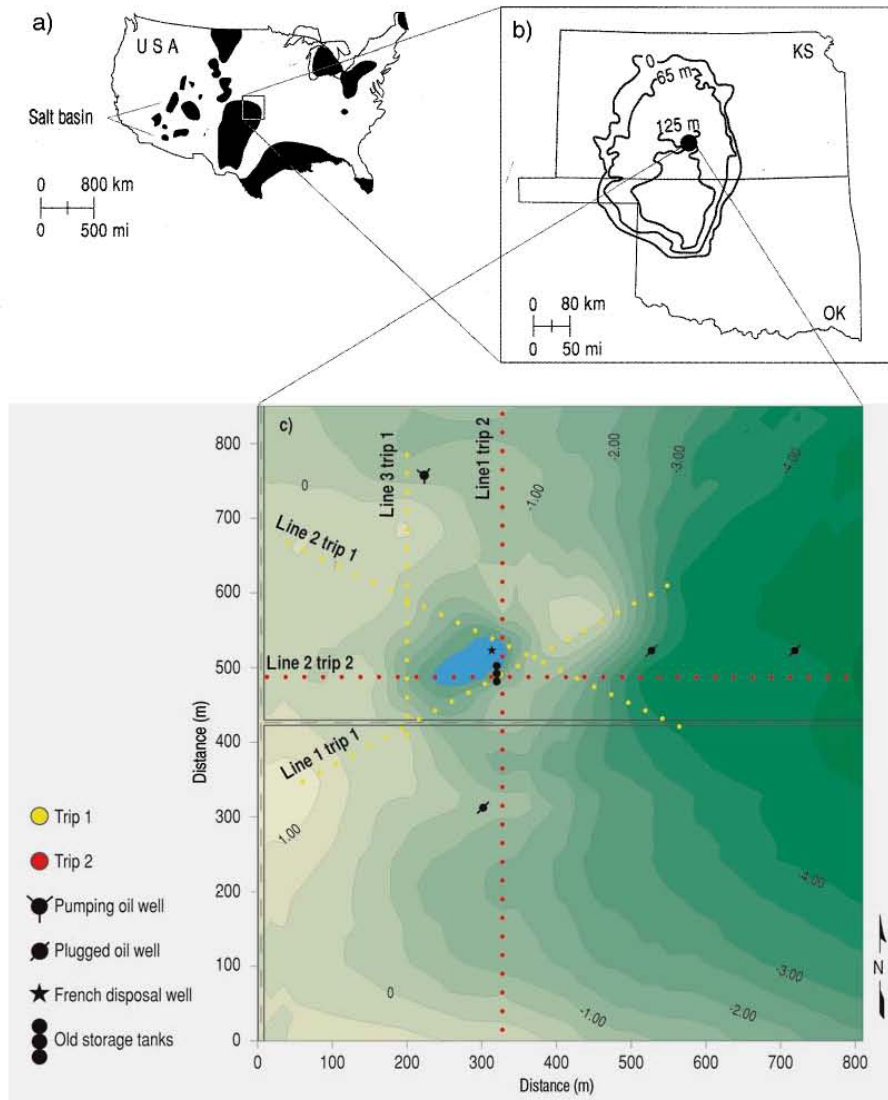
depth window of interest for this study ranged from the approximately 102 m thick sequence of marine limestones, dolomites, shales, and siltstones 570 m BGS that make up the Chase Group (Watney et al., 1988) to the sandstones and shales of the Nippewalla Group that represent bedrock less than 70 m BGS.

Most of the upper 750 m of rock at this site is Permian-aged shale (Merriam, 1963) (Figure 2). The currently disputed Permian/Pennsylvanian age boundary is about 1 km deep and seismically represented by a strong sequence of cyclic reflecting events. The Chase Group (top at 570 m deep), Lower Wellington Shales (top at 425 m deep), Hutchinson Salt (top at 380 m deep), Upper Wellington Shales (top at 325 m deep), Ninnescah Shale (top at 275 m deep), Stone Corral Anhydrite (top at 250 m), Harp-

er Sandstone (top at 200 m), and Salt Plain Formation (top at 70 m) all make up an easily identifiable and segregated packet of reflecting events within the Permian portion of the section.

The Hutchinson Salt Member, which occurs in central Kansas, northwestern Oklahoma, and the northeastern portion of the Texas Panhandle, has an extensive history of dissolution and formation of sinkholes. In Kansas, the Hutchinson Salt possesses an average net thickness of 76 m, reaching a maximum of over 152 m in the northeastern part of the basin (Figure 1). Deposition occurring during fluctuating sea levels caused numerous halite beds, 0.15 to 3 m thick, interbedded with shale, minor anhydrite, and dolomite/magnesite. Individual salt beds may be continuous for only a few kilometers despite the remarkable

Figure 1. Site map showing relative locations of (a) major salt basins in the United States (Ege, 1984) with (b) a generalized isopach map of the Hutchinson Salt Member in Kansas and Oklahoma (Walters, 1978), and (c) a ground surface contour map showing the location of seismic lines and the water-filled portion of French sinkhole, SW 1/4, Section 17, T23 S, R13 W, Stafford County, Kansas.



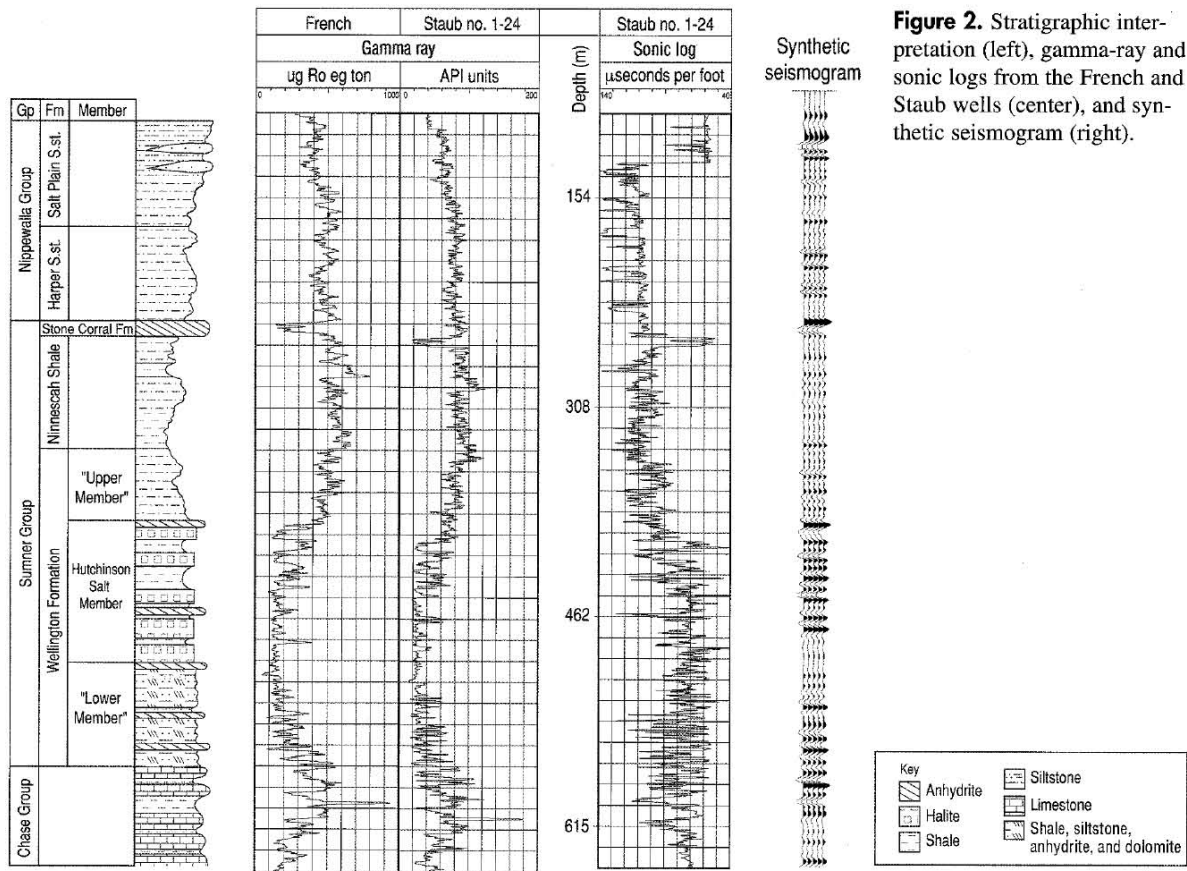


Figure 2. Stratigraphic interpretation (left), gamma-ray and sonic logs from the French and Staub wells (center), and synthetic seismogram (right).

lateral continuity of the salt as a whole (Walters, 1978). Thin anhydrite beds within the halite succession have a strong acoustic response and aided the interpretation of stacked sections in this study.

The French "A" no. 1 well was drilled and completed as a production well in 1955, after which it was permitted in 1978 as a disposal well. Brine introduction was well-head rated at a minimum of 800 barrels per day and a maximum of 1000 barrels per day under gravity pressure from a large receiving and settling tank. Subsidence at the French site was first documented in 1991. Since 1991, about 3 m of subsidence has been measured at the site. The rate of subsidence at the well is currently about one-third meter per year.

Redbed evaporites that overlay the Hutchinson Salt Member represent the roof-rock interval and therefore a key target for unraveling the past, current, and future subsidence associated with salt dissolution, mechanisms controlling sinkhole development, and the risk of those sinkholes to the environment and human activity. Failure and subsidence of this thick sequence of Permian shales and sandstones control formation rates and dimensions of sink-

holes. Maybe more important, breaching these nonpermeable layers opens pathways for groundwater to gain access to the Hutchinson Salt. Seismic reflection studies used to delineate localized structures in this area have relied heavily for structural control on the 12 m thick dolomite and anhydrite Stone Corral Formation, 250 m BGS. The Stone Corral anhydrite is stratigraphically just above the Hutchinson Salt, laterally continuous with widespread regional distribution, and well documented as an acoustic marker (McGuire and Miller, 1989).

Rock salt under a depositional load is almost incompressible, highly ductile, and easily deformed by creep (Baar, 1977). Plastic deformation of the salt associated with creep is expected to occur naturally in these salts (Miller, 2002; Anderson et al., 1995). Thin anhydrite beds within the halite succession have a strong acoustic response and therefore are very seismically imageable. These beds provide a measure of mechanical deformation within the salt interval. Considering the extreme range of possible strain rates the salt can experience during creep deformation, these thin interbeds can possess quite dramatic geometries, especially high amplitude, short wavelength folding.

Anthropogenically Induced Salt Dissolution and Associated Sinkhole Formation

Prior to the introduction of drilling, natural dissolution of the Permian-aged basin evaporites was the sole process responsible for the formation of sinkholes, subsidence troughs, and collapse structures. Invasive human activities without sufficient controls (e.g., overmining salt deposits and inadequate seals between casing and borehole walls) have allowed or enhanced the development of dissolution-related features in areas of Kansas with thick evaporite layers. Evaporite dissolution occurs very rapidly when relatively fresh fluids get access to and can escape from evaporite materials. The high dissolution rate of evaporites is due to their high solubility relative to other dissolution-prone rocks [i.e., gypsum and salt being, respectively, 150 and 7500 times more soluble than limestone (Martinez et al., 1998)].

Since its discovery in 1923, oil in central Kansas has been produced from aquifer reservoirs containing large amounts of brine. Approximately 75 percent of the oil produced in central Kansas in the 1930s and 1940s came from Arbuckle dolomite reservoirs. These reservoirs have a very strong water drive and, at times, five barrels of salt water was being produced for every barrel of oil. Evaporation ponds were used to dispose of these brines in the 1930s. Starting in the 1940s shallow well disposal (SWD) techniques (Walters, 1991) became the preferred disposal method. The convenience and apparent cleanliness of subsurface disposal weighed strongly in its industry-wide acceptance. However, one compelling negative was overlooked or maybe ignored: These brines contain highly corrosive H_2S .

Large volumes of unsaturated brine flowing at high energy in SWD systems long after casing confinement was breached set up an environment conducive to evaporite dissolution. Without the confinement of casing, borehole walls were exposed to large flow volumes that developed a pathway to and from rock exposed in the borehole walls and allowed the dissolution process to flourish. As the dissolution of the salt layers progressed unchecked, large cavities formed with roof spans that taxed the strength of the overlying rocks. Roof rock failure in these oversized cavities resulted in the successive collapse of individual rock layers, moving progressively from layer to layer at variable rates toward the ground surface. This domino effect culminated in surface subsidence and the formation of sinkholes.

Subsidence can occur at rates ranging from gradual to catastrophic, continuous to segmented. To some extent, subsidence rates are controlled by the type of deformation in the salt (ductile or brittle), the strength of rocks immediately above the salt layer, and the depth to the top of salt. As salt is leached, pore space is created. As this pore space

grows, it eventually gets large enough to provide the differential pressure necessary to support creep (Carter and Hansen, 1983). If this pore space continues to grow, it can attain a size that exceeds the strength of the roof rock, the undersupported span will fail, and subsidence occurs.

Strength of the roof rock and size of the void dictate rock failure characteristics within and just above the salt, and therefore, control how the void progresses upward. In general, gradual surface subsidence is associated with ductile deformation accommodating both vertical and radial growth of the sinkhole, forming an ever-enlarging bowl-shaped depression with bed geometries and offsets constrained by normal fault geometries (Steeple et al., 1986; Anderson et al., 1995). When rapid to catastrophic subsidence rates are observed, failure within the salt is usually brittle with the void area migrating toward the surface as an ever-narrowing cone defined by bed offsets and controlled by rock failure along reverse-type fault planes (Davies, 1951; Walters 1980; Rokar and Staudtmeister, 1985).

Subsidence rates are difficult to predict and deformation sequences associated with subsidence are generally complex. Overmining (dissolution style) of the Hutchinson Salt and the resulting subsidence associated with salt jugs has been suggested to form along reverse faults extending from the salt voids to the surface (Walters, 1978). High-resolution seismic reflection surveys over collapsed salt jugs, oil field brine-induced subsidence, and natural subsidence during the last quarter of the twentieth century were only able to conclusively map normal faults defining a series of blocks stepping away from the salt void (Steeple et al., 1986; Miller et al., 1995).

Seismic Acquisition

Seismic data for this study were acquired during two separate visits. During the preliminary site visit in 1995, three fixed 96-station spreads were deployed in a triangular pattern centered on the sinkhole (Figure 1). Two more orthogonal profiles crossing near the borehole were acquired during the follow-up trip in 1997. To extend the findings of the first trip, the two orthogonal profiles were designed and acquired based on the results.

Acquisition parameters for the first survey were selected based on a series of walkaway tests along line 1. Three Mark Products L28E 40Hz geophones separated by .5 m (forming a 1.5 m linear array) were deployed at 5-m intervals along each survey line. Geophones were deeply seated into tilled fields after the top few centimeters of loose soil and vegetation were removed to maximize coupling. Two 48-channel, 24-bit Geometrics StrataView networked seismographs allowed the recording of each 96-station fixed spread without rolling. An IVI Minivib delivered three 10-s, 30–300 Hz upsweeps at each shot location (separated by 5 m). A single unrecorded sweep was run at each shot location to insure the vibrator pad was well seated. The ground

force pilot was telemetered from the vibrator to the seismograph where it was correlated with each trace. The three recorded shots per station were vertically stacked and stored in the seismograph.

The two lines collected during the second trip used end-on spreads and a roll-along acquisition method (Mayne, 1962). The acquisition and processing flows for the second trip were modified from the first to optimize the data and its interpretability based on the findings of the first trip. As well, the two-year time separation in these data sets allowed for any subsurface changes related to growth to be identified and for appraisal of the significance of those changes to this sinkhole's development. Shot and receiver stations and source parameters were the same as the first trip. To enhance flexibility and resulting data quality during processing, the seismic data were recorded uncorrelated and unstacked on the second trip. The north-south profile was extended south through a harvested cornfield that was unharvested during the first trip to intersect a plugged well. Lines acquired on the second survey were each approximately 1 km long. Extending the line lengths allowed the edge of the subsidence to be clearly located in all directions around the sinkhole. By extending the east-west line, the east CMP section intersected two nearby plugged wells with sufficient fold to correlate reflections to borehole logs (Figure 1).

Synthetic Seismogram

The closest sonic log available in the vicinity of the French site was from the Staub no. 1-24 well, about 3 km away (Figure 2). The Staub well had sonic and gamma ray logs acquired in 1991 that included the depth interval of interest. The similarity between the gamma ray curve from the Staub well and the French gamma curve was the basis for asserting that the sonic log from the Staub well would represent a reasonable stand-in for a sonic log at the French well. After a 10-m shift, an extremely high correlation can be observed between the French and Staub gamma curves. The synthetic seismogram inserted into the stacked section is the product of convolving a Klauder seismic wavelet with the reflectivity series obtained from the sonic log for a constant density and frequency filtering (Figure 2).

Since the sonic log recorded instantaneous velocity as a function of depth, a simple transformation from depth to two-way traveltime was used to match the synthetic seismogram with the CMP stacks. In the absence of a check-shot survey, an estimated replacement velocity of 1500 m/s was used to account for the material from the surface down to 100 m of depth.

Seismic Processing

The basic processing flow was consistent with routine 2D shallow high-resolution reflection methodologies (Steeple and Miller, 1990). All lines were processed using

ProMAX™ 2D seismic data processing software from Landmark Graphics, Inc.

The data volume acquired during the first trip was approximately 3% of that stored during the second trip. The difference is the correlating and vertical stacking done in the field during the 1995 trip and individually saving three 10-s uncorrelated shot records at each shot location during the 1997 campaign. Data saved uncorrelated allowed the use of precorrelation processing techniques designed to increase the signal-to-noise ratio and resolution potential (Doll and Çoruh, 1995). Enhancement of signal and some improvement in bandwidth was achieved using precorrelation processing, but at a significant increase in acquisition and processing time. In this case the improvement in signal-to-noise was well worth the cost.

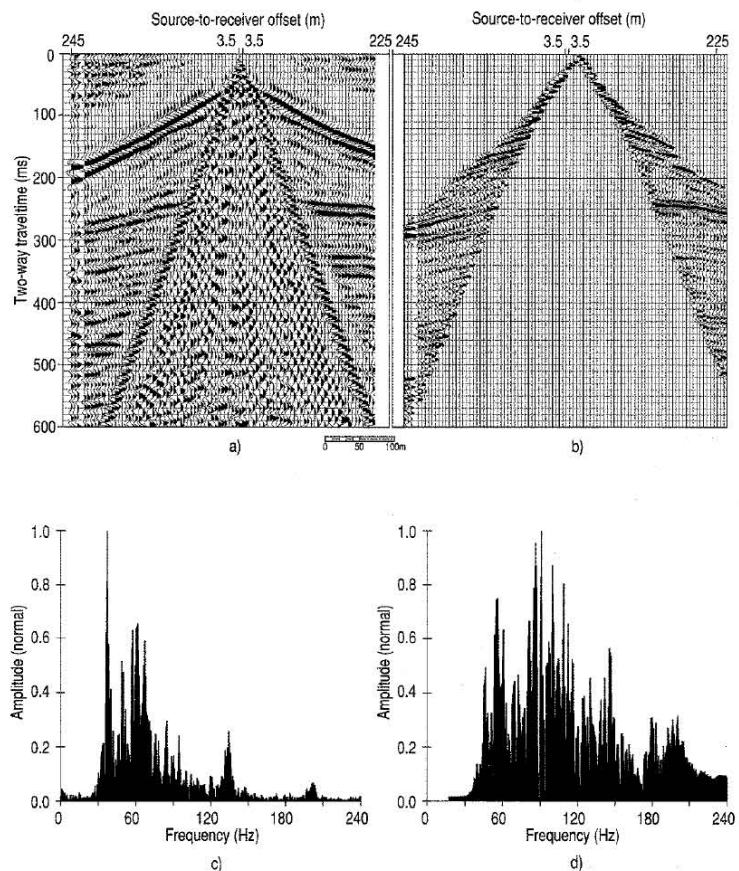
Approximately 60% of the total processing time was spent in the shot-gather domain. Time, frequency, and $f-k$ domain analysis of shot records targeted identification of coherent noise contaminating the data and any unique characteristics of the noise. Coherent noise commonly found in these data, not cancelled or sufficiently suppressed by CMP stacking, include power-line noise, refraction (first) arrivals, air-coupled wave, ground roll, and correlation noise (Figure 3).

Much of the analysis concentrated on defining the unique characteristics distinguishing noise from signal in the different domains. The air-coupled wave velocity is considerably slower than the refraction and reflection arrivals, and therefore, airwaves map in a distinct area in the $f-k$ domain. Linear arriving energy with frequencies above 100 Hz and low apparent linear velocities are most susceptible to spatial aliasing from undersampling the higher frequency components of the energy. To avoid aliasing problems, a bottom mute was applied on a shot-by-shot basis to remove the air-coupled wave.

Ground roll is the most dominant coherent linear noise present in the data. Its characteristic low-frequency and high-amplitude waveforms makes it easily recognizable on shot gathers (Figure 3). Because ground roll energy is dispersive, it transforms into a large portion of the low frequency section of the $f-k$ spectrum. $F-k$ filtering is therefore not an effective tool for removing ground roll from most data sets. Considering the incident angle and frequency properties of returning high-frequency reflections, a receiver array large enough to suppress the ground roll would tend to suppress much of the recoverable high-frequency signal at close offsets (Knapp and Steeples, 1986). It is therefore common practice for shallow reflection data processing to mute ground roll from shot gathers (Baker et al., 1998). Bottom mute zones were chosen so that both ground roll and the air-coupled wave were eliminated from shot records.

Routine trapezoid frequency filtering was not effective in removing or suppressing nonlinear noise from a nearby pump jack. With the offline location of the pump jack,

Figure 3. (a) Scaled raw data, FFID 2340, line 2, trip 2 ; (b) processed and spectral balanced (a); (c) frequency spectrum of (a); (d) frequency spectrum of (b).



recorded noise appears to have hyperbolic moveout. This noise can be seen on traces across the entire record and is evident before the first breaks. For this nonlinear pump-jack noise case, a noise adaptive filter was designed using a window prior to the first breaks to avoid any source-energy contamination of the filter.

CMP domain processing

CMP analysis allows isolation of many shot station specific characteristics and allows data signature arrivals consistent across a spread length to be identified and enhanced. Spectrally balancing (band-limited spiking decon) frequencies in the 30–40–150–225-Hz frequency range broadened the frequency spectrum sufficiently to compress the wavelet and suppress some of the ringy character of the data. The optimum stacking-velocity field was a smoothed combination of velocity picks from both velocity picking of supergathers containing five adjacent CMPs and constant-velocity stack analysis. Stretch mute was carefully selected to prevent wavelet distortion and amplitude and frequency spectrum degradation, especially at large offsets (Miller, 1992).

The true, time-varying fold of the stacked sections is significantly lower than nominal fold calculated from acquisition parameters alone. This difference is significant for shallow reflection data where most of the optimum window is sandwiched between large components of noise. Therefore, large mute zones are defined, leaving many of the traces in a CMP gather zeroed out and not contributing to the final stacked trace. Asymmetry and sporadic high or low fold areas can dramatically affect interpretations in structurally altered or complex geologies. Visibly higher signal-to-noise ratio between CMPs 4200 and 4260 (Figure 4) on the second survey could be due to either geology or variations in fold.

Higher signal-to-noise ratios coincide with the highest fold between CMPs 4200 and 4260 (Figures 4 and 5). True-fold maps were created to evaluate the true fold distribution of each stacked section (Liberty and Knoll, 1998). Because the signal-to-noise ratio varies proportionally with the square root of fold, the improved coherency in these zones could be an artifact of data processing and independent of geology. Decimated stacked sections were produced to ascertain the nature of these changes in lateral coherency (Figure 6). Stacked sections with even data-fold distribution

(Figure 6) possessed signal-to-noise ratios, frequency content, trace-to-trace event coherency, and amplitude characteristics very similar to the original irregular-fold stacks. Lateral variations in the coherency of reflections on Figure 6 are likely related to true variations in geology.

Seismic Interpretation

Several key reflecting interfaces or packets of reflections proved important in gaining an understanding of the stratigraphic relationships, structural framework, and subsidence chronology associated with the French well. These reflections can be correlated to shallow Permian redbed sequences, the Stone Corral anhydrite, the top and bottom of the salt section, and the top of the Chase Group (Figures 7, 8, and 9). Identifying these key reflecting horizons on shot gathers and tracking them through the processing flow was of the utmost importance in ensuring only true reflections, and not stacked coherent noise, were interpreted on CMP sections. The synthetic seismogram provided the generalized ground-truth starting point for stratigraphic interpretations.

The most striking feature common to all CMP sections is the distinctive synform on the 250 m deep Stone Corral anhydrite (Figures 7, 8, and 9). The Stone Corral is the strongest (highest amplitude with consistent waveform) reflection observed in these data with lateral continuity that allows confident correlations despite the structural complexities observed across the subsidence feature. The Stone Corral seems to have experienced both brittle and plastic deformation (Figure 8, red event).

The faulted synform geometry is evident below and surrounding the disposal well location (CMP 2192) on the north-south profile (line 1) from the second trip (Figure 8). Faulting of the Stone Corral along the synform defines several distorted rock segments resulting from nonuniform failure rates and distribution of prefailure stresses. Approximately 40 m of vertical displacement in the Stone Corral anhydrite can be observed near the disposal well location on this profile. Reflections on CMP stacks from the first trip possess the same structural traits and geometries as from the second trip, but are much more subdued with lower signal-to-noise ratios and lower dominant and upper corner frequencies (Figure 7).

A collapsed portion of the Stone Corral reflection between CMPs 4080 and 4140 on line 2, trip 2, centered at the disposal well is a striking example of the deformation characteristics of these kinds of collapse features (Figure 9). A sitewide maximum of approximately 50 m of vertical displacement is estimated to be coincident with the collapsed slab of anhydrite between CMPs 4080 and 4140. Deformation of the Stone Corral along line 2 from trip 2 seems to extend from CMP 4040 on the west side to CMP 4200 on the east side of the profile. This synform devel-

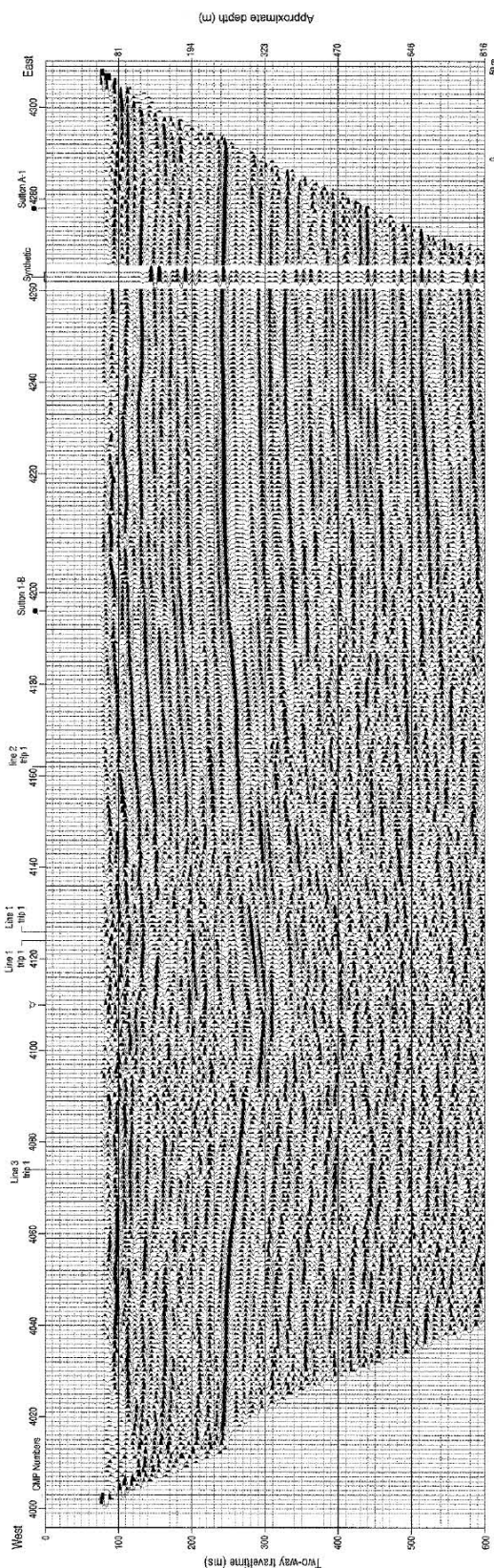


Figure 4. CMP stack from line 2, trip 2.

oped as a result of roof failure and collapse of the Stone Corral into the void left after the salt was leached away.

The top-of-salt reflection occurs at approximately 325 ms (390 m of depth). This salt reflection is not as prominent (amplitude and/or coherency characteristics) as the Stone Corral reflection, even away from the well where no leaching has occurred. The amplitude difference is due to the smaller contrast in acoustic impedance between the Hutchinson Salt and the overlying shale compared to the

Stone Corral and its overlying shales. Drill evidence, based on cores and drillers' logs, suggests the contact between the salt and overlying Permian shales is sometimes characterized by a thin rubble zone. Such a rubble zone will likely represent a gradational and laterally variable change in acoustic impedance, and therefore be responsible for the more diffuse, lower frequency reflections with strong lateral variability in waveform characteristics. Variability of this kind could be related to compaction, grain size of rub-

Figure 5. True-fold map from line 2, trip 2, based on true processing fold (a) when all traces are stacked and just live data areas considered. Decimation of fold based on consistent offset and data windows produces a more uniform fold (b), ranging from 25 to 10.

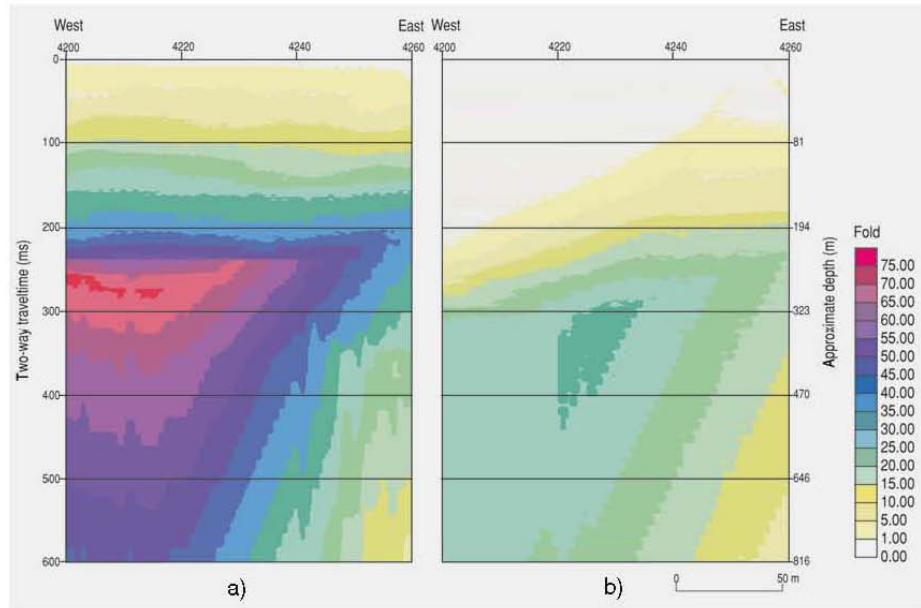
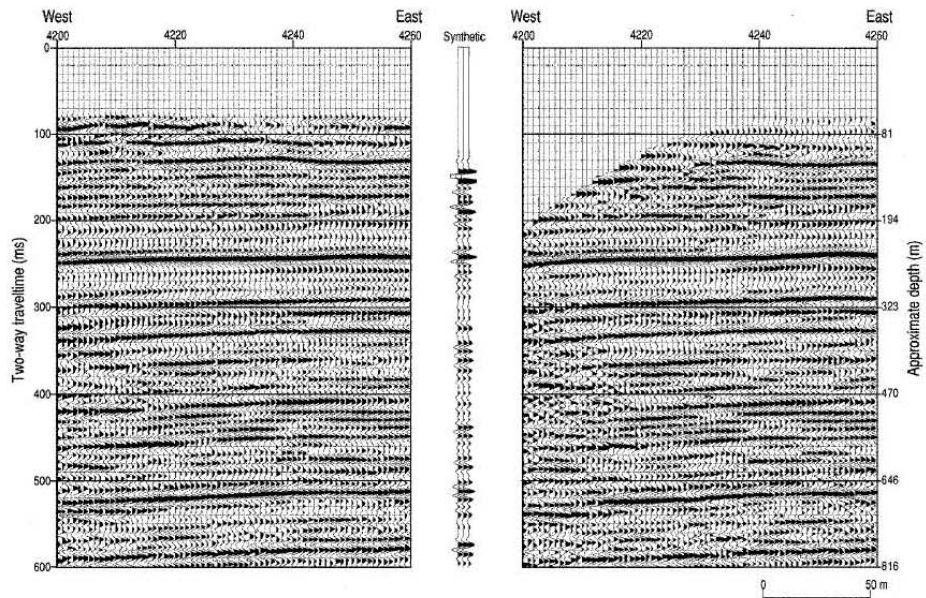


Figure 6. CMP stack from line 2, trip 2, with all the data traces (a) without concern for fold or offset distribution. CMP stack (b) decimated to balance fold and offset distributions within the live data areas.



ble, thickness of rubble layer, and lateral extent of the rubble layer. Any of these physical characteristics could relate to subsidence or a remnant of original deposition.

Reflections from within the salt interval are from laterally discontinuous (in a regional sense) thin anhydrite and shale layers interbedded with the halite. Intrasalt reflections and reflections from the top of the salt become locally discontinuous toward the center of the sink. Termination, distortion, or degradation of these intrasalt reflections is likely indicative of the collapse of these less soluble intrasalt anhydrite and shale layers into voids left by leaching (Miller et al., 1997). The dissolved or partially dissolved salt volume is characterized seismically by a lack of laterally coherent reflections and higher levels of scattered

seismic energy within the salt interval. Segmented reflections within this dissolution zone, some with extreme geometries, are probably from larger remnants of intrasalt shale/anhydrite layers and possibly shale beds (which overlay the salt) that have fallen or slumped into dissolution voids.

The reflection at around 460 ms (570 m) is interpreted to be from the top of the Chase Group (Figures 7, 8, and 9). As expected and consistent with previous seismic studies, this subsalt reflection loses coherency and possesses a time sag (drape) below the disturbed zone (Anderson et al., 1995). The loss of coherency is related to the attenuation and scattering of the seismic energy as it passes through the disturbed cone (defined by subsidence-altered reflectors above the salt) and is due to lateral changes in compaction, bed terminations, rubble zones, and nonsymmetric reflection raypaths.

The top of the Chase Group reflection possesses a synform geometry generally similar to reflections from within the lower Wellington interval immediately above the Chase Group. Since layers in this area are generally considered flat on the scale of this study (1 to 2° westward dip), apparent small scale, localized subsalt synclinal structures on seismic sections beneath a dissolution zone must be the result of decreases in average velocity within and above the dissolution zone. If the Chase Group is flat, the nearly 20 ms difference in two-way traveltimes below the sinkhole equates to about a 100-m/s decrease in average velocity between the Chase Group reflector and ground surface. This dramatic change in average velocity must be compensated for during time-to-depth conversions for true structural geometries to be identified and delineated. This 100-m/s slowdown in NMO velocity is not distinguishable on the velocity function as defined using constant-velocity stacks

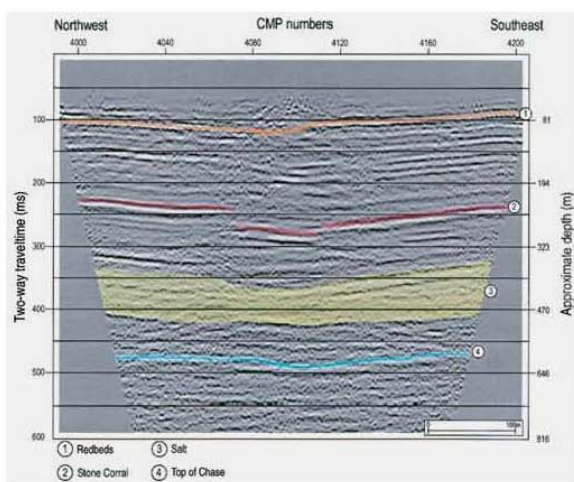


Figure 7. Interpreted CMP stack from line 2, trip 1.

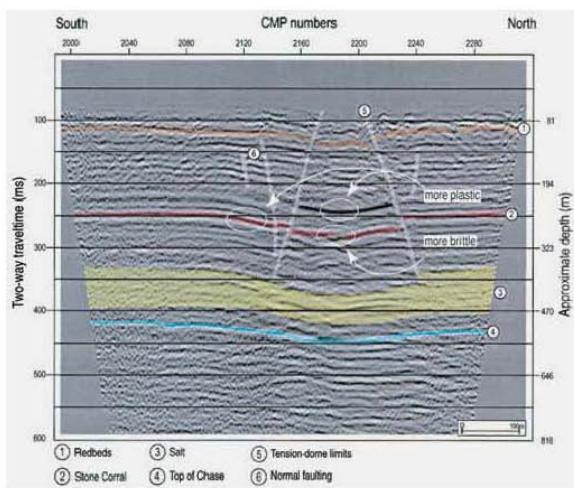


Figure 8. Interpreted CMP stack from line 1, trip 2.

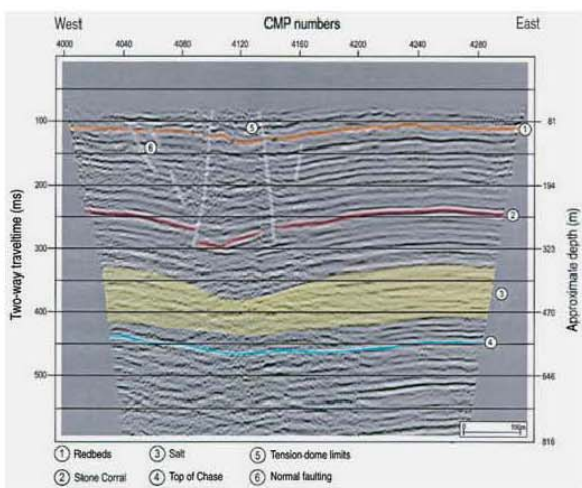


Figure 9. Interpreted CMP stack from line 2, trip 2.

and CMP-gather curve analysis (Figure 10). The inability of standard velocity analysis routines to identify and quantify this change in velocity is not particularly surprising, considering the length of the spread relative to the size of the disturbed volume. This observation raises concerns on any high-resolution survey that apparent small-scale structures could be the result of uncompensated lateral velocity variations. These velocity variations interpreted as real structures could go completely undetected when spread lengths are consistent with or larger than the velocity anomaly.

Finally, many shallow reflections evident between the ground surface and Stone Corral anhydrite appear to bridge over (flat reflections overlying draped or slumping reflections) small areas with synform geometries (e.g., Figure 8, CMPs 2160 to 2180 @ 275 ms). It is reasonable to suggest that these very localized bridging features are an indication that the subsidence process is not complete. These small subvoids are manifestations of the upward movement of the void left from salt leaching. These microstructures are the result of nonuniform failure and will eventually fill with overlying rock through gravity compaction or roof failure and subsidence of overlying materials. Continued subsidence of rocks above and around these bridged subvoids continues to change the forces and loads and therefore the dynamics in the subsurface. This complex interaction of rubble zones, voids, and competent rock accounts for the slow, yet continuous, development of sinkholes above some areas where leaching of the salt has long since stopped.

Structural Interpretation

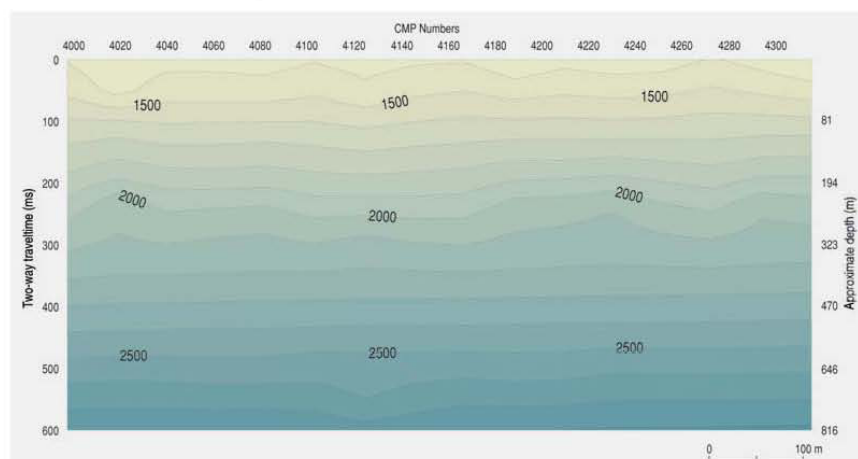
The main structural features of the French sink are similar to other sinkholes studied in this area (Steeple et al., 1986; Walters, 1978). Principal failure planes bounding the initial collapsed earth volume below sinkholes have

been suggested to resemble reverse faults (Walters, 1978). These failure planes are generally centered on the disposal well and diverge downward from the surface (Figure 11). Borehole evidence alone has been the basis for descriptions of this process. Little other evidence—geophysical or physical—has existed prior to this study supporting extrapolation of borehole observations into the surrounding earth volume. For these subsidence wedges or inverted dome-type geometries to be feasible, the volume of salt dissolved to form the initial void at the salt depth must be much greater than the volume of the depression at the ground surface after overburden failure and sinkhole formation is complete.

Interpreted on the CMP sections from this study are subdued indications of a fault-defined wedge or cone-shaped collapse structure centered at the French well (Figures 7, 8, and 9). This cone structure is interpreted to define the initial subsidence zone, which likely collapsed at a rate greater than inferred from recent elevation surveys made during the more mature stages of sinkhole development. This initial failure mechanism was likely similar to failure en masse of the roof or walls of caverns (Davies, 1951). The stress regime acting on cavern roofs and walls prior to collapse should be reasonably analogous to the forces observed around dissolution void structures at or near failure.

Lithostatic load is key to the development of cavern breakdown and the primary factor controlling mass failure of subsurface voids (Davies, 1951). Before a cavern forms, the vertical and horizontal components of stress acting on any point in the subsurface are in equilibrium. Once an opening develops, these forces are no longer in equilibrium and a new stress regime develops which tries to overcome the strength of the rock to force the roof and walls into the void opening. Vertical stresses cause beds to drape (sag) and separate at physical contacts above the cavern. The extent of this separation and sag is defined in three dimen-

Figure 10. Stacking velocity field, in m/s, from line 2, trip 2.



sions by a tension dome (Figure 12). The amount of sag before failure depends on the strength of the material. Assuming horizontal beds of similar physical strength, sag is greatest around a vertical axis centered on the opening (or cavity) and lessens upward with decreasing depths. After separation, lithostatic load cannot be transmitted within the tension dome, and stress is then transferred to adjacent rocks and to the walls of the cavity. Rock outside the tension dome has no direct impact on the mechanics of breakdown; the weight and strength of the rock units within the dome alone cause collapse. Failure generally occurs first on a sagging bed closest to the wall where shear forces are the greatest.

Collapse of rocks within the tension dome can occur anywhere layer sag extends to the point of failure. Depending on the rock properties and void specifics, massive breakdown usually results in the failure of successive beds within the dome. Depending on material properties and

stress levels, the lowest bed may collapse first, with failure then gradually progressing upward into overlying units, or collapse can be initiated by layer failure within the dome moving downward toward the void. Most breakdowns can be attributed to the latter mechanism where a sagging bed somewhere within the dome fails, transferring the weight of the layer onto to the bed below. Rapid transfer of this weight initiates successive failure of underlying units proceeding down through the tension dome much like dominos. Such a sequence of failures extends over a considerable vertical distance and typically culminates in roof collapse of the void itself.

Subsidence rates are difficult to predict and the associated deformation sequences are generally complex. Failure of intermediate layers within the dome is the most plausible mechanism for catastrophic subsidence observed in select sinkholes throughout central Kansas (Walters, 1978). Catastrophic sinkhole development requires the ground surface, or at a minimum the top of consolidated bedrock, be within the tension dome. Due to the high-stress environment within the tensional dome, it is possible the linearity of stress and strain, as defined by Young's Modulus, is violated such that localized increases in shear-wave velocities may be indicative of material within the tensional dome and therefore representing a measurable property diagnostic of collapse, potential prefailure. We speculate that shear-wave velocity surveying in suspect areas could provide critical early warning of subsidence risk.

Disturbed reflections within 50 m of the French well are from beds distorted by excessive stress and/or failure within the arched boundary generally consistent with a tension dome (Davies, 1951) (Figure 8). This arched bound-

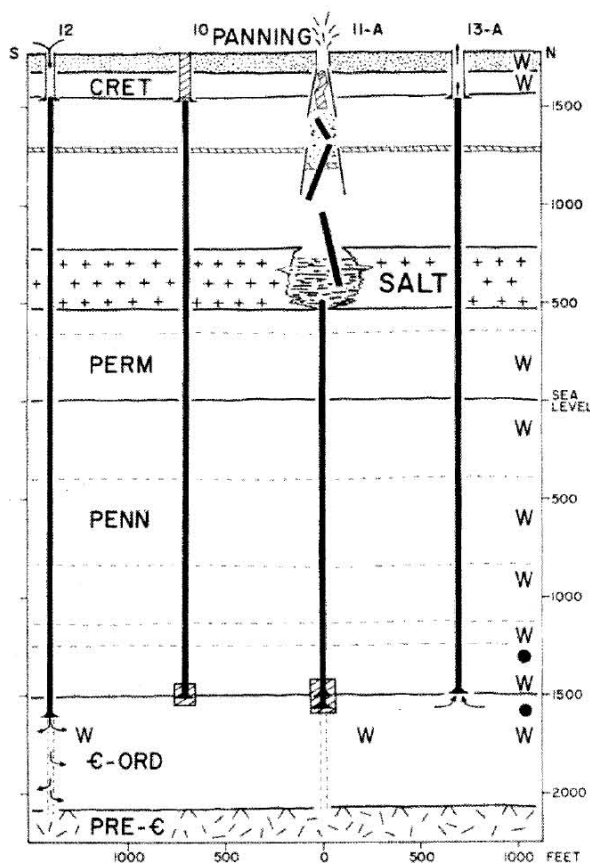


Figure 11. Cartoon to show the conceptual model of the subsurface below a newly formed sinkhole (Panning Sinkhole from Walters, 1978).

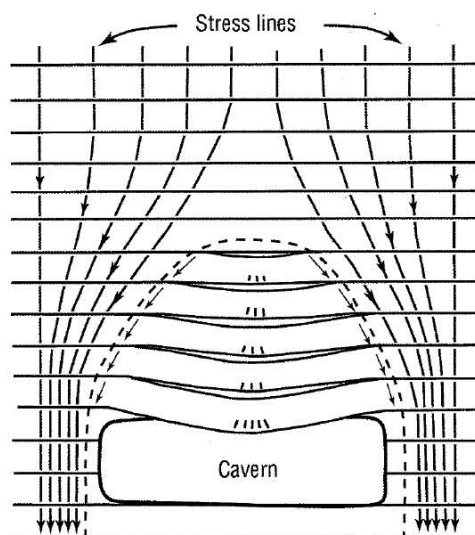


Figure 12. Tension dome and distribution of stress lines around a cavern opening in horizontal strata (Davies, 1951).

ary is defined on seismic data by a decrease in signal-to-noise ratio, apparent bed offsets, and loss of coherency attributed to attenuation and scattering of energy along the planes (or in this case “zones”) of failure. The dome is defined by a series of reverse fault planes (Figure 8, ⑤), extends vertically from the base of the salt interval to near the top of the section, and is roughly symmetric in shape centered on the French well. The beds within this dome have undergone differing amounts of plastic and brittle deformation attributed to differences in strength of the various lithologies or to strain rates within the dome.

In all CMP stacks, evidence exists supporting initial failure of the Stone Corral Formation along the tension dome boundary, defined by the reverse faults (Figures 7, 8, and 9). Lines 1 and 2 of the second trip image significant tensional offsets on the lower surface of the sagging anhydrite layer within the tensional dome. This supports the suggestion that failure occurred in the area of maximum tension.

Lines 1 and 2 from trip 2 to the French sinkhole conclusively demonstrate that reverse faulting is present and likely does control initial subsidence within the tensional dome (Figures 8 and 9). Normal faulting is interpretable in the layers above the salt extending outward beyond any apparent disturbed salt. These normal faults seem to define blocks that dropdown toward the center of the tensional dome from outside the reverse faults defining the dome. These normal faults likely formed as part of a lower strain rate affecting layers near the edge of the dissolution zone but outside the trace of the tensional dome.

Reverse and normal faulting are associated with the subsidence process above dissolution voids in the Hutchinson Salt, each defining a different stress regime, period of sinkhole development, and rate of stress normalization and subsidence.

Discussion

The French sink was formed as a direct result of dissolution of the Hutchinson Salt by uncontrolled brine release into the salt interval at the French “A” no. 1 well. The dissolution cavity at the time of collapse encompassed no less than 1 000 000 m³. Since about 30% of this volume contains altered shale and anhydrite layers, the amount of dissolved salt is estimated at around 700 000 m³. Considering the amount of time the French “A” no. 1 was used as a disposal well, the amount of brines injected, and the typical salinity values for brines in the area, disposed fluids alone cannot account for all the dissolved salt. Groundwater from above the salt gained access to and transported salt away from the French well dissolution front.

Once a pathway has been established for waste water to reach the salt through casing and grout failure, the salt void grows based on the salinity and volume of fluid ex-

posed to the salt. The borehole integrity and isolation of shallow groundwater from the salt was breached once the casing and grout in the upper part of the borehole collapsed into the void area. From that point the French well bore served as a conduit for previously confined or perched groundwater to reach the salt interval. Fresh water moving through the well bore probably entered the well bore from the redbed sequence of the upper Permian. In general, the Stone Corral, when undisturbed, acts as an impermeable layer preventing water in shallower aquifers from reaching the salt; however, once the Stone Corral is penetrated by a well, a potential path for fluids is established.

Leaching mechanisms and associated void development changed once rock failure occurred. The initial stage was responsible for forming a cavity large enough to instigate failure and collapse of the overlying units as defined by the tension dome. This first stage of the subsidence process occurred when the gradual outward movement of the dissolution front reached the point exceeding the strength of the roof rock and the roof rock failed. Collapse probably originated in units directly above the cavity, progressing slowly upward toward the surface, engulfing layer by layer as it moved upward.

A second stage or mechanism of dissolution is inferred by deformed units outside the tension dome. This later stage of dissolution probably involved two different subsidence mechanisms. First, freshwater gained access to the salt through pathways opened after first stage failure, especially along the fracture planes. Second, subsidence of rock layers outside the tensional dome along normal faults progressed as rock layers weakened during the initial failure ruptured from overburden load and material breakdown. Normal faulting characterizes both these two mechanisms that are active during these later phases of subsidence. Normal fault blocks are clearly present on these seismic data and define the gradual outward progression of subsidence.

Information about the hydrostatic history of the French well provided crucial information necessary to understand the dynamics of the dissolution process at this site. Since the hydrostatic level of the borehole was below the salt interval once the casing was breached there could be a 100% man-made flow-through system. This system would provide a continuous source of unsaturated brines (perched groundwater) reaching the salt from above and a ready outlet for saturated brine to leave the salt area where the casing/borehole penetrated the base of the salt. Without a man-made outlet (open borehole) for saturated brine to leave the salt interval, a natural feature such as a fault, fracture, or paleo-sinkhole would be necessary to instigate and sustain the leaching process. No evidence exists to support a natural inlet or escape route for fluids.

The active dissolution front seems to extend outward from the center of the sink radially between 200 and 250 m. Two abandoned wells located approximately 200 m

south and west of the French well were reported to have communication with the French during plugging procedures. A large void was encountered in the salt interval during plugging of the well 200 m east of the French well. Based on seismic and borehole data, dissolution is actively occurring within confined, preferential halite horizons in the salt unit and is advancing faster laterally between shale and anhydrite layers with the salt than vertically through the salt interval.

Conclusions

With ever-improving resolution potential and signal-to-noise ratio of high-resolution seismic reflection data comes a better understanding of many small-scale geologic processes. Evaluating the mechanisms associated with land subsidence instigated by dissolution provides invaluable insights into these processes and therefore their risk to humans and the environment. Subsidence at the French sinkhole in Stafford County, Kansas, was initially the result of well-casing failure. This initial failure provided the pathway and transport mechanisms for continued dissolution by uncontrolled downward migration of groundwater. Current subsidence is associated with localized failure of rock layers moving progressively farther from the well bore. Stopping the dissolution will require elimination of fluid transport away from the salt (i.e., plugging the old well bore at the base of the salt).

The subsidence process at the French sinkhole clearly was driven by two separate stress regimes. An initial failure process began when the first salt was leached by borehole fluids. This first phase saw the formation of a tensional dome, which defined the failure mechanics, and the rocks determined the rate. The failure of rocks during the initial stage was controlled by reverse fault planes at the edges of the tension dome. This initial failure was then followed by a period of relaxation characterized by sagging rock layers and failure along a sequence of normal faults interpreted in rock layers above the salt. These normal-fault oriented ruptures begin outside the tensional dome and step away from the edge of the dissolution zone in general to form a synform. Stress relaxation through sagging rock layers is not surprising, considering the plastic nature of layered salt deposits, and as the salt is squeezed and moves into void areas overlying rocks will sag and try to stabilize this high-energy environment. Both reverse and normal faulting are associated with the subsidence process above dissolution voids in the Hutchinson Salt.

References

- Anderson, N. L., R. W. Knapp, D. W. Steeples, and R. D. Miller, 1995, Plastic deformation and dissolution of the Hutchinson Salt Member in Kansas, *in* N. L. Anderson and D. E. Hedke, eds., *Geophysical atlas of selected oil and gas fields in Kansas*: Kansas Geological Survey Bulletin 237, 66–70.
- Baker, G. S., D. W. Steeples, and M. Drake, 1998, Muting the noise cone in near-surface reflection data: An example from southeastern Kansas: *Geophysics*, **63**, 1332–1338.
- Baar, C. A., 1977, *Applied salt-rock mechanics 1*: Elsevier Scientific Publishing Co.
- Carter, N. L., and F. D. Hansen, 1983, Creep of rock salt: *Tectonophysics*, **92**, 275–333.
- Davies, W. E., 1951, Mechanics of cavern breakdown: *The National Speleological Society Bulletin*, **13**, 36–43.
- Doll, W. E., and C. Çoruh, 1995, Spectral whitening of impulsive and swept-source shallow seismic data: 60th Annual International Meeting, SEG, Expanded Abstract, 398–401.
- Ege, J. R., 1984, Formation of solution-subsidence sinkholes above salt beds: U.S. Geological Survey Circular 897, 1–11.
- Knapp, R. W., and D. W. Steeples, 1986, High-resolution common depth point seismic reflection profiling: Field acquisition parameter design: *Geophysics*, **51**, 283–294.
- Knapp, R. W., D. W. Steeples, R. D. Miller, and C. D. McElwee, 1989, Seismic reflection surveys at sinkholes in central Kansas, *in* D. W. Steeples, ed., *Geophysics in Kansas*: Kansas Geological Survey Bulletin 226, 95–116.
- Liberty, L. M., and M. Knoll, 1998, Time varying fold in high-resolution seismic reflection data: A recipe for optimized acquisition and quality control processing and interpretation: *Proceedings of the Symposium on the Application of Geophysics to Engineering and Environmental Problems (SAGEEP 98)*, 745–751.
- Martinez, J. D., K. S. Johnson, and J. T. Neal, 1998, Sinkholes in evaporite rocks: *American Scientist*, **86**, 38–51.
- Mayne, W. H., 1962, Horizontal data stacking techniques: *Geophysics*, **27**, 927–938.
- McGuire, D., and B. Miller, 1989, The utility of single-point seismic data, *in* D. W. Steeples, ed., *Geophysics in Kansas*: Kansas Geological Survey Bulletin 226, 1–8.
- Merriam, D. F., 1963, *The geologic history of Kansas*: Kansas Geological Survey Bulletin 162.
- Miller, R. D., 1992, Normal moveout stretch mute on shallow reflection data: *Geophysics*, **57**, 1502–1507.
- Miller, R. D., 2002, High resolution seismic reflection investigation of the subsidence feature on U.S. highway 50 at Victory Road near Hutchinson, Kansas: Kansas Geological Survey Open-file Report 2002-17.
- Miller, R. D., D. W. Steeples, L. Schulte, and J. Davenport, 1993, Shallow seismic reflection study of a salt dissolution well field near Hutchinson, Kansas: *Mining Engineering*, October, 1291–1296.
- Miller, R. D., D. W. Steeples, and T. V. Weis, 1995, Shal-

- low seismic-reflection study of a salt-dissolution subsidence feature in Stafford County, Kansas, *in* N. L. Anderson and D. E. Hedke, eds., *Geophysical atlas of selected oil and gas fields in Kansas*: Kansas Geological Survey Bulletin 237, 71–76.
- Miller, R. D., A. C. Villella, and J. Xia, 1997, Shallow high-resolution seismic reflection to delineate upper 400 m around a collapse feature in central Kansas: *Environmental Geosciences*, **4**, 119–126.
- Rokar, R. B., and K. Staudtmeister, 1985, Creep rupture criteria for rock salt, *in* B. C. Schreiber, and H. L. Harner, eds., *Sixth International Symposium on Salt*, Salt Institute Inc., **1**, 455–462.
- Sheriff, R. E., and L. P. Geldart, 1995, *Exploration Seismology*, 2nd ed.: Cambridge University Press.
- Steeple, D. W., R. W. Knapp, and C. D. McElwee, 1986, Seismic reflection investigation of sinkholes beneath interstate highway 70 in Kansas: *Geophysics*, **51**, 295–301.
- Steeple, D. W., and R. D. Miller, 1990, Seismic reflection methods applied to engineering, environmental, and groundwater problems, *in* S. H. Ward, ed., *Geotechnical and Environmental Geophysics*, SEG Investigations in Geophysics No. 5, 1–30.
- Walters, R. F., 1978, Land subsidence in central Kansas related to salt dissolution: *Kansas Geological Survey Bulletin* 214, 1–82.
- 1980, Solution and collapse features in the salt near Hutchinson, Kansas: South-central Section, Geological Society of America, Field Trip Notes.
- Walters, R. F., 1991, Gorham oil field: *Kansas Geological Survey Bulletin* 228, 1–112.
- Watney, W. L., J. A. Berg, and S. Paul, 1988, Origin and distribution of the Hutchinson Salt (lower Leonardian) in Kansas: *Midcontinent SEPM Special Publication*, **1**, 113–135.

Miller, R.D., D.W. Steeples, and J.L. Lambrecht, 2006, High-resolution seismic-reflection imaging 25 years of change in I-70 sinkhole, Russell, County, Kansas [exp. abs.]: Society of Exploration Geophysicists (published on CD).

High-resolution seismic-reflection imaging 25 years of change in I-70 sinkhole, Russell County, Kansas

Richard D. Miller, * Kansas Geological Survey; Don W. Steeples, Department of Geology, University of Kansas; Jamie L. Lambrecht, Kansas Geological Survey; and Neil Croxton, Kansas Department of Transportation

Summary

Time-lapse seismic reflection imaging improved our understanding of the consistent, gradual surface subsidence ongoing at two sinkholes in the Gorham Oilfield discovered beneath a stretch of Interstate Highway 70 through Russell and Ellis Counties in Kansas in 1966. With subsidence occurring at a rate of around 10 cm per year since discovery, monitoring has been beneficial to ensure public safety and optimize maintenance. A miniSOSIE reflection survey conducted in 1980 delineated the affected subsurface and successfully predicted development of a third sinkhole at this site. In 2004 and 2005 a high-resolution vibroseis survey was completed to ascertain current conditions of the subsurface, rate and pattern of growth since 1980, and potential for continued growth. With time and improved understanding of the salt dissolution affected subsurface in this area it appears that these features represent little risk to the public from catastrophic failure. However, from an operational perspective the Kansas Department of Transportation should expect continued subsidence, with future increases in surface area likely at a slightly reduced vertical rate. Seismic characteristics appear empirically consistent with gradual earth material compaction/settling.

Introduction

A high-resolution seismic reflection study began in 1980 targeting rock layers in the upper Permian portion of the geologic section beneath an approximately 4.5 km stretch of Interstate 70 (I-70) in western Russell County, Kansas. Surface subsidence along this stretch of highway had caused public concern and a transportation headache since 1966 (Figure 1). The principal goal of this study was to delineate rock layers within and above the Hutchinson Salt Member, specifically beneath three salt dissolution sinkholes centered at approximately mile marker 179.

It has been the consistent goal of this lengthy study to appraise the subsurface extent, overall surface growth rate, and subsidence mechanism and chronology. State-of-the-art shallow high-resolution seismic reflection techniques were used for both surveys. Advancements in the technology are obvious between the 1980 and 2004 data sets. However, even with markedly different resolution and signal-to-noise ratios, both surveys accomplished their objectives of mapping and evaluating the locally complex structures associated with the dissolution of the salt, structural failure of overlying sediments, and the resulting sinkhole.

Surface subsidence in this part of Kansas can range from gradual (an inch per year) to catastrophic (tens of feet per second) and can represent a significant risk to public safety.

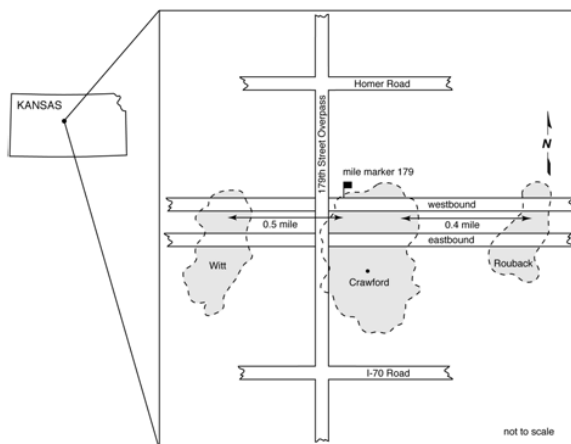


Figure 1. Site map of the study area showing location of the three sinkholes in relation to Interstate 70 in Russell County, Kansas.

The unstable nature of the ground around mile marker 179 is due almost exclusively to anthropogenic salt dissolution resulting from containment failure in brine disposal wells within the Gorham oil field (Walters, 1978). Considering the high density of wells penetrating the salt layer in this area, lateral subsurface growth to known sinkholes as well as the potential for subsidence features yet to be discovered to grow large enough to be a problem is very likely. With that in mind, it seemed prudent to seismically monitor the subsurface volume where unstable ground was evident (i.e., the three known sinkholes) and could hinder travel on I-70.

Shallow, high-resolution seismic reflection techniques have been successful delineating stratigraphic and structural features associated with several salt dissolution features throughout Kansas (Steeple, 1980; Steeples et al., 1986; Miller et al., 1993; Miller et al., 2005). Seismic reflection has proven to be a very effective tool to map structural aberrations in proximity of sinkholes. No less than a dozen sinkholes have been examined with shallow seismic reflection in Kansas, generally resulting in a detailed structural map of significant layers above the salt as well as some suggestion of the amount and extent of future subsidence.

Geologic and Geophysical Setting

The Permian Hutchinson Salt Formation underlies a significant portion of south central Kansas (Walters, 1978). The distribution and stratigraphy of the salt is well documented

High-resolution time-lapse seismic-reflection imaging

(Dellwig, 1963; Holdoway, 1978; Kulstad, 1955; Merriam, 1963). Variation in salt thickness throughout central and south central Kansas is due to a combination of increased salt and more and thicker interbedded anhydrites. The Stone Corral Anhydrite (a well documented acoustic marker) overlies the salt throughout Kansas (McGuire and Miller, 1989) and represents a primary marker reflector imaged during the I-70 seismic monitoring program. Directly above the salt is a thick sequence of Permian shales overlain by a portion of the lower Cretaceous section. At this location the Hutchinson Salt is approximately 400 m deep and about 100 m thick.

Subsidence within the Gorham oilfield in western Russell County has been a nuisance, source of substantial repair expense, and focus of much public concern for KDOT over most of the last forty years. Most significant has been the multiple meters of subsidence at the Crawford sinkhole that has affected the paved superhighway and cement overpass located within the western half of that sinkhole. Uncontrolled release of unsaturated oil field brine and the resulting indiscriminate leaching of large volumes of salt around the Crawford disposal well bore occurred when the casing failed more than fifty years ago (Walters, 1978).

Once the salt void left from this leaching process grew to exceed the strength of the roof rock, failure occurred and subsidence began. Even after wastewater disposal was halted, leaching continued as overlying fresh water gained access to the salt when borehole confinement (casing-to-borehole seal) was lost. Natural confining properties of the rock layers surrounding the well bore were compromised when strain manifested itself as large faults generally centered around the well bore (Steeple et al., 1986). With failure and subsidence of rock layers surrounding the well bore and above the salt, natural new conduits for vertical migration of fresh water were established and the process proceeded unchecked.

Acquisition/Processing

Improvements in high-resolution data acquisition and processing techniques occurring over the last twenty years are evident in the dramatic increase in signal-to-noise ratio and data fidelity. Comparing and contrasting the 1980 and 2004 seismic surveys, it is evident that the biggest improvements come in source, number of recording channels, dynamic range of seismograph, and pre-stack processing steps.

Seismic reflection data acquired in 1980 used the Mini-SOSIE method (Barbier et al., 1976) to minimize the effects of traffic noise and avoid the expense and increased safety concerns of using high explosives. Vibroseis was employed in 2004 to increase the total energy, maintain non-invasive and non-destructive requirements, and tailor the amplitude spectra. Both are coded sources and reduce the effects of traffic noise compared to impulsive sources.

Both 1980 and 2004 surveys were 4.5 km long and approximately centered on the Crawford sinkhole. Increased fold and improved amplitude spectra of the source was the most substantial improvement in the 2004 data set. No doubt

	1980	2004
seismograph	12 channel I/O	240channel Geometrics
	12-bit A/D fixed-gain amplifiers	24-bit A/D floating-point gain amplifiers
source	MiniSOSIE 1 Wacker (earth compactor)	vibroseis minivibII (10,000 lbs)
receivers	-28 Hz	-40 Hz
station spacing	16 m	5 m
spread	split	fixed, asymmetric
source offset	64 m to 160 m	5 m to 600-900m

doubling the size of the seismograph's A/D converter also played a significant role in overall data quality improvements. The 1980 survey included 130 shot stations and took three days to acquire. In 2004 the survey included over 450 shot stations and took two days to acquire. Data were acquired between mile markers 177 and 181.

The basic architecture and sequence of processing steps followed during the generation of the final stacked sections was similar to conventional petroleum exploration flows (Yilmaz, 1987). All records and files from the 1980 survey for both data and processing flow and the ability to match display parameters were lost, so comparisons of processing approaches and steps are not possible. High-resolution seismic reflection data, by its very nature, lends itself to over-processing, inappropriate processing, and minimal involvement processing. Interpretations of high-resolution shallow reflection data must take into consideration not only the geologic information available, but also each step of the processing flow and the presence of reflection events on raw unprocessed data.

Discussion

Comparison of seismic data characteristics from the legacy and monitor seismic data clearly demonstrates the advancements in high-resolution shallow seismic reflection imaging in this extremely challenging setting. From the analog displays available for the 1980 survey it is possible to interpret the extent and degree of subsurface collapse at the time of the survey (Figure 2). In the 25 years following the 1980 survey the horizontal expression of the sinkhole has only increased slightly, but the character of the reflections from within the subsidence feature have changed dramatically.

The drop in dominant frequency and velocity beneath the sinkhole as well as the lack of consistency in wavelet character across the subsidence-affected area is indicative of changes in material above the salt (Figure 3). Major surface changes are related to KDOT filling the sinkhole twice prior to the 1980 survey and then once more between the 1980 and 2004 survey; however, these surface activities do not totally account for the kinds of changes observed on the seismic sections.

High-resolution time-lapse seismic-reflection imaging

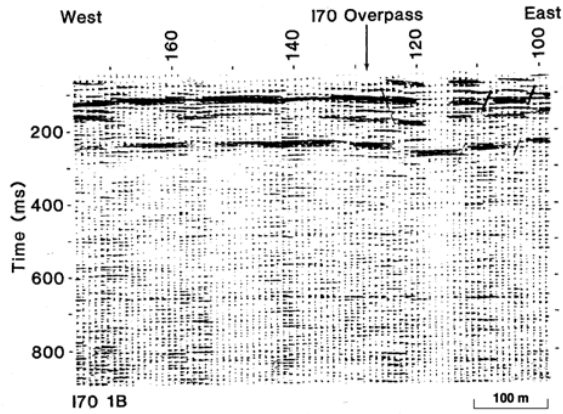


Figure 2. Interpreted seismic section from 1980 survey at the Crawford sinkhole located at station 110 (from Steeples et al., 1986).

Two of the three confirmed subsidence features have cone-like vertical development and notable seismic characteristics consistent with several unique paleosubsidence features discovered on a seismic reflection profile acquired 200 m away along the eastern dissolution front of the Hutchinson Salt (Figure 4). These paleosubsidence features appear near vertical on seismic data and have been interpreted as remnants

of catastrophic collapse of overburden into naturally occurring salt dissolution voids.

There are notable differences between these two time-lapse seismic subsidence images, the most obvious being the degree of wavelet character change within the affected area (Figures 2 and 3). Also noteworthy are the relatively flat reflections within the subsidence feature that define a much larger subsurface-affected area than surface expression. This is also evident in the upward-narrowing disturbed zone defining the tensional dome. If the interpretation of paleocatastrophic failure is correct on reflection sections from the dissolution front (Figure 4), then wavelet stretching, cone-shaped geometry, and flat-laying reflections within the disturbed volume observed on seismic data from the Crawford/Witt sinkholes could be indicative of a slower rate of vertical rock movement into voids in the salt.

The cone-shaped appearance of the I-70 sinkholes on seismic data is consistent with active dissolution and subsidence as interpreted on several seismic investigations at similar sinkholes in Kansas. Based on a tensional dome failure mechanism, the two primary sinkholes at this site are still active with reverse faults defining the major collapse structures. Once horizontal roof rock failure of the salt interval slows or subsides, strain should begin to manifest itself as normal faults defining an ever-shallowing bowl structure. Subtle indications are evident in the salt overburden that this transition might have begun.

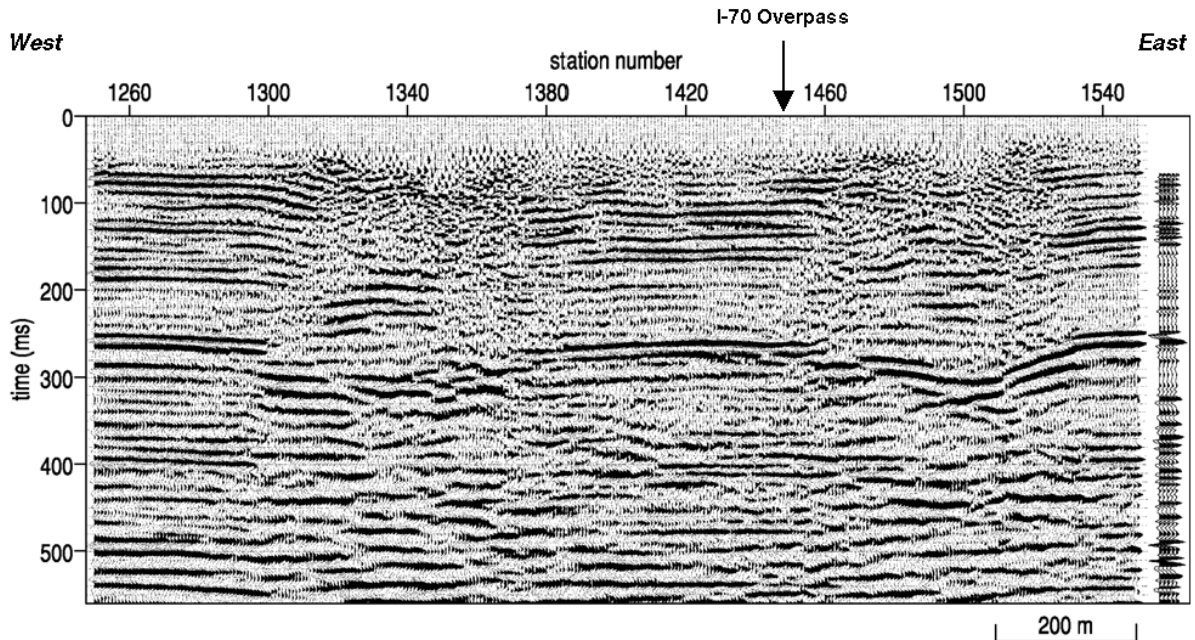


Figure 3. Witt sinkhole is located at station 1340 and the Crawford is at 1500. The high amplitude event at 260 ms is the 300-m deep Stone Corral Anhydrite. Top of salt is at about 340 ms and is approximately 400 m below ground surface. The synthetic at the right was used to verify reflection identification

High-resolution time-lapse seismic-reflection imaging

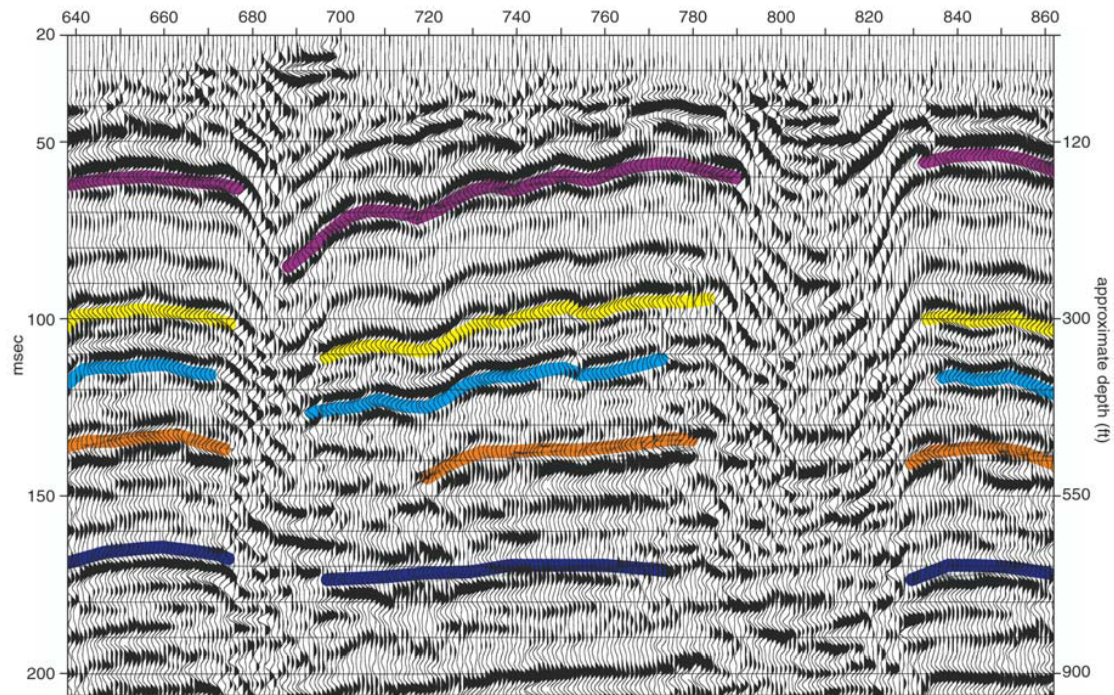


Figure 4. Seismic profile from along the eastern dissolution front of the Hutchinson Salt near Punkin Center in Reno County, Kansas.

Conclusions

An improved understanding of the subsidence process associated with failure of casing integrity was gained through seismic time-lapse investigations of the Witt, Crawford, and Rouback sinkholes beneath I-70. Improvements in methodology and equipment in the last 25 years for applications to near-surface high-resolution problems is clearly evident. It appears the dissolution process is still active at both the Crawford and Witt sinkholes and therefore the full surface expanse of these sinkholes is still unknown as well as a likely time-frame for surface stabilization.

Acknowledgments

Kansas Department of Transportation provided financial support for this project. We thank the KGS acquisition crew, led by David Laflen for their work in the field, and Mary Brohammer for her assistance in manuscript preparation.

References

- Barbier, M.G., P. Bondon, R. Mellinger, and J. Viallix, 1976, Mini-SOSIE for land seismology: *Geophysical Prospecting*, 24, 518-527.
- Dellwig, L.F., 1963, Environment and mechanics of deposition of the Permian Hutchinson Salt Member of the Wellington Shale. Symposium on Salt, Northern Ohio Geological Society, Cleveland, p. 74-85.
- Holdaway, K.A. 1978, Deposition of evaporites and red beds of the Nipewalla Group, Permian, western Kansas: Kansas Geological Survey Bulletin 215.
- Kulstad, R.O., 1959, Thickness and salt percentage of the Hutchinson Salt: Symposium on Geophysics in Kansas, Kansas Geological Survey Bulletin 137, p. 241-247.
- McGuire, D., and B. Miller, 1989, The utility of single-point seismic data: Geophysics in Kansas, D.W. Steeples, ed., Kansas Geological Survey Bulletin 226, p. 1-8.
- Merriam, D.F., 1963, The geologic history of Kansas: Kansas Geological Survey Bulletin 162, 317 p.
- Miller, R.D., D.W. Steeples, L. Schulte and J. Davenport, 1993, Shallow seismic-reflection feasibility study of the salt dissolution well field at North American Salt Company's Hutchinson, Kansas, facility: *Mining Engineering*, October, p. 1291-1296.
- Miller, R.D., A. Vilella, J. Xia, and D.W. Steeples, 2005, Seismic investigation of a salt dissolution feature in Kansas: Soc. Explor. Geophys., Investigations in Geophysics no. 13, Dwain K. Butler, ed., *Near-Surface Geophysics*, p. 681-694.
- Steeples, D.W., 1980, Seismic reflection investigations of sinkholes in Russell and Ellis counties, Kansas: Progress report to the Kansas Department of Health and Environment and the Kansas Department of Transportation, 14 p.
- Steeples, D.W., R.W. Knapp, and C.D. McElwee, 1986, Seismic reflection investigations of sinkholes beneath interstate highway 70 in Kansas: *Geophysics*, v. 51, p.295-301.
- Walters, R.F., 1978, Land subsidence in central Kansas related to salt dissolution: Kansas Geological Survey Bulletin 214, 82 p.
- Yilmaz, O., 1987, Seismic data processing; S.M. Doherty, ed; *in* Series: Investigations in Geophysics, no. 2, E.B. Neitzel, series ed.: Soc. Explor. Geophys

Miller, R.D., and K. Millahn, 2006, High-resolution seismic reflection investigations of dissolution sinkholes [ext. abs.]: European Association of Geoscientists and Engineers (EAGE) 68th Conference and Exhibition, Vienna, Austria, June 12-15, 4 p. (published on CD).

Summary

Seismic reflection images of dissolution subsidence features that have not yet developed any surface expression provide insights into potential growth mechanisms, development rates, and sinkhole risk. Vertical growth of small depressions or drapes in reflectors several hundred meters below ground surface and in proximity to major salt dissolution sinkholes appear to be controlled by active dissolution in deeper salt layers and the size and competence of the unsupported span of roof rock. Gradual failure and continued upward movement of voids characterized by reflector drape are confined to the inverted cone geometry defining the stress regime or tensional dome. Time-lapse imaging of these yet-to-emerge sinkholes could provide key parameters for developing empirical models of sinkhole development. Ideally, these models would allow reasonable estimations of growth rates and mature sinkhole areal expressions.

Introduction

Sinkholes resulting from rock dissolution (karst) can develop at rates ranging from gradual (mm in years) to catastrophic (meters in seconds). Unexpected sinkhole formation represents a potential risk to property and safety the world over (Beck 1984). Detection prior to surface subsidence is preferable, but appraising the risk a juvenile subsidence feature represents is essential for minimizing the impact of these hazards on human habitation and the environment (Ruth et al. 1985). Disruption of ground stability by dissolution-instigated subsidence has affected transportation facilities, residences, manufacturing facilities, commercial buildings, underground utilities, as well as groundwater and aspects of the ecosystem (Beck 1987).

Dissolution of rock responsible for subsidence and ultimately the formation of a sinkhole can be initiated and/or influenced by natural or anthropogenic processes (Steeple et al. 1986; Wilson 1995; Brink 1984). Understanding the site-specific temporal variability of the mechanisms controlling subsidence as a function of changes in the surface and subsurface hydrologic and structural characteristics and the generalized failure process of a specific rock column is key to understanding and hopefully reducing the risk of unexpected or accelerated development of surface depressions (Kemmerly 1993).

Numerical models populated with uniform/generalized rock characteristics are a reasonable means for understanding the mechanism and potential risk for a subsidence prone area (Augarde et al. 2003). However, under field conditions small scale inhomogeneities in rocks not adequately defined through borehole measurements or generalized site geology predicate using generalized numerical model predictions as a high-confidence means of estimating the risk a particular site represents to public safety. Risk estimations from site-specific monitoring and empirically based predictions are preferable to generalized numerical model-based appraisals.

Dissolution of carbonates is extremely slow in comparison to the same process for evaporites. Evaporites, therefore, represent a much greater risk for anthropogenic errors to instigate or accelerate the dissolution process. However, human activity can be the catalyst for accelerated collapse in any karst setting through alteration of the unconsolidated overburden, such as changes in hydrology (Bell 1988; Kannan 1999; Tharp 1999).

Dissolution to the point of subsidence occurs in an evaporite unit at a much accelerated rate relative to limestones. Imaging changes in evaporite rocks at various stages through the dissolution (leaching) and failure (stress to strain) process can provide a greater range of empirical evidence to support generalizations about the maturation process for a given observation time than for equivalent studies in known limestone karst areas. Observing a relatively large number of sinkholes through various stages of their maturation within a relatively short time window allows some degree of confidence in qualitative statements and estimates of uniformity or commonality in the dissolution-related subsidence process. However, to more completely generalize failure due to dissolution of a rock, it is important to relate and contrast subsidence characteristics of both limestone and evaporite dissolution.

Geologic Setting

Several major salt basins exist throughout North America (Ege 1984). The Hutchinson Salt Member occurs in central Kansas, northwestern Oklahoma, and the northeastern portion of the Texas panhandle, and is prone to and has an extensive history of dissolution and formation of sinkholes. In Kansas, the Hutchinson Salt possesses an average net thickness of 76 m and reaches a maximum of over 152 m in the southern part of the basin. Deposition occurring during fluctuating sea levels caused numerous halite beds, 0.15 to 3 m thick, to be formed interbedded with shale, minor anhydrite, and dolomite/magnesite. Individual salt beds may be continuous for only a few miles despite the remarkable lateral continuity of the salt as a whole (Walters 1978).

Permian shale layers overlaying the Hutchinson Salt Member are a primary target of any study looking at salt dissolution sinkhole development and associated risks to the environment and human activity in Kansas. Failure and subsidence of these shale units are responsible for many of the physical characteristics observed in modern sinkholes. Once failure occurs, the impermeable shales provide the pathways for groundwater to gain access to the salt. In proximity to the dissolution front fractures, faults, and collapse structures compromise the confining properties of the Permian shale bedrock and put the major fresh water aquifer (Plio-Pleistocene Equus Beds) in this part of southern Kansas at risk. Along the eastern boundary (dissolution front) the salt ranges in thickness from 0 to over 100 m and is buried beneath about 120 m of Permian red bed shales.

Seismic Data Acquisition and Processing

In general, data used in this study were acquired and processed as 2-D CMP sections, focusing primarily on high resolution and optimal signal-to-noise ratio. Most data included as part of this study have been acquired using the Vibroseis technique. Source and recording methodology were based on best fit to the individual survey requirements. Signal generated by high-sensitivity geophones were recorded on a Geometrics seismograph supporting from 96 to 240 channels.

Data processing relied on confident identification of reflections on shot gathers. Critical is the identification and awareness of a reflection event's optimum time window. Equally as important is the understanding and isolation/elimination of noise from signal. Noise for reflection data includes source generated (refractions, surface waves, air wave, and diffraction/scatter) and environmental (vehicles, facilities, power lines, wind, animals, etc.) noise. Minimal processing has proven beneficial in ensuring signal is being enhanced with little distortion and without the creation of artifacts common with overprocessing or inappropriate processing.

Discussion

Time-lapse images capturing a collapse feature's maturation through the stages of void development, initial roof rock failure of the void, migration of subsidence through the overburden, and eventual formation of a sinkhole would provide essential empirical characteristics necessary to refine site-specific theoretical models. Most numerical collapse models are based on uniform void geometries (sphere, ellipsoids, etc.) and laterally homogeneous layers between void and ground surface. Prediction of collapse rates and affected volumes at a particular site would require realistic models populated with parameters deduced from seismic images of subsurface subsidence recorded at representative sites.

Capturing earth material movement associated with roof rock failure of a dissolution void prior to subsidence is generally a matter of coincidence or reasoning through vague clues from borehole data or responses. Considering, in the best case scenario, borehole measurements (fluid levels and pressures) provide only subtle hints of containment problems in or around a well bore, it is not surprising the prefailure information has been extremely limited. To date, there are no cases reported in the scientific literature of time-lapse seismic images capturing an unintentional (natural or anthropogenic) subsurface collapse event.

As with many acts of nature, acquiring seismic images of pre-sinkhole subsidence is more a matter of coincidence than planning. On two occasions "juvenile" subsidence features have

been interpreted on seismic data at sites where the target of the seismic reflection survey has been adjacent to active sinkholes. These apparent subsidence features have several distinctive characteristics both seismic and in relation to the geologic setting, suggestive of future sinkholes: first, presence of dissolvable rocks; second, bed distortion not attributable to tectonics; third, history of local dissolution; fourth, an available source of fluid and possible mechanism for moving saturated brine away from the dissolution front; and fifth, bed distortion observed only above the dissolvable rock.

An attempt to evaluate the growth of a series of sinkholes along a major four-lane interstate in central Kansas, USA, using seismic reflection has produced images of what could be a collapse feature actively migrating toward the ground surface. The target of this survey was the 150-m-wide sinkhole centered on station 1340 that has a subsurface seismic expression on the CMP section consistent with other sinkholes from this area (Figure 1). Top of Hutchinson Salt in this area is about 350 ms two-way travel time. A series of high amplitude and relatively high resolution reflections are prevalent throughout the predominantly Permian shale section, Jurassic, and the lower part of the Cretaceous section. The 270 ms Stone Corral Anhydrite is a regional seismic marker bed and lies around 150 m above the salt section. Diffracted seismic energy and relatively low velocity and low frequency reflections from within and adjacent to the subsidence feature beneath station 1340 could be artifacts of tight bed folding (ductile deformation and a “bow tie” resulting for extreme synclinal geometries) or scattered energy re-radiated from bed terminations resulting from brittle deformation.

Apparent drape in a series of reflections around station 1250 between the Stone Corral Anhydrite and a shallow Cretaceous layer about 100 m below ground surface is characteristic of subsidence features seismically mapped in this region. No surface expression was present at this location at the time of the seismic survey. It is, therefore, reasonable to suggest that this is a collapse feature resulting from dissolution of the Hutchinson Salt and migrating toward the ground surface. Improved processing and associated data enhancements will be necessary to determine the dominant failure mechanism at this site. It is assumed that casing failure in an oil field well opened a pathway for fluids to access the salt and initiated the dissolution process.

At a second site approximately 300 m shallower in the geologic section and 200 km southeast of the previous site (Figure 1), a gradually developing sinkhole with apparent subsurface ties to paleosubsidence features is adversely affecting a two-lane highway through south central Kansas. Several different subsidence mechanisms are and/or have been at work at this site (Figure 2). Clearly, the subsurface dissolution responsible for the current sinkhole is an order of magnitude or more larger than the sinkhole dimensions. Also, the predominant structures controlling at least the initial subsidence are a set of reverse faults.

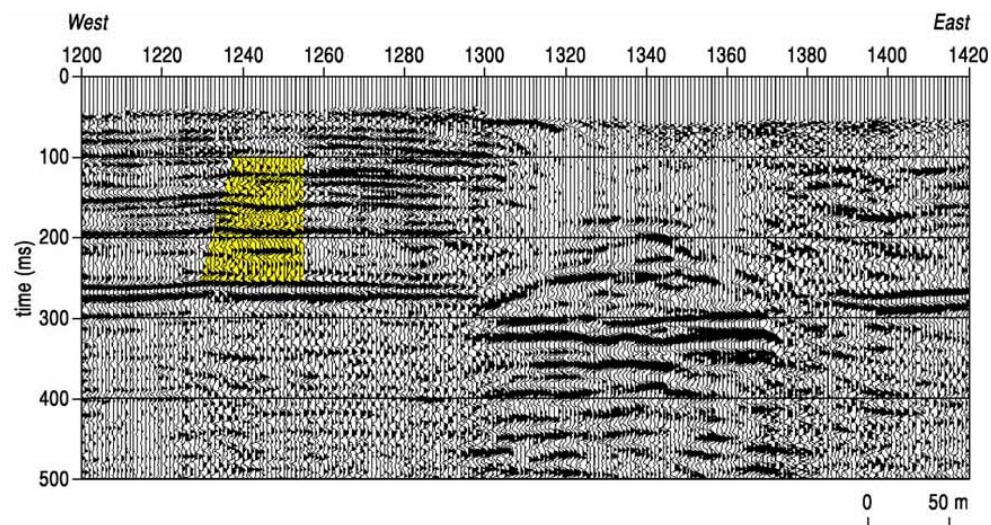


Figure 1. Possible collapse feature (highlighted). An existing sinkhole is centered at station 1340.

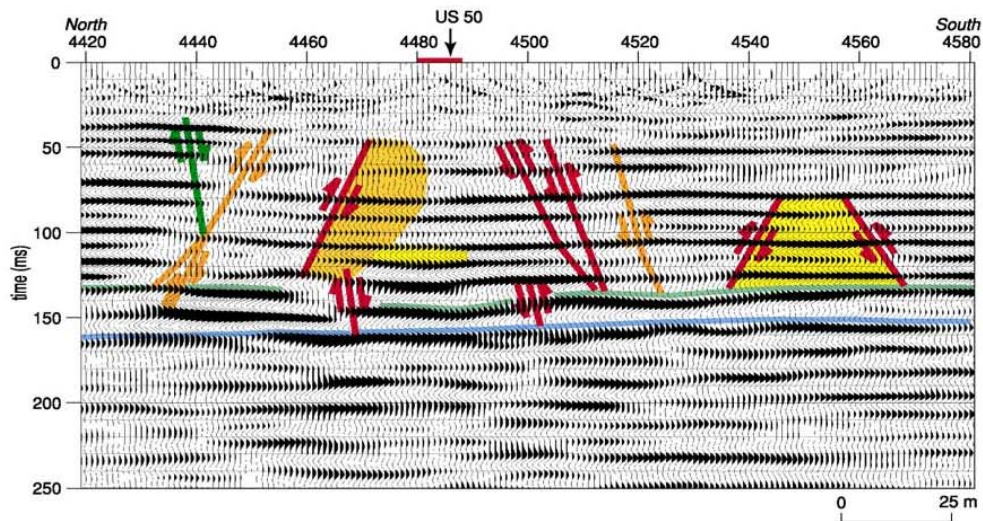


Figure 2. Gradually developing sinkhole with associated paleosubsidence features affecting a highway.

Adjacent to the sinkhole and its related dissolution and subsidences are a set of reflections from within the Permian shales that appears to drape. This drape is contained within an area defined by an inverted cone and truncates against a relatively high-amplitude reflection interpreted to be a dolomite separating the Upper Wellington Shale from the Ninescah Shale (Figure 2). If this is an active feature, growth of the dissolution void in the salt will eventually result in an unsupported roof span at the base of the Ninescah Shale that surpasses the strength of the dolomite and failure will result. Key will be how large the roof span becomes prefailure and the strength/resistance to failure of rocks 50 m below bedrock.

Conclusions

Capturing dissolution-related subsidence features at different stages of vertical expression can provide key stress/strain relationships key to predicting growth rates and maximum dimensions of mature sinkholes for different geologic settings. If these kinds of growth predictions can be made with reasonable confidence, it becomes possible to develop remediation strategies after the onset of dissolution but before the stoping advances to the point of sinkhole development. Key to these predictions is understanding the geology of the host rock and overburden as well as the fluid source (inlet) and departure point(s). By capturing seismic images at different stages of growth, empirical and numerical models can be developed predicting growth. Examples of "juvenile" subsidence features at stages of intermediate development exist for both anthropogenic and natural induced dissolution subsidence.

References

- Augarde, C.E., Lyamin, A.V., and Sloan, S.W. [2003] Prediction of undrained sinkhole collapse. *Journal of Geotechnical and Geoenvironmental Engineering* 129(3), 197-205.
- Beck, B.F. [1984] *Sinkholes: Their Geology, Engineering, and Environmental Impact*. Balkema, Rotterdam.
- Beck, B.F., and Wilson, W.L. (eds.) [1987] *Karst Hydrogeology: Engineering and Environ. Applications*. Balkema, Rotterdam.
- Bell, F.G. [1988] Subsidence associated with the abstraction of fluids. *Engineering Geology of Underground Movements*, F.G. Bell et al. (eds.), 363-376. The Geological Society, London.
- Brink, A.B.A. [1984] A brief overview of the South African sinkhole problem. *Proceedings, First Multidisciplinary Conference on Sinkholes*. Balkema, Rotterdam.
- Ege, J.R. [1984] Formation of solution-subsidence sinkholes above salt beds. U.S. Geological Survey Circular 897, 1-11.
- Kannan, R.C. [1999] Designing foundations around sinkholes. *Engineering Geology (Amsterdam)* 52, 75-82.
- Kennerly, P.R. [1993] Sinkhole hazards and risk assessment in a planning context. *Journal of the American Planning Association* 59(2), 221-229.
- Ruth, B.E., Beggs, T.F., and Degner, J.D. [1985] Predicting sinkhole collapse. *Civil Engineering* 55(11), 58-60.
- Steeple, D.W., Knapp, R.W., and McElwee, C.D. [1986] Seismic reflection investigations of sinkholes beneath Interstate Highway 70 in Kansas. *Geophysics* 51, 295-301.
- Tharp, T.M. [1999] Mechanics of upward propagation of cover-collapse sinkholes. *Engineering Geology (Amsterdam)* 52, 23-33.
- Walters, R.F. [1978] Land subsidence in central Kansas related to salt dissolution. *Kansas Geological Survey Bulletin* 214, 1-32.
- Wilson, W.L. [1995] Sinkhole and buried sinkhole densities and new sinkhole frequencies of Northwest Peninsular Florida. *Proceedings, 5th Multidisciplinary Conference on Sinkholes*. Balkema, Rotterdam.

Miller, R.D., J. Xia, and C.B. Park, 2005, Seismic techniques to delineate dissolution features (karst) at a proposed power plant site; in D.K. Butler, ed., *Near-Surface Geophysics*: Society of Exploration Geophysicists, Investigations in Geophysics No. 13, p. 663-679.

Seismic Techniques to Detect Dissolution Features (Karst) at a Proposed Power-Plant Site

Richard D. Miller¹, Jianghai Xia¹, and Choon B. Park¹

Introduction

Population growth in southern Alabama and in the panhandle of northwestern Florida has taxed the current electric grid to the point that many critical services could be in jeopardy during peak demand times. Surplus or overflow electric power generation facilities are critical to small power cooperatives that must buy power when peak demand exceeds their maximum production capacities. Locating sites for power generation facilities has historically relied on the convergence of three things: fuel delivery system (pipeline, railroad, harbor, etc.), water (river, lake, etc.), and power grid (high-tension regional distribution electric lines), with concerns for the site geology being secondary or not considered at all.

Power-plant designers could provide significant cost savings to power cooperatives if site-specific characteristics could be considered during the engineering of turbine frames, fuel storage tanks, pipelines, and the like. Many times overdesign of facilities is necessary to accommodate potential hazards that are possible based on geography or have been suggested using isolated or even single borehole material test. Sitewide borings that encountered rubble, fractures, or lost circulation zones within 1 km of a proposed power-plant site near Damascus, Alabama (PPDA), prompted concerns for future plant safety and necessary design constraints (Figure 1). Seismic methods (reflection and surface wave analysis) were used to examine the competence of shallow rock layers and search for anomalies (Miller and Xia, 1999).

Seismic reflection and surface-wave imaging can be used in conjunction with boring logs to confidently identify and map disturbed strata and anomalous zones (faults, fractures, subsidence features, etc.) within the upper 100 m of the earth's surface. Success of high-resolution seismic reflection imaging of the shallow subsurface depends on several key conditions (Steeple and Miller, 1990). Fore-

most among these is the existence of acoustic velocity and/or density contrasts that generally correspond to geologic interfaces. The second relates to the ability of the near surface to propagate high-frequency seismic signals. Finally, the acquisition parameters, recording equipment, and processing flow must be compatible with the proposed target and resolution requirements of the survey (Hunter et al., 1984).

Seismic surveys are generally designed to image structural and stratigraphic features with a high degree of resolution and accuracy. On such surveys, surface waves are generally considered noise. For our application, however, the objective is to exploit the sensitivity of the surface wave to changes in material velocities associated with voids in the half-space it travels through. Surface-wave propagation depends on frequency (depth of penetration), phase velocity (compressional and shear), and density. Each of these properties will affect the surface-wave dispersion curve (phase velocity versus frequency) in a predictable fashion. Of all the earth's seismic properties, shear-wave velocity has the greatest influence on the propagation of a surface wave (Xia et al., 2000). By making a reasonable assumption about Poisson's ratio, it is possible to invert the surface-wave dispersion curve to obtain the shear-wave velocity as a function of depth (Xia et al., 1999) with an accuracy better than 20%. Disturbances or perturbations in the surface-wave energy appear as anomalies in the otherwise uniform shear-wave velocity field for a layered earth.

Imaging using continuous multichannel analysis of surface waves (Park et al., 1999; Xia et al., 1999) is a new technique that relies on the same properties of surface waves as well-founded surface-wave techniques (Nazarian et al., 1983; Stokoe et al., 1994) that have been used for years in civil engineering applications to estimate shear-wave velocity as a function of depth. Mapping the two- or three-dimensional shear-wave velocity field provides insight into subsurface variability, in particular, changes in strength properties. A real advantage to this imaging method over other seismic methods is that it can be applied

¹Kansas Geological Survey, 1930 Constant Avenue, The University of Kansas, Lawrence, KS 66047-3726, E-mail: rmiller@kgs.ku.edu.

with no assumptions about the subsurface (i.e., layered earth, increasing velocity with depth, geologic/hydrogeologic contacts/interfaces possessing a velocity and/or a density contrast, etc.). The shear-wave velocity field mapping technique, as applied here, is sensitive to abrupt changes in near-surface materials (e.g., bedrock interface, voids, fracture zones, etc.), especially the absence or alteration of otherwise competent rock.

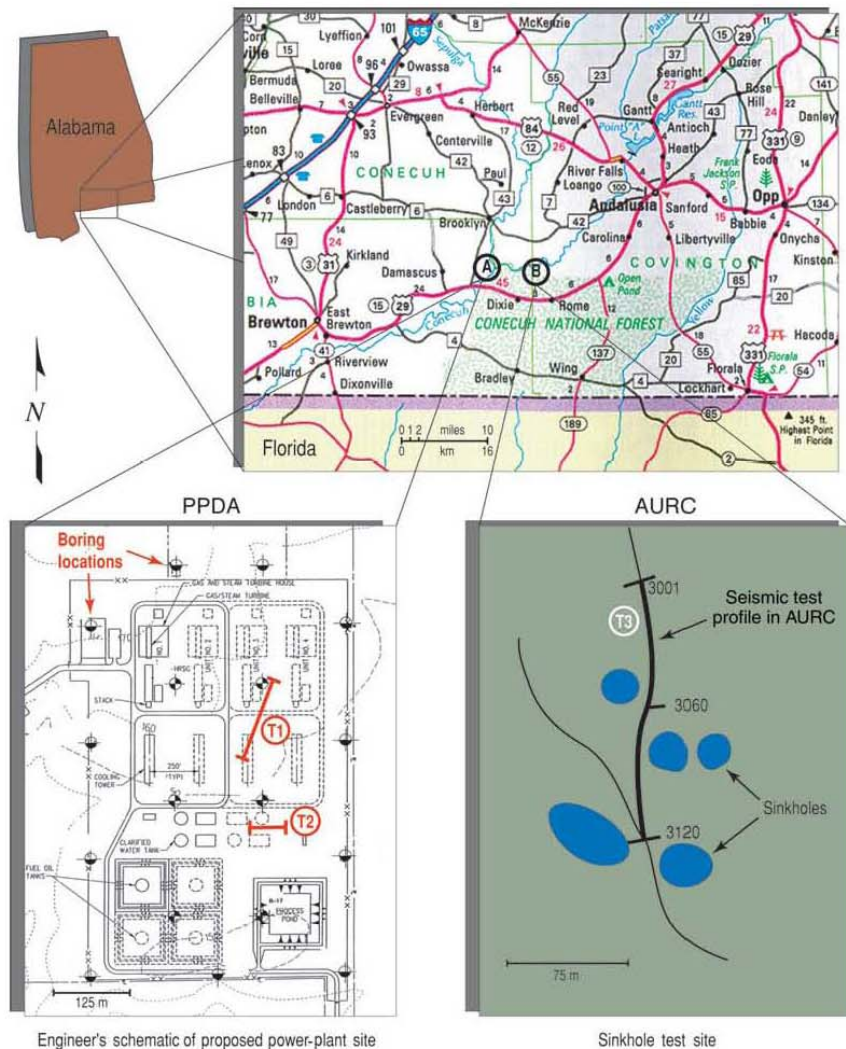
With no indications on the ground surface that dissolution was active, the proposed power plant at the Damascus site was not originally designed with concerns about subsidence. Surface investigations of surrounding properties following site selection uncovered sinkholes liberally scattered between this site and the Conecuh River (Figure 1). A near-surface seismic investigation was initiated to

determine if designers should be concerned about subsidence features smaller than the borehole spacing of the grid drill program. Feasibility testing was performed within Auburn University's Forestry Research Center (AURC) several kilometers away from PPDA, to evaluate the effectiveness of these geophysical methods to detect presubsidence features. AURC is plagued with swarms of active subsidence and exposed karst features as well as subterranean tunnels with flowing water.

Geology

Subsidence features within the Bucatunna Clay and river terrace deposits throughout this part of southern Alabama and nearby northern Florida have formed from

Figure 1. Site map of (A) proposed power-plant site near Damascus, Alabama (PPDA), and (B) test run in the Auburn University Research Center (AURC). Test lines 1 (T1) and 2 (T2) overlay the proposed layout of the power facility. The AURC line (T3) was located between sinkholes (blue). The borings were completed at the time of the survey.



collapse of voids from karsting processes in the Glendon and Marianna limestones (Figure 2). These limestones are particularly susceptible to dissolution and have been responsible for sinkholes in this area throughout the Quaternary. Incorporating seismic reflection and surface-wave profiling with lithology and material characteristics interpreted from gridded boreholes allowed extension of one-dimensional geologic interpretations into three dimensions. Seismic methods provided insight into the lateral coherency of geologic anomalies encountered during drilling.

Near-surface geology (the upper 200 m) is characterized locally by relatively flat-lying, predominantly limestone and shale (clay) sequences overlain by a relatively thin veneer of unconsolidated materials less than 10 m thick and composed predominantly of clay and sandy-clay (Figures 2 and 3). The Bucaturna Clay separates river terrace deposits from the sculptured surface of the Glendon Limestone (bedrock). Dissolution and erosion of the bedrock surface has produced the short wavelength pinnacle-type topography observed in outcrop and interpreted from drill data. This highly irregular bedrock surface provided a resolution challenge to both reflection and surface-wave imaging with neither having the potential to reliably resolve the pinnacle features as observed in outcrop.

The Glendon Limestone overlays the Mariana Limestone and together are around 10 to 20 m thick. The Mariana Limestone is in direct contact with the Red Bluff Clay, which overlays the Ocala Limestone. The top of the Ocala Limestone is generally thought to be around 30 m below ground surface (BGS) and was thought to represent the shallowest sitewide unit that might be a consistent seismic reflection marker that could be identified on all seismic reflection sections.

The Ocala Limestone is also thought to be responsible for karst-related sinkholes in northern and central Florida

(Figure 2). The Glendon, Marianna, and Ocala limestones should all be present within the upper 50 m at this site and all have a history of local dissolution. Critical to safe construction and operation of the proposed power station is the presence of an intact geologic section from at least the top of the river terrace deposits (ground surface) down to the base of the Ocala Limestone. Detailed knowledge of the physical properties and lateral continuity of rocks in the upper 50 m could, should, and likely will be an aid in engineering designs.

Lithologies have been identified based on drill characteristics (such as changes in stiffness), cuttings, and from the core samples. Most rock layers sampled during drilling were extremely altered, resulting in reduced core recovery in many holes (Figure 3). With the exception of bedrock, no unique geologic interfaces or markers (units) within 50 to 60 m of the ground surface were identified in drill cuttings or cores that could be correlated between boreholes. Confident ground truth correlations between rock layers and seismic data require clean, abrupt contacts and consistency in the properties of rock layers from borehole to borehole. Every borehole drilled penetrated zones with fractures, voids, extremely low blow counts, water loss, and/or vugs. Considering the regional continuity of the near-surface geologic units expected to be present at this site, the lack of any consistently distinguishable limestone and clay units between those closely spaced borings suggests most of the rock within the upper 60 m has been highly altered.

Phase 1: Feasibility Testing

Evaluating the feasibility of seismic techniques and the necessary considerations to optimize each methodology requires analysis of a variety of parameters and equip-



Figure 2. Generalized geologic profile of the proposed power-plant site based on drilling and field studies.

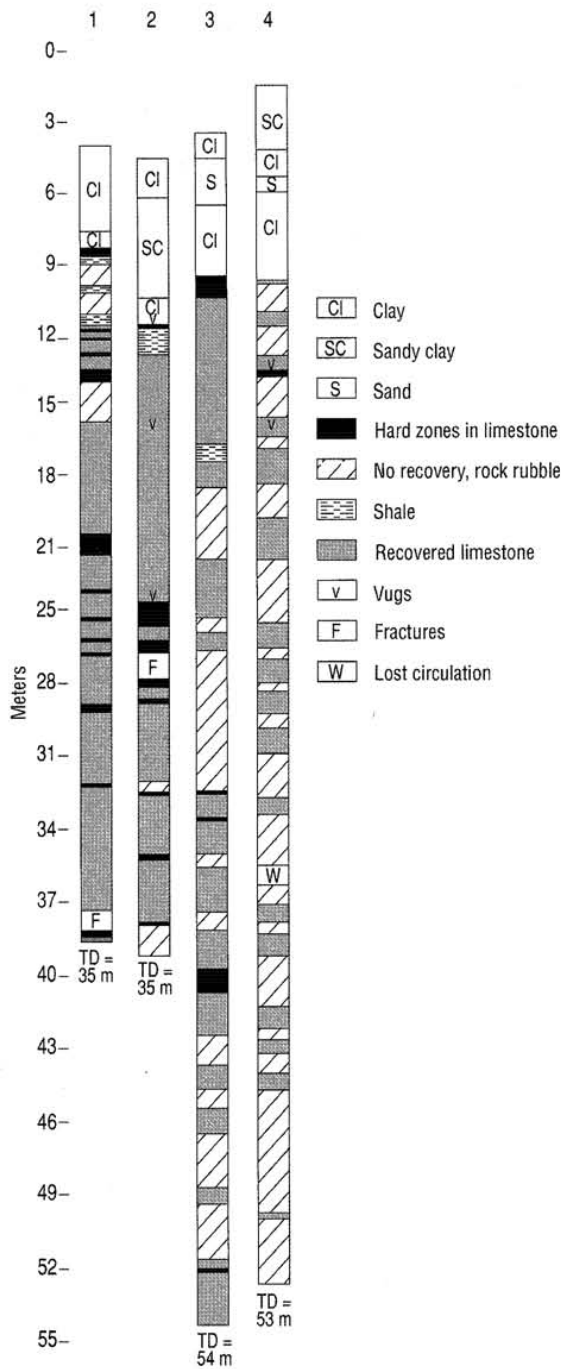


Figure 3. Selected boring logs with geologist description (Laura Moore, B&M).

ment (Steeple and Miller, 1990; Park et al., 1999). The primary objective of these seismic surveys was to characterize the subsurface sufficiently for engineering designs to be developed that would compensate for or tolerate potential subsidence features during construction and future plant operations. For seismic techniques to be considered feasible, they must be capable of detecting volumes of disturbed subsurface materials indicative of subsidence as small as a few meters in diameter tens of meters below bedrock. At PPDA, general site properties were established, while at AURC the objective was identification of unique seismic characteristics of developing sinkholes.

Testing at PPDA focused on wavelet characteristics, velocities, and offset dependence without concern for discriminating undisturbed from altered earth materials. A total of 206 strings of 40-Hz geophones (three phones per string) were deployed at 0.6-m spacing along T1, located near boring 4 (Figures 1 and 3). Data were recorded from five different sources (two projectile, two explosive, and one impact). End-on and split-spread geometries provided several unique surface locations for the single fixed spread of receivers. This source configuration offered an opportunity to observe significant seismic properties of the wavefield and their dependence on source and changes in source location.

In addition to high-resolution seismic reflection testing at PPDA, surface-wave imaging was evaluated at two different spots at PPDA (T1, T2) and in one area in AURC (T3) (Figure 1). Production of a 1D shear-wave velocity profile requires the inversion of the almost 60-m spread into a 1D shear-wave velocity trace that is a function of depth. This approach averages the 2D slice of earth materials beneath the spread during the estimation of the dispersion curve. This averaging smears anomalies in the shear-wave velocity field and therefore the length of the spread affects the resolution of the technique.

Feasibility of the seismic reflection technique

Seismic reflection testing was conducted along a single 125 m profile (T1) within the PPDA (Figure 1). Source and receiver testing focused on resolution and signal-to-noise ratio. Of the five sources tested, the downhole 50-cal. rifle (Steeple et al., 1987) showed the greatest potential to image features from 15 m to over 200 m of depth (Figure 4). Source evaluation criteria were based on shallowest discernable reflection, overall frequency content, depth of penetration, number of shots necessary to properly condition the hole, and percentage of noise (ground roll, air-coupled wave, and guided waves).

Hole conditioning has long been known to improve the coupling of high-frequency seismic reflection data (Miller et al., 1986). The benefits of hole conditioning are extremely evident on walkaway data from this site. Down-

sizing the source in hopes of increasing the dominant frequency and signal-to-noise ratio and possibly reducing the shallowest imageable depth would have required detonation of at least two and likely three 30.06 shots at each location (Figure 5). With each shot fired into the same hole, the frequency content, signal-to-noise ratio, and depth of signal penetration increases. Data from the 50-cal. downhole did not appear to benefit from multiple shots in a single hole.

With the imageable depth range based on velocities calculated from NMO curves and two-way reflection times well within the objectives of this survey, questions about resolution are all that remain in evaluating the feasibility of seismic reflection. The empirically derived half-wavelength criteria for vertical resolution (Miller et al., 1995) suggests 2.4 m is reasonable for the shallower part of the section (10 m to 30 m) and 4.5 m for the deeper part of the section (70 m to 200 m). Horizontal resolution of these data, calculated using Ricker criteria (Brühl et al., 1996), allows detection of beds laterally separated by more than about 3.5 m at 20 m of depth and around 15 m at 200 m depth. Any feature larger than 2.4 m tall and 3.5 m wide at 20 m of depth and 4.5 m tall and 15 m wide at 200 m of

depth should be detectable with these reflection data. It is, of course, possible to detect features much smaller, but only through wavelet interference or indirect methods closely related to borehole data and associated modeling (Gochioco, 1992).

Feasibility of the surface-wave imaging technique

Surface waves, when used to estimate shear-wave velocity, provide a relatively rapid and straightforward method of detecting changes in material properties of the shallow subsurface. Interpretations of the two-dimensional shear-wave velocity field derived from inversion of the surface-wave dispersion curve do not possess the resolution routinely observed in shallow seismic reflection sections (e.g., Baker et al., 1999). However, the shear-wave velocity field derived from surface waves is quite sensitive to even small changes in shear-wave velocity. In this setting, it is reasonable to expect most voids, caverns, or collapse features to be defined by discernible changes in shear-wave velocity compared to intact rock.

A swarm of sinkholes in AURC, less than 8 km from

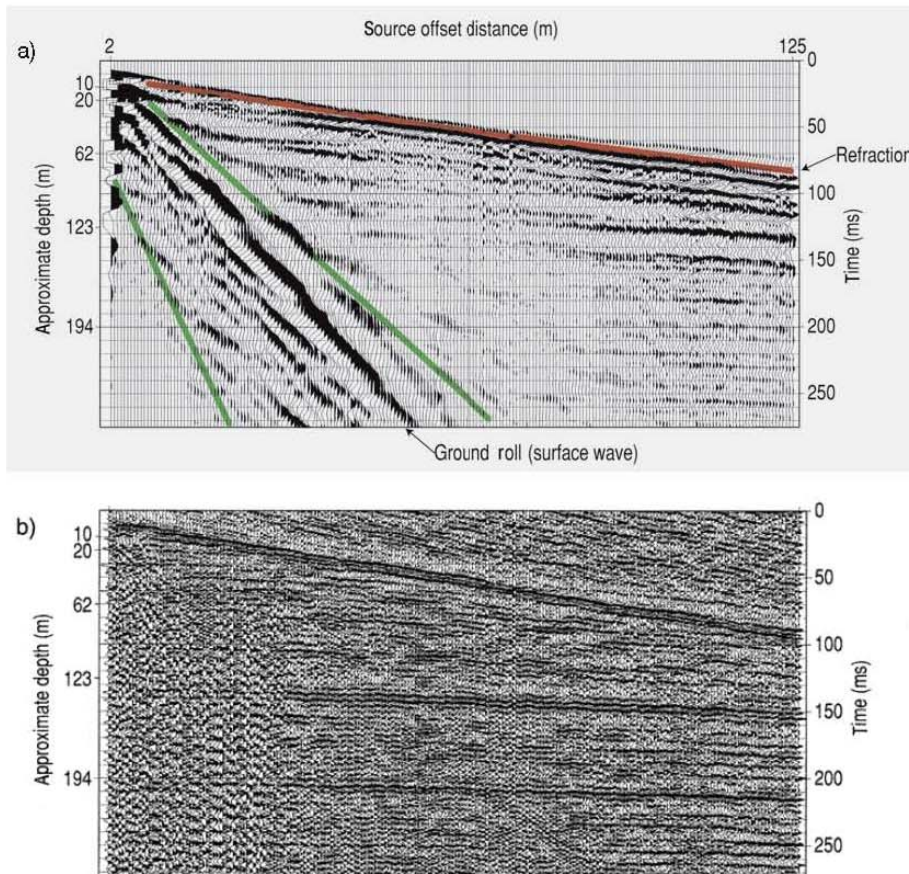
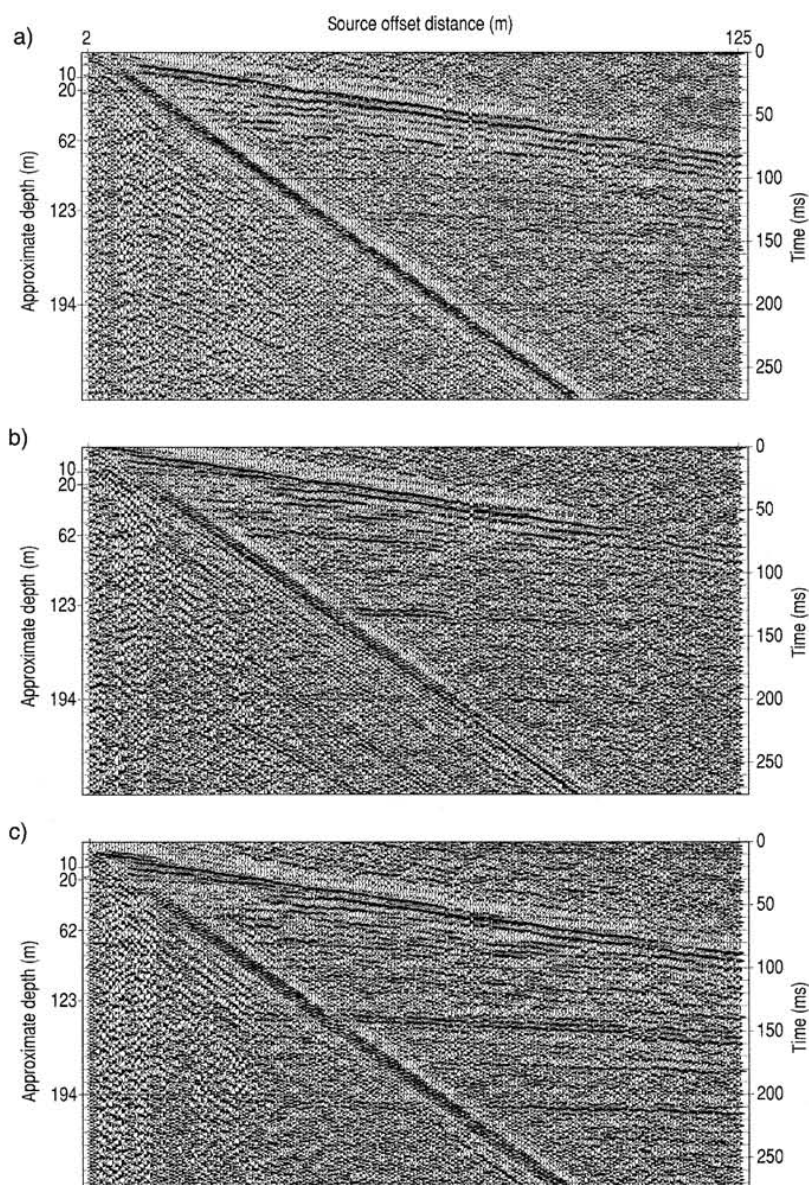


Figure 4. Raw shot gathers (a) have a strong ground roll component, complemented by high-amplitude refractions and associated guided waves. Reflection arrivals as shallow as 20 ms and covered by ground roll are easily interpretable on the spectral balanced downhole 50-cal. data (b).

PPDA, provided an ideal setting to study and characterize the seismic properties of presubsidence earth (Figure 1). A short spread acquired south of boring 3 (T2) at PPDA established the dispersive properties of the near-surface material and helped select optimum source offsets and receiver spacing (Figure 6). A second profile acquired using continuous acquisition methods in the AURC allowed examination of subsurface character beneath a well-defined sinkhole swarm (Figure 7). Tests designed to identify seismic signatures of developing sinkholes targeted areas alongside obvious sinkholes with no apparent surface expression.

Establishing a karst seismic template that allows areas with subsidence potential to be distinguished from natural or undisturbed areas on seismic sections was an important component of the feasibility phase. A tight cluster of sinkholes in the AURC aligned generally along an east-west trend provided optimum density and distribution to test the capability of this method to identify subsidence prone areas. Since drilling in the national forest was prohibited, a survey line was located so that half was on solid ground away from a cluster of sinkholes and the other half was in close proximity to a high concentration of sinkholes. For

Figure 5. An example of hole conditioning. One shot into the hole (a) produces good reflection and refraction arrivals and a strong air-coupled wave component. A second shot into the same hole (b) produces a higher signal-to-noise record. The best data recorded (c) was by the third projectile fired into the same hole.



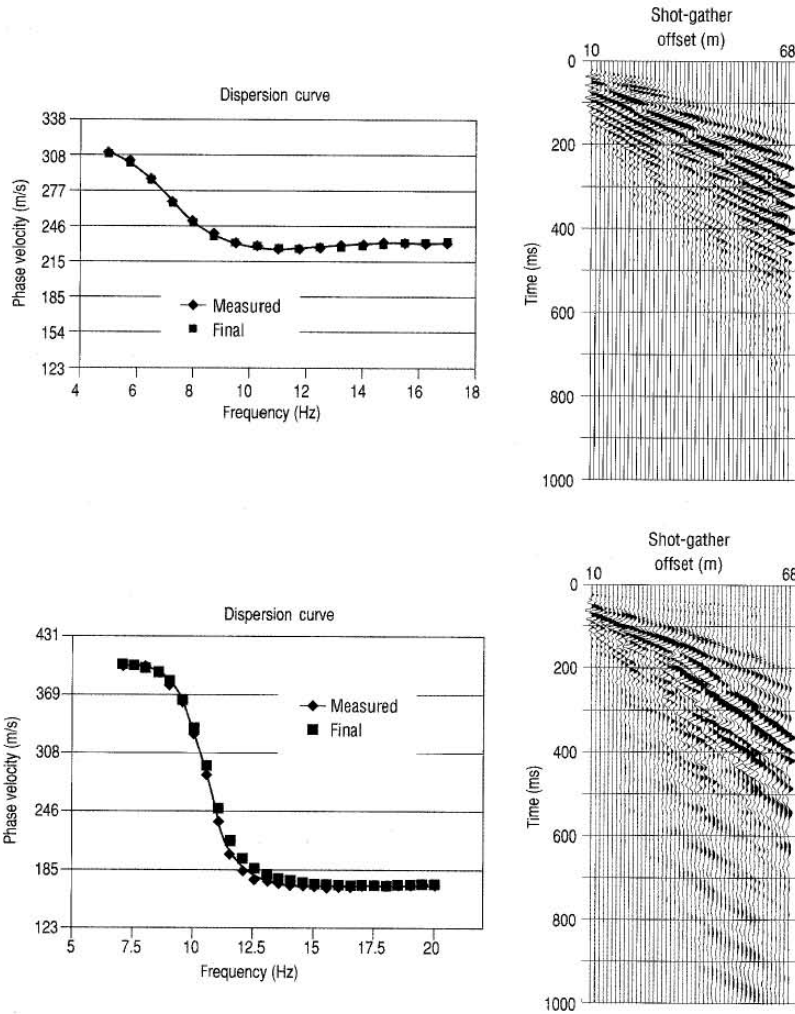


Figure 6. Data from the two sites (PPDA and AURC) have different dispersive properties, but both have very well-behaved dispersion curves consistent with model data, and depths of penetration (imageable depths) exceed 23 m.

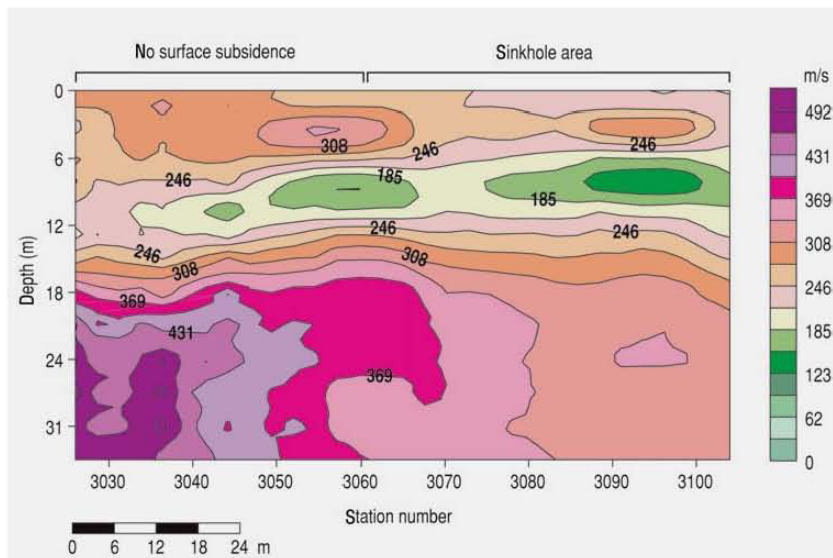


Figure 7. Shear-wave velocity field from surface inversion of data acquired from the sinkhole test. The bull's-eye characteristic of sinkholes is evident between stations 3050 and 3060 as well as between stations 3090 and 3100. Contour interval is 30 m/s.

purposes of our evaluation, receiver stations immediately adjacent to the sinkholes were considered over subsidence prone areas. Low-velocity anomalies in proximity to sinkholes were classified as diagnostic of dissolution features with subsidence potential.

Several questions concerning the processed section from AURC need to be addressed so criteria can be established for identification of sinkhole-susceptible areas (Figure 7). The most important is whether subsurface anomalies associated with sinkholes have a unique seismic expression in the shear-wave velocity field. Based on preliminary analysis of these data, subsurface anomalies associated with sinkholes seem to have a characteristic high-velocity "bull's-eye" or contour closure directly over a low-velocity "bull's-eye" or closure. This unique combination is evident between stations 3055 and 3060 as well as between 3090 and 3100. Correlation between sinkholes identified near the survey line (Figure 1) and the high-velocity over low-velocity closures on the shear-wave velocity sections (Figure 7) appears to be the unique seismic signature needed to locate subsidence prone areas with this technique.

Phase 2: Production

Acquisition

Since the grid-style drilling program at PPDA was based on proposed engineering designs in place prior to the seismic survey, to maximize control, the seismic lines were laid out in a 2D grid intersecting as many borings as possible. This deployment scheme allowed a 2.5D evaluation of the subsurface. In this context, 2.5D implies coincident interpretation of 2D profiles that tie (common station) with enough redundancy to allow contiguous interpretations between the adjoining lines and into unsampled space.

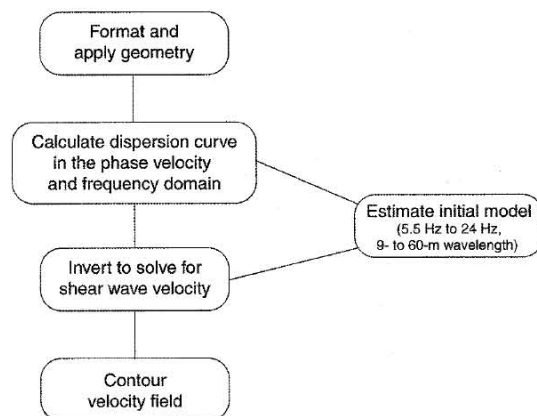
Data for the gridded 2D survey were acquired using state-of-the-art near-surface imaging equipment and techniques. A Geometrics StrataView R60 seismograph was used in a 240-channel configuration for the shallow reflection data and in a 48-channel configuration with a 240-channel roll-along switch for surface-wave data. Receivers for the shallow reflection survey were a group of three Mark Products L28E 40 Hz geophones wired in series with 14-cm spikes. For the surface-wave surveys, single Geospace GS-11D 4.5 Hz geophones with 8-cm spikes were deployed. Both surveys used receiver station spacings of 1.2 m and source station spacings of 2.4 m. Three ground impacts from a rubber-band accelerated weight drop (RAWD) were vertically stacked in the seismograph for the surface-wave profiles, while a single shot from a 50-cal. downhole rifle provided the energy for most of the shallow reflection data (both sources were developed at the Kansas Geological Survey).

Processing

Processing of these data was consistent with current methodologies and flows. Software used to process the CMP data was specially designed and written for high-resolution seismic surveys. High-resolution shallow reflection data were processed into CMP stacked sections using WinSeis, a commercially available software package. Shallow reflection data were nominal 60-fold with the actual fold ranging from 2 to over 120, depending on location of stations along profiles relative to start and end points and number of traces within the optimum offset window. Ample traces were recorded within the optimum window to capture reflections returning from depths as shallow as 12 m and as deep as 300 m. Processing the reflection data for this survey required abnormally high attention to near-surface static corrections. Variability of several milliseconds directly related to conditions at the geophone was observed between adjacent traces. Since these data possess dominant frequencies as high as 200 Hz in some locations, less than 3 ms of mismatch between traces within a CMP would result in cancellation of reflected wavelets.

Surface-wave data processing involved fewer individual steps and about one-fifth as many traces as the reflection data (Table 1). Shear-wave velocity field cross sections were produced using SurfSeis, a commercially available software package. Processing surface-wave data involves transformation of the surface wave from a time-distance format on shot gathers into a frequency-phase velocity domain curve (dispersion curve) followed by inversion to a shear-wave velocity trace (shear-wave velocity as a function of depth). Each shot gather produces a unique 1D velocity function or trace, so by moving the source and receiver spread incrementally along each profile line, a single trace was produced for each unique spread and separated by the

Table 1. Surface-wave processing flow.



source interval (2.5 m). A 2D contour map of the velocity field as a function of station location and depth was generated for each profile line.

Interpretation

Reflection data from this survey possess excellent resolution potential and very high signal-to-noise ratio to depths in excess of 300 m. Several high-quality reflection events are evident sitewide in the upper 90 m. Time to depth conversions were made based on stacking velocities that ranged from around 1250 m/s at around 25 ms to 2000 m/s at 300 ms. These velocities are consistent with the VSP collected at a boring near the center of the site and were used for estimating reflector depths.

Reflection events as shallow as 25 ms (~12 m) are interpretable at various locations across the site. The 100-ms reflection (~90 m) is a sitewide marker bed that provides a reference for structures interpreted in the shallow portion of the sections. Based on drill data, this reflection is significantly below the basal contact of the Yazoo Shale at about 50 m. Assuming this high amplitude, continuous (at least within the survey area) reflection at 100 ms is below the competent and regionally flat Ocala Limestone, shallower structures related to dissolution or erosion can be confidently separated from static that is the result of the highly altered near surface.

Several distinctive features on the shear-wave velocity cross sections are indicative of a karst setting and consistent with the fracture and loss circulation zones noted on drill logs. A high shear-wave velocity gradient observable sitewide between 6 and 12 m BGS at velocities around 250 m/s appears to be generally consistent with the depth of bedrock on boring logs (Figure 3). A very rapid and relatively uniform transition between about 225 m/s and 300 m/s is consistent with expectations of changes from

unconsolidated to consolidated sediments and borehole shear-wave velocity measurements.

Considering the length of the receiver spread, used to calculate the dispersion curve, shallower anomalies will appear more diffuse in the shear-wave velocity domain than in a geologic cross section. In general, within zones of anomalous bedrock, dissolution features will likely be elongated downward and away from the source laterally. This elongation artifact, inherent to the propagation of surface waves, will impact how well each line ties in the presence of anomalies, the resolvability of particular anomalies, and the estimation of the velocity change with the anomaly. Velocity changes associated with anomalies can be interpreted confidently if the spread length is tuned for the depth and length of the anomaly. Physical and digital model analysis beyond the scope of this study is necessary to quantify the resolution and smearing characteristics of this new imaging method.

Line 1

Reflection

Flat reflections below about 100 ms on the CMP stacked section of line 1 provide a reference for interpreting the structural variations evident in the shallow portion of the section (Figure 8). Probably the most striking feature on line 1 is the paleostructure centered around station 1390 (Figure 9). This bowl-shaped depression in reflections shallower than 70 m is striking evidence supporting suggestions that subsidence has been active in this area for a significant portion of the past. The lack of discernible flat-lying undisturbed reflection events above this paleosinkhole prohibits estimation of subsidence rates, length of activity, or even when subsidence ended. With no current surface expression, it is reasonable to suggest the dissolution process responsible for this paleosinkhole is currently inactive.

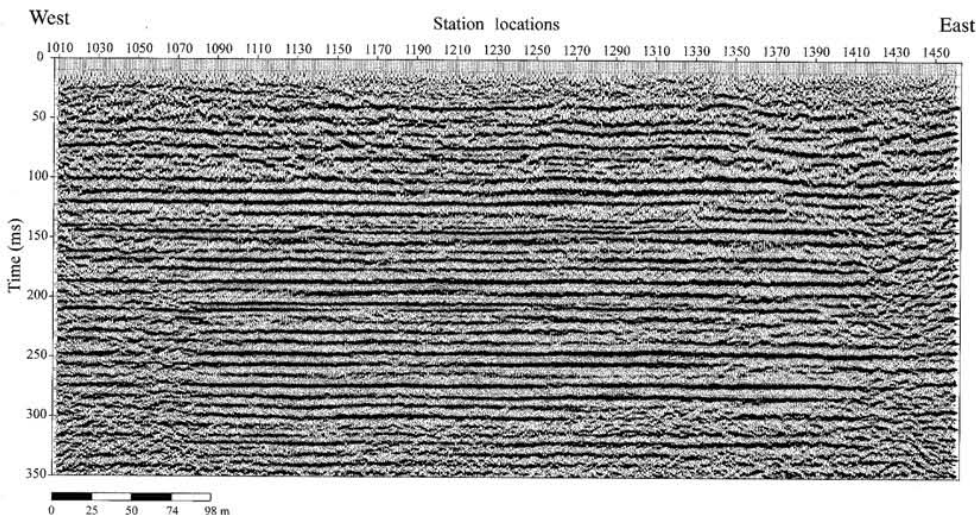
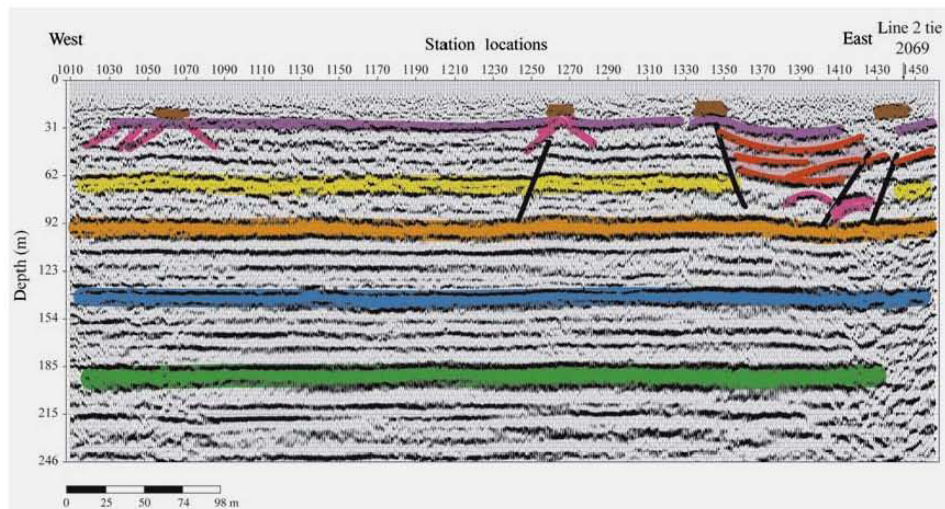


Figure 8. CMP stacked section of line 1.

Figure 9. Interpreted line 1 time-to-depth converted using NMO velocity calculated during reflection data processing.



The relative locations and orientations of the various coherent reflection events within the depression at station 1390 suggest this sinkhole has undergone several distinguishable periods of activity (dissolution, subsidence, and sedimentation). Even though subsidence rates cannot be estimated with these seismic data, it is possible to approximate the size and geometry of this depression when it was visible at the ground surface. Based on seismic stacking velocities and unmigrated sections, it is reasonable to suggest this sinkhole encompasses a total of 20 to 25 m of subsidence since it first formed. Interpretations using this line alone suggest this feature was about 60 m across and 15 m deep prior to the last episode of sedimentation. Even with indications that this feature is presently dormant, the several periods of dissolution, subsidence, dormancy, and reactivation it has previously experienced makes it a threat that cannot be fully dismissed.

Disturbed, chaotic-looking reflection events between stations 1115 and 1190 within the 40 to 80 ms (25 to 60 m) time window could be indicative of karst deeper than currently a concern for the stability of surface installations. Between station 1130 and about station 1240 the shallowest reflector (9 to 12 m) appears to be either missing or extremely disturbed. This may suggest the dissolution processes responsible for the paleosinkhole beneath station 1390 is or has been active along various portions of this profile.

Several small diffraction events are interpreted on stacked sections. Diffractions are key indicators of point source features, generally related to bed terminations, extreme geometries (tight syncline), small independent offset blocks, fracture zones, etc. The apexes of the diffraction events interpreted on this line are at stations 1060, 1265, and 1390. The 1060 event has characteristics consistent with a shallow dissolution feature. Based on offsets in reflections mapped (black) as deep as 90 m beneath station 1265, it is reasonable to suggest that faulting might be

responsible for the diffraction arrival at 1265 (Figure 9). The abrupt termination at 90 m BGS in the apparent bed offset of this fault could indicate the base of the dissolution feature is at the 90-m reflector or it could be an artifact of insufficient resolution. Reflections below 60 m have not been drilled and are therefore interpreted based on coherency and amplitude.

Surface wave

The 2D shear-wave velocity field maps (Figures 10, 13, and 16) were produced independent of supporting information (drill data, reflection results, etc.). This was intentionally done to avoid biasing the processing parameters or flows. Several distinct features are interpreted to be localized zones of very disturbed materials at or just below the bedrock surface along line 1 (Figure 10). A lower velocity anomaly between station 1030 and about station 1080 within a depth range of 12 to about 30 m is consistent with rock retrieved from boreholes. This anomaly, represented by the 10 to 20% drop in shear-wave velocity relative to other depth-equivalent rocks is likely (20-25% or more) smaller than suggested by these data, due to the elongation characteristic of this technique. A fracture system or void area is likely present in bedrock beneath surface stations 1040 to 1060 as evidenced by the pull-down in the 369 m/s contour near station 1050. This feature is probably less than 12 m across (~.25 spread length) and extends from the surface of bedrock down to around 25 m BGS.

It is not possible to accurately define the dimensions of a deep (relative to survey limits) and broad subbedrock low-velocity zone centered about station 1270 considering the resolution limits of these data. From shear-wave velocity alone, the material between the top of bedrock (at about 6 m) and 30 to 32 m beneath stations 1280 to 1290 possesses less strength (decreased stiffness, reduced blow counts, etc.) than the more native and competent materials beneath station 1130, for example. Logs from boring 4,

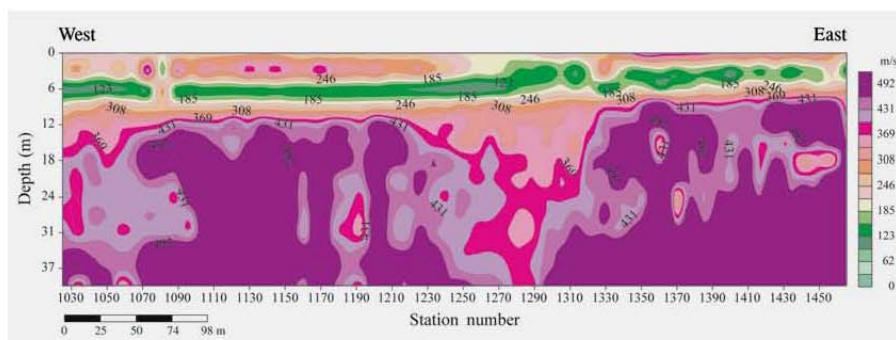


Figure 10. Shear-wave velocity contours along line 1. Contour interval is 30 m/s.

located near station 1300, are very consistent with the general appearance of the shear-wave velocity cross section in that area.

The paleosinkhole interpreted on the stacked reflection section (Figure 9) can only be inferred on the shear-wave velocity profile (Figure 10). This lack of a clear expression suggests subsidence artifacts that define the paleosinkhole were in place and well compacted prior to the deposition of the unconsolidated sediments that overlie bedrock. It is likely subsidence features such as those observed on CMP stacked sections may be imageable using surface-wave inversion techniques during or shortly after the conclusion of the dissolution, subsidence, and deposition process.

A paleosinkhole interpreted beneath station 1390 on reflection data may manifest itself as the sparsely distributed lower velocity anomalies near the east end of line 1 (Figure 10). Features possibly correlating to the paleosinkhole are beneath station 1360 at 16 m, station 1370 at 22 m, and station 1440 at 17 m. These three anomalies have the characteristic shape of the paleosinkhole observed on reflection data. An alternate or compounding reason for the lack of similarity between the two data sets is the depth of features each is tuned to image.

Line 2

Reflection

Stacked data from line 2 (Figure 11) have captured the same paleostructure interpreted on line 1 (Figure 8). Line 2 intersects line 1 orthogonally at around station 2070. Subsidence structures interpreted on line 2 correlate with line 1 from about station 2030 to station 2130 (a distance of about 120 m) (Figure 12). The deepest single subsidence event produced about 12 to 15 m of drop in reflectors defining the base of the sinkhole. Two high-amplitude reflections interpretable within the paleosinkhole possess distinctly different attributes compared to surrounding "native" reflections (inside the structure the reflections are of higher amplitude and lower frequency). These reflections from inside the structure are obviously a different age and/or lithology than those outside the paleostructure.

This paleosinkhole or, more generically, synform has a remarkable similarity to cut-and-fill channel features observed on seismic data in Miocene sediments along the Atlantic Coastal Plain (Miller et al., 1999). Considering no pull-down is observed in deeper reflections, the synform is not completely consistent with modeled seismic signatures of sinkholes (Anderson et al., 1995), therefore making channels a real possibility. Based on lines 1 and 2, the synform is 60 by 120 m, elongated along its north-south axis, and has had a total of around 22 m of subsidence, likely occurring during at least two different episodes.

A feature with apparent active dissolution and associated subsidence potential is located beneath station 2235. Offset in otherwise coherent events can be interpreted down to around 120 m BGS. This feature is about 15 to 18 m wide and does not seem to extend through the entire imaged section, and therefore is likely related to a fracture zone and/or dissolution. Events from within this zone possess distinctively different seismic characteristics in comparison to surrounding rock layers. This chaotic zone could be the image of a dissolution void and therefore should be considered an area of questionable stability. Diffraction-looking events indicative of termination points are evident within this zone characterized by chaotic reflection coherency, curved reflection geometries, and abrupt changes in wavelet characteristics.

A monocline observed between stations 2290 and 2350 has all the classic characteristics of a 50 m wide normal fault zone (Figure 12). Analysis of these data did not uncover sufficient evidence to confidently interpret this feature. The lack of interpretable faulting on other lines in proximity raises the biggest concerns. The geometry of this monocline, its lack of vertical uniformity, and the flat 30-m-deep reflection that overlies this feature support its being a real structure and not a static artifact. However, without some suggestion of three-dimensionality a confident fault interpretation is not possible.

Reflections from within the upper 50 m near the intersection with line 3, on the south end of this line, possess geometries and diffractions consistent with the paleosinkhole/paleochannel on the opposite end of the profile at 2070. Draping of the shallow reflections and the apparent

Figure 11. CMP stacked section of line 2.

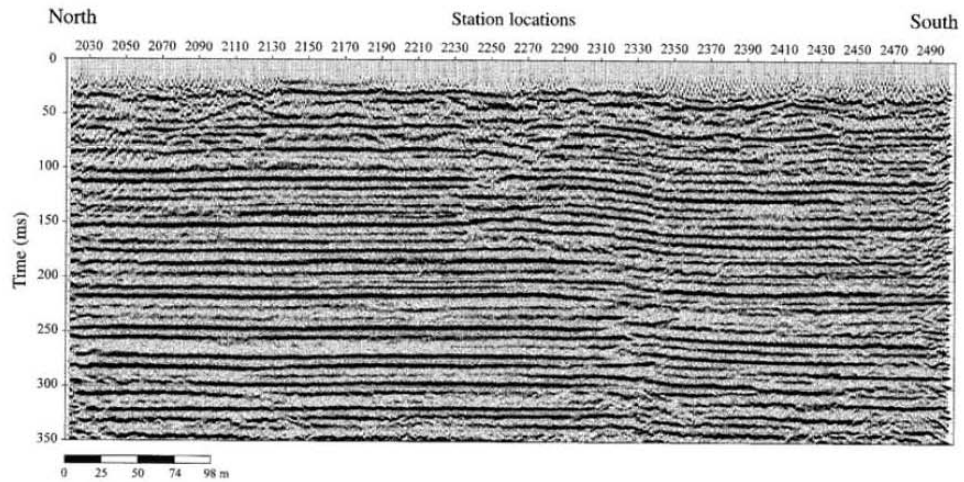
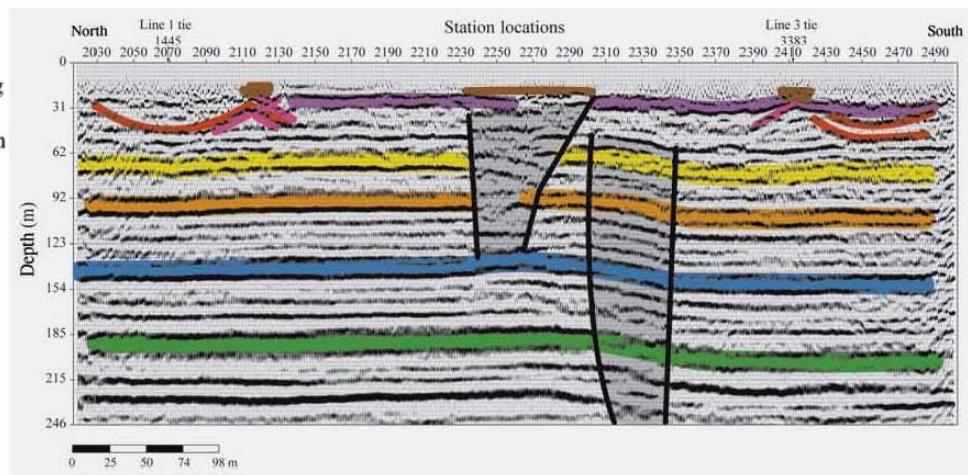


Figure 12. Interpreted line 2 time-to-depth converted using NMO velocity calculated during reflection data processing.



diffraction centered on station 2415 mirror characteristics of the 2070 paleosinkhole/paleochannel. Any abnormality in the lateral continuity of reflections defining the synform justifies subsidence concerns. The highly disturbed zone observed beneath station 2270 also warrants concern. Diffractions and disturbed bedding can be indicative of voids and fractures in otherwise competent rock, such as that observed in drill data from borings 1, 3, and 4. The combination of these void or rubble areas, identified on borings with the apparent bridging of the 30 m reflection over this disturbed area, represents a risk to surface structures.

Noteworthy features on line 2 include the channel or diffraction apex beneath station 2130, the paleochannel/sinkhole under stations 2070 and 2455, disturbed reflections between 2230 and 2270, and the monocline at 2330. All these reflections have geometries that can be explained by either high energy erosion and deposition and/or disso-

lution, subsidence, and sedimentation. If dissolution and subsidence produced these geometrically extreme features, it is reasonable to suggest some settling due to compaction should be expected over time above these irregularities.

Surface wave

A very thin layer of higher velocity material and extremely disturbed subbedrock materials are evident on the northern end of the line (Figure 13). From about station 2260 south, the material in the upper 3 m possesses higher shear-wave velocities in comparison to the northern portion of line 2 and most of line 1. Associated with this change in near-surface shear-wave velocity is a stunning change in the uniformity of the rock below 6 m (interpreted bedrock).

Bedrock appears to be extremely altered at the northern end of this line (Figure 13). This very erratic appear-

ance of the velocity structure in the first 18 m below bedrock is consistent with drill cuttings from borings 1, 3, and 4. Bedrock lows interpreted at stations 2050 and 2090 are consistent with the subsidence feature interpreted on reflection data (Figure 12). The drape observed in the bedrock is slightly less than that evident in the deeper beds imaged on reflection data, but the lateral extent and general shape of the subsidence/channel features match well.

Disturbed bedrock between stations 2150 and 2250 is beneath a marshy low area on the ground surface. Anomalous bedrock material defined by the lower shear-wave velocities beneath stations 2150 to 2250 is within one of the few parts of the line 2 seismic reflection section that can be classified as *undisturbed*. Only one of the two paleo-features interpreted on the reflection profiles is apparent on the shear-wave velocity data. Markedly higher velocity shear-wave values above 3 m at the south end of the profile are consistent with drillers' observations of noticeable increases in drill bit pressure and difficulty drilling in the

upper 3-5 m on both deep borings and seismic shot holes. From station 2250 south, bedrock appears very uniform, with no indication of anomalous velocity materials below the bedrock surface.

Line 3

Reflection

Excellent reflection arrivals are evident between about 40 and 300 ms along line 3 (Figure 14). The general character of reflections across this profile is very similar to that observed on other seismic lines from PPDA. The most obvious and largest noteworthy feature on line 3 is the paleo-sinkhole/channel on the eastern half of the survey line (Figure 15). Reflection arrival geometries at depths less than 50 ms (35 m) on the eastern end of the line appear to have imaged reflectors sculpted during several periods of subsidence and deposition and/or cut and fill. Coherent events on the western portion of the profile have some

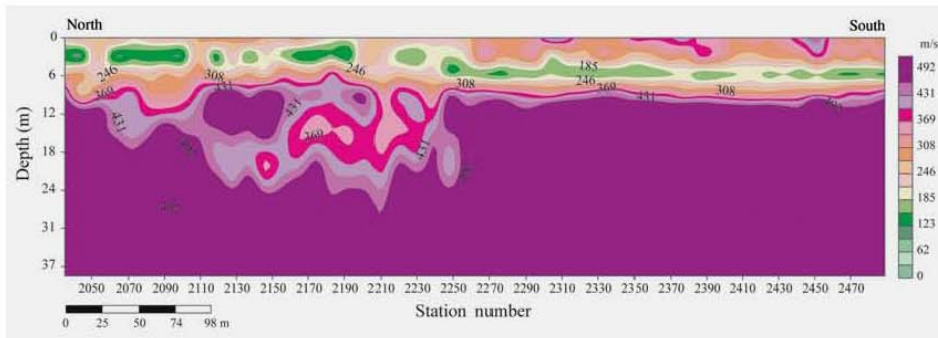


Figure 13. Shear-wave velocity contours along line 2. Contour interval is 30 m/s.

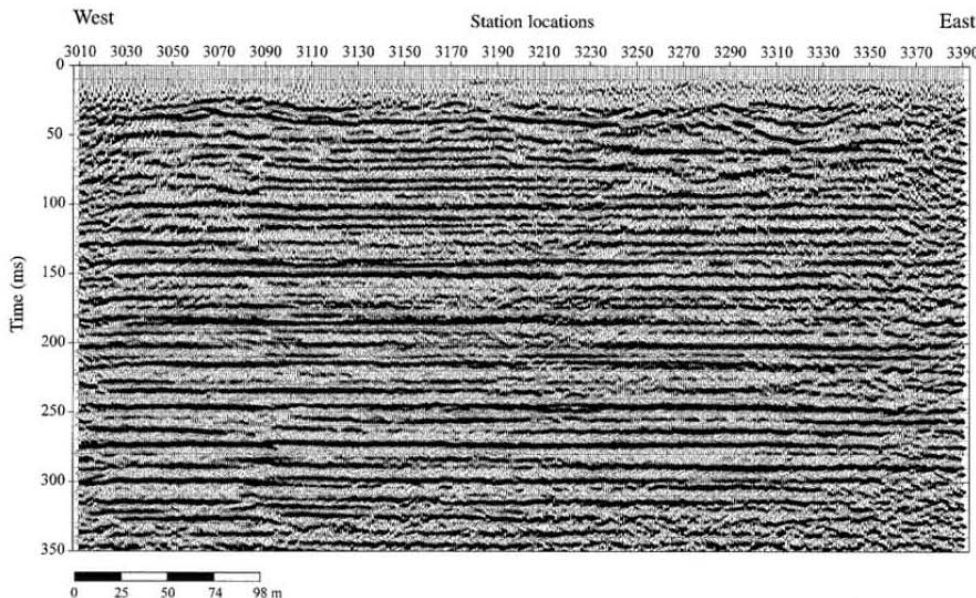


Figure 14. CMP stacked section of line 3.

subtle characteristics suggestive of erosion and deposition. Reflections arriving below 35 m are relatively flat without variations that might suggest reduced rock strengths or a risk of subsidence.

Reflection arrivals between stations 3190 and around 3400 and down to about 100 ms (90 m) possess geometries and attributes expected from an area that has experienced several episodes of dissolution, subsidence, and sedimentation over hundreds of thousands of years. Wavelet characteristics, reflection geometries, and apparent depth of this paleosinkhole are consistent with the properties and characteristics of this same paleosinkhole imaged on line 2. Consistent with the interpretation on the northeastern end of lines 1 and 2, there appears to have been at least two unique periods of subsidence as defined by the two lower frequency, higher amplitude events. Reactivation of dissolution and/or subsidence in this area has resulted in a secondary sinkhole 5 m deep and about 75 m wide centered on station 3320. This shallower and small-

er sinkhole area appears to be capped by a flat reflection indicative of a period without subsidence. At its maximum, the original sinkhole spanned more than 250 m and was around 15 m deep along the trace of this profile. There does not appear to have been any subsidence within this complex of paleosinkholes since the deposition of the unconsolidated sediments above the current bedrock surface.

A small disturbed zone centered on station 3070 (Figure 15) resembles the disturbed zone identified beneath station 2250 on the line 2 reflection section (Figure 12). As with the one on line 2, this zone is characterized by a drop in reflection coherency and increase in the amplitude of coherent lower frequency events. Common to both these areas are marshy surface conditions and similar descriptions in geologist logs of nearby borings. It is reasonable to suggest this area (3070) and the area surrounding station 2250 on line 2 are experiencing minor subsidence related to dissolution within a localized fracture system.

Figure 15. Interpreted line 3 time-to-depth converted using NMO velocity calculated during reflection data processing.

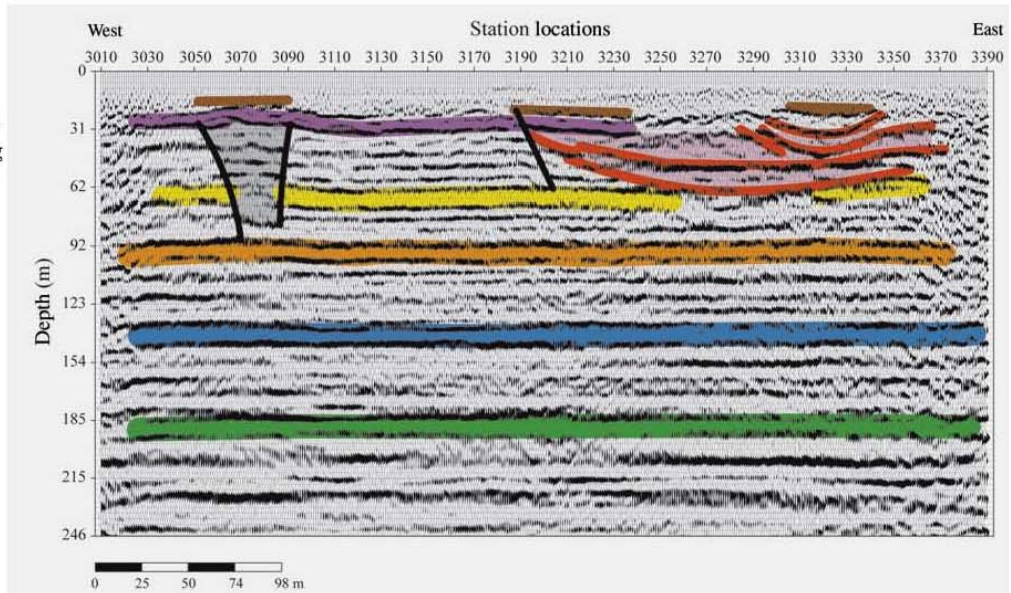
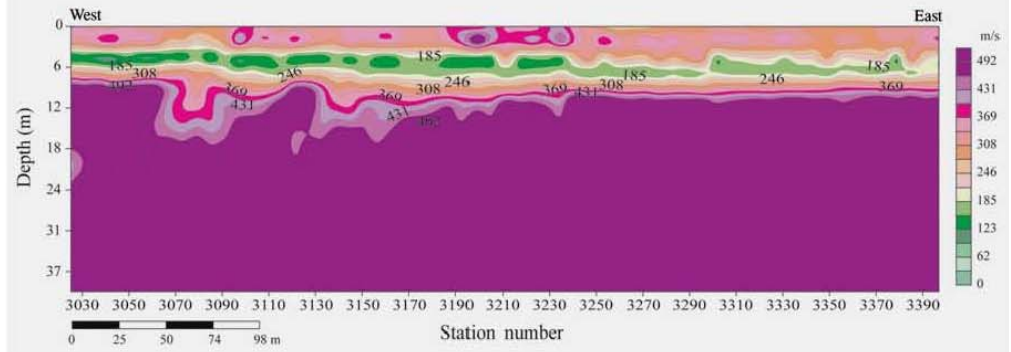


Figure 16. Shear-wave velocity contours along line 3. Contour wave is 30 m/s.



Surface wave

Shear-wave velocity data along line 3 portray a relatively undisturbed bedrock east of station 3230 (Figure 16). This observation is consistent with the interpretation of line 2 (Figure 13), which intersects line 3 near its eastern end. Most of the obviously altered layers at and below bedrock are located between stations 3060 and 3230. These disturbed features have a more subdued shape consistent with the edges of the deeper, more pronounced velocity lows on line 1 (Figure 10). Considering the local geology and drill data, it is reasonable to suggest that these lower velocity zones within bedrock are related to fractures and/or dissolution activities.

With the uniformity of the clay unit consistently encountered in boreholes above the bedrock surface, it is unlikely these low-velocity anomalies in rock are the result of infilling by clays and sandy clays originally deposited above bedrock. Considering that no draping/subsidence can be seen in layers above 6 m, it is reasonable to suggest that these subbedrock features are older and were, for the most part, in place prior to deposition of the river terrace deposits above bedrock. Low shear-wave velocity areas based on drilling are likely partially filled with rubble remnants of the bedrock scattered within a clay and sandy clay fill (possibly described as shale on geologist boring logs). In this setting, there will likely be small void or collapse areas present within this unconsolidated sediment fill. These lower shear-wave velocity patterns are likely karst and are, therefore, zones of inherent weakness in the limestone below the top of bedrock, preferentially oriented along highly variable and localized pre-existing fracture systems.

Discussion

Clearly, in various places around this site the entire depth interval from bedrock at about 6 m to the top of the flat-lying undisturbed rock layers at about 90 m has been affected by dissolution and/or erosion that has been active over a long period of time. There have been several times in the past when significant erosional and depositional forces had been at work here.

The ramifications of the noted and more pronounced anomalies need to be evaluated more with considerations made during the engineering of a surface facility (Figure 17). Trying to correlate paleosinkholes, chaotic zones, cut-and-fill channels, and disturbed areas line to line using reflection geometry, wavelet characteristics, drill logs, and shear-wave velocity gradients demonstrates the extremely variable nature of near-surface anomalies and their very localized uniqueness across this site. The seismic lines correlated quite well at their intersections or tie points. However, matching specific features from line to line across portions of the site without seismic coverage was specula-

tive in many cases. This lack of more large-scale structures is probably due to the unique and localized nature of each dissolution-induced geometry. If faulting or regional fracture systems had been responsible for or controlled the formation of these features, correlating between lines would have been possible using a simple linear relationship. Reflection events below 90 m appeared coherent and uniform, with the exception of the single monocline observed on line 2.

Some of the more extreme geometries interpreted as synforms could be paleosinkholes resulting from subsidence over karst features, or they could be associated with stream/river erosion. Synforms interpreted on data from this site have similar geometry and dimensions as both paleochannels routinely observed on seismic data in Miocene sediments along the Atlantic Coastal Plain (Miller et al., 1999) and paleosinkholes resulting from dissolution of the thick bedded Permian salts of Central Kansas (Miller and Xia, 2002). If these features are cut-and-fill channels rather than dissolution-related, their significance as a subsidence risk or fluid pathway is greatly reduced.

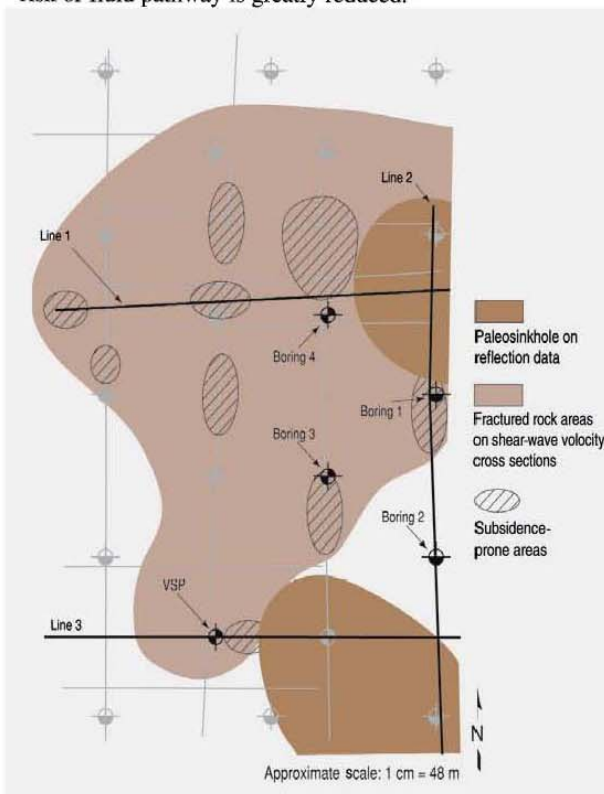


Figure 17. Paleosinkholes, fractured/karst rock, and subsidence-prone areas interpreted from seismic data. Lines are located on this diagram in approximate relative locations across this roughly 40-acre tract of land, with notable features interpreted.

Surface-wave data (shear-wave velocity profiles) in general appear more disturbed in the north and west relative to the south and east. Using the deeper, more substantial shear-wave velocity anomalies as indicators of major breaches in the confining characteristics and rigidity of the bedrock materials, the northern half of the site becomes an immediate area of concern. Most swamp and marshy areas on the ground surface seem correlated with the more dramatic anomalies in the shear-wave velocity field, suggesting some common link. Several isolated features are evident where competent bedrock has clearly deteriorated, leaving a zone of chaotic shear-wave velocities. Paleosinkholes, as interpreted on reflection sections, were not clearly evident on shear-wave velocity profiles.

Comparing and contrasting the features interpreted on the two data sets provides a picture of the subsurface indicative of a history of karst, karst-related instability, and/or cut-and-fill processes. These data highlight areas with reduced bedrock competence. Clearly, reflection sections provide a glimpse of an older segment of the earth. Reflection sections are key indicators that the ground in this area has been unstable for hundreds of thousands of years. Surface-wave data which produced the shear-wave velocity profiles targeted the more recent dissolution/erosion and deposition and their detrimental effects on the stiffness of rock from bedrock down to about 20 m.

The nonuniqueness of units, intervals, and anomalies identified on boring logs from this site inhibited well-to-well correlations. After studying the seismic data, this observation is not surprising considering the vast number of relatively small anomalies, all similar in nature but each with unique characteristics. When both shallow (surface wave) and deep (reflection) images possess disturbed or laterally inconsistent zones, changes in the surface expression should be considered possible within a short window of geologic time. Future subsidence potential is greatest in areas with both near-surface expression and deeply disturbed rock layers.

Looking at areas on both reflection and surface-wave data with the greatest risk of future subsidence, a few locations appear most susceptible to ground movement (Figure 17). The edges of paleosinkholes interpreted on these reflection data are consistent with the edges of subbedrock disturbed zones interpreted on surface-wave data. Overlap of these anomalies is generally consistent with surface features such as ponds, wet holes, and swampy areas. These overlapping features appear to be most active at their edges.

Conclusions

Shallow seismic reflection and surface-wave profiling improved the understanding and interpretations of the grid drilling program. Subsurface features large enough to produce sinkholes capable of damaging surface facilities

based on engineering designs were located with this survey. A unique velocity signature interpreted on shear-wave velocity field data was indirectly (in proximity of recently developed sinkholes) correlated to the dissolution (active or dormant) of limestone. Reflection imaging successfully detected reflectors from 15 m to over 200 m deep while surface-wave imaging provided a glimpse of the first 30 m of the earth. Boring logs show a reasonably consistent bedrock surface, however below bedrock no two logs have descriptions that permit the matching of individual units or markers. Seismic data provided cross sections explaining this lack of well-to-well consistency and a picture of dissolution, cut-and-fill erosion, subsidence, and sedimentation prevalent across this very complex site.

Acknowledgments

Invaluable field and technical support for this study were provided by Bill Shefchik and Laura Moore from Burns & McDonnell; we greatly appreciate their efforts. The authors would like to thank David Laflen and Chad Gratton of the Kansas Geological Survey and Danny Morgan and Oui Sheldon from Burns & McDonnell for their assistance during acquisition of this data. Assistance from Mary Brohammer in manuscript and graphic preparation is also greatly appreciated.

References

- Anderson, N. L., W. L. Watney, P. A. Macfarlane, and R. W. Knapp, 1995, Seismic signature of the Hutchinson Salt and associated dissolution features: *Kansas Geological Survey Bulletin* 237, 57–65.
- Baker, G. S., C. Schmeissner, and D. W. Steeples, 1999, Seismic reflections from depths of less than two meters: *Geophysical Research Letters*, **26**, 279–282.
- Brühl, M., G. J. O. Vermeer, and M. Kiehn, 1996, Fresnel zones for broadband data: *Geophysics*, **61**, 600–604.
- Gochioco, L. M., 1992, Modeling studies of interference reflections in thin-layered media bounded by coal seams: *Geophysics*, **57**, 1209–1216.
- Hunter, J. A., et al., 1984, Shallow seismic-reflection mapping of the overburden-bedrock interface with the engineering seismograph—Some simple techniques: *Geophysics*, **49**, 1381–1385.
- Miller, R. D., N. L. Anderson, H. R. Feldman, and E. K. Franseen, 1995, Vertical resolution of a seismic survey in stratigraphic sequences less than 100 m deep in southeastern Kansas: *Geophysics*, **60**, 423–430.
- Miller, R. D., S. E. Pullan, J. S. Waldner, and F. P. Haeni, 1986, Field comparison of shallow seismic sources: *Geophysics*, **51**, 2067–2092.
- Miller, R. D., and J. Xia, 1999, Feasibility of seismic techniques to delineate dissolution features in the upper

- 600 ft at Alabama Electric Cooperative's proposed Damascus site: Kansas Geological Survey Open-file Report 99-3.
- 2002, High-resolution seismic reflection investigation of a subsidence feature on US highway 50 near Hutchinson, Kansas: Presented at the Symposium on the Application of Geophysics to Engineering and Environmental Problems, (SAGEEP), Paper 13CAV6, published on CD.
- Miller, R. D., J. Xia, C. B. Park, and J. M. Ivanov, 1999, Multichannel analysis of surface waves to map bedrock: *The Leading Edge*, **18**, 1392–1396.
- Nazarian, S., K. H. Stokoe II, and W. R. Hudson, 1983, Use of spectral analysis of surface waves method for determination of moduli and thicknesses of pavement systems: *Transportation Research Record No. 930*, 38–45.
- Park, C. B., R. D. Miller, and J. Xia, 1999, Multichannel analysis of surface waves: *Geophysics*, **64**, 800–808.
- Sheriff, R. E., 1988, *Encyclopedic dictionary of exploration geophysics*: SEG.
- Steeple, D. W., R. D. Miller, and R. W. Knapp, 1987, Downhole .50-caliber rifle—An advance in high-resolution seismic sources: Presented at the 57th Annual International Meeting, SEG, Expanded Abstracts, 76–78.
- Steeple, D. W., and R. D. Miller, 1990, Seismic-reflection methods applied to engineering, environmental, and groundwater problems, *in* S. H. Ward, ed., *Geotechnical and Environmental Geophysics*, v. 1: Review and Tutorial: SEG, Investigations in Geophysics No. 5, 1–30.
- Stokoe, K. H., II, S. G. Wright, J. A. Bay, and J. M. Roësset, 1994, Characterization of geotechnical sites by SASW method, *in* R. D. Woods, ed., *ISSMFE Technical Committee*, **10**, Oxford Publishers.
- Xia, J., R. D. Miller, and C. B. Park, 1999, Estimation of near-surface shear-wave velocity by inversion of Rayleigh waves: *Geophysics*, **64**, 691–700.
- Xia, J., et al., 2000, Comparing shear-wave velocity profiles from MASW with borehole measurements in unconsolidated sediments, Fraser River Delta, B.C., Canada: *Journal of Environmental and Engineering Geophysics*, **5**, no. 3, 1–13.

Miller, R.D., 2006, High-resolution seismic reflection to identify areas with subsidence potential beneath U.S. 50 Highway in eastern Reno County, Kansas: Symposium on the Application of Geophysics to Engineering and Environmental Problems (SAGEEP 2006), Seattle, Washington, April 2-6, Paper 28, 13 p. **Awarded Best of SAGEEP 2006; presented as an invited paper at EAGE NS in Helsinki, Finland, June 2006.**

HIGH-RESOLUTION SEISMIC REFLECTION TO IDENTIFY AREAS WITH SUBSIDENCE POTENTIAL BENEATH U.S. 50 HIGHWAY IN EASTERN RENO COUNTY, KANSAS

Richard D. Miller, Kansas Geological Survey, Lawrence, KS

Abstract

High-resolution seismic reflections were used to map the upper 200 m along an approximately 22 km stretch of U.S. 50 highway in Reno County, Kansas, where natural and anthropogenic salt dissolution is known to threaten ground stability. Surface subsidence in this part of Kansas can range from gradual (an inch per year) to catastrophic (tens of feet per second), representing a significant risk to public safety. Primary objectives of this study were to delineate the Permian Hutchinson Salt layer beneath the proposed alignment of the new U.S. 50 bypass around the City of Hutchinson. Of secondary interest were any features with subsidence potential beneath U.S. 50 east of the City of Hutchinson in Reno County, a distance of around 15 km crossing the dissolution front of the salt beds. The high signal-to-noise ratio and resolution of these seismic reflection data allowed detection, delineation, and evaluation of several abnormalities in the rock salt layer and overlying Permian sediments. Locations were identified where failure and associated episodes of material collapse into voids left after periodic and localized leaching of the 125 m deep, 40 m thick Permian Hutchinson Salt member were evident. Anomalies were identified within the salt and overlying rock layers with seismic characteristics consistent with collapse structures. Of particular interest were features with the potential to migrate to the surface in areas where no subsidence has been previously observed. Anhydrite and shale layers several meters thick within the salt are uniquely distinguishable and appear continuous for distances of several kilometers. High noise levels from the heavy traffic load carried on U.S. 50 and maintaining continuous subsurface coverage beneath the Arkansas River presented significant challenges to both the acquisition and processing of these data. Over a dozen unique features potentially related to subsidence risk were identified.

Introduction

Sinkholes are common hazards to property and human safety the world over (Beck et al., 1999). Their formation is generally associated with subsurface subsidence that occurs when overburden loads exceed the strength of the roof rock bridging voids or rubble zones formed as a result of dissolution or mining. Understanding sinkhole processes and what controls their formation rate is key to reducing their impact on human activities, and in the case of anthropogenic, potentially avoiding their formation altogether. Sinkholes can form naturally or anthropogenically from the dissolution of limestone (karst), gypsum, or rock salt, or from mine/tunnel collapse. With the worldwide abundance of limestone, karst-related sinkholes are by far the most commonly encountered and studied. Both simple and complex sinkholes have formed catastrophically and/or gradually, as the result of dissolution of limestone or rock salt, and by natural and man-induced dissolution processes in many parts of Kansas (Merriam and Mann, 1957).

In central Kansas most sinkholes are the result of leached out volumes of the Permian Hutchinson Salt member of the Wellington Formation (Watney et al., 1988) (Figure 1). Sinkholes forming above salt layers have been studied throughout Kansas (Frye, 1950; Walters, 1978) and the United States (Ege, 1984). Studies of subsidence related to mining of the salt around Hutchinson, Kansas (Walters, 1980),

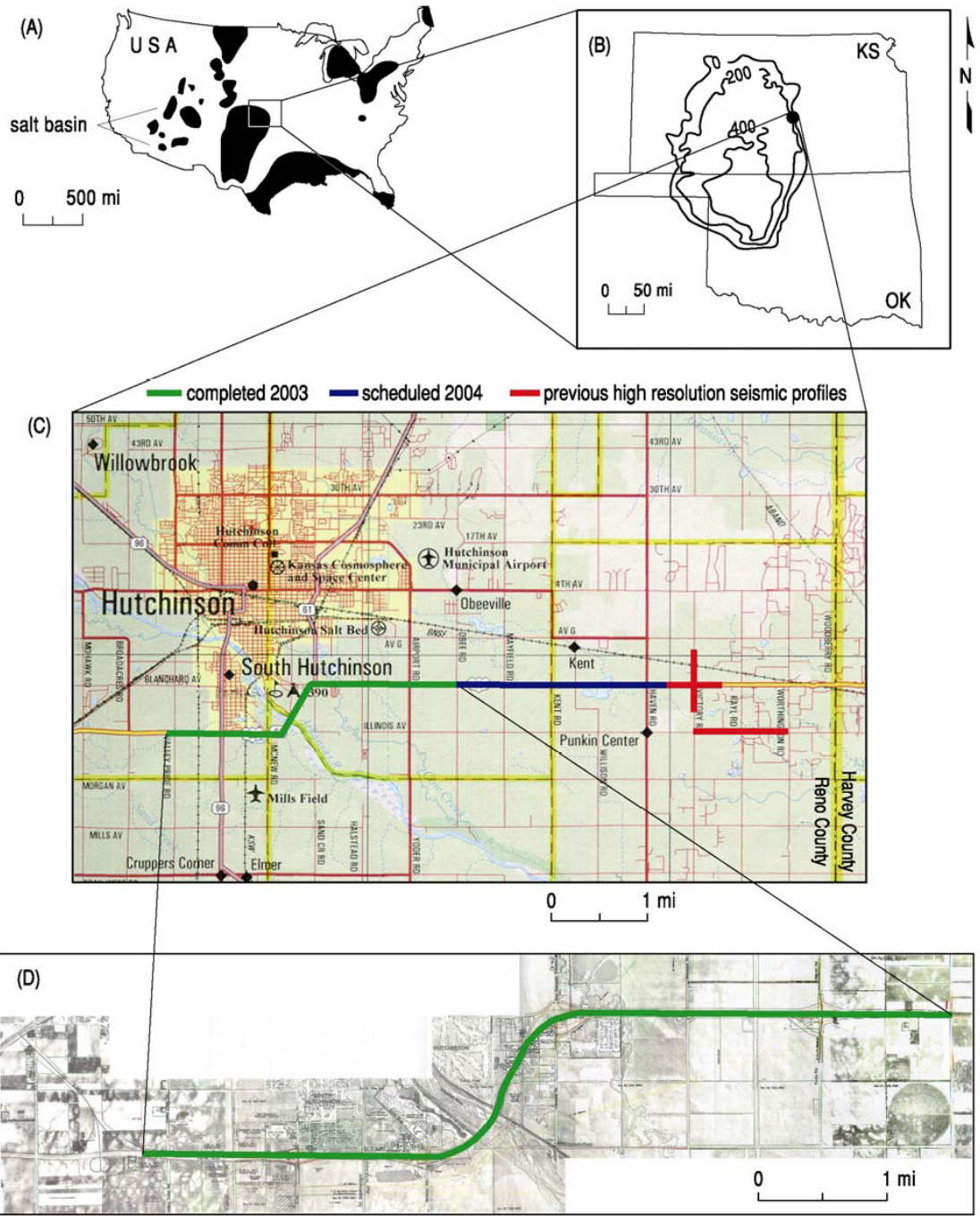


Figure 1: Site map for seismic reflection study along proposed new U.S. 50 bypass around Hutchinson, Kansas. Major salt basins of North America (A). Areas extent and thickness of the Permian Hutchinson Salt member in Kansas and Oklahoma (B). Seismic profiles acquired and planned along and near Highway U.S. 50 and the dissolution front (C). Seismic profile map along the proposed U.S. 50 bypass around Hutchinson (D).

disposal of oil field brine near Russell, Kansas (Walters, 1991), and natural dissolution through fault/fracture-induced permeability (Frye and Schoff, 1942) have drawn conclusions about the mechanism responsible for subsidence geometries and rates based on surface and/or borehole observations. Using only surface observations and borehole data, a great number of assumptions and a good deal of geologic/mechanical sense must be drawn on to define and explain these features and their impact. High-resolution seismic reflection profiling has proven an effective tool in 3-D mapping the subsurface expression and predicting future surface deformation associated with dissolution of the Hutchinson Salt in Kansas (Steeple et al., 1986; Miller et al., 1993; Anderson et al., 1995a; Miller et al., 1995; Miller et al., 1997).

Salt dissolution sinkholes are found in all areas of Kansas where the Hutchinson Salt is present in the subsurface. Sinkholes have been definitely correlated to failed containment of disposal wells injecting oil field brine wastewater using stem pressure tests and/or seismic reflection investigations at a variety of sites throughout central Kansas (Steeple et al., 1986; Knapp et al., 1989; Miller et al., 1995; Miller et al., 1997). Sinkholes that have formed by natural dissolution and subsidence processes are most commonly documented at the depositional edges on the west and north and erosional boundary on the east of the Hutchinson Salt (Frye and Schoff, 1942; Frye, 1950; Merriam and Mann, 1957; Anderson et al., 1995a). The vast majority of published works studying the source of localized leaching of salt in Kansas directly contradict suggestions that recent land subsidence in Kansas is mostly natural in origin (Anderson et al., 1995a).

Natural dissolution of the Hutchinson Salt is not uncommon in Kansas and has been occurring for millions of years (Ege, 1984). Faults extending up to Pleistocene sediments containing fresh water under hydrostatic pressure are postulated as the conduits instigating salt dissolution and subsidence along the western boundary of the salt in Kansas (Frye and Schoff, 1942). Paleosinkholes resulting from dissolution of the salt before Pleistocene deposition have been discovered previously with high-resolution seismic surveys (Anderson et al., 1998).

Subsidence can occur at rates ranging from gradual to catastrophic. Subsidence rates are to some extent related to the type of deformation in the salt (ductile or brittle) and the strength of rocks immediately above the salt layer. As salt is leached, the resulting pore space provides the differential pressure necessary to support creep (Carter and Hansen, 1983). If this pore space gets large enough to exceed the strength of the roof rock, the unsupported span will fail and subsidence occurs (Figure 2). Depending on the strength of the roof rock and therefore the size of the void, characteristics of the failure within and just above the salt will dictate how the void progresses upward until it eventually reaches the ground surface. In general, gradual surface subsidence is associated with ductile deformation that—besides vertically sinking—progresses outward, forming an ever-growing bowl-shaped depression with bed geometries and offsets constrained by normal fault geometries (Steeple et al., 1986; Anderson et al., 1995b). When rapid to catastrophic subsidence rates are observed, failure within the salt is usually brittle with void area migrating to surface as an ever-narrowing cone with bed offsets and rock failure controlled by reverse-type fault planes (Davies, 1951; Walters, 1980; Rokar and Staudtmeister, 1985).

Seismic reflection data targeting beds altered by dissolution and subsidence in this area have ranged in quality and interpretability from poor (Miller et al., 1995) to outstanding (Miller et al., 1997). Interpretations when data quality is poor have unfortunately been relegated to indirect inference of structural processes and subsurface expression (mainly from interpretations of structural deformation in layers above the salt) due to low signal-to-noise ratios. However, data with excellent signal-to-noise ratios and resolution have allowed direct detection of structures and geometries that appear characteristic of complex sinkholes. Resolution potential and signal-to-noise ratio of seismic data from this study are superior to any previously published that have targeted the salt interval. These data provide conclusive images of important structural features and unique characteristics that control sinkhole development.

Concerns for public safety and elevated maintenance costs associated with potential future surface subsidence along a newly proposed four-lane bypass around the city of Hutchinson, Kansas, are

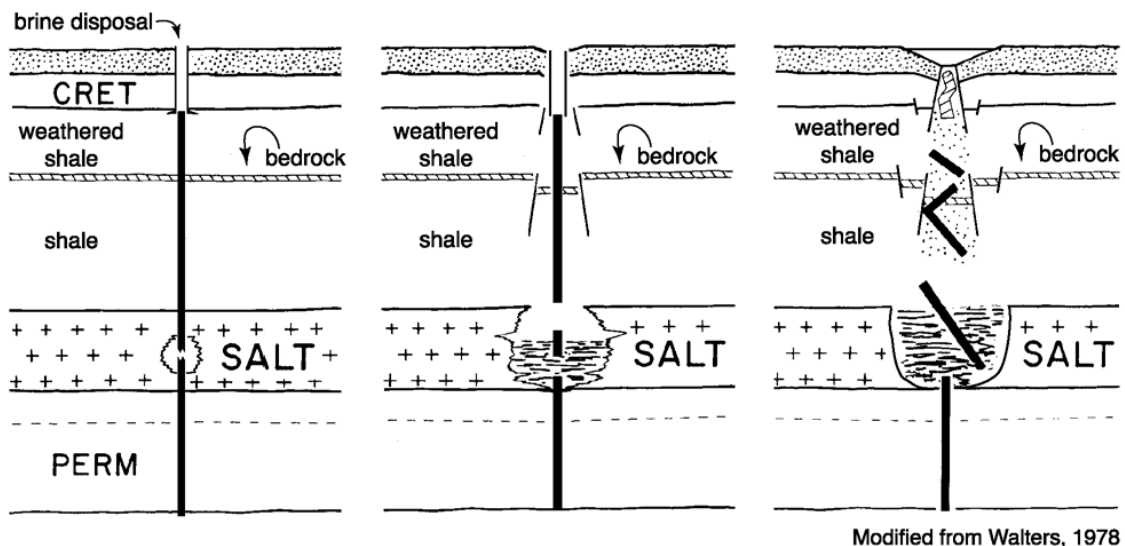


Figure 2: Cartoon of the dissolution and subsidence process across time when instigated by fluids introduced by lost containment in a disposal well.

justified considering the tendency for sinkholes to form in eastern Reno County, Kansas, associated with the natural dissolution front, aging oil field wells, and voids (jugs) remaining from salt dissolution mining practices. As an example, the formation of a sinkhole just 15 km east of the proposed bypass on U.S. 50 has become a nuisance for maintenance crews, vehicle traffic, and public officials trying to calm the concerns of local residence. Subsidence of U.S. 50 below construction grade at its intersection with Victory Road totaled 30 cm when first measured during a 1998 elevation survey. Routine elevation surveys conducted since that time have monitored the pattern and rate of subsidence. At an average subsidence rate of around 20 cm/yr, the highway surface at its centerline has sunk about 1 m since its construction. The current sinkhole is symmetric, with a very regular bowl-shaped geometry around 100 m in diameter that retains water most of the year.

Geologic Setting

Several major salt basins exist throughout North America (Ege, 1984). The Hutchinson Salt Member occurs in central Kansas, northwestern Oklahoma, and the northeastern portion of the Texas panhandle, and is prone to and has an extensive history of dissolution and formation of sinkholes (Figure 1). In Kansas, the Hutchinson Salt possesses an average net thickness of 76 m and reaches a maximum of over 152 m in the southern part of the basin. Deposition occurring during fluctuating sea levels caused numerous halite beds, 0.15 to 3 m thick, to be formed interbedded with shale, minor anhydrite, and dolomite/magnesite. Individual salt beds may be continuous for only a few miles despite the remarkable lateral continuity of the salt as a whole (Walters, 1978).

Rock salt under a depositional load is almost incompressible, highly ductile, and easily deformed by creep (Baar, 1977). Plastic deformation of the salt associated with creep is expected naturally to occur in these salts (Anderson et al., 1995b). Thin anhydrite beds within the halite succession have a strong acoustic response. Considering the extreme range of possible strain rates the salt can experience during creep deformation, these thin interbeds can possess quite dramatic, high frequency folds within relatively short distances.

Redbed evaporites overlaying the Hutchinson Salt Member are a primary target of any study in Kansas looking at salt dissolution sinkhole development and associated risks to the environment and human activity. Failure and subsidence of these evaporite units are responsible for the eventual formation of sinkholes and provide a pathway for groundwater to gain access to the salt. In proximity to the dissolution front fractures, faults, and collapse structures compromise the confining properties of the Permian shale bedrock and put the major fresh water aquifer (Plio-Pleistocene Equus Beds) in this part of southern Kansas at risk. Along the eastern boundary (dissolution front), the salt, which ranges from 0 to over 100 m thick, is buried beneath about 120 m of Permian redbed evaporites.

The eastern margin of the salt was exposed during late Tertiary where erosion and leaching began the 30 km westward progression of the front to its present day location (Bayne, 1956). The ability of the front to migrate while under as much as 100 m of sediments was a direct consequence of ready access to an abundant supply of groundwater (Watney et al., 1988). Subsidence of Permian, Cretaceous, and Tertiary rocks has progressed along the migration front as the salt has been leached away. While this subsidence was going on, Quaternary alluvium was being deposited in volumes consistent with the salt that was being removed. This processes resulted in today's moderate to low surface relief that masks the extremely distorted (faulted and folded—non-tectonic) rock layers within the upper Wellington and Ninnescah shales (Anderson et al., 1998).

Seismically, all Permian and younger reflectors are important to accurate interpretation of the stacked sections. Model studies show significant time delays (static) and geometric distortions that are to be expected below recent subsidence (Anderson et al., 1995b). "Pull downs" in time result from the localized decreases in material velocities within a sinkhole. The velocity structure and small radius of curvature of the synforms, characteristic of salt dissolution and subsidence in this area, can produce diffractions and distort reflections on vertically incident reflection sections. Reflections from beneath the salt will have a subdued expression of the post-salt subsidence. Estimations of subsidence and therefore volume of rock salt removed based on time section estimations alone (without compensation for velocity variability) may exceed actual by as much as 25 to 50 percent in this area. Considering this geologic setting, it is reasonable to compensate for compaction-related static causing this lateral decrease in velocity by "flattening" on the top of the Chase Group.

Most of the upper 700 m of rock at this site is Permian shales (Merriam, 1963). The currently disputed Permian/Pennsylvanian boundary is about 700 m deep and seismically marked by a strong sequence of cyclic reflecting events. The Chase Group (top at 250 m deep), Lower Wellington Shales (top at 175 m deep), Hutchinson Salt (top at 125 m deep), Upper Wellington Shales (top at 70 m deep), and Ninnescah Shale (top at 25 m deep) make up the packets of reflecting events easily identifiable and segregated within the Permian portion of the section. Bedrock is defined as the top of the Ninnescah Shale with the unconsolidated Plio-Pleistocene Equus Beds making up the majority of the upper 30 m of sediment. Thickness of Quaternary alluvium that fills the stream valleys and paleosubsidence features goes from 0 to as much as 100 m depending on the dimensions of the features.

Seismic Acquisition

A continuous profile, a little over 10 km in length was acquired along the existing U.S. 50 highway right-of-way around Hutchinson, Kansas (Figure 1). In moving to meet the ever-growing vehicle load on the current highway, engineers proposed several possible transects skirting the southern edge of Hutchinson intended to accommodate a new four-lane limited access highway generally consistent with the current two-lane road that is there. With the known threat sinkholes in this area represents—both naturally occurring and as a result of dissolution mining—the subsurface between the base of the salt and bedrock beneath the proposed highway transect was examined using high resolution seismic reflection. The objective of this survey was to expose any feature lurking below ground that might someday

threaten the stability of the road surface. These data were acquired using a rolling fixed-spread design that eliminated the need for a roll-along switch and extended the range of far offsets available during processing. This survey design provided the wide range of source offsets necessary for detailed velocity analysis, close receiver spacing for improved confidence in event identification, and maximized the range of imageable depths.

Even though no sinkholes were visible at the ground surface, evidence for historical dissolution and subsidence not visible at the ground surface has been observed in several locations around eastern Reno County, Kansas. This historical dissolution and subsidence, referred to as “paleosinkholes,” is an indication that fresh water has had access to the salt in this area previously and has found a pathway to carry the dissolved salt away from the dissolution front. Several naturally forming sinkholes in this area have seen recent reactivation and formation of a surface depression. Therefore, looking for paleo-sinkholes and old salt mine dissolution jugs will be critical to final placement of this proposed bypass around Hutchinson.

Acquisition parameters were defined based on experience and walkaway tests near the start of the profile on the western end of the survey. Twin Mark Products L28E 40Hz geophones were planted at 2.5 m intervals in approximate 1 m arrays. Geophones were planted into firm to hard soil at the base of the road ditch in small divots left after the top few inches of loose material were removed to insure good coupling. Four 60-channel Geometrics StrataView seismographs were networked to simultaneously record 240 channels of data. An IVI Minivib1 using a prototype Atlas valve delivered three 10-second, 25-250 Hz up-sweeps at each 5 m spaced shot location. Experiments at this site were consistent with bench tests, which suggested this new rotary valve design will produce up to four times the peak force of conventional valves at 250 Hz. The pilot was telemetered from the vibrator to the seismograph and recorded as the first trace of each shot record. Each of the three sweeps generated per shot station was individually recorded and stored in an uncorrelated format with the ground force pilot-occupying channel 1.

All sweeps were recorded into the fixed 240-channel spread with the source incrementally moving from shot station to shot station through the middle half of the spread. Once the center 120 receiver stations (60 shot stations) were shot through, the back 120 receiver stations were moved to the front and the process repeated. Since all shot records were recorded uncorrelated, QC involved visual inspection of the recorded pilot trace, audio monitoring of the pilot trace on an RF scanner, inspection of the vibrator power spectra after each shot, and review of a correlated shot record after every 5 to 10 shot stations. With the exception of receiver stations not instrumented due to excess or thick gravel or asphalt or stations taken off-line when their offset exceeded 300 m, the survey was recorded with 98 percent live receivers within the optimum recording window (Hunter et al., 1984).

Seismic Processing

A basic common midpoint (CMP) processing flow was used in a fashion consistent with well-established 2-D high-resolution seismic reflection methodologies (Steeple and Miller, 1990). All lines were processed using WinSeis2, beta seismic data processing software (next generation of WinSeis Turbo) from the Kansas Geological Survey. Any reflection data acquired in this highly disturbed subsurface setting will be plagued with static problems and subject to dramatic swings in NMO velocity over relatively short distances; this data set was no exception.

Data were recorded and stored uncorrelated to allow precorrelation processing in hopes of increasing the signal-to-noise ratio and resolution potential (Doll and Çoruh, 1995). Removal of noisy traces and amplitude scaling were precorrelation processing steps that significantly enhanced signal-to-noise and resolution potential. Attempts to improve the data quality precorrelation through frequency filtering, spectral whitening, and frequency-wave number (F-k) filtering were unsuccessful. Storing data

uncorrelated also allowed tests to be run with different methods of correlation and correlating with different pilot traces. These data were optimally correlated using the synthetic drive signal. Storing data uncorrelated and unstacked required 30 times more storage space, about 50 percent more acquisition time, and 5 times more data transfer time. Improvements in signal-to-noise ratio and resolution made these increases cost effective.

Emphasis was placed on noise suppression, maintaining true amplitude, and compensating for velocity irregularities. Noise suppression focused on vehicle noise from the highway, livestock along the lines, powerline noise, surface waves, first arrivals, and air-coupled waves. Muting and hum filtering (Xia and Miller, 2000) improved signal-to-noise appreciably. The three individual shot gathers acquired at each shotpoint were vertically stacked after all the noise suppression operations were complete. With the exception of the 1 sec AGC used precorrelation and display gains, only spherical divergence was used to adjust trace amplitudes. With the large depth window of interest, a relatively wide optimum offset window was maintained, which after noise mutes resulted in true trace folds ranging from 1 to a maximum of 30 (Liberty and Knoll, 1998). Velocity was defined in groups of 20 CMPs with at least one control point for each 100 ms time window and a minimum of five points selected in the first 200 ms. Each line is defined by a velocity function with over 400 time/velocity pairs determined with the aid of several iterations of correlation static corrections and velocity analysis.

Even when reflections were interpretable within the noise cone an inside mute was applied after the air-coupled wave to avoid signal degradation of reflection wavelets on CMP stacked sections. Inside mutes are a common practice for shallow (upper 1 km) seismic reflection processing (Baker et al., 1998). It is however, uncommon and counterintuitive to remove confidently identifiable reflection events regardless of where they are relative to other energy arrivals. The likelihood of wavelet distortion sufficient to reduce the resolution potential or lose the trace-to-trace coherency of reflections is significantly increased when surgically muting noise immersed in signal. Analogous to inoperable tumors, attempts to precisely remove just noise—especially air-wave noise—at tolerances of a millisecond or two run the risk of cutting too severely and/or defining mute tapers that are too steep, thereby irreparably altering the reflection waveform. Stacking waveforms into the fold that have been distorted by overly aggressive mutes will compromise the accuracy of the information contained in the waveform, and in some cases produce artifacts that can be misinterpreted as true earth response.

Powerline noise was pronounced on shot gathers where power lines were located along the south side of the road. A complex combination of 60 Hz, 120 Hz, and 180 Hz noise bleeding from overhead power lines masked most of the seismic energy even after correlation along portions of the road. A hum filter was very effective in eliminating powerline noise without affecting the amplitude or phase of the seismic data (Xia and Miller, 2000). This predictive filter produced a noticeable increase in signal-to-noise without loss of resolving potential.

Interpretation

Confidently interpretable reflections on shot gathers are essential to optimizing the acquisition, processing, and interpretation of high-resolution seismic reflection data. Reflections can be interpreted on raw, correlated shot records (scaled for display purposes) from around 50 ms to two-way time depths in excess of 500 ms (Figure 3). Considering the optimum window for these data, it was imperative to keep a wide range of offsets to insure the entire target zone was imaged. Reflections with dominant frequencies of around 200 Hz can be interpreted as deep as 200 ms, while the dominant frequency of reflections at 500 ms have dropped to around 100 Hz. With dominant frequencies of some reflections exceeding 200 Hz, a 2.5 ms static between adjacent traces represents a 180° phase shift and complete cancellation. Therefore, it is critical that static irregularities be compensated for before the data are CMP stacked. Reflection events can be traced through the air-coupled wave and just into the ground roll

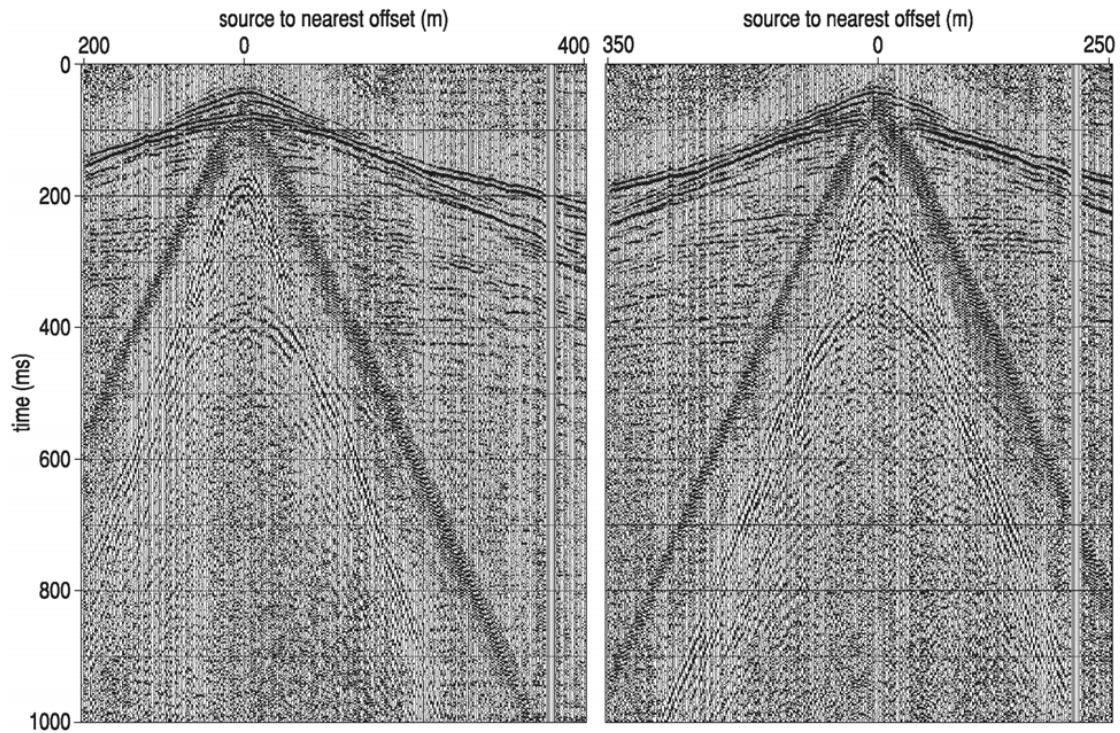


Figure 3: Correlated shot gathers from along profile. Reflection events have diagnostic curvature and high frequency wavelets.

wedge. To avoid any contamination by air-coupled wave, all energy after the airwave was removed during processing.

For quality control reasons it is important that reflections interpreted at two-way times less than 50 ms on CMP stacks can be correlated with equivalent 50 ms reflection hyperbolae on shot gathers. Identification of these reflections on field files and tracking of them throughout the processing flow was necessary to ensure CMP sections were correctly stacked and interpreted. Ultra shallow reflections (< 50 ms) were a critical aspect in discerning the periods since Permian that these sediment-filled sinkholes may have been active.

From interpretations of reflection from raw shot gathers it can be estimated that reflectors from 15 m to over 1 km were imaged by these data (Figure 3). Even under these extremely noisy conditions, contending with wind, vehicles, and power lines along with an extremely variable near surface at overpasses, access road fill, the Arkansas River, and railroad grade, the data are of exceptional quality. Bed resolution using the half-wavelength criteria is around 2 m at the top of the salt unit. Reflections identified on the shot gather extend from the Permian through the upper Pennsylvanian.

CMP stacked section from this 10+ km survey are all of excellent quality (Figure 4). Data from the western extreme of the profile provide an excellent look at the seismic character of a segment of Permian rocks not disturbed by dissolution-induced subsidence. The salt interval has been identified using a combination of nearby well logs and depth estimates from NMO velocity conversions. Two-way travel time to the top of the salt is around 170 ms with a salt interval that is clearly distinguishable on seismic data from the surrounding Permian rocks.

Critical to identifying areas of disturbed salt and any overburden that might be susceptible to collapse due to irregularities within the salt is a clear understanding of how native, undisturbed salt and

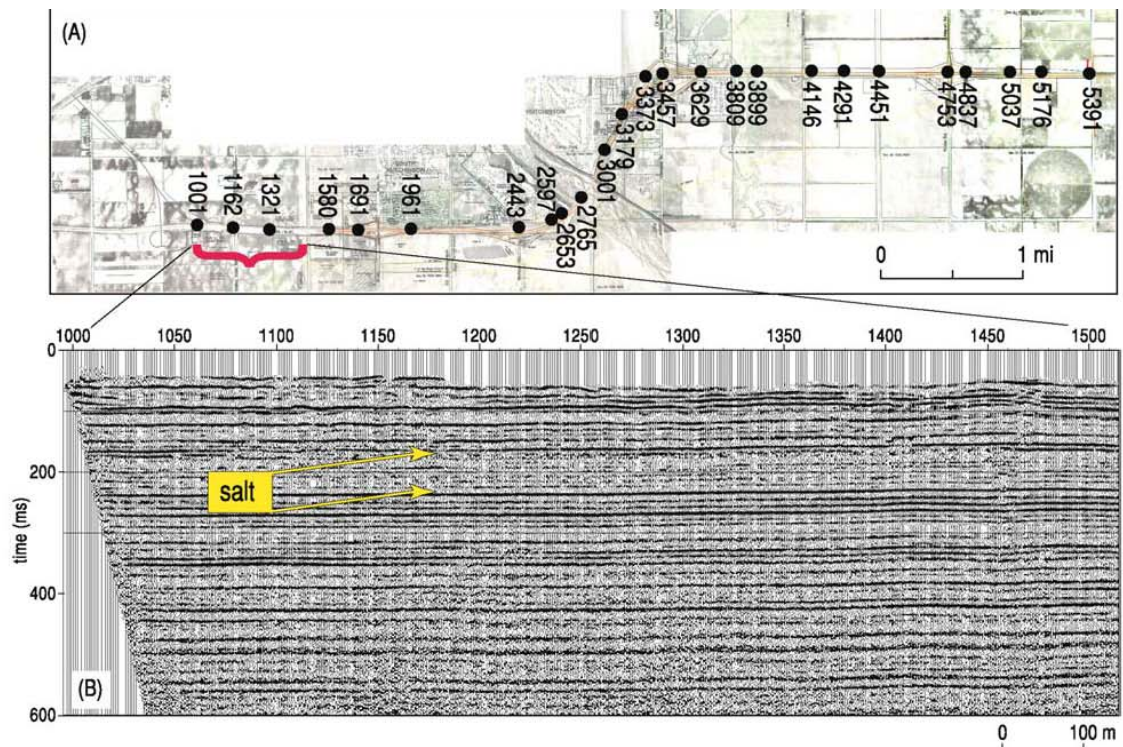


Figure 4: Seismic stations were DGPS located to within ± 2 cm (x, y, z) (A). Seismic section from first 1.25 km clearly demonstrates the data quality and signature of undisturbed salt (B).

overburden appear on CMP stacked seismic sections. A strong reflection at about 170 ms interpreted to be the Milan Limestone marks the top of the salt, followed by a subdued set of relatively discontinuous reflections to about 230 ms where another high amplitude reflection, likely the Carlton Limestone, is interpreted to be the basal contact between the salt and surrounding rocks of the Sumner Group (Figure 5). Reflections from within the salt layer possess geometries consistent with channel-cut-and-fill deposition. These intra-salt beds are likely shales and anhydrites.

A somewhat unusual feature interpreted on these seismic data is a small area of disturbed salt with a volume of rock extending upward from the salt to near the bedrock surface that appears to be disturbed and possibly offset with some related subsidence (Figure 6). The disturbed area within the salt can be identified by the loss of continuity of the intra-salt reflections. Immediately below the basal salt contact at about 230 ms is a slightly disturbed zone that increases in area with depth that is likely the shadow effect (scatter and decreased overburden velocity) related to the disturbed reflections within the salt and is an artifact. A chimney feature extending toward the bedrock surface appears to be a fracture zone associated with the anomaly in the salt. Localized layers above the salt and this anomaly appear to form a very subdued syncline. This fracture zone could well be related to salt creep and not dissolution. With the many zones where water is confined in the Permian redbeds between the salt and bedrock surface, this fracture zone could well have allowed water access to the salt, but without an exit point for the saturated brine solution to leave the salt. The leaching process started but was halted before sufficient salt was dissolved to create a void of sufficient size for large-scale subsidence to occur.

The only clearly identifiable paleosinkhole across the 10 km profile was identified near the intersection of U.S. Highway 50 and Kansas state Highway 96 (Figure 7). Reflection characteristics of the salt and overlying sediments across the almost 1 km between the anomaly identified beneath station

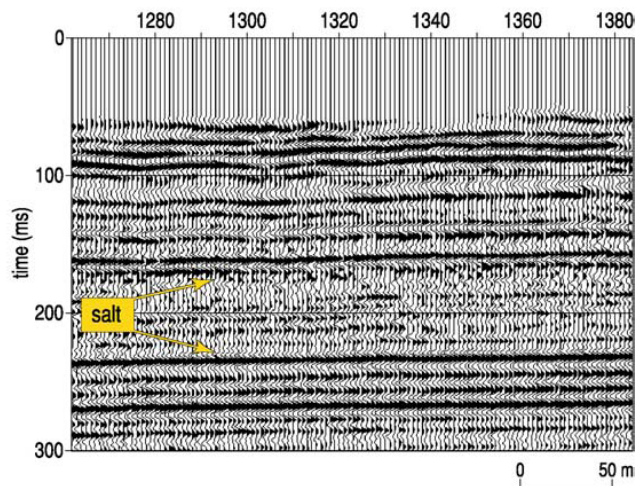


Figure 5: Expanded view of salt interval and layers above and immediately below. Reflections from within the salt are unique in comparison to those from surrounding Permian layers.

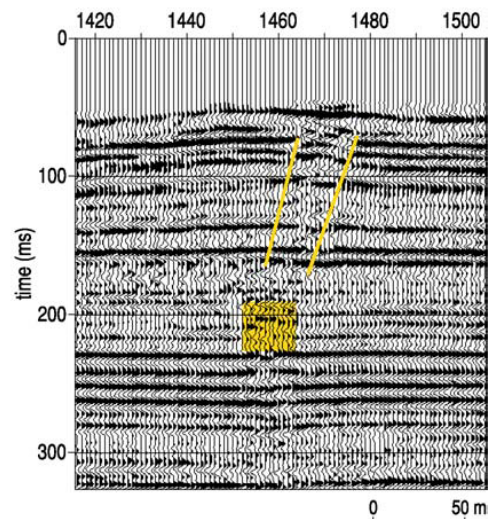


Figure 6: Disturbed area within the salt and associated chimney where rocks between the salt and bedrock appear altered.

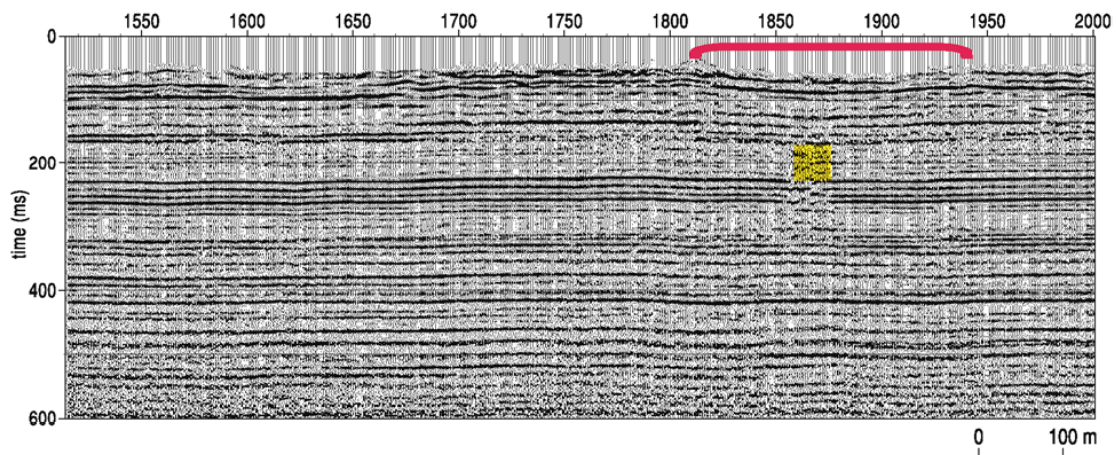


Figure 7: Paleosinkhole evident about 2 km from the beginning of profile and approximately beneath the stretch of highway that includes the overpass of Highway 96.

1470 and 1800 appear very undisturbed with “normal” depositional features interpretable in reflections within the upper 300 m. Between stations 1800 and 1950 a very pronounced depression in the shallower sediments is evident. In general, this anomaly possesses the classical reflection drape above the salt indicative of plastic deformation that occurs as salt gradually dissolves and overlying sediments subside into the void. The only significant faulting evident in this feature is at the edges of the bowl-shaped structure indicative of more brittle deformation.

A close-up of the paleosinkhole beneath station 1870 provides a very intriguing view of this ancient, yet potentially dangerous feature (Figure 8). Clearly all the leached salt responsible for this more than 300 m wide feature at the bedrock surface came from little more than a 50 m wide stretch of salt. Key to this discovery is what appear to be competent layers within the salt that are beneath the

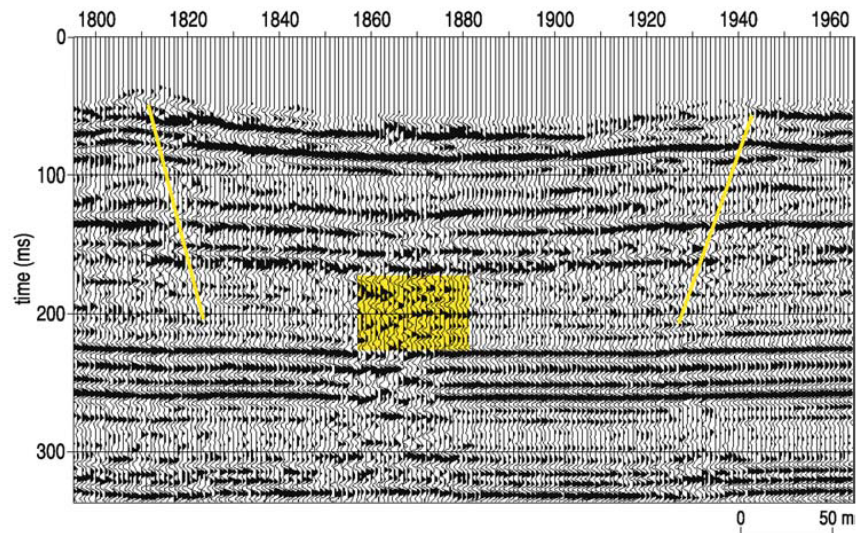


Figure 8: An area of active dissolution from where the salt was previously dissolved, allowing creep and the formation of a much larger surface depression than salt void volume.

bedrock expression of the sinkhole. This implies dissolution occurred within a relatively small volume, then due to salt creep this 50 m wide zone of dissolution reduced the pressure regime and affected salt more than 100 m away. As salt crept toward this low-pressure area, wide expanses of unsupported roof rock began forming until subsidence occurred, with the edges of salt creep defined by faults that extended to the bedrock surface.

Probably one of the most intriguing, yet least significant feature for highway planners, is what appears to be a large fault zone beneath station 4430 (Figure 9). This fault zone appears to have minimal vertical offset, but possesses a marked change in character of reflections across this zone. The reflection identified as from the top of the salt changes in both frequency and amplitude, as well most events above about 250 ms appear to have changes in character across this fault that range from dramatic to subtle. Below 250 ms the fault zone is still evident but lacks as much change in seismic wavelet characteristics

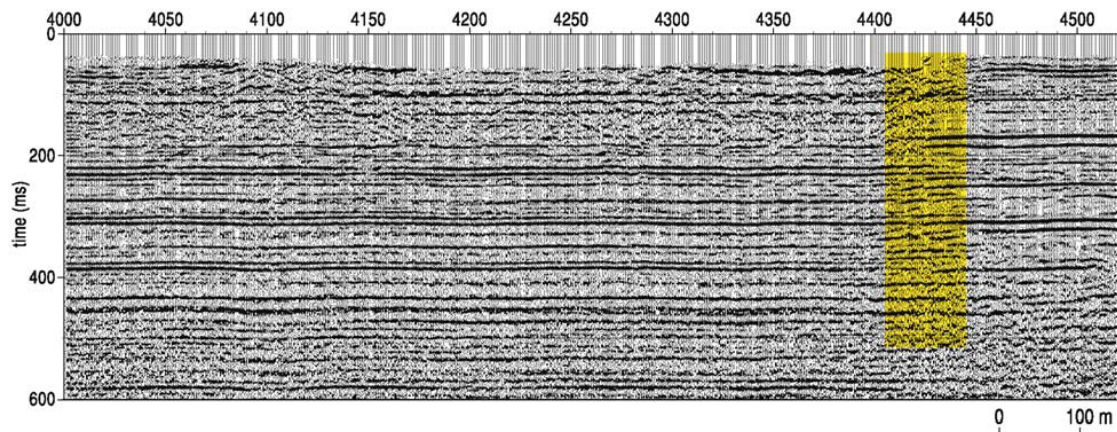


Figure 9: A fault is clearly evident on these data beneath station 4430. An abrupt change in reflection characteristic, diffraction, and apparent bed offset are all key indicators of faulting.

as shallower in the section. From a purely speculative perspective this fault has all the characteristics expected from a predominantly strike-slip fault. Correlations with local geology are not yet complete, but will likely provide key insights into this feature.

Conclusions

High-resolution seismic reflection provided a relatively continuous view of key rock layers above the base of the Hutchinson Salt beneath the proposed new alignment of the U.S. 50 bypass south of the city of Hutchinson, Kansas. Several features with the potential to affect the ground surface along or beneath the future highway were discovered. A paleosinkhole with indications of reactivation since it originally formed represents a risk of gradual subsidence in the highway surface at some point in time. Also, chimney features associated with salt creep are areas for monitoring. A fault intersecting the highway alignment cannot be avoided by the new highway and it has not provided a conduit for fresh water to gain access to the salt at this time. The area above the fault will also require monitoring for any indication of ground subsidence, but does not represent a significant threat to highway stability. Diffraction or scatter associated with bed terminations or point source re-radiation was identified in two locations adjacent to known areas where dissolution salt mining has been active previously. It is not unreasonable to suggest these features might be related to that mining activity. If they are related to dissolution mining activity, they represent the most significant risk of accelerated failure and subsidence in this area. More study of these diffraction/scatter features is needed to better define their source.

References

- Anderson, N.L., W.L. Watney, P.A. Macfarlane, and R.W. Knapp, 1995a, Seismic signature of the Hutchinson Salt and associated dissolution features: *Kansas Geol. Survey Bulletin 237*, p. 57-65.
- Anderson, N.L., R.W. Knapp, D.W. Steeples, and R.D. Miller, 1995b, Plastic deformation and dissolution of the Hutchinson Salt Member in Kansas: *Kansas Geol. Survey Bulletin 237*, p. 66-70.
- Anderson, N.L., A. Martinez, and J.F. Hopkins, 1998, Salt dissolution and surface subsidence in central Kansas: A seismic investigation of the anthropogenic and natural origin models: *Geophysics*, v. 63, p. 366-378.
- Baar, C.A., 1977, *Applied salt-rock mechanics 1*: Elsevier Scientific Publishing Company, 294 p.
- Baker, G.S., D.W. Steeples, and M. Drake, 1998, Muting the noise cone in near-surface reflection data: An example from southeastern Kansas: *Geophysics*, v. 63, p. 1332-1338.
- Bayne, C.K., 1956, *Geology and ground-water resources of Reno County, Kansas*: Kansas Geological Survey Bulletin 120.
- Beck, B.F., A.J. Pettit, and J.G. Herring, eds., 1999, *Hydrogeology and engineering geology of sinkholes and Karst-1999*: A.A. Balkema.
- Carter, N.L., and F.D. Hansen, 1983, Creep of rock salt: *Tectonophysics*, v. 92, p. 275-333.
- Doll, W.E., and C. Çoruh, 1995, Spectral whitening of impulsive and swept-source shallow seismic data [Exp. Abs.]: *Soc. Explor. Geophys.*, p. 398-401.
- Davies, W.E., 1951, *Mechanics of cavern breakdown*: National Speleological Society, v. 13, p. 6-43.
- Ege, J.R., 1984, Formation of solution-subsidence sinkholes above salt beds: *U.S. Geological Survey Circular 897*, 11 p.
- Frye, J.C., 1950, Origin of Kansas Great Plains depressions: *Kansas Geological Survey Bulletin 86*, pt. 1, p. 1-20.
- Frye, J.C., and S.L. Schoff, 1942, Deep-seated solution in the Meade Basin and vicinity, Kansas and Oklahoma: *American Geophysical Union Transactions*, v. 23, pt. 1, p. 35-39.
- Hunter, J.A., S.E. Pullan, R.A. Burns, R.M. Gagne, and R.S. Good, 1984, Shallow seismic-reflection

- mapping of the overburden-bedrock interface with the engineering seismograph—Some simple techniques: *Geophysics*, v. 49, p. 1381-1385.
- Knapp, R.W., D.W. Steeples, R.D. Miller, and C.D. McElwee, 1989, Seismic reflection surveys at sinkholes in central Kansas: *Geophysics in Kansas*, D.W. Steeples, ed.: Kansas Geological Survey Bulletin 226, p. 95-116.
- Liberty, L.M., and M. Knoll, 1998, Time varying fold in high-resolution seismic reflection data: a recipe for optimized acquisition and quality control processing and interpretation: *Proceedings of the Symposium on the Application of Geophysics to Engineering and Environmental Problems (SAGEEP 98)*, March 22-26, Chicago, p. 745-751.
- Merriam, D.F., 1963, The geologic history of Kansas: *Kansas Geol. Survey Bulletin* 162, 317 p.
- Merriam, D.F., and C.J. Mann, 1957, Sinkholes and related geologic features in Kansas: *Transactions Kansas Academy of Science*, v. 60, p. 207-243.
- Miller, R.D., D.W. Steeples, L. Schulte, and J. Davenport, 1993, Shallow seismic reflection study of a salt dissolution well field near Hutchinson, Kansas: *Mining Engineering*, October, p. 1291-1296.
- Miller, R.D., D.W. Steeples, and T.V. Weis, 1995, Shallow seismic-reflection study of a salt-dissolution subsidence feature in Stafford County, Kansas: in N.L. Anderson and D.E. Hedke, eds., *Geophysical Atlas of Selected Oil and Gas Fields in Kansas*: Kansas Geological Survey Bulletin 237, p. 71-76.
- Miller, R.D., A.C. Villella, and J. Xia, 1997, Shallow high-resolution seismic reflection to delineate the upper 400 m around a collapse feature in central Kansas: *Environmental Geosciences*, v. 4, n. 3, p. 119-126.
- Rokar, R.B., and K. Staudtmeister, 1985, Creep rupture criteria for rock salt: *Sixth International Symposium on Salt*, B.C. Schreiber and H.L. Harner, eds., Salt Institute Inc., Virginia, v. 1, p. 455-462.
- Steeple, D.W., R.W. Knapp, and C.D. McElwee, 1986, Seismic reflection investigation of sinkholes beneath interstate highway 70 in Kansas: *Geophysics*, v. 51, p. 295-301.
- Steeple, D.W., and Miller, R.D., 1990, Seismic reflection methods applied to engineering, environmental, and groundwater problems: *Soc. Explor. Geophys., Geotechnical and Environmental Geophysics*, Stan Ward, ed., Vol. 1: Review and tutorial, p. 1-30.
- Walters, R.F., 1978, Land subsidence in central Kansas related to salt dissolution: *Kansas Geological Survey Bulletin* 214, p. 1-32.
- Walters, R.F., 1980, Solution and collapse features in the salt near Hutchinson, Kansas: *South-central Section, Geological Society of America, Field Trip Notes*, 10 p.
- Walters, R.F., 1991, Gorham Oil Field: *Kansas Geological Survey Bulletin* 228, p. 1-112.
- Watney, W.L., J.A. Berg, and S. Paul, 1988, Origin and distribution of the Hutchinson Salt (lower Leonardian) in Kansas: *Midcontinent SEPM Special Publication No. 1.*, p. 113-135.
- Xia, J., and R.D. Miller, 2000, Design of a hum filter for suppressing power-line noise in seismic data: *Journal of Environmental and Engineering Geophysics*, v. 5, n. 2, p. 31-38.

Acknowledgments

We greatly appreciate the assistance provided by KDOT geologists and maintenance staff keeping the work area safe for both motorist and seismic crew members, fearlessly facing down angry and sometimes dangerous motorists. Assistance was provided by Jim Burns and Ryan Duling, Chanute Geology Office; Neil Croxton, Jeff Geist, and Scott Sherman, Abilene Geology Office; Tom Johnson, Matt Cuthbertson, and Jason Ressor, El Dorado Geology Office; Ryan Salber, Lawrence Geology Office; Randy Billenger and Josh Welge, Topeka Geology Office; and Cindy Behnke, John Goset, Tracy Barragan, Shannon Jones, Pam Newlin, Terry Elliott, Ron Nusz, and Dave Peters, Hutchinson Maintenance Group. Also, we would like to thank Mary Brohammer for her help with editing and graphics, she made our life a lot easier.



Environmental and Engineering Geophysical Society

July 7, 2006

Dear Rick,

Congratulations on the selection of your presentation “High-Resolution Seismic Reflection to Identify Areas with Subsidence Potential beneath U.S. 50 Highway in Eastern Reno County, Kansas” as one of the top SAGEEP2006 Best Presentations at the recent SAGEEP in Seattle, WA.

As a SAGEEP2006 Best Paper, you are invited to present your paper at the European Association of Geoscientists and Engineers (EAGE) Near Surface Geoscience Division (NSGD) conference, Near Surface 2006. The conference will be held September 4-6, 2006 in Helsinki, Finland. A complimentary registration to the conference is provided by NSGD. You will be required to provide your own air and ground transportation, lodging, and meals. Information on the conference can be accessed at the following web site:
<http://www.eage.org/events/index.php?eventid=5&Opendivs=s2>.

A four (4) page abstract is required to submit to NSGD. The abstract is generally a modification of that submitted to SAGEEP. Please refer to the attached .zip file and additional information provided in the cover letter for guidance in preparing the abstract.

Please provide me today, Friday, 7 July 2006, with the information listed on the attached sheet. I apologize for the short notice and appreciate your immediate attention. The NSGD requires the information immediately so that it can be included in the conference proceedings. If you have any questions, contact me by email or telephone at the number listed below. Thank you for your assistance and again, congratulations. I am sure you will enjoy the NSGD conference and especially enjoy Helsinki.

Micki Allen

SAGEEP2006, Liason
Phone: +905-474-9118
Fax: +905-474-1968
Mobile: +647-401-8758

Miller, R.D., J. Ivanov, S. Hartung, and L. Block, 2004, Seismic investigation of a sinkhole on Clearwater Dam: Symposium on the Application of Geophysics to Engineering and Environmental Problems (SAGEEP 2004), Colorado Springs, Colorado, February 22-26, Paper KAR01, p. 1082-1098.

SEISMIC INVESTIGATION OF A SINKHOLE ON CLEARWATER DAM

*Richard D. Miller, Kansas Geological Survey, Lawrence, KS
Julian Ivanov, Kansas Geological Survey, Lawrence, KS
Steve Hartung, U.S. Army Corps of Engineers, Little Rock, AR
Lisa Block, U.S. Bureau of Reclamation, Denver, CO*

Abstract

A 10 ft wide and 10 ft deep sinkhole that catastrophically formed approximately 120 ft upstream of the crest of Clearwater Dam in southeastern Missouri was the target of a high-resolution seismic imaging program including reflection, surface wave analysis, and crosshole tomography. The primary goals were to determine the general subsidence geometry and integrity of the core and help ascertain the involvement of bedrock and native alluvium beneath this earthen dam. Reflection data from this survey possess excellent frequency content (dominant >150 Hz) and provide high-resolution images of layers within the pervious shell. Using tightly spaced surface wave profiles, an elongated low shear-wave velocity chimney-like feature was delineated and interpreted to represent the root of the sinkhole. Based on seismic, construction, drill, and borehole tracer data, a borehole geophysics program was designed to identify fractures/joints that might provide seepage pathways. Crosshole seismic data detected a large low-velocity zone within the bedrock and an associated low-velocity zone within the pervious fill consistent with the surface seismic interpretations. A comprehensive appraisal of the risk this disturbed zone represents to the overall integrity of the dam and whether it is a symptom of a larger, yet undetermined subsurface leaching problem is being developed.

Summary

A sinkhole that formed catastrophically on Clearwater Dam during January of 2003 was the target of a high-resolution seismic imaging program that included both seismic reflection and surface wave analysis. The primary goals of this surface seismic investigation was to determine the general subsidence geometry within the dam (the "root or chimney" of the sinkhole) and help ascertain if and to what extent bedrock and native alluvium was involved with the sinkhole. This sinkhole formed approximately 120 ft on the upstream side of the dam crest and when first discovered measured 10 ft across and 10 ft deep. Seismic data provide insights into the areal extent and approximate affected volume of dam material. Based on seismic, construction, drill, and borehole tracer data, a borehole geophysics program was designed to identify fractures/joints that might provide pathways for upstream water to flow through the pervious fill material and leak past the impervious core. A comprehensive appraisal of the risk this disturbed zone represents to the overall integrity of the dam and whether it is a symptom of a larger, yet undetermined subsurface leaching problem should be developed once all surface and borehole data are assimilated and collectively interpreted.

High-resolution seismic reflection and full-wavefield seismic studies targeted key areas within and below this earthen dam. The high-resolution seismic reflection portion of the program focused on bedrock and layering within the impervious core and lower portion of pervious fill in a depth range from about 40 to 130 ft below the dam surface. Surface wave analysis provided shear wave velocity measurements in the upper 60 ft of the pervious fill material that overlays the impervious dam core. These two, unique seismic measurement techniques provided key details about the materials associated with and responsible for the sinkhole.

Analysis of the shear wave velocity profiles significantly improved our understanding of the material strengths, affected shallow subsurface, and the area with the greatest risk of continued subsidence. Surface wave data from this site supports the suggestion that the sinkhole formed at the left extreme of a chimney-like structure as characterized by reduced shear wave velocities (related to stiffness) within the pervious fill. This chimney of disturbed material within the pervious fill is predominantly a left/right feature, appears quite limited in its upstream/ downstream extent, and is most pronounced on profiles crossing directly through the surface depression. On profile C3 at depths greater than 40 ft below the surface of the dam the disturbed zone is approximately 40 ft wide and extends from about 5 ft left of the left edge of the sinkhole to 30 ft or so right of the sinkhole center. Located just 8 ft away, profile C4 possesses a similar reduced velocity zone more closely centered on the sinkhole and significantly less elongated to the right in comparison to C3. The 3-D geometry of this feature in the pervious fill material based on the six 2-D surface wave profiles, appears to have the greatest width in the upstream/ downstream direction near the surface, narrowing with depth. In contrast, the structure appears extremely elongated in the right/left “fingering” right from the center of the sinkhole as much as 30 ft.

High-resolution reflection sections provide a detailed image of the pervious fill, core, native alluvium, and bedrock surface in the depth range of about 40 ft to just over 130 ft below the surface of the dam. Not all reflections returning from within and below the dam can be correlated to known acoustic contrasts identifiable on construction records. Reflections within the pervious fill are likely related to undocumented changes in construction materials and/or compaction practices. Cement grout and placed clay layers were unexpectedly encountered in cores from intervals construction records indicate “native alluvium” should be present. Cement layers, unplanned placed clay layers, and variations in impervious core dimensions were likely used to remedy problems with cutoff trench stability or to improve the uniformity of the clay core. Offset in reflections at two-way traveltimes consistent with the pervious core zone is likely related to subsidence after dam completion. It is possible some subsidence occurred during construction as evidence by the reflection droop observed in places where overlying layers appear flat. If subsidence occurred during construction extra fill material would have been used to level the working surface bring it back up to grade. Distortion observed in the reflection events interpreted as defining the core wedge is likely the result of stability problems during construction, subsidence after completing construction, or horizontal sampling smear.

The bedrock surface appears to have an irregular topography. Undulations on the bedrock surface are likely due to material (and therefore sediment) variability above bedrock. If the velocity function is accurate time-to-depth conversions should compensate for these changes in material properties. However, due to the very short wavelength nature of the materials changes around the disturbed area it was not possible to fully compensate for these lateral changes in material properties using NMO velocity alone. Dramatic drops in amplitude are likely related to fracture/joint zones in bedrock. It is not possible to determine if these fracture/joint systems are open or are grout sealed from construction. Subsidence below 40 ft in proximity to the sinkhole appears to be non-vertical and directionally consistent with the “fingering” interpreted on surface wave data. The core wedge appears to become more uniform upstream. Two areas with apparent fracture/joints systems and associated subsurface subsidence are interpreted with the system right of the sinkhole correlated to the sinkhole formation.

Once the drilling program is complete and crosshole seismic data interpreted, it should be possible to more definitively correlate the surface seismic data with a realistic model of the current dam interior and subgrade. Seismic techniques have rarely provided high resolution, high signal-to-noise ratio images of the interior of an earthen dam. Reflections interpretable on shot gathers are outstanding in quality and some of the best in quality and consistency we have ever recorded on the upstream slope of a dam. Irregularities in reflections on CMP sections from within the pervious fill were used as indicative of disturbed areas within the dam that resulted from sediment erosion, transport, and

subsidence, specifically those disturbed areas related to the sinkhole. Inversion of surface wave dispersion curves into vertical shear wave velocity profiles along a series of lines that intersected the sinkhole and ran parallel to the strike of the upstream dam surface provided low-resolution yet interpretable images highlighting areas with low/ reduced compaction. Subsidence of layers within the dam volume, likely the result of erosion within the alluvium and pervious dam fill, appear to be directly responsible for the sinkhole.

Disturbed areas are evident on seismic reflection images in the rip-rap layer, pervious fill, impervious core, and natural alluvium from about 100 ft right and 80 ft or so left of the sinkhole. There are two reasonably well defined and unique subsidence trends or areas that are interpretable on reflection data below about 40 ft. Subsidence features interpreted right of the sinkhole are the most pronounced and appear to best connect with the vertical chimney structure encountered during trenching of the sinkhole and imaged on shear wave velocity cross-sections. Two smaller structures are interpreted left of the sinkhole with the larger of the two appearing to intersect bedrock near the location of an enlarged joint mapped during construction of the cutoff trench. This more extensive feature left of the sinkhole appears to have only affected the lower portion of the pervious fill material. The smaller of the two features seems either dormant or not yet large enough to have migrated vertically into the very near-surface material.

Based on data collected from borings drilled after the reflection data were collected, processed, and initially interpreted, it seems likely some irregularities observed on CMP stacked sections could be related to construction abnormalities not documented in the historical records. If the cutoff trench and core were dug and placed uniformly and the overlying pervious shell laid down in a horizontally consistent fashion, undulations in reflections from about 40 below ground surface down to the bedrock must have come as a result of differential settling related to either poor compaction or dissolution/erosion and subsidence. However, layers of concrete and placed clay were unexpected encountered in at least two of the borings. Speculation is that these materials were placed to help stabilize the cutoff trench or seal smaller joints adjacent to the two enlarged joints known to be cement filled. Borings were all placed offline and away from the areas identified as disturbed on the CMP stacked seismic sections to best accommodate the crosshole seismic study of the bedrock. The crosshole study is designed to investigate the most likely areas where interpretations of seismic reflection data indicate disturbed bedrock. As evident on the two seismic profiles separated by just over 40 ft, the material above bedrock changes quite dramatically across a very short distance within a 100 ft radius of the sinkhole.

Confirming key seismic interpretations will require borings be made directly on seismic line 1 at the following locations: about 50 ft right of the sinkhole, 30 ft right of the sinkhole, and 40 ft left of the sinkhole. The six-boring pattern completed at the time of this writing was designed to surround the fractured or altered limestone bedrock area. This pattern optimizes the crosshole tomography survey but provides little or no ground truth for the surface seismic data. Enhanced confidence and improved interpretations will be possible with borings dedicated to the surface seismic reflection and surface wave data.

This study was extremely successful in optimally applying non-invasive, high-resolution seismic techniques to target internal features of an earthen dam, a goal not routinely accomplished. Reflection data from this survey possess excellent frequency content and provide high-resolution images of the pervious shell as well as impervious core. A unique, optimized acquisition geometry was used to overcome the significant physical limitations imposed on this survey as a result of working on the dam face. Layers within the pervious shell separated by distances no more than several feet were delineated and mapped. Using the tightly spaced surface wave profiles it was possible to delineate the elongated chimney-like feature which represented the root of the sinkhole. If two or more boreholes are placed in key locations along seismic reflection line 1 it will be possible to develop an accurate map of the dam

structure which should be generally consistent with the construction records, but possess significantly more detail about internal geometries than possible with construction logs alone.

Introduction

In support of the U.S. Army Corps of Engineer’s strong commitment to dam safety, new and/or adaptations of existing technologies are being identified and evaluated at sites with both physical characteristics conducive to those technologies and failure potential. Proven correlation between acoustic properties and stiffness/rigidity is the basis for developing and implementing field-efficient, laterally continuous, non-invasive methods to accurately measure the seismic wavefield. As well, routine non-invasive appraisal of dam/dike core integrity is feasible and could prove quite valuable in some settings. Ultimately, the goal is to identify localized anomalous material zones—indicative of either dissolution activity or non-uniform compaction/ settling—prior to surface subsidence or the formation of vertically extensive chimney features. Seismic techniques hold vast potential for imaging and measuring materials in a fashion applicable to evaluations of dam integrity.

Clearwater Lake Dam, 30 miles northwest of Poplar Bluff, Missouri, was designed and constructed in the early 1940s as a control structure across the Black River (Figure 1). During the design



Figure 1: Aerial photo of Clearwater Dam. Sinkhole and seepage are indicated. Dikes extending into the lake were part of the 1989 retrofitting for seismic stability and seepage control.

and building of the cutoff trench two distinct and unique sets of enlarged joints were discovered in the limestone bedrock. Additional drilling suggested the joints were extremely localized and inferred to only extend several tens of feet beyond the cutoff trench excavation. Based on the trench and drill findings, the joints were filled with concrete consistent with the dam building practices of that time.

Sinkhole Chronology and Actions

On January 14, 2003, project personnel working at Clearwater Lake found a 10 ft diameter by 10 ft deep sinkhole (Figure 2). A sinkhole of this nature and location represented a threat to dam integrity and prompted a response by the dam owner. On January 17, 2003, a backhoe excavated the sinkhole down to 25 ft below ground surface where the diameter of the subsidence feature narrowed to 3 ft. The 25 ft deep excavation was backfilled with a clay plug, returning the dam surface to original grade. On February 15, 2003, with the first sizeable rainfall (1.2 in) since the installation of the clay plug came subsidence of the clay plug (3 in around the perimeter and 6 in at the center). The backfilled sinkhole has been under constant surveillance since it formed with no evidence of downstream seepage, upstream slumps, cracks, or whirlpools. Soil engineers describe the 6-ft thick clay blanket covering the upstream slope as being very compacted and probably hiding a void that likely formed during the summer of 2002 and then finally collapsed in January, forming the sinkhole.

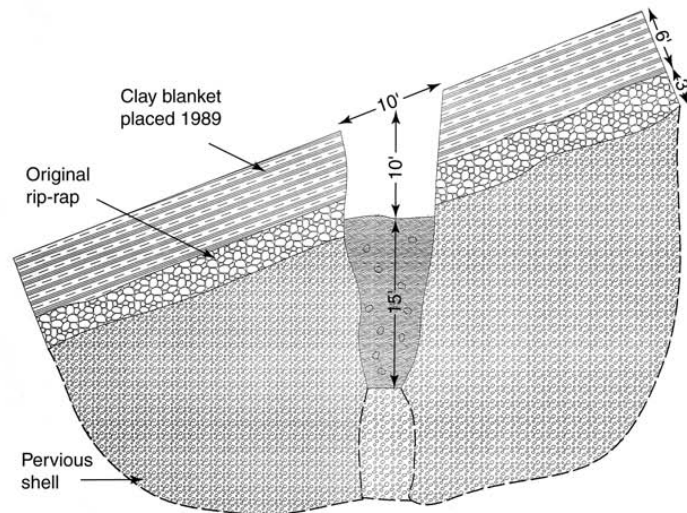


Figure 2: Material cross-section of sinkhole perpendicular to the axis of the dam. Dimensions and material classifications are based on findings of the excavation and backfill (figure from Hartung, 2003, USACE).

Program Objectives

Geophysics used during site characterization routinely involves relatively noisy measurements of earth properties, qualitatively incorporated into working subsurface models with ground truth provided by observational data sets (e.g., drilling, outcrop studies, etc.). Evaluation of dam and dike integrity and internal structures complicates and usually eliminates effective use of many geophysical tools due to layer geometries, conductive materials used during construction, utilities and operational workings, depth of investigations, and resolution requirements. Body wave seismic techniques have not been extensively used due to survey costs and resolution requirements. With equipment improvements and technique developments and the wealth of information contained in the seismic wavefield (body waves and surface waves), seismic measurement or imaging data are routinely underutilized (Steeple et al., 1995).

This applied research project was designed to evaluate the applicability of several seismic techniques to identify, evaluate, and delineate key physical characteristics and/or material properties

associated with failure risk within and beneath Clearwater Dam. High-resolution seismic reflection has been reasonably successful imaging unconsolidated materials from about 30 ft below ground surface to depths in excess of several hundred feet. As well, detection of fractures in sedimentary rocks has been a routine objective of seismic reflection surveys. Multichannel surface wave inversion techniques (MASW) have proven capable of detecting anomalous shear wave velocity zones within and below fill materials (Miller et al., 1999). Shear wave velocity studies of fill materials provides a general understanding of key engineering properties like stiffness and Poisson's ratio, leading to an increased awareness of areas susceptible to ground failure.

Program Components

Reflection

For the reflection data to be useful delineating bedrock fractures it is imperative to maximize the resolution potential, interpretability, and signal-to-noise ratio of reflection returning from within the dam. Intra-dam reflections provide improved time-to-depth conversions and a relative guide for determining real structures and anomalies observed on reflections from bedrock from artifacts. To maximize the chance of recording reflections from within the dam and alluvium beneath the dam, two CMP profiles (Mayne, 1962) were acquired using a single source line (located just above the sinkhole, along the access road at the top of the clay blanket) and two parallel 120-channel fixed spreads (one through the sinkhole and one below the terrace built around the sinkhole) offset from the source by 10 ft and 45 ft (Figure 3). This geometry was designed to maintain the optimum recording window and image the subsurface parallel to the dam axis, straddling the sinkhole's subsurface expression (Hunter et al., 1984). Data were acquired and processed to delineate local irregularities in stratigraphy, structure, and material properties from about 40 ft below ground surface to as deep as 250 ft below ground surface.

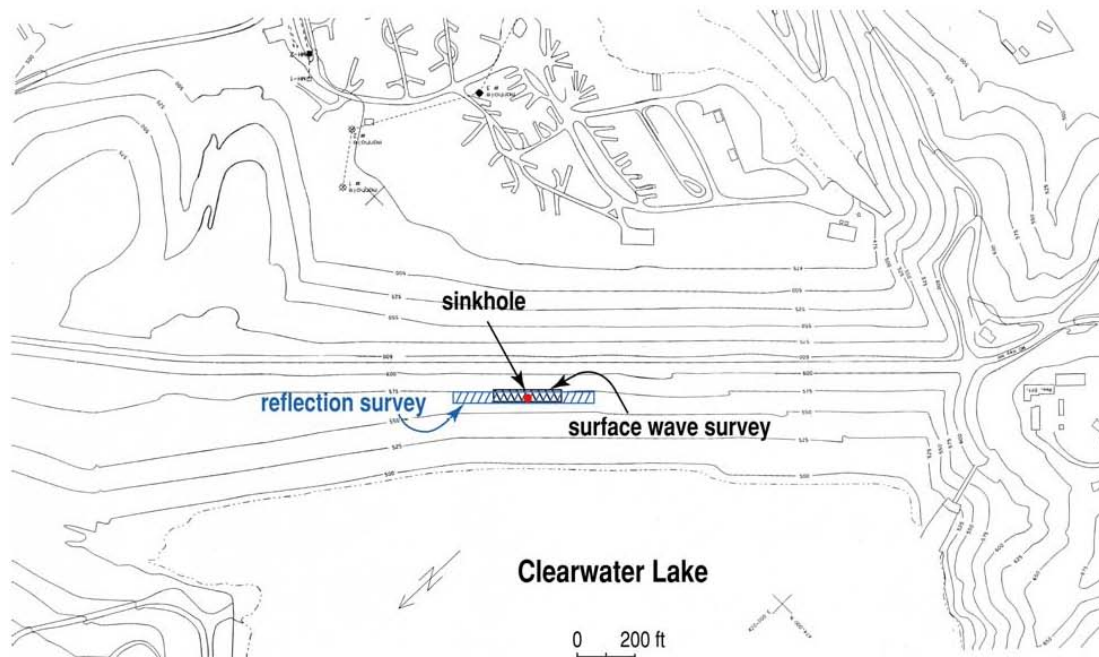


Figure 3: Site map with elevation contours, sinkhole, and planned locations of two seismic profiles (surface wave/tomography and high-resolution reflection).

Data acquisition and processing for the 2-D profile data generally followed well-established shallow high-resolution data acquisition methodologies, emphasizing correlation with ground truth, shear wave velocity profiles, and optimized velocity control for reflection coherency and resolution and accuracy of time-to-depth conversions (Hunter et al., 1984; Knapp and Steeples, 1986; Steeples and Miller, 1990).

Surface Wave Inversion

Surface wave data were acquired on six lines crossing the sinkhole parallel to the dam axis (Figure 3). Data were acquired simultaneously on two adjacent 120-station lines with the energy source moving incrementally from shot station to shot station between the two recording lines. Each profile used the same spread geometry and numbering sequence relative to a line perpendicular to the dam axis that split the sinkhole in half. Acquiring these data in this fashion permitted excellent line-to-line correlation and made it possible for 2½-D interpretations of the shear wave velocity field. With the unique requirements of surface wave measurements it was imperative to use an accelerated weight drop source, low frequency receivers, and close receiver spacing.

Data Acquisition

Data were acquired using different spread geometries for the two different types of data. All source and receiver lines were generally centered on the sinkhole (Figure 3). Energy recorded by two sub-parallel receiver lines was from a single energy source moving along an offset source line (Figure 4). This orientation provided twice the number of subsurface sample points per shotpoint, thereby improving the economics and the spatial sampling interval of the resulting sections. Two receiver lines and one source line were used for the reflection data and six receiver lines and three source lines provided the best subsurface coverage for surface wave data, considering the site limitations (Figure 5).

For ease in working on the sinkhole with heavy equipment, a clay bench was constructed to provide a level working surface on the side of the dam. This clay bench complicated the data processing some due to the nearly 3 ft change in elevation for receivers placed on the bench versus those into the clay blanket.

Unique geometries and equipment were necessary to optimize these two techniques for different portion of the subsurface, physical earth properties, and resolution requirements. For the reflection data, a pair of 120-channel lines with two 40 Hz L28E geophones per receiver station recorded three 10 second, 25 to 250 Hz IVI minivib sweeps at each shot station. All reflection ground stations were separated by 4 ft. Surface wave data are four shot vertical stacks of RAWD impacts that were recorded by two 120-station receiver lines each with a single GS11D 4.5 Hz geophone at each



Figure 4: View of RAWD traveling between two surface wave profiles (C1 and C2).

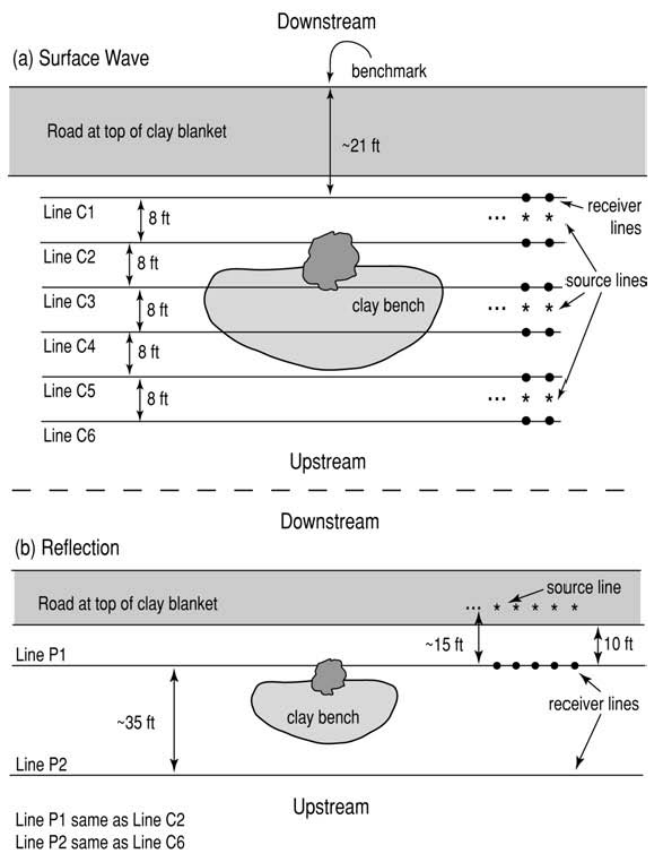


Figure 5: Line layout for surface wave data (a) and reflection data (b).

$\frac{1}{2}$ -wavelength and the radius of the Fresnel Zone as the fully resolvable horizontal limit, beds as thin as 4 ft and objects as small as 30 to 40 ft in diameter can be resolved.

Fundamental surface wave energy possesses excellent dispersive characteristics with a frequency range from 35 Hz down to as low as maybe 3 Hz, providing excellent penetration and near-surface resolution. Shot records of surface wave energy (Figure 7) are markedly different in appearance and wave properties in comparison to reflection shot gathers (Figure 6). The dominant energy traveling across the record is the surface wave also known as ground roll. With the excellent dispersive characteristics and frequency content evident in the shot gather it is no surprise that the dispersion curve is well formed and can be concisely interpreted (Figure 8). Penetration depths based on the half wavelength estimates could reach 50 to 60 ft providing reliable shear wave velocities to those depths.

Data points were surveyed in using a differential GPS unit sold by Trimble. The system included a 4700 base and 4800 rover unit providing x, y, and z accuracy of less than 1 inch. Line placement was dictated by location of the sinkhole, steepness of the upstream dam face, geometry of the sinkhole, and construction information. GPS readings were taken at key benchmarks and as many of the receiver and source stations as possible.

receiver station. Source and receiver stations for surface wave data were separated by 2 ft. Surface wave lines were about 240 ft long and extended about 50 ft upstream from the edge of the road at the top of the clay blanket. Reflection lines were almost 500 ft long with the upstream most line about 50 ft from the upstream edge of the road at the top of the clay blanket. All data for this study were recorded on a 24-bit, 240-channel Geometrics Strataview seismograph with a StrataVisor NZC controller. These acquisition parameters provided dense subsurface coverage over that area that appeared from surface investigations and construction documentation to be the most likely volume responsible for the sinkhole (Figure 5).

Several reflecting events are easily interpretable at times between 40 and 120 msec (Figure 6). Considering the velocity and near-surface conditions of this earthen dam structure, these reflections are of outstanding quality and quantity. With dominant frequencies around 200 Hz, normal moveout velocities (NMO) of 1500 ft/sec to 2500 ft/sec, and reflection hyperbolae that extend completely through the noise cone, resolution and signal-to-noise are much higher than expected. Using a practical vertical resolution limit of

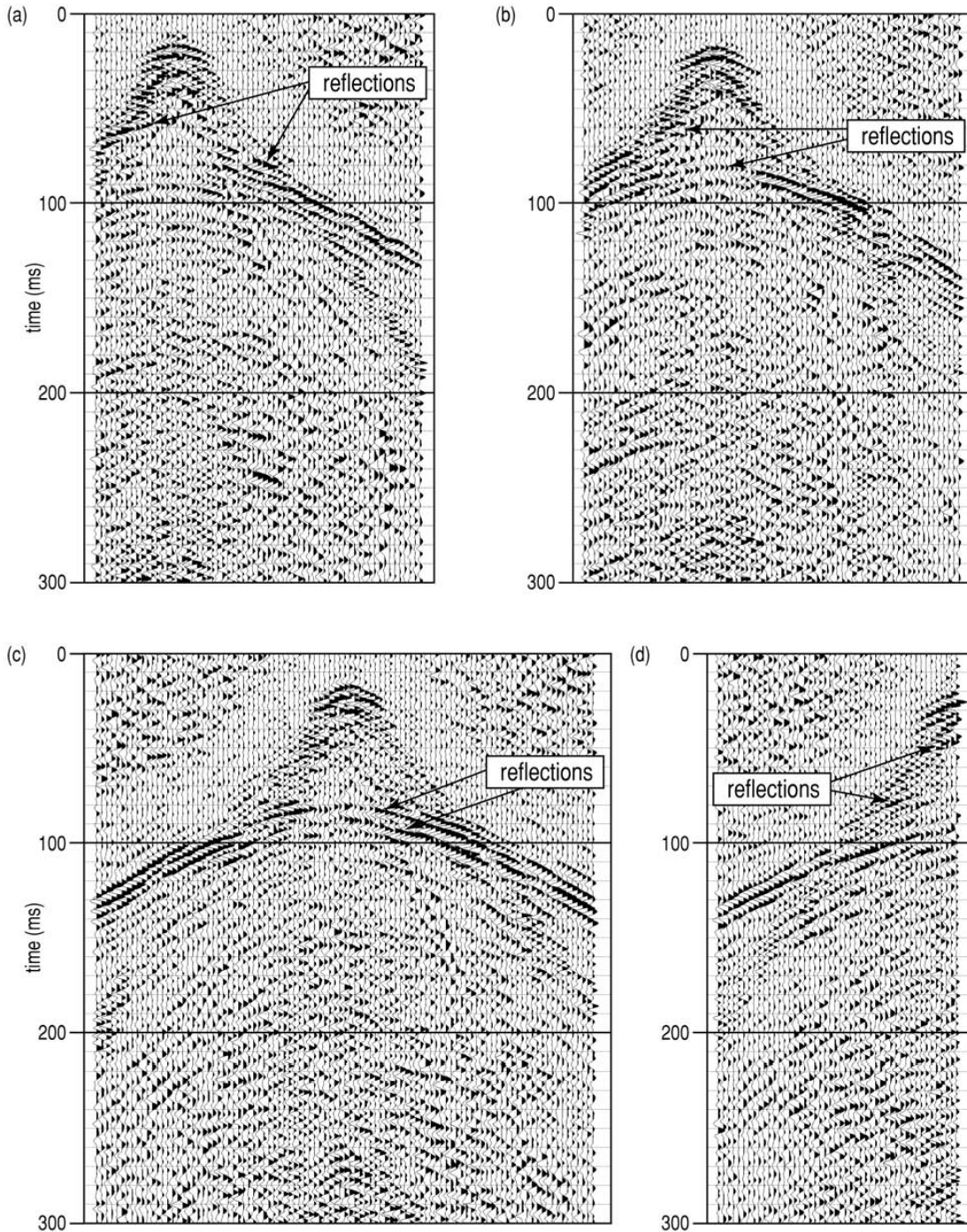


Figure 6: Representative shot gathers from across line P1. Reflections are evident on all these spectral balanced shot gathers. Based on stacking velocities, reflections from 80 msec are approximately 100 ft deep.

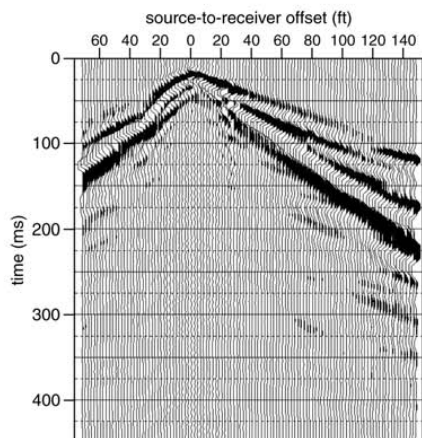


Figure 7: Surface wave shot gather.

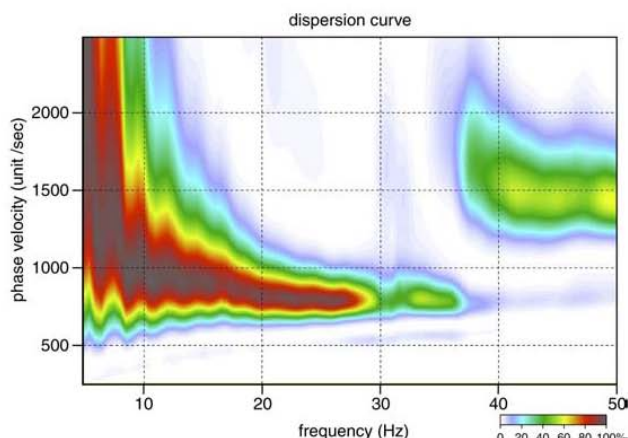


Figure 8: Surface wave dispersion curve.

Data Processing

Seismic Reflection

High-resolution seismic reflection data, by its very nature, lends itself to over-processing, inappropriate processing, and minimal involvement processing. Interpretations of high-resolution shallow reflection data must take into consideration not only the geologic information available, but also each step of the processing flow and the presence of reflection events on raw unprocessed data. Processing for the reflection portion of this study included only operations or processes that enhanced signal-to-noise-ratio and/or resolution as determined by evaluation of high confidence reflections interpreted directly on shot gathers (Figure 9). For the most part, processing of high resolution shallow reflection data is a matter of scaling down conventional processing techniques and methods; however, without extreme attention to details, conventional processing approaches will produce undesirable artifacts. In-field processing of the reflection data resulted in correlated shot gathers that were subject to a variety of scaling and filtering operations. In-field processing was coincident with data acquisition and did not impact the full day field schedules.

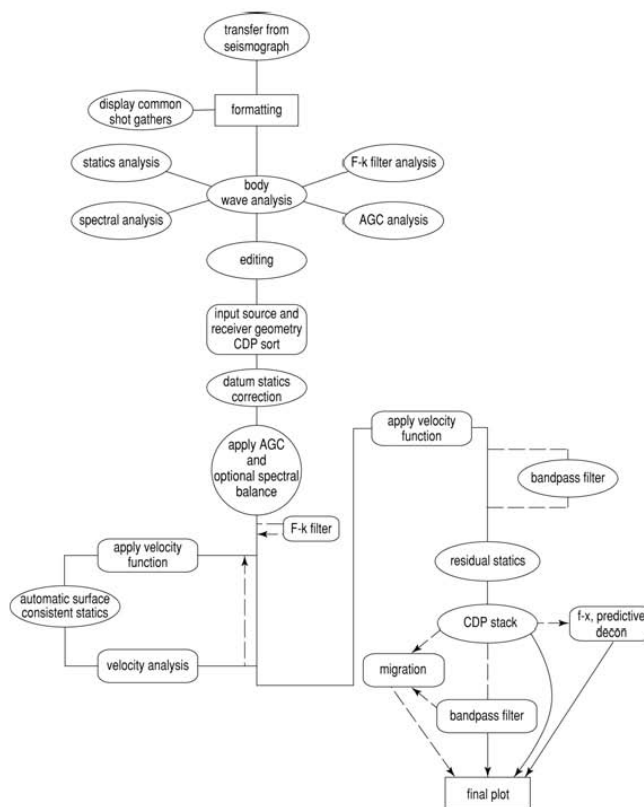


Figure 9: Generalized processing flow.

The basic architecture and sequence of processing steps followed during the generation of the final stacked sections were similar to conventional petroleum exploration flows (Yilmaz, 1987). The primary exceptions related to the step-by-step QC necessary for the highest confidence interpretations of shallow features and realization of full resolution potential (Miller et al., 1989; Miller et al., 1990; Miller and Steeples, 1991) (Figure 9). Specific distinctions relate to the emphasis placed on velocity analysis (Miller, 1992), lack of extensive wavelet processing, care and precision placed on muting, step-by-step analysis of effects of each operation on reflected energy, limiting statics operations to maximum shifts no greater than one-quarter wavelength of the dominant reflection energy with large correlation windows, and coincident iterative velocity and statics analysis.

Production Processing Surface Wave

To ensure accurate and consistent MASW results it is imperative to process only the optimum traces (selection based on source-to-receiver distance for a particular target interval) from each shot gather. For these data about 30 traces per gather were analyzed using the software package SurfSeis. Each shot gather (Figure 7) was transformed to produce one dispersion curve and assigned a surface location corresponding to the middle point of the spread (Figure 8). Care was taken to ensure that the spectral properties of the t-x data (shot gathers) were consistent with the maximum and minimum $f \cdot v_c$ values (v_c is the phase velocity of surface waves) contained in the dispersion curve. Estimating the dispersion curve in this fashion is both robust and allows identification and removal of coherent source noise on both the shot gather and dispersion curve (Park et al., 1998). Inverting the dispersion curve produces a shear-wave velocity profile as a function of depth (Figure 10). Assumptions necessary for this inversion, such as Poisson's ratio, density, and layer model, can be made with confidence considering the dependence of each on the shear wave velocity profile (Xia et al., 2000). Each shot gather produces a single velocity with depth trace that, when combined with velocity traces from all the shots along the survey line, produced 2-D shear wave velocity maps.

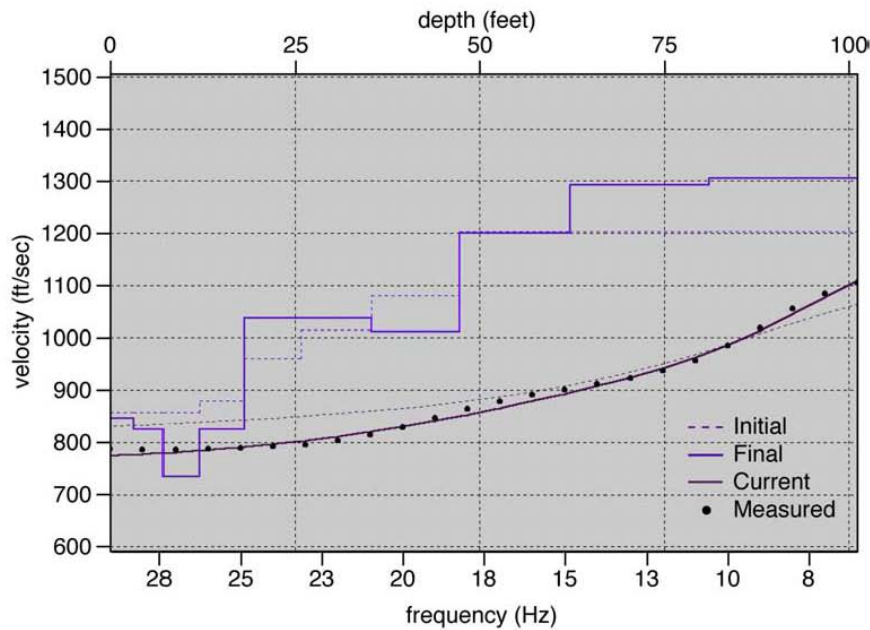


Figure 10: Shear wave velocity profile determined by inverting surface wave dispersion curves.

Interpretation

Interpretations for this paper are limited to identifying changes in subsurface layer geometry; amplitude, frequency, and phase characteristics that appear to relate to subsurface non-uniformities; and lateral variations in seismic properties. Shear wave velocity is commonly used as a measure of material rigidity or stiffness. Lateral changes in material properties are most obvious on 2-D shear wave images produced using continuous profiling techniques. Interpretation of shear wave velocity profiles for this investigation mainly focused on drops in shear wave velocity that could be correlated to the sinkhole location. Considering the age and construction of this earthen dam, compaction is going to naturally vary independent of any current or previous dissolution/erosion related activities. Changes in compaction could manifest themselves in reflection droop or shear wave velocity changes unrelated to the subsidence responsible for the sinkhole formation.

Shear wave velocity profiles targeted the upper 40 ft or so of the dam, focusing predominantly on areas near and below the sinkhole currently exhibiting characteristic consistent with zones of potential structural weakness. Data on some lines possessed sufficient low frequencies to allow interpretations of features as deep as 80 to 90 ft. The upstream extent of the subsurface disturbed zone associated with the sinkhole was of the greatest interest. One surface wave line was recorded downstream of the sinkhole, two over the sinkhole, and three were recorded upstream of the sinkhole. There appears to be little or no abnormality in the shear wave velocity downstream of the sinkhole. Only the first profile upstream (C4) seems to have a subsurface signature consistent with predicted subsidence effects on shear-wave velocity. Clearly from the surface wave data, the “root” of the sinkhole is a chimney-type structure and evident on profiles that cross directly through the the sinkhole and one immediately upstream of the sinkhole.

Line C3 provides the most dramatic view of the sinkhole “root” (Figure 11). From the line C3 cross-section it appears as though the affected subsurface is around 40 ft wide predominantly in the

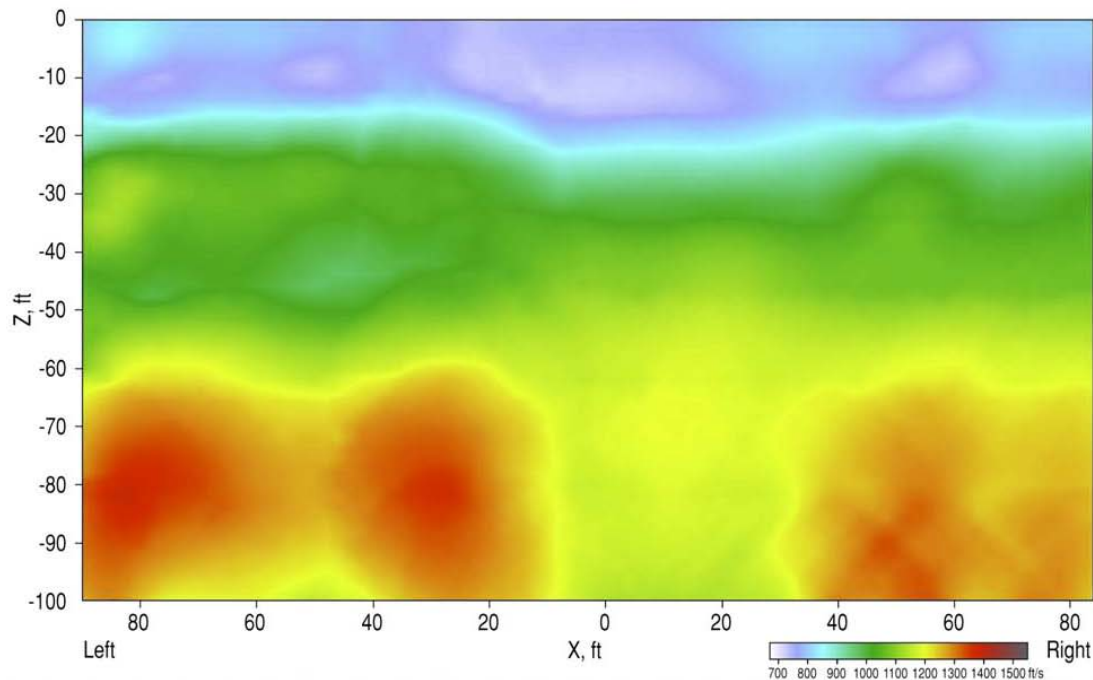


Figure 11: Clearwater Dam, Line C3, Vs, ft/s, 6-28 Hz frequency range.

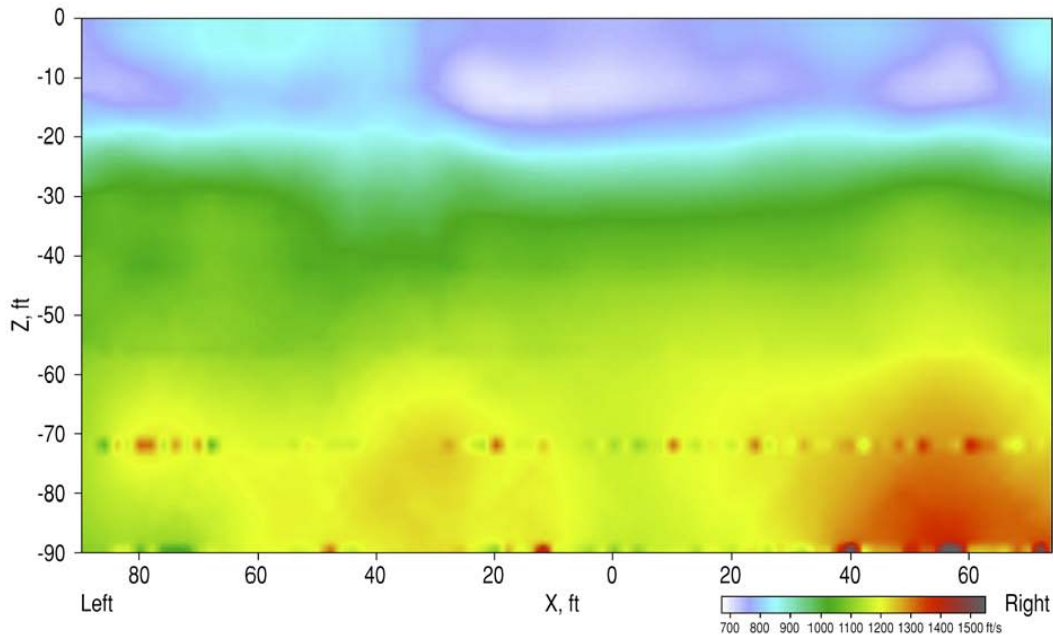


Figure 12: Clearwater Dam, Line C4, Vs, ft/s, 6-28 Hz frequency range.

right/left directions. Near-surface (upper 20 ft) the subsurface footprint of the sinkhole is well constrained and appears to be maybe 10 ft wide with some minor velocity reductions extending as far as 20 ft from the sinkhole center to the right. This wide zone of influence is not unexpected or inconsistent with the trenching that was completed near the time the sinkhole was first discovered. Vertical trenching suggested the subsidence was 10 ft wide at the ground surface narrowing to a diameter of just a few feet at around 20 ft below ground surface. This disturbed cone has a zone outside the physical subsidence area that will have altered shear wave velocities much larger than the subsidence feature itself. Clearly below 30 ft the zone of marked influence increases to almost 40 ft, asymmetric to the right of the sinkhole itself.

Mapping just the lowest velocity material and therefore looking at the largest lateral shear wave velocity gradient on line C4, the 10 ft diameter sinkhole appears well defined and very vertical (Figure 12). However, at increasing depths below 20 ft the footprint of the sinkhole becomes more pronounced with a more complex failure pattern below 60 ft than the simple sagging layers as apparent above about 20 ft. Without line C3 (Figure 11) it would be difficult to accurately place the subsurface area associated with the sinkhole on line C4 (Figure 12). Some of the variability in shear velocity is clearly related to non-uniform construction practices (e.g. drop in shear velocity at 25 ft below station 40 ft to 20 ft left of the center of the sinkhole). A localized drop in shear velocity below 60 ft is interpreted as related to the sinkhole. It is likely the subsurface expression of the sinkhole becomes irregular at these depths and in this case begins to enlarge upstream, but to a much smaller degree than it extends right at these same depths as evidenced on line C3.

Common midpoint (CMP) stacked sections provide an excellent glimpse into the internal layer geometry from bedrock to about 40 ft below ground surface. To insure the safety of the operation, the IVI minivib was used only along the road at the top of the clay blanket and therefore reflection data were acquired using a single source line (along the access road at the top of the clay blanket) and two parallel lines offset from the source 15 ft and 50 ft and straddling the sinkhole (Figure 5). Reflection frequencies were quite high considering the nature of the man made fill that composes this dam. Inter-

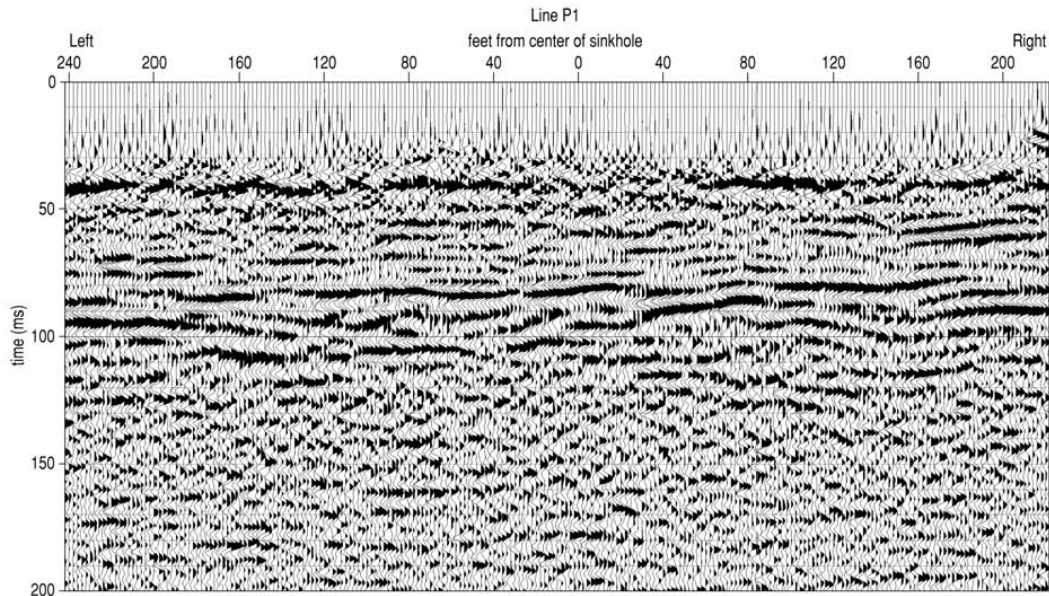


Figure 13: CMP stacked section from line P1. Reflections from the alluvium/clay core contact with the pervious fill is evidenced by the dramatic change in reflection character at about 80 ms.

pretable reflections are evident from about 50 ms to more than 100 ms on line P1, translating to a depth range from around 30 ft to 140 ft (Figure 13). While line P2 has reflections that can be interpreted from about 60 to 70 ms down to around 90 ms. This difference is related to source offset and therefore sampling of reflection points from uniquely different portions of the dam's internal structure. The coherent low frequency event on P1 at about 40 msec is a refraction artifact.

Data quality and resolution potential along line P1 are very good with coherent reflections returning from within the pervious fill and core/alluvium that possess dominant frequencies from 100 Hz to over 200 Hz (Figure 13). An obvious change in reflection characteristics marks the top of the impervious core at about 80 msec. Reflections from the top of the core are very irregular in geometry and coherency seeming to imply a lack of uniformity in the pervious fill/core contact. Considering where the subsurface sampling points are for this line, it is very likely some of this disturbed looking surface is a result of smear along the upstream face of the impervious core and the upstream toe of the core. With the reflection wavelet having a horizontal dimension that exceeds 50 ft, each reflection wavelet returning from the core surface is actually the average of not only the CMP on the sampling plane, but also information from points all along the upstream wedge (core toe) and the 1-to-1 slope of the clay core above the top of the alluvium across the entire 50+ ft sampling area. The wide sampling area effectively smears the information returning in the reflection wavelet so all the features within about a 50 ft circle around the reflecting point will be averaged into the reflection wavelet recorded from a particular CMP. With this resolution limitation in mind, distinguishing breaks in reflection coherency related to failure from artifacts related to non-uniform construction practices is very difficult.

Three areas can be identified on line P1 with reflection geometries that imply subsidence and therefore reduced compaction of the fill (Figure 14). Most significant is the apparent subsidence, mapped through reflection droop, that originates beneath the sinkhole and angles to the right through the pervious fill and clay core ending at the top of bedrock where reduced amplitudes and scattered seismic energy seem to suggest fracturing. This is clearly the most pronounced and likely candidate volume possibly representing the "root" of the sinkhole. Another volume that appears to have reflection

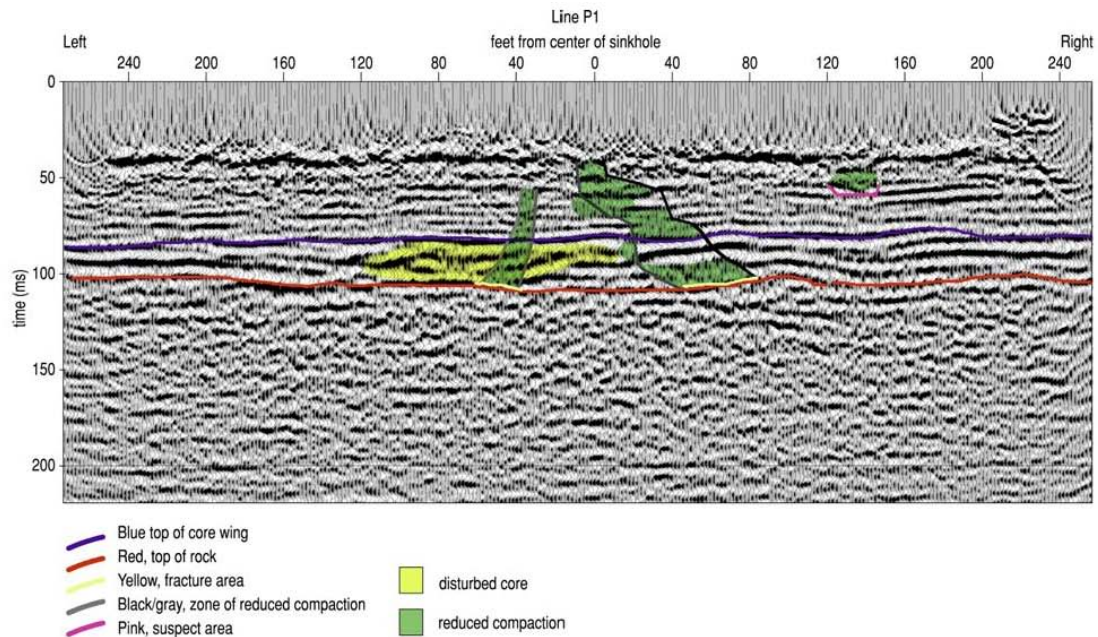


Figure 14: Interpreted CMP stack of line P1 showing key layers and abnormalities.

geometries consistent with the subsurface model of subsidence features is about 30 ft left of the sinkhole and can be described as a relatively narrow chimney like feature that appears to correlate to a section of the bedrock characterized by disturbed reflections with reduced coherency, signal-to-noise, and minor scattering. This feature does not have a direct tie to the sinkhole location nor to the trenching that was done to over 20 ft tracking the sinkhole into the subsurface. A third and final area with unusual reflection geometries is about 130 ft right of the sinkhole and appears to be a construction remnant. It relates to an area of the core (based on reflections) that possesses some sag, similar in nature to those observed beneath gradual subsidence features.

One more area on line P1 that bears monitoring and possibly further investigation is located within what is interpreted as the impervious core toe or wedge between the sinkhole and about 120 ft left of the sinkhole (Figure 14). This zone is characterized by lower frequency and highly undulating reflection events. Considering the size of the horizontal sampling zone, it is not possible to say definitely that this unusual character is due to reduced competence or if this is a construction artifact associated with the apparent trouble that was experienced in grouting the enlarged joints and retaining the integrity of the core trench. However, until an invasive sample is taken, it will not be possible to constrain the interpretation further.

Combining the interpretations of all the seismic data, the sinkhole appears to have formed as a result of dissolution/erosion of materials right of the sinkhole itself following a path that leads to the horizontal extension of the known enlarged joint pattern. It is therefore imperative to find the path fluids took when moving sediment out of the dam interior and downstream if there is any hope of effectively remediating the structure. A cross-hole seismic survey has investigated the apparent fractures observed on seismic reflection data on the bedrock surface. Construction materials (neat grout and placed clay layers) were encountered in boreholes drilled based on seismic data in places not expected from construction records alone. These unexpected encounters implies the core trench was likely much larger in this area than planned and possibly responsible for some of the irregular reflection arrivals interpreted as disturbed materials.

One boring encountered concrete above bedrock and a river gravel and two others placed clay layers inside alluvial zone and neat grout just above rock. These abnormalities are indicative of real-time fixes to problems encountered during construction but not reported in any known surviving documentation. If these materials are laterally continuous across distance as short as a few 10s of feet they could produce reflections with irregular wavelet attributes, possess characteristics potentially indicative of subsidence (droop, amplitude variability, extreme dips, etc.), and/or difficult to correlate with dam designs and therefore assumed related to changes in internal dam structure since construction.

Conclusions

It appears from the two data sets that the narrow “chimney” that has been observed to depth in excess of 20 ft through vertical trenching is significantly wider below about 30 or 40 ft from the ground surface and trends to the right along a narrow finger like corridor. This elongated to the right and very irregular pattern is for the most part associated with a predominantly vertical meander pattern. The overall seismic data quality appears excellent with greater penetration of the surface wave data than expected and shallower imaging with the P-wave data than planned. Disturbed bedrock and dam materials are interpretable on seismic data and provide insight into the mechanism responsible for the remove of sediment and eventual subsidence within the dam.

Surface Wave Analysis

Data from the shallow portion of the sections (upper 15 ft) is not nearly as accurate as was planned. For the most part this is due to the presence of the sinkhole and its effect on wave propagation associated with the 25 Hz to 60 Hz frequency band. The deeper data however does possess very good signal-to-noise and therefore equally as good convergence to a solution.

P-wave Reflection Data

The reflection data were excellent and much better than expected. With upper corner frequencies extending well beyond 300 Hz the data resolution was sufficient to all the detection of layering within the dam shell material (pervious fill), likely indicative of the layering and compaction sequences used during construction. This higher than expected resolution also allows the expression of the sinkhole to be tracked from about 40 ft below the ground surface down to the top of bedrock with unusual accuracy and associated confidence.

Starting at the top of the section beneath the sinkhole, a downdropped reflection can be seen at about 50 ms with equates to about 45 ft. This zone is about 15 ft wide and extends from about station 8 ft right to 8 ft left of the sinkhole, from here it drifts strongly to the right side. At about 70 ft it appears to widen from 10 ft left of the sinkhole to over 40 ft right of the sinkhole. Looking deeper into the section the “chimney” or subsidence-altered zone appears to meander around stronger or more resistant layers, with these stronger layers forming bridges or in some cases subsiding intact. At the top of the clay core, interpreted at about 80 ms (~100 ft) the subsiding materials have left either the top or a reflective layer near the top offset a bit. The void or less competent area in the subsurface continues to move right where at the bedrock surface correlates with a set of what appear to be fractures located between 80 ft and 20 ft right of the sinkhole. These inferred fractures correlated quite closely to the projection of the enlarged joints observed during dam construction.

References

- Hunter, J.A., S.E. Pullan, R.A. Burns, R.M. Gagne, and R.L. Good, 1984, Shallow seismic reflection mapping of the overburden-bedrock interface with the engineering seismograph—Some simple techniques: *Geophysics*, v. 49, p. 1381-1385.
- Knapp, R.W., and D.W. Steeples, 1986, High-resolution common-depth-point, seismic-reflection profiling: Field acquisition parameter design: *Geophysics*, v. 51, p. 283-294.
- Mayne, W.H., 1962, Horizontal data stacking techniques: Supplement to *Geophysics*, v. 27, p. 927-938.
- Miller, R.D., 1992, Normal moveout stretch mute on shallow-reflection data: *Geophysics*, v. 57, p. 1502-1507.
- Miller, R.D., D.W. Steeples, and M. Brannan, 1989, Mapping a bedrock surface under dry alluvium with shallow seismic reflections: *Geophysics*, v. 54, p. 1528-1534.
- Miller, R.D., and D.W. Steeples, 1991, Detecting voids in a 0.6-m coal seam, 7 m deep, using seismic reflection: *Geoexploration*, Elsevier Science Publishers B.V., Amsterdam, The Netherlands, v. 28, p. 109-119.
- Miller, R.D., D.W. Steeples, and P.B. Myers, 1990, Shallow seismic-reflection survey across the Meers fault, Oklahoma: *GSA Bulletin*, v. 102, p. 18-25.
- Miller, R.D., J. Xia, and C.B. Park, 1999, MASW to investigate subsidence in the Tampa, Florida area: Kansas Geological Survey Open-file Report 99-33.
- Park, C.B., R.D. Miller, and J. Xia, 1998, Imaging dispersion curves of surface waves on multi-channel record [Exp. Abs.]: Soc. Expl. Geophys., p. 1377-1380.
- Steeple, D.W., and R.D. Miller, 1990, Seismic reflection methods applied to engineering, environmental, and groundwater problems: Soc. Explor. Geophys. Investigations in Geophysics no. 5, Stan H. Ward, ed., *Volume 1: Review and Tutorial*, p. 1-30.
- Steeple, D.W., C.M. Schmeissner, and B.K. Macy, 1995, The evolution of shallow seismic methods: *Journal of Environmental and Engineering Geophysics*, v. 0, n. 1, p. 15-24 (invited paper).
- Xia, J., R.D. Miller, and C.B. Park, 2000, Advantages of calculating shear-wave velocity from surface waves with higher modes: [Exp. Abs.]: Soc. Expl. Geophys., p. 1295-1298.
- Yilmaz, O., 1987, Seismic data processing; S.M. Doherty, ed.; in Series: Investigations in Geophysics, no. 2, E.B. Neitzel, series ed.: Soc. Explor. Geophys.

Miller, R.D., 2003, High-resolution seismic-reflection investigation of a subsidence feature on U.S. Highway 50 near Hutchinson, Kansas; in K.S. Johnson and J.T. Neal, eds., Evaporite karst and engineering/environmental problems in the United States: Oklahoma Geological Survey Circular 109, p. 157-167.

High-Resolution Seismic-Reflection Investigation of a Subsidence Feature on U.S. Highway 50 near Hutchinson, Kansas

Richard D. Miller

Kansas Geological Survey
Lawrence, Kansas

ABSTRACT.—High-resolution seismic reflections were used to map the upper 150 m of the ground surface around and below an actively subsiding sinkhole currently affecting the stability of U.S. Highway 50 in Reno County, Kansas. Primary objectives of this study were to delineate the subsurface expression of this growing sinkhole induced by salt dissolution and appraise its threat to highway stability and the characteristically heavy commercial traffic load. The high signal-to-noise ratio and resolution of these seismic-reflection data allowed detection, delineation, and evaluation of rock failure and associated episodes of material collapse into voids left after periodic and localized leaching of the 125-m-deep, 40-m-thick Hutchinson Salt Member of the Wellington Formation (Permian).

Mechanisms and gross chronology of structural failures as interpretable from stacked seismic sections suggest that initial subsidence and associated bed offset occurred as accumulated stress was rapidly released and was constrained to a tensional dome defined by reverse-fault planes. As the downward movement (settling, relaxation) of sediments slowed with little or no incremental buildup of stress, gradual subsidence continued in the subsurface, advancing as an ever-expanding bowl, geometrically defined by normal-fault planes.

INTRODUCTION

Sinkholes are common hazards to property and human safety the world over (Beck and others, 1999). Their formation is generally associated with subsurface subsidence that occurs when overburden loads exceed the strength of the roof rock bridging voids or rubble zones formed as a result of dissolution or mining. Understanding sinkhole processes and what controls their formation rate is key to reducing their impact on human activities, and in the case of anthropogenic causes, potentially avoiding their formation altogether. Sinkholes can form naturally or anthropogenically from the dissolution of limestone (karst), gypsum, or rock salt, or from mine/tunnel collapse. With the worldwide abundance of limestone, karst-related sinkholes are by far the most commonly encountered and studied. Both simple and complex sinkholes have formed catastrophically and/or gradually as the result of dissolution of limestone or rock salt, and by natural and man-induced dissolution processes in many parts of Kansas (Merriam and Mann, 1957).

In central Kansas, most sinkholes are the result of leached-out volumes of the Permian Hutchinson Salt Member of the Wellington Formation (Watney and others, 1988). Sinkholes that have formed above salt layers have been studied throughout Kansas (Frye, 1950; Walters, 1978) and the United States (Ege, 1984). Studies of subsidence related to mining of the

salt around Hutchinson, Kansas (Walters, 1980), disposal of oil-field brine near Russell, Kansas (Walters, 1991), and natural dissolution through fault/fracture-induced permeability (Frye and Schoff, 1942) have drawn conclusions about the mechanism responsible for subsidence geometries and rates based on surface and/or borehole observations.

Using only surface observations and borehole data, a great number of assumptions and a good deal of geologic/mechanical sense must be drawn on to define and explain these features and their impact. High-resolution seismic-reflection profiling has proven an effective tool in three-dimensional (3-D) mapping of the subsurface expression and predicting future surface deformation associated with dissolution of the Hutchinson Salt in Kansas (Steeple and others, 1986; Miller and others, 1993, 1995, 1997; Anderson and others, 1995a).

Salt-dissolution sinkholes are found in all areas of Kansas where the Hutchinson Salt is present in the subsurface. Sinkholes have been definitely correlated to the failed containment of disposal wells into which oil-field brine was injected. This correlation was determined by means of stem pressure tests and/or seismic-reflection investigations at a variety of sites throughout central Kansas (Steeple and others, 1986; Knapp and others, 1989; Miller and others, 1995, 1997). Sinkholes that have formed by natural dissolu-

Miller, R. D., 2003, High-resolution seismic-reflection investigation of a subsidence feature on U.S. Highway 50 near Hutchinson, Kansas, in Johnson, K. S.; and Neal, J. T. (eds.), *Evaporite karst and engineering/environmental problems in the United States*: Oklahoma Geological Survey Circular 109, p. 157-167.

tion and subsidence processes are most commonly documented at the depositional edges on the west and north and at the erosional boundary on the east of the Hutchinson Salt (Frye and Schoff, 1942; Frye, 1950; Merriam and Mann, 1957; Anderson and others, 1995a). The vast majority of published works studying the source of localized leaching of salt in Kansas directly contradict suggestions that recent land subsidence in Kansas is mostly natural in origin (Anderson and others, 1995a).

Natural dissolution of the Hutchinson Salt is not uncommon in Kansas and has been occurring for millions of years (Ege, 1984). Faults extending up to Pleistocene sediments containing fresh water under hydrostatic pressure are postulated as the conduits that instigated salt dissolution and subsidence along the western boundary of the salt in Kansas (Frye and Schoff, 1942). Paleosinkholes resulting from dissolution of the salt before Pleistocene deposition were discovered previously with high-resolution seismic surveys (Anderson and others, 1998).

Subsidence can occur at rates ranging from gradual to catastrophic. These rates are, to some extent, related to the type of deformation in the salt (ductile or brittle) and the strength of rocks directly above the salt layer. As salt is leached, the resulting pore space provides the differential pressure necessary to support creep (Carter and Hansen, 1983). If this pore space gets large enough to exceed the strength of the roof rock, the unsupported span will fail, and subsidence occurs. Depending on the strength of the roof rock, and therefore the size of the void, characteristics of the failure within and just above the salt will dictate how the void progresses upward until it eventually reaches the ground surface. In general, gradual surface subsidence is associated with ductile deformation that, besides vertically sinking, progresses outward, forming an ever-growing bowl-shaped depression with bed geometries and offsets constrained by normal-fault geometries (Steeple and others, 1986; Anderson and others, 1995b). When rapid to catastrophic subsidence rates are observed, failure within the salt is usually brittle, with the void area migrating to the surface as an ever-narrowing cone with bed offsets and rock failure controlled by reverse-type fault planes (Davies, 1951; Walters 1980; Rokar and Staudtmeister, 1985).

Seismic-reflection data targeting beds altered by dissolution and subsidence in this area have ranged in quality and interpretability from poor (Miller and others, 1995) to outstanding (Miller and others, 1997). Interpretations from poor-quality data have unfortunately been relegated to indirect inference of structural processes and subsurface expression (mainly from interpretations of structural deformation in layers above the salt) owing to low signal-to-noise ratios. However, data with excellent signal-to-noise ratios and resolution have allowed direct detection of structures and geometries that appear characteristic of complex sinkholes. The resolution potential and signal-to-noise

ratio of seismic data from this study are superior to those of any studies previously published that have targeted the salt interval. These data provide conclusive images of important structural features and unique characteristics that control sinkhole development.

The sinkhole that is the subject of this study is centered a few tens of meters northwest of the intersection of U.S. Highway 50 and Victory Road in Reno County (Fig. 1). The symmetry and compact nature of the sinkhole, as well as its subsidence rate, are consistent with conceptual models of sinkhole formation when salt is leached by borehole-released fluids (Miller and others, 1997). These similarities in geometry and subsidence rates raise suspicions that this feature might somehow be related to the disposal of oil-field wastewater, even though no records or surface installations exist to support that suggestion. Two seismic-reflection profiles acquired orthogonally, and centered on the intersection of the highway and county road, provided optimal coverage for mapping bed geometries, growth potential, and future surface footprints for identifying structural characteristics that might someday put vehicle traffic at risk.

GEOLOGIC SETTING

Several major salt basins exist throughout North America (Ege, 1984). The Hutchinson Salt Member of the Wellington Formation is present in central Kansas, northwestern Oklahoma, and the northeastern part of the Texas Panhandle and is prone to, and has an extensive history of, dissolution and formation of sinkholes (Fig. 1). In Kansas the Hutchinson Salt possesses an average net thickness of 76 m and reaches a maximum of >152 m in the southern part of this salt basin. Deposition that occurred during fluctuating sea levels caused numerous halite beds, 0.15 to 3 m thick, to be interbedded with shale, minor anhydrite, and dolomite/magnesite. Individual salt beds may be continuous for only a few miles, despite the remarkable lateral continuity of the salt as a whole (Walters, 1978).

Rock salt under a depositional load is almost incompressible, highly ductile, and easily deformed by creep (Baar, 1977). Plastic deformation of the salt associated with creep is expected naturally to occur in these salts (Anderson and others, 1995b). Thin anhydrite beds within the halite succession have a strong acoustic response. Considering the extreme range of possible strain rates the salt can undergo during creep deformation, some of these thin interbeds possess quite dramatic, high-frequency folds within relatively short distances.

Red-bed evaporites that overlie the Hutchinson Salt are a primary target of any study in Kansas that looks at salt-dissolution sinkhole development and associated risks to the environment and human activity. The failure and subsidence of these evaporite units are responsible for the eventual formation of sinkholes and provide a pathway for ground water to gain access to

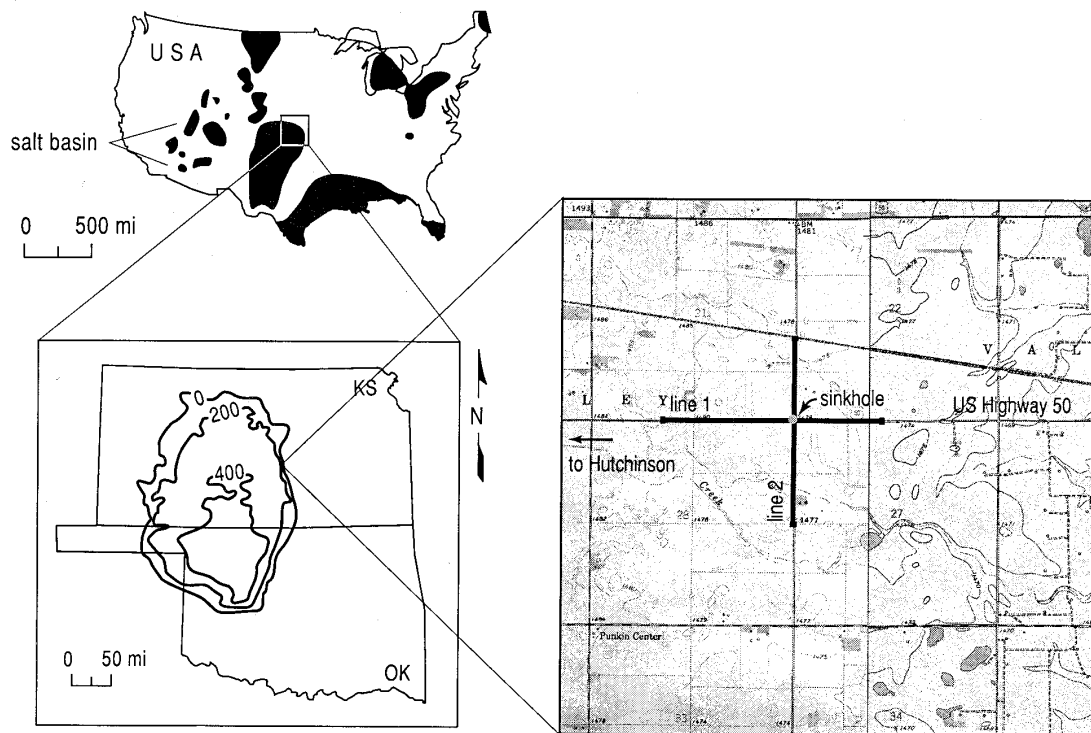


Figure 1. Site map relative to bedded salt deposits. The Hutchinson Salt is a bedded salt deposit extending from central Oklahoma across most of south-central Kansas. Along the eastern extremity of the salt bed is the currently active dissolution front responsible for many natural dissolution features, both sinkholes and paleosubsidence. Two 1.2-km seismic profiles tie at the intersection of U.S. Highway 50 and Victory Road in Reno County, Kansas.

the salt. In proximity to the dissolution front, fractures, faults, and collapse structures compromise the confining properties of the Permian shale bedrock and put the major freshwater aquifer (the Pliocene–Pleistocene Equus Beds) in this part of southern Kansas at risk. Along the eastern boundary (dissolution front), the salt, which ranges from 0 to >100 m thick, is buried beneath ~120 m of Permian red-bed evaporites.

The eastern margin of the salt was exposed during the late Tertiary Period, when erosion and leaching began the 30-km westward progression of the front to its present-day location (Bayne, 1956). The ability of the front to migrate while under as much as 100 m of sediments was a direct consequence of ready access to an abundant supply of ground water (Watney and others, 1988). The subsidence of Permian, Cretaceous, and Tertiary rocks has progressed along the migration front as the salt has been leached away. While this subsidence was going on, Quaternary alluvium was being deposited in volumes consistent with the amount of salt that was being removed. These processes resulted in today's moderate to low surface relief that masks the extremely distorted (faulted and folded but non-tectonic) rock layers within the upper Wellington Formation and the overlying Ninnescah Shale (Anderson and others, 1998). About 30 m of salt is still in

place at the U.S. 50–Victory Road site, where a maximum of ~85 to 100 m once existed.

Most of the upper 700 m of rock at this site consists of Permian shales (Merriam, 1963). The currently disputed Permian–Pennsylvanian boundary is ~700 m deep and seismically marked by a strong sequence of cyclic reflecting events. The Chase Group (top at 250 m deep), Lower Wellington shales (top at 175 m deep), Hutchinson Salt (top at 125 m deep), Upper Wellington shales (top at 70 m deep), and Ninnescah Shale (top at 25 m deep) make up the packets of reflecting events easily identifiable and segregated within the Permian portion of the section. Bedrock is defined as the top of the Ninnescah Shale, with the unconsolidated Pliocene–Pleistocene Equus Beds making up most of the upper 30 m of sediment. The thickness of Quaternary alluvium that fills the stream valleys and paleosubsidence features ranges from 0 to as much as 100 m, depending on the dimensions of the features.

SEISMIC ACQUISITION

To ensure that the entire subsurface “root” of the sinkhole was clearly imaged, the survey was designed with two seismic lines, each possessing at least 1.0 km of full-fold subsurface coverage centered on the sinkhole (Fig. 1). With the sinkhole conveniently lo-

cated at the intersection of U.S. 50 and Victory Road, two orthogonal seismic lines were acquired along the roads where surface materials and coupling were relatively consistent. These data were acquired using a rolling fixed-spread design that eliminated the need for a roll-along switch and extended the range of far offsets available during processing. This survey design provided the wide range of source offsets necessary for detailed velocity analysis, and the close receiver spacing for improved confidence in event identification; and it maximized the range of imageable depths.

Acquisition parameters were defined on the basis of experience and walkaway tests along line 1 (Fig. 1). Twin Mark Products L28E 40-Hz geophones were planted at 2.5-m intervals in approximate 1-m arrays. They were planted into firm to hard soil at the base of the road ditch in small divots left after the top few inches of loose material was removed to ensure good coupling. Four 60-channel Geometrics StrataView seismographs were networked to simultaneously record 240 channels of data. An IVI Minivib using a prototype Atlas valve delivered three 10-s, 25–250-Hz upsweeps at each 5-m spaced shot location. Experiments at this site were consistent with bench tests, which suggested that this new rotary-valve design will produce up to 4 times the peak force of conventional valves at 250 Hz. The pilot was telemetried from the vibrator to the seismograph and recorded as the first trace of each shot record. Each of the three sweeps generated per shot station was individually recorded and stored in an uncorrelated format with the ground-force pilot occupying channel 1.

Reflections can be interpreted on raw, correlated shot records (scaled for display purposes) from ~30 ms to two-way-traveltime depths >500 ms (Fig. 2). Considering the optimum window (Hunter and others, 1984) these data possess, it was imperative to keep a wide range of offsets to ensure that the entire target zone was imaged. Reflections with dominant frequencies of ~200 Hz can be interpreted as deep as 200 ms, whereas the dominant frequency of reflections at 500 ms have dropped to ~100 Hz. Several milliseconds of reflection “chatter” observable between traces in proximity to the sinkhole is indicative of the dramatic localized changes in material velocities associated with rock-layer failure and subsidence. Considering that the dominant frequency of some reflections exceeds 200 Hz, a 2.5-ms static between adjacent traces represents a 180° phase shift and complete cancellation. Therefore, it is critical that these static irregularities be compensated for before the data are CMP (common-midpoint) stacked.

SEISMIC PROCESSING

The basic CMP processing flow was consistent with 2-D high-resolution seismic-reflection methodologies (Steeple and Miller, 1990). All lines were processed using WinSeis2, beta seismic-data-processing software

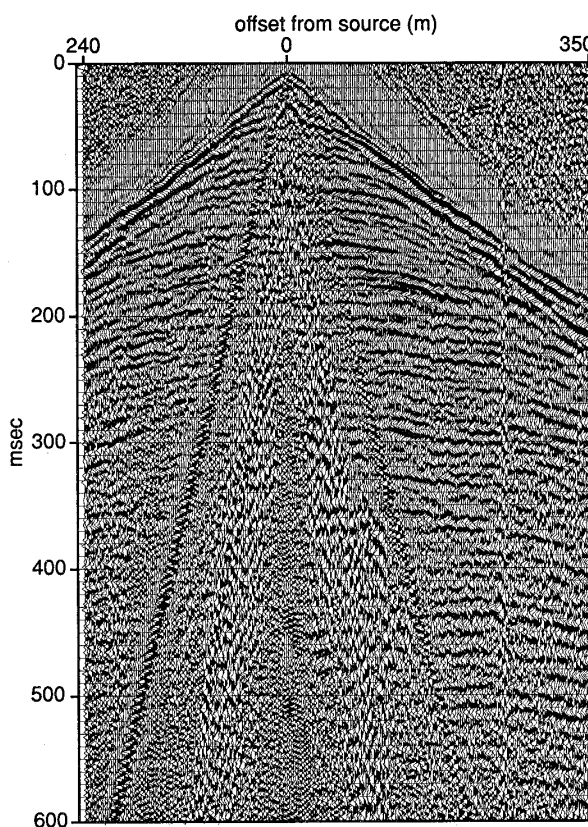


Figure 2. Representative 240-channel shot gather with 2.5-m receiver spacing and IVI Minivib source, scaled for display. Dozens of reflections are interpretable in the upper 600 ms. The top of salt is indicated by the high-amplitude reflection at ~130 ms.

(next generation of WinSeis Turbo) from the Kansas Geological Survey. Any reflection data acquired in this highly disturbed subsurface setting will be plagued with static problems and subject to dramatic swings in NMO (normal-moveout) velocity over relatively short distances; this data set was no exception. For the purposes of this survey the surface topography was flat with the exception of the 1-m-deep low associated with the 100-m-wide sinkhole. Changes in velocity related to differentially compacted fill, anomalous rubble zones, and distorted rock layers produced several millisecond fluctuations in event-arrival times across distances of 5 to 10 m. In extreme cases, shifts of 10 ms can be measured across a span of <10 m.

SEISMIC INTERPRETATION

The confident interpretation of reflections on shot gathers is essential to optimizing the acquisition, processing, and interpretation of high-resolution seismic-reflection data. Dozens of reflections dominate the average shot gather from this site (Fig. 2). Reflections throughout the primary time–depth target window

(50–200 ms) possess broad spectral bandwidths and sufficient coherency to interpret reflections clearly across several to tens of traces. The irregular seesaw (zigzag) pattern evident in reflections across several traces denotes static related to lateral velocity irregularities. The nonlinear pattern observed in the first arrivals is the result of velocity irregularities, either at or very near the bedrock surface or between bedrock and the ground surface. Reflection events can be traced through the air-coupled wave and just into the ground-roll wedge. To avoid any contamination by the air-coupled wave, all energy after the air wave was removed during processing.

For quality-control reasons, it is important that reflections interpreted at two-way traveltimes <30 ms on CMP stacks can be correlated with equivalent 30-ms reflection hyperbolae on shot gathers. This consistency between shot records and stacked sections can be seen at various places along both lines of this survey (Fig. 3). Identification of these reflections on field files, and tracking them throughout the processing flow, were necessary to ensure that CMP sections were correctly stacked and interpreted. Ultra-shallow reflections (<30 ms) were a critical aspect in discerning the times since the Permian that these sediment-filled sinkholes may have been active. Besides the reflection “chatter” indicative of lateral variations in material velocity, a striking characteristic of these seismic data is the contradictory effects of AVO (amplitude variation with offset), depending on source and receiver orientation (Fig. 3B). Changes in reflection amplitude in this setting could be indicative of changes in acoustic impedance of the reflector itself and/or lateral variations in attenuation owing to rock failure and collapse. True amplitude analysis intended to search for localized changes in material properties, possibly indicative of changes indicating increased loading, does not seem to be an effective first-order tool at this site.

High signal-to-noise ratio and bed-resolution potential of observed reflections on shot and CMP gathers between ~20 and 350 m deep suffer little degradation as a result of horizontal stacking (Figs. 4, 5). Bed resolution on the order of 2 to 4 m, depending on specific reflections, was more than sufficient for confident delineation of rock layers distorted by collapse into voids left after rock salt was leached away. The Permian bedrock surface varies in and around the subsidence features from 25 to as much as 50 m below ground surface with drape in the Equus Beds clearly interpretable within the upper 40 ms beneath station 2400 (Fig. 4). Between the surface of bedrock and the top of salt is a 125-ft-thick sequence of red-bed evaporites comprising mostly shales. The highly plastic nature of these shale units is evident in the conformal nature of the folding that overlies the highly altered beds of the salt unit. Amplitude changes across these folded units are interpreted only in a very general fashion as related to compaction, bridging, and energy scatter-

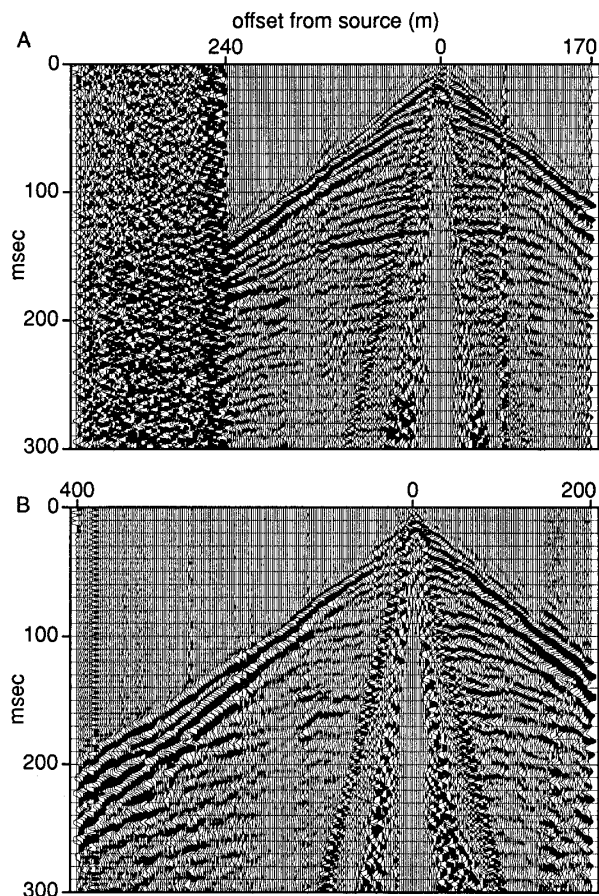


Figure 3. (A) True-amplitude shot gathers (24 dB/s spherical-divergence correction) demonstrate the highly variable reflection waveforms that do not seem to correlate to a single change in physical or seismic characteristics (velocity, attenuation, offset, or density) but more likely represent some complex combination of several. (B) Apparent anisotropic characteristics (in this case, attenuation), pronounced on some shot gathers, are directly related to the near surface in close proximity to the source.

ing. Interpreting migrated data provided only minor improvement in differentiating the subsidence mechanisms and their sequence, but migration did focus much of the energy distortion associated with very localized (30- to 40-m) undulations at the salt–upper Wellington contact (Fig. 4B). Dramatic subsidence structures revealed on CMP-stacked sections allude to a complex chronology of nonlinear interaction between salt leaching and associated roof-rock failure.

The current sinkhole expression and associated distortion of rock layers are the result of a minor episode of dissolution and subsidence in the history of this site. Rock layers disturbed by subsidence span >350 m along the transect cut by line 1 (Fig. 4). Changes in bed dip across this feature provide the key criteria for deciphering the sequence of dissolution and subsid-

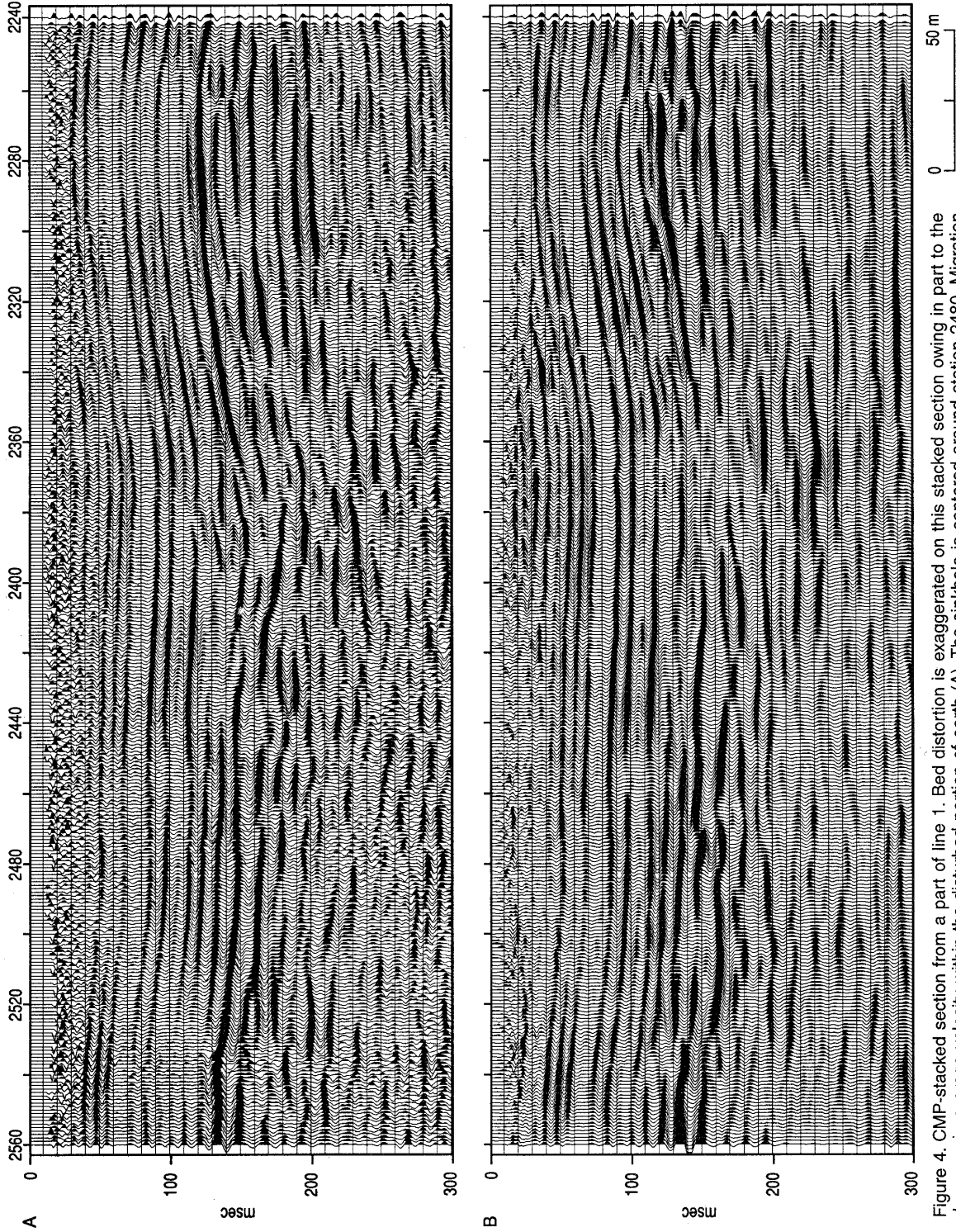


Figure 4. CMP-stacked section from a part of line 1. Bed distortion is exaggerated on this stacked section owing in part to the decrease in average velocity within the disturbed portion of earth (A). The sinkhole is centered around station 2480. Migration corrected for much of the optical distortion that results from dipping beds but reduced the resolution potential a bit (B).

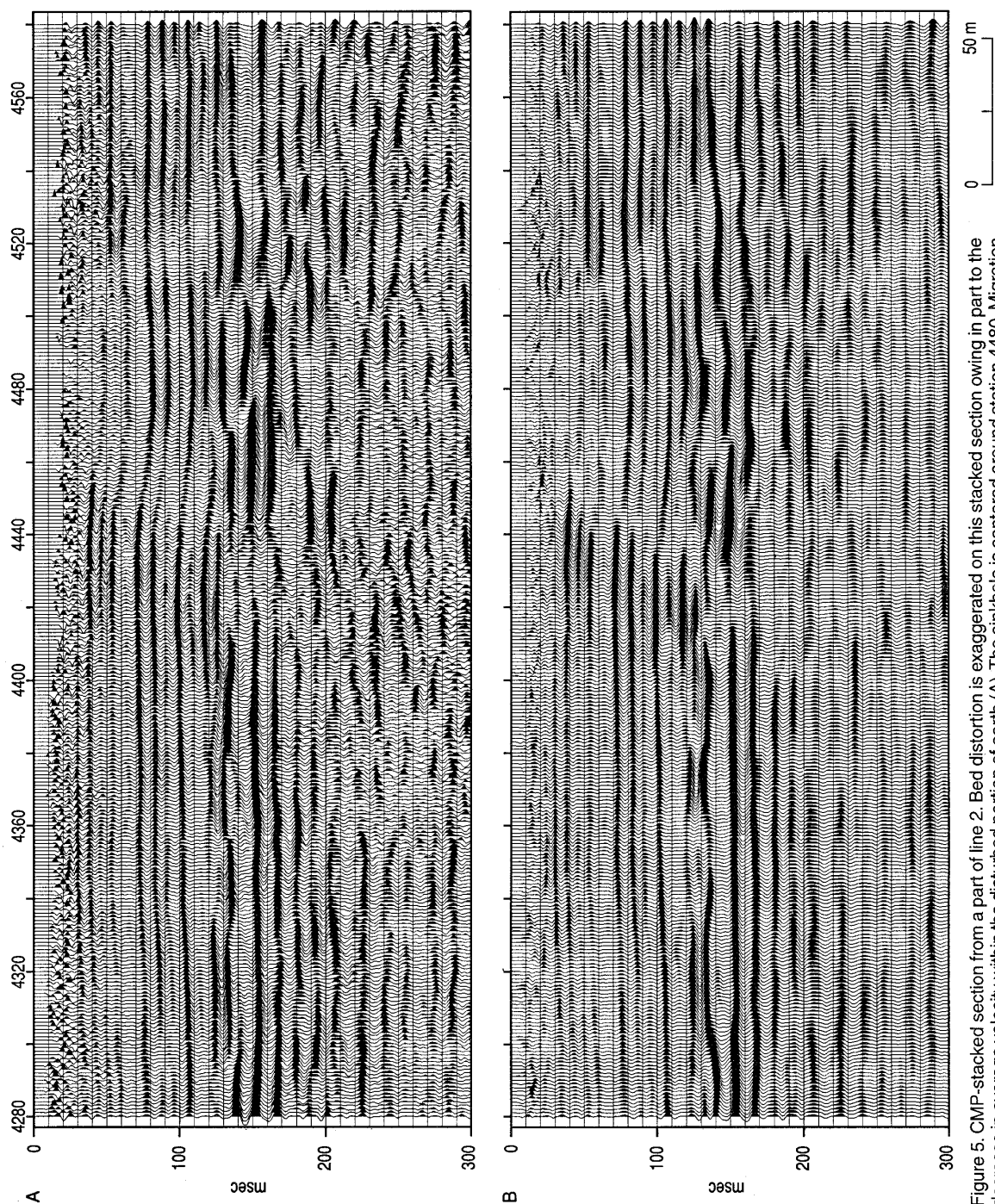


Figure 5. CMP-stacked section from a part of line 2. Bed distortion is exaggerated on this stacked section owing in part to the decrease in average velocity within the disturbed portion of earth (A). The sinkhole is centered around station 4480. Migration corrected for much of the optical distortion that results from dipping beds but reduced the resolution potential a bit (B).

ence events that led to the current sinkhole. The north-south slice through the sinkhole provides a complementary but significantly different picture of the subsurface (Fig. 5). The root of the sinkhole along line 2 is only ~125 m across and appears to be related to two periods of activity. Both the individual features and gross structure of the subsidence along line 2 is consistent with dissolution failures formed after a breach in borehole confinement or overmining. The subsidence structure does not rule out natural dissolution, but the line 2 feature alone more closely fits the anthropogenic model for the instigation of salt leaching. The coincident interpretation of lines 1 and 2 strongly supports natural dissolution.

Several episodes of subsidence are evident in most dissolution-related features (current and paleo) imaged on these two 1-km-long seismic profiles. Current surface subsidence at the intersection of U.S. 50 and Victory Road is probably related to the reactivation of natural salt-dissolution processes, which produced the seismically imaged, 350-m-wide subsidence feature. Focusing on the area likely active at the current time,

at least in relationship to the sinkhole, allows an understanding of the current processes (Fig. 6). The original subsidence in proximity to the current sinkhole was likely at the very end of the Tertiary Period or just prior to deposition of the Pliocene-Pleistocene Equus Beds, which appear as the much subdued draping layers within the deepest part of the bedrock low. With this as the backdrop, a well-defined set of faults can be interpreted, which likely defines the formation of the original sinkhole. The westernmost of these faults is about 50 m west of the current sinkhole. After this initial collapse came a period of gradual plastic deformation, when the rock layers were releasing stress in the form of an ever-growing synform defined by faults with normal geometry.

The current sinkhole is one of possibly many minor reactivations of dissolution and subsidence or oscillations between times of high and low stress release. During times of high strain rates, material above the salt subsided along reverse-fault planes, which defined an ever-narrowing cone structure extending to the ground surface. Alternately, the current development

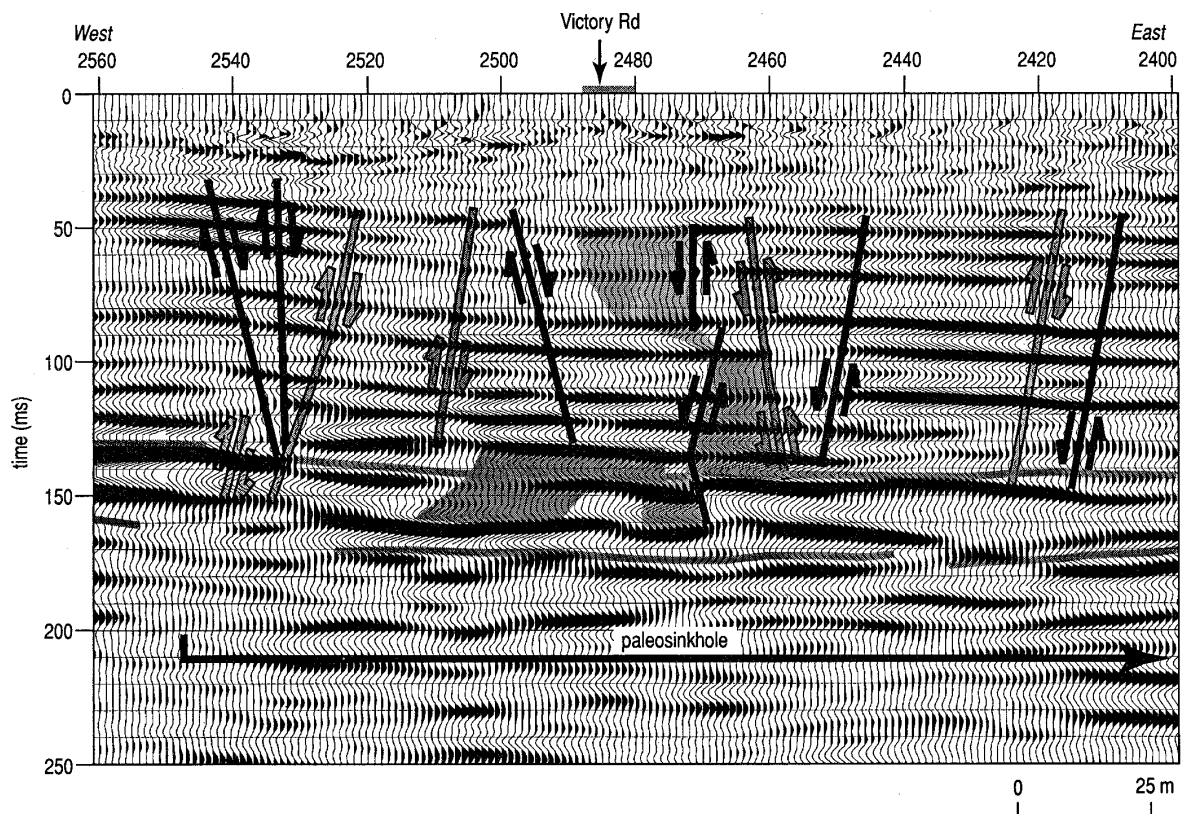


Figure 6. An interpreted part of line 1, showing two different paleosinkhole margins as reverse-oriented faults (light gray) that formed after rapid strain release in a brittle-rupture fashion. This was followed by a low-velocity, low-stress release that formed a synform (bowl-shaped depression) bounded by normal-type faults (black). The most recent subsidence was again the result of rock failure and rapid strain release that formed the tensional dome that caused beds to subside along reverse-fault planes (darker gray, toward center). Lighter shading (above) represents areas currently active, whereas darker shading (below) indicates areas for future concern.

of this sinkhole could be explained as recent failure of Permian rock layers above the salt that had bridged (roof-rock) void or rubble areas that remained following the Tertiary to Quaternary subsidence, as imaged on the seismic sections.

Using changes in amplitude and subtle breaks in rock-layer slopes, the high-angle reverse faults and subsidence cone (volume) can be defined (Fig. 6). Drapes in the bedrock beneath station 2480, with a noticeable change in amplitude, is interpreted to define the top of the subsidence cone. The subsidence volume, based on amplitude and synforms, appears to be nonsymmetrical, likely following a path of least strength. Faulting and differential compaction of materials within and above the salt represent a highly unsettled section of earth with a variety of areas indicative of bridging and the upward progression of subsidence. Areas of apparent bridging above the salt within the dissolution zone are good candidates for infilling by collapsing red-bed sediments. With the volume of undercompacted earth (possibly void or rubble) suggested by the seismic section and the proximity of the dissolution front, this area will continue

to experience variable rates of subsidence significantly into the future.

The complexity and diversity of subsidence patterns along line 2 are markedly different from those observed across line 1 (Fig. 7). The sinkhole appears symmetrically located within the subsurface subsidence zone and possesses a "root" consistent in size with subsidence features observed on seismic data from other sites that were induced by leaking oil-field brine from injection wells. This subsidence feature appears to have a well-defined zone where salt has been or is being leached, with an associated offset in intra-salt anhydrite or shale units. Reverse faults, which define the cone of disturbed sediments associated with the original subsidence at this site, are well defined by the amplitude zones near the points of greatest offset in the red-bed reflections. This area has undergone at least one period of gradual, low-stress relief, as the normal-fault geometries indicate. Consistent with line 1, the active cone of subsidence is bounded by reverse-fault planes centered on the sinkhole.

Mechanisms and gross chronology of structural failures, as interpreted from stacked seismic sections,

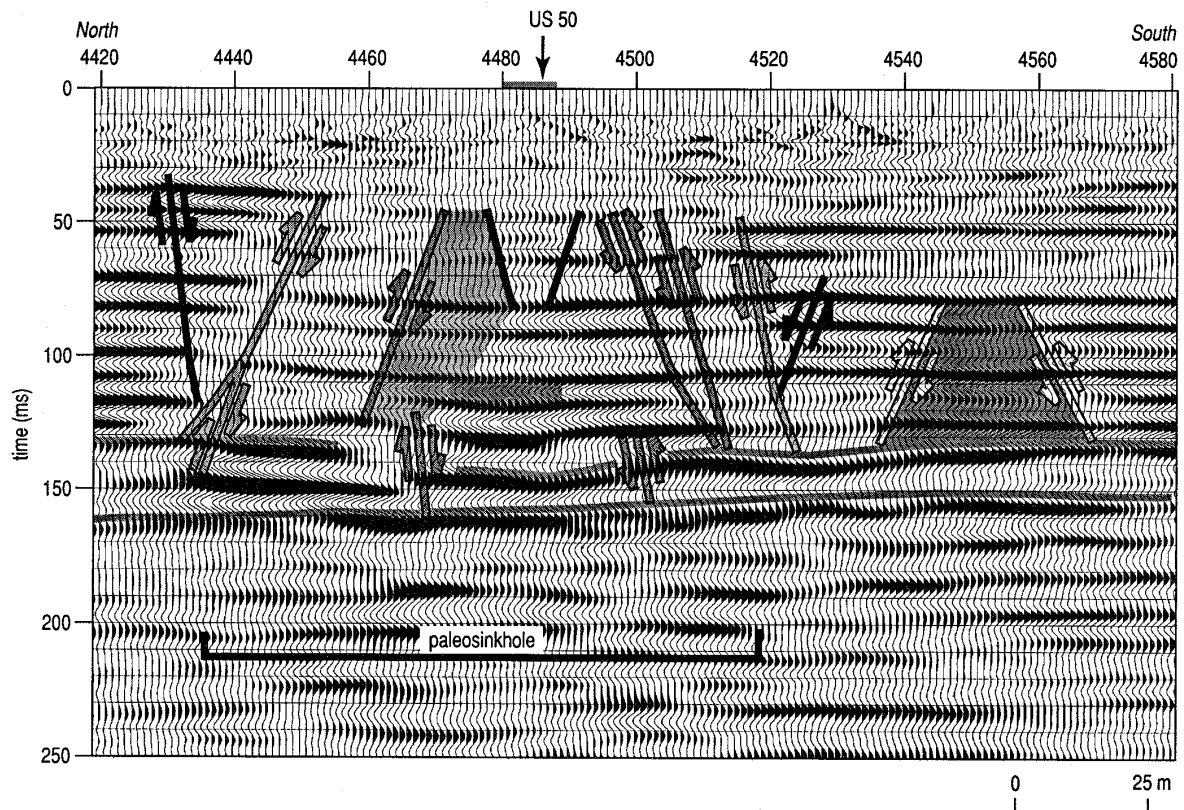


Figure 7. An interpreted part of line 2, with the original sinkhole margins indicated by reverse-oriented faults (light gray), which formed during rapid stress release during brittle-rock failure. This was followed by low-velocity, low-stress release forming a synform (bowl-shaped depression) bounded by normal-type faults (black). The most recent subsidence was again the result of rock failure and rapid stress release that formed the tensional dome that caused beds to subside along reverse-fault planes (darker gray, toward center). Darker shading bounded by white reverse faults indicates an area for future concern.

suggest that initial subsidence and associated bed offset occurred at high strain rates and were confined to a cone defined by reverse-fault planes. This process was active at least twice: once when the current 100-m-wide sinkhole developed, and initially as the 350-m-wide dissolution feature originally formed as a single, relatively continuous event. This 350-m-wide footprint could also be the result of dozens of uniquely segregated events occurring throughout the last million or so years. Separating each of the periods of rapid subsidence was a long period (not necessarily represented by uniform or continuous rates) of the downward movement (settling, relaxation) of sediments when little or no stress was building up on rock layers. These episodes of gradual subsidence continued in the subsurface, advancing as an ever-expanding bowl, geometrically defined by normal-fault planes until roof-rock failure above the salt reactivated high stress-relief processes. The rate of destabilization and failure, as well as the load-bearing potential of the rock layers above zones of dissolution, strongly influenced both the original subsidence geometries and dimensions as well as the subsequent reactivation of subsidence along the profiles.

SUMMARY AND CONCLUSIONS

Several episodes of subsidence are evident in most dissolution-related features (current and paleo) imaged on these two 1-km-long seismic profiles. The rate of destabilization and failure, as well as the load-bearing potential of the rock layers above zones of dissolution strongly influenced both the original subsidence geometries and dimensions as well as the subsequent reactivation of subsidence along the profiles. Current surface subsidence at the intersection of U.S. 50 and Victory Road is probably related to the reactivation of natural salt-dissolution processes that produced the seismically imaged, 300-m-wide subsidence feature interpreted to have been active during Tertiary and/or Quaternary time. Alternately, recent failure of Permian rock layers above the salt-bridging (roof-rock) void or rubble areas that remained after most of the Tertiary to Quaternary subsidence had slowed or stopped could explain the most recent sinkhole development.

With a subsidence history at this site potentially extending as far back as mid-Tertiary time, it is unlikely that subsidence will end within the next millennium. Until the highway started sinking here during 1998, little if any subsidence seems to have been associated with this paleosinkhole throughout late Quaternary time. This long period of inactivity, followed by the localized, rapid subsidence observed at this site, makes it reasonable to expect other small sinkholes to form without warning above this paleo-feature or other similar paleofeatures in this area. Considering the interpreted bed geometries, surface subsidence at the current sinkhole site will likely continue gradually along its northern and eastern edges,

elongating the sinkhole in those directions. Besides the obvious disruption to the road system, this subsidence feature unfortunately provides a pathway between the fresh waters of the Equus Beds and the more brackish waters of the Permian rocks. Surface subsidence will likely continue at a gradual rate for some time into the future. Sufficient bridging and undercompacted rock layers still exist beneath this sinkhole to sustain the current subsidence rate of ~ 0.3 m/yr for several years.

The interpretation of reflections from key stratigraphic horizons suggests that plastic deformation of rock layers over dissolution voids was followed by roof-rock failure along reverse-fault planes within an earth volume known as the tension dome. The original tensional dome was centered on the dissolution volume and extended from the base of the salt interval to near the surface. A long period of low strain, evident in layers outside the tensional dome, occurred along normal-fault planes for a significant part of the late Tertiary and early Quaternary. A much smaller tensional dome at the western extremity of the original tensional dome has controlled recent subsidence. Subsidence, associated with failure defined by this most recent dome, has followed a somewhat asymmetric path from salt to surface.

This study evaluated the effectiveness of using high-resolution vibroseis techniques on the shoulder of U.S. 50 when traffic was slowed but not stopped. Previous data collected in this area were acquired 1.5 km south along a quiet, east-west county road using a small recording-channel seismograph and an invasive, low-energy, impulsive-source survey. Equivalent dominant frequencies were recorded on both surveys, but recent efforts resulted in significantly greater energy penetration and a signal-to-noise ratio that resulted in usable data regardless of cultural noise levels. The bed resolution, coherency of bedding within subsidence features, and overall signal-to-noise ratio were greatly improved using minivibroseis-survey techniques.

If salt dissolution—anthropogenic or natural—has begun at this site, it is not possible with these data alone to identify definitively a fluid source or pathway. However, with the superimposition of this modern sinkhole and the mid-Tertiary to early Quaternary subsidence feature, and considering that the nearest disposal well with a history of fluid-containment problems is >2 km away, the sinkhole is likely natural in origin. Unfortunately, considering the long history of oil-field disposal-well-induced dissolution in this area and the proximity of this particular site to the natural dissolution front, neither catalyst can be completely ruled out.

ACKNOWLEDGMENTS

The author would like to thank Charles Ludders of the Kansas Department of Transportation, Mike Dealy from Groundwater Management District 2, and

Morris Korphage and Doug Lewis from the Kansas Corporation Commission for their support of this project. Also, thanks go to Rex Buchanan of the Kansas Geological Survey, who provided assistance during media coverage, and the field crew on this project: David Laflen, Joe Anderson, Mitchell Fiedler, and Chad Gratton.

REFERENCES CITED

- Anderson, N. L.; Watney, W. L.; Macfarlane, P. A.; and Knapp, R. W., 1995a, Seismic signature of the Hutchinson Salt and associated dissolution features: *Kansas Geological Survey Bulletin* 237, p. 57–65.
- Anderson, N. L.; Knapp, R. W.; Steeples, D. W.; and Miller, R. D., 1995b, Plastic deformation and dissolution of the Hutchinson Salt Member in Kansas: *Kansas Geological Survey Bulletin* 237, p. 66–70.
- Anderson, N. L.; Martinez, A.; and Hopkins, J. F., 1998, Salt dissolution and surface subsidence in central Kansas: a seismic investigation of the anthropogenic and natural origin models: *Geophysics*, v. 63, p. 366–378.
- Baar, C. A., 1977, *Applied salt-rock mechanics 1*: Elsevier, 294 p.
- Bayne, C. K., 1956, Geology and ground-water resources of Reno County, Kansas: *Kansas Geological Survey Bulletin* 120, 130 p.
- Beck, B. F.; Pettit, A. J.; and Herring, J. G. (eds.), 1999, *Hydrogeology and engineering geology of sinkholes and karst—1999*: Balkema, Rotterdam, 130 p.
- Black, R. A.; Steeples, D. W.; and Miller, R. D., 1994, Migration of shallow seismic reflection data: *Geophysics*, v. 59, p. 402–410.
- Carter, N. L.; and Hansen, F. D., 1983, Creep of rock salt: *Tectonophysics*, v. 92, p. 275–333.
- Davies, W. E., 1951, *Mechanics of cavern breakdown*: National Speleological Society, v. 13, p. 6–43.
- Ege, J. R., 1984, Formation of solution-subsidence sinkholes above salt beds: U.S. Geological Survey Circular 897, 11 p.
- Frye, J. C., 1950, Origin of Kansas Great Plains depressions: *Kansas Geological Survey Bulletin* 86, pt. 1, p. 1–20.
- Frye, J. C.; and Schoff, S. L., 1942, Deep-seated solution in the Meade Basin and vicinity, Kansas and Oklahoma: *American Geophysical Union Transactions*, v. 23, pt. 1, p. 35–39.
- Hunter, J. A.; Pullan, S. E.; Burns, R. A.; Gagne, R. M.; and Good, R. S., 1984, Shallow seismic-reflection mapping of the overburden–bedrock interface with the engineering seismograph—some simple techniques: *Geophysics*, v. 49, p. 1381–1385.
- Knapp, R. W.; Steeples, D. W.; Miller, R. D.; and McElwee, C. D., 1989, Seismic reflection surveys at sinkholes in central Kansas, in Steeples, D. W. (ed.), *Geophysics in Kansas: Kansas Geological Survey Bulletin* 226, p. 95–116.
- Merriam, D. F., 1963, The geologic history of Kansas: *Kansas Geological Survey Bulletin* 162, 317 p.
- Merriam, D. F.; and Mann, C. J., 1957, Sinkholes and related geologic features in Kansas: *Transactions of Kansas Academy of Science*, v. 60, p. 207–243.
- Miller, R. D.; Steeples, D. W.; Schulte, L.; and Davenport, J., 1993, Shallow seismic reflection study of a salt dissolution well field near Hutchinson, Kansas: *Mining Engineering*, October, p. 1291–1296.
- Miller, R. D.; Steeples, D. W.; and Weis, T. V., 1995, Shallow seismic-reflection study of a salt-dissolution subsidence feature in Stafford County, Kansas, in Anderson, N. L.; and Hedke, D. E. (eds.), *Geophysical atlas of selected oil and gas fields in Kansas: Kansas Geological Survey Bulletin* 237, p. 71–76.
- Miller, R. D.; Vilella, A. C.; and Xia, J., 1997, Shallow high-resolution seismic reflection to delineate upper 400 m around a collapse feature in central Kansas: *Environmental Geosciences*, v. 4, no. 3, p. 119–126.
- Rokar, R. B.; and Staudtmeister, K., 1985, Creep rupture criteria for rock salt, in Schreiber, B. C.; and Harner, H. L. (eds.), *Sixth International Symposium on Salt: Salt Institute, Inc., Virginia*, v. 1, p. 455–462.
- Steeples, D. W.; and Miller, R. D., 1990, Seismic reflection methods applied to engineering, environmental, and groundwater problems, in Ward, S. (ed.), *Geotechnical and environmental geophysics*, v. 1: review and tutorial: *Society of Exploration Geophysicists*, p. 1–30.
- Steeples, D. W.; Knapp, R. W.; and McElwee, C. D., 1986, Seismic reflection investigation of sinkholes beneath Interstate Highway 70 in Kansas: *Geophysics*, v. 51, p. 295–301.
- Walters, R. F., 1978, Land subsidence in central Kansas related to salt dissolution: *Kansas Geological Survey Bulletin* 214, p. 1–32.
- , 1980, Solution and collapse features in the salt near Hutchinson, Kansas: *Geological Society of America, South-Central Section, Field Trip Notes*, 10 p.
- , 1991, Gorham oil field: *Kansas Geological Survey Bulletin* 228, p. 1–112.
- Watney, W. L.; Berg, J. A.; and Paul, S., 1988, Origin and distribution of the Hutchinson Salt (lower Leonardian) in Kansas: *Society of Economic Paleontologists and Mineralogists, Mid-Continent Section, Special Publication* 1, p. 113–135.

